

# **Epigenetic regulation of gene expression in colorectal cancer cells**

by

**Saira Rose Ali**

*Thesis  
Submitted to Flinders University  
for the degree of*

**Doctor of Philosophy**  
College of Medicine and Public Health  
February 2020

---

# Table of Contents

---

<b>Table of Contents .....</b>	<b>ii</b>
<b>List of Figures .....</b>	<b>ix</b>
<b>List of Tables .....</b>	<b>xiii</b>
<b>List of Abbreviations.....</b>	<b>xv</b>
<b>Summary .....</b>	<b>xviii</b>
<b>Declaration.....</b>	<b>xx</b>
<b>Publications and Presentations .....</b>	<b>xxi</b>
Peer-reviewed Publications.....	xxi
Poster Presentations .....	xxi
Oral presentations .....	xxii
<b>Acknowledgements.....</b>	<b>xxiii</b>
<b>Chapter 1. Introduction.....</b>	<b>25</b>
1.1 Epigenetic regulation of gene expression.....	25
1.2 Colorectal cancer.....	26
1.2.1 Epidemiology of colorectal cancer.....	26
1.2.2 Colorectal cancer pathogenesis.....	27
1.2.3 Genetic and epigenetic changes in colorectal cancer.....	30
1.2.4 Risk Factors .....	32
1.2.5 Screening and diagnostics .....	33
1.2.6 Current treatment .....	33
1.3 Dietary effects on colorectal cancer.....	34
1.3.1 Diet and colorectal cancer .....	34
1.4 Butyrate .....	34
1.4.1 Butyrate and colorectal cancer .....	35
1.4.2 Effects of butyrate on gene expression in colorectal cancer cells .....	35
1.4.3 Mechanisms of action of butyrate in CRC.....	38
1.5 MicroRNAs in colorectal cancer .....	52

## TABLE OF CONTENTS

1.5.1 MicroRNA discovery .....	52
1.5.2 MicroRNA biogenesis and function .....	53
1.5.3 MicroRNAs in tumorigenesis and colorectal cancer .....	56
1.5.4 MicroRNAs as biomarkers of tumorigenic states and therapeutic agents.....	59
1.5.5 Effects of butyrate on microRNAs in colorectal cancer.....	60
1.6 lncRNAs in colorectal cancer.....	61
1.6.1 lncRNA discovery.....	62
1.6.2 lncRNA biogenesis and function.....	62
1.6.3 lncRNAs in tumorigenesis and colorectal cancer.....	68
1.6.4 lncRNAs as biomarkers of tumour stages and therapeutic agents .....	73
1.6.5 Effects of HDAC inhibitors on lncRNAs in cancer .....	75
1.7 Aims and hypotheses .....	75
1.7.1 General hypotheses and aims.....	75
1.7.2 Chapter 3 Aim .....	77
1.7.3 Chapter 4 Aim .....	77
1.7.4 Chapter 5 Aim .....	77
1.8 Chapter 1: Preliminary data.....	77
1.8.1 Summary.....	77
<b>Chapter 2. Materials and Methods .....</b>	<b>82</b>
2.1 Cell culture.....	82
2.1.1 Cell lines .....	82
2.1.2 Storage and revival.....	83
2.1.3 Mycoplasma testing .....	83
2.2 Transfections and treatments with miRNA mimics, lncRNA siRNAs and target gene siRNAs .....	84
2.2.1 High-throughput functional screen experiments .....	84
2.2.2 Proliferation and apoptosis assays.....	86
2.3 Bioinformatics .....	89

## TABLE OF CONTENTS

2.3.1 miRNA target prediction .....	89
2.3.2 KEGG Mapper .....	90
2.4 mRNA expression analysis .....	90
2.4.1 TRIzol RNA extraction .....	90
2.4.2 RNA quantification .....	91
2.4.3 RNA quality analysis.....	91
2.5 Relative quantitation real-time reverse transcriptase PCR.....	91
2.5.1 Real-time RT-PCR for microRNAs .....	91
2.5.2 Real-time RT-PCR for mRNAs.....	92
2.6 Protein analysis.....	94
2.6.1 Protein purification and quantification.....	94
2.6.2 Western blotting.....	94
2.6.3 Protein expression normalisation and analysis .....	95
2.7 WNT signalling: TOPflash and FOPflash assays .....	95
2.7.1 Forward transfection .....	95
2.7.2 TOPflash/FOPflash assay analysis .....	96
2.8 Total and small RNA-seq .....	96
2.9 Network and pathway analysis.....	97
2.9.1 Protein-protein interaction (PPI) network construction.....	97
2.9.2 Gene ontology (GO) analysis.....	97
2.9.3 miRNA-mRNA network analysis.....	98
2.9.4 lncRNA-miRNA-mRNA network analysis.....	98
2.10 Flow cytometry .....	98
2.10.1 Cell cycle analysis.....	99
2.10.2 Cell death analysis.....	99
2.10.3 Flow cytometry analysis.....	99
2.11 Reagents and equipment used for experiments .....	100
<b>Chapter 3. High-throughput functional microRNA screen and validation.....</b>	<b>104</b>
3.1 Introduction.....	104

## TABLE OF CONTENTS

3.2 Results .....	105
3.2.1 Butyrate-sensitising miRNA selection .....	105
3.2.2 Further validation of miRNA and butyrate growth and death effects in CRC cells using flow cytometry .....	106
3.2.3 Validation of viability and apoptosis in LIM1215 CRC cells after miRNA mimic transfection and butyrate treatment .....	111
3.2.4 Investigation of miR-125b in KRAS mutant disrupted cells, Hke3..	112
3.2.5 Investigation of viability and apoptosis in HFF ‘normal’ fibroblasts after miRNA mimic transfection and butyrate treatment .....	113
3.2.6 miRNA target prediction using bioinformatics analysis.....	115
3.2.7 mRNA expression analysis .....	120
3.2.8 Protein expression analysis .....	126
3.2.9 miRNA target gene suppression in the butyrate response and effect on proliferation.....	134
3.2.10 WNT signalling activity.....	136
3.3 Discussion.....	139
3.3.1 Summary.....	139
3.3.2 Butyrate-sensitising miRNAs regulate CRC cell proliferation, apoptosis and the cell cycle .....	139
3.3.3 Butyrate-sensitising miRNAs regulate cell viability and apoptosis in LIM1215 CRC cells.....	143
3.3.4 Butyrate-sensitising miRNAs regulate cell viability and death in ‘normal’ cell line models.....	144
3.3.5 Validation of predicted miRNA target genes.....	146
3.3.6 <i>PIK3R3</i> knockdown mimics miR-181a cellular response .....	151
3.3.7 miR-181a regulates WNT signalling.....	151
3.3.8 Conclusion .....	153
<b>Chapter 4. Integrative transcriptome network analysis in butyrate treated CRC cells .....</b>	<b>154</b>
4.1 Introduction.....	154

## TABLE OF CONTENTS

4.2 Results .....	155
4.2.1 Identification of butyrate regulated mRNAs .....	155
4.2.2 Identification of butyrate regulated miRNAs .....	155
4.2.3 Butyrate regulated protein-protein interaction (PPI) network analysis .....	157
4.2.4 Functional gene ontology (GO) analysis of butyrate regulated genes .....	159
4.2.5 Pathway enrichment analysis of butyrate regulated genes .....	162
4.2.6 Integrative network construction using miRNA target prediction....	165
4.2.7 Investigation of key miRNA-mRNA interactions involved in cell growth and death pathways in the butyrate response .....	167
4.2.8 Validation of the butyrate effect on miRNA and mRNA target gene expression .....	169
4.2.9 Effect of miRNA nodes on both cell cycle and cell growth in CRC in the presence of butyrate .....	170
4.2.10 Effects of miR-139 and miR-542 on cell growth and death in other cell types.....	176
4.2.11 miRNA target confirmation using miRNA mimics in HCT116 cells .....	178
4.2.12 Effect of miRNA target gene silencing and butyrate treatment on CRC cell proliferation and the cell cycle .....	179
4.3 Discussion.....	182
4.3.1 Summary.....	182
4.3.2 Butyrate regulated gene expression .....	182
4.3.3 Butyrate regulated PPI networks .....	183
4.3.4 GO and pathway enrichment analysis .....	184
4.3.5 Integrative network analysis .....	186
4.3.6 Butyrate-sensitising miRNAs regulate CRC cell proliferation, apoptosis and cell cycle.....	188
4.3.7 Butyrate-sensitising miRNAs regulate cell viability and apoptosis in LIM1215 cells.....	192

## TABLE OF CONTENTS

4.3.8 Butyrate-sensitising miRNAs regulate cell viability and apoptosis in ‘normal’ cell line models .....	193
4.3.9 Butyrate regulates target gene expression.....	193
4.3.10 Effect of target gene knockdown and butyrate treatment on cell proliferation and the cell cycle.....	194
4.3.11 Conclusion .....	195
<b>Chapter 5. High-throughput functional lncRNA screen and validation .....</b>	<b>196</b>
5.1 Introduction.....	196
5.2 Results .....	196
5.2.1 Primary high-throughput screen.....	196
5.2.2 Secondary lncRNA-targeting siRNA screen.....	200
5.2.3 lncRNA-miRNA-mRNA interaction networking using Cytoscape ..	202
5.2.4 MALAT1 functional investigation .....	204
5.3 Discussion.....	215
5.3.1 Summary.....	215
5.3.2 Primary high-throughput screen.....	216
5.3.3 Secondary screen investigating RNA interference of lncRNAs.....	216
5.3.4 Integrative network and pathway analyses .....	217
5.3.5 MALAT1 butyrate regulation and knockdown .....	219
5.3.6 Effects of MALAT1 knockdown on proliferation, apoptosis and the cell cycle .....	220
5.3.7 Effect of MALAT1 RNAi on miRNA and mRNA interactors.....	222
5.3.8 Conclusion .....	223
<b>Chapter 6. Summary and conclusions .....</b>	<b>225</b>
6.1 Thesis summary .....	225
6.2 Functional high-throughput screen identifies miRNAs sensitise CRC cells to butyrate .....	225
6.3 Systems biology approach reveals butyrate-sensitising miRNAs and their involvement in the cell cycle.....	226
6.4 Functional RNAi screen identifies butyrate-sensitising lncRNAs in CRC cells	227

## TABLE OF CONTENTS

6.5 Future directions and applications .....	228
6.6 Conclusion.....	235
<b>Appendix 1 Canonical pathway analysis for miR-125b predicted target genes ..</b>	<b>237</b>
<b>Appendix 2: Canonical pathway analysis for miR-181a predicted target gene ...</b>	<b>241</b>
<b>Appendix 3: Protein loading images .....</b>	<b>245</b>
<b>Appendix 4: Differentially expressed mRNA genes.....</b>	<b>246</b>
<b>Appendix 5: Protein-protein interaction network interactors .....</b>	<b>248</b>
<b>Appendix 6: GO analysis Molecular Functions and Cellular Components .....</b>	<b>256</b>
<b>Appendix 7: WikiPathways and Reactome GO pathway analysis .....</b>	<b>259</b>
<b>Appendix 8: Differentially expressed miRNA list .....</b>	<b>261</b>
<b>Appendix 9: lncRNA screen quality control.....</b>	<b>263</b>
<b>Appendix 10: lncRNA-miRNA interactions .....</b>	<b>264</b>
<b>Appendix 11: MALAT1 RNA-seq data .....</b>	<b>265</b>
<b>References.....</b>	<b>266</b>

# List of Figures

---

Figure 1-1 Colonic crypt structure .....	29
Figure 1-2 Colorectal adenoma-carcinoma development.....	32
Figure 1-3 Mechanism of action: HDAC inhibition.....	39
Figure 1-4 Mechanisms of action of butyrate in colorectal cancer.....	52
Figure 1-5 MicroRNA biogenesis pathway.....	55
Figure 1-6 lncRNA transcript origins .....	63
Figure 1-7 lncRNA archetypes.....	68
Figure 1-8 Therapeutic targeting of lncRNA molecules .....	74
Figure 3-1 Flow cytometry analysis of apoptosis in miRNA transfected HCT116 cells after 24 h of butyrate treatment.....	107
Figure 3-2 Flow cytometry analysis of apoptosis in miRNA transfected HCT116 cells after 24 h of butyrate treatment.....	108
Figure 3-3 Flow cytometry analysis of the cell cycle in miRNA transfected HCT116 cells after 24 h of butyrate treatment.....	109
Figure 3-4 Flow cytometry analysis of the cell cycle in miRNA transfected HCT116 cells after 24 h of butyrate treatment.....	110
Figure 3-5 Cell viability and apoptosis in miRNA transfected LIM1215 cells after 24 h of butyrate treatment.....	112
Figure 3-6 Cell proliferation in miR-125b transfected Hke3 cells after 24 h of butyrate treatment .....	113
Figure 3-7 Butyrate response of immortalised ‘normal’ cells .....	114
Figure 3-8 Cell viability and apoptosis in miRNA transfected HFF ‘normal’ cells after 24 h of butyrate treatment .....	115
Figure 3-9 KEGG mapper canonical pathway analysis for miR-125b: Pathways in Cancer.....	118
Figure 3-10 KEGG mapper canonical pathway analysis miR-181a: PI3K-Akt Signalling Pathway .....	119
Figure 3-11 Real-time RT-PCR analysis of predicted miR-593 target gene mRNA levels in HCT116 cells after 24 h of butyrate treatment.....	121
Figure 3-12 Real-time RT-PCR analysis of predicted miR-1227 target gene mRNA levels in HCT116 cells after 24 h of butyrate treatment.....	122
Figure 3-13 Real-time RT-PCR analysis of predicted miR-125b target gene mRNA levels in HCT116 cells after 24 h of butyrate treatment.....	123

## LIST OF FIGURES

Figure 3-14 Real-time RT-PCR analysis of predicted miR-181a target gene mRNA levels in HCT116 cells 72 h post-transfection.....	124
Figure 3-15 Real-time RT-PCR analysis of predicted miR-181a target gene mRNA levels in HCT116 cells after 24 h of butyrate treatment. ....	126
Figure 3-16 Protein expression of miR-593 predicted targets .....	128
Figure 3-17 Protein expression of miR-1227 predicted targets .....	130
Figure 3-18 Protein expression of miR-125b predicted targets .....	131
Figure 3-19 Protein expression of miR-181a predicted targets.....	133
Figure 3-20 DVL3 and PIK3R3 siRNA knockdown efficiency in HCT116 .....	135
Figure 3-21 Cell proliferation in DVL3 and PIK3R3 siRNA transfected HCT116 cells after 24 h of butyrate treatment.....	135
Figure 3-22 Butyrate responsive miRNAs and butyrate alter WNT reporter activity in HCT116 cells .....	137
Figure 3-23 Butyrate responsive miRNAs and butyrate alter WNT reporter activity in RKO cells.....	138
Figure 4-1 Volcano plot representing the differential expression of butyrate responsive mRNAs.....	155
Figure 4-2 Volcano plot representing the differential expression of butyrate responsive miRNAs.....	156
Figure 4-3 Butyrate regulated PPI network for DE protein-coding genes .....	158
Figure 4-4 Gene Ontology Enrichment analysis for butyrate DE genes .....	160
Figure 4-5 KEGG, WikiPathways and Reactome pathway analysis of differentially expressed butyrate responsive mRNAs .....	163
Figure 4-6 Integrative miRNA-mRNA interaction network of butyrate regulated genes in CRC .....	166
Figure 4-7 Real-time RT-PCR analysis of networking miRNAs and predicted target gene expression validation in HCT116 cells treated with 2.5 mM butyrate for 24 h.....	169
Figure 4-8 Flow cytometry analysis of the cell cycle in miRNA transfected HCT116 cells after 24 h of butyrate treatment.....	171
Figure 4-9 Cell cycle analysis using flow cytometry in miRNA transfected HCT116 cells after 24 h of butyrate treatment.....	172
Figure 4-10 Proliferation of HCT116 cells after transfection with miRNA mimics and butyrate treatment for 24 h .....	173
Figure 4-11 Flow cytometry analysis of apoptosis in miRNA transfected HCT116 cells after 24 h of butyrate treatment.....	175

## LIST OF FIGURES

Figure 4-12 Apoptosis analysis of networking miRNAs using Cytoflex flow cytometry .....	176
Figure 4-13 Cell viability and apoptosis in miRNA transfected LIM1215 cells after 24 h of butyrate treatment.....	177
Figure 4-14 Cell viability and apoptosis in miRNA transfected HFF normal cells after 24 h of butyrate treatment .....	178
Figure 4-15 Real-time RT-PCR analysis of miRNA target gene expression in HCT116 cells treated with butyrate for 24 h.....	179
Figure 4-16 <i>EIF4G2</i> siRNA knockdown efficiency in HCT116 cells .....	180
Figure 4-17 siRNA knockdown of miR-139 target gene <i>EIF4G2</i> .....	181
Figure 4-18 Flow cytometry analysis of the cell cycle in siRNA transfected HCT116 cells after 24 h of butyrate treatment.....	181
Figure 4-19 Cell cycle analysis of <i>EIF4G2</i> siRNA transfected HCT116 cells using flow cytometry.....	182
Figure 5-1 High-throughput screen workflow summary .....	197
Figure 5-2 Summary of primary screen data.....	199
Figure 5-3 lncRNA siRNA secondary screen SMARTpool validation of apoptosis data .....	202
Figure 5-4 Integrative apoptotic lncRNA-miRNA-mRNA interaction network of butyrate regulated genes in CRC .....	203
Figure 5-5 Real-time RT-PCR analysis of MALAT1 expression in HCT116 CRC cells .....	205
Figure 5-6 MALAT1 siRNA knockdown efficiency in HCT116 CRC cells.....	205
Figure 5-7 Cell viability and apoptosis in MALAT1 siRNA transfected HCT116 cells after 24 h of butyrate treatment.....	207
Figure 5-8 Flow cytometry analysis of apoptosis in siRNA transfected HCT116 cells after 24 h of butyrate treatment.....	208
Figure 5-9 Apoptosis analysis of MALAT1 siRNA using Cytoflex flow cytometry.....	209
Figure 5-10 Proliferation of HCT116 cells after transfection with MALAT1 siRNAs and 24 h butyrate treatment.....	209
Figure 5-11 Viability of HCT116 cells after transfection with MALAT1 siRNAs and 24 h butyrate treatment .....	210
Figure 5-12 Flow cytometry analysis of the cell cycle in siRNA transfected and butyrate treated HCT116 cells.....	210
Figure 5-13 Cell cycle analysis using flow cytometry in butyrate treated HCT116 cells.....	211

## LIST OF FIGURES

Figure 5-14 mRNA and miRNA expression changes in HCT116 cells exposed to MALAT1 siRNAs and butyrate.....	215
Figure 6-1 Summary of non-coding RNA interactions contributing to butyrate sensitisation of CRC cells .....	233
Figure A1-1 KEGG mapper canonical pathway analysis miR-125b: RAS Signalling Pathway .....	237
Figure A1-2 KEGG mapper canonical pathway analysis miR-125b: MAPK Signalling Pathway .....	238
Figure A1-3 KEGG mapper canonical pathway analysis miR-125b: PI3K-AKT Signalling pathway.....	239
Figure A1-4 KEGG mapper canonical pathway analysis miR-125b: WNT Signalling pathway.....	240
Figure A2-1 KEGG mapper canonical pathway analysis miR-181a: Pathways in Cancer .....	241
Figure A2-2 KEGG mapper canonical pathway analysis miR-181a: MAPK Signalling Pathway .....	242
Figure A2-3 KEGG mapper canonical pathway analysis miR-181a: RAS Signalling Pathway .....	243
Figure A2-4 KEGG mapper canonical pathway analysis miR-181a: Apoptosis.....	244
Figure A3-1 Protein loading for total protein normalisation .....	245
Figure A9-1 Correlation analysis of lncRNA-targeting siRNA primary high-throughput screen.....	263
Figure A11-1 MALAT1 RNA-seq data .....	265

# List of Tables

---

Table 1-1 Summary of key oncogenic and tumour suppressor miRNAs involved in colorectal cancer cell growth and death.....	58
Table 1-2 Summary of dysregulated lncRNAs involved in growth, death and migration in colorectal cancer cells. ....	71
Table 1-3 Butyrate-sensitising miRNAs from an unbiased high-throughput functional screen.....	78
Table 1-4 Summary of results collated during Honours year 2014.....	79
Table 2-1: Chemicals, consumables and reagents .....	100
Table 2-2 Equipment and Software .....	101
Table 2-3: Primers and Oligonucleotides .....	101
Table 2-4: Antibodies .....	103
Table 2-5: Buffers and Solutions .....	103
Table 3-1 Coefficient of drug interaction values for miRNA and butyrate interactions for xCELLigence proliferation data.....	106
Table 4-1 Top three 'Biological processes' identified in GO enrichment analysis .....	161
Table 4-2 Enriched pathway terms identified using KEGG in ClueGO.....	164
Table 4-3 Cell cycle related miRNA-mRNA interactions identified by interactive network analysis .....	168
Table 4-4 Apoptosis related miRNA-mRNA interactions identified by interactive network analysis .....	168
Table 4-5 Coefficient of drug interaction values for miRNA and butyrate interactions for xCELLigence proliferation data.....	174
Table 5-1 Selected lncRNA hits from the primary high-throughput functional siRNA screen.....	200
Table 5-2 Secondary screen hits .....	201
Table 5-3 Interaction table representing anti-correlating lncRNA-miRNA-mRNA interactors only.....	204
Table 5-4 Binding sites for miR-200b in MALAT1.....	212
Table 5-5 Binding sites for miR-200c in MALAT1 .....	213
Table 5-6 Binding sites for miR-335 in MALAT1 .....	214
Table A4-1 Top 100 mRNA differentially expressed genes.....	246
Table A5-1 Protein-protein interaction network interactions.....	248
Table A6-1 Top three enriched Molecular Functions identified in ClueGO.....	256

## LIST OF TABLES

Table A6-2 Top three enriched Cellular Components identified in ClueGO .....	257
Table A7-1 Enriched pathway terms identified using WikiPathways in ClueGO.....	259
Table A7-2 Enriched pathway terms identified using Reactome in ClueGO.....	260
Table A8-1 Differentially expressed miRNA genes selected for network analysis .....	261
Table A10-1 lncRNA-miRNA interactions .....	264

# List of Abbreviations

---

<i>ACTB</i>	beta-actin
<i>AKT3</i>	AKT serine/threonine kinase 3
<i>ANRIL</i>	antisense non-coding RNA in the INK4 locus
<i>APC</i>	adenomatous polyposis coli
<i>B2M</i>	beta-two microglobulin
<i>BAK1</i>	BCL2 antagonist/killer 1
<i>BAX</i>	BCL2 associated X, apoptosis regulator
<i>BCL2</i>	B-cell lymphoma 2
<i>BCL9</i>	B-cell CLL/lymphoma 9
<i>BIRC5</i>	baculoviral IAP repeat-containing protein 5
<i>BMI1</i>	BMI1 proto-oncogene, polycomb ring finger
<i>BMP</i>	bone morphogenetic protein
bp	base pair
<i>BRAF</i>	B-Raf proto-oncogene, serine/threonine kinase
<i>C.elegans</i>	<i>Caenorhabditis elegans</i>
<i>CAC</i>	Citric acid cycle
<i>CCND1</i>	cyclin D1
<i>CDK4</i>	cyclin-dependent kinase 4
<i>CDK19</i>	cyclin-dependent kinase 19
<i>CDKN2A</i>	cyclin-dependent kinase inhibitor 2A
<i>CDX2</i>	caudal type homeobox 2
<i>CIMP</i>	CpG island methylator phenotype
<i>CIN</i>	chromosomal instability
<i>CK1a</i>	casein kinase 1 alpha
<i>c-MYC</i>	MYC proto-oncogene, bHLH transcription factor
<i>COX2</i>	cyclooxygenase 2
<i>CRC</i>	colorectal cancer
<i>Ct</i>	threshold cycle
<i>CTCL</i>	cutaneous T-cell lymphoma
<i>CV1</i>	cell viability 1
<i>CV2</i>	cell viability 2
<i>DCC</i>	DCC netrin 1 receptor
<i>DE</i>	differentially expressed
<i>DGCR8</i>	DiGeorge syndrome critical region gene 8
<i>DNMT</i>	DNA methyltransferase
<i>dsRNA</i>	double stranded RNA
<i>DTT</i>	dithiothreitol
<i>DUSP1</i>	dual specificity phosphatase 1
<i>DVL3</i>	dishevelled segment polarity protein 3
<i>EEF2K</i>	eukaryotic elongation factor 2 kinase
<i>EGFR</i>	epidermal growth factor receptor
<i>EIF4G2</i>	eukaryotic translation initiation factor 4 gamma 2
<i>EphB2</i>	Eph receptor B2
<i>EphB3</i>	Eph receptor B3
<i>ERBB2</i>	Erb-b2 receptor tyrosine kinase 2
<i>ERK1</i>	extracellular signal-regulated kinase 1
<i>ERK2</i>	extracellular signal-regulated kinase 2
<i>FAP</i>	familial adenomatous polyposis
<i>FN1</i>	fibronectin 1
<i>FOBT</i>	faecal occult blood test

## LIST OF ABBREVIATIONS

<i>FOS</i>	fos proto-oncogene, AP-1 transcription factor
<i>FZD4</i>	frizzled class receptor 4
<i>GAB2</i>	GRB2 associated binding protein 2
<i>GADD45A</i>	growth arrest and DNA damage inducible alpha
<i>GAPDH</i>	glyceraldehyde-3-phosphate dehydrogenase
gFOBT	guaiac faecal occult blood test
GO	gene ontology
<i>GRB2</i>	growth factor receptor bound protein 2
<i>GSK3<math>\beta</math></i>	glycogen synthase kinase 3 beta
HAA	heterocyclic aromatic amine
HATs	histone acetyltransferases
HCV	hepatitis C virus
HDAC	histone deacetylase
HDACi	histone deacetylase inhibitor
HDI	human development index
HDM	histone demethylase
Hi	high
HMT	histone methyltransferase
HNPCC	hereditary non-polyposis colorectal cancer
HRP	horse radish peroxidase
hsa	<i>Homo sapiens</i>
HWA	high induction of WNT activity
iFOBT	immunohistochemical faecal occult blood test
<i>IGF1R</i>	insulin like growth factor 1 receptor
IPA	ingenuity pathway analysis
<i>JUN</i>	jun proto-oncogene, AP-1 transcription factor
KD	knockdown
KEGG	Kyoto Encyclopedia of Genes and Genomes
LC	lethal cell viability
<i>LEF</i>	lymphoid enhancer binding factor
lncRNA	long non-coding RNA
Log2FC	Log2 fold change
<i>LRP6</i>	LDL receptor related protein 6
LWA	lower changes in WNT activity levels
<i>MALAT1</i>	metastasis associated lung adenocarcinoma transcript
<i>MAP3K8</i>	mitogen-activated protein kinase kinase kinase 8
<i>MAPK</i>	mitogen-activated protein kinase
<i>MCT1</i>	monocarboxylate transporter 1
miRNA	microRNA
miRAGE	miRNA serial analysis of gene expression
M-MLV RT	Moloney Murine Leukemia Virus Reverse Transcriptase
<i>MLH1</i>	mutL homolog 1
MM	multiple myeloma
mRNA	messenger RNA
<i>MSH2</i>	mutS homolog 2
<i>MSH6</i>	mutS homolog 6
<i>MSI</i>	microsatellite instability
<i>mTOR</i>	mechanistic target of rapamycin kinase
NC	negative control
NGS	next generation sequencing
<i>NLK</i>	nemo like kinase
NOC	n-nitroso compounds
<i>NRAS</i>	NRAS proto-oncogene, GTPase

## LIST OF ABBREVIATIONS

<i>NUP62</i>	nucleoporin 62
OE	overexpression
<i>PAH</i>	polycyclic aromatic hydrocarbons
<i>PAK2</i>	p21 (RAC1) activated kinase 2
PcG	polycomb-group proteins
PCNA	proliferating cell nuclear antigen
<i>PIK3R3</i>	phosphoinositide-3-kinase regulatory subunit 3
<i>PMS2</i>	PMS1 homolog 2, mismatch repair system component
PPI	protein-protein interaction
PRC1	polycomb repressive complex 1
Pre-miRNA	precursor microRNA
Pri-miRNA	primary microRNA
<i>PRKAA2</i>	protein kinase AMP-activated catalytic subunit alpha 2
PTCL	peripheral T-Cell lymphoma
<i>PTEN</i>	phosphatase and tensin homolog
<i>PUMA</i>	p53 upregulated modulator of apoptosis
PVDF	polyvinylidene fluoride
Real-time RT-PCR	real-time reverse transcriptase polymerase chain reaction
RIN	RNA integrity number
RISC	RNA induced silencing complex
RNAi	RNA interference
rRNA	ribosomal RNA
RS	resistant starch
RTCA	real time cell analysis
<i>S6K1</i>	ribosomal protein S6 kinase
SAHA	suberoylanilide hydroxamic acid
SEM	standard error of the mean
shRNA	short hairpin RNA
siRNA	small interfering RNA
<i>SMAD4</i>	SMAD family member 4
<i>SMCT1</i>	sodium monocarboxylate transporter 1
<i>STAT3</i>	signal transducer and activator of transcription 3
<i>TCF4</i>	transcription factor 4
TERC	telomerase RNA component
TERT	telomerase reverse transcriptase
<i>TGF-<math>\beta</math></i>	transforming growth factor beta
TRBP	TAR RNA binding protein
<i>TRIM29</i>	tripartite motif containing 29
TUG1	taurine upregulated 1
VPA	valproic acid
<i>WEE1</i>	WEE1 G2 checkpoint kinase
<i>WNT3A</i>	Wnt family member 3A
<i>WNT8A</i>	Wnt family member 8A
WT	wild type
<i>ZEB1</i>	zinc finger E-box binding homeobox 1
3'UTR	three prime untranslated region
5'UTR	five prime untranslated region

# Summary

---

Despite improvements in colorectal cancer (CRC) diagnosis and therapy, CRC remains the second leading cause of cancer-related deaths worldwide; hence, there is a need for innovative and novel treatment approaches. CRC development and progression involves several epigenetic alterations including changes in histone modification patterns, DNA methylation and dysregulated non-coding RNA expression (microRNAs (miRNAs) and long non-coding RNAs (lncRNAs)). Dietary molecules, including the gut fermentation product butyrate, can alter CRC cell gene expression and consequently cell behaviour through epigenetic mechanisms. While specific miRNAs have been shown to sensitise CRC cells to butyrate by increasing its anticancer potential (Humphreys et al. 2014b), there have been no reports of an unbiased process to discover butyrate-sensitising ncRNAs. Using functional high-throughput screening and sequencing technologies, the role of miRNAs and other ncRNAs in the butyrate sensitisation of CRC cells was investigated by exploring proliferative and apoptotic cell changes. The roles of downstream interactors were also investigated in the butyrate response of CRC cells.

Unbiased high-throughput screening revealed 13 miRNAs with butyrate-sensitising properties in CRC cells. miR-125b, miR-181a, miR-593 and miR-1227 increased the anti-proliferative and pro-apoptotic potential of butyrate in CRC cells by a synergistic mechanism. Predicted miRNA target genes were identified as regulators of cell growth and death pathways including WNT signalling, PI3K-AKT signalling and apoptosis. miR-181a was identified as a potential regulator of the WNT signalling pathway. The silencing of a PI3K subunit, *PIK3R3*, revealed potent anti-proliferative effects in combination with butyrate in CRC cells.

In addition, a systems biology approach was used to examine butyrate-regulated transcriptomic changes and complex RNA interactions contributing to the butyrate response of CRC cells. Total and small RNA-seq analyses revealed thousands of butyrate-regulated protein-coding and ncRNA species. Differentially expressed (DE) protein-coding transcripts were enriched for genes encoding components of the cell cycle pathway. Network analyses highlighted key miRNA-target pairs, including tumour suppressor miRNAs, miR-139 and miR-542, that were upregulated by butyrate and consequently reduced cell cycle regulators, *EIF4G2* and *BIRC5*, respectively. miR-139 and miR-542 sensitised cells to butyrate through synergistic mechanisms. miR-542 was a

## SUMMARY

potent inhibitor of CRC cell growth. *EIF4G2* RNAi in CRC cells resulted in potent anti-proliferative effects in combination with butyrate.

Unbiased high-throughput screening using a lncRNA-targeting siRNA library revealed that silencing of several lncRNAs in combination with butyrate affected CRC cell apoptosis. Network and pathway analyses investigating lncRNA-miRNA-mRNA axes revealed that oncogenic MALAT1 was highly connected in the constructed apoptosis network. MALAT1 was predicted to interact with miR-200b and miR-200c which potentially targeted *DUSP1*, *FN1* and *JUN*, and miR-335 which potentially targeted *PRK4A2*. Apoptosis was enhanced when CRC cells were exposed to MALAT1 siRNAs in combination with butyrate. Further investigation is required to confirm regulation of downstream targets.

In summary, these data contribute to the growing knowledge of the role of ncRNAs in the response of CRC cells to butyrate and the cellular pathways that are involved. These results provide the basis for further investigation of a novel therapeutic approach combining RNAi and HDACi treatment in CRC. Further investigation is also warranted in other cancer models due to the broad-acting effects of these epigenetic molecules.

# Declaration

---

I certify that this thesis does not incorporate without acknowledgment any material previously submitted for a degree or diploma in any university; and that to the best of my knowledge and belief it does not contain any material previously published or written by another person except where due reference is made in the text.

Saira Rose Ali

# Publications and Presentations

---

## Peer-reviewed Publications

Ali SR, Humphreys KJ, McKinnon RA, Michael MZ. 2015. Impact of Histone Deacetylase Inhibitors on microRNA Expression and Cancer Therapy: A Review. *Drug Dev Res*, vol. 76, no. 6, pp. 296-317.

## Poster Presentations

Ali SR, Humphreys KJ, McKinnon RA, Michael MZ. The role of butyrate-sensitising microRNAs in colorectal cancer cells. 2015 PhD Day School of Medicine, Flinders Centre for Innovation in Cancer, South Australia, Australia, 9 October 2015.

Ali SR, Humphreys KJ, McKinnon RA, Michael MZ. The role of butyrate-sensitising microRNAs in colorectal cancer cells. The Australian Society for Medical Research 54th National Scientific Conference, the Stamford Plaza, Adelaide, South Australia, Australia, 17 November 2015.

Ali SR, Humphreys KJ, McKinnon RA, Michael MZ. Epigenetic regulation of gene expression in colorectal cancer cells. 2016 ASMR South Australian annual scientific meeting, Adelaide Convention Centre, Adelaide, South Australia, Australia, 8 June 2016.

Ali SR, Humphreys KJ, McKinnon RA, Michael MZ. Epigenetic regulation of gene expression in colorectal cancer cells. 2016 EpiCSA 1<sup>st</sup> Scientific Meeting, SAHMRI, Adelaide, South Australia, Australia, 13 October 2016. **Best Student Poster Talk.**

Ali SR, Humphreys KJ, McKinnon RA, Michael MZ. MicroRNAs enhance anticancer properties of butyrate in colorectal cancer. 2017 Noncoding RNAs: From Disease to Targeted Therapeutics (J5) Keystone Symposia Conference, Fairmont Banff Springs, Banff, Alberta, Canada, 5 February 2017.

Ali SR, Humphreys KJ, McKinnon RA, Michael MZ. MicroRNAs enhance anticancer properties of butyrate in colorectal cancer. 2017 Flinders Health Research Week, Flinders Centre for Innovation in Cancer, Adelaide, South Australia, Australia, 5 February 2017.

## PUBLICATIONS AND PRESENTATIONS

Ali SR, Humphreys KJ, McKinnon RA, Michael MZ. MicroRNAs enhance anticancer properties of butyrate in colorectal cancer. 2017 ComBio2017, Adelaide Convention Centre, Adelaide, South Australia, Australia, 2 October 2017.

Ali SR, Orang A, McKinnon RA, Michael MZ. Long non-coding RNA knockdown and butyrate sensitisation of colorectal cancer cells. 2017 EpiCSA 2<sup>nd</sup> Scientific Meeting 2017, The University of Adelaide Ingkarni Wardli Building, Adelaide, South Australia, Australia, 6 October 2017.

Ali SR, Orang A, McKinnon RA, Michael MZ. Long non-coding RNA knockdown and butyrate sensitisation of colorectal cancer cells. 2018 ComBio2018, International Convention Centre, Sydney, New South Wales, Australia, 23 September 2018.

### **Oral presentations**

Ali SR, Humphreys KJ, McKinnon RA, Michael MZ. High-throughput functional screen: Identification of ncRNAs that sensitise colorectal cancer cells to butyrate. 2016 EpiCSA Workshop -Studying Epigenetics using Functional High-throughput Screening, Flinders Centre for Innovation in Cancer, Adelaide, South Australia, Australia, 9 November 2016.

Ali SR, Humphreys KJ, McKinnon RA, Michael MZ. Involvement of non-coding RNAs in the butyrate response of colorectal cancer cells. 2017 Colorectal Cancer Research Day, Flinders Centre for Innovation in Cancer, Adelaide, South Australia, Australia, 29 June 2017.

Ali SR, Orang A, McKinnon RA, Michael MZ. High-throughput functional screen: Identification of ncRNAs that sensitise colorectal cancer cells to butyrate. 2017 EpiCSA & Adelaide RNA Special Interest Group Monthly Seminar Series, Adelaide Health & Medical Sciences Building, Adelaide, South Australia, Australia, 29 September 2017.

Ali SR, Orang A, McKinnon RA, Michael MZ. Transcriptomic integrative network and pathway analysis to identify butyrate-sensitising miRNAs in colorectal cancer cells. 2018 EpiCSA, University of Adelaide Health and Medical Sciences Building, Adelaide, South Australia, Australia, 3 October 2018.

Various presentations at the Flinders Centre for Innovation in Cancer annual research days and the Flinders Clinical and Molecular Medicine cluster seminar series.

# Acknowledgements

---

I would like to thank my PhD supervisors, Associate Professor Michael Michael, Associate Professor Robyn Meech and Professor Ross McKinnon, for their advice and support during my candidature. Thank you to Associate Professor Michael Michael for allowing me to undertake my research in his laboratory and Professor Ross McKinnon for providing me with much needed funds during the final stages of my PhD. Special thanks to Robyn Meech for providing helpful guidance and perspectives on my work, even after joining the supervisory team part way through my candidature.

Thank you to the researchers from the Victorian Centre for Functional Genomics (VCFG) at the Peter MacCallum Cancer Centre including Associate Professor Kaylene Simpson, Dr. Iva Nikolic, Jennii Luu, Piyush Madhamshettiwar and Daniel Thomas for assisting me in completing my high-throughput functional screen.

I would like to especially thank my lab members Kym McNicholas, Ayla Orang, Annette Mazzone, Dr. Ann-Sophie Mehdorn, Dr. Darling Rojas-Canales, Dr. Amanda Aloia and Marie Lowe for providing emotional support, encouragement and guidance throughout my PhD. I would have found it very difficult to complete the work of this thesis without you all. Kym McNicholas was always there to provide me with words of wisdom, kindness and advice that I needed to give me confidence to believe in myself. Ayla Orang went above and beyond her role as my fellow PhD student and provided valuable guidance and support whenever I was unsure. Annette Mazzone and Ann-Sophie Mehdorn are two of the most hilarious people I know, and they always made me laugh. They made my PhD bearable during the most stressful stages with their funny jokes and opinions. Darling Rojas-Canales provided me with valuable advice, guidance and support. Thank you for seeing the potential in me and continuing to support me in the development of my research career. Amanda Aloia always provided me with encouragement, helpful guidance and advice especially for my screening work. Marie Lowe always listened when I needed someone to talk to and ensured we would have everything we needed in the lab. Thank you to Dr. Karen Humphreys who greatly helped me during the early stages of this project.

Thank you to my family and friends for their love and support during my PhD. Thank you to my mum and dad, and my siblings Jaraad, Daniaal and especially my sister, Sofia, who always supported me when I was stressed out. Thank you to my friends Cat,

## ACKNOWLEDGEMENTS

Garwai, Alice and Chai-Hoon for encouraging me and always lending an ear when I needed someone to talk to.

Finally, but most importantly, thank you to my partner, Chris, for always providing me with the love, support and encouragement I needed to complete my PhD. Having someone close also doing their PhD alongside meant I could confide in you and you understood how I really felt and the stress I faced. I really could not have completed it without you.

# Chapter 1. Introduction

---

## 1.1 Epigenetic regulation of gene expression

Colorectal cancer (CRC) is a common cause of cancer related deaths worldwide (Bray et al. 2018). Although a small number of CRC cases develop from genetic factors, most cases develop sporadically due to environmental and lifestyle factors such as diet (Hagggar & Boushey 2009; Stoffel & Kastrinos 2014). The development and progression of CRC is associated with several epigenetic alterations such as altered histone modification patterns, DNA methylation and dysregulated non-coding RNA expression (Danese & Montagnana 2017; Lao & Grady 2011).

Epigenetic regulation is characterised as the alteration in gene expression or activity induced by non-DNA sequence related changes (Jaenisch & Bird 2003). Chromatin remodelling is a key epigenetic mechanism by which gene expression is altered and includes changes in DNA methylation and post-translational covalent histone modifications. Chromatin is composed of DNA wrapped around core histone proteins which create structures called nucleosomes. Nucleosomes are octamers composed of 8 histone proteins including two H2A–H2B dimers and a H3–H4 tetramer as well as amino acid histone tails; nucleosomes are linked by H1 proteins (Keppler & Archer 2008). Histone modifications, including acetylation, methylation and phosphorylation, are primarily located on the amino acid tails of core histone proteins that project out from the chromatin structure. The presence of these structures can either promote open or closed chromatin configurations and this regulates gene expression through the transcription of target genes. Several enzymes are involved in the histone modification process. Histone acetyl transferases (HATs) and histone deacetylases (HDACs) increase and decrease acetylation, respectively. Histone acetylation, in general, encourages open chromatin configurations as the presence of an acetyl group causes the neutralisation of positive lysine molecules which then lose electrostatic attraction to the negative phosphate backbone of the DNA (Mariadason 2008). This promotes transcription as the chromatin is more accessible to transcription machinery. Reducing the number of acetylation marks promotes a closed chromatin configuration due to the strong electrostatic attraction between the negative backbone of the DNA and positive lysine residues, which hinders transcription. Alternatively, histone methyltransferases (HMTs) and histone demethylases (HDMs) increase and decrease methylation, respectively. Methylation of lysine residues on the histone tails does not affect the charge. However,

the number of methyl groups can be differentiated by proteins with lysine recognition domains, resulting in gene activating or repressive marks (Rice & Allis 2001). Histone phosphorylation is regulated by a range of kinases and phosphatases which add and remove phosphate groups, respectively. Similarly, phosphorylation promotes an open chromatin configuration due to the negative charge of the phosphate group which repels the negatively charged phosphates in the DNA backbone and therefore promotes gene transcription (Rossetto et al. 2012).

DNA methylation is regulated by DNA methyltransferase (DNMT) proteins and contributes to regulation of chromatin structure and transcriptional repression. DNA methylation is the mechanism by which methyl groups are added to cytosine residues which are paired with guanine nucleotides (CpG dinucleotides). CpG dinucleotides are generally concentrated in specific regions of the genome (CpG islands) and are commonly found in the promoter regions of genes. DNA methylation is associated with gene silencing as the methyl groups interfere with the binding of transcription machinery and prevent gene expression (Lim & Maher 2011). DNA methylation also regulates chromatin remodelling through interactions with transcription co-repressor complexes (Brenner et al. 2005; Lim & Maher 2011).

Other epigenetic related molecules, including non-coding RNAs such as miRNAs and lncRNAs, are involved in the regulation of gene expression. miRNAs are short non-coding RNA molecules with the ability to post-transcriptionally regulate protein-coding and non-coding RNA molecules through complementary binding sites. Alternatively, lncRNAs are long non-coding RNAs with the ability to regulate gene expression through several mechanisms involving interactions with DNA, RNA and protein molecules. These non-coding RNAs are epigenetic regulators but can also be epigenetically regulated themselves by each other and other epigenetic mechanisms. As highlighted throughout this literature review, these epigenetic mechanisms are critical contributors to the development and progression of CRC and are regulated by dietary molecules.

## **1.2 Colorectal cancer**

### **1.2.1 Epidemiology of colorectal cancer**

Colorectal cancer is the third most common cancer and the second leading cause of cancer-related deaths worldwide, with approximately 1.8 million new cases and 881,000 deaths in 2018 (Bray et al. 2018). The global distribution of CRC has high geographical

variation, with the disease incidence being the greatest in Southern and Eastern Europe and the lowest in Western Africa and South Central Asia (Bray et al. 2018). CRC cases occur approximately 3-fold greater in transitioned countries compared to transitioning countries as the disease appears to be an indicator of socioeconomic development with the incidence of CRC rising in those countries with increased human development index (HDI) scores (Bray et al. 2018). Although CRC incidence has stabilised or is decreasing in countries classified with the highest HDI scores, such as Australia, New Zealand and several Western European countries; the incidence is still rapidly increasing in other medium to high HDI scored countries in Eastern Europe, Asia and South America (Center et al. 2009a). Those countries in which CRC incidence is greatest also experience the greatest human loss from the disease, with 60% of deaths occurring in countries with high or very high HDI scores (Center et al. 2009a). Mortality rates have decreased in some developed countries, due to improved prevention, early detection and treatment strategies; however, rates have increased in numerous developing countries (Center et al. 2009b).

In Australia, CRC is the third most commonly diagnosed cancer in the population, with 15,604 people newly diagnosed with the disease in 2015 (AIHW 2018). The age-standardised incident rate in 2015 was 57 cases per 100,000 people (AIHW 2018). In 2019, the number of new cases of CRC is expected to be 16,398 (11 % of all cancer cases) (AIHW 2019). In 2016, CRC was the most common cause of cancer related deaths in Australia, with 5,375 deaths recorded in 2016 (AIHW 2019). The age-standardised mortality rate was 19 deaths per 100,000, in 2016 (AIHW 2019). Deaths from CRC are projected to increase in 2019 to 5,597 persons, with risk of dying from CRC before age 85 at 1 in 43 (AIHW 2019). The five-year survival rate for those diagnosed with CRC was 70 % between 2011-2015 (AIHW 2018).

### **1.2.2 Colorectal cancer pathogenesis**

The colorectum consists of the ascending, transverse, descending, sigmoid sections and rectum. The colon normally functions to absorb remaining nutrients, salts and water, store waste, breakdown undigested food via bacterial fermentation using colonic flora and secrete residual waste products (Milla 2009). CRC develops from sporadic or inherited mutations leading to disordered DNA replication and accelerated colonocyte proliferation. With the progressive accumulation of mutations, normal colonic epithelial cells may develop a malignant phenotype (Cappell 2005). However, CRC often takes from years to decades to develop (Fearon 2011).

## CHAPTER 1

Due to the exposure of the colorectum to carcinogenic substances through food consumption, high epithelial cell turnover is required, and cell growth and death must be tightly regulated to avoid the development of a malignant phenotype. The colon is lined with villus structures that are composed of differentiated colorectal epithelial cells including enterocytes, goblet and enteroendocrine cells, which are maintained by multipotent stem cells and progenitor cells at the base of the crypts. The stem cells produce a population of transit amplifying cells which migrate up through the crypts, proliferate and differentiate into the aforementioned cell types (Khalek et al. 2010; Stoian et al. 2016). This is regulated by several signalling pathways including WNT, Notch, Hedgehog, BMP, EGFR and Eph–ephrin signalling (Figure 1-1) (Spit et al. 2018). WNT signalling regulates intestinal stem cell maintenance and size. It is most active at the base of the crypt and gradually lessens as cells become differentiated (Farin et al. 2016). Notch signalling regulates cell fate and stemness within the crypts, where it is steadily expressed, and is critical in determining if a cell will follow absorptive or secretory cell type lineages (Fre et al. 2005). Hedgehog signalling (mostly Indian Hedgehog (Ihh)) regulates and maintains the intestinal mesenchymal cells in the surrounding smooth muscle and myofibroblasts of the crypts and villi (Buller et al. 2012). BMP signalling (TGF- $\beta$  family of molecules) regulates crypt formation and, specifically, terminal differentiation by restricting proliferation and promoting differentiation of progenitor cells; therefore, signalling activity is greatest in differentiated epithelia (luminal surface) (He et al. 2004). BMP antagonists also regulate BMP signalling in the crypt (He et al. 2004). EGFR signalling regulates intestinal cell proliferation, growth and differentiation within the crypts (where it is steadily expressed) through the activation of several cascades including MAPK, PI3K/AKT, JNK, Jak/STAT signalling (Jorissen et al. 2003). Eph–ephrin signalling regulates cell positioning within the crypts and villi through cell-cell signalling through EphB2 and EphB3 in the crypts (expression induced by WNT signalling) (Batlle et al. 2002) and ephrin-B1 in differentiated intestinal cells (expression induced by Notch signalling) (Koo et al. 2009). This influences adhesion and integrin molecules as well as cytoskeleton organisation which affects cell morphology, adhesion and migration within the intestine (Pasquale 2010).

The origin of CRC is unclear. Mutations, due to DNA replication repair errors, cellular stress and exposure to carcinogens may occur in the epithelial cells; however, they are often lost due to a high-turnover of 4-5 days, unless migration is impeded (Huels & Sansom 2015). Stem-cells may also acquire mutations through similar mechanisms;

however, ‘neutral drift’ often results in replacement of the mutated cell with a normal stem cell before it can form a malignancy, and unless the mechanism is faulty, this may explain the long development time of CRC (Huels & Sansom 2015; Khalek et al. 2010). These mutations may result in gain of function or constitutively active oncogenes or loss of function in tumour suppressor genes that lead to a growth advantage and progression to a more malignant phenotype.

Abnormal cell growth may lead to the formation of a polyp structure, which projects from the mucosal membrane. Polyps may be classified as hyperplastic or adenomatous. In general, hyperplastic polyps do not form CRC, while adenomatous polyps are more likely to progress to CRC (Singh et al. 2016). Serrated polyps may also form in the colorectum though they transform into CRC via an alternate serrated pathway (Singh et al. 2016).

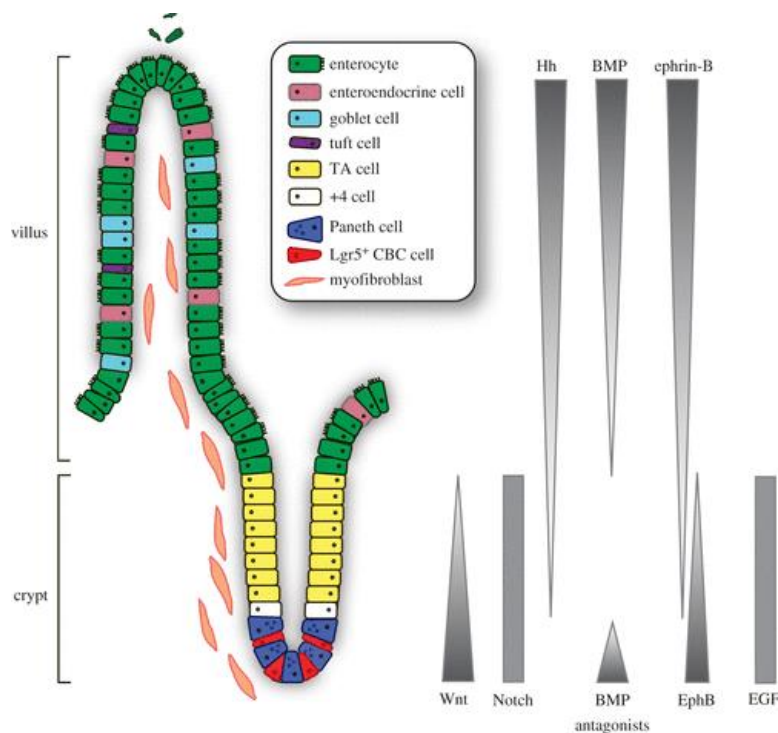


**Figure 1-1 Colonic crypt structure**

Illustration depicting cell type location in colonic crypt and villus structures as well as level of WNT signalling activity and differentiation distribution. WNT signalling activity is high in the crypt to promote stemness, but decreases as cell differentiate, while BMP signalling increases as cells differentiate near the top of the villus. (Image from OpenBiol, CC-BY: (Spit et al. 2018)).

### 1.2.3 Genetic and epigenetic changes in colorectal cancer

CRC has been observed as a multi-step process, involving various epigenetic changes and mutations in critical tumour suppressor genes and oncogenes, resulting in dysregulation of key pathways involved in cell proliferation, apoptosis and differentiation (Fearon & Vogelstein 1990). Colonic cell homeostasis is normally tightly controlled through key cell growth and death pathways such as WNT, PI3K/AKT and TGF- $\beta$  signalling (Armaghany et al. 2012). Therefore, it is no surprise that the genes in these pathways are often mutated in CRC.

Inherited genetic mutations account for approximately 5% of CRC cases, while about 95% of CRCs are caused by a mixture of acquired genetic mutations, environmental and lifestyle factors (Stoffel & Kastrinos 2014). The most common CRC genetic syndrome is Hereditary non-polyposis colorectal cancer (HNPCC) or Lynch syndrome (Davies et al. 2005). HNPCC is an autosomal dominant syndrome involving the inheritance of germ-line mutations in *MLH1*, *MSH2*, *MSH6* or *PMS2*, which encode critical DNA mismatch repair proteins (Papadopoulos & Lindblom 1997). Familial adenomatous polyposis (FAP) is the second most common CRC syndrome. FAP is an autosomal dominant syndrome, involving the germ-line inheritance of a mutated adenomatous polyposis coli (*APC*) gene; a key tumour suppressor in WNT signalling (Olschwang et al. 1993).

The multi-step process of CRC development (Figure 1-2) frequently begins with the loss of the tumour suppressor, *APC* (70-80% of adenoma and carcinoma cases), resulting in dysregulation of WNT signalling (Fearon & Vogelstein 1990; Fodde 2002). *APC* normally regulates cell adhesion, migration, signal transduction and chromosomal segregation; however, its most critical role in negative regulation of cellular  $\beta$ -catenin in WNT signalling is often lost in CRC (Fodde 2002). The loss of a functional *APC* gene allows  $\beta$ -catenin to enter the nucleus of cells and promote transcription factors which target genes involved in cell proliferation, differentiation and migration (Goss & Groden 2000). Later stages of tumour development are often followed by activating mutations in oncogenes such as *KRAS* and *PI3K*, which may result in a constitutively active protein (Yashiro et al. 2001). These genes are involved in promotion of cell proliferation and survival via RAS/RAF/MAPK and PI3K/AKT signalling pathways; therefore, activating mutations can lead to enhanced cell growth, and further development of an adenoma (Armaghany et al. 2012; Yashiro et al. 2001). Adenoma progression is accompanied by increase in the loss of various tumour suppressors, including SMAD4,

## CHAPTER 1

a signal transduction protein involved in cell proliferation inhibition in TGF-beta signalling (Handra-Luca et al. 2011), and DCC which promotes apoptosis, further promoting the transformation of the colorectal tumour to a late stage adenoma (Cappell 2005). This is often followed by the loss of critical tumour suppressors such as p53, 'the Guardian of the Genome', which is involved in cell cycle arrest, apoptosis and senescence, and most importantly preventing mutations in the genome (Rodrigues et al. 1990). As protective tumour suppressors are lost and oncogenes become over-active, this promotes colorectal carcinoma formation, a malignant tumour formation which can invade surrounding tissue (Bodmer 2006). Metastasis may occur, if critical genes in the Epithelial-Mesenchymal pathway become over-active, such as *ZEB1/2*, promoting the mobility of tumour cells (Fearon 2011). Other genes affected may include *PTEN*, *BAX*, *HER2*, *BRAF*, *NRAS* and *c-MYC* (Fearon 2011). Many CRC models have been suggested. However, the accumulation of multiple mutations is a highly critical factor in CRC development rather than the specific order of mutations acquired (Fearon 2011).

The genetic and epigenetic changes observed in the development of CRC have been attributed to three major pathways of genomic instability including the Chromosomal Instability (CIN), Microsatellite Instability (MSI) and CpG Island Methylator Phenotype (CIMP) pathways (Armaghany et al. 2012). The CIN pathway involves defects in chromosomal segregation, telomere stability and DNA damage response, resulting in an imbalance in chromosomal number (aneuploidy) and loss of heterozygosity (Pino & Chung 2010). The MSI pathway involves inadequate DNA repair of short tandem repeat sequences called microsatellites. Normally when DNA polymerase makes a mistake the mismatch repair enzymes, expressed from genes including *MLH1*, *MSH2*, *MSH6* and *PMS2*, will proofread and repair the DNA (Boland & Goel 2010). This does not occur when these genes acquire mutations. The CIMP pathway reflects epigenetic instability in CRC. This pathway involves the hypermethylation of CpG island in promoter regions of tumour suppressor genes in order to silence them (Mojarad et al. 2013). Such genes affected by this mechanism include *CDKN2A* tumour suppressor and *MLH1* DNA repair gene (Mojarad et al. 2013).

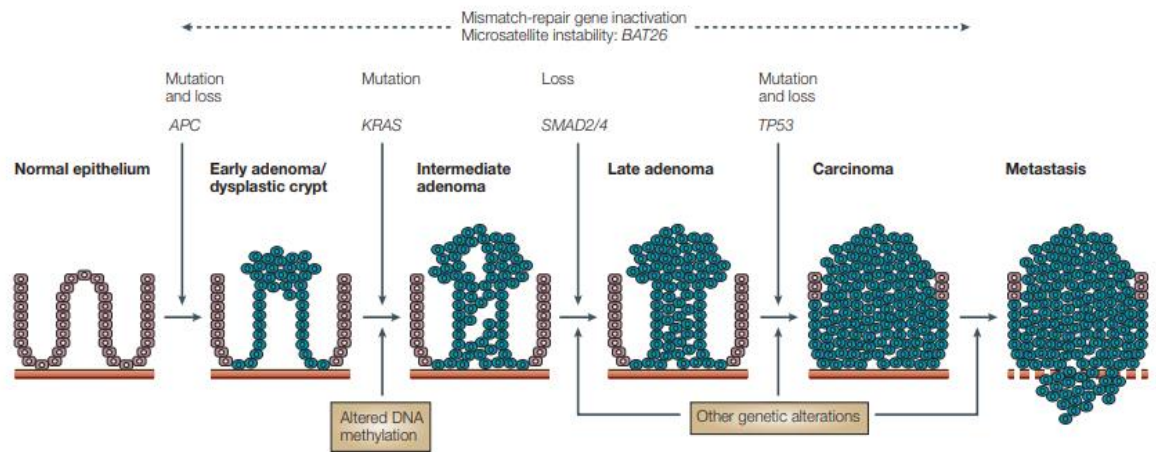


**Figure 1-2 Colorectal adenoma-carcinoma development**

The transformation of the normal epithelium to adenoma and then colorectal carcinoma is characterized by the accumulation of mutation in genes involved in various signalling pathways. Mutations in mismatch-repair genes cause microsatellite instability and can be accompanied by various mutations in tumour suppressor genes and oncogenes. Microsatellite region (*BAT26*) that is altered in almost all mismatch-repair-deficient CRCs. (Image reproduced with permission: (Davies et al. 2005)).

### 1.2.4 Risk Factors

The development of CRC is influenced by a multitude of factors, both genetic and environmental. Familial history of CRC increases CRC risk. Those with a first degree relative who has suffered from CRC, without an inherited disorder, have a 2-3 fold greater chance of suffering from CRC themselves (Winawer 2007). Personal history of adenomatous polyps also increases CRC risk, with approximately 95% of sporadic cases forming from these types of polyps, while inflammatory bowel disease, including ulcerative colitis and Crohn's disease, increases risk 4-20 fold (Janout & Kollarova 2001). Inherited genetic mutations can also result in the formation of colorectal carcinomas, although they only contribute to a small number of CRC cases, while the rest are caused by a mixture of acquired genetic mutations, environmental and lifestyle factors (Stoffel & Kastrinos 2014).

Lifestyle choices, which are modifiable factors, such as diet, body weight, physical activity, smoking and alcohol consumption are a primary influence on CRC development (Hagggar & Boushey 2009). The risk of developing CRC also changes with age and sex, with risk increasing in those who are greater than 60 years old and are male (Davies et al. 2005). A primary influence in CRC development is diet. Previous studies have shown that consumption of high resistant starch foods may help prevent CRC by production of chemo-protective butyrate in the colon, while diets high in red meat can

promote the production of cytotoxic adducts promoting CRC formation (Humphreys et al. 2014a; Lewin et al. 2006).

### 1.2.5 Screening and diagnostics

Detection of CRC is generally via routine screening strategies including stool tests (faecal occult blood tests) and structural examinations (colonoscopies and sigmoidoscopies). Some cases may be detected by presentation of symptoms, which is more commonly observed in advanced stages of CRC rather than early stages. Early stage CRC is often first detected by a positive faecal occult blood test, followed by structural examination using colonoscopy (Levin et al. 2008). Colonoscopies not only provide a method for detecting CRC, but also a means of removing pre-cancerous growths (polyps) thus preventing CRC development (Von Renteln et al. 2017). The development of the TNM staging system allows the general classification of cancers, including colorectal cancer, into malignancy stages based on degree of primary tumour spread (T), involvement of lymph nodes (N) and the presence of metastatic spread (M) (Amin et al. 2017). Cancers are classified into five general stages i.e. Stage 0 (cancer in situ), stage I (localised cancer), stage II and III (localised cancer with some lymph node involvement) and stage IV (metastasised cancer to other organs) (Amin et al. 2017).

### 1.2.6 Current treatment

CRC treatment is based on the stage of cancer. Generally, treatment can include minor to major surgical procedures, chemotherapy and/or radiotherapy. During pre-cancerous stages, such as the formation of adenomatous polyps and sessile polyps, from which 70-90% and 10-30 % of CRCs form, respectively (Rudy & Zdon 2000), screening can help identify the formation of abnormal growths that can be surgically removed via colonoscopic polypectomy (Winawer et al. 1993). Once CRC has developed, surgical and chemotherapeutic techniques are often required. Stage 0-2 of CRC may require anything from local excision and colonoscopic polypectomies to wide bowel resections and anastomosis to remove parts of the bowel, while more aggressive stages 3-4 may require surgery, chemotherapy or radiotherapy and local ablation (National Cancer Institute 2014). Biological agents such as miRNAs are starting to make their way into the clinic, due to their high level of target specificity and ability to knock down gene expression in multiple pathways. A phase 1 clinical trial demonstrated that miR-16 replacement therapy in patients with mesothelioma resulted in the objective and partial responses of some patients (van Zandwijk et al. 2017). Further investigation is required for use in CRC.

## 1.3 Dietary effects on colorectal cancer

### 1.3.1 Diet and colorectal cancer

The consumption of certain dietary components can result in direct changes in the human genome and indirect changes due to epigenetic alterations of histone acetylation and methylation patterns, DNA methylation and non-coding RNA expression (miRNA and lncRNA). Due to the exposure of the colonic epithelium to carcinogenic substances via food consumption, this is a likely factor affecting CRC development. Red meat, processed meat and charred meat consumption has been associated with an increase in CRC risk. Various studies have identified carcinogenic substances that are present or formed in meat during the cooking process including heterocyclic aromatic amines (HAA) (cooking at high temperatures) (Nagao et al. 1977), polycyclic aromatic hydrocarbons (PAH) (charred meat) (Fretheim 1983), N-nitroso compounds (NOC) (processed meat) (Lijinsky 1999) and heme iron (red meat) (Igene et al. 1979). HAA, PAH and NOC have been found to induce point mutations in DNA include base substitutions, deletions and insertions, while heme iron can promote colonic hyperproliferation and DNA damage (Ishikawa et al. 2010; Lewin et al. 2006; Pratt et al. 2011). On the other hand, fibre-based foods may have some benefits in protecting the gut from CRC. One mechanism of protection is thought to be through faecal bulking to decrease transit time through the colon thereby decreasing exposure of the colon to carcinogenic substances contained in the stools. Another mechanism is by the bacterial fermentation of dietary fibre which results in the production of protective short chain fatty acids including butyrate, acetate and propionate.

### 1.4 Butyrate

Butyrate is a short chain fatty acid molecule produced in the proximal colon of mammals, by the anaerobic bacterial fermentation of dietary fibre, such as insoluble resistant starch (RS) (Cummings 1981). Bacteria specifically in the phylum, Firmicutes, including *Faecalibacterium prausnitzii*, *Eubacterium rectale*, *Roseburia* spp. and *Anaerostipes* spp. among others are responsible for butyrate production in the mammalian colon (Louis et al. 2014). Butyrate provides approximately 60% of the daily energy requirements for normal healthy colonocytes and has been shown to be the primary and preferential fuel used during colonocyte metabolism (butyrate>glucose>ketone bodies>glutamine) (Cummings 1984; Roediger 1982). In the normal colon, butyrate has been shown to be involved in maintenance of homeostasis in the colonic mucosa and regulation of colonic

mobility, inflammation, immune response, fluid and electrolyte flux and mucosal barrier integrity as well as regulation of cell growth, apoptosis, differentiation in normal colonocytes (Fung et al. 2012).

#### 1.4.1 Butyrate and colorectal cancer

Interestingly, butyrate is also a well-known histone deacetylase inhibitor (HDACi) which has the ability to prevent tumour formation (Hinnebusch et al. 2002; Sealy & Chalkley 1978). Other short chain fatty acids are also produced from dietary fibre including acetate and propionate; however, they are less potent HDAC inhibitors. The anti-tumorigenic properties of butyrate include its ability to strongly induce intrinsic apoptosis and differentiation, inhibit cell proliferation and block the cell cycle in cancer cell lines, including HCT116 CRC cells, through epigenetic regulation of genes involved in these processes as shown in microarray studies (Daly & Shirazi-Beechey 2006; Hague et al. 1997; Mariadason 2008). The ability of butyrate to promote healthy colonic cells while eliminating cancerous cells is a phenomenon called the 'butyrate paradox' (Gibson et al. 1999).

#### 1.4.2 Effects of butyrate on gene expression in colorectal cancer cells

The effects of butyrate on CRC cells and gene expression have been studied in both *in vitro* and in non-human *in vivo* studies. *In vitro* studies, in several colorectal carcinoma cell lines, including HCT116 cells, have shown that butyrate alters gene expression and exerts anti-tumorigenic responses at concentrations as low as 0.5 mM, which is much lower than faecal butyrate at around 20 mM and predicted physiological concentrations in the gastrointestinal system (Fung et al. 2012; Humphreys et al. 2014a; Singh et al. 1997; Yu et al. 2010a). An early study demonstrated that butyrate can alter gene expression in CRC cells as early as 30 minutes after exposure and up to 48 h in the SW480 cells (Mariadason et al. 2000). Gene and protein expression changes in CRC cells, caused by butyrate, have been characterised by using microarrays and proteomic techniques. A large microarray study determining gene expression changes in the CRC cell line HT29, after exposure to 5 mM butyrate over 24 h, demonstrated the ability of butyrate to alter the expression of a large number of genes (Daly & Shirazi-Beechey 2006). A total of 1983 genes were found to be differentially expressed (796 upregulated and 1187 downregulated) and of those, 221 genes were found to be involved in apoptosis, proliferation and differentiation (Daly & Shirazi-Beechey 2006). Analysis of real-time RT-PCR data revealed the upregulation of cell cycle inhibitors, *CDKN1A* and *GADD45A* and the pro-apoptotic gene, *BAK1*, and the downregulation of anti-

apoptotic and cell cycle progression genes, *BIRC5* and *CCND1*, which reflects the anti-tumorigenic abilities of butyrate (Daly & Shirazi-Beechey 2006). An earlier transcriptomics study revealed similar results, with the downregulation of 21 oncogenes involved in cell proliferation and cell cycle regulation and upregulation of 39 apoptotic and DNA repair genes in HT29 cells, after 24 h periods of 4 mM butyrate exposure (Iacomino et al. 2001). Butyrate has also demonstrated the ability to induce gene expression changes in specific canonical pathways, including WNT signalling, which is a critical pathway in CRC development (Polakis 2000). WNT signalling becomes hyper-activated by butyrate, which promotes induction of apoptosis in cancer cells (Bordonaro et al. 2008). A more recent study demonstrated that exposure of HCT116 cells to 5 mM of butyrate resulted in the dysregulation of 1008 genes modulated by butyrate in a WNT signalling-specific manner (Lazarova et al. 2014). Many proteomic studies support mRNA analysis studies, revealing the ability of butyrate to alter the protein levels of many proteins, in HCT116 and HT29 cells, involved in cell signalling, tumour suppression, apoptosis, and proteasomal degradation (Fung et al. 2009; Tan et al. 2008; Tan et al. 2002).

The chemo-protective effects of butyrate have been demonstrated using *in vivo* models. Using rat models of CRC, high fibre diets associated with butyrate were demonstrated to significantly decrease colon tumour mass and number when implemented over a period of 30 weeks, with up to 2 more tumours present in low fibre diet rats than high fibre diet rats (McIntyre et al. 1993). Le Leu et al. (2007) also demonstrated that the dietary supplementation of RS in CRC rat models over 4 weeks, caused a significant decrease in intestinal neoplasms and colorectal adenocarcinomas ( $P < 0.01$ ) compared to rats on non-RS diets. Later studies have demonstrated that a butyrylated-RS diet protects rat colonocytes from DNA damage; butyrylated-RS diets were shown to be twice as effective as high protein diets in protecting rats against genetic damage (Bajka et al. 2008). Clarke et al. (2012) demonstrated that the exposure to high levels of butyrylated-RS, in the diet, caused an increase in apoptosis of the colonocytes in carcinogen treated rats. More recently, Donohoe et al. (2014) demonstrated that BALB/c inbred mice with chemically-induced CRC tumours had less aggressive, smaller and fewer tumours when fed with high-fibre diets. It must be noted that some of the gnotobiotic mice were colonised with butyrate producing bacteria, *Butyrivibrio fibrosolvens*, which demonstrated the importance of having the correct bacteria present in order to achieve the most beneficial results when eating a high-fibre diet (Donohoe et al. 2014).

## CHAPTER 1

Dietary alterations, including RS, appear to be efficacious in decreasing CRC tumour growth and protecting colonocytes against genetic damage in animal models.

Currently, few studies have investigated the effects of butyrate within humans. More human *in vivo* studies are required in order to support the observed efficacy of butyrate in eliminating CRC cells in both *in vitro* and non-human *in vivo* studies. A randomised, controlled cross-over trial involving diet interventions in 23 healthy volunteers demonstrated that a diet incorporating butyrylated-RS with red meat increased faecal butyrate compared to a high red meat diet (Humphreys et al. 2014a). Increased concentrations of faecal butyrate may counteract the carcinogenic effects caused by consumption of red meat (Humphreys et al. 2014a). The oncogenic miR-17-92a cluster was also increased in those with the high-red meat diet, but all miRNAs, except miR-21, were restored to baseline levels when butyrylated-RS was also consumed (Humphreys et al. 2014a). Le Leu et al. (2015b) also showed that butyrylated-RS helped to reduce the formation of DNA adducts in these volunteers. A larger study investigating the effects of RS on the adenomas of young FAP sufferers indicated that RS does not significantly decrease the number of polyps or proliferation of crypts (Burn et al. 2011). In contrast, results from an earlier randomised control trial involving RS supplementation in CRC patients for 4 weeks reported that crypt proliferation decreases after RS exposure and *GADD45A* and *CDK4* genes become upregulated (Dronamraju et al. 2009), which are butyrate responsive genes and important cell cycle regulators (Daly & Shirazi-Beechey 2006). This highlights the need for further investigation of the butyrate response in humans.

Direct delivery of butyrate to humans is also problematic due to the current delivery techniques and short half-life of butyrate within the human body (Miller et al. 1987). Currently, butyrate may be administered via pills, enemas, or indirectly through diet alterations (Hamer et al. 2008). Release of butyrate from a pill needs to be within the tumour area which can be hindered by gastric enzymes, while butyrate enemas have low compliance rates due to the discomfort and result in only a short exposure to butyrate (Breuer et al. 1997). Clarke et al. (2007) demonstrated that the supplementation of butyrate via butyrylated-RS in humans resulted in an approximately 75% delivery rate beyond the small intestine, due to the fermentation of RS into butyrate, and the presence of the conjugated butyrate molecules. Therefore, this may be an ideal delivery system.

### 1.4.3 Mechanisms of action of butyrate in CRC

Butyrate functions through various mechanisms including histone acetylation, histone and DNA methylation, phosphorylation, Polycomb and Trithorax complexes and acetylation of non-histone proteins to regulate gene and protein expression in CRC cells.

#### **Histone acetylation**

After dietary fibre has been processed to produce butyrate in the lumen, it is thought to be absorbed into normal colonocytes by electroneutral transporters MCT1 ( $H^+$  coupled) and SMCT1 ( $Na^+$  coupled) (Sivaprakasam et al. 2017). Butyrate is converted into acetyl-CoA through  $\beta$ -oxidation and processed by the citric acid cycle (CAC) for energy. This does not allow butyrate to accumulate in the nucleus and exert HDACi effects (Donohoe et al. 2012). Interestingly, not all intestinal cells are immune to the effects of butyrate as it was identified to be a potent inhibitor of intestinal stem cell and progenitor proliferation in mice studies (Kaiko et al. 2016). It was demonstrated that the colon structure protects stem and progenitor cells as differentiated colonocytes at the top of the villus metabolise butyrate before it can reach the crypt base (Kaiko et al. 2016).

Alternatively, CRC cells act metabolically different to normal colonocytes and are thought to rely on the Warburg effect (Warburg 1956). Even in the presence of oxygen, cancer cells primarily rely on 'aerobic glycolysis' (glucose to lactate) instead of oxidative phosphorylation via the mitochondria (Vander Heiden et al. 2009). Aerobic glycolysis produces far less ATP (2 molecules) compared to oxidative phosphorylation (up to 36 ATP) (Warburg 1956). The reason for cancer cells switching to this metabolic pathway is unknown. Most convincingly, it has been argued that proliferating cells require nucleotides, amino acids, and lipids to grow, particularly rapidly growing cancer cells (Vander Heiden et al. 2009). So cancer cells bypass oxidative phosphorylation to avoid using important substrates (such as acetyl-CoA and ATP) that are required for production of these growth molecules (Vander Heiden et al. 2009). In CRC cells, therefore, butyrate accumulates in the cytoplasm, which allows it to exert its effects primarily as an HDACi (Figure 1-3). Butyrate inhibits the removal of acetyl groups from lysine residues of histone tails leading to hyperacetylation of H3 and H4 histones (Mariadason 2008). This results in open chromatin configuration allowing transcription proteins to access the DNA, therefore, promoting transcription of genes involved in the cell cycle, apoptosis and differentiation (Gu & Roeder 1997). Supporting this argument,

butyrate was shown to significantly increase the activating histone mark, H3K9ac (acetylation) in HT29 CRC cells (Bartova et al. 2005).

Histone acetyl transferases (HATs) also contribute to the butyrate response in CRC cells, as their activity can be promoted by acetyl-CoA. Acetyl-CoA is produced from  $\beta$ -oxidation of butyrate which is then converted to citrate via the CAC (Wellen et al. 2009). Citrate is shuttled out of the mitochondria for conversion back to acetyl-CoA by ATP citrate lyase (ACLY) in the nucleus (Wellen et al. 2009). Acetyl-CoA is an important donor of acetyl groups for histone acetylation (Wellen et al. 2009). Citrate and acetate can also diffuse through nuclear pores, so acetyl-CoA production may also occur in the nucleus (Paine et al. 1975). Therefore, acetyl-CoA produced from butyrate can act as a HAT co-factor and acetyl group donor (Donohoe et al. 2012). The balance between HDACi and HAT activity is regulated by butyrate concentration in CRC cells (Donohoe et al. 2012). When low doses of butyrate are used (0.5 mM), it does not accumulate at high enough concentrations to cause HDACi, but it can alter HAT activity through the above mechanism (Donohoe et al. 2012). At higher concentrations (5 mM), the HDACi function dominates and is the primary cause of gene expression changes (Donohoe et al. 2012). This is due to cancer cells reaching a metabolic threshold for oxidative phosphorylation around 1-2 mM butyrate; therefore, butyrate is no longer metabolised and accumulates (Andriamihaja et al. 2009).

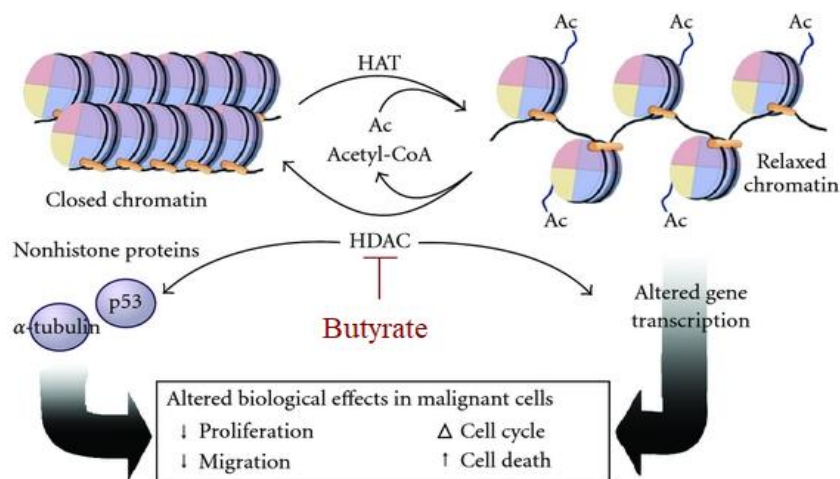


**Figure 1-3 Mechanism of action: HDAC inhibition**

Butyrate regulates histone acetylation patterns by inhibiting histone deacetylases (HDACs), thereby; preventing the removal of acetyl groups from lysine residues on core histones. This contributes to hyperacetylation of the histones and consequently, a more open and transcriptionally active chromatin structure. Along with induced changes in non-histone proteins, gene transcription becomes altered to promote several anticancer effects. (Adapted image from Lymphoma, CC-BY: (Rodd et al. 2012)).

### **Histone and DNA methylation**

Butyrate has been shown to regulate lysine histone methylation in order to exert its anticancer effects (Boffa et al. 1981). In CRC, decreases in the activating mark, H3K9me2, is associated with poor survival rate (Tamagawa et al. 2012). However, butyrate has been shown to increase H3K4me2 in HT29 CRC cells (Bartova et al. 2005). Furthermore, butyrate was shown to decrease protein expression of DNA methyltransferase 1 (DNMT1), which can silence genes by marking CpG structures with methyl groups, in RKO, HCT116 and HT29 CRC cells (Saldanha et al. 2014).

### **Phosphorylation**

Butyrate can also selectively inhibit the phosphorylation of histones 1 and 2A by an indirect targeting effect of substrate accessibility or modulation of systems involved in kinase protein activity (Boffa et al. 1981). The phosphorylation (negative charge) of histone tails neutralises positive lysine groups, leading to decreased interaction with negative DNA backbones, resulting in a more open configuration to promote transcription (Grant 2001). Butyrate can inhibit non-histone protein phosphorylation by inhibiting protein kinases, ERK1 and ERK2 (Davido et al. 2001). ERK1 and ERK2 phosphorylate and activate proteins involved in cell proliferation so butyrate can inhibit cell proliferation (Davido et al. 2001).

### **Polycomb and Trithorax complexes**

Butyrate has been shown to decrease expression of BMI1, a protein from the Polycomb Group (PcG) involved in regulation of cell proliferation and differentiation, which is often overexpressed in cancer (Bommi et al. 2010; Li et al. 2014b). Polycomb proteins are transcriptional repressors that epigenetically modify chromatin through processes such as methylation (Bommi et al. 2010). Conversely, Trithorax proteins oppose the actions of Polycomb proteins and are often involved in gene activation. Trithorax proteins function by rearranging nucleosomes, interacting with transcription machinery and modifying selected histones (Kingston & Tamkun 2014), although the effects of butyrate on these proteins requires further investigation.

### **Non-histone proteins**

Non-histone proteins such as DNA binding transcription factors and signal transduction proteins can also be affected by butyrate, thereby promoting transcription (Wilson et al. 2010). Butyrate (0.5 and 5 mM) can also increase p53 protein acetylation

in HCT116 CRC cells which results in increased DNA binding activity and target activation (Donohoe et al. 2012). p53 is important in intrinsic apoptosis and cell cycle regulation as it activates key pro-apoptotic genes (*PUMA*) (Nakano & Vousden 2001) and cell cycle inhibitors (*P21*) (He et al. 2005). Butyrate was demonstrated to decrease SP1 transcription factor acetylation, which resulted in decreased binding affinity for the *P21* and *BAX* promoters and increased their expression to promote cell cycle arrest and apoptosis (Waby et al. 2010). S6K1 acetylation was also found to be increased by butyrate (Cao et al. 2019), which inhibits the kinase that normally promotes mTOR signalling for cell growth and protein synthesis (Hong et al. 2014).

#### 1.4.3.1 Butyrate regulation of signalling pathways

Butyrate regulates several key pathways and molecules involved in cell growth, death and migration in order to inhibit the development of CRC. Listed below are some key dysregulated pathways and molecules involved in the butyrate response (Figure 1-4).

##### **Canonical WNT signalling**

Canonical WNT signalling is a key dysregulated pathway in CRC in which various mutations accumulate. This pathway is exploited by CRC cells due to its critical role in normal colonocytes, whereby WNT signalling is involved in intestinal stem cell maintenance by regulating cell growth, differentiation, and cell-fate (Gregorieff & Clevers 2005). The WNT pathway is activated by the binding of WNT ligands (e.g. WNT3A) to specific Frizzled (FZD) and LRP co-receptors. This leads to LRP co-receptor phosphorylation by glycogen synthase kinase 3 $\beta$  (GSK3 $\beta$ ) and casein kinase (CK1 $\alpha$ ), resulting in recruitment and activation of Dishevelled (DVL) protein complexes at the cell membrane. The DVL complexes inactivate the destruction complex and subsequently  $\beta$ -catenin is stabilised and accumulates before translocating into the nucleus.  $\beta$ -catenin complexes with T-cell factor (TCF) and lymphoid enhancer factor (LEF) transcription factors by displacing transducing-like enhancer protein (TLE)/Groucho complexes, which hinders recruitment of histone modifying co-activators (BRG1, BCL9, CBP/p300) (Hecht et al. 2000; Kramps et al. 2002). This results in the expression of key genes involved in promotion of cell growth and survival such as *CCND1*, *c-MYC* and *BIRC5* (He et al. 1998; Kim et al. 2003; Tetsu & McCormick 1999). When WNT ligands are absent, this results in the phosphorylation and deactivation of  $\beta$ -catenin within the destruction complex, which includes components: APC, scaffold protein AXIN, kinases CK1 $\alpha$  and GSK3 $\beta$ ) (Liu et al. 2002).  $\beta$ -catenin is ubiquitinated by  $\beta$ -TrCP and processed by proteasomal degradation (Latres

et al. 1999). Lack of nuclear  $\beta$ -catenin promotes repression of target gene expression through a nuclear repressive complex (TCF/LEF and TLE/Groucho) which recruit HDACs to silence genes.

As previously mentioned, FAP is an autosomal dominant inherited disorder whereby a key suppressor of WNT signalling, *APC*, has a truncation mutation (95% of cases) resulting in abnormal function of the protein (Fearhead et al. 2001). *APC* is mutated or a wild-type allele lost in 80% of sporadic CRC cases (Fearhead et al. 2001). These mutations can inhibit binding of APC to AXIN and  $\beta$ -catenin which can affect the formation and function of the destruction complex allowing  $\beta$ -catenin to accumulate in the nucleus and alter transcription (Fearhead et al. 2001). *APC* mutations may also be involved in dysregulating  $\beta$ -catenin ubiquitination (Kawahara et al. 2000; Yang et al. 2006). Other WNT signalling mutations can contribute to CRC development including activating mutations in the transcriptional activator,  $\beta$ -catenin. This can lead to functional changes in phosphorylation sites that prevent its inhibition by the destruction complex resulting in  $\beta$ -catenin pooling in the cytoplasm and nucleus, thereby promoting gene expression and cell growth (Morin et al. 1997). WNT signalling genes including *AXIN1* and *AXIN2* (Mazzoni & Fearon 2014), *GSK3 $\beta$*  (Shakoori et al. 2005), *LRP6* (de Voer et al. 2016) have also been found to be mutated and contribute to CRC development.

Butyrate is a known regulator of WNT signalling, with early studies identifying the link with this pathway through the increased induction of TCF activity in luciferase constructs containing TCF wild type (TOPflash) binding sites in SW620 CRC cells (Bordonaro et al. 2002; Bordonaro et al. 1999). Daly and Shirazi-Beechey (2006) revealed that WNT signalling inhibitors, such as AXIN2 and NLK, were upregulated by butyrate, while WNT signalling activators, such as WNT8A, were downregulated by butyrate in HT29 cells. More recently, 5 mM sodium butyrate was shown to regulate the expression of 1008 WNT signalling specific genes in HCT116 cells through microarray analysis (Lazarova et al. 2014). WNT hyperactivation is a key mechanism by which butyrate reduces growth and induces apoptosis in CRC cells; however, the mechanism by which this happens is poorly understood (Bordonaro et al. 2002; Bordonaro et al. 2008; Lazarova et al. 2014). Lazarova et al. (2004) identified a linear relationship between WNT activity levels and apoptosis in ten CRC cell lines when they were treated with 5 mM sodium butyrate. CRC cell lines showing high induction of WNT activity (HWA) included HCT116 cells with mutant  $\beta$ -catenin and E-cadherin and DLD-1 cells with mutant APC (Lazarova et al. 2004). RKO cells were classified in the lower changes

in WNT activity levels (LWA) group as they had the smallest change in WNT activity (Lazarova et al. 2004). Notably, RKO cells only had a mutation in *CDX2*, which is known to bind  $\beta$ -catenin to inhibit its interaction with TCF proteins (Guo et al. 2010b; Lazarova et al. 2004). The WNT activity levels correlated with apoptosis whereby HCT116 and DLD-1 cells were among those cells to have the greatest increase and change in apoptosis compared to RKO cells which had the lowest induction (Lazarova et al. 2004). The WNT-apoptosis relationship was reinforced by experimentation with HCT116 and DLD-1 cells with dominant negative *TCF4*, which demonstrated that repression of WNT specific transcriptional activity positively correlated with a reduction in apoptosis (Lazarova et al. 2004).

### **MAPK signalling**

Mitogen-activated protein kinase (MAPK) signalling is another key dysregulated pathway in several cancers, including CRC, due to its regulation of proliferation, apoptosis, differentiation and migration (Fang & Richardson 2005). MAPK signalling involves three subfamilies of molecules including extracellular-regulated kinases (ERK and MAPK); c-jun N-terminal kinases (JNK); p38 $\alpha$  (MAPK14) (Fang & Richardson 2005). The ERK/MAPK pathway is important in contributing to dysregulated proliferation in many cancer types, specifically CRC, due to key mutations found in *KRAS* and *BRAF* molecules in this pathway. ERK/MAPK signalling is activated by the binding of growth factors or mitogens to receptor tyrosine kinases (RTKs), which initiates the recruitment of adaptor proteins (SHC and GRB2) to hydrolyse GDP to GTP on the GTPase protein RAS (HRAS, NRAS, and KRAS) (Imajo et al. 2006). Protein kinase C (PKC) is also responsible for promoting GTP binding to RAS to trigger a similar down-stream cascade (Rusanescu et al. 2001). A phosphorylation cascade is initiated resulting in activation of RAF proteins (ARAF, BRAF, and CRAF), which serine phosphorylate MEK1/2 followed by ERK1/2 phosphorylation and activation (Imajo et al. 2006). ERK can act by phosphorylating cytoplasmic proteins or move into the nucleus to phosphorylate and activate several transcription factors such as c-FOS and ELK1 (Treisman 1994). This promotes transcription of genes, such as cell cycle regulators *CCND1* (Lavoie et al. 1996) and anti-apoptotic genes *MCL1* (Domina et al. 2004), and inhibits pro-apoptotic genes such as *BIM* (Biswas & Greene 2002), which promote cell proliferation and protect cells against apoptosis. The JNK and MAPK14 signalling pathways regulate cell proliferation and apoptosis but are also regulated by stress and cytokines. The JNK proteins (MAPK8, MAPK9, and MAPK10) are activated by a phosphorylation cascade involving protein kinase G (PKG) activation

of MEKK1, followed by SEK1 and finally JNK protein activation (Soh et al. 2001). Active JNK proteins can enter the nucleus and activate several transcription factors such as activating protein 1 (AP1) (Ip & Davis 1998). Alternatively, MAPK14 signalling can be initiated by ASK1 activation which phosphorylates MKK3/6, followed by MAPK14 (Kyriakis & Avruch 2012). Activated MAPK14 enters the nucleus to activate transcription factors such as MEF2, STAT1 and ELK1 (Kyriakis & Avruch 2012).

As previously mentioned, *KRAS* and *BRAF* are commonly mutated genes which contribute to CRC development and progression. Their constitutive activation contributes to sustained proliferation and survival of cancer cells through MAPK signalling pathways. *KRAS* mutations occur in around 40% of CRC cases (Di Fiore et al. 2007; Karapetis et al. 2008; Lievre et al. 2006), while *BRAF* mutations are in 5-15% of CRC cases (Davies et al. 2002; Rajagopalan et al. 2002; Yuen et al. 2002). Activating mutations in *KRAS* result in inability to deactivate the protein due to physical changes in the active site, that lead to impaired GTPase function and therefore GTP cannot be hydrolysed back to GDP (Scheffzek et al. 1997). *KRAS* becomes constitutively active. *BRAF* mutations in CRC and other cancers (~80%) are most commonly caused by amino acid substitution of valine to glutamate at residue 600 (*BRAF*<sup>Val600Glu</sup>) (Davies et al. 2002). This mutation is situated between two phosphorylation sites in the activation segment of the protein and is thought to mimic phosphorylation of the protein (phosphomimetic substitution), resulting in constitutively active BRAF (Lavoie & Therrien 2015; Zhang & Guan 2000).

Butyrate has also been shown to regulate MAPK signalling. Daly and Shirazi-Beechey (2006) demonstrated that after 5 mM butyrate treatment of HT29 cells, ERK3 expression was decreased while MAPK12 expression was upregulated. Butyrate treatment (10 and 40 mM) was shown to decrease RKO CRC cell proliferation and induce apoptosis (Zhang et al. 2010). A butyrate dose dependent increase of pro-apoptotic protein, BAX, and decrease of anti-apoptotic protein, BCL2, was observed in RKO cells (Zhang et al. 2010). Further investigation revealed that butyrate activated JNK protein via increased phosphorylation and inhibition of JNK reversed the anti-apoptotic effects of butyrate (Zhang et al. 2010). ERK1/2 phosphorylation was also reduced by butyrate, indicating that ERK signalling is likely inhibited to allow JNK signalling pathways to promote cell death (Zhang et al. 2010). A later study revealed the involvement of endocan in ERK signalling in the butyrate response (Zuo et al. 2013). Endocan is a dermatan sulfate proteoglycan that is released by endothelial cells and is involved in a range of cellular processes including inflammation, cell proliferation

migration, adhesion and angiogenesis (Kali & Shetty 2014). Previous studies have shown that endocan expression is correlated with CRC stage and that it is highly expressed in normal colonic and rectum mucosa, but downregulated in colorectal cancer (Zuo et al. 2008). Butyrate has been shown to upregulate endocan mRNA and protein expression in RKO CRC cells (Zuo et al. 2013). Further investigation revealed endocan overexpression decreased cell cycle progression, migration and growth, while knockdown of endocan reversed the inhibitory effects of butyrate on RKO migration and growth (Zuo et al. 2013). Butyrate was also shown to regulate ERK2/MAPK signalling molecule protein expression in order to reduce cell proliferation and migration, while *ERK* shRNA demonstrated increased endocan expression in RKO cells, reiterating the endocan and ERK/MAPK signalling connection with butyrate (Zuo et al. 2013).

Another study demonstrated that butyrate treatment regulates MAPK signalling and apoptosis by ERK and sphingosine kinase (SphK2) (Xiao et al. 2014). SphKs are important in regulating sphingolipid metabolites, which are involved in cell growth and apoptosis (Xiao et al. 2014). ERK inhibitors sensitised butyrate-treated HCT116 cells to apoptosis and blocked SphK2 from being exported from the nucleus to the cytoplasm (Xiao et al. 2014), indicating a key role of ERK in the butyrate response. The importance of ERK in the butyrate response was further highlighted by Li et al. (2017b) who demonstrated that butyrate reduced migration and invasion of CRC cells (HCT116, HT29, LOVO and HCT8) by preventing phosphorylation and, thereby, activation of ERK1/2 and AKT1.

### **PI3K/AKT signalling**

PI3K/AKT is another signalling pathway dysregulated in various cancers, including CRC, which accumulates mutations to promote cancer development and progression. PI3K/AKT signalling regulates proliferation, apoptosis and cytoskeleton rearrangement (Vivanco & Sawyers 2002). RTKs, such as MET, are activated by hepatocyte growth factor (HGF) ligand binding, which results in receptor dimerization and autophosphorylation. Inactive PI3K molecules can be recruited by interactions between phospho-tyrosine residues on RTKs and SRC-homology 2 (SH2) domains on the PI3K p85 regulatory subunit. Alternatively, adaptor proteins (IRS1 and IRS2) are recruited and the activated RTK phosphorylates IRS1 and IRS2, creating binding sites for the SH2 domains of p85 and inducing formation of the signalling complex (Metz & Houghton 2011). SH2–phospho-tyrosine interactions position PI3K closely to its

substrate at the cell membrane and activate the PI3K p110 catalytic subunit (released the inhibitory action of p85) which converts phosphatidylinositol 4,5-bisphosphate (PIP<sub>2</sub>) into phosphatidylinositol (3,4,5)-trisphosphate (PIP<sub>3</sub>) (Ahmed & Prigent 2017). Another activation pathway involves RTK recruitment of adaptor proteins SHC, GRB2 and GAB2 to activate RAS and help bring PI3K close to the cell membrane for catalysis of PIP<sub>2</sub> to PIP<sub>3</sub> (Ahmed & Prigent 2017). PIP<sub>3</sub> can then recruit and help activate AKT by directly interacting with its PH domain followed by phosphorylation at Thr308 by 3-phosphoinositide-dependent protein kinase-1 (PDK1) (Vanhaesebroeck & Alessi 2000). AKT must be phosphorylated at this site to be activated; however, maximal activation requires phosphorylation at the Ser473 site by PDK2 (Alessi et al. 1997). PTEN is a phosphatase that helps regulate the activity of this pathway by dephosphorylating PIP<sub>3</sub> to form PIP<sub>2</sub>.

Activated AKT has several molecular targets involved in various cellular processes such as BAD, FKHR, NF- $\kappa$ B (apoptosis); GSK3 $\beta$  (cell cycle); mTOR (growth, protein translation), MDM2 (cell cycle arrest, apoptosis) (Vivanco & Sawyers 2002). Pro-apoptotic proteins, such as BAD and caspase 9, can be phosphorylated and inhibited by AKT. BAD proteins normally promote cell death by forming non-functional protein complexes with the anti-apoptotic protein, BCLXL; however, AKT inhibition of BAD can release BCLXL to inhibit apoptosis (Datta et al. 1997). Furthermore, AKT can target and inhibit FKHR transcription factors to inhibit expression of its pro-apoptotic target genes, BIM and FAS ligand (Brunet et al. 1999). AKT can also phosphorylate and inhibit I $\kappa$ B kinase (IKK), which normally inhibits NF- $\kappa$ B transcription factor, in order to promote cell survival (Romashkova & Makarov 1999). The tumour suppressor, p53, is indirectly and negatively regulated by AKT, which phosphorylates its inhibitor MDM2 (promotes p53 proteasomal degradation through ubiquitination) resulting in more efficient translocation of the protein into the nucleus and greater p53 degradation (Mayo & Donner 2001; Zhou et al. 2001). AKT can also regulate cell proliferation by promoting activity of cell cycle regulators such as CCND1. Glycogen synthase kinase-3 $\beta$  (GSK3 $\beta$ ), which normally phosphorylates CCND1 and promotes its degradation (proteasome), is phosphorylated and inhibited by AKT which promotes CCND1 accumulation (Diehl et al. 1998). AKT can negatively regulate expression of cyclin-dependent kinase inhibitors (CKIs) such as CDKN1B (p27) and CDKN1A (p21). As previously mentioned, FKHR transcription factors are inhibited by AKT phosphorylation (Brunet et al. 1999). CDKN1B is another target gene repressed as a result of this effect and AKT can also negatively regulate CDKN1A phosphorylation

and activity (Dijkers et al. 2000; Medema et al. 2000). AKT also regulates cell growth through the mammalian target of rapamycin (mTOR) signalling pathway which responds to changes in nutrient availability by regulating protein synthesis. mTOR activates S6 kinase (RSK) to promote translation of mRNAs and inhibits translational repressors of mRNAs such as EIF4EBP1. mTOR is regulated by AKT53, however the exact mechanism requires further investigation (Nave et al. 1999).

Mutations in this pathway are also commonly found in several cancers including CRC. RAS mutations have been previously mentioned. Mutations are also found in p110 $\alpha$  catalytic subunit of PI3K (*PIK3CA*) in 10-15% of CRC cases; *PIK3CB* and *PIK3CD* (p110 $\beta$  and p110 $\delta$ , respectively) in approximately 2–3% of CRCs; *PIK3CG* (p110 $\gamma$ ) in 4% of CRCs, *PIK3R1* (p85 $\alpha$  regulatory subunit) in around 2–8% of CRCs; *PTEN* in around 2-10% of CRCs; and *AKT1* in around 1% (Bleeker et al. 2008; Danielsen et al. 2008; Day et al. 2013; Forbes et al. 2011; Huang et al. 2007; Philp et al. 2001; Tamborero et al. 2013). These mutations promote aberrant PI3K/AKT signalling. For example, *PIK3CA* mutations mostly result in changes in the helical and kinase domains that likely contribute to enhanced kinase activity (Samuels et al. 2004). *PTEN* mutations seem to destroy the phosphatase activity of the protein which means it cannot convert PIP3 back to PIP2 resulting in the inability to shutdown PI3K/AKT signalling (Leslie & Downes 2004).

Butyrate has been shown to control components of PI3K/AKT signalling, including AKT itself and downstream molecules such as mTOR (Cao et al. 2019; Wang et al. 2002). An early study revealed that exposure of KM20 CRC cells to 5 mM sodium butyrate and PI3K inhibitors (Wortmannin or LY294002) induced a significant pro-apoptotic and anti-proliferative effect (Wang et al. 2002). Interestingly, butyrate increased AKT phosphorylation alone, although the reason is unknown, but the PI3K inhibitors reduced it further when combined with butyrate (Wang et al. 2002). Butyrate has also been shown to regulate mTOR/S6K1 signalling in HCT116 cells by decreasing the phosphorylation of key targets including mammalian target of rapamycin (mTOR), ribosomal protein S6 kinase  $\beta$ 1 (S6K1), S6 and expression of silent mating type information regulation 2 homolog (SIRT1) (Cao et al. 2019). Butyrate increased the acetylation of S6K1 (Cao et al. 2019). SIRT1 inhibition had similar effects to the butyrate response whereby growth was inhibited, apoptosis induced and S6K1 acetylation increased, thereby reducing mTOR/S6K1 signalling (Cao et al. 2019). Butyrate increased the anticancer effects of SIRT1 inhibition through reducing cell proliferation and activity of mTOR/S6K1 further (Cao et al. 2019). The activation of

mTOR/S6K1 signalling and upregulation of cell proliferation, mediated by overexpression of SIRT1, were blocked by butyrate (Cao et al. 2019).

### **VEGF signalling pathway**

Angiogenesis, which is the development of new blood vessels, is an important process in the promotion of tumour growth and metastasis (Nishida et al. 2006). This process is regulated by proteins called vascular endothelial growth factors (VEGFs), which includes VEGFA (also known as VEGF), VEGFB, VEGFC, VEGFD, and placenta growth factor (PlGF) (Hoeben et al. 2004). Binding of these ligands to their corresponding receptors triggers cascades to promote angiogenesis (VEGFA, VEGFB, VEGFC, VEGFD, PlGF bind NRP1/2 receptors; VEGFA, VEGFC, VEGFD bind VEGFR2; VEGFA, VEGFB and PlGF binds VEGFR1) (Cao 2009). VEGFA, the most well studied growth factor, is commonly upregulated in several cancer types including CRC and is associated with poor prognosis in CRC patients (Bendardaf et al. 2017; George et al. 2001; Goel & Mercurio 2013). NRP1, which is a receptor for VEGF, is also highly expressed in many tumour types including CRC tumour tissue when compared to normal mucosa (Parikh et al. 2004). NRP1 has also been associated with poor prognosis and survival in CRC patients (Staton et al. 2013). CRC patients with high NRP1 levels also had less apoptotic cells indicating that NRP1 may also be involved in apoptosis suppression (Ochiumi et al. 2006).

Several studies demonstrated the ability of butyrate to induce a dose-dependent decrease in VEGF and NRP1 mRNA and protein expression in HCT116, Caco2 and HT29 CRC cells (Pellizzaro et al. 2002; Yu et al. 2010b). Interestingly normal mucosa samples had decreased NRP1 expression when the individual that the sample was taken from had high levels of butyrate in their gut (Yu et al. 2011). Butyrate was also found to cause a dose-dependent decrease in DNA binding affinity of SP1 transcription factors to the NRP1 promoter region (Yu et al. 2010b). This explains decreased NRP1 expression and likely contributes to its anti-angiogenic effect (Yu et al. 2010b). Interestingly, butyrate has also been shown to reduce angiogenesis by reversing the effects of VEGF stimulation by reducing *COX2* expression in human intestinal microvascular endothelial cells, which reinforces its strong antiangiogenic properties (Ogawa et al. 2003).

### **Apoptosis**

A hallmark of cancer is to resist cell death. In CRC, the ability of cells to apoptose is progressively lost during the acquisition of various genetic mutations (Wong 2011). Apoptosis functions through two key pathways: the intrinsic mitochondrial pathway and

extrinsic death receptor pathway. The intrinsic pathway is initiated by several internal stimuli such as DNA damage, hypoxia, radiation and oxidative stress. These stimuli induce increased mitochondrial permeability by promoting oligomerisation of BAX and BAK to allow for the release of cytochrome-c from the mitochondria into the cytoplasm (Danial & Korsmeyer 2004). Cytochrome-c forms an apoptosome protein complex with APAF-1 and pro-caspase 9, in order to assist in the activation of the initiator caspase 9. Once active, caspase 9 can cleave and activate executioner caspases 3 and 7 which initiate apoptosis. The BCL2 family proteins are key regulators of intrinsic apoptosis and include the pro-apoptotic proteins such as BAX, BAK, BAD, BID and BIM and the anti-apoptotic proteins such as BCL2, BCLXL, and MCL1 (Levine et al. 2008). As the release of cytochrome-c is a critical initiator of intrinsic apoptosis, anti-apoptotic proteins function by inhibiting release of cytochrome-c while pro-apoptotic proteins function by promoting release from the mitochondria. Other apoptosis regulators include second mitochondria-derived activator of caspase (SMAC)/direct IAP Binding protein with Low pI (DIABLO), apoptosis inducing factor (AIF), and Omi/high temperature requirement protein A (HTRA2) (van Loo et al. 2002). These proteins can promote caspase activation by interfering with caspase and inhibitor of apoptosis proteins (IAPs) binding (van Loo et al. 2002).

The extrinsic pathway is initiated when death ligands bind to a death receptor e.g. FAS ligand (FASL) binds to FAS receptors (CD95) (Itoh et al. 1991) and TNF ligands bind to type 1 TNF receptor (TNFR1) (Fuchs et al. 1992). Intracellular death domains for each receptor recruits their corresponding adapter proteins including FAS-associated death domain (FADD) and TNF receptor-associated death domain (TRADD) and pro-caspase 8 and altogether these protein complexes are referred to as death-inducing signalling complexes (DISCs) (Schneider & Tschopp 2000). The DISCs promote pro-caspase 8 activation to form initiator caspase 8, which initiates the apoptosis pathway by cleaving executioner caspases such as caspase 3 (Kruidering & Evan 2000).

As previously mentioned, butyrate can regulate WNT signalling to induce apoptosis. However, there are other mechanisms by which apoptosis is induced by butyrate. The loss of the tumour suppressor gene, *TP53*, occurs in around 50% of CRC cases (Liu & Bodmer 2006). p53 is involved in regulating processes like apoptosis, but most importantly preventing mutations in the genome. However, when mutated, p53 cannot perform its function and regulate the apoptosis-related target genes *p21<sup>waf1</sup>* and *BAX* (Rodrigues et al. 1990). An early study demonstrated that 3 mM butyrate induced the expression of pro-apoptotic gene *BAX* in DiFi colorectal cancer cells (Mandal et al.

1998), while anti-apoptotic *BCL2* expression was reduced in SW480 and HCT116 cells (Tailor et al. 2014). This was also confirmed using microarray analysis of HT29 cells treated with 5 mM butyrate, which resulted in upregulation of *BAK1*, a pro-apoptotic gene and downregulation of anti-apoptotic genes *BIRC5*, *CFLAR* and *BCLXL* (Daly et al. 2005; Daly & Shirazi-Beechey 2006). Butyrate also increased the levels of cleaved-PARP and cleaved-caspase-3 (Tailor et al. 2014). Dynamin-related protein 1 (DRP1), which is involved in mitochondrial fusion and fission during the cell cycle, may also have a role in the pro-apoptotic effects of butyrate (Tailor et al. 2014). *DRP1* expression was reduced by butyrate but increased again when CRC cells were treated with a pan-caspase inhibitor (Tailor et al. 2014).

### **Cell cycle regulation**

The dysregulation of the cell cycle is critical in promoting uncontrolled cell division and contributing to the development of cancer. The cell cycle is regulated by interactions between cyclin proteins and cyclin-dependent kinases (CDK) which are regulated by CDK inhibitors (CKIs). During growth phase 1 (G1), CDK4/cyclin D and CDK2/cyclin E complexes phosphorylate retinoblastoma protein (Rb), which activates E2F transcription factors and E2F target genes (Lim & Kaldis 2013). E2F target genes regulate G1/S transition of the cell cycle such as cyclin E, cyclin A and CDK1, enzymes involved in nucleotide synthesis (thymidine kinase) and DNA replication machinery (CDC6 and ORC1) (Lim & Kaldis 2013). The S-phase checkpoint includes the activation of CDK2/cyclin A (He et al. 2005). The G2 phase involves protein complexes CDK1/cyclin A and CDK1/cyclin B which phosphorylate and activate FOXM1 and recruit histone deacetylase p300/CREB binding protein (CBP) (Lim & Kaldis 2013). FOXM1 target genes include cell cycle regulators for mitosis initiation (cyclin B) and chromosomal segregation regulators (centromere protein F) (Major et al. 2004). Cell cycle progression is regulated by cyclin-dependent kinase inhibitors (CKIs), which slow progression by binding to and inhibiting the cyclin-CDK complexes. CKIs are divided into two groups INK4 and CIP/KIP families (Molinari 2000). INK4 includes p16 (INK4a), p15 (INK4b), p18 (INK4c) and p18 (INK4d) inhibiting CDK4 and CDK6 (Molinari 2000). CIP/KIP families include p21 (CIP1), p27 (KIP1) and p57 (KIP2) which can inhibit cyclin D dependent kinases (CDK) as well as CDK2/cyclin E and CDK2/cyclin A complexes (Vermeulen et al. 2003).

p53 is a critical protein involved in cell cycle regulation and DNA repair during this process. As previously mentioned, the *TP53* gene is mutated in many cancers including

CRC (~50%) (Liu & Bodmer 2006). p53 normally regulates the expression of cell cycle regulators such as p21 and GADD45A (Carrier et al. 1994). Mariadason et al. (2000) demonstrated that gene expression changes occur as early as 30 minutes in SW480 cells exposed to 5 mM butyrate. The maximal response of cell cycle related genes (arrest and progression) occurred at 16 h when SW480 cells were treated with 5 mM butyrate and was most like the synthetic HDACi TSA (1  $\mu$ M) at 12 h (Mariadason et al. 2000). Genes such as c-FOS (cell cycle transcription factor) were induced, while CDK6 (cell cycle regulator) were reduced. Mariadason et al. (2000) also noted that butyrate induces G0-G1 cell cycle arrest in CRC cells SW480 and Caco2.

Interestingly, 5 mM butyrate was demonstrated to cause cell cycle arrest in the G1 phase as well as inhibit mRNA expression of cyclin D1 (*CCND1*) (no change in protein), increase protein expression of cyclin D3 (no change in mRNA) and induce mRNA and protein expression of p21 expression in HT29 cells (Siavoshian et al. 2000). A later study determined that genes involved in cell cycle regulation and arrest were upregulated (*CDKN1A*, *PAK2*, *FOS*, *GADD45A*) whereas those involved in cell cycle progression were downregulated (*CCND1*, *CCNA2*, *CCNC*, *CDK4*, *CCT5*) by 5 mM butyrate in HT29 cells (Daly et al. 2005; Daly & Shirazi-Beechey 2006). Interestingly, butyrate treatment (1-5 mM) decreased cell viability and induced G2-M phase cell cycle arrest in HCT116 and SW480 CRC cells (Tailor et al. 2014) rather than arrest in the G1 phase as mentioned above (Siavoshian et al. 2000); the difference may be due to mutational status, but SW480 cells were also tested by Mariadason et al. (2000). Another study also demonstrated that 5 mM butyrate induced G2-M cell cycle arrest in HCT116 and RKO cells but not HT29 cells in which butyrate induced G1 arrest (Saldanha et al. 2014). *P21* mRNA expression was induced in RKO cells by butyrate but *BIRC5* levels were reduced, while p53 nuclear protein was increased (Saldanha et al. 2014). ChIP assays using p53 antibodies identified interactions with the p21 promoter indicating p53-dependent regulation with butyrate (Saldanha et al. 2014). This change was accompanied by decreases in protein expression of G2-M cell cycle regulators: cyclin B1, CDK1 and CDC25C (Tailor et al. 2014).

### **Regulation of non-coding RNAs**

Butyrate has been shown to regulate the expression of various transcription factors and non-coding RNAs including miRNAs to induce changes in CRC cell proliferation, migration and death. MicroRNAs are short non-coding RNAs with the ability to silence gene expression. They are involved in various cellular processes including cell

proliferation, apoptosis, cell cycle and differentiation (Bartel 2004). Dysregulated miRNAs contribute to the development and progression of numerous cancers, including CRC, due to their important role in regulation of tumour suppressors and proto-oncogenes (Lee & Dutta 2009; Orang & Barzegari 2014). Butyrate regulation of microRNAs is summarised in Section 1.5.5.

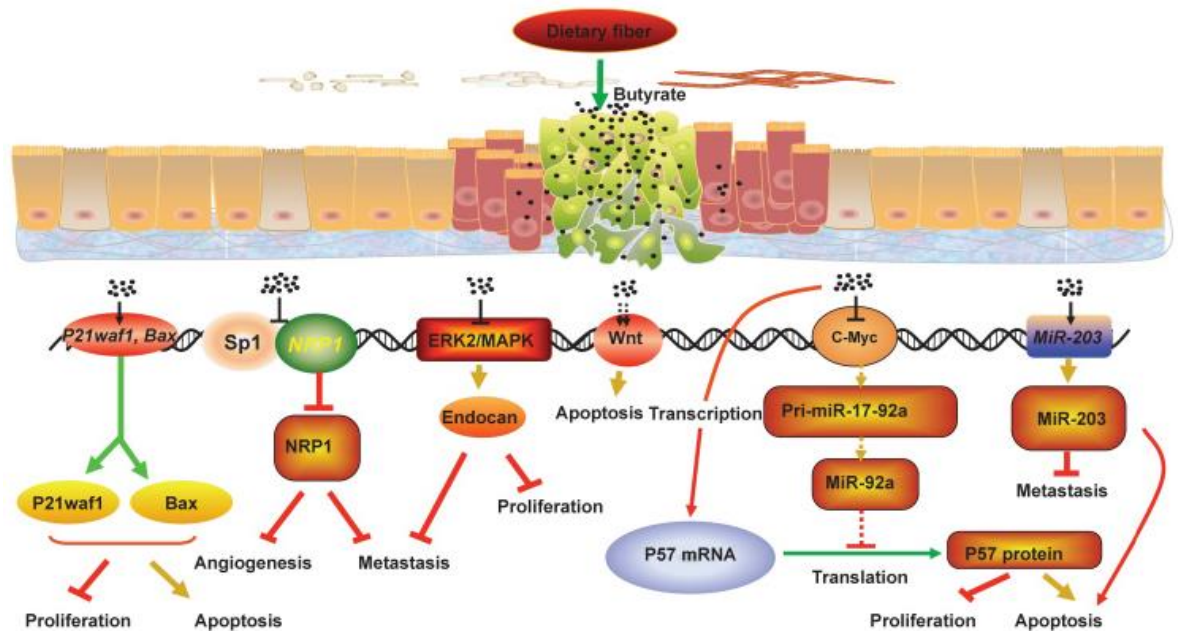


**Figure 1-4 Mechanisms of action of butyrate in colorectal cancer**

Butyrate-mediated regulation of several key growth, death and migration related pathways and molecules to promote CRC cell apoptosis and inhibit proliferation, angiogenesis and metastasis. This includes the upregulation of pro-apoptotic genes *P21* and *BAX*, inhibition of NRP1 growth receptor via SP1 transcription factor inhibition, ERK2/MAPK signalling inhibition, WNT hyperactivation promoting apoptosis and oncogenic miRNA downregulation. (Image from J Cancer, CC-BY-NC: (Wu et al. 2018c)).

## 1.5 MicroRNAs in colorectal cancer

As previously mentioned, HDAC inhibitors, such as butyrate, can regulate key cell proliferation, apoptotic and differentiation pathways. miRNAs are another form of epigenetic regulators, which also target similar pathways.

### 1.5.1 MicroRNA discovery

miRNAs are endogenous small non-coding (19-25 nucleotide) RNA molecules. They can post-transcriptionally regulate target gene expression by binding to complementary mRNA molecules and, thereby, inhibiting translation of mRNAs into proteins. miRNAs represent a small component of non-coding RNA molecules, which also includes long

non-coding RNAs (lncRNAs), PIWI RNAs (piRNAs), small nuclear RNAs (snoRNAs) and other non-coding RNAs of various lengths.

miRNAs were first discovered in 1993 in the nematode, *C.elegans* (Lee et al. 1993; Wightman et al. 1993). The heterochronic gene *lin-4* was found to be involved in early postembryonic development of *C.elegans*, by regulation of translation through antisense RNA-RNA interaction with the complimentary *lin-14* mRNA 3'UTR region (Lee et al. 1993; Wightman et al. 1993). Later, *lin-4* was also found to regulate LIN-28 protein levels, by the same mechanism (Moss et al. 1997). *Let-7*, another heterochronic gene, was the second miRNA to be discovered in *C.elegans* (Reinhart et al. 2000). This miRNA is involved in developmental timing, specifically adult cell fate, in the nematode (Reinhart et al. 2000). The importance of this miRNA was confirmed through investigation of loss-of-function mutants in *C.elegans*, whereby the nematodes failed to reach the correct larval stages (Reinhart et al. 2000). Further investigation in other organisms has revealed that both *lin-4* and *let-7* are conserved across multiple species, including *Drosophila* and humans (Pasquinelli et al. 2000).

Since the discovery of these miRNAs, many more have been identified in a range of organisms including plants and viruses (Skalsky & Cullen 2010; Zhang et al. 2006a). The miRBase miRNA database (version 20) now holds records of 28645 entries representing hairpin precursor miRNAs, which produce 35828 mature miRNA products, in 223 different species of organisms (Kozomara & Griffiths-Jones 2014). Of those miRNAs, currently 1881 precursors and 2588 mature miRNAs belong to the human species (Kozomara & Griffiths-Jones 2014). These miRNAs can not only regulate multiple gene targets, but also multiple miRNAs can regulate a single gene. It is estimated that miRNAs regulate approximately 60% of protein-coding genes in humans (Friedman et al. 2009).

### 1.5.2 MicroRNA biogenesis and function

miRNA genes are structurally similar to protein-coding genes with an upstream promoter region, transcription start site and RNA-coding sequence. miRNA biogenesis is initiated with the transcription of miRNA genes, by RNA polymerase II, to produce primary-miRNAs (pri-miRNAs) (Figure 1-5) (Lee et al. 2004). miRNA genes can be intronic (alone or clustered), intergenic (alone or clustered), exonic and can be mirtrons (located in introns) (Kapinas & Delany 2011; Kim et al. 2009). Pri-miRNAs form hairpin structures which have imperfect stem base-pairing and may contain one, or more commonly, multiple miRNA sequences (Hwang & Mendell 2006). Drosha (RNase

III endonuclease enzyme) and DiGeorge syndrome Critical Region gene 8 (DGCR8) (mammalian double-stranded RNA binding protein) form a complex and process the pri-miRNA into a precursor-miRNA (pre-miRNA) (Landthaler et al. 2004; Tomari & Zamore 2005). A pre-miRNA is a hairpin structured molecule approximately 70-100 nucleotides in length with a two nucleotide 3' overhang (characteristic of RNase III endonuclease processing) which is transported into the cytoplasm via Exportin 5 (RanGTP-dependent double-stranded RNA (dsRNA) binding protein) (Bartel 2004; Denli et al. 2004; Yi et al. 2003). The pre-miRNA undergoes maturation in the cytoplasm involving cleavage of the hairpin loop by a protein complex composed of RNase III-type endonuclease Dicer, TAR RNA binding protein (TRBP) and protein activator of PKR (PACT) to form a miRNA duplex approximately 19-25 nucleotides in length (Filipowicz et al. 2008; Lee et al. 2013). Further processing by this complex results in two mature miRNA strands, one of which is a passenger strand, degraded by enzymes, and a primary strand which is incorporated into the RNA induced silencing complex (RISC) with the help of the associated proteins Dicer, TRBP and PACT (Bartel 2004; MacFarlane & Murphy 2010). The RISC is a ribonucleoprotein which contains 1 of the 4 Argonaute proteins that are involved in miRNA mediated gene repression (Fabian et al. 2010). Argonaute proteins contain conserved domains including PAZ, MID and PIWI (Fabian et al. 2010). However, Argonaute 2 is the only protein which contains an enzymatically active PIWI domain with the ability to cleave miRNA-mRNA complexes when perfect base pairing is achieved, resulting in mRNA cleavage (Fabian et al. 2010). miRNA targets are identified through the binding of the conserved miRNA seed sequence to the complementary target mRNA 3'UTR; they are classified into multiple groups. There are two kinds of 7mer sites, including 7mer-m8 sites, which have exact matches to the seed sequence and position 8 (positions 2-8 match) of the mature miRNA; 7mer-1A sites which have exact matches to the seed sequence (positions 2-7 match) of the mature miRNA with an Adenine at position 1 (Bartel 2004; Lewis et al. 2005); 8mer sites have perfect matches to the seed sequence and position 8 (positions 2-8) of the mature miRNA and an Adenine base at position 1 (Bartel 2004; Friedman et al. 2009). Imperfect base pairing of the miRNA-mRNA duplex within RISC can result in translational inhibition or mRNA destabilisation which is mediated by interference of cap recognition and ribosomal subunit recruitment (Guo et al. 2010a). Destabilisation of the mRNA molecule involves de-capping by DCP1/DCP2 de-capping complexes and de-adenylation by CCR4:NOT deadenylase proteins; thereby, initiating the mRNA destabilisation process (Behm-Ansmant et al. 2006). miRNA mediated silencing is known to occur inside P-bodies, which are aggregates of proteins containing machinery

involved in translational inhibition and mRNA decay (Patel et al. 2016). mRNAs may be degraded or stored and released from P-bodies for translation at a later time (Parker & Sheth 2007).

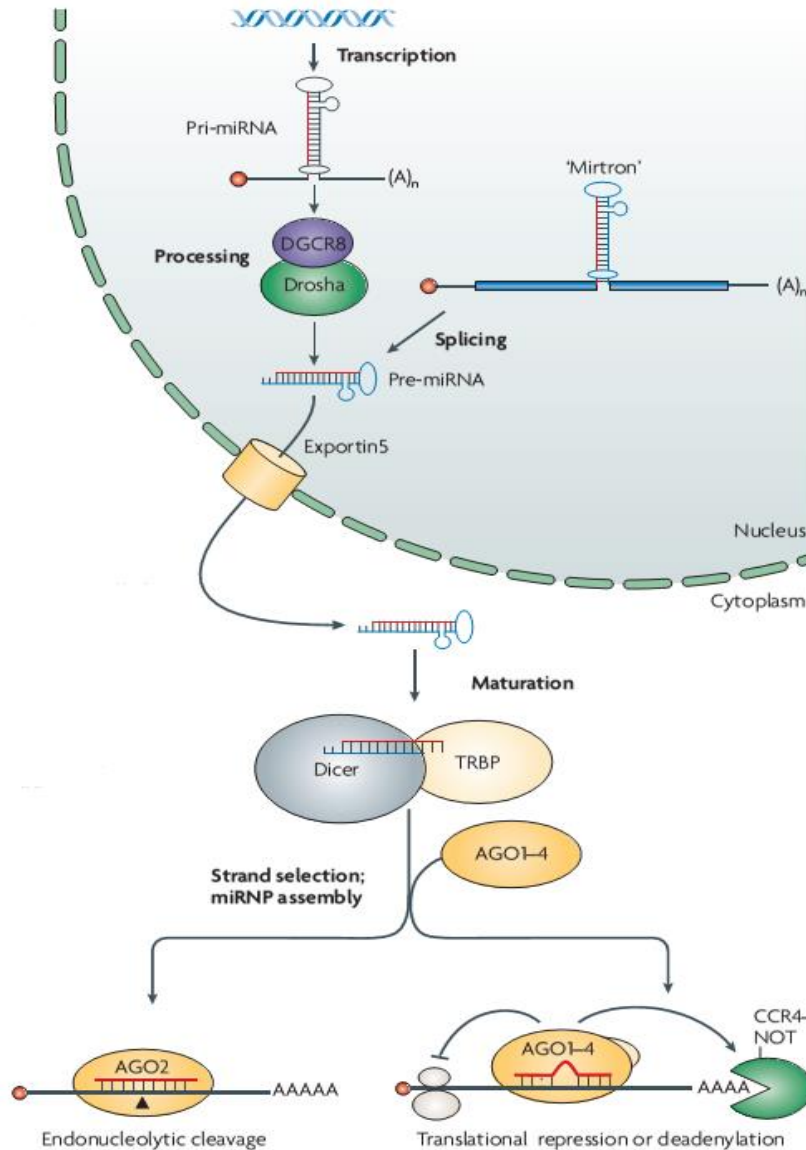


**Figure 1-5 MicroRNA biogenesis pathway**

Transcribed pri-miRNAs are processed by the Drosha and *DGCR8* complex in the nucleus, which produce pre-miRNAs that are exported into the cytoplasm by Exportin5. Pre-miRNAs are processed by the Dicer and TRBP complex to form a miRNA duplex. The primary miRNA strand is incorporated into RISC, which mediates miRNA-mRNA binding through Argonaute proteins. Argonaute 2 is the only protein that can cleave miRNA-mRNA complexes when perfect base pairing is achieved resulting in mRNA degradation, while all Argonaute proteins can mediate translational inhibition or mRNA destabilisation due to imperfect base pairing of the miRNA-mRNA complex. (Image reproduced with permission: (Filipowicz et al. 2008))

### 1.5.3 MicroRNAs in tumorigenesis and colorectal cancer

miRNAs have been demonstrated to have critical roles in several cellular processes and pathways, including cell proliferation, apoptosis and differentiation (Lee & Dutta 2009; Peng & Croce 2016). Consequently their dysregulation is important in the development and progression of numerous cancer types including CRC (Cummins et al. 2006; Lu et al. 2005; Volinia et al. 2006). Calin et al. (2002) identified the first key connection between miRNA dysregulation and cancer when they revealed that miR-15 and miR-16 were frequently deleted in B-cell chronic lymphocytic leukaemia. Several other mechanisms have since been shown to contribute to miRNA dysregulation including changes in the DNA methylation status of miRNA gene promoters, histone modifications (acetylation or methylation), changes in transcription factor activity and global or miRNA specific changes in miRNA processing (Saito et al. 2009). Many miRNA genes are located within genomic fragile sites and cancer associated regions such as regions of amplification, loss of heterozygosity or breakpoints which are commonly amplified, deleted or rearranged in cancer (Calin et al. 2004). Zhang et al. (2006b) reported that miRNA and miRNA associated genes (*Dicer1*, *Argonaute 2*) had high copy number alterations in ovarian and breast cancers and melanoma, which may be attributed to amplification or deletion mutations.

miRNAs can act as tumour suppressors or oncogenes, by altering gene expression and regulating signalling pathways to suppress or promote tumour development, respectively. They do not require one or both alleles to have a gain or loss of function respectively, as do typical oncogenes and tumour suppressor genes (Garzon et al. 2006; Kent & Mendell 2006). Across numerous cancers, the expression of specific miRNAs is frequently increased or decreased. Commonly dysregulated oncogenic and tumour suppressor miRNAs involved in the growth and death pathways of CRC are presented in Table 1-1. miR-143 and miR-145 were the first miRNAs to be consistently detected at lower levels in adenomatous and CRC tissues when compared to normal mucosa (Michael et al. 2003). Large scale expression analyses have identified even more dysregulated miRNAs in CRC. Cummins et al. (2006) identified 200 known miRNA genes, 133 novel miRNA candidates and 112 previously uncharacterised miRNAs in CRC cells using miRNA serial analysis of gene expression (miRAGE). Another profiling study, involving comparison of miRNA expression in colon tumour tissue and normal mucosa using high-throughput sequencing, revealed the dysregulation of 37 miRNAs; 19 were downregulated while 18 were upregulated (Hamford et al. 2012). miRNAs previously shown to be involved in CRC development including miR-1, miR-96 and

miR-145 were identified as well as miRNAs newly associated with CRC including miR-3163 and miR-1827 (Hamfjord et al. 2012). Schee et al. (2013) used deep sequencing to identify 523 miRNAs expressed similarly across 88 CRC tumours of which miR-10a-5p, miR-21-5p, miR-22-3p and miR-192-5p were the most highly abundant. A more recent study using small RNA-seq revealed 2245 known miRNAs and 515 novel miRNAs and of them 222 were dysregulated (135 upregulated and 87 downregulated) in paired CRC tumour tissue versus matched normal tissue (Neerinx et al. 2015). Other profiling studies, using real-time RT-PCR and microarrays, have also demonstrated dysregulation of miRNA expression in CRC (Bandrés et al. 2006; Guo et al. 2009; Koduru et al. 2017; Ng et al. 2009b; Reid et al. 2012; Rohr et al. 2013).

Individual miRNAs and miRNA clusters which are commonly upregulated in CRC often exhibit oncogenic properties. miR-21 is an oncogenic miRNA that is normally upregulated in CRC (Table 1-1). miR-21 silences *PTEN*, which is particularly important in inhibiting the PI3K signalling pathway that normally promotes growth, in order to promote CRC growth and metastasis (Wu et al. 2017b). Higher expression of this miRNA is also associated with a worse clinical outcome in CRC patients (Mima et al. 2016). The oncogenic miR-17-92 cluster (miR-17, 18a, 19a, 20a, 19b-1 and 92a-1) has been associated with colorectal cancer development and progression, whereby these molecules are almost always upregulated in the disease state. Key tumour suppressor target genes of this cluster include *PTEN* (miR-17, 19a, 20a and 19b-1), *BCL2L1* (miR-92a-1) and *CDKN1A* (miR-17 and 20a) which are involved in inhibiting cell growth by pathways such as PI3K signalling and promoting apoptosis and cell cycle arrest respectively. Interestingly, miR-18a has been demonstrated to display tumour suppressor properties even amongst an oncogenic cluster. Humphreys et al. (2014b) demonstrated that miR-18a targets *CDC42*, which is a key Rho GTPase involved in promoting growth via PI3K signalling pathway. Expression of the entire cluster is also upregulated and has oncogenic properties including the ability to promote cell proliferation and survival and inhibit differentiation in many other cancers (Olive et al. 2010).

Individual miRNAs and miRNA clusters, which are commonly downregulated in CRC, often exhibit tumour suppressor properties. miR-34a is often downregulated in CRC (Table 1-1) and normally acts as a tumour suppressor by inhibiting CRC cell proliferation (Tazawa et al. 2007). This miRNA silences the transcription factor E2F, which normally promotes the cell cycle, as well as increases p53 protein expression (Tazawa et al. 2007). miR-143 and miR-145 are a cluster of miRNAs commonly

downregulated in CRC (Table 1-1). These miRNAs are putative tumour suppressors shown to silence a range of genes involved in cell proliferation and survival, reflecting their anti-tumorigenic properties (Akao et al. 2010). miR-143 and miR-145 have been shown to decrease expression of MDM2, a ubiquitin ligase that normally promotes degradation of tumour suppressor p53, resulting in decreased cell proliferation and increased apoptosis (Zhang et al. 2013). miR-143 can also silence oncogenes including *ERK5* and *KRAS* which are strongly involved in cell proliferation via the MAPK signalling pathways (Chen et al. 2009; Clapé et al. 2009). Alternatively, miR-145 has been shown to target oncogenes *FLI1* and *c-MYC*, which are involved in chromosomal translocations and transcriptional regulation of genes involved in cell proliferation, development and differentiation (Sachdeva et al. 2009; Zhang et al. 2011a). Interestingly, c-MYC is a transcription factor that regulates the miR-17-92 cluster which is also dysregulated in CRC (Diosdado et al. 2009).

**Table 1-1** Summary of key oncogenic and tumour suppressor miRNAs involved in colorectal cancer cell growth and death.

miRNA	Examples of key target genes in CRC	Reference
<b>Tumour suppressor miRNAs downregulated</b>		
let-7	KRAS	(Akao et al. 2006; Cappuzzo et al. 2014; Saridaki et al. 2014)
miR-15a	BCL2, BMI1, DCLK1, YAP1	(Cimmino et al. 2005; Fesler et al. 2017; Gopalan et al. 2018; Wu et al. 2016a)
miR-16	BCL2	(Cimmino et al. 2005; Young et al. 2012)
miR-25	SMAD7	(Li et al. 2013b)
miR-29b	BCL9L	(Subramanian et al. 2014)
miR-30a	CD73, ITGB3, MTDH, PIK3CD	(Jin et al. 2018; Wei et al. 2016; Xie et al. 2017; Zhong et al. 2013)
miR-34a	E2F, HMGB1	(Chandrasekaran et al. 2016; Tazawa et al. 2007)
miR-93	SMAD7	(Tang et al. 2015)
miR-101	COX2, ZEB1	(Strillacci et al. 2009; Xiong et al. 2018)
miR-137	CDC42	(Liu et al. 2011b)
miR-143	ERK5, KRAS, MDM2	(Chen et al. 2009; Clapé et al. 2009; Zhang et al. 2013)
miR-145	c-MYC, FLI-1, MDM2	(Sachdeva et al. 2009; Zhang et al. 2011a; Zhang et al. 2013)
miR-342	DNMT1, NAA10	(Wang et al. 2011; Yang et al. 2015a)
miR-365	BCL2, CCND1	(Nie et al. 2012a)
miR-675	RB1	(Tsang et al. 2010a)
<b>Oncogenic miRNAs upregulated</b>		
miR-17-92 cluster	BCL2L11 (17, 18a, 20a, and 92a), CDKN1A (17, 20a), E2F1 (17, 20a), PTEN (17, 19a, 19b, 20a), TGFBR2 (20a)	(Humphreys et al. 2013; Humphreys et al. 2014b; Kanaan et al. 2012)
miR-21	PTEN, PDCD4, RHOB, TPM1	(Chang et al. 2011; Wu et al. 2017b)
miR-31	RASA1, SATB2	(Sun et al. 2013; Yang et al. 2013c)
miR-96	TP53INP1, FOXO1, FOXO3a	(Gao & Wang 2015)
miR-106a	ATG7, RB1	(Catela Ivkovic et al. 2013; Hao et al. 2017)
miR-135a	APC, MTSS1	(Nagel et al. 2008; Zhou et al. 2012a)
miR-135b	APC	(Nagel et al. 2008)
miR-146	PDHB	(Zhu et al. 2017)
miR-155	E2F2, NTR, PTEN, SOCS1	(Bakirtzi et al. 2011; Li et al. 2014a)
miR-301a	DLC1, RUNX3	(Zhang et al. 2019b)

### 1.5.4 MicroRNAs as biomarkers of tumorigenic states and therapeutic agents

miRNAs have been investigated as both biomarkers and therapeutic agents for various disease states, due to their dysregulation within various cancer cell types. Large profiling studies, involving the use of microarrays, were the first to highlight the dysregulation of a number of miRNAs in cancers including breast, prostate, lung, pancreatic and colon cancer (Lu et al. 2005; Volinia et al. 2006). Due to the limitations of microarrays, such as difficulty normalising data and inability to detect novel miRNAs (Pritchard et al. 2012), Next Generation Sequencing (NGS) is becoming more widely used for the profiling of RNA molecules in disease states. NGS can profile miRNA expression changes in cancer cells with greater sensitivity, accuracy and range of detection than microarrays (Tam et al. 2014). Recently, Peng et al. (2015) acquired and analysed RNA-seq results from The Cancer Genome Atlas (TCGA) for 4043 cancer types and designed cancer specific panels to differentiate between cancer and normal cells, highlighting the power of these NGS techniques.

Currently, cancer diagnosis is performed following the biopsy of cancer tissue. However, this technique is invasive and uncomfortable for patients. Detecting biomarkers within human fluids including urine, saliva or blood is easier and less invasive. miRNAs as biomarkers of CRC presence and stage have shown great potential in serum and faecal samples (Huang et al. 2010; Link et al. 2010; Ng et al. 2009a). Many studies have shown that members of the oncogenic clusters miR-17-92a and miR-18b-106a are upregulated in CRC patients. (Ng et al. 2009a) revealed that miR-92 is significantly increased in the plasma of people suffering from CRC, while (Link et al. 2010) demonstrated that both miR-21 and miR-106a are increased in faecal matter of those with adenomas and CRC. miRNAs have also been detected in the exosomes of CRC patients. More recently, exosomal miR-19a was found to be upregulated in the serum of CRC patients compared to healthy people (Matsumura et al. 2015). These miRNAs have the potential to be non-invasive CRC biomarkers.

miRNA replacement therapies and anti-miR therapy have been of great interest as future disease treatments due to the known dysregulation and causative roles of miRNAs in various disease states. Re-introduction of a miRNA, which has decreased expression in a disease state (normally tumour suppressor miRNAs), may inhibit the progression of the disease when healthy miRNA levels are regained. miRNA replacement therapy in CRC mouse models demonstrated that the introduction of miR-

145, which has decreased expression in CRC, caused reduced tumour proliferation and induced apoptosis (Ibrahim et al. 2011). Li et al. (2013b) also demonstrated that restoration of miR-25 in CRC mouse models, which is normally downregulated in CRC, resulted in suppressed growth of CRC xenografts *in vivo*. Many animal studies strongly support the protective effects of the master tumour suppressor, miR-34a, in animal models, including the ability to decrease tumour growth and survival and induce apoptosis in a variety of cancer types e.g. pancreatic cancer (Pramanik et al. 2011), lung cancer (Kasinski et al. 2015; Trang et al. 2011; Wiggins et al. 2010; Xue et al. 2014) and prostate cancer (Liu et al. 2011a). miR-34a (MRX34) replacement therapy has also been delivered to hepatocellular carcinoma sufferers in phase 1 clinical trials and demonstrated efficacy in some patients including 1 partial response and 6 stable disease states (Beg et al. 2017). When a miRNA has increased expression in a disease, the inhibition of that miRNA using antagomirs may also inhibit disease progression. ZR-75-30 breast cancer cells transfected with antagomir-20b were subcutaneously delivered to BALB/c nude mice which resulted in delayed tumour formation and reduced tumour size compared to negative controls (Zhou et al. 2014). Anti-miR-122 (Miravirsen) entered phase 2 clinical trials in individuals suffering from Hepatitis C Virus (HCV); this treatment was used to block miR-122 which is highly expressed in the liver and used for HCV RNA stability and propagation (Janssen et al. 2013). Janssen et al. (2013) demonstrated that anti-miR-122 treatment caused dose-dependent reductions in HCV RNA levels in patients and there has been no viral resistance. Sicard et al. (2013) demonstrated that the use of lentiviral vectors in pancreatic cancer *in vitro* and *in vivo* models, decreases miR-21 expression. As previously mentioned, it was demonstrated that miR-16 replacement therapy in humans with mesothelioma resulted in the objective and partial responses of some patients (van Zandwijk et al. 2017). Further investigation is required for use of miRNA therapies in CRC.

### 1.5.5 Effects of butyrate on microRNAs in colorectal cancer

Butyrate has been shown to regulate individual miRNAs, as well as clusters of miRNAs, to exert its anticancer effects (Han et al. 2016b). miR-203 is a known tumour suppressor miRNA in CRC, which has decreased expression and has been shown to inhibit CRC cell proliferation, migration and invasion (Deng et al. 2016; Fu et al. 2016). Butyrate treatment was shown to restrict cell proliferation, colony formation, cell invasion, and induce cell apoptosis in CRC cells (HT29 and Caco2) through upregulating the expression of miR-203, which resulted in the downregulation of its target gene NEDD9

(Han et al. 2016b). The knockdown of NEDD9 induced similar effects to the observed butyrate response (Han et al. 2016b).

A key dysregulated cluster in CRC is the miR-17-92 cluster (miR-17, miR-18a, miR-19a, miR-20a, miR-19b-1, and miR-92a-1), which is known to contribute to CRC development and progression (Diosdado et al. 2009). Hu et al. (2011) demonstrated that 1 mM butyrate treatment, over 24 h, altered the expression of 44 miRNAs in HCT116 colorectal carcinoma cells. Oncogenic clusters members miR-17, miR-20a, miR-20b, miR-93, miR-106a and miR-106b (from clusters miR-17-92a, miR-106a-363, and miR-106b-25), which are normally upregulated in CRC, were decreased by exposure to butyrate (Hu et al. 2011). Hu et al. (2011) also reversed the anti-proliferative effects of butyrate by overexpressing miR-106b, which decreased p21 expression induced by butyrate. Later, Humphreys et al. (2013) confirmed the downregulation of the miR-17-92 and miR-106a-363 (miR-18b, miR-19b, miR-20b, miR-92a, miR-106a, miR-363) cluster by exposing HT29 and HCT116 CRC cells to 5 mM butyrate. Contradictory data have been presented in terms of how butyrate regulates the miR-17-92 cluster. c-MYC, a transcription factor, is thought to be a key player because it upregulates the miR-17-92 cluster in various cancers including CRC (Diosdado et al. 2009; Fuziwara & Kimura 2015). Humphreys et al. (2013) demonstrated that c-MYC expression was unchanged in HT29 but significantly increased in HCT116 cells, which does not support the hypothesis that the miR-17-92 cluster is regulated by c-MYC in all CRC cell lines. Another study found that miR-92a expression was significantly decreased by 2 mM butyrate treatment in HCT116 and HT29 cells, while c-MYC decreased in HCT116 cells (Hu et al. 2015). In HCT116 cells, the other miR-17-92 cluster members were also found to decrease in expression following 2 mM butyrate exposure, as well as exposure to other HDAC inhibitors, SAHA and valproic acid in HCT116 cells (Hu et al. 2015). Further investigation also revealed that miR-92a mimics rescued the cells from butyrate by inhibiting the tumour suppressor p57 which is normally upregulated by butyrate (Hu et al. 2015). Butyrate treatment also reduced miR-135a/b, miR-24, and miR-106b expression in LT97 CRC cells (Schlormann et al. 2015). Clearly miRNA interactions have a role in the butyrate response.

## 1.6 lncRNAs in colorectal cancer

As previously mentioned, miRNAs and the HDACi, butyrate, have a role in the regulation of key cell growth and death pathways through post-transcriptional and/or chromatin regulation. lncRNAs are another form of RNA-mediated gene regulation,

often with epigenetic involvement, which also target similar pathways through the regulation of chromatin, RNA and protein.

### 1.6.1 lncRNA discovery

lncRNAs were unknowingly discovered in the 1980s. In 1984, Pachnis et al. (1984) identified the H19 imprinted maternally-expressed transcript in foetal mouse liver and it was noted that a corresponding protein was not identified. Further investigation in the 1990s revealed that H19 was likely non-coding because it lacked conserved open reading frames (ORFs) between human and mouse transcripts, did not associate with ribosomes, formed cytoplasmic particles and most importantly, did not produce a detectable protein (Brannan et al. 1990). H19 was later confirmed to be non-coding and involved in epigenetic regulation through its parental imprinting patterns with the *igf2* mouse gene (Bartolomei et al. 1993; Bartolomei et al. 1991). A lncRNA called X inactive specific transcript (XIST), which is involved in X-inactivation, was also discovered during the early 1990s (Brockdorff et al. 1992). XIST also lacked conserved ORFs that were long enough to produce a protein and the RNA transcripts were mostly localised to the nucleus and associated with the inactivated X-chromosome in females; this confirmed its function as a non-coding RNA with a role in X-inactivation (Brown et al. 1992; Clemson et al. 1996).

### 1.6.2 lncRNA biogenesis and function

lncRNAs are long non-coding RNA molecules, which lack the ability to produce proteins. They are generally classified to be >200 nt in length and may have short ORFs <300 nt (<100 amino acids) (Dinger et al. 2008; Prasanth & Spector 2007). There are notably some exceptions where small conserved peptides have been identified as being expressed from lncRNAs with short ORFs (Choi et al. 2018; Ji et al. 2015). lncRNAs are produced from various regions of the genome and are classified based on their proximity to a gene including intronic, exonic, intergenic and intragenic regions, the 3' and 5' UTR, and promoter and enhancer sequences (Figure 1-6) (Nie et al. 2012b). They may also be expressed in both sense and antisense orientations in relation to the host gene or in a bidirectional manner (Nie et al. 2012b). The canonical biogenesis of lncRNAs is similar to mRNA transcription and processing. lncRNAs are generally transcribed by RNA polymerase II, but some have been reported to be produced by RNA polymerase III (Nie et al. 2012b). They are often spliced (98%), produced with a poly(A) tail and 5'cap and they often contain multiple exons, although of unusual structure, with a bias toward two exons (48%) (Derrien et al. 2012). Interestingly,

lncRNA promoters are almost as conserved as protein-coding gene promoters; lncRNA exons are conserved to a lesser extent (Derrien et al. 2012). lncRNAs are generally enriched in the chromatin and cell nucleus; however, some function in the cytoplasm (Derrien et al. 2012). An example of a lncRNA with a typical structure is XIST, which is spliced, has a poly (A) tail and 5'cap (Brown et al. 1992; Hong et al. 2000).

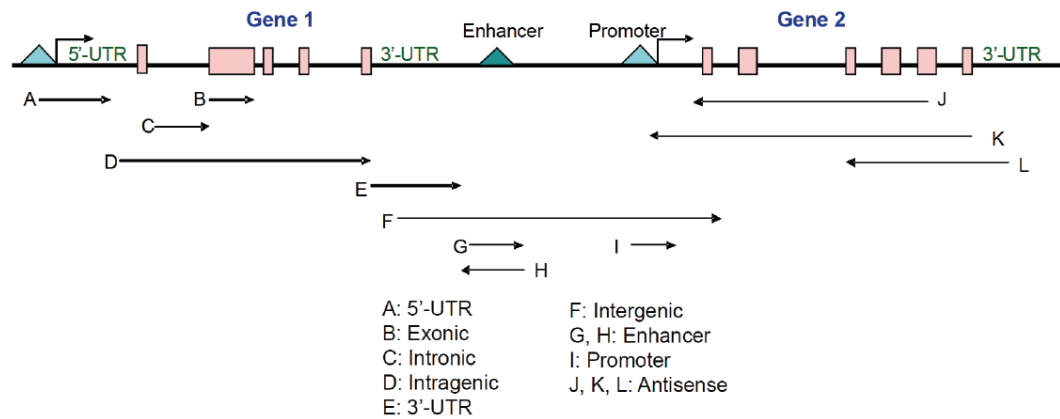


**Figure 1-6 lncRNA transcript origins**

lncRNAs can originate from various locations in relation to other genes. (Image from Am J Transl Res, CC-BY-NC: (Nie et al. 2012b)).

The secondary and tertiary structures formed during lncRNA production appear to be particularly important in the function of some lncRNAs. Interestingly, 40% of long unannotated transcripts are thought to be precursors for small RNAs less than 200 nt (Kapranov et al. 2007). Metastasis associated lung adenocarcinoma transcript 1 (MALAT1), for example, contains a tRNA-like secondary structure, which is removed during processing and localised to the cytoplasm (Wilusz et al. 2008). The small 61 nt molecule is broadly expressed in human tissues (Wilusz et al. 2008). H19 has been found to be a precursor for the microRNA, miR-675, which is involved in placental growth during development (Keniry et al. 2012). lncRNA structures are also important in the primary function of lncRNAs. HOX transcript antisense RNA (HOTAIR), which functions as a scaffold for chromatin modifying complexes such as Polycomb Repressive Complex 2 (PRC2), is composed of complex RNA structural motifs, which help recruit and bind enzymes that alter the chromatin structure (Tsai et al. 2010). lncRNA steroid receptor RNA activator (SRA) has also been shown to have a complex structural arrangement of four domains with an array of secondary elements, to perform its function in co-activation of hormone receptors (Kino et al. 2010).

Many lncRNAs are also spliced, resulting in the production of lncRNA variants. The lncRNA colorectal neoplasia differentially expressed (CRNDE), for example, has been

## CHAPTER 1

reported to have at least 10 different splice variants due to the CRNDE gene containing 6 exons (Graham et al. 2011). Interestingly, CRNDE-h, which is associated with colorectal cancer prognosis, has 5 out of 6 CRNDE protein-coding gene exons, although it still functions as a non-coding RNA (Liu et al. 2016b).

Genes encoding lncRNAs are produced with similar epigenetic marks associated with protein-coding transcripts. These include histone modifications H3K4me3, H3K4me2, H3K9ac, H3K27ac active and H3K36me3 repressive marks around the transcriptional start sites, and H3K36me3 repressive marks throughout the gene body (Derrien et al. 2012; Guttman et al. 2009; Sati et al. 2012), which assists in lncRNA regulation at the chromatin level. Interestingly, the abundance of H3K27me3 repressive and H3K36me3 active marks were discovered in slight excess in lncRNA transcription start sites compared with those of protein-coding transcripts (Derrien et al. 2012). DNA methylation also regulates lncRNA expression, and changes in these DNA modifications are commonly seen in cancer states. Chen et al. (2018c) revealed that long intergenic non-protein coding RNA 472 (LINC00472), a lncRNA which may be involved in cell growth, was downregulated in several CRC cell lines (HCT116, SW620, HT29, and COLO 205) due to DNA hypermethylation of its promoter region. lncRNA genes are also regulated by the transcription factors and chromatin remodelling enzymes that also regulate protein-coding gene expression (Prensner & Chinnaiyan 2011).

lncRNAs may also be produced via non-canonical biogenesis pathways, which results in them lacking a poly (A) tail, 5'cap or both structural features. MALAT1, a lncRNA first discovered as a prognostic marker for non-small cell lung cancer (Ji et al. 2003), lacks polyadenylation (Wilusz et al. 2012). However, this is replaced by a uracil and adenine rich triple helical structure, which provides the transcript with greater stability at the 3'end of the transcript, normally provided by a poly(A) tail (Wilusz et al. 2012). This triple helical structure has also been observed on the 3'end of the multiple endocrine neoplasia  $\beta$  (MEN- $\beta$ ) lncRNA (Brown et al. 2012). Interestingly, lncRNAs have also been discovered to have sno-RNAs on the 5' and 3' ends, in place of a 5'cap and poly(A) tail, which likely contributes to transcript stability (Yin et al. 2012). The lncRNAs that host miRNAs can be processed by the Microprocessor complex resulting in the production of a lnc-pre-miRNA molecule with a 3' cap, rather than a poly(A) tail (Dhir et al. 2015). Further processing can result in production of the miRNA and unstable, non-polyadenylated lncRNA (Dhir et al. 2015). A genome wide analysis of RNA stability in a mouse cell line revealed that lncRNA stability is comparable to that

of mRNA; however, on average the half-lives of lncRNAs are shorter than those of mRNAs (Clark et al. 2012).

### 1.6.2.1 Post-transcriptional regulation of lncRNAs

lncRNAs can also be regulated by post-transcriptional mechanisms such as miRNA-mediated degradation. Although the exact mechanism is not well understood, key RNA-binding proteins including HuR and Ago2 (RISC complex catalytic unit) have been implicated in lncRNA decay (Leucci et al. 2013; Yoon et al. 2012). For example, lincRNA-p21 was found to be associated with HuR and let-7/Ago2 (ribonucleoprotein immunoprecipitation) in human cervical carcinoma cells (Yoon et al. 2012). Upon silencing of HuR and Ago2, lincRNA-p21 transcripts became more stable but this also reduced the interaction of the non-silenced RBP (HuR or Ago2) with lincRNA-p21, indicating a coordinated and key role of HuR and Ago2 in lincRNA-p21 destabilisation (Yoon et al. 2012). Over-expression of let-7 also reduced lincRNA-p21 expression levels (Yoon et al. 2012). Similarly, RNA immunoprecipitations revealed an interaction with MALAT1 and miR-9/Ago2 in the cytoplasm and nucleus (Leucci et al. 2013). Knockdown of Ago2 in Hodgkin's lymphoma and glioblastoma cell lines increased expression of MALAT1 and overexpression of miR-9 decreased MALAT1 expression indicating an Ago2-dependent and miR-9 regulated mechanism of MALAT1 stability (Leucci et al. 2013).

### 1.6.2.2 lncRNA basic archetypes

The functions of lncRNAs are widely varied and as a result, they are involved in an array of cellular processes. lncRNAs may be classified into five basic archetypes including decoys, scaffolds, guides, signalling and enhancer molecules (Figure 1-7). Some lncRNAs may exhibit activity through more than one of these archetypes.

#### Scaffolding Molecules

lncRNAs categorised in the scaffold archetype are involved in providing a structural motif for RNA or protein molecules to assemble into complexes or spatial proximity required for various cellular processes in the nucleus or cytoplasm. The lncRNA, telomerase RNA component (TERC), assists in the assembly of the telomerase complex in the nucleus by providing a scaffold for the enzyme components, including telomerase reverse transcriptase (TERT) and other accessory proteins such as dyskerin (Wang & Chang 2011). lncRNAs such as antisense non-coding RNA in the INK4 locus (ANRIL) and taurine upregulated 1 (TUG1) are also known to interact and provide scaffolds for

chromatin modifying complexes polycomb repressive complex 1 (PRC1) and PRC2 in order to promote gene silencing through the addition of repressive chromatin marks like H3K27me3 (Aguilo et al. 2011; Khalil et al. 2009; Yang et al. 2011a).

### **Enhancers**

lncRNAs defined as the enhancer archetype function by regulating the formation of chromosomal loop structures in an enhancer-loop model. For example, the lncRNA HOTTIP binds the adaptor protein, WDR5, resulting in the recruitment of the MLL/Trx chromatin modifying complex to the HOXA locus for chromatin modification (Guil & Esteller 2012; Hung et al. 2011). In combination with chromosomal looping, the HOTTIP/chromatin modifying complex is moved into close proximity to the HOXA genes, allowing for the addition of H3K4me3 methylation marks to activate gene expression *in cis* (Guil & Esteller 2012; Hung et al. 2011).

### **Signalling Molecules**

lncRNAs classified in the signalling archetype may function as molecular signals in response to particular stimuli such as cellular stress or markers of biologically significant events such as developmental stage (Wang & Chang 2011). lincRNA-p21 and PANDA, for example, are molecular markers of cellular stress (Huarte et al. 2010; Hung et al. 2011). When a cell experiences DNA damage, p53-dependent induction of lincRNA-p21 and PANDA occurs in order to trigger apoptosis through regulation of apoptotic genes (Huarte et al. 2010) and regulate cell cycle arrest and cell survival respectively (Hung et al. 2011). Upon silencing of lincRNA-p21 in mouse embryonic fibroblasts, cell viability increased, apoptosis decreased, pro-apoptotic genes (*NOXA* and *PERP*) decreased in expression and cell survival genes (*BCL2B* and *STAT3*) increased in expression, highlighting the importance of lincRNA-p21 in apoptosis induction (Huarte et al. 2010). PANDA regulates the NF- $\kappa$ B transcription factor to reduce the expression of pro-apoptotic genes such *FAS* and *BIK* to repress apoptosis, and interestingly this results in cell cycle arrest and cell survival after DNA damage (Hung et al. 2011).

### **Guides**

lncRNAs classified under the guide archetype function by guiding ribonucleoprotein complexes (RNA and protein complexes) to regulate target genes. This can occur *in cis* (genes in close genomic proximity to the site of lncRNA production) or *in trans* (genes that are distant in genomic location relative to the site of lncRNA production) e.g. the guidance of chromatin modification enzymes toward the target DNA strand. HOTAIR

is a well-studied guide lncRNA involved in recruiting the chromatin remodelling complex, PRC2, in *trans* to specific genomic locations such as the HOXD locus in order to regulate gene expression through repressive methylation marks (H3K27me3) (Gupta et al. 2010; Rinn et al. 2007). lncRNA AIR represses the expression of its target genes (Slc22a3, Slc22a2, and Igf2r) in *cis* by guiding G9a histone methyltransferase to the promoter region of the target genes to add H3K9me3 repressive marks (Nagano et al. 2008).

### **Decoys**

A lncRNA defined as a decoy archetype functions by binding or sequestering RNA or protein molecules (e.g. transcription factors, chromatin modifiers, miRNAs and other regulatory proteins) to inhibit interactions with their target molecule to regulate gene expression within the nucleus and cytoplasm. For example, lncRNAs in this category can function by binding to multiple miRNA molecules through a sequestration effect to inhibit miRNA target gene expression. MALAT1 is a well-known sponge for the tumour suppressor miR-200c in several cancers (Li et al. 2016e; Liang et al. 2017; Pa et al. 2017). This interaction results in the promotion of migration and invasion in cancers due to the increase in the miR-200c target gene ZEB1, which promotes epithelial to mesenchymal transition (EMT) (Zhuo et al. 2018).

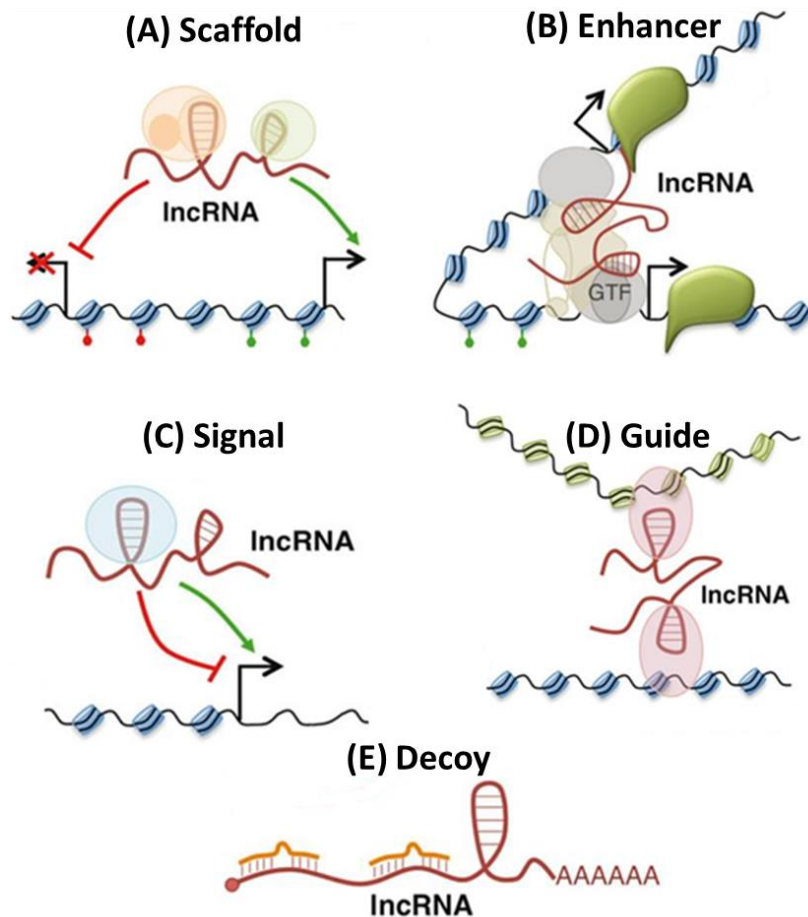


**Figure 1-7 lncRNA archetypes**

lncRNAs have several functions: (A) scaffolding molecules provide structural motifs for RNA/protein complexes to form on; (B) enhancers form chromosomal loop structures to regulate gene expression, (C) signals respond to particular stimuli such as cellular stress to promote or repress gene expression (D) guides recruit ribonucleoprotein complexes (RNA and protein complexes) to regulate target genes in *cis* or in *trans* and (E) decoys bind or sequester RNA or protein molecules such as miRNAs to inhibit interactions with their target molecule to regulate gene expression. (Adapted image from Front Med (Lausanne), CC-BY: (Morlando et al. 2015)).

### 1.6.3 lncRNAs in tumorigenesis and colorectal cancer

lncRNAs have been reported to be involved in many fundamental cellular processes such as cellular development, differentiation, apoptosis and growth, and unsurprisingly they are important in both normal development and disease progression. The link between lncRNAs and cancer was first discovered by Hibi et al. (1996) through the investigation of lncRNA H19 which was significantly over expressed in CRC and oesophageal cancer. Later, Bussemakers et al. (1999) identified lncRNA DD3 which was significantly dysregulated in prostate cancer, followed by Srikantan et al. (2000) who discovered dysregulation of lncRNA PCGEM1 also in prostate cancer. Large profiling studies involving human tissues have confirmed that lncRNAs are dysregulated in many

cancer types (Chen et al. 2015; Ronchetti et al. 2016; Yang et al. 2016b). Further investigation of lncRNAs in cell lines and mouse models have revealed that lncRNAs are implicated in tumorigenesis (Chai et al. 2016), with the ability to function with oncogenic and tumour suppressor properties in a tissue specific manner (Hajjari & Salavaty 2015; Zhou et al. 2012b). The increased or reduced expression of specific lncRNAs can lead to tumour formation and progression (Huarte 2015; Schmitt & Chang 2016).

The mechanisms by which lncRNAs become dysregulated can include genomic alterations such as mutations in regulatory regions (enhancer or promoter sequence) as well as changes in chromatin states including histone acetylation and methylation and DNA methylation (Yan et al. 2015). Interestingly, Calin et al. (2007) identified several genomic loci, commonly mutated in leukaemias and carcinomas, which encode ultra-conserved noncoding sequences found to be dysregulated in cancer. Other studies have also identified that some lncRNAs span the same region as single nucleotide polymorphisms (SNPs) associated with increased CRC risk such as the CRC associated rs6983267 SNP (8q24.21 chromosomal region) that is encompassed by the dysregulated lncRNA, CCAT (Ling et al. 2013). At the chromatin level, it has been demonstrated that changes in histone acetylation can increase or decrease lncRNA expression in cancer. The lncRNA TINCR has increased expression in breast cancer due to H3K27 acetylation at the TINCR promoter region (Dong et al. 2019). Another study demonstrated that hypoxic conditions can reduce histone acetylation in the promoter region of the anti-metastatic lncRNA-LET to reduce its expression and promote metastasis in hepatocellular carcinoma (Yang et al. 2013a). DNA methylation is also particularly important in the repression of genes. Through the analysis of DNA methylation microarray profiles, Yan et al. (2015) revealed that lncRNA promoters can be hypermethylated in cancer and this corresponds to a decrease in RNA expression in tumour tissue compared to normal tissues.

lncRNAs have also been found to be dysregulated in colorectal cancer (Luo et al. 2017; Yang et al. 2017d). Through a high-throughput microarray assay, comparing paired non-cancerous and colorectal cancer tissue, Xue et al. (2015b) demonstrated that 762 lncRNAs (390 upregulated and 372 downregulated) were significantly dysregulated in colorectal cancer. Of these lncRNAs, 56.8% were aberrantly expressed from protein-coding regions and 43.2% from intergenic regions of the genome (Xue et al. 2015b). More recently, Yamada et al. (2018) performed RNA-seq comparing matched normal mucosa and CRC tissue samples and identified 27 upregulated and 22 downregulated

lncRNAs confirmed using The Cancer Genome Atlas (TCGA) dataset. An extensive computational analysis done on 566 CRC samples (microarray) from the Gene Expression Omnibus (GEO) public repository revealed 282 lncRNAs associated with CRC heterogeneity (James de Bony et al. 2018). Since then, many more lncRNAs have been identified to promote or inhibit tumorigenesis in CRC by regulating key cellular processes including cell proliferation, apoptosis, invasion and migration (Table 1-2).

lncRNAs that are commonly upregulated in CRC often exhibit oncogenic properties. MALAT1 is a well-studied oncogenic lncRNA that is upregulated in many cancers, including CRC cells and tissues, and is associated with poor prognosis (Ji et al. 2014b; Zheng et al. 2014). MALAT1 promotes tumour growth, migration and invasion through several mechanisms. MALAT1 acts to sponge miR-200c to promote migration and invasion of cancer cells via ZEB1 and ZEB2 transcription factors as well as sequestering other miRNAs including miR-663a to regulate *JUND* and *PIK3CD* to induce proliferation, migration, and invasion in CRC (Li et al. 2016e; Liang et al. 2017; Pa et al. 2017; Tian et al. 2018). MALAT1 can also bind to the tumour suppressor protein SFPQ, thereby releasing the oncogenic protein PTBP2 from the SFPQ/PTBP2 complex and promoting growth and migration (Ji et al. 2014b). MALAT1 has also been shown to regulate anchor protein AKAP-9 to exert its pro-cancer effects in CRC (Yang et al. 2015c). Colon cancer-associated transcript 2 (CCAT2) is another key oncogenic lncRNA which is upregulated in CRC cells and tissues (Ling et al. 2013; Wang et al. 2019a). Interestingly, CCAT2 indirectly increases the expression of *c-MYC*, miR-17 and miR-20a (oncogenic miR-17-92 cluster) by interacting with the TCF7L2 transcription factor to increase the activity of WNT signalling, thereby, promoting growth and metastasis in CRC cells (Ling et al. 2013).

lncRNAs that are commonly downregulated in CRC often exhibit tumour suppressor properties. GAS5 is a well-known tumour suppressor lncRNA in many cancers which is downregulated in CRC cells and tissues and associated with poor prognosis in patients (Li et al. 2018b; Yin et al. 2014). GAS5 represses proliferation, migration and invasion and promotes apoptosis in CRC cells (Li et al. 2018b). GAS5 functions by regulating a key CRC related miRNA, miR-21, that normally represses tumour suppressors *PTEN* and *PDCD4*, in order to promote its anticancer effects (Hu et al. 2016a). GAS5 has also been shown to increase the expression of the tumour suppressor *TP53* and decrease the transcription factor *E2F1* in order to promote apoptosis and inhibit proliferation (Shi et al. 2015a). MEG3, another tumour suppressor lncRNA that is reduced in CRC, is also involved in inhibiting growth in CRC cells and low expression is associated with poor

## CHAPTER 1

prognosis in CRC patients (Yin et al. 2015). MEG3 functions by promoting the expression and enhancing the binding of tumour suppressor p53 to the GDF15 gene promoter region in order to inhibit proliferation (Zhou et al. 2007).

**Table 1-2 Summary of dysregulated lncRNAs involved in growth, death and migration in colorectal cancer cells.**

KD = knockdown and OE = overexpression.

lncRNA	Expression in CRC cells	Function in CRC cells	Reference
AFAP1-AS1	Upregulated	KD inhibits growth, promotes cell cycle arrest	(Han et al. 2016c)
ANRIL	Upregulated	KD inhibits proliferation, migration and invasion, promotes apoptosis	(Naemura et al. 2016; Sun et al. 2016c; Yu et al. 2018a)
ATB	Upregulated	KD inhibits proliferation	(Yue et al. 2016)
BANCR	Upregulated and downregulated	KD inhibits proliferation and invasion, induces apoptosis	(Guo et al. 2014; Ma et al. 2018; Shi et al. 2015b; Wang et al. 2016b)
BC200	Upregulated	KD inhibits proliferation, promotes cell cycle arrest and apoptosis	(Wu et al. 2018a)
BLACAT1	Upregulated	KD promotes apoptosis and cell cycle arrest, inhibits proliferation	(Su et al. 2017)
CCAL	Upregulated	KD decreases cell proliferation, OE promotes proliferation, migration and invasion	(Ma et al. 2015)
CASC2	Downregulated	OE inhibits proliferation	(Huang et al. 2016)
CASC7	Downregulated	OE inhibit proliferation, migration and invasion, and promote apoptosis	(Zhang et al. 2017d)
CASC11	Upregulated	KD inhibits proliferation and metastasis, OE promotes growth and migration	(Zhang et al. 2016b)
CASC19	Upregulated	OE promotes proliferation, migration and invasion, inhibits apoptosis, KD inhibits proliferation, migration and invasion, promotes apoptosis	(Wang et al. 2019b)
CCAT1	Upregulated	OE promotes proliferation, invasion and metastasis	(Alaiyan et al. 2013; He et al. 2014; Kam et al. 2014; Nissan et al. 2012; Yao et al. 2018; Ye et al. 2015)
CCAT1-L	Upregulated	OE promotes growth	(Xiang et al. 2014)
CCAT2	Upregulated	OE promotes growth and metastasis	(Ling et al. 2013)
CLMAT3	Upregulated	KD inhibits growth and cell cycle, induces apoptosis	(Ye et al. 2016b)
CRCAL-3	Upregulated	KD inhibits growth and migration	(Chang et al. 2019)
CRNDE	Upregulated	KD inhibits proliferation, promotes apoptosis, OE promotes proliferation	(Ding et al. 2017; Ellis et al. 2012; Graham et al. 2011)
CTNNAP1	Downregulated	OE inhibits cell proliferation	(Chen et al. 2016b)
DQ786243	Upregulated	KD induced cell cycle arrest and apoptosis, reduced cell proliferation and invasion	(Sun et al. 2016b)
FER1L4	Downregulated	OE Inhibits proliferation, migration and invasion	(Yue et al. 2015)
FEZF1-AS1	Upregulated	OE promotes proliferation, migration and invasion, KD inhibits proliferation	(Bian et al. 2018; Chen et al. 2016a)
GAS5	Downregulated	OE inhibits cell proliferation	(Wang et al. 2016b; Yin et al. 2014)
GHET1	Upregulated	KD inhibited proliferation, migration, and invasion	(Zhou et al. 2016a)
H19	Upregulated	KD inhibits growth and promotes cell cycle arrest	(Han et al. 2016a; Liang et al. 2015a; Tsang et al. 2010b; Yang et al. 2017b)
HOTAIR	Upregulated	KD promotes apoptosis and inhibits cell proliferation, migration and invasion	(Kogo et al. 2011; Lu et al. 2018; Padua Alves et al. 2013; Svoboda et al. 2014; Wu et al. 2014; Xue et al. 2015a; Xue et al. 2015c; Yang et al. 2015e)
HOTAIRM1	Downregulated	KD promotes cell proliferation	(Wan et al. 2016)
HOTTIP	Upregulated	KD inhibits migration and invasion	(Liu et al. 2018b; Ren et al. 2015; Rui et al. 2018)
KCNQ1OT1	Upregulated	KD inhibits proliferation and induces apoptosis	(Li et al. 2019b)
LINC00659	Upregulated	KD inhibits proliferation and induces apoptosis	(Tsai et al. 2018)
LINC00959	Downregulated	OE inhibits proliferation, invasion, and migration, KD opposite effects	(Sun et al. 2017)
LINC01194	Upregulated	KD inhibits proliferation, migration and invasion	(Wang et al. 2019c)
lincRNA-p21	Up- or Downregulated	OE promotes apoptosis	(Wang et al. 2014a; Wang et al. 2015; Zhai et al. 2013)
lincRNA-PINT	Downregulated	OE inhibits migration and invasion	(Marin-Bejar et al. 2013)
lincRNA-ROR	Upregulated	KD inhibits proliferation, migration and invasion	(Zhou et al. 2016b)
lincRNA-422	Downregulated	OE inhibited cell proliferation, migration, and	(Shao et al. 2018; Xue et al. 2015c)

## CHAPTER 1

		invasion	
<b>lncRNA-91H</b>	Upregulated	KD inhibits proliferation, migration, and invasion	(Deng et al. 2014)
<b>lncRNA-ATB</b>	Upregulated	KD inhibits proliferation and promotes apoptosis	(Yue et al. 2016)
<b>lncRNA-FTX</b>	Upregulated	KD inhibits proliferation, migration and invasion	(Guo et al. 2015; Yang et al. 2018c)
<b>lncRNA-kcna3</b>	Downregulated	OE inhibits proliferation, migration and invasion, and induces apoptosis, KD opposite effects	(Zhong et al. 2018)
<b>lncRNA-uc002kmd.1</b>	Upregulated	OE promotes proliferation	(Wu et al. 2016c)
<b>lncTCF7</b>	Upregulated	OE promotes proliferation, migration and invasion, KD opposite effects	(Li et al. 2017c)
<b>LOC285194</b>	Downregulation	OE inhibits proliferation	(Liu et al. 2013a; Qi et al. 2013)
<b>LOC554202</b>	Downregulated	OE promotes apoptosis and cycle arrest and inhibits proliferation	(Ding et al. 2015)
<b>LSINCT5</b>	Upregulated	OE promotes proliferation, KD opposite effects	(Xu et al. 2014)
<b>MAFG-AS1</b>		OE promotes cell cycle and invasion, inhibits apoptosis	(Cui et al. 2018)
<b>MALAT1 (NEAT2)</b>	Upregulated	OE promotes proliferation, migration, invasion and metastasis	(Furi et al. 2015; Ji et al. 2013; Ji et al. 2014b; Sun et al. 2019b; Wang et al. 2016b; Xu et al. 2011; Yang et al. 2015c; Zheng et al. 2014)
<b>MEG3</b>	Downregulated	OE promotes apoptosis and inhibits proliferation	(Yin et al. 2015)
<b>ncRAN</b>	Downregulated	OE inhibits cell migration and invasion	(Qi et al. 2015)
<b>NEAT1</b>	Upregulated	OE promotes proliferation and invasion, KD inhibits proliferation and invasion	(Li et al. 2015b; Wu et al. 2015)
<b>NORAD</b>	Upregulated	KD inhibits proliferation, migration and invasion, promotes apoptosis	(Zhang et al. 2018b)
<b>OCC-1</b>	Upregulated	OE inhibits proliferation, KD promotes proliferation	(Lan et al. 2018; Pibouin et al. 2002)
<b>PANDAR</b>	Upregulated	KD inhibits proliferation, migration and invasion, promotes apoptosis	(Lu et al. 2016a, 2017a)
<b>PCAT-1</b>	Upregulated	KD inhibits proliferation and promotes cell cycle arrest and apoptosis	(Ge et al. 2013; Qiao et al. 2017; Wang et al. 2016b)
<b>PRNCR1</b>	Upregulated	KD inhibits proliferation and cell cycle progression	(Li et al. 2013a; Yang et al. 2015b, 2016a)
<b>PVT1</b>	Upregulated	OE inhibits apoptosis, KD inhibits proliferation and cell survival	(Fan et al. 2018; Ping et al. 2018; Takahashi et al. 2014; Tseng et al. 2014; Wang et al. 2018; Yu et al. 2018c; Zhang et al. 2018c)
<b>SLC25A25-AS1</b>	Downregulated	OE inhibits cell proliferation, KD promotes proliferation	(Li et al. 2016f)
<b>SNHG1</b>	Upregulated	KD inhibits proliferation, invasion and migration, promotes apoptosis	(Yang et al. 2018a)
<b>SNHG7</b>	Upregulated	OE promotes proliferation, migration, and invasion, KD inhibits invasion and proliferation	(Shan et al. 2018)
<b>SNHG15</b>	Upregulated	OE promotes proliferation and invasion, KD inhibits proliferation and invasion	(Sacinasab et al. 2019)
<b>SNHG20</b>	Upregulated	KD inhibited proliferation and promotes cell cycle arrest	(Li et al. 2016a)
<b>Sox2ot</b>	Upregulated	KD inhibits proliferation and promotes cell cycle arrest	(Liu et al. 2016a)
<b>SPRY4-IT1</b>	Upregulated	KD inhibits proliferation, migration and invasion, induces cell cycle arrest	(Cao et al. 2016; Shen et al. 2017)
<b>TINCR</b>	Downregulated	OE inhibits cell proliferation, migration and metastasis, KD promotes cell proliferation, migration and metastasis	(Zhang et al. 2016c)
<b>TUG1</b>	Upregulated	KD decreases proliferation	(Sun et al. 2016a; Wang et al. 2016a; Zhai et al. 2016)
<b>TUSC7</b>	Upregulated	OE promotes migration and invasion	(Zhang et al. 2019a)
<b>UCA1</b>	Upregulated	KD inhibits proliferation and migration and promotes apoptosis	(Bian et al. 2016; Cui et al. 2019; Han et al. 2014; Ni et al. 2015; Yang et al. 2018b)
<b>XIAP-AS1</b>	Upregulated	KD inhibits proliferation and induces cell cycle arrest	(Lu et al. 2019)
<b>XIST</b>	Upregulated	KD inhibits proliferation and invasion	(Sun et al. 2018a)
<b>ZDHHC8P1</b>	Upregulated	OE promotes proliferation and metastasis, KD inhibits proliferation and promotes cell cycle arrest	(Li et al. 2019a)
<b>ZFAS1</b>	Upregulated	OE promotes proliferation, migration and invasion	(Thorenoor et al. 2015; Wang & Xing 2016)

#### 1.6.4 lncRNAs as biomarkers of tumour stages and therapeutic agents

As knowledge of lncRNA involvement in disease states is expanding, so is their potential as new disease biomarkers. lncRNAs have been shown to be dysregulated in many cancers including breast, colon, lung and pancreatic cancer (Yan et al. 2015). A key study implicating lncRNAs in CRC development involved the analysis of HOTAIR expression in CRC tissues (Kogo et al. 2011). Kogo et al. (2011) discovered that HOTAIR was over-expressed in CRC and it was associated with metastasis and poor prognosis. lncRNAs have been detected in extracellular vesicles, plasma and serum of cancer patients, highlighting the possibility of their use as biomarkers (Dong et al. 2016; Duan et al. 2016). Recently, PVT1 was discovered in extracellular vesicles isolated from CRC cells and was also found to be upregulated in CRC tissues compared to normal tissue (Guo et al. 2017). In the plasma of CRC patients, CCAT1 and HOTAIR were upregulated and lincRNA-p21 downregulated when compared to the plasma of healthy controls (Zhao et al. 2015). lncRNA HULC was found to be highly expressed in the serum of patients with gastric cancer compared to normal controls and indicative of poorer overall survival in patients with high versus low HULC expression (Jin et al. 2016). BLACAT1 was also found to be a potential plasma biomarker for CRC as it was significantly upregulated in CRC patient plasma versus non-cancer plasma (Dai et al. 2017). Most recently, CCAT2 which is normally over expressed in CRC, was shown to be highly expressed in the serum and exosomes of CRC patients and associated with advanced CRC (Wang et al. 2019a). Together these studies highlight the potential of lncRNAs as promising disease biomarkers.

lncRNAs are also being investigated as therapeutic targets using a range of therapeutic molecules such as toxic DNA plasmids (Figure 1-8). H19 is a paternally imprinted, oncofoetal lncRNA which is upregulated in many cancers including CRC (Smaldone & Davies 2010). BC-819 is a double-stranded DNA plasmid that produces the A subunit of the diphtheria toxin, which is regulated by the H19 gene promoter (Smaldone & Davies 2010). When the H19 promoter is activated upon cell entry, diphtheria toxin is produced in cancer cells due to high H19 expression, resulting in protein synthesis inhibition (Sidi et al. 2008). A study investigating BC-819 as an aerosol treatment for lung cancer cells and mouse models demonstrated that BC-819 decreases lung cancer cell proliferation and intrabronchially induced tumour growth in mice (Hasenpusch et al. 2011). This molecule has demonstrated low toxicity in Phase I and II clinical trials in bladder, ovarian, peritoneal and pancreatic cancer patients (Hanna et al. 2012; Lavie et

al. 2017; Sidi et al. 2008). BC-819 intravesical treatment in bladder cancer patients resulted in 4/18 complete responses (tumour completely disappeared) and 3/18 partial (50% tumour disappeared) and incomplete partial responses (tumour completely disappeared but new tumours) (Sidi et al. 2008).

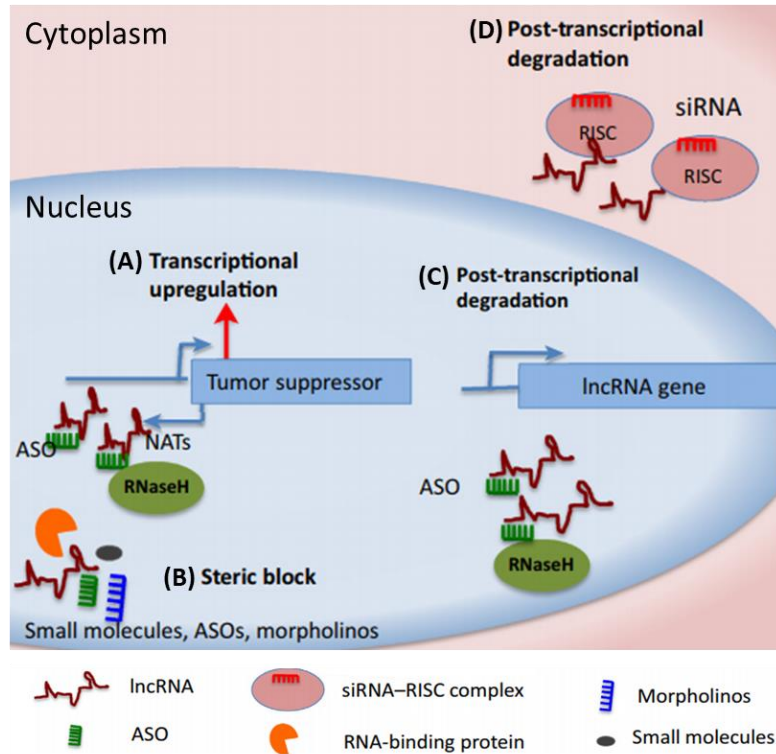


**Figure 1-8 Therapeutic targeting of lncRNA molecules**

Summary of potential lncRNA therapeutic approaches including (A) ASOs can knockdown NATs can promote transcriptional upregulation of their target (tumour suppressor) (B) steric blocks such as morpholinos can block binding of regulatory molecules to RNAs (C) ASOs can be used to knockdown over-expressed oncogenic lncRNAs in cancer (D) siRNAs can induce post-transcriptional degradation of oncogenic lncRNAs through RISC. (Image reproduced with permission: (Arun et al. 2018)).

Antisense oligonucleotides (ASOs), Antago-Natural Antisense transcripts (AntagoNATs), siRNAs, and lncRNA replacement therapy using gene therapy vectors are other avenues of investigation for lncRNA therapeutics that are currently in pre-clinical stages. ASOs are single stranded oligonucleotides which repress lncRNAs by the formation of RNA: DNA complexes, whereby the RNA molecule is degraded by RNase H activity. For example, ASOs targeting MALAT1 in mouse models with lung cancer xenografts resulted in decreased metastasis (Gutschner et al. 2013), while ASOs targeting TUG1 in mouse models with glioma demonstrated reduced tumour growth (Katsushima et al. 2016). AntagoNATs are single stranded oligonucleotides that repress the gene inhibitory effects of antisense lncRNAs or Natural Antisense Transcripts

(NATs) (Wahlestedt 2013). Modarresi et al. (2012) demonstrated that using siRNAs, which function via RISC, and AntagoNATs, which induce RNase H activity, against *BDNF-AS*, restored *BDNF* expression in HEK293T cells and C57BL/6 mouse brains, respectively and induced neuronal outgrowth and differentiation. lncRNA replacement therapies are also another area of investigation, whereby lncRNA gene therapy vectors can be introduced into cells to restore lncRNA expression. lncRNA-422 lentiviral vectors, in CRC *in vitro* models, induced apoptosis and suppressed migration and invasion and reduced tumour growth in mouse xenograft models (Shao et al. 2018). Another therapeutic possibility is morpholinos. Morpholino oligomers are chemically modified DNA analogues that can regulate RNAs by inhibiting translation, splicing, as well as miRNA-mediated silencing by blocking binding sites on their target RNA. These molecules were originally designed for knockdown studies in zebrafish (Nasevicius & Ekker 2000) but can also be used to regulate lncRNA expression in mammalian models (Wu et al. 2019). Morpholinos have been used to regulate splicing of dystrophin mRNA in Duchenne muscular dystrophy sufferers (Aartsma-Rus et al. 2003; Alter et al. 2006), although more investigation is required for their use against lncRNAs in cancer treatment. With the ability to reduce oncogenic lncRNA expression, re-activate gene expression by targeted inhibition and increase tumour suppressor lncRNA expression, these molecules certainly show therapeutic potential.

### 1.6.5 Effects of HDAC inhibitors on lncRNAs in cancer

Currently there are no studies investigating the effects of butyrate on lncRNAs in colorectal cancer. However, other HDAC inhibitors have been shown to regulate lncRNAs to mediate their anticancer effects. Yang et al. (2013b) identified 447 upregulated and 512 downregulated lncRNAs (microarray) in liver cancer cells after 1  $\mu$ M treatment of the HDACi, TSA. The lncRNA, uc002mbe.2, was induced by more than 300-fold after TSA treatment, indicating a strong regulatory effect (Yang et al. 2013b). Another study demonstrated that XIST lncRNA expression can predict the response of breast cancer cells to HDACi, abexinostat (Salvador et al. 2013)

## 1.7 Aims and hypotheses

### 1.7.1 General hypotheses and aims

The development and progression of CRC is associated with alterations in epigenetic modifications such as histone acetylation and dysregulation of key ncRNA genes. It is known that the dietary molecule and HDACi, butyrate, can alter miRNA expression to

exert some of its anticancer properties. However, there is a small amount of evidence indicating that the manipulation of miRNA levels can also regulate this response. The aim of this study was to systematically identify miRNAs with the ability to promote the anticancer properties of butyrate in CRC cells and to further examine the role of miRNAs in the butyrate response. It was hypothesised that specific miRNAs can synergistically enhance the anti-proliferative and pro-apoptotic effects of butyrate in CRC cells. To address this hypothesis, the validation of an unbiased, high-throughput, functional screen utilising a synthetic miRNA mimic library in combination with butyrate treatment was performed.

While butyrate is known to alter global histone acetylation patterns and consequently the expression of genes involved in apoptosis, proliferation and the cell cycle to exert its anticancer properties, there is still the need for a wholistic understanding of this response. To the best of our knowledge, a systems biology approach has not yet been employed to gain a comprehensive understanding of the complex RNA interactions occurring and contributing to the butyrate response of CRC cells. This study, therefore, aimed to examine the diverse effects of butyrate on the transcriptomic profile of CRC cells and to investigate the role of key miRNA-target interactions in butyrate-specific signalling networks to further elucidate the butyrate response. It was hypothesised that the manipulation of miRNA levels in CRC cells may contribute to the anticancer properties of butyrate in cell growth and death-related signalling pathways. To address this hypothesis, total and small RNA sequencing was performed on butyrate-treated CRC cells and integrative network and pathways analyses and experimental validation were used to identify key miRNA-mRNA interactions involved in the butyrate response.

To further elucidate the role of complex RNA interactions and biological pathways in the butyrate response of CRC cells, a second class of RNA molecules was examined; lncRNAs. lncRNAs have not been studied in the context of butyrate. However, they may regulate miRNA expression, specifically by functioning as miRNA sponges, to regulate miRNA target genes. As lncRNAs directly regulate key genes involved in cancer cell growth and death, they may influence the butyrate response of CRC cells. This study, therefore, aimed to systematically identify lncRNAs that enhance the anticancer effects of butyrate and reveal critical lncRNA-miRNA-mRNA interactions involved in butyrate regulated biological pathways in CRC cells. It was hypothesised that knockdown of specific lncRNAs would lead to synergistic enhancement of the anti-proliferative and pro-apoptotic effects of butyrate in CRC cells. To address this hypothesis, a high-throughput RNAi functional screen utilising a lncRNA-targeting

## CHAPTER 1

siRNA library in combination with butyrate treatment was performed as well as integrative network and pathway analyses and experimental validation.

As previously discussed, there is an urgent need to develop novel CRC therapies that target a broader range of biological capabilities of cancer cells. Therefore, the combination of HDAC inhibitors with RNAi technology could reveal a valuable dual-acting therapy to reduce toxic side effects and increase anti-tumour effects of a single therapeutic agent. This study could form the basis for further exploration of these innovative combinations as potential cancer treatments as well as reveal novel therapeutic targets and pathways.

### 1.7.2 Chapter 3 Aim

To systematically identify miRNAs with the ability to enhance the anticancer properties of butyrate, including inhibition of cell proliferation and promotion of apoptosis, in CRC cell lines through the validation of an unbiased, high-throughput, functional screen.

### 1.7.3 Chapter 4 Aim

To investigate the diverse effects of butyrate on the transcriptome profile of CRC cells and to identify key miRNA-target interactions within biological signalling pathways that contribute to the anticancer effects of butyrate.

### 1.7.4 Chapter 5 Aim

To use high-throughput RNAi functional screening and networking analyses to systematically identify lncRNAs that enhance the anti-cancer effects of butyrate and reveal critical lncRNA-miRNA-mRNA interactions involved in the butyrate response of CRC cells.

## 1.8 Chapter 1: Preliminary data

### 1.8.1 Summary

The miRNA high-throughput screen validation component of this project was commenced during my Honours year in 2014 (Ali 2014). This data must be included in the current thesis in order to justify and understand the continuation of the project in chapter 3. Work from my Honours is currently unpublished.

In 2013, Research Associate Dr. Karen Humphreys performed an unbiased high-throughput functional screen, at the Peter MacCallum Cancer Centre in Victoria,

involving the analysis of 1280 miRNAs in HCT116 colorectal carcinoma cells. The aim was to identify miRNAs with the ability to enhance the anticancer properties of butyrate. The cells were reverse transfected with a Human miRIDIAN miRNA Mimic Library V16 (GE Healthcare Dharmacon) for 48 h and treated with 0 mM or 2.5 mM butyrate for 24 h. The 2.5 mM butyrate concentration was chosen because it caused ~20-30% cell death after 24 hours and therefore enabled the study of combinatorial effects of miRNA mimics to be observed in addition to butyrate exposure (data not shown). Other butyrate doses were not suitable for this study. High doses of butyrate (5 mM) were found to induce excessive cell death (Humphreys et al. 2013), while low doses of butyrate (0.5 mM) induce alternative mechanisms (HAT activity) not investigated in this study (Donohoe et al. 2012). An endpoint assay, ApoLive-Glo Multiplex assay (Promega), was used to determine cell viability and apoptosis changes. miRNA mimics were selected for validation based on their ability to sensitise CRC cells to butyrate by further reducing cell viability and increasing apoptosis. This high throughput screen resulted in the identification of 13 butyrate-sensitising miRNAs (Table 1-3), which were further investigated in the current study.

**Table 1-3 Butyrate-sensitising miRNAs from an unbiased high-throughput functional screen**

Butyrate-sensitising miRNAs selected from an unbiased high-throughput functional screen based on their ability to decrease cell viability and increase cell apoptosis in HCT116 cells, particularly those treated with butyrate. Cell viability results were categorised as  $Hi > 1.15$  (increase),  $CV1 > 0.8-1.15$  (no change),  $CV2 < 0.8-0.5$  (decrease),  $LC < 0.5$  (lethal effect). Caspase data were analysed using Z-score distribution, with a Z-score  $> 2$  indicating significant caspase activity and an average fold change ratio, a positive ratio ( $> 1$ ) indicating increased apoptosis when the miRNA was used with butyrate treatment compared to the negative control (Ali, 2014).

MicroRNA mimic	Normalised viability (mimic vs NC) 0 mM butyrate		Normalised viability (mimic vs NC) 2.5 mM butyrate		Normalised caspase activity (mimic vs NC) 0 mM butyrate	Z-score (caspase activity)	Normalised caspase activity (mimic vs NC) 2.5 mM butyrate	Z-score (caspase activity)	Average fold change ratio (caspase activity)
miR-29b-2-5p	CV1	0.8	CV2	0.71	1.31	0.3	2.1	2.59	1.6
miR-125b-1-3p	CV1	0.88	CV2	0.74	1.43	0.6	1.66	1.45	1.16
miR-181a-5p	CV1	0.84	CV2	0.78	1.27	0.2	1.7	1.56	1.34
miR-509-5p	CV1	0.86	CV2	0.69	1.5	0.77	1.75	1.69	1.17
miR-593-3p	CV1	0.88	CV2	0.76	1.23	0.1	1.48	0.99	1.2
miR-1227-3p	CV1	0.82	CV2	0.74	1.66	1.17	2.04	2.44	1.23
miR-1231	CV1	0.85	CV2	0.73	2.97	4.45	2.19	2.83	0.74
miR-1256	CV1	0.91	CV2	0.77	1.94	1.87	1.9	2.08	0.98
miR-1265	CV1	0.84	CV2	0.76	1.5	0.77	1.92	2.13	1.28
miR-3151	CV1	0.88	CV2	0.7	4.02	7.07	2	2.33	0.5
miR-3179	CV1	0.8	CV2	0.55	2.57	3.45	2.19	2.83	0.85
miR-3654	CV1	0.82	CV2	0.67	3.16	4.92	1.88	2.02	0.59
miR-4252	CV1	0.92	CV2	0.64	1.21	0.05	1.58	1.25	1.31

In 2014, validation of the 13 miRNAs commenced. The project aim was to validate butyrate-sensitising miRNAs and identify key target genes involved in cell growth and death pathways. With the use of the xCELLigence and Incucyte real-time systems, all miRNAs were demonstrated to significantly enhance the butyrate response of CRC cells by further increasing the anti-proliferative and pro-apoptotic effects of butyrate. miR-593 and miR-1227 were identified to have the most significant and lethal effects on CRC cell proliferation both alone and in combination with butyrate (Ali, 2014). Of all the miRNAs, miR-1227 was shown to have the greatest ability to induce apoptosis in the presence of butyrate, while miR-593 alone had the greatest pro-apoptotic effect (Table 1-4) (Ali 2014). miR-1227 also significantly induced apoptosis alone and miR-593 significantly enhanced apoptosis in the presence of butyrate (Table 1-4) (Ali 2014).

**Table 1-4 Summary of results collated during Honours year 2014**

miRNA	miRNA effect alone	miRNA effect in combination with butyrate	IPA Pathway analysis (Top pathways)	Target genes investigated
<b>miR-593-3p</b>	↓ proliferation, ↑ apoptosis	Enhanced ↓ proliferation and ↑ apoptosis	Molecular Mechanisms of Cancer, Epithelial-Mesenchymal Transition pathway, TGF-β signalling, PTEN signalling, Colorectal Cancer Metastasis signalling	<i>BCL2, BIRC5, CBL, FZD7, JUN, KRAS, MDM2, MET</i>
<b>miR-1227-3p</b>	↓ proliferation, ↑ apoptosis	Enhanced ↓ proliferation and ↑ apoptosis	WNT signalling, PTEN signalling, STAT3 signalling, Epithelial-Mesenchymal Transition pathway, TGF-β signalling, Colorectal Cancer Metastasis signalling, Molecular Mechanisms of Cancer	<i>BIRC5, CBL, DVL3, HNF1A, KSR2, MTHFR, NUP62, PRKCi, XRCC2</i>

Further investigation of these miRNAs using miRNA target prediction programs (miRWalk) identified 2914 predicted target genes of miR-593 and 1019 predicted target genes of miR-1227 (Ali, 2014). Predicted target genes were then analysed using Ingenuity Pathway Analysis (IPA), which is a multifaceted database used to analyse and represent data in various molecular networks and canonical signalling pathways, and categorise data based on cellular functions and diseases. The bioinformatics analysis revealed that their target genes were involved in key cell growth and death pathways. miR-593 predicted target genes were primarily involved in 'Molecular Mechanisms of Cancer' (33 molecules), the 'Epithelial-Mesenchymal Transition pathway' (22 molecules) and 'TGF-β signalling' (15 molecules) among others (Table 1-4) (Ali, 2014). miR-1227 predicted target genes were found to be associated with CRC development, survival and metastasis. As an example, some miR-1227 predicted target genes were involved in 'WNT signalling' (11 molecules) (Table 1-4) (Ali 2014). WNT signalling has been strongly implicated in CRC and is often over-active in CRC, promoting cell proliferation (Polakis 2000). Other genes were also involved in 'PTEN signalling' (9 molecules),

## CHAPTER 1

'STAT3 signalling' (7 molecules), 'Epithelial-Mesenchymal transition pathway' (10 molecules) and 'TGF- $\beta$  signalling' (7 molecules) (Table 1-4) (Ali 2014).

Based on canonical pathways and relevant cellular functions, including cell death, survival, growth and proliferation, a more specific gene list for each miRNA was identified for further analysis. Oncogenic molecules were specifically selected from this list as they were thought to be likely targets inhibited by the miRNA in order to decrease cell proliferation or increase cell apoptosis in HCT116 cells. A final gene list for miR-593 predicted target genes included *BCL2*, *BIRC5*, *CBL*, *FZD7*, *JUN*, *KRAS*, *MDM2* and *MET* and for miR-1227 target genes included *BIRC5*, *CBL*, *DVL3*, *HNF1A*, *KSR2*, *MTHFR*, *NUP62*, *PRKCi* and *XRCC2* (Table 1-4) (Ali 2014).

These genes were then validated for mRNA expression changes using real time RT-PCR. HCT116 cells, which were reverse transfected with miR-593 or miR-1227 mimics, showed altered mRNA expression levels of some miRNA predicted target genes, when compared with NC mimic transfected cells not treated with butyrate (Ali 2014). As for miR-593 predicted targets, *BCL2*, *KRAS* and *MET* had significantly reduced transcript levels, while *FZD7* was significantly increased and *BIRC5*, *CBL*, *JUN* and *MDM2*, did not significantly change after miR-593 mimic transfection in CRC cells (Ali 2014). Only those genes with reduced expression were further investigated in the context of butyrate. When miR-593 mimic transfection with butyrate treatment *BCL2*, *KRAS* and *MET* had significantly reduced transcript levels (Ali 2014). As for miR-1227, predicted target genes, *DVL3* and *NUP62* had significantly reduced transcript levels, while *XRCC2* was significantly increased and *HNF1A* and *MTHFR* transcript levels had an increasing trend; however, the changes were not significant (Ali 2014). The transcript levels of predicted target genes, including *BIRC5*, *CBL*, *KSR2* and *PRKCi* did not significantly change (Ali 2014). Interestingly, when miR-1227 was combined with butyrate treatment there were no significant decreases in *DVL3* or *NUP62* transcript levels; however, *DVL3* mRNA levels had a decreasing trend (Ali 2014). Butyrate significantly decreased levels of *DVL3* and *NUP62* (Ali 2014).

Some of the targets which appeared to be regulated by miR-593 or miR-1227 were then investigated for protein expression changes. MET protein expression was significantly decreased when exposed to 2.5 mM butyrate (Ali 2014). When cells were exposed to miR-593 in combination with butyrate, protein expression levels significantly decreased compared to the NC transfected cells (Ali 2014). MET expression in the cells did not respond to miR-593 mimics alone (Ali 2014).

## CHAPTER 1

In conclusion, this study identified 13 butyrate-sensitising miRNAs with the ability to further enhance the anti-proliferative and pro-apoptotic effects of butyrate in CRC cells. miR-593 and miR-1227 were selected for further validation and their target genes were identified to be involved in key cell growth and death pathways involved in CRC. Potential new targets were identified for miR-593 (*BCL2*, *KRAS*, *MET*) and miR-1227 (*NUP62* and *DVL3*).

# Chapter 2. Materials and Methods

---

## 2.1 Cell culture

### 2.1.1 Cell lines

HCT116, LIM1215 and RKO human colorectal carcinoma and HaCaT human keratinocytes, HEK293 human embryonic kidney, HFF human foreskin fibroblast, MCF10A human mammary gland cell lines were used for *in vitro* experiments. All cell lines were acquired from ATCC, Virginia, USA, except LIM1215 cells which were acquired from Sigma-Aldrich, Missouri, USA. HCT116 cells are an adherent epithelial cell line that originated from a colorectal carcinoma tumour surgically removed from an adult male (Brattain et al. 1981). HCT116 cells have mutant *KRAS* (G13D) and *PIK3CA* (H1047R) and wild-type (WT) phenotypes for *BRAF*, *PTEN*, *TP53* and *APC* (Ahmed et al. 2013; Brink et al. 2003; Samuels et al. 2005; Yeh et al. 2009). LIM1215 cells are an adherent epithelial cell line that originated from a primary lesion in the ascending colon of a 34 year old male (Whitehead et al. 1985). LIM1215 cells have mutant  $\beta$ -catenin and have WT phenotypes for *TP53* and *KRAS*. RKO cells are an adherent epithelial cell line that originated from a colorectal carcinoma tumour surgically removed from an adult (Brattain et al. 1984). RKO cells have mutant *BRAF* (V600E) and *PIK3CA* (H1047R) and WT phenotypes for *KRAS*, *TP53* and *PTEN* (Ahmed et al. 2013). HaCaT cells are an adherent epidermal cell line that originated from adult skin (Boukamp et al. 1988). HEK293 cells are an adherent epithelial cell line that originated from embryonic kidney tissue surgically removed from a foetus (Graham et al. 1977). HFF cells are an adherent fibroblast cell line that originated from foreskin tissue surgically removed from a newborn male (Compton 1993). MCF10A cells are an adherent epithelial cell line that originated from mammary gland tissue surgically removed from a 36 year old female (Soule et al. 1990).

Cells were maintained at 37°C and 5% CO<sub>2</sub> in McCoy's 5A (Modified) Medium (HCT116), Dulbecco's Modified Eagle's Medium 1X (HaCaT, HEK293, HFF, LIM1215, RKO) (Invitrogen, New South Wales, Australia) or Mammary Epithelial Cell Growth Medium (Lonza, Basel, Switzerland) (MCF10A) containing 10% foetal bovine serum (Bovogen Biologicals, Victoria, Australia). Cells were grown to <85% confluence and passaged approximately 1-2 times per week using 3 ml of 1X PBS (Sigma-Aldrich) prepared in the laboratory and 1.5 ml of TrypLE (trypsin-EDTA) (Invitrogen). Cells

were used between passages 15-25; cells were disposed of beyond passage 25 to limit changes in the clonal population.

### 2.1.2 Storage and revival

Cells were stored in a cryopreservation mixture composed of the appropriate cell media, foetal bovine serum (FBS) and DMSO in a ratio of 5:3:1 respectively, in cryovials at -80°C (for short term storage) or liquid nitrogen (for long term storage). A container of isopropanol was used to slowly freeze cells to avoid ice crystal formation (Mr. Frosty™, Thermo Fisher Scientific, Massachusetts, USA). When required, cells were resuscitated by thawing cryovials in a 37°C water bath.

### 2.1.3 Mycoplasma testing

Cells were routinely tested for mycoplasma using AmpliTaq Gold DNA polymerase (Applied Biosystems, Massachusetts, USA) and mycoplasma specific primers. A 200 µl aliquot of cells was collected, diluted in 1 ml sterile saline to and centrifuged at 6500 rpm for 5 minutes. Supernatant was removed and the pellet was resuspended in 90 µl of 0.05 M NaOH and vigorously mixed. Tubes were heated at 98°C for 10 minutes to lyse cells and when cool, 10 µl of 1M Tris pH 7.5 was added to each tube to neutralize. A 1:10 dilution was prepared by adding 10 µl of DNA to 90 µl of sterile water. A master mix was prepared: 2.5 µl 10X PCR Buffer II, 1 µl 50 mM MgCl<sub>2</sub>, 0.5 µl 10 mM dNTPs, 0.2 µl AmpliTaq Gold DNA polymerase, 15.8 µl sterile H<sub>2</sub>O, 2 µl DNA, mycoplasma genus specific primer pairs (1 µl 100 ng/µl GPO-1 and 1 µl 100 ng/µl MGSO) and internal control primer pairs (0.5 µl 100 ng/µl HRAG-I-F and 0.5 µl 100 ng/µl HRAG-I-R). The Veriti© thermal cycler (Applied Biosystems) was used to detect the presence of mycoplasma DNA using the following cycling conditions: denaturation for 1 cycle at 94°C for 10 minutes, annealing for 50 cycles at 94°C for 30 seconds, 53°C for 1 minute and 72°C for 1 minute and extension for 1 cycle at 72°C for 5 minutes. Products were then separated using a 1% agarose gel and imaged using a 1:1000 dilution of GelRed dye (Biotium, California, USA).

## 2.2 Transfections and treatments with miRNA mimics, lncRNA siRNAs and target gene siRNAs

### 2.2.1 High-throughput functional screen experiments

#### 2.2.1.1 lncRNA siRNA primary screen: reverse transfection

The lncRNA siRNA screen was performed in duplicate, with two replicates for the butyrate treatment plates and two for no butyrate treatment plates; no butyrate treatment plates were termed A and B, and butyrate treatment plates were termed C and D. Reverse transfection was performed in 384 well plates with the Human Lincode siRNA SMARTpool Library V54 (2231 lncRNA siRNAs) (Dharmacon, Colorado, USA), as well as controls on each plate (positive death control siRNA: siPLK1) (Dharmacon); positive miRNA mimic control: miR-18a (GenePharma, Shanghai, China); negative control siRNA: ON-TARGETplus Non-targeting Control siRNAs (OTP-NT) (Dharmacon) and mock transfection control. PLK1 was used as a positive control as it is a potent repressor of growth and inducer of death in CRC (Driscoll et al. 2014). miR-18a was selected as mimic control as previous studies demonstrated its pro-apoptotic and anti-proliferative effects in HCT116 cells (Humphreys et al. 2014b). The controls and lncRNA inhibitors were tested at a final concentration of 20 nM in each well. Transfections were performed with DharmaFECT 2 lipid (Dharmacon) in Opti-MEM (Thermo Fisher Scientific), using volumes of 0.06  $\mu\text{l}$  /well in 10.94  $\mu\text{l}$  Opti-MEM/well. The BioTek EL406 liquid dispenser (BioTek, Vermont, USA) was used to dispense 4 x lipid (44  $\mu\text{l}$  for siRNA) into A plates. The SciClone ALH3000 Lab Automation Liquid Handler (Caliper Lifesciences, Massachusetts, USA) was used to dispense 4 x siRNA (6  $\mu\text{l}$  of 0.5  $\mu\text{M}$  library i.e. 1.5  $\mu\text{l}$  /well for 20 nM concentration) from library plates into A plates (final volume 50  $\mu\text{l}$ ), and to then distribute 12.5  $\mu\text{l}$  to each of B, C and D plates. Plates were incubated at room temperature (RT) for 20 min. Cells were counted on the Countess (Thermo Fisher Scientific) and diluted appropriately, to seed the cells at 1400/well for a 72 h experiment. The BioTek liquid dispenser was used to dispense 25  $\mu\text{l}$  cells/well, and plates were then incubated at 37°C for 24 h. Media was changed on all assay plates 24 h after transfection using the BioTek liquid dispenser, followed by the addition of 50  $\mu\text{l}$  pre-warmed fresh growth medium with 10% FBS to each well. Plates were incubated for a further 24 h.

### 2.2.1.2 Secondary lncRNA screen: reverse transfection

A similar protocol was performed compared to the primary lncRNA screen; however, each individual duplex from each SMARTpool was tested for efficacy in lncRNA knockdown. Each individual duplex was tested at 25 nM as recommended and the SMARTpools were used for comparison and tested at the primary screening concentration of 20 nM. The same controls were used as above.

### 2.2.1.3 Butyrate treatment

Media was removed from wells as above and replaced with 15  $\mu$ l of butyrate-containing or plain McCoy's 5A (Modified) Medium. Cells were treated with butyrate at a concentration of 4.166 mM to achieve a final concentration of 2.5 mM per well. Vehicle treated wells received medium without butyrate. Plates were incubated for a further 24 h.

### 2.2.1.4 ApoLive-Glo™ Multiplex Assay for cell viability and apoptosis

The ApoLive-Glo™ Multiplex Assay was performed at 72 h post transfection. Cell Titre Fluor (CTF) is a fluorescent viability assay involving a cell-permeable, peptide substrate. Live cells take up the substrate and normal protease activity cleaves it to produce a molecule, which generates a fluorescent signal proportional to the number of live cells. For the high-throughput screen, the BioTek liquid handler was used to dispense 5  $\mu$ l of CTF per well prior to incubation at 37°C for 1 h. Plates were read with the Cytation 3 or Synergy H4 plate readers (BioTek) at an excitation level of 380-400 nm and emission at 505 nm. For validation experiments, 20  $\mu$ l of CTF was added to 96 well plates prior to incubation at 37°C for 30 minutes and read using the EnSight plate reader (PerkinElmer, Massachusetts, USA). Caspase-Glo 3/7 is a luminescent endpoint assay which measures the activity of caspases 3 and 7; executioner caspases involved in intrinsic and extrinsic apoptosis pathways. The luciferase reaction releases light, which is proportional to the amount of caspase activation in the well. For the high-throughput screen, the BioTek was used to dispense 12  $\mu$ l of Caspase-Glo 3/7, prior to incubation at RT for approximately 30 minutes. Luminescence was measured using the plate readers mentioned above. For validation experiments, 100  $\mu$ l of Caspase-Glo 3/7 was added to 96 well plates prior to incubation at RT for 30 minutes and read using the EnSight.

### 2.2.1.5 Screen data analysis and hit selection

Quality control analysis was performed to determine the quality and reliability of the screen data, including the dynamic range between the positive and negative controls

## CHAPTER 2

using the  $Z'$  factor and coefficient of variation. For cell viability (CV) data from the lncRNA screen, wells were binned based on viability fold change to OTP-NT (lethal cell viability (LC) is  $<0.5$  viability, CV2  $<0.8 - 0.5$ , CV1  $>0.8 - 1.15$ , Hi  $>1.15$ ). For synthetic lethality, hit 1 was classified as without butyrate CV1 and with butyrate CV2, hit 2 was classified as without butyrate CV1/CV2 and with butyrate LC, hit 3 was classified as without butyrate CV1/Hi and with butyrate CV2/CV1, and hit 4 was classified as without butyrate Hi and with butyrate CV1. For caspase data the robust  $Z$ -score was used with a score  $>1.5$  indicating a significant increase in apoptosis in butyrate treated groups compared to without treatment and a score  $<-1.5$  indicating reduced apoptosis comparing the same groups. The robust  $Z$ -score normalisation method takes into account the sample value, median and median absolute deviation which is less sensitive to outliers compared with  $Z$ -score.

Screen quality control was also performed to determine the performance and reliability of the screen using the  $Z'$  factor, Pearson correlation and coefficient of variation. The  $Z'$  factor indicates the dynamic range between positive and negative controls. If the difference is too small between positive and negative controls this will increase the number of false positives. Plate values were considered as excellent between  $0.5- >1$ , good  $0.3-0.5$ , acceptable  $0- >3$  and too much overlap between positive and negative controls  $<0$ . The coefficient of variation was also determined, and this indicates control variability ( $\sim 10\%$  good,  $>24\%$  unacceptable). The Pearson correlation coefficient indicates reproducibility of the data between replicate plates and  $0.6-0.8$  is acceptable while  $>0.8$  is good.

### 2.2.2 Proliferation and apoptosis assays

#### 2.2.2.1 Proliferation and apoptosis validation: reverse transfections

Proliferation experiments were performed using 16 well E plates (ACEA Biosciences, California, USA) and the xCELLigence RCTA platform (ACEA Biosciences) which measures electrical impedance in cell media in a well, proportional to cell proliferation, morphology and adhesion. Apoptosis experiments were performed with Greiner 96 well plates (Greiner Bio-One, Frickenhausen, Germany) and the Incucyte FLR (Essen BioScience, Michigan, USA) which uses phase contrast imaging to determine cell confluence changes and fluorescence imaging for assays including for apoptosis assays (wells were equivalent in size in both types of well plates). Reverse transfections were performed using Lipofectamine 2000 (Thermo Fisher Scientific) to deliver miRNAs, siRNAs, negative control (NC) mimics/siRNAs (a scrambled sequence with no reported

## CHAPTER 2

biological significance) (GenePharma) and target gene siRNAs or NC siRNAs (Qiagen, California, USA) to CRC cells. All transfections were performed in triplicate or quadruplicate per miRNA mimic per treatment group. Prior to transfection, xCELLigence E plates were blanked using 50  $\mu$ l of growth medium, contributing to part of the total well volume of 150  $\mu$ l; 50  $\mu$ l of growth medium was also added to 96 well plates prior to transfections to maintain consistency in Incucyte studies, although not required for blanking. Transfections were performed using 0.25  $\mu$ l of Lipofectamine 2000 in 25  $\mu$ l of Opti-MEM per well which was combined with 0.15  $\mu$ l of 20  $\mu$ M mimic in 25  $\mu$ l of Opti-MEM per well. The final concentration of miRNA and NC mimics in each well was 20 nM each. Cells were passaged and counted by using a Brightline Hemocytometer (Sigma-Aldrich). Cells were diluted and seeded at 7500 cells in 50  $\mu$ l of growth media per well in 16 well E plates or 96 well plates. The total well volume was 150  $\mu$ l. Plates were incubated at RT for 20 minutes before being placed in the xCELLigence instrument (cell proliferation studies) or Incucyte (apoptosis studies) for a 48 h post-transfection period at 37°C and 5% CO<sub>2</sub>.

Reverse transfections were also performed using Greiner 24 well plates (Greiner Bio-One), to generate enough cells for RNA or protein extraction. These transfections involved using 1  $\mu$ l of Lipofectamine 2000 in 50  $\mu$ l of Opti-MEM per well which was combined with 0.6  $\mu$ l of 20  $\mu$ M mimic (stock) in 50  $\mu$ l of Opti-MEM per well. Cells were seeded at 75,000 per well in 500  $\mu$ l of growth medium, to make a total well volume of 600  $\mu$ l. Cells for the RNA-seq and flow cytometry (cell cycle and apoptosis) were collected from 6 well plates (Greiner Bio-One). These transfections involved using 3  $\mu$ l Lipofectamine 2000 in 250  $\mu$ l of Opti-MEM per well which was combined with 2  $\mu$ l of mimic in 250  $\mu$ l of Opti-MEM per well. Cells were seeded at 200,000 per well in 1.5 mL of growth medium, to make a total well volume of 2 ml.

### **2.2.2.2 Butyrate treatment**

CRC cells were exposed to 0 mM or 2.5 mM sodium butyrate (Sigma-Aldrich) treatment after the 48 h transfection period. Sodium butyrate powder was dissolved in the appropriate volume of McCoy's 5A (Modified) Medium to make a 1 M solution of butyrate. The solution was filtered using a 0.2  $\mu$ M filter and a 2 ml syringe. To avoid disturbing cells, the butyrate solution was diluted to 5 mM in growth medium and used to replace half of the total volume in each well to reach a final concentration of 2.5 mM.

### 2.2.2.3 xCELLigence proliferation data analysis

Cell index data points were collated from the xCELLigence software and represented graphically over the 72 h incubation period in time plots and at 72 h post-transfection in bar-graphs (endpoint of the experiment) using GraphPad Prism (GraphPad Software Inc, California, USA). Unpaired t-tests ( $P < 0.05$ ) were performed on data sets to compare differences between the NC and miRNA mimic transfected CRC cells within each treatment group to determine changes in cell proliferation; graphs display the mean of replicates  $\pm$  standard error of the mean (SEM).

### 2.2.2.4 Coefficient of drug interaction (CDI)

The coefficient of drug interaction was calculated for xCELLigence proliferation data using the calculation  $CDI = AB / (A \times B)$ , whereby A = miRNA mimic/inhibitor/siRNA to negative control ratio, B = 2.5 mM butyrate treatment to negative control, AB = combination of miRNA mimic/inhibitor/siRNA and 2.5 mM butyrate treatment to negative control ratio (Cao & Zhen 1989).  $CDI < 1$ , = 1 or  $> 1$  indicates that the drugs are synergistic, additive or antagonistic, respectively and a  $CDI < 0.7$  indicates that the drug is significantly synergistic (Cao & Zhen 1989).

### 2.2.2.5 Caspase 3/7 Reagent assay for apoptosis studies

Apoptotic changes in CRC cells were measured using CellPlayer™ 96-well Caspase 3/7 reagent (Essen BioScience) which fluoresces when cleaved by executioner caspases 3 and 7 during intrinsic and extrinsic apoptosis. The Incucyte FLR was used to detect fluorescent changes in cells. Cells were exposed to the apoptosis reagent 48 h post transfection. The Caspase 3/7 reagent, provided in a 5 mM stock solution, was diluted to 5  $\mu$ M in 4 ml of growth medium. A 1 M butyrate solution was diluted to 5 mM in 2 ml of Caspase 3/7 reagent solution by adding 10  $\mu$ l of butyrate. As mentioned above, 75  $\mu$ l of the butyrate and Caspase 3/7 reagent, or just Caspase 3/7 reagent solution, were used to replace growth medium in each well, to create a final concentration of 2.5 mM or 0 mM of butyrate and 2.5  $\mu$ M of Caspase 3/7 reagent in appropriate wells. The plates were incubated for a further 24 h in the Incucyte FLR instrument.

Due to background fluorescence and confluence variation between wells, apoptosis changes were normalised. Objects per image (fluorescent cell points) and confluence data were obtained using the Incucyte Object Counting v2.0 analysis software (Essen BioScience). Objects per image were normalised to confluence and represented as Normalised Caspase Activity graphically. Normalised data was statistically analysed

using unpaired t-tests ( $P < 0.05$ ) at 72 h post-transfection (endpoint of the experiment) to compare apoptotic changes between experimental groups. Graphs display the mean of replicates  $\pm$  standard error of the mean (SEM).

#### 2.2.2.6 Crystal violet assay

For some experiments, crystal violet was used to examine viability changes. Crystal violet is a viability assay used to quantify the changes in cellular adherence in a culture plate through the staining of DNA. A 10X concentrated crystal violet solution was made by dissolving 1 g crystal violet powder (Sigma-Aldrich) in 500 ml of buffered-formalin (Orion Labs, California, USA), followed by further dilution to a 1X solution in buffered-formalin. The assay was performed in 96 well plates and cell media was removed from the wells gently and the plate washed twice with 150  $\mu$ L 1 $\times$ PBS. To each well, 50  $\mu$ l of 1X crystal violet solution was added and incubated at RT for 20 minutes. The plate was then washed once by immersion in a tray of water and air dried. To each well, 100  $\mu$ l of 1% SDS (Sigma-Aldrich) was added in order to solubilize the crystal violet stained DNA followed by agitation on an orbital shaker until a uniform colour was achieved. To quantify the stained cells, the absorbance at 570 nm was measured using the Infusion plate reader (PerkinElmer). Data was analysed and represented in bar-graphs (endpoint of the experiment) using GraphPad Prism (GraphPad Software Inc). Unpaired t-tests ( $P < 0.05$ ) were performed on data sets to compare differences between the NC and miRNA mimic transfected CRC cells within each treatment group to determine changes in cell viability. Graphs display the mean of replicates  $\pm$  standard error of the mean (SEM).

## 2.3 Bioinformatics

### 2.3.1 miRNA target prediction

miRWalk (Dweep et al. 2011), an online target prediction program, was used to collate information about predicted miRNA target genes using eight prediction programs including DIANA-mT (Maragkakis et al. 2009), miRanda (Enright et al. 2003; John et al. 2004), miRDB (Wang 2008), miRWalk (Dweep et al. 2011), PICTAR5 (Krek et al. 2005), PITA (Kertesz et al. 2007), RNA22 (Miranda et al. 2006) and TargetScan (Grimson et al. 2007; Lewis et al. 2005). These prediction programs use complex mathematical algorithms to determine the probability of a miRNA binding to a target mRNA based on several criteria including conservation of canonical binding sites (complete pairing in the seed sequence), free energy of binding and mRNA 3'UTR

secondary structures (Kertesz et al. 2007; Miranda et al. 2006; Witkos et al. 2011). Predicted target genes were labelled as hits if 4 or more prediction programs identified those genes as possible miRNA targets (specifically if miRNAs had 3'UTR binding sites for those genes). Microsoft Excel 2007 (Microsoft Corporation, Washington, USA) was used to compile the gene lists and they were transferred into the KEGG Mapper (Kanehisa & Goto 2000; Kanehisa et al. 2016) online program for pathway analysis.

### 2.3.2 KEGG Mapper

The KEGG Mapper pathway mapping tool (Kanehisa & Goto 2000; Kanehisa et al. 2016) is a basic pathway analysis online program used to present molecular datasets in key canonical signalling pathways, based on the KEGG PATHWAY database. Predicted target genes were analysed using KEGG Mapper to investigate CRC relevant canonical signalling pathways, specifically oncogenes involved in CRC cell growth and death.

## 2.4 mRNA expression analysis

### 2.4.1 TRIzol RNA extraction

RNA was collected for mRNA expression analysis of miRNA predicted target genes using TRIzol Reagent extraction methods (Thermo Fisher Scientific). After the 72 h incubation period, including miRNA transfection and butyrate treatment, each well was exposed to 400  $\mu$ l (24 well plate) or 1 ml (6 well plate) of TRIzol reagent to lyse the CRC cells and inhibit RNase activity. The cells were vigorously scraped from the base of the wells. The lysate of each replicate was stored at  $-20^{\circ}\text{C}$  in separate microcentrifuge tubes for RNA extraction or RNA was extracted immediately.

TRIzol RNA extraction from 24 well plates or 6 well plates involved the addition of 80  $\mu$ l or 200  $\mu$ l of chloroform (Chem-supply) respectively to each tube, followed by vigorous mixing and 2 minute incubation at RT. Tubes were centrifuged at 12,000 g for 15 minutes at  $4^{\circ}\text{C}$  and the top aqueous phase containing the RNA was removed into new tubes. Isopropanol (Chem-supply) (200  $\mu$ l- 24 well plate/500  $\mu$ l- 6 well plate) was added to each tube to precipitate the RNA, followed by a 10 minute RT incubation. Tubes were centrifuged at 12,000 g for 20 minutes at  $4^{\circ}\text{C}$  to form an RNA pellet and 500  $\mu$ l (24 well plate) or 1 ml (6 well plate) of 70% ethanol (Chem-supply) was used to clean the RNA pellet. Tubes were centrifuged at 7,500 g for 5 minutes at  $4^{\circ}\text{C}$ , the wash was removed, and the remaining RNA pellet dried on ice. RNA was resuspended in 15  $\mu$ l (24 well plate) or 40  $\mu$ l (6 well plate) of RNase free water.

### 2.4.2 RNA quantification

The Nanodrop8000 spectrophotometer (Thermo Fisher Scientific) was used to quantify RNA samples. The Nanodrop8000 was blanked with 1  $\mu$ l of sterile water, followed by quantification of 1  $\mu$ l of RNA represented as a concentration in ng/ $\mu$ l. The ratios of absorbance, 260/280 and 260/230, were analysed to determine the presence of contaminants including phenols (from TRIzol) and proteins.

### 2.4.3 RNA quality analysis

The Agilent 2100 Bioanalyzer (Agilent Technologies, California, USA) was used to determine the integrity of RNA samples used for mRNA analysis, based on the ratio of 18s and 28s ribosomal subunits. The instrument analyses samples using micro-fluidics and capillary electrophoresis (Schroeder et al. 2006). One sample, from each treatment group, was used to represent each RNA extraction performed. RNA samples were diluted (using sterile water) to a concentration between 25-500 ng/ $\mu$ l, to ensure they were within the quantitative range of the instrument. A gel-dye mix was prepared using 65  $\mu$ l of RNA 6000 Nano Gel Matrix (Agilent Technologies) and 1  $\mu$ l of RNA 6000 Nano Dye concentrate (Agilent Technologies) which was centrifuged at 13,000 g for 10 minutes. Diluted RNA samples were heated to 70°C for 2 minutes using a heating block. An Agilent RNA 6000 Nano chip (Agilent Technologies) was placed into the chip priming station and 9  $\mu$ l of gel-dye mix was loaded into the appropriate well. The syringe plunger in the chip priming station was positioned at 1 ml and the gel was set for 30 seconds, and then 9  $\mu$ l of gel-dye mix was added to appropriate wells. Each sample well and the ladder well was loaded with 5  $\mu$ l of the RNA 6000 Nano marker (Agilent Technologies), followed by 1  $\mu$ l of the RNA 6000 ladder (Agilent Technologies) in the ladder well and 1  $\mu$ l of RNA into corresponding sample wells. The chip was vortexed in the IKA vortex mixer (IKA-works, North Carolina, USA) at 2400 rpm for 1 minute and then placed in the Agilent 2100 Bioanalyzer for approximately 30 minutes for analysis.

## 2.5 Relative quantitation real-time reverse transcriptase PCR

### 2.5.1 Real-time RT-PCR for microRNAs

#### 2.5.1.1 cDNA synthesis

miRNA expression was determined using RNA from control and butyrate treated (2.5 mM) CRC cells. cDNA was synthesised from 20-100 ng of RNA using microRNA or RNU6B (endogenous control) specific primers as specified by the TaqMan MicroRNA

Assay protocol (Applied Biosystems). For the reverse transcriptase (RT) step each reaction contained 3.5  $\mu\text{l}$  master mix (0.075  $\mu\text{l}$  100 mM dNTPs, 0.5  $\mu\text{l}$  MultiScribe™ RT enzyme, 0.75  $\mu\text{l}$  10X RT buffer, 0.095  $\mu\text{l}$  RNase inhibitor, 2.08  $\mu\text{l}$  water), 2.5  $\mu\text{l}$  RNA, and 1.5  $\mu\text{l}$  RT primer. After the reaction components were combined and added to the wells of eight-strip tubes, samples were loaded into the Veriti Thermal Cycler (Applied Biosystems). The RT program included 30 minute incubation at 16°C, a 30 minute incubation at 42°C and finally a 5 minute incubation at 85°C.

### 2.5.1.2 Real-time PCR

Real-time PCR was performed as specified by the TaqMan MicroRNA Assay protocol. PCR amplification reactions of 10.84  $\mu\text{l}$ , containing 5  $\mu\text{l}$  TaqMan Universal PCR Master Mix No AmpErase UNG, 0.5  $\mu\text{l}$  miRNA-specific primers and probe assay mix and 3.84  $\mu\text{l}$  water, were pipetted into four-strip PCR tubes. Each sample was performed in triplicate. Tubes were loaded into the Qiagen Rotorgene Q (Qiagen) and the program included a 10 min incubation at 95°C, then 50 cycles of a 15 sec denaturing step at 95°C and a 60 sec annealing/ extension step at 60°C.

miRNA levels were normalised relative to the levels of the endogenous small nuclear RNA gene RNU6B. Expression levels were calculated from Ct values using Qgene (Muller et al. 2002). Data was represented graphically using GraphPad Prism, to represent changes in mRNA levels of predicted targets and statistically analysed using unpaired t-tests ( $P < 0.05$ ). Graphs display the mean of triplicates  $\pm$  standard error of the mean (SEM). Refer to Table 2-3 for primer sequences.

## 2.5.2 Real-time RT-PCR for mRNAs

### 2.5.2.1 DNase treatment

Quantified RNA samples were diluted to 0.1  $\mu\text{g}/\mu\text{l}$  in 22.5  $\mu\text{l}$  of sterile water. To each sample, 2.5  $\mu\text{l}$  of DNase buffer (Promega, Wisconsin, USA) and 1  $\mu\text{l}$  of 1u/ $\mu\text{l}$  DNase enzyme (Promega) was added to remove remnant DNA, followed by a 20 minute incubation period at 37°C. The DNase buffer and enzyme were from the RQ1 RNase free DNase kit (Promega). Samples were resuspended in 2.5  $\mu\text{l}$  of DNase inactivation slurry (DNA-free™ Kit) (Ambion, California, USA), to inactivate DNase enzymes and then incubated at RT for 2 minutes. Tubes were centrifuged at 10,000 g for 1.5 minutes to pellet slurry and the RNA solution was removed. A 10  $\mu\text{l}$  aliquot of DNase treated sample was used for cDNA synthesis.

### 2.5.2.2 cDNA synthesis

cDNA synthesis was initiated with the addition of 1  $\mu$ l of Random Primer 6 (New England Biolabs, Massachusetts, USA) to 10  $\mu$ l of DNase treated sample, followed by an incubation period of 5 minutes at 70°C and 5 minutes on ice. A master mix consisting of 5  $\mu$ l of 200u/ $\mu$ l Moloney Murine Leukemia Virus Reverse Transcriptase (M-MLV RT) buffer (Promega), 1.25  $\mu$ l of dNTP mix, 1  $\mu$ l of M-MLV RT enzyme (Promega) and 6.75  $\mu$ l of sterile water was added to each sample i.e. 14  $\mu$ l of master mix. Tubes were incubated for 10 minutes at RT and then placed in the Programmable Thermal Controller 100 (PTC100) (MJ Research, Quebec, Canada) with the following RT-PCR conditions: 50°C for 50 minutes; 70°C for 15 minutes and 4°C hold. The cDNA was diluted to a 1:3 ratio by adding 50  $\mu$ l of sterile water to each sample.

### 2.5.2.3 Real-time PCR

mRNA expression of miRNA predicted target genes were analysed using Power SYBR green quantitative real-time RT-PCR (Applied Biosystems) and the Qiagen Rotorgene Q real-time PCR cycler. Standard curves for each of the predicted target genes and 3 reference genes including Glyceraldehyde-3-Phosphate Dehydrogenase (GAPDH), Beta-2 Microglobulin (B2M) and Beta-Actin (ACTB) were prepared for mRNA expression normalisation by using normal colon or CRC cell line RNA. Real-time PCR was performed as per the Power SYBR green protocol provided by Thermo Fisher Scientific. PCR amplification reactions were performed in triplicate using 20  $\mu$ l reactions of 10  $\mu$ l of Power SYBR green reagent, 2  $\mu$ l of forward primer, 2  $\mu$ l of reverse primer, 4  $\mu$ l of water and 2  $\mu$ l of cDNA. Primers were prepared at 3  $\mu$ M dilutions for final concentrations of 300 nM in the reaction mix. Refer to Table 2-3 for primer sequences. Cycling conditions included 95 °C hold for 10 minutes, 90 °C for 15 seconds for denaturation and 60 °C for 1 minute for annealing and extension.

### 2.5.2.4 mRNA expression normalisation and analysis

mRNA levels were normalised using relative quantitation. The 3 reference genes used for mRNA normalisation included GAPDH, B2M and ACTB. Relative quantitation was used to convert threshold cycle (Ct) values of the reference genes and predicted target genes to relative quantities with the highest relative quantity for each gene set to 1 i.e. the sample with the earliest Ct value. The geometric mean of the 3 reference genes was calculated from the raw values to produce a gene expression normalization factor. The predicted target gene means were normalised using the normalisation factor for each sample. Data was represented graphically using GraphPad Prism, to represent changes

in mRNA levels of predicted targets and statistically analysed using unpaired t-tests ( $P < 0.05$ ). Graphs display the mean of replicates  $\pm$  standard error of the mean (SEM).

## 2.6 Protein analysis

### 2.6.1 Protein purification and quantification

Protein was extracted from a 24 well plate of CRC cells transfected with miRNAs or NC mimics and treated with 0 mM or 2.5 mM of butyrate, with 6 replicate wells per plate. Protein lysis buffer was prepared using 1.5 ml of RIPA buffer (Table 2-5), 300  $\mu$ l of protease solution (Complete mini protease inhibitor cocktail tablet, Roche Applied Science, Basel, Switzerland) and 2  $\mu$ l of 1 M DL-Dithiothreitol (DTT) (Sigma-Aldrich). Cell medium was removed from each well and replaced with 100  $\mu$ l of 1X PBS to wash cells. The PBS was removed and replaced with 55  $\mu$ l of protein lysis buffer and cells were vigorously scraped from the wells. Two replicates were pooled, per tube, to increase protein yield ( $n=3$ ) and stored at  $-20^{\circ}\text{C}$  for Western blotting.

Protein quantification was performed using an EZQ Protein Quantification kit (Thermo Fisher Scientific) as per manufacturer's instructions using a total of 1  $\mu$ l of protein per sample, which were diluted to a 1:2 ratio using 2.5  $\mu$ l of RIPA buffer. The ChemidocMP Imaging System (BioRad) was used to image the prepared EZQ assay paper. Image lab 4.1 (BioRad) was used to quantify protein concentrations based on image analysis of EZQ Protein Quantification assay results. Average protein concentrations were collected for each sample and used to calculate protein loading for Western blotting.

### 2.6.2 Western blotting

Protein extracts were analysed for changes in selected protein levels. Protein extracts were prepared at 10-50  $\mu$ g per tube, combined with 1:5 ratio of 1M DTT to 3X blue loading dye (New England Biolabs). The total volume of 13  $\mu$ l was reached with RIPA buffer. These mixtures were boiled at  $98^{\circ}\text{C}$  for 3-5 minutes and then loaded into 15 well 15  $\mu$ l mini PROTEAN TGX precast gels (BioRad) along with 5  $\mu$ l of Pre-stained Protein Marker 7-190 kDa or 11-195 kDa (p7708s or p7706s) (New England Biolabs). BioRad PROTEAN TGX precast gels contain trihalo compounds that react with tryptophan residues in proteins in a UV-induced 1-minute reaction to produce fluorescence. No additional staining is required. Gels were submerged in 1X SDS Running buffer (Table 2-5). Protein was separated at 150 V for 30-35 minutes using a PowerPac<sup>TM</sup>Basic (BioRad). Protein transfer was performed using a 0.2  $\mu$ M

## CHAPTER 2

Polyvinylidene Fluoride (PVDF) membrane (BioRad) and the Trans-blot Turbo Transfer System (BioRad) for 7 minutes at a constant current of 1.3 A. The gels and membranes were imaged, after transfer, using the ChemidocMP Imaging System and Image Lab 4.1 imaging system (BioRad) for transfer efficiency and total protein loading. Membranes were then blocked with 5 % BSA (Sigma-Aldrich) or Diploma skim milk powder (Fonterra, Victoria, Australia) in TBS-T buffer (Table 2-5) prior to being exposed to primary antibodies (Table 2-4) in an overnight incubation period. Corresponding horse-radish peroxidase (HRP)-conjugated secondary antibodies (Table 2-4) were used with Enhanced Chemiluminescence (ECL) substrate (BioRad) to develop the membrane which was imaged using the ChemiDoc MP imaging system.

### 2.6.3 Protein expression normalisation and analysis

Image lab 4.1 (BioRad) was used to collate band intensity data for proteins of interest and normalise data. The band intensity data were normalised to total protein loading and presented graphically using GraphPad Prism as normalised mean intensity. Total protein normalisation was determined to be the most reliable method of protein expression normalisation (Aldridge et al. 2008). GAPDH and alpha-actinin were initially tested as loading controls; however, they were deemed unreliable as they are dysregulated in CRC and regulated by butyrate (Hu et al. 2016b). Data were statistically analysed using unpaired t-tests ( $P < 0.05$ ). Graphs display the mean of replicates  $\pm$  standard error of the mean (SEM).

## 2.7 WNT signalling: TOPflash and FOPflash assays

### 2.7.1 Forward transfection

TOPflash and FOPflash (Merck, New Jersey, USA) are firefly luciferase reporters that can be transfected into mammalian cells and used to determine beta-catenin-mediated transcriptional activation in WNT signalling. TOPflash has three wild type TCF transcription factor binding sites, while FOPflash has three mutant TCF binding sites. When  $\beta$ -catenin enters the nucleus during canonical WNT signalling activation, it can bind to the functional TCF binding sites of TOPflash and induce the production of luciferase mRNA and eventually luciferase protein is translated. The amount of luminescence from this protein is directly proportional to the activation of this pathway. FOPflash is negative control plasmid which should not bind  $\beta$ -catenin and if changes in luminescence are detected non-specific pathway activity may be occurring.

## CHAPTER 2

CRC cells were seeded at 7500 per well in 96-well clear Greiner plates and incubated at 37°C for 24 h. Cells were then forward transfected with 50 ng per well TOPflash/FOPflash vector (Firefly), 5 ng per pRL Null vector (Renilla control) and 20 nM microRNA mimics, using 0.15 µl Lipofectamine 2000 and Opti-MEM. Cells were incubated for a further 24 h at 37°C. Conditioned media from L-cells with and without WNT3A was combined with the appropriate volume of 1 M sodium butyrate solution to make a 5 mM solution. Half of the total well volume was removed (75 µl) and replaced with conditioned media to make a final concentration of 2.5 mM sodium butyrate in selected wells. Control wells did not have butyrate added to conditioned media. Cells were incubated for a further 24 h at 37°C. At 72 h a Dual Luciferase Reporter Assay was performed (Promega). All media was removed, and cells were lysed using 20 µl of Passive Lysis Buffer (PLB) per well for 15 minutes on a plate shaker. Cell lysate (10 µl) was transferred to a white-walled 96-well plate and 25 µl of LARII was added to each well and Firefly luminescence was read using the EnSight plate reader. Stop&Glo reagent (25 µl) was added to each well and the plate was read again for luminescence (Renilla).

### 2.7.2 TOPflash/FOPflash assay analysis

The TOPflash and FOPflash Firefly luminescent readings were normalised to pRL Null Renilla luminescent readings. Luminescent values were collected and presented as mean  $\pm$  standard error of the mean (SEM) including a minimum of four replicates. Data were statistically analysed using GraphPad Prism using an unpaired Student's t-test, with a P value  $< 0.05$  considered statistically significant. Graphs display the mean of replicates  $\pm$  standard error of the mean (SEM).

### 2.8 Total and small RNA-seq

Total RNA and small RNA expression was determined using RNA from HCT116 control and butyrate treated (2.5 mM) cells. The cells were treated over 48 h. Prior to sequencing preparation, samples were analysed for quality using the Agilent 2100 Bioanalyzer system as previously mentioned. The RNA-Seq libraries were prepared and sequenced at the Flinders Genomics Facility (Flinders University, Adelaide, Australia). Samples underwent rRNA depletion (only total RNA-seq), adapter ligation and PCR amplification using the TruSeq Stranded Total RNA Sample Preparation Kit (Illumina Inc., California, USA) for total RNA-seq and TruSeq small RNA Library Preparation (Illumina Inc.) for small RNA-seq, refer to manufacturer's instructions. For total RNA-seq, aliquots (1 µg) of the 4 RNA samples (duplicate samples for the control and

untreated experimental groups), were subjected to paired-ends 100 bp sequencing using the Illumina Nextseq sequencing platform (Illumina Inc.) and approximately 30 million reads were generated per sample. While 6 RNA samples (triplicate samples for the control and untreated experimental groups) for small RNA-seq generated approximately 10 million reads each.

RNA-seq data were analysed by the bioinformatician, Dr. Shashikanth Marri, from the Flinders Genomics Facility (Flinders University, Adelaide, Australia). Data were trimmed for adaptors using the Trimmomatic (Bolger et al. 2014) program, followed by quality analysis of reads using FASTQC and assembly, mapping and alignment of reads to Ensembl human genome (Grch38.p5\_v24) using STAR (Dobin et al. 2013). Aligned reads were then converted to raw counts using HTseq (Anders et al. 2015) and differential expression analysis performed using DESeq2 (Love et al. 2014).

## 2.9 Network and pathway analysis

### 2.9.1 Protein-protein interaction (PPI) network construction

miRNA-mRNA networks were produced from the top differentially expressed miRNAs and mRNAs selected from small RNA-seq and total RNA-seq data respectively. Criteria used to select differentially expressed miRNAs included  $\log_2FC < -1$  or  $\log_2FC > 1$ ,  $p_{adj} < 0.05$  and mean raw counts  $> 25$ . Criteria used to select differentially expressed mRNAs included  $\log_2FC < -1.5$  or  $\log_2FC > 1.5$ ,  $p_{adj} < 0.01$  and mean raw counts per group  $> 25$ . The final protein-coding gene list was refined using the biological network analysis and visualisation tool, Network analyst (Xia et al. 2014; Xia et al. 2015), to define interactors with degree interactions (node connections)  $> 1$ . Only zero-order networks were investigated as these show direct interactions with the input list (seed proteins). The protein-protein interaction network was visualized using the open source network construction software, Cytoscape (Version 3.4.0) (Shannon et al. 2003) and then analysed (undirected network) using the in-built NetworkAnalyser tool to determine the network properties.

### 2.9.2 Gene ontology (GO) analysis

Gene ontology (GO) enrichment analysis allows the classification and interpretation of gene lists based on their functional characteristics including molecular function, biological processes and cellular components. GO enrichment analysis was used to examine dysregulated genes identified in the PPI network. ClueGO (Bindea et al. 2009)

is a Cytoscape plug-in which can be used for GO enrichment analysis of gene lists. ClueGO was used to identify the enriched GO terms for dysregulated mRNA genes for each of the following classifications: Biological Processes, Molecular Functions, and Cellular Compartments.

### 2.9.3 miRNA-mRNA network analysis

miRNA-mRNA networks were then constructed based on miRNA target predictions. miRNA target predictions were collated from multiple target prediction programs including TargetScan Human Release 7.0 (total context++ score  $\leq -0.3$ ) (Agarwal et al. 2015), miRDB (prediction score  $\geq 85$ ) (Wong & Wang 2015), DIANA Tools microT-CDS (miTG score  $\geq 0.95$ ) (Paraskevopoulou et al. 2013), miRTarBase (strong evidence) (Chou et al. 2018b) and miRecords (strong evidence) (Xiao et al. 2009b). The Cytoscape application, CluePedia (Bindea et al. 2013), was used to perform network construction for differentially expressed mRNAs and miRNAs, including only those with predicted interactions and with anti-correlating expression values. Gene ontology analysis (section 2.10.2) and literature review was then used to further refine the list and identify key, relevant interactions in colorectal cancer for further investigation.

### 2.9.4 lncRNA-miRNA-mRNA network analysis

lncRNA-miRNA-mRNA networks were produced from the top lncRNA hits selected during high-throughput screening and miRNA-mRNA interactions found in section 2.10.3. lncRNA-miRNA interactions were predicted using a sequence based algorithm called DIANA-LncBase V2 (threshold  $\geq 0.6$ ) (Paraskevopoulou et al. 2016). Some lncRNAs were excluded as they were not listed within the prediction program or their targets were not within the list of butyrate dysregulated miRNAs. The Cytoscape application, Cluepedia (Bindea et al. 2013), was then used to construct a network based on these interactions with miRNAs and their target genes due to the known role of lncRNAs as miRNA sponges and the ability of miRNAs to regulate lncRNAs (section 1.5.2). Literature review was then used to further refine the list and identify key, relevant interactions in colorectal cancer for further investigation.

## 2.10 Flow cytometry

CRC cells were further investigated for changes in cell growth and death using flow cytometry. HCT116 cells were reverse transfected with NC or miRNA mimics as per previous protocols for 48 h followed by 24 h butyrate treatment. Cells were seeded at 200,000 cells per well in a 6 well plate. Supernatant was collected in 2 ml

microcentrifuge tubes and combined with 200  $\mu$ l trypsinised cells from the corresponding well.

### 2.10.1 Cell cycle analysis

Cells were spun at 300 g for 5 minutes and resuspend in 1 ml of 1X PBS in a 1.5 ml microcentrifuge tube. The pellet was resuspended in 200  $\mu$ l of 1X PBS by pipetting vigorously several times to create a single cell suspension. Cells were vortexed and 800  $\mu$ l of 100% cold ethanol was added dropwise to get a final concentration of 80% ethanol. Samples were transferred to -20°C for 2 h and then immediately centrifuged at 300 g for 10 minutes. Cells were washed with 1 ml of cold 1X PBS and spun at 600 g for 10 minutes at 4°C. Cells were resuspended in 400  $\mu$ l staining PI/RNase/Triton-x solution (Table 2-5) and passed through cell strainer FACS tube tops (Thermo Fisher Scientific). Cells were incubated for 30 minutes in the dark at RT and analysed or stored at 4°C and read within 48 h. The cells were not synchronised as there are several disadvantages in synchronising cells including the induction of cell death and alterations to their metabolic state (Davis et al. 2001). As butyrate and miRNAs regulate these pathways and cell death was a particular focus of this project, synchronisation would not have led to a true representation of the cellular response; therefore, cells were not serum starved (Davis et al. 2001).

### 2.10.2 Cell death analysis

Cells were centrifuged at 10000 rpm for 5 min at 4°C. The media was removed, and the pellet resuspend in 1 ml 1X PBS. Centrifugation and resuspension steps were repeated once. Pellets were resuspended in 100  $\mu$ l 1X annexin V binding buffer (BD Biosciences, New South Wales, Australia). To each tube 2  $\mu$ l of annexin V (BD Biosciences) and 5  $\mu$ l of PI (BD Biosciences) were added. Tubes were gently vortexed and incubated for 15 minutes at RT in the dark. After incubation, 100  $\mu$ l of 1X Binding Buffer was added to each tube. Tubes were stored on ice and analysed within 1 h.

### 2.10.3 Flow cytometry analysis

Cell cycle and cell death data were analysed using the flow cytometry analysis program, CytExpert (Beckman Coulter, California, USA). Cell percentages were collected and presented as mean  $\pm$  standard error of the mean (SEM) including a minimum of three biological replicates. Data were statistically analysed using GraphPad Prism using an unpaired Student's t-test, with a P value < 0.05 considered statistically significant.

## 2.11 Reagents and equipment used for experiments

Table 2-1: Chemicals, consumables and reagents

Reagent	Supplier
Agilent RNA 6000 Nano chip	Agilent Technologies, California, USA
Agilent RNA 6000 Nano kit	Agilent Technologies, California, USA
AmpliTaq Gold DNA polymerase	Applied Biosystems, California, USA
Annexin V	BD Biosciences, New South Wales, Australia
Annexin V Binding Buffer	BD Biosciences, New South Wales, Australia
ApoLive-Glo Multiplex assay	Promega, Wisconsin, USA
Bovine serum albumin	Sigma-Aldrich, Missouri, USA
Buffered Formalin (10%)	Orion Labs, California, USA
CellPlayer™ 96-well Caspase 3/7 reagent	Essen Bioscience, Michigan, USA
Chloroform	Chem-supply, South Australia, Australia
Complete Mini Protease Inhibitor Cocktail Tablets	Roche, Basel, Switzerland
Crystal Violet	Sigma-Aldrich, Missouri, USA
DharmaFECT 2 Transfection Reagent	Dharmacon, Colorado, USA
Dimethyl sulfoxide	Sigma-Aldrich, Missouri, USA
DL-Dithiothreitol	Sigma-Aldrich, Missouri, USA
DNase inactivation slurry	Ambion, California, USA
dNTP mix	Promega, Wisconsin, USA
Dual Luciferase Reporter Assay	Promega, Wisconsin, USA
Dulbecco's Modified Eagle Medium	Thermo Fisher Scientific, New South Wales, Australia
Enhanced chemiluminescence reagents	BioRad, California, USA
E-plate 16	Roche, Basel, Switzerland
Ethanol	Chem-supply, South Australia, Australia
EZQ Protein Quantitation kit	Thermo Fisher Scientific, New South Wales, Australia
Foetal bovine serum	Bovogen Biologicals, Victoria, Australia
Glycine	Sigma-Aldrich, Missouri, USA
Greiner 96/24/6 well plates	Greiner Bio-One, Frickenhausen, Germany
Human Lincode siRNA SMARTpool Library V54	Dharmacon, Colorado, USA
Human miRIDIAN miRNA Mimic Library V16	Dharmacon, Colorado, USA
Hydrochloric acid	Chem-supply, South Australia, Australia
Isopropanol	Chem-supply, South Australia, Australia
Lipofectamine 2000 Transfection Reagent	Thermo Fisher Scientific, New South Wales, Australia
Mammary Epithelial Cell Growth Medium	Lonza, Basel, Switzerland
McCoy's 5A (Modified) Medium	Thermo Fisher Scientific, New South Wales, Australia
M-MLV Reverse Transcriptase, RNase H minus, Point mutant	Promega, Wisconsin, USA
Opti-MEM Reduced Serum Medium	Thermo Fisher Scientific, New South Wales, Australia
Ovalbumin (2mg/ml)	BioRad, California, USA
Phosphate Buffer Saline	Sigma-Aldrich, Missouri, USA
Polyvinylidene Fluoride (PVDF) membrane	BioRad, California, USA
Power SYBR Green Master Mix	Applied Biosystems, California, USA
Pre-stained protein markers (7-190 kDa or 11-195 kDa)	New England Biolabs, Massachusetts, USA
Propidium Iodide (PI)	BD Biosciences, New South Wales, Australia
Protein loading dye	New England Biolabs, Massachusetts, USA
Random Primer 6	New England Biolabs, Massachusetts, USA
RQ1 RNase-Free DNase kit	Promega, Wisconsin, USA
Skim milk powder	Fonterra, Victoria, Australia
Sodium butyrate	Sigma-Aldrich, Missouri, USA
Sodium chloride	Chem-Supply, South Australia, Australia
Sodium dodecyl sulfate	Sigma-Aldrich, Missouri, USA
TaqMan MicroRNA Reverse Transcription Kit	Applied Biosystems, California, USA
TOPflash and FOPflash vectors	Merck, New Jersey, USA
Triton X-100	Sigma-Aldrich, Missouri, USA
Trizma Base	Sigma-Aldrich, Missouri, USA
TRIzol Reagent	Thermo Fisher Scientific, California, USA
TruSeq small RNA Library Preparation	Illumina Inc., California, USA
TruSeq Stranded Total RNA Sample Preparation Kit	Illumina Inc., California, USA
TrypLE Express (trypsin)	Thermo Fisher Scientific, New South Wales, Australia
Tween-20	Sigma-Aldrich, Missouri, USA
Whatman filter paper	Whatman, Kent, UK

## CHAPTER 2

**Table 2-2 Equipment and Software**

Equipment	Supplier
Agilent 2100 Bioanalyzer	Agilent Technologies, California, USA
Allegra X-22 R centrifuge	Beckman Coulter, California, USA
BioTek EL406 Liquid Handler	BioTek, Vermont, USA
Brightline Hemocytometer	Sigma-Aldrich, Missouri, USA
ChemiDoc Image System	BioRad, California, USA
CO2 water jacketed cell incubator	Forma Scientific, Ohio, USA
Cytation 3 plate readers	BioTek, Vermont, USA
CytExpert	Beckman Coulter, California, USA
Cytoscape software (version 3.4.0)	National Institute of General Medical Sciences, Maryland, USA
Dry block heater	Thermoline L+M, New South Wales, Australia
Ensiht Multimode Plate Reader	Perkin Elmer, Massachusetts, USA
FCS Express 6	De Novo Software, California, USA
Gel tank blotting system	BioRad, California, USA
GraphPad Prism	GraphPad Software Inc, California, USA
IKA vortexer	Applied Biosystems, California, USA
Illumina Nextseq sequencing platform	Illumina Inc., California, USA
Image Lab 4.1	BioRad, California, USA
IncuCyte FLR System	Essen Bioscience, Michigan, USA
IncuCyte Object Counting v2.0 analysis software	Essen Bioscience, Michigan, USA
αInfusion plate reader	Perkin Elmer, Massachusetts, USA
Ingenuity Pathway Analysis Software	Ingenuity Systems, Redwood City, CA, USA
Microcentrifuge 5424	Eppendorf, Hamburg, Germany
Mr. Frosty	Thermo Fisher Scientific, New South Wales, Australia
Nanodrop-8000	Thermo Fisher Scientific, New South Wales, Australia
Power-Pac Basic	BioRad, California, USA
Programmable Thermal Controller	MJ Research, Massachusetts, USA
Rocking platform	Ratek, Victoria, Australia
Rotorgene Q and machine software	Qiagen, California, USA
SciClone ALH3000 Lab Automation Liquid Handler	Caliper Lifesciences, Massachusetts, USA
Synergy H4 plate readers	BioTek, Vermont, USA
Tempette Junior TE-85 water bath	Techne, Staffordshire, UK
Turbo Semi-wet Transfer System	BioRad, California, USA
Ultra-low temperature freezer (-80°C)	Thermo Scientific Revco, Massachusetts, USA
Veriti Thermocycler	Applied Biosystems, California, USA
Weigh scales	Shimadzu, Kyoto, Japan
xCELLigence RTCA DP instrument	Roche, Basel, Switzerland

**Table 2-3: Primers and Oligonucleotides**

Assay	Assay ID	Supplier
Random primer 6	S1230S (5' d (N <sub>6</sub> ) 3' [N=A,C,G,T])	New England Biolabs, Massachusetts, USA
<b>Taqman assays:</b>	<b>Assay ID</b>	<b>Supplier</b>
hsa-miR-139-5p	005364_mat	Applied Biosystems, Foster City, CA, USA
hsa-miR-200b-3p	002251	
hsa-miR-200c-3p	002300	
hsa-miR-335-3p	002185	
hsa-miR-381-3p	000571	
hsa-miR-542-3p	001284	
RNU6B	001093	
<b>miRNA oligonucleotide duplexes:</b>	<b>Sequences</b>	<b>Supplier</b>
hsa-miR-125b-1-3p sense	5' ACGGGUUAGGCUCUUGGGAGCU 3'	GenePharma, Shanghai, China
hsa-miR-125b-1-3p antisense	5' CUCCCAAGAGCCUAACCCGUUU 3'	
hsa-miR-139-5p sense	5' UCUACAGUGCACGUGUCUCCAGU 3'	
hsa-miR-139-5p antisense	5' UGGAGACACGUGCACUGUAGAUU 3'	
hsa-miR-181a-5p sense	5' AACAUUCAACGCUGUCGGUGAGU 3'	
hsa-miR-181a-5p antisense	5' UCACCGACAGCGUUGAAUGUUUU 3'	
hsa-miR-200b-3p sense	5' UAAUACUGCCUGGUAUUGAUGA 3'	
hsa-miR-200b-3p antisense	5' AUCAUUACCAGGCAGAUUUUU 3'	
hsa-miR-200c-3p sense	5' UAAUACUGCCGGGUAUUGAUGGA 3'	
hsa-miR-200c-3p antisense	5' CAUCAUUACCGGCAGUAUUUU 3'	
hsa-miR-335-3p sense	5' UUUUUAUUUUGCUCUCCUGACC 3'	
hsa-miR-335-3p antisense	5' UCAGGAGCAAUUAUGAAAAUUU 3'	
hsa-miR-542-3p sense	5' UGUGACAGAUUGAUAAACUGAAA 3'	
hsa-miR-542-3p antisense	5' UCAGUUAUCAUCUGUCACAAU 3'	
hsa-miR-593-3p sense	5' UGUCUCUGCGGGGUUUUCU 3'	

CHAPTER 2

hsa-miR-593-3p antisense	5' AAACCCAGCAGAGACAUU 3'	
hsa-miR-1227-3p sense	5' CGUGCCACCCUUUUCGCCAG 3'	
hsa-miR-1227-3p antisense	5' GGGGAAAAGGGUGGCACGUU 3'	
Negative control sense	5' UUCUCCGAACGUGUCACGUTT 3'	
Negative control anti-sense	5' ACGUGACACGUUCGGAGAATT 3'	
<b>Gene specific primers</b>	<b>Sequences</b>	<b>Supplier</b>
ACTNB Forward	5' TTGCCGACAGGATGCAGAAG 3'	Sigma–Aldrich, Missouri, USA
ACTNB Reverse	5' GCCGATCCACACGGAGTACT 3'	
AKT3 Forward	5' CCTTCCAGACAAAAGACCGTT 3'	GeneWorks Thebarton, South Australia
AKT3 Reverse	5' CGACAAAATGGAAAAACAGCTCG 3'	
B2M Forward	5' GCCGTGTGAACCATGTGACTTT 3'	
B2M Reverse	5' CCAAATGCGGCATCTTCAA 3'	
BCL2 Forward	5' CAGGATAACGGAGGCTGGGATG 3'	
BCL2 Reverse	5' AGAAATCAAACAGAGGCCGCA 3'	
BIRC5 Forward	5' ACTGAGAACGAGCCAGACTTG 3'	
BIRC5 Reverse	5' TGTTCTCTATGGGGTCGTC 3'	
CBL Forward	5' ATCCAGAGTTCACGAGCAT 3'	
CBL Reverse	5' GCTCTCGGTGATAGATGGCG 3'	
CCND1 Forward	5' GATCAAGTGTGACCCGACTG 3'	
CCND1 Reverse	5' CCTTGGGGTCCATGTTCTGC 3'	
CDK19 Forward	5' TATGGGGGAAGCAGACAATGG 3'	
CDK19 Reverse	5' AACAAAATCCTCCACCCGCTC 3'	
COX2 Forward	5' GCTGTTCCACCCATGTCAA 3'	
COX2 Reverse	5' AAATTCGGTGTGAGCAGT 3'	
DUSP1 Forward	5' AGGACAACCACAAGGCAGAC 3'	Integrated DNA Technologies, Iowa, USA
DUSP1 Reverse	5' TCCAGCATCTTGATGGAGTCTATG 3'	
DVL3 Forward	5' TGGACGACGATTTCCGGAGTG 3'	GeneWorks Thebarton, South Australia
DVL3 Reverse	5' GCTCCGATGGGTTATCAGCA 3'	
EEF2K Forward	5' CAGCTCTGGACGGGTATGTG 3'	
EEF2K Reverse	5' CCCCCAAAATGGACTTCCCGA 3'	
EIF4G2 Forward	5' TGTTCCAGTGAAATCAGTGGC 3'	Integrated DNA Technologies, Iowa, USA
EIF4G2 Reverse	5' GCAGTGGTTAGGTCAAATGCAG 3'	
ERBB2 Forward	5' AGATTGCCAAGGGATGAGC 3'	GeneWorks Thebarton, South Australia
ERBB2 Reverse	5' GCCAGCCCGAAGTCTGTAAT 3'	
FN1 Forward	5' ACAAACACTAATGTTAATTGCCCA 3'	Integrated DNA Technologies, Iowa, USA
FN1 Reverse	5' CGGGAATCTTCTGTGACCC 3'	
FOS Forward	5' GGAGAATCCGAAGGGAAAGGA 3'	GeneWorks Thebarton, South Australia
FOS Reverse	5' AGTTGGTCTGTCTCCGCTTG 3'	
FZD4 Forward	5' AACGTGACCAAGATGCCCA 3'	
FZD4 Reverse	5' TAAACAGAACAAAGGAAGAAGTGC 3'	
GAB2 Forward	5' CCCACCGCAAGCCATCTA 3'	
GAB2 Reverse	5' TCTCCTTGTCCACCTGAACG 3'	
GAPDH Forward	5' TGCACCACCACTGCTTAGC 3'	
GAPDH Reverse	5' GGCATGGACTGTGGTCATGAG 3'	
GPO1	5' ACTCTACGGGAGGCAGCAGTA 3'	
GRB2 Forward	5' GCAAAAATCCCGAGGCCAAG 3'	
GRB2 Reverse	5' TTCCAAACTTGACAGAGAGGGAG 3'	
HNF1A Forward	5' TATGCTCATCACCGACACCAC 3'	
HNF1A	5' TGAGGTGAAGACCTGCTTGG 3'	
HRAG-1 Forward	5' AGGAATTTAACTCACAACTGC 3'	
HRAG-1 Reverse	5' GCCATGAAGAGCAGTGAATTA 3'	
IGF1R Forward	5' AAGGGATGAAGTCTGGCTCCG 3'	
IGF1R Reverse	5' CCCGAGATTTCTCCACTCG 3'	
JUN Forward	5' CCGGCTGGAGGAAAAAGTGA 3'	
JUN Reverse	5' GCGTTAGCATGAGTTGGCAC 3'	
KRAS Forward	5' GGTGAGGGAGATCCGACAAT 3'	
KRAS Reverse	5' AGGCATCATCAACACCAGATT 3'	
LRP6 Forward	5' TTTGGATGGGACAGAACGGG 3'	
LRP6 Reverse	5' TCCGGTTAGCACTGAGAGA 3'	
MALAT1 Forward	5' GTTCAGTGTCTTTAGTGCATTGTT 3'	Integrated DNA Technologies, Iowa, USA
MALAT1 Reverse	5' GCTGAGTGTCTTGCATGT 3'	
MAP3K8 Forward	5' TGGCGTGTAACCTGATCCCA 3'	GeneWorks Thebarton, South Australia
MAP3K8 Reverse	5' CCCTCGCTGCTTCCATAAA 3'	
MET Forward	5' ACCAAGTCAGATGTGTGGTCC 3'	
MET Reverse	5' GTCTGGGCAGTATTCGGGTT 3'	
MGSO	5' TGCACCATCTGTCACTCTGTTAACCTC 3'	
NUP62 Forward	5' TTCTCTGTTGCAGAAACCCAC 3'	
NUP62 Reverse	5' GCCTTGGGAAGATTCGCTC 3'	
PAK2 Forward	5' CCGGGAGCTCTGACCGA 3'	
PAK2 Reverse	5' TCAGAATTATGAAATGGCCCCG 3'	

## CHAPTER 2

<b>PIK3R3 Forward</b>	5' CTTGCTGCTCTGTGGCCGAT 3'	
<b>PIK3R3 Reverse</b>	5' TGGAGCACTAGCTCCTCAGA 3'	
<b>PRKAA2 Forward</b>	5' GGCAAAGTGAAGATTGGAGAACA 3'	
<b>PRKAA2 Reverse</b>	5' TCCAACAACATCTAAACTGCCA 3'	
<b>STAT3 Forward</b>	5' GAAACAGTTGGGACCCCTGA 3'	
<b>STAT3 Reverse</b>	5' AGGTACCGTGTGTCAAGCTG 3'	
<b>TRIM29 Forward</b>	5' GCCACGTTGAGAAGATGTGC 3'	
<b>TRIM29 Reverse</b>	5' GATGGTCACCACCGTTCTCC 3'	
<b>WEE1 Forward</b>	5' AAGTGTGTGAAGAGGCTGGA 3'	Integrated DNA Technologies, Iowa, USA
<b>WEE1 Reverse</b>	5' TCTCAAAGCGTTCTGTCATC 3'	
<b>ZEB1 Forward</b>	5' GATGACCTGCCAACAGACCA 3'	GeneWorks Thebarton, South Australia
<b>ZEB1 Reverse</b>	5' TCTTGCCTTCCCTTCTGTCA 3'	
<b>siRNAs</b>	<b>Sequence</b>	<b>Supplier</b>
<b>DVL3_7 FlexiTube siRNA</b>	5' CTGCGGGAGATTGTGCACAAA 3'	Qiagen, California, USA
<b>EIF4G2_5 FlexiTube siRNA</b>	5' ACGATCAATCAAATTCGTCAA 3'	
<b>PIK3R3_8 FlexiTube siRNA</b>	5' CAGGGCTGTAGTATTTCAGTAA 3'	
<b>Negative control siRNA</b>	5' AATTCTCCGAACGTGTACACGT 3'	

**Table 2-4: Antibodies**

Antibody	Dilution	Supplier
<b>CCND1 (92G2)</b>	1:1000	Cell Signalling Technology, Massachusetts, USA
<b>COX2</b>	1:1000	Cell Signalling Technology, Massachusetts, USA
<b>DVL3</b>	1:1000	Cell Signalling Technology, Massachusetts, USA
<b>eEF2K</b>	1:1000	Cell Signalling Technology, Massachusetts, USA
<b>NUP62 (ab140651)</b>	1:1000	Abcam, Massachusetts, USA
<b>PI3 Kinase p55 (D2B3)</b>	1:1000	Cell Signalling Technology, Massachusetts, USA
<b>TRIM29 (GTX115749)</b>	1:500	GeneTex, California, USA

**Table 2-5: Buffers and Solutions**

Buffer/ solution	Formula
<b>RIPA buffer</b>	Final concentrations: 10 mM Tris/HCl pH 7.4, 150 mM NaCl, 1 mM EGTA, 1% Triton X-100, 1% deoxycholate, 0.1% SDS, 1 mM DDT. For 50 mM: 0.5 ml 1M Tris/HCl, 6.25 ml 1.2 M NaCl, 1 ml 50 mM EGTA, 0.5 ml Triton X-100, 5 ml 10% deoxycholate, 0.5 ml 10% SDS, 50 µl 1M DTT, water to 50 ml.
<b>5× SDS Running buffer</b>	Final concentrations: 125 mM Tris Base, 1 M Glycine, 0.5% SDS. For 500 ml: 7.57 g Tris/HCl, 37.5 g Glycine, 25 ml of 10% SDS, water to 500 ml.
<b>Western Transfer buffer</b>	For 1 L: 200 ml of 5x BioRad Transfer buffer, 600 ml 100% ethanol, water to 1 L.
<b>10× TBS</b>	Final concentrations: 0.2 M Tris Base, 1.37 M NaCl. For 500 ml: 12.1 g Tris Base, 40 g NaCl, water to 500 ml. pH adjusted to 7.6 using conc. HCl.
<b>1× TBS-T</b>	Final concentrations: 1× TBS, 0.1% Tween-20 For 500 ml: 50 ml 10× TBS, 5 ml 10× Tween-20, water to 500 ml.
<b>Cell cycle staining solution</b>	Final concentrations: 200 µg/ml RNASE A, 50 µg/ml PI, 0.1% Triton X-100, 1×PBS For 1 ml: 200 µl 1mg/ml RNASE A, 50 µl 1mg/ml PI, 100 µl 1% Triton X-100, 650 µl 1× PBS

# Chapter 3. High-throughput functional microRNA screen and validation

---

## 3.1 Introduction

Butyrate is a naturally occurring HDACi with the ability to decrease proliferation and increase apoptosis in CRC cells by altering global histone acetylation and consequently global gene expression. This chemo-protective fermentation product has been found to alter the expression of non-coding RNAs, including miRNAs, in order to mediate its anticancer effects in CRC cells through various cellular pathways including apoptosis and the cell cycle (Wu et al. 2018c). Interestingly, it has been shown that the manipulation of tumour suppressor miRNAs in a combined cell treatment with butyrate, including the oncogenic miR-17-92a cluster member miR-18a, can enhance the anticancer properties of butyrate in CRC cells (Humphreys et al. 2014b). miRNAs are known to regulate similar pathways and molecules compared to butyrate, so this is not unexpected. This novel finding warranted the further investigation of other miRNAs with the ability to enhance the anticancer properties of butyrate given that miRNA replacement therapy has shown promising results (Beg et al. 2017) and this may reveal novel therapeutic miRNAs. In this study, enhancement of the butyrate response in CRC cells by non-coding RNAs refers to the greater decrease in proliferation or increase in apoptosis observed in the combination treatments, which may be synergistic or additive in nature. Both combinatorial effects were considered as they could potentially be useful in the development of different therapeutic approaches. The investigation of these functional RNA molecules may also further reveal how butyrate influences key cell growth and death pathways in CRC and assist in identification of potential therapeutic miRNA target genes.

To investigate butyrate-sensitising miRNAs with the ability to enhance the anticancer properties of butyrate, unbiased high-throughput functional screening (performed by Dr. Karen Humphreys) was used to identify miRNAs for further investigation (section 1.9). miRNA and predicted miRNA target gene validation was completed using real-time cell analysis assays, pathway analysis, real-time RT-PCR, western blotting and pathway specific assays. This chapter contains data collected during this candidature, but

it is based on the continuation of an undergraduate Honours project outlined in section 1.9.

## 3.2 Results

### 3.2.1 Butyrate-sensitising miRNA selection

Based on the functional high-throughput screen performed (Ali 2014), 13 butyrate-sensitising miRNAs were identified (refer to section 1.9) and of those four were further validated in this study. miR-593 and miR-1227 butyrate-sensitising miRNAs were previously selected for validation (section 1.9); however, the candidate miRNA and gene lists were expanded to also include miR-125b and miR-181a. miRNAs were initially selected based on their significance in which those candidate miRNAs with the lowest P-values had the greatest butyrate-sensitising ability (Ali 2014). However, as the project progressed, coefficient of drug interaction (CDI) was substituted as it was found to be a more suitable indicator of synergistic interactions with butyrate (Table 3-1). miR-1227 had the lowest CDI value at 0.19 indicating significant synergism with butyrate. miR-125b had the second lowest CDI value, 0.40. miR-181a was the miRNA with the third lowest CDI value at 0.43. miR-593 was considered borderline synergistic with a CDI value of 0.92; however, as mentioned in section 1.9, it had the most potent ability to decrease growth and increase death alone. This miRNA was therefore selected for further validation due to its individual therapeutic potential. Based on the overall CDI calculations all miRNAs displayed significantly synergistic ( $CDI < 0.7$ ) or synergistic ( $CDI < 1$ ) behaviour when combined with 2.5 mM butyrate treatment. Of the 13 miRNAs identified in the high-throughput screen none had an additive or antagonistic effect when combined with butyrate (Table 3-1).

**Table 3-1 Coefficient of drug interaction values for miRNA and butyrate interactions for xCELLigence proliferation data**

Coefficient of drug interaction values were calculated as described in the methods section. CDI <1, = 1 or >1 indicates that when the miRNA mimic and butyrate combined, they behave synergistically, additively or antagonistically, respectively. CDI <0.7 indicates that the drug is significantly synergistic.

miRNA	CDI value	Classification
miR-29b-2-5p	0.61	Significantly synergistic
miR-125b-1-3p	0.40	Significantly synergistic
miR-181a-5p	0.43	Significantly synergistic
miR-509-5p	0.53	Significantly synergistic
miR-593-3p	0.92	Synergistic
miR-1227-3p	0.19	Significantly synergistic
miR-1231	0.73	Synergistic
miR-1256	0.52	Significantly synergistic
miR-1265	0.50	Significantly synergistic
miR-3151	0.76	Synergistic
miR-3179	0.46	Significantly synergistic
miR-3654	0.54	Significantly synergistic
miR-4252	0.72	Synergistic

### 3.2.2 Further validation of miRNA and butyrate growth and death effects in CRC cells using flow cytometry

#### 3.2.2.1 Effect of miRNAs on apoptosis in CRC in the presence of butyrate

The effect of miRNAs on apoptosis and viability was further investigated using the Cytoflex Flow Cytometer. HCT116 cells were reverse transfected with miRNA mimics (miR-125b, miR-181a, miR-593 or miR-1227) or controls for 48 h; followed by 0 mM or 2.5 mM butyrate treatment for 24 h. Cells were stained with annexin V and propidium iodide to differentiate between viable, early and late apoptotic cells and dead cells as described in Chapter 2. No miRNA alone had a significant effect on viability, which was in contrast to previous observations; however, miR-125b, miR-593 and miR-1227 significantly enhanced the reduction in viability induced by butyrate (Figure 3-1, 3-2). In terms of early apoptosis, miR-125b and miR-181a appeared to have anti-apoptotic effects alone and not have any significant effect in the presence of butyrate. Only miR-593 significantly increased early apoptosis alone; however, both miR-593 and miR-1227 significantly enhanced the pro-apoptotic properties of butyrate. None of the miRNAs influenced late apoptosis alone; however, miR-125b, miR-593 and miR-1227 enhanced the pro-apoptotic effect of butyrate. miR-125b and miR-181a also slightly, but significantly, increased the number of dead cells in the absence of butyrate.

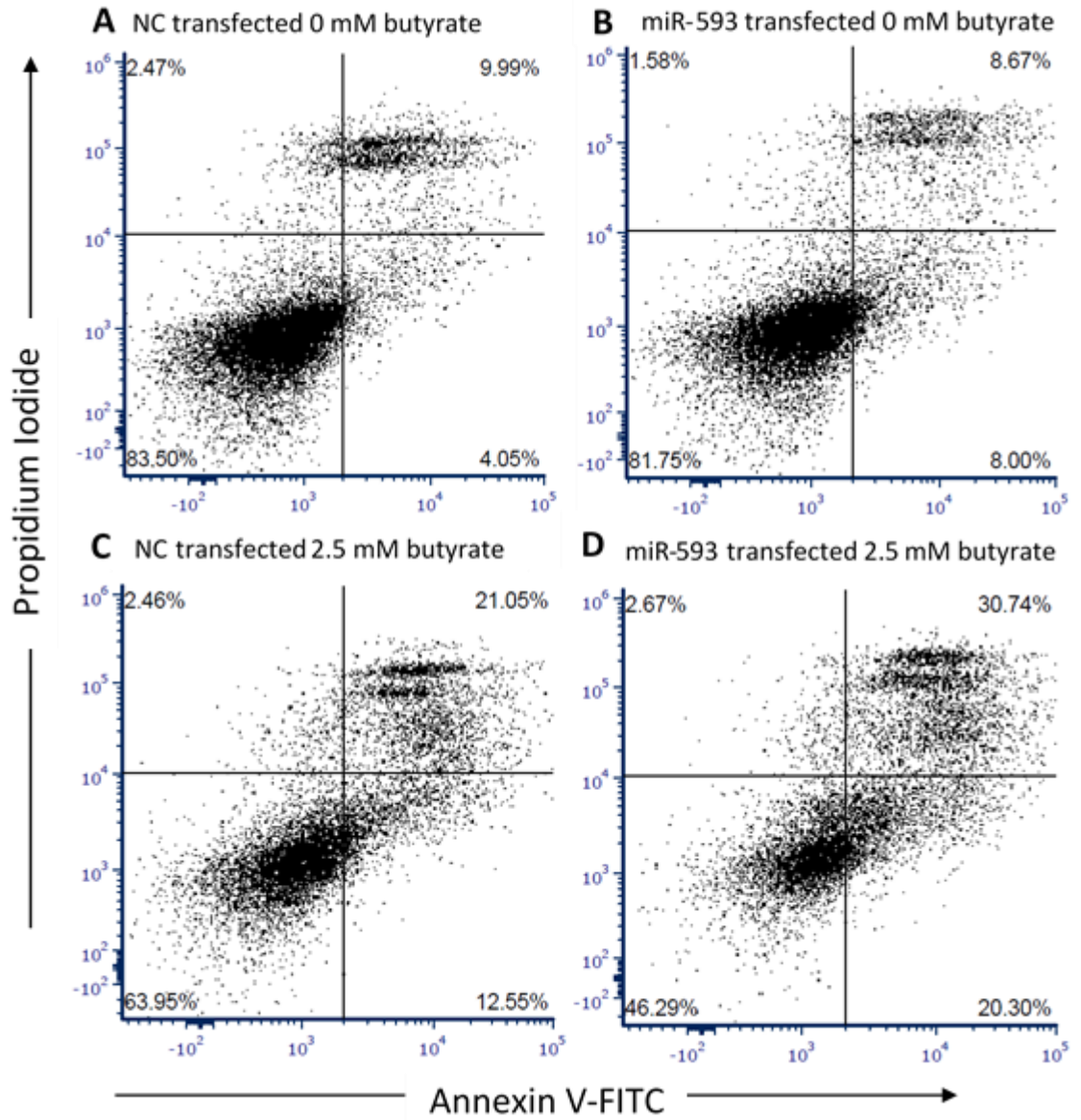


**Figure 3-1** Flow cytometry analysis of apoptosis in miRNA transfected HCT116 cells after 24 h of butyrate treatment

Examples of flow charts depicting the apoptosis analyses of HCT116 cells reverse transfected with NC or miRNA mimics for 48 h, followed by 24 h of treatment with 0 mM or 2.5 mM butyrate, over a 72 h post-transfection period (A) NC transfected 0 mM butyrate, (B) miR-593 transfected 0 mM butyrate, (C) NC transfected 2.5 mM butyrate, (D) miR-593 transfected 2.5 mM butyrate. Cells were stained with propidium iodide and annexin V stain and measured using the Cytoflex Flow Cytometer. NC= Negative Control mimic.

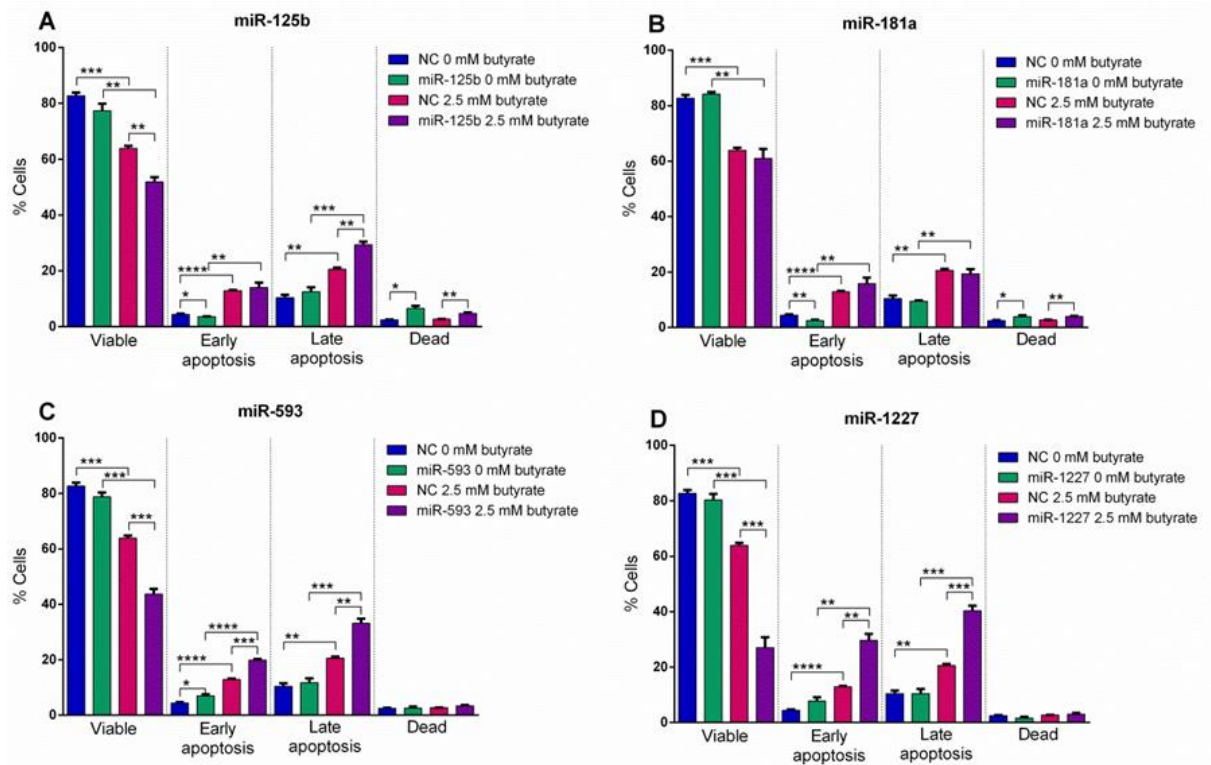


**Figure 3-2** Flow cytometry analysis of apoptosis in miRNA transfected HCT116 cells after 24 h of butyrate treatment

Bar chart showing viability and apoptosis analysis of HCT116 cells reverse transfected with miRNA mimics (A) miR-125b, (B) miR-181a, (C) miR-593, (D) miR-1227 for 48 h, followed by 24 h of treatment with 0 mM or 2.5 mM butyrate, over a 72 h post-transfection period. Cells were stained with propidium iodide and annexin V stain and measured using the Cytoflex Flow Cytometer. The mean  $\pm$  SEM of 3 replicate wells is shown. Significant results are indicated by \*  $P < 0.05$ , \*\*  $P < 0.01$ , \*\*\*  $P < 0.001$ , \*\*\*\*  $P < 0.0001$ . NC= Negative Control mimic.

### 3.2.2.2 Effect of miRNAs on the cell cycle in CRC in the presence of butyrate

miRNAs were further investigated for their role in the butyrate response of CRC cells by determining their effects on the cell cycle. Earlier studies (section 1.9) demonstrated that butyrate-sensitising miRNAs induced cell proliferation changes using the xCELLigence instrument; however, as these changes may have been the result of cell cycle regulation among other cellular effects, it was important to investigate these responses. HCT116 cells were reverse transfected with miRNA mimics or controls for 48 h, followed by 24 h of 0 mM or 2.5 mM butyrate treatment. The Cytoflex Flow Cytometer and propidium iodide staining were used to measure changes in percentage of cells in each cell cycle phase in the CRC cells. The results demonstrated that miR-125b had no effects on any phases alone or in combination with butyrate (Figure 3-4 A). miR-593 or miR-1227 alone significantly increased the percentage of cells in the G<sub>0</sub>/G<sub>1</sub> phase, while miR-181a had no significant effect (Figure 3-3, 3-4 B, C, D). In the

presence of butyrate miR-1227 and miR-181a significantly reduced the percentage of cells in the G<sub>0</sub>/G<sub>1</sub> phase, while miR-593 increased cells in this phase. miR-593 and miR-1227 alone had no significant effects on the S phase; however, miR-181a significantly increased the percentage of cells in the S phase. Interestingly, the combination of butyrate and miR-181a or miR-593 significantly reduced the percentage of cells in the S phase. miR-181a and miR-1227 alone significantly reduced percentage of cells in the S phase. miR-181a and miR-1227 alone significantly reduced percentage of cells in the G<sub>2</sub>/M phase, while miR-593 had no effect. In combination with butyrate, miR-181a and miR-593 significantly increased the percentage of cells in G<sub>2</sub>/M, but miR-1227 combined with butyrate significantly reduced cells in this phase.

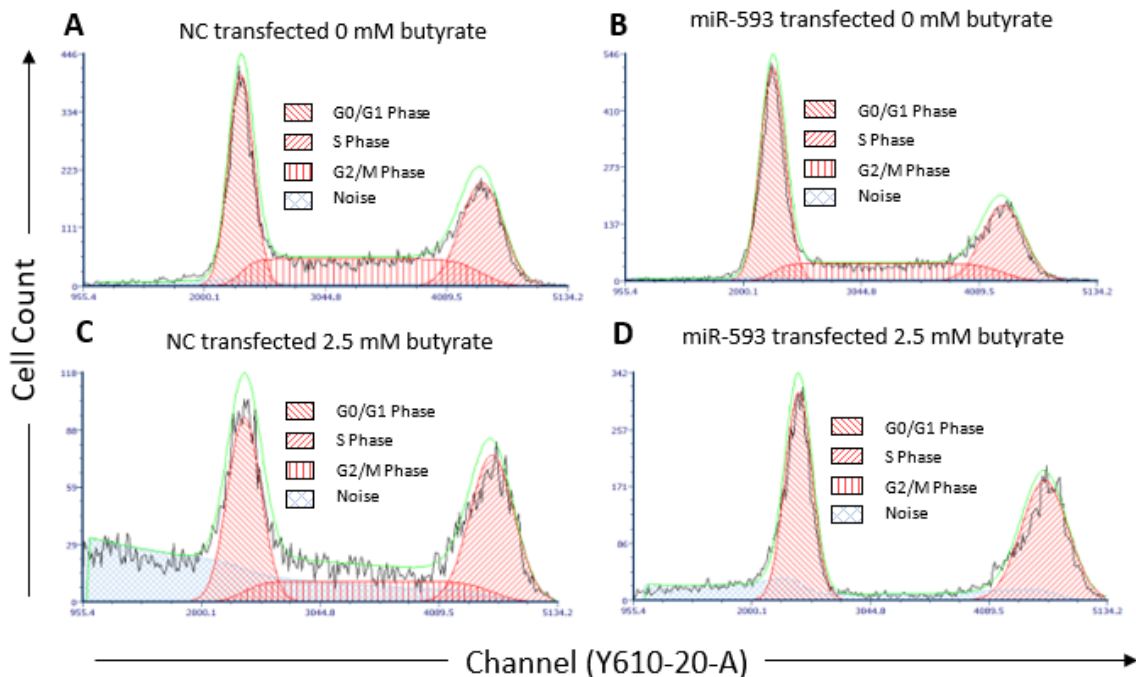


**Figure 3-3** Flow cytometry analysis of the cell cycle in miRNA transfected HCT116 cells after 24 h of butyrate treatment

Examples of flow charts depicting cell cycle analyses of HCT116 cells reverse transfected with NC or miR-593 mimics for 48 h, followed by 24 h of treatment with 0 mM or 2.5 mM butyrate, over a 72 h post-transfection period (A) NC transfected 0 mM butyrate, (B) miR-593 transfected 0 mM butyrate, (C) NC transfected 2.5 mM butyrate, (D) miR-593 transfected 2.5 mM butyrate. Cells were stained with propidium iodide and measured using the Cytoteflex Flow Cytometer. NC= Negative Control mimic.

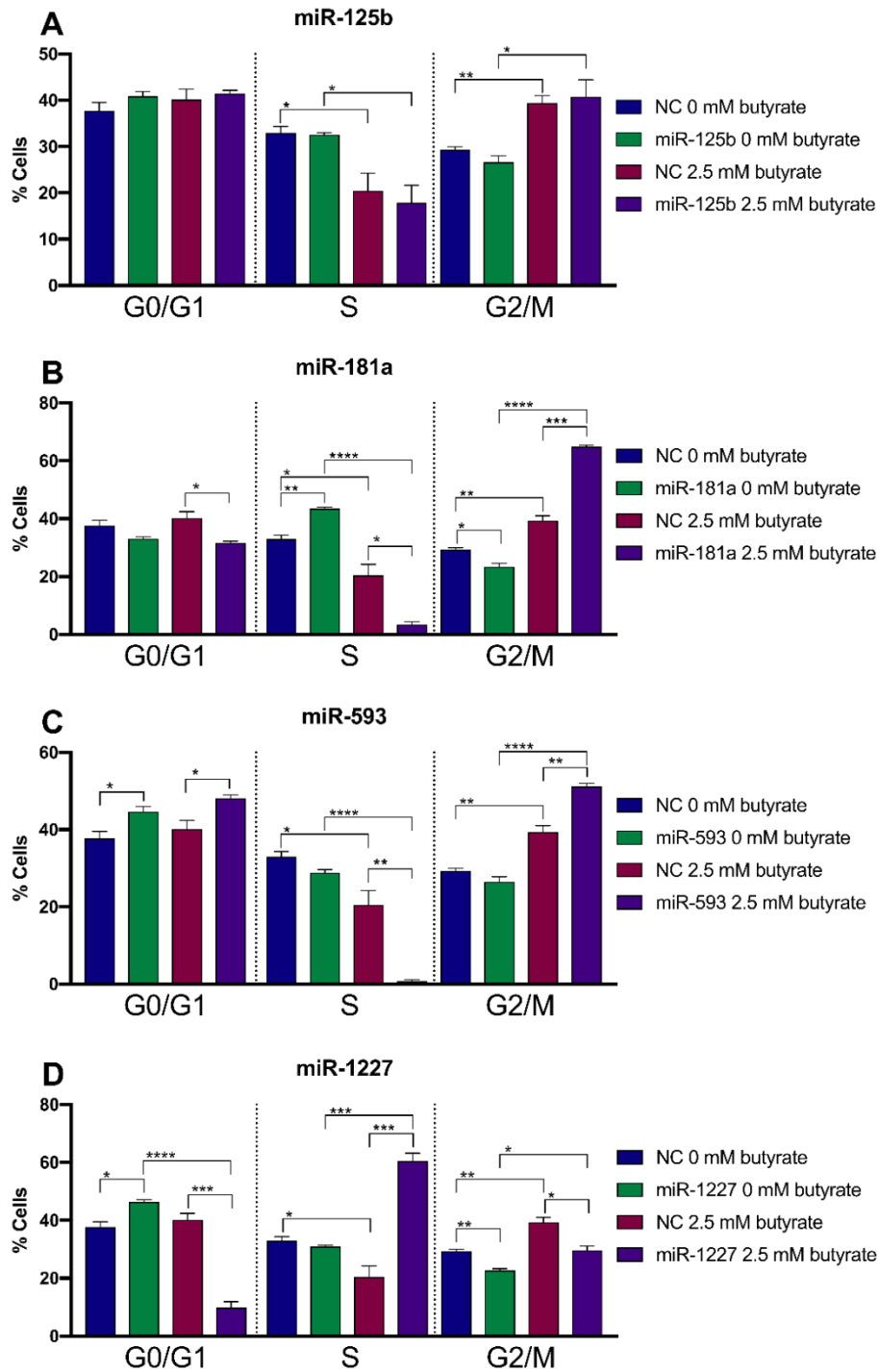


**Figure 3-4** Flow cytometry analysis of the cell cycle in miRNA transfected HCT116 cells after 24 h of butyrate treatment

Bar chart showing cell cycle analysis of HCT116 cells reverse transfected with miRNA mimics (A) miR-125b, (B) miR-181a, (C) miR-593, (D) miR-1227 for 48 h, followed by 24 h of treatment with 0 mM or 2.5 mM butyrate, over a 72 h post-transfection period. Cells were stained with propidium iodide and measured using the Cytoflex Flow Cytometer. The mean  $\pm$  SEM of 3 replicate wells is shown. Significant results are indicated by \*  $P < 0.05$ , \*\*  $P < 0.01$ , \*\*\*  $P < 0.001$ , \*\*\*\*  $P < 0.0001$ . NC = Negative Control mimic.

### 3.2.3 Validation of viability and apoptosis in LIM1215 CRC cells after miRNA mimic transfection and butyrate treatment

The cellular effects of the miRNAs studied were further tested in another CRC cell line, LIM1215, to determine if their effects were consistent in different CRC models. LIM1215 cells have wild type *TP53*, *KRAS*, *BRAF* and *PIK3CA* but mutant  $\beta$ -catenin. As butyrate more readily hyperactivates WNT signalling in CRC cells with high WNT levels in order to induce apoptosis (Lazarova et al. 2004), similar responses to HCT116 cells were expected even with a differing mutational status. The ApoLive-Glo™ Multiplex Assay was used to confirm cell viability and apoptotic changes. Transfection of LIM1215 cells with miRNA mimics, combined with 2.5 mM butyrate treatment, led to significantly decreased viability when compared to NC transfected cells (2.5 mM butyrate) over a 72 h time period for all miRNAs, except miR-125b (Figure 3-5). miRNAs that significantly decreased viability of LIM1215 cells independently of butyrate (NC 0 mM butyrate vs. miRNA 0 mM butyrate) included miR-181a, miR-593 and miR-1227. miR-181a induced the greatest reduction in viability of LIM1215 cells alone ( $P < 0.0001$ ). miR-125b alone significantly increased LIM1215 cell viability. Butyrate alone was able to significantly decrease cell viability within all miRNA experiments (NC 0 mM butyrate vs. NC 2.5 mM butyrate and miRNA 0 mM butyrate vs. miRNA 2.5 mM butyrate) ( $P < 0.01$ ).

Cell apoptosis changes were measured following viability measurements. miRNAs which induced significant increases in apoptosis of LIM1215 cells, both independently of butyrate (NC 0 mM butyrate vs. miRNA 0 mM butyrate), and by enhancing the butyrate effect (NC 2.5 mM butyrate vs. miRNA 2.5 mM butyrate) included miR-181a, miR-593 and miR-1227 (Figure 3-5). miR-125b did not affect apoptosis alone; however, a slight enhancement effect was observed in the presence of butyrate. miR-181a and miR-1227 induced the greatest increases in apoptosis in LIM1215 cells independently ( $P < 0.0001$ ). miR-1227 induced a dramatic increase in apoptosis in the presence of butyrate. Butyrate alone was able to significantly increase apoptosis within all miRNA experiments (NC 0 mM butyrate vs. NC 2.5 mM butyrate and miRNA 0 mM butyrate vs. miRNA 2.5 mM butyrate) ( $P < 0.01$ ).

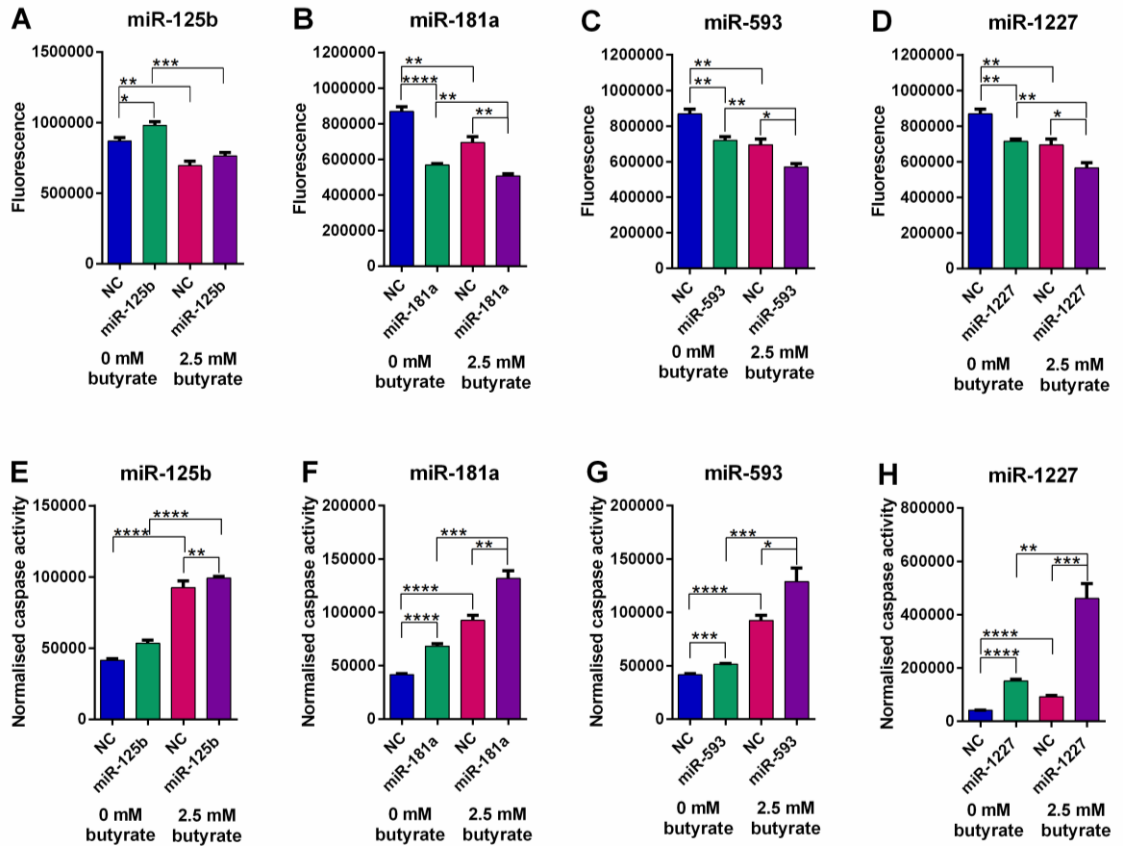


**Figure 3-5 Cell viability and apoptosis in miRNA transfected LIM1215 cells after 24 h of butyrate treatment**

ApoLive-Glo™ Multiplex Assay: fluorescence signal for viability changes (A) miR-125b, (B) miR-181a, (C) miR-593, (D) 1227 and luminescent signal for normalised caspase activity for apoptosis changes (E) miR-125b, (F) miR-181a, (G) miR-593, (H) 1227 in LIM1215 cells transfected with butyrate-sensitising miRNAs for 48 h, followed by 24 h of treatment with 0 mM or 2.5 mM butyrate, over a 72 h post-transfection period. The mean  $\pm$  SEM of 4 replicate wells is shown. Significant results are indicated by \*  $P < 0.05$ , \*\*  $P < 0.01$ , \*\*\*  $P < 0.001$ , \*\*\*\*  $P < 0.0001$ . NC = Negative Control mimic.

### 3.2.4 Investigation of miR-125b in KRAS mutant disrupted cells, Hke3

As previously mentioned, miR-125b induced pro-proliferative effects in LIM1215 cells (Figure 3-5 A) in contrast to the anti-proliferative effects seen in HCT116 cells (Ali 2014). The key difference between these cell lines is *KRAS* status. As previously described, *KRAS* is a commonly mutated gene which contributes to CRC development and progression. The constitutive activation of this GTPase protein contributes to sustained proliferation and survival of cancer cells through aberrant MAPK signalling. *KRAS* mutations occur in around 40% of CRC cases (Di Fiore et al. 2007; Karapetis et al. 2008; Lievre et al. 2006). HCT116 cells have a *KRAS* wild type allele and *KRAS*<sup>G13D</sup> mutant allele, resulting in constitutively activated *KRAS* protein, whereas LIM1215 cells only have *KRAS* wild type alleles. It was hypothesised that the cell growth response of

CRC cells to miR-125b may be KRAS dependent. Hke3 cells are derived from HCT116 cells in which the mutant allele has been knocked out via homologous recombination (Shirasawa et al. 1993), while the wild type allele remains active. The real-time cell analysis platform, xCELLigence, was used to measure cell index over time as a representation of cell proliferation changes in Hke3 cells. miR-125b mimics had no effect alone on Hke3 cell proliferation (Figure 3-6), in contrast to the changes seen in HCT116 and LIM1215 cells. Transfection of Hke3 cells with miR-125b mimics and treatment with 2.5 mM butyrate in combination led to significantly decreased proliferation (NC 2.5 mM butyrate vs. miRNA 2.5 mM butyrate). This requires further investigation.

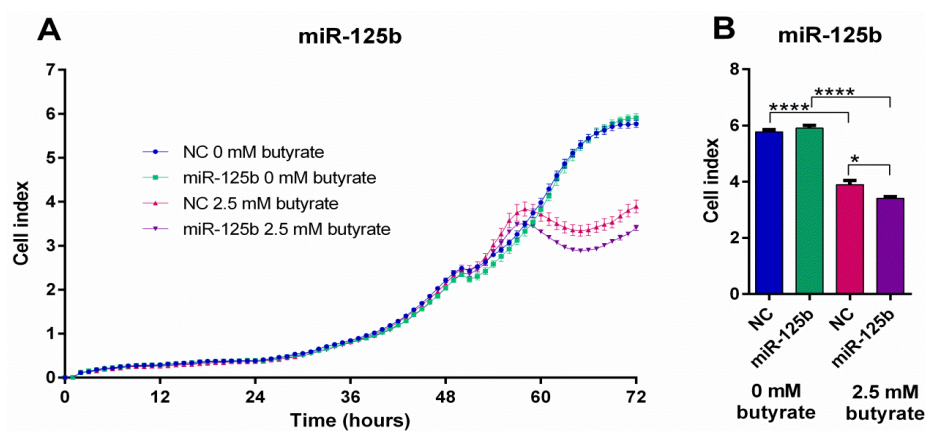


**Figure 3-6 Cell proliferation in miR-125b transfected Hke3 cells after 24 h of butyrate treatment**

Real-time cell index measurements using the xCELLigence RTCA platform, in Hke3 cells transfected with (A) miR-125b for 48 h, followed by 24 h of treatment with 0 mM or 2.5 mM butyrate, over a 72 h post-transfection period. The mean  $\pm$  SEM of 4 replicate wells is shown at 72 h post-transfection (B) miR-125b. Significant results are indicated by \*  $P < 0.05$ , \*\*  $P < 0.01$ , \*\*\*  $P < 0.001$ , \*\*\*\*  $P < 0.0001$ . NC= Negative Control mimic.

### 3.2.5 Investigation of viability and apoptosis in HFF ‘normal’ fibroblasts after miRNA mimic transfection and butyrate treatment

To ensure that the effects of miRNA and butyrate treatments were cancer specific, it was important to assess their toxicity in normal cells. For this purpose, a noncancerous cell line was selected for further investigation. Crystal violet assays were used to assess the viability of a panel of immortalised ‘normal’ human cells to a range of butyrate concentrations (0.5-20 mM) for 24 h (Figure 3-7). HFF cells, which are human foreskin fibroblasts, were the only cell line that did not have a significant response to butyrate, except at the 5 mM concentration. HaCaT human keratinocytes and MCF10A human

breast cells showed a dose-dependent decrease in cell viability when exposed to butyrate. HEK293 human embryonic kidney cells showed a significant decrease in viability in response to butyrate; however, the effect was not dose-dependent.

HFF cells were selected for further validation with the four selected miRNAs due to lack of response to butyrate. HFF cells were reverse transfected with NC or miRNA mimics for 48 h, followed by 2.5 mM butyrate treatment for 24 h for a total growth period of 72 h. The ApoLive-Glo™ Multiplex Assay was performed to determine the changes in cell viability and apoptosis. HFF cell viability did not significantly change in response to any miRNA mimics or butyrate alone or in combination treatments except for the combination of miR-1227 and butyrate which slightly but significantly increased growth (Figure 3-8). Apoptosis data revealed that all miRNAs alone were able to significantly increase apoptosis, while miR-181a, miR-593 and miR-1227 significantly increased growth in combination with butyrate.

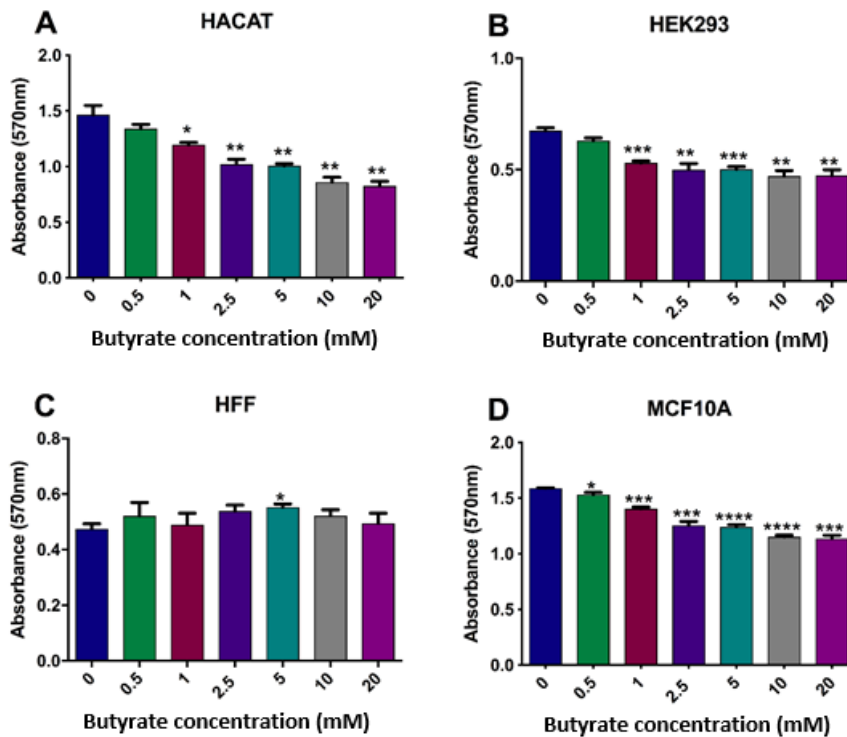


**Figure 3-7 Butyrate response of immortalised 'normal' cells**

Crystal violet assay: Absorbance signal at 570 nm for viability changes in 'normal' cells treated with a range of butyrate concentrations 0, 0.5, 1, 2.5, 5, 10 and 20 mM (A) HaCaT, (B) HEK293, (C) HFF, (D) MCF10A and treated with 0 mM or 2.5 mM butyrate at 48 h, over a 72 h growth period. The mean  $\pm$  SEM of 4 replicate wells is shown. Significant results are indicated by \* P<0.05, \*\* P<0.01, \*\*\* P<0.001, \*\*\*\*P<0.0001. NC= Negative Control mimic.

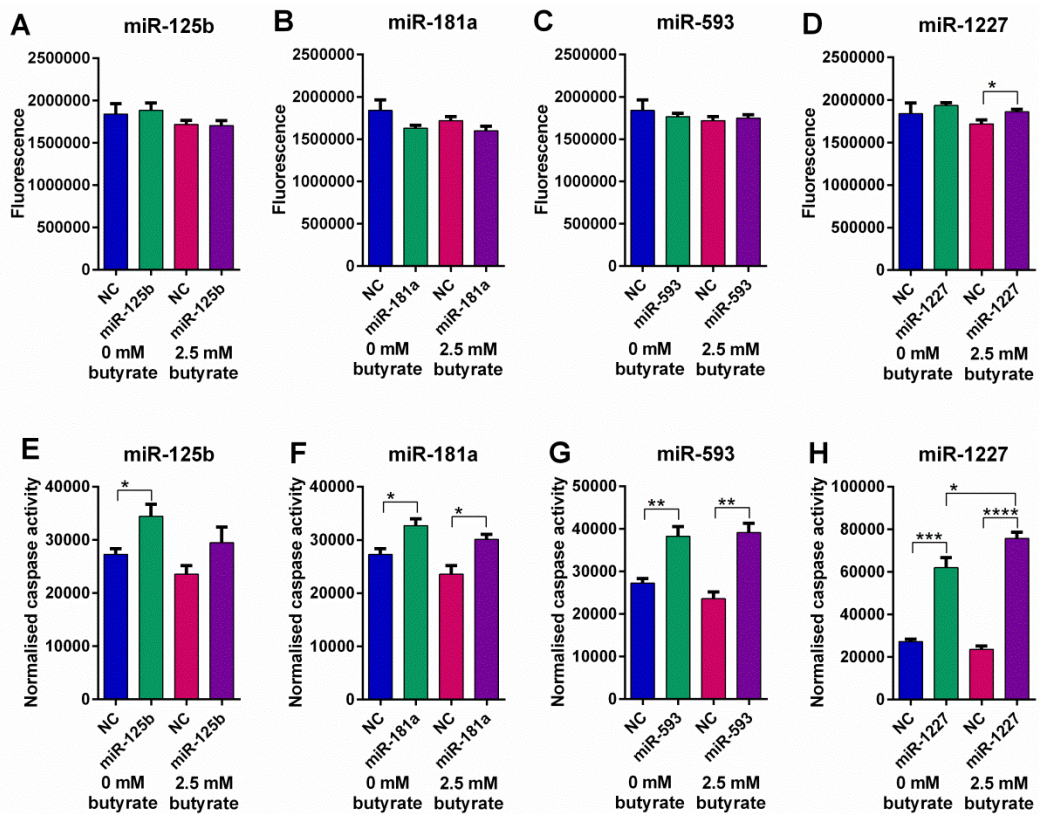


**Figure 3-8 Cell viability and apoptosis in miRNA transfected HFF ‘normal’ cells after 24 h of butyrate treatment**

ApoLive-Glo™ Multiplex Assay: fluorescence signal for viability changes (A) miR-125b, (B) miR-181a, (C) miR-593, (D) 1227 and luminescent signal for normalised caspase activity for apoptosis changes (E) miR-125b, (F) miR-181a, (G) miR-593, (H) 1227 in HFF ‘normal’ cells transfected with butyrate-sensitising miRNAs for 48 h, followed by 24 h of treatment with 0 mM or 2.5 mM butyrate, over a 72 h post-transfection period. The mean  $\pm$  SEM of 4 replicate wells is shown. Significant results are indicated by \*  $P < 0.05$ , \*\*  $P < 0.01$ , \*\*\*  $P < 0.001$ , \*\*\*\*  $P < 0.0001$ . NC = Negative Control mimic.

### 3.2.6 miRNA target prediction using bioinformatics analysis

Following the expanded validation of butyrate-sensitising miRNAs, by analysis of cell proliferation and apoptosis in other cell lines, predicted miRNA target genes were investigated to determine their involvement in the cellular responses observed. Predicted target genes with known oncogenic functions were the primary focus. miR-593 and miR-1227 pathway analyses had already been previously performed using IPA (Ali 2014). Therefore, a new subset of cell growth and death related genes was selected from these analyses as well as some based on their association with CRC for further investigation. miR-125b and miR-181a target genes were identified using the miRWalk target prediction program. This involved collating a list of genes for each miRNA from eight prediction programs, based on a four-hit minimum i.e. four or more programs predict that the mRNAs have 3'UTRs with binding sites for those miRNAs (refer to chapter 2). An open source pathway analysis tool, KEGG Mapper, was utilised to

analyse canonical pathways of miR-125b and miR-181a target genes as IPA was no longer available.

### 3.2.6.1 miR-593 and miR-1227 predicted target genes

As previously mentioned, a new subset of predicted target genes associated with cell growth and death pathways were selected from earlier IPA analyses (Ali 2014). The literature was also used to help refine the final gene list. The new target gene list for miR-593 included *CCND1* (1 predicted binding site), *PAK2* (1 predicted binding site), *EEF2K* (3 predicted binding site), *ERBB2* (1 predicted binding site). The new target gene list for miR-1227 included *CDK19* (1 predicted binding site), *GRB2* (1 predicted binding site) and *PAK2* (1 predicted binding site).

### 3.2.6.2 KEGG mapper analysis of miR-125b predicted target genes

miRWalk analysis involved the collation of 82 predicted target genes of miR-125b for further bioinformatics analysis. The predicted target gene list was refined by selecting the top CRC cell growth and death related pathways with the largest representation of target genes including Pathways in Cancer (5 molecules) (Figure 3-9), RAS Signalling Pathway (4 molecules), MAPK Signalling Pathway (3 molecules), PI3K-AKT signalling (3 molecules) and WNT signalling (3 molecules) (refer to Appendix 1). Target genes were further investigated through reviewing the literature and selected if they were reported to be involved in promoting cell proliferation and inhibiting apoptosis in CRC. Due to the small number of target genes collated from pathway analysis, other target genes that were not in KEGG Mapper pathways were selected based on the literature for relevance in CRC as well as their oncogenic potential. A small list of target genes was assembled with the above criteria and 3'UTR binding site information collected from miRanda. These genes included *TRIM29* (1 predicted binding site), *IGF1R* (1 predicted binding site) and *ZEB1* (1 predicted binding sites). Refer to Table 2-3 for primer sequences.

### 3.2.6.3 KEGG mapper analysis of miR-181a predicted target genes

miRWalk analysis involved the collation of 4270 predicted target genes of miR-181a for further bioinformatics analysis. The predicted target gene list was refined by selecting the top CRC cell growth and death related pathways with the largest representation of target genes including Pathways in cancer (30 molecules), PI3K-AKT signalling pathway (16 molecules), MAPK signalling pathway (15 molecules), RAS signalling pathway (13 molecules) and Apoptosis (8 molecules). As an example, some genes were found to be involved in the PI3K-AKT signalling pathway (Figure 3-10). Other signalling pathways

## CHAPTER 3

previously described can be found in Appendix 2. The gene list was further refined by investigating oncogenic predicted target genes through reviewing the literature for relevance to CRC as previously described. Oncogenic molecules involved in promoting proliferation or inhibiting apoptosis were selected as targets for further investigation. A small list of target genes was assembled using the above criteria and 3'UTR binding site information collected from miRanda. These genes included *BCL2* (1 predicted binding site), *PIK3R3* (2 predicted binding sites), *FZD4* (2 predicted binding sites), *FOS* (1 predicted binding site), *LRP6* (1 predicted binding site), *PTGS2* (alias *COX2*; 2 predicted binding sites), *GAB2* (1 predicted binding site), *AKT3* (1 predicted binding site) and *MAP3K8* (1 predicted binding site).

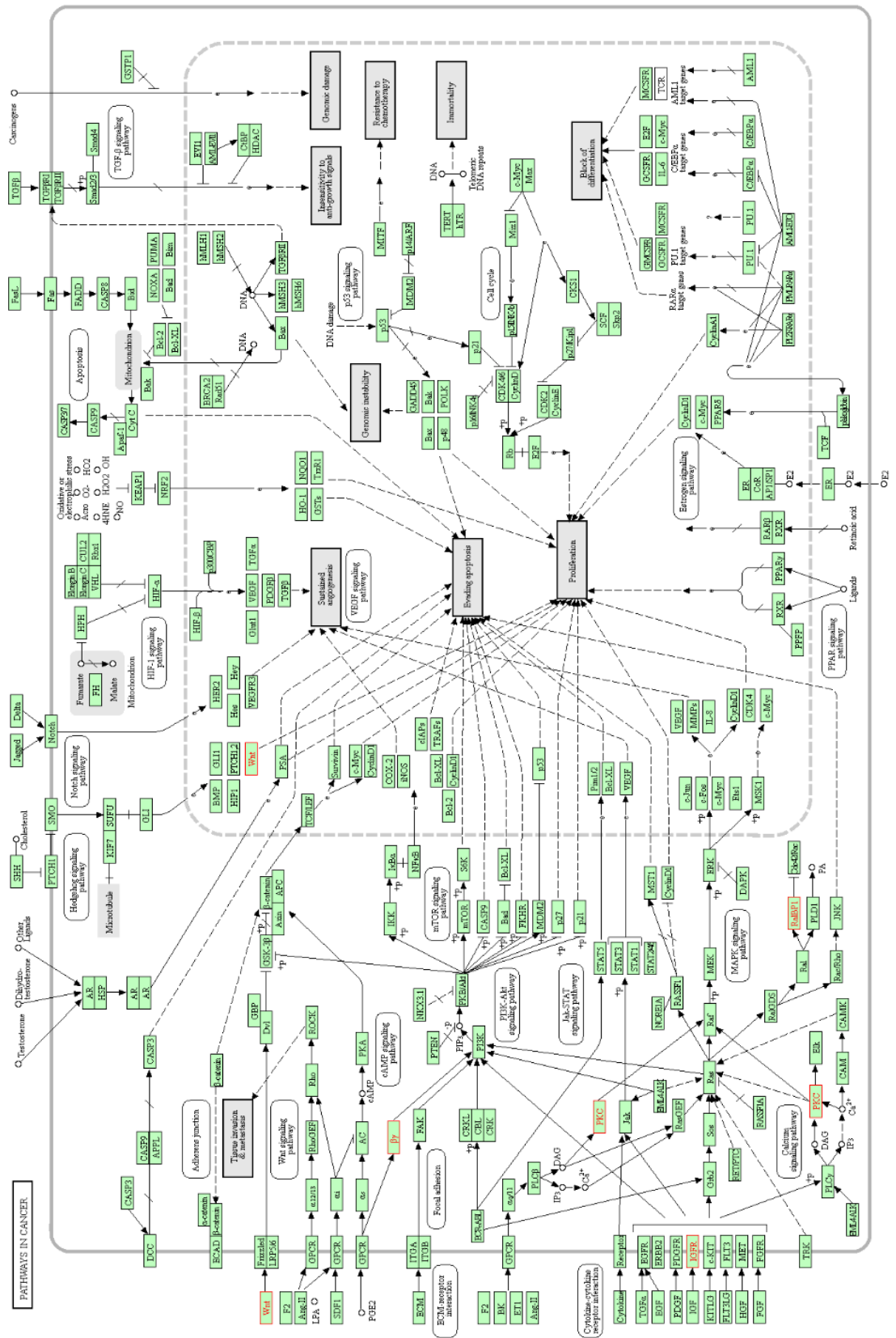


**Figure 3-9 KEGG mapper canonical pathway analysis for miR-125b: Pathways in Cancer**

Highlighted molecules represent the predicted target genes of miR-125b analysed in KEGG Mapper. The following genes involved in Pathways in Cancer include *GNG4*, *IGF1R*, *PRKCA*, *RALBP1* and *WNT8B*.

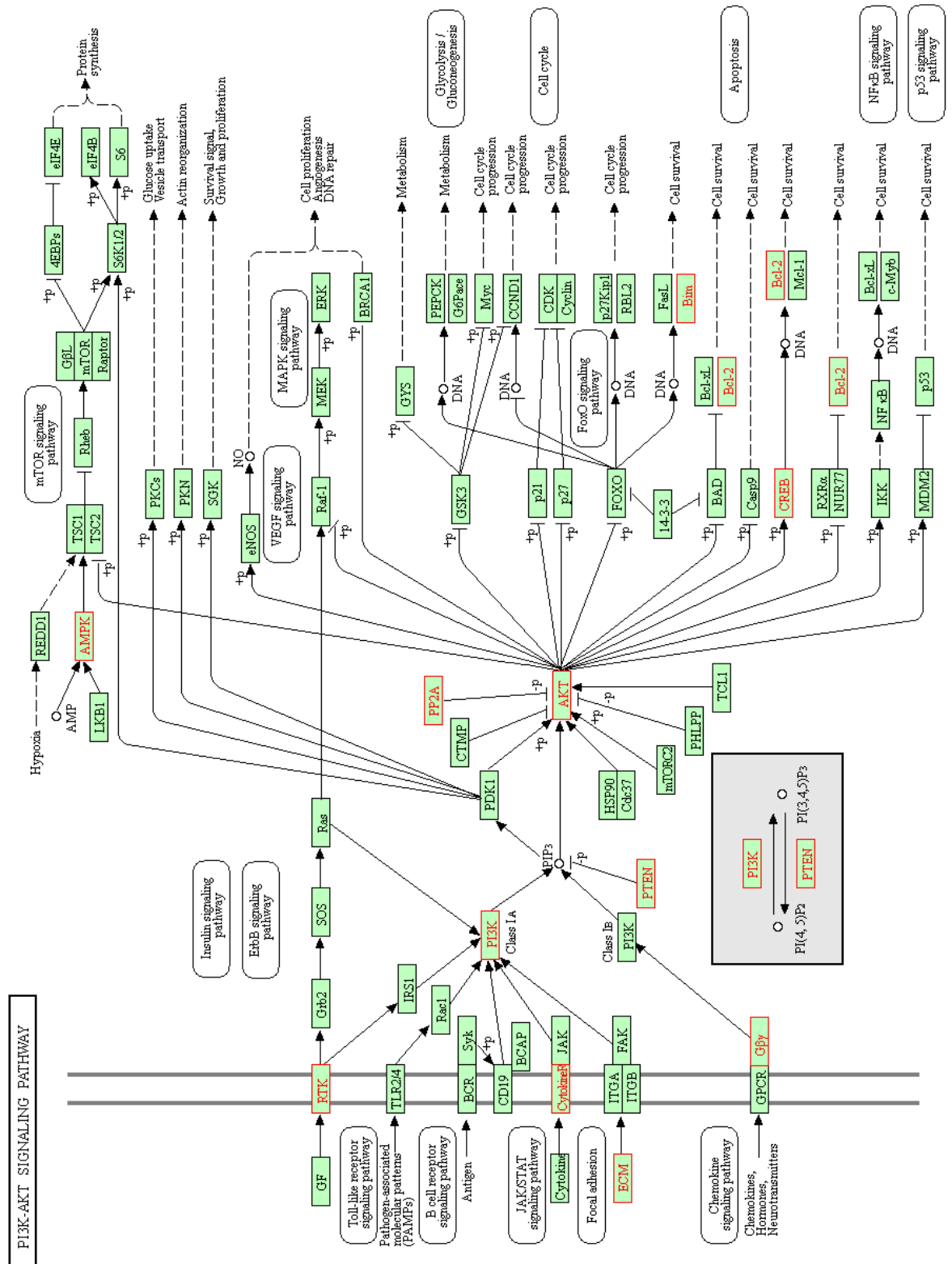


**Figure 3-10 KEGG mapper canonical pathway analysis miR-181a: PI3K-Akt Signalling Pathway**

PI3K-Akt Signalling Pathway was present in the top canonical pathways related to CRC for miR-181a predicted target genes. Predicted target genes are highlighted in red. Example target genes in PI3K-Akt Signalling Pathway include *PIK3R3*, *PTEN*, *CREB5* and *MAP3K8*.

### 3.2.7 mRNA expression analysis

Based on the aforementioned criteria, 3 predicted target genes were selected for miR-125b, 9 predicted target genes were selected for miR-181a, 4 predicted target genes for miR-593 and 3 predicted target genes for miR-1227 for further investigation by real-time RT-PCR to determine if their mRNA level could be altered by the selected miRNAs (refer to Table 2-3 for primer sequences). The investigation of these genes was primarily performed to determine molecules which may be involved in the cellular responses mediated by miR-125b, miR-181a, miR-593 and miR-1227. HCT116 cells were transfected with miRNA or NC mimics and treated with 0 mM or 2.5 mM butyrate as per previous experiments. Due to the larger number of candidate targets, only non-butyrate treated HCT116 samples (NC or miRNA mimic transfected; 0 mM butyrate treated) were used to initially identify miR-181a binding transcripts. These targets were defined as mRNAs that had significantly decreased levels after transfection with the selected miRNA. Some targets were selected for further validation if the P-value was close to  $P < 0.05$ , but not significant, as the number of experimental replicates was increased in the second validation experiment. Those predicted targets which had no change or increased expression were not further investigated. The validated targets of miRNAs were further analysed to examine if the miRNAs and butyrate synergistically altered transcript levels. The same screening process was not applied to targets for miR-125b, miR-593 or miR-1227 due to the small number of targets. Predicted target genes which showed decreased expression following transfection with the miRNA alone and enhanced the response to butyrate were selected for protein expression analysis.

#### 3.2.7.1 Effects of miR-593 and butyrate on predicted target gene transcript levels

To determine the effects of miR-593 and butyrate on predicted target gene transcript levels, HCT116 cells were reverse transfected with miR-593 mimics or controls for 48 h, followed by 24 h of 0 mM or 2.5 mM butyrate treatment. miR-593 transfection alone significantly decreased the transcript levels of *CCND1* ( $P=0.0001$ ) and *EEF2K* ( $P=0.0214$ ), while *ERBB2* and *PAK2* transcript levels had a non-significant decreasing trend (Figure 3-11). When HCT116 cells were exposed to miR-593 mimics in combination with 2.5 mM butyrate, *EEF2K* ( $P=0.0178$ ) transcript levels were significantly reduced; however, the other transcripts did not significantly change. Butyrate alone significantly decreased all transcript levels when comparing 0 mM butyrate and 2.5 mM butyrate treated NC transfected cells as well as 0 mM butyrate and 2.5 mM butyrate treated miR-593 transfected cells ( $P \leq 0.0029$ ). As *CCND1* and *EEF2K*

were the only genes to significantly respond to the miRNA, they were selected for further validation at the protein level.

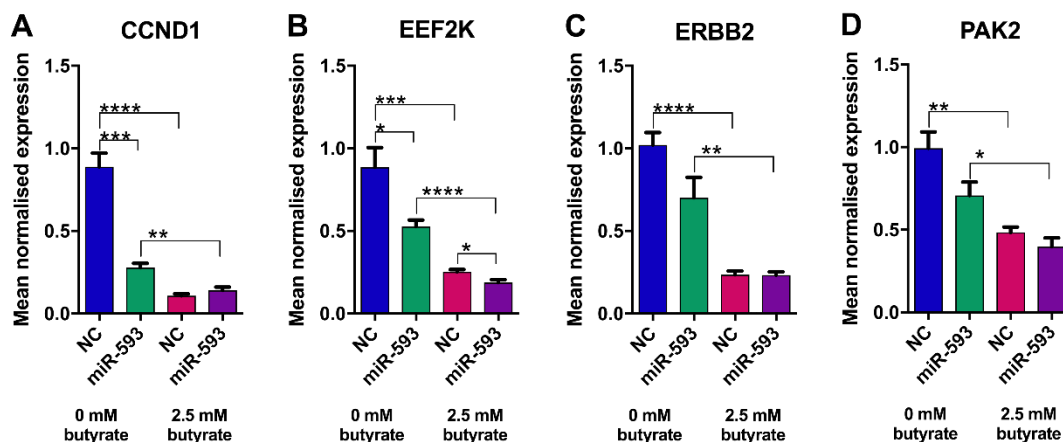


**Figure 3-11 Real-time RT-PCR analysis of predicted miR-593 target gene mRNA levels in HCT116 cells after 24 h of butyrate treatment**

mRNA levels of miR-593 predicted target genes (A) *CCND1*, (B) *EEF2K*, (C) *ERBB2* and (D) *PAK2* in HCT116 cells transfected with miR-593 or NC mimics for 48 h, followed by 24 h of treatment with 0 mM or 2.5 mM butyrate, over a 72 h post-transfection period. The mean mRNA levels  $\pm$  SEM of 5 replicates is represented and their expression is normalised to the geometric mean of three reference genes, *ACTB*, *B2M* and *GAPDH*. Significant values are indicated by \* $P < 0.05$ , \*\* $P < 0.01$ , \*\*\* $P < 0.001$ , \*\*\*\* $P < 0.0001$ . NC= Negative Control mimic.

### 3.2.7.2 Effect of miR-1227 and butyrate on predicted target gene transcript levels

To determine the effects of miR-1227 and butyrate on predicted target gene transcript levels, HCT116 cells were reverse transfected with miR-1227 mimics or controls for 48 h, followed by 24 h of 0 mM or 2.5 mM butyrate treatment. miR-1227 alone and in combination with butyrate did not significantly affect the transcript levels of *CDK19* or *GRB2*; however, a non-significant decreasing trend was seen in *GRB2* transcript levels when cells were exposed to miR-1227 (Figure 3-12). *STAT3* transcript levels significantly increased when cells were exposed to miR-1227 alone ( $P = 0.0310$ ) and this increase was further enhanced in the presence of butyrate ( $P = 0.0086$ ). Butyrate significantly increased the transcript levels of *GRB2* ( $P \leq 0.0021$ ) and *STAT3* ( $P \leq 0.0001$ ) when comparing NC 0 mM butyrate versus 2.5 mM butyrate treated and miR-1227 0 mM butyrate versus 2.5 mM butyrate treated; however, no significant changes were observed with *CDK19* transcript levels. Analyses of *DVL3* and *NUP62* were repeated with a greater number of replicates to confirm previous results (Ali 2014). miR-1227 alone significantly decreased expression of *DVL3* ( $P = 0.0132$ ) and *NUP62* ( $P = 0.0278$ ).

After HCT116 cells were exposed to miR-1227 and 2.5 mM butyrate in combination, there were no further significant decreases in *DVL3* or *NUP62* transcript levels; however, *DVL3* mRNA levels had a decreasing trend. Butyrate significantly decreased levels of *DVL3* when comparing miR-1227 0 mM butyrate versus 2.5 mM butyrate treated cells and *NUP62* transcript levels decreased when comparing NC 0 mM butyrate versus 2.5 mM butyrate treated cells. As only *DVL3* and *NUP62* responded significantly to miR-1227 alone, they were selected for further validation through protein analysis (section 3.2.8.2).

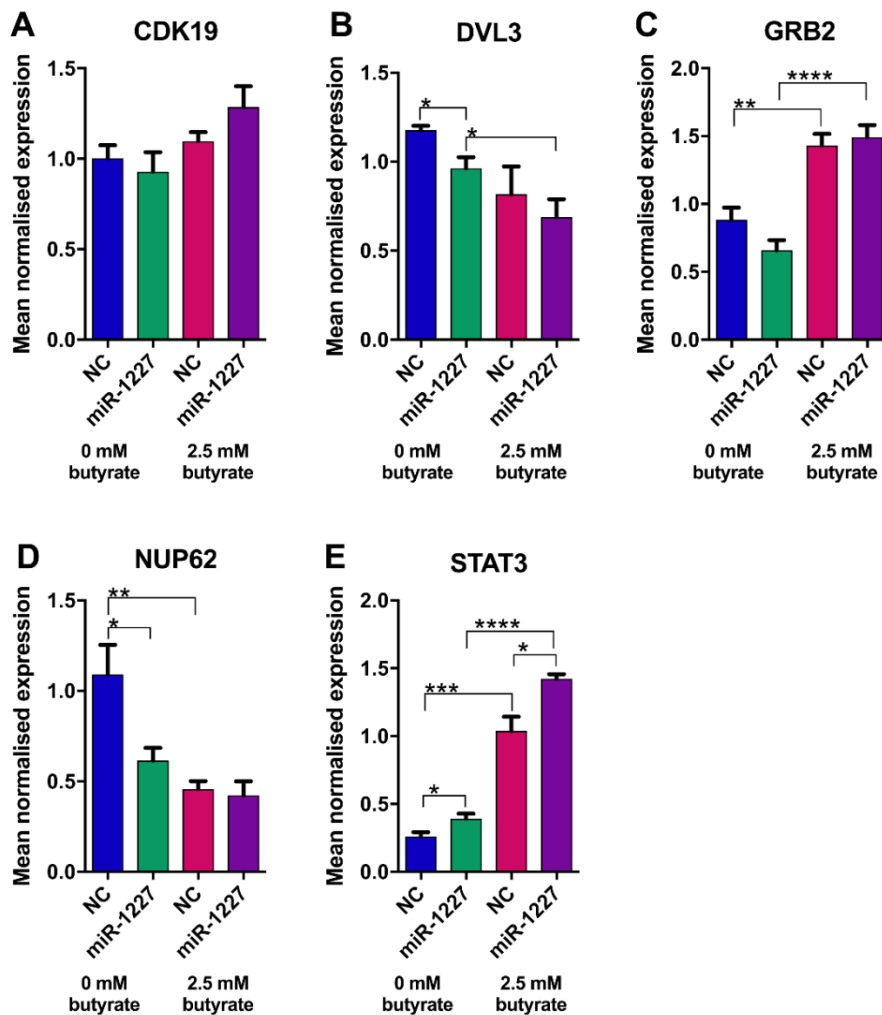


**Figure 3-12 Real-time RT-PCR analysis of predicted miR-1227 target gene mRNA levels in HCT116 cells after 24 h of butyrate treatment**

mRNA levels of miR-1227 predicted target genes (A) *CDK19*, (B) *DVL3* (C) *GRB2*, (C) *NUP62*, (E) *STAT3* in HCT116 cells transfected with miR-1227 or NC mimics for 48 h, followed by 24 h of treatment with 0 mM or 2.5 mM butyrate, over a 72 h post-transfection period. The mean mRNA levels  $\pm$  SEM of 5 replicates is represented and their expression is normalised to the geometric mean of three reference genes, *ACTB*, *B2M* and *GAPDH*. Significant values are indicated by \* $P < 0.05$ , \*\* $P < 0.01$ , \*\*\* $P < 0.001$ , \*\*\*\* $P < 0.0001$ . NC= Negative Control mimic.

### 3.2.7.3 Effect of miR-125b and butyrate on predicted target gene transcript levels

To determine the effects of miR-125b and butyrate on predicted target gene transcript levels, HCT116 cells were reverse transfected with miR-125b mimics or controls for 48 h, followed by 24 h of 0 mM or 2.5 mM butyrate treatment. miR-125b alone significantly reduced the transcript levels of *TRIM29* ( $P=0.0034$ ) in HCT116 cells; however, *IGF1R* and *ZEB1* transcript levels did not significantly change (Figure 3-13). After CRC cells were exposed to miR-125b and 2.5 mM butyrate in combination, *TRIM29* transcript levels significantly increased ( $P=0.0484$ ) when compared to 2.5 mM butyrate treated NC transfected cells; there was no significant change in *IGF1R* or *ZEB1* transcript levels when comparing the same groups. Butyrate significantly increased the transcript levels of all genes ( $P\leq 0.0001$ ) when comparing NC 0 mM butyrate versus 2.5 mM butyrate treated as well as miR-125b 0 mM butyrate versus 2.5 mM butyrate treated cells. As *TRIM29* was the only gene to respond to miR-125b alone, it was further investigated as a target using protein analysis (section 3.2.8.3).

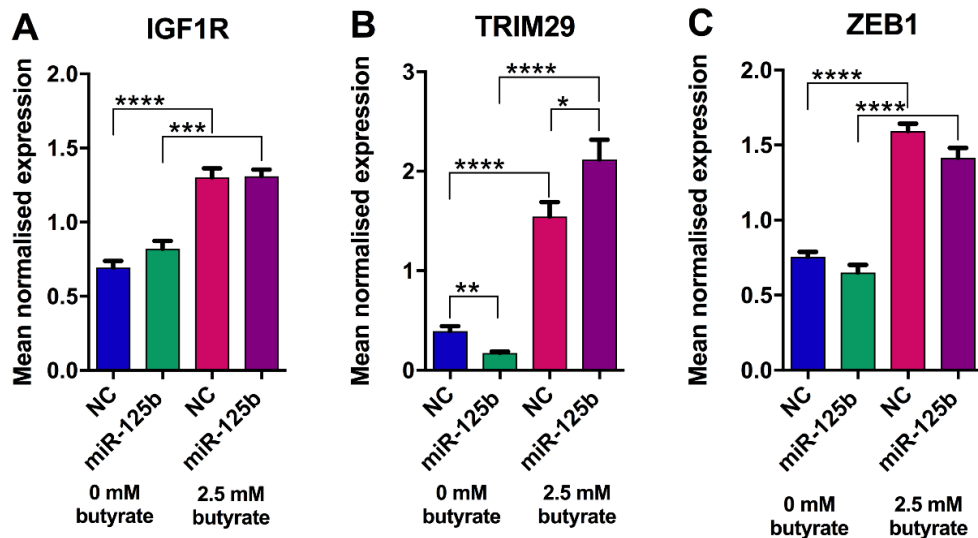


**Figure 3-13 Real-time RT-PCR analysis of predicted miR-125b target gene mRNA levels in HCT116 cells after 24 h of butyrate treatment**

mRNA levels of miR-125b predicted target genes (A) *CDK19*, (B) *GRB2* and (C) *STAT3* in HCT116 cells transfected with miR-125b or NC mimics for 48 h, followed by 24 h of treatment with 0 mM or 2.5 mM butyrate, over a 72 h post-transfection period. The mean mRNA levels  $\pm$  SEM of 5 replicates is represented and their expression is normalised to the geometric mean of three reference genes, *ACTB*, *B2M* and *GAPDH*. Significant values are indicated by \* $P<0.05$ , \*\* $P<0.01$ , \*\*\* $P<0.001$ , \*\*\*\* $P<0.0001$ . NC= Negative Control mimic.

### 3.2.7.4 Effects of miR-181a on predicted target gene transcript levels

HCT116 cells that were transfected with miR-181a mimics showed altered expression levels of some predicted miR-181a target genes, when compared with NC mimic transfected cells (0 mM butyrate) (Figure 3-14). *COX2* ( $P=0.0118$ ) and *FZD4* ( $P=0.0215$ ) had significantly decreased transcript levels in HCT116 cells when exposed to miR-181a mimics alone. In addition, *LRP6* ( $P=0.0717$ ), *MAP3K8* ( $P=0.0821$ ) and *PIK3R3* ( $P=0.0644$ ) transcript levels showed a non-significant decreasing trend. *AKT3* transcript levels did not change after exposure to miR-181a mimics, while *BCL2*, *FOS* and *GAB2* showed slight, non-significant increases in transcript levels.

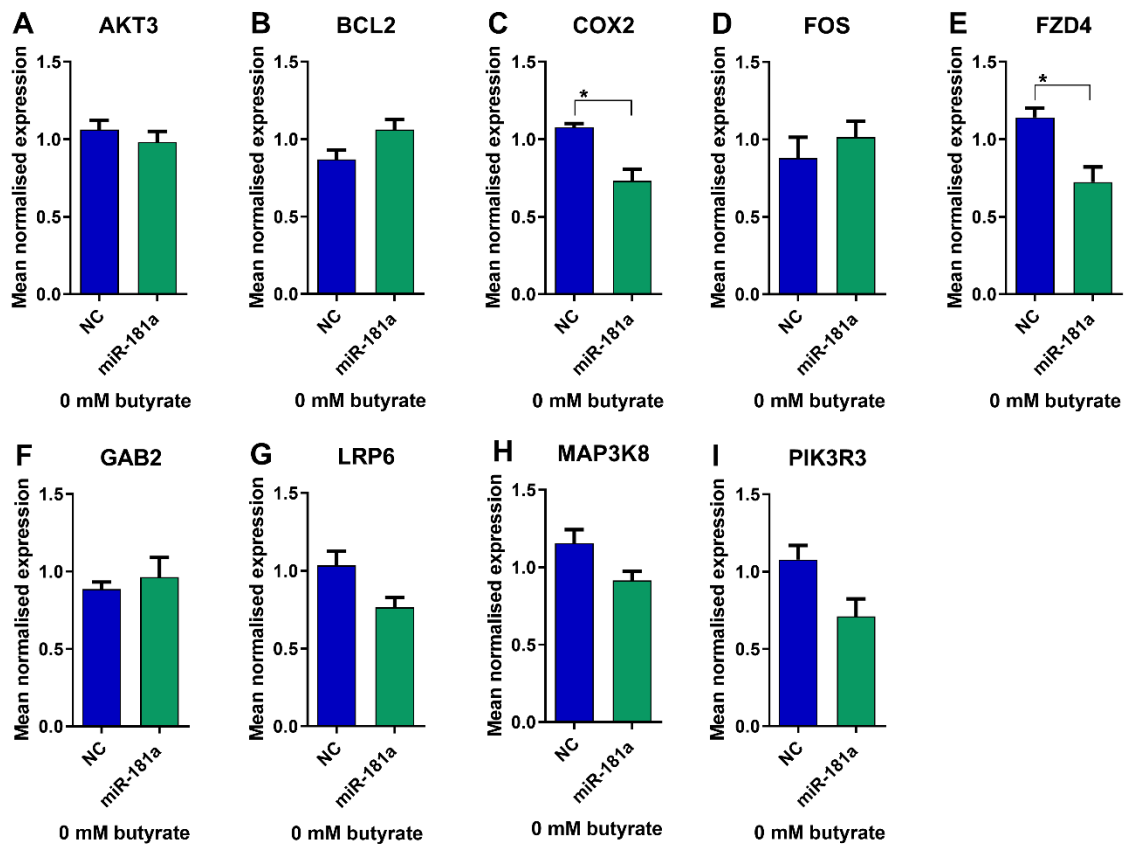


**Figure 3-14** Real-time RT-PCR analysis of predicted miR-181a target gene mRNA levels in HCT116 cells 72 h post-transfection.

mRNA levels of miR-181a predicted target genes (A) *AKT3*, (B) *BCL2*, (C) *COX2* (D) *FOS*, (E) *FZD4*, (F) *GAB2*, (G) *LRP6*, (H) *MAP3K8* and (I) *PIK3R3* in HCT116 cells transfected with miR-181a or NC mimics, and treated with 0 mM butyrate, over a 72-h post-transfection period. The mean mRNA levels  $\pm$  SEM of the triplicates is represented, and their expression is normalised to the geometric mean of three reference genes, *ACTB*, *B2M* and *GAPDH*. Significant values are indicated by \* $P<0.05$ , \*\* $P<0.01$ , \*\*\* $P<0.001$ , \*\*\*\* $P<0.0001$ . NC= Negative Control mimic.

### 3.2.7.5 Effect of miR-181a and butyrate on predicted target gene transcript levels

To examine the effects of miR-181a and butyrate on predicted target gene transcript levels, HCT116 cells were reverse transfected with miR-181a mimics or controls for 48 h, followed by 24 h of 0 mM or 2.5 mM butyrate treatment. miR-181a alone significantly decreased mRNA levels of *COX2* (P=0.0014), *FZD4* (P=0.0120), *MAP3K8* (P=0.0001) and *PIK3R3* (P=0.0395); however, *LRP6* transcript levels significantly increased (P=0.0494) (Figure 3-15). Following exposure of HCT116 cells to 2.5 mM butyrate, transcript levels of all predicted target genes dramatically and significantly increased when compared to the NC 0 mM butyrate cells. With the addition of miR-181a and 2.5 mM butyrate, *COX2* (P=0.0490), *LRP6* (P<0.0001) and *PIK3R3* (P=0.0018) levels significantly increased again; however, *FZD4* (P=0.0429) levels significantly decreased compared to 2.5 mM butyrate treated NC cells. *MAP3K8* mRNA levels did not significantly change after CRC cells were exposed to miR-181a and butyrate; however, there was a decreasing trend. All transcript levels were significantly increased by butyrate treatment (P≤0.009) as shown by the comparison of the NC transfected 0 mM butyrate and 2.5 mM butyrate treated groups and the miRNA mimic transfected 0 mM butyrate and 2.5 mM butyrate treated groups. All genes, except *LRP6*, had significantly reduced transcript levels when cells were exposed to miR-125b; therefore, they were selected for further investigation through protein analysis (section 3.2.8.4).

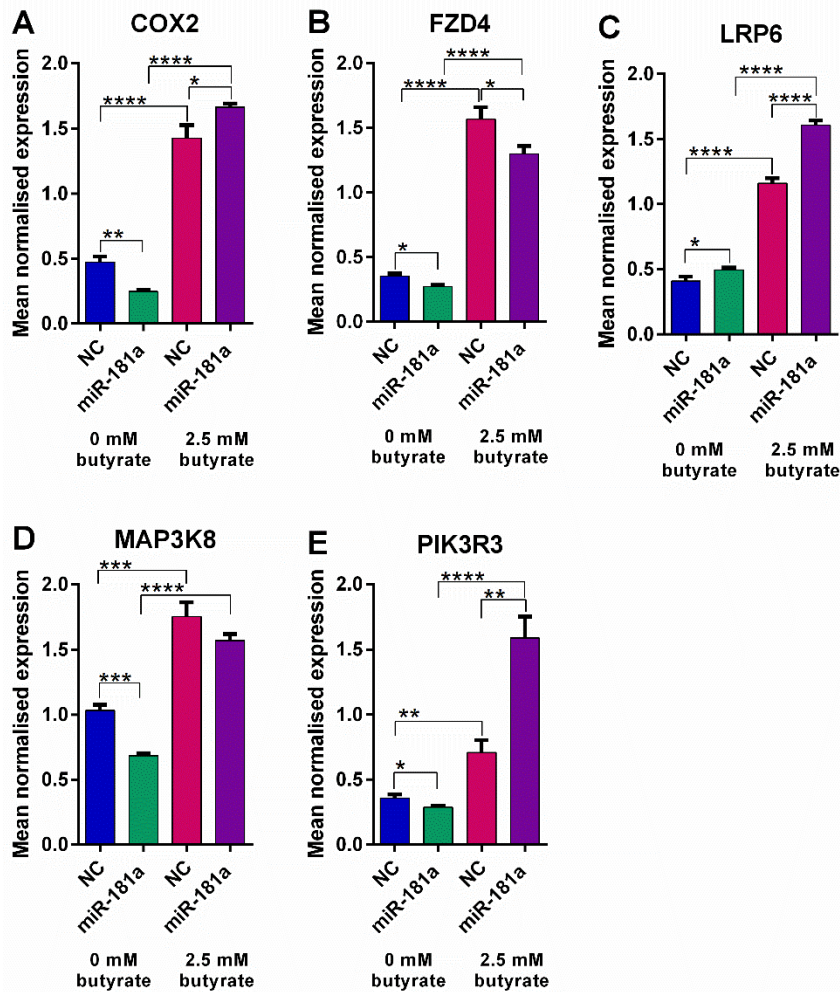


**Figure 3-15** Real-time RT-PCR analysis of predicted miR-181a target gene mRNA levels in HCT116 cells after 24 h of butyrate treatment.

mRNA levels of miR-181a predicted target genes (A) *COX2*, (B) *FZD4*, (C) *LRP6* (D) *MAP3K8* and (E) *PIK3R3* in HCT116 cells transfected with miR-181a or NC mimics for 48 h, followed by 24 h of treatment with 0 mM or 2.5 mM butyrate, over a 72 h post-transfection period. The mean mRNA levels  $\pm$  SEM of 5 replicates is represented and their expression is normalised to the geometric mean of three reference genes, *ACTB*, *B2M* and *GAPDH*. Significant values are indicated by \*P<0.05, \*\*P<0.01, \*\*\*P<0.001, \*\*\*\*P<0.0001. NC= Negative Control mimic.

### 3.2.8 Protein expression analysis

Selected predicted target genes, including miR-593 targets *CCND1* and *EEF2K*; miR-1227 targets *DVL3* and *NUP62*; miR-125b target *TRIM29* and miR-181a targets *COX2*, *FZD4*, *PIK3R3* and *MAP3K8* were further investigated to determine if the miRNAs affect the level of corresponding target proteins in CRC cells. HCT116 cells were transfected and butyrate treated as per previous experiments; however, protein lysates were prepared, separated using SDS-PAGE and subjected to immunoblotting.

**3.2.8.1 Effect of miR-593 on predicted target gene protein expression**

CCND1 protein expression was significantly decreased when exposed to miR-593 mimics alone ( $P = 0.0102$ ) (Figure 3-16 A, C). When cells were exposed to miR-593 mimics and butyrate in combination, CCND1 expression significantly increased ( $P = 0.0495$ ). Butyrate was able to reduce CCND1 protein expression when comparing NC 0 mM butyrate to NC 2.5 mM butyrate treated ( $P=0.0168$ ) and miR-593 transfected 0 mM butyrate to miR-593 transfected 2.5 mM butyrate treated cells ( $P=0.0153$ ). Protein loading across all lanes was consistent when compared to reference lane 1 (Figure 3-16 E) (Appendix 3).

EEF2K protein expression was unaffected by miR-593 (NC 0 mM butyrate vs miRNA 0 mM butyrate) or butyrate alone when comparing NC 0 mM butyrate to NC 2.5 mM butyrate treated cells; however, EEF2K expression showed a non-significant decreasing trend when comparing miRNA 0 mM butyrate to miRNA 2.5 mM butyrate treated conditions (Figure 3-16 B, D). EEF2K protein expression was slightly but significantly decreased when cells were exposed to miR-593 and butyrate alone ( $P=0.0348$ ). Protein loading across all lanes was consistent when compared to reference lane 1, except lane 4 which appeared to be under loaded (Figure 3-16 F) (Appendix 3).

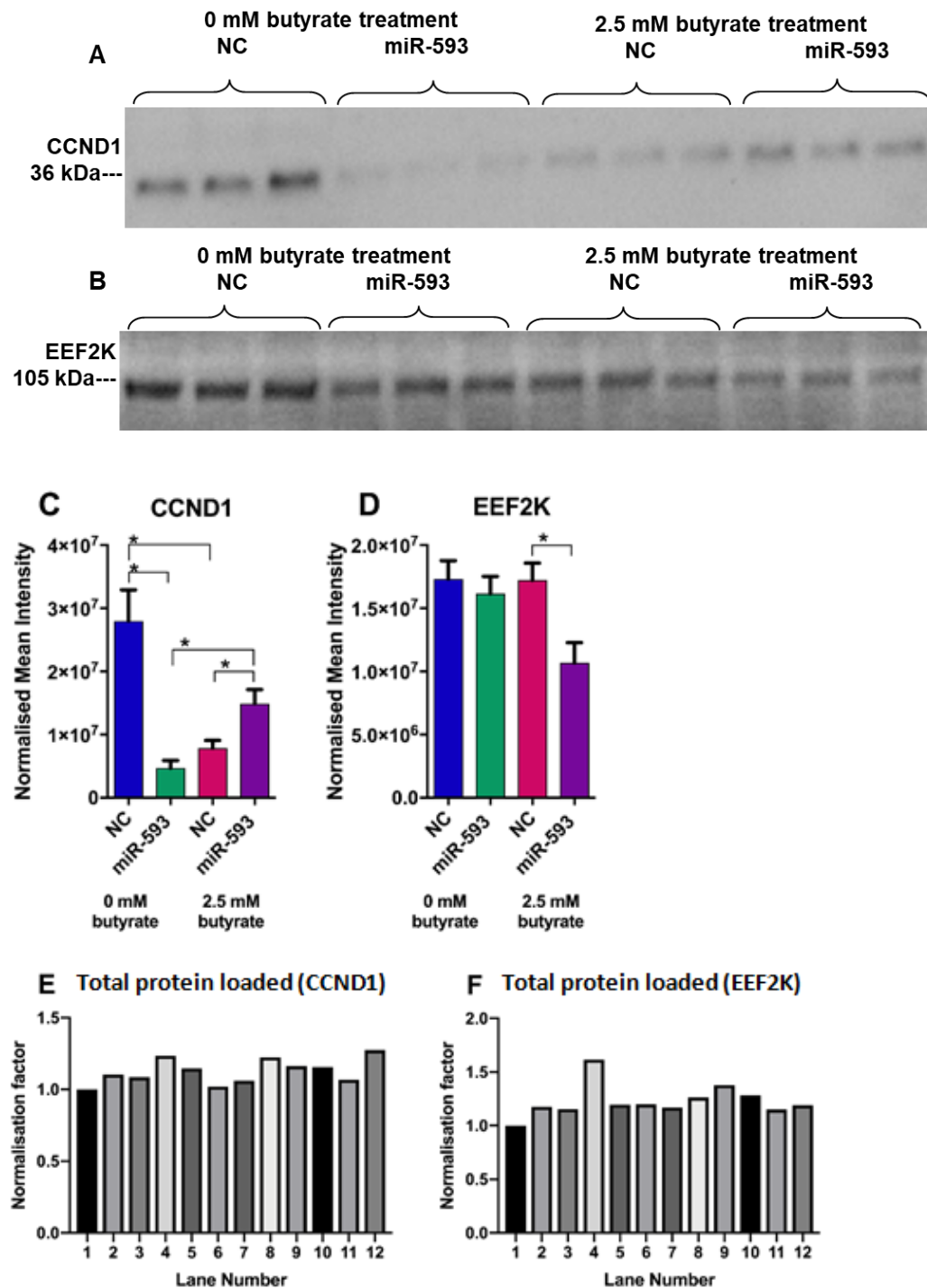


**Figure 3-16 Protein expression of miR-593 predicted targets**

Western blots of (A) CCND1 and (B) EEF2K in HCT116 cells transfected with miR-1227 or NC mimics for 48 h, followed by 24 h of treatment with 0 mM or 2.5 mM butyrate, over a 72 h post-transfection period. The mean normalised intensity of bands  $\pm$  SEM of the triplicates is represented for the protein analysis of (C) CCND1 and (D) EEF2K and their expression is normalised to (E) total protein loaded (CCND1) and (F) total protein loaded (EEF2K) respectively. All significant results are indicated by \* $P < 0.05$ , \*\* $P < 0.01$ , \*\*\* $P < 0.001$ , \*\*\*\* $P < 0.0001$ . NC= Negative Control mimic.

**3.2.8.2 Effect of miR-1227 on predicted target gene protein expression**

DVL3 protein expression did not significantly change in HCT116 cells when exposed to miR-1227 alone (Figure 3-17 A, C). When CRC cells were exposed to both miR-1227 and butyrate in combination, protein levels significantly decreased ( $P=0.0106$ ). Butyrate was also able to significantly reduce DVL3 protein expression when comparing NC 0 mM butyrate to NC 2.5 mM butyrate treated cells ( $P=0.0005$ ) and miRNA 0 mM butyrate to miRNA 2.5 mM butyrate treated cells ( $P= 0.0081$ ). Protein loading across all lanes was consistent when compared to reference lane 1; however, lane 12 was slightly underloaded (Figure 3-17 E) (Appendix 3).

NUP62 protein expression was significantly reduced when CRC cells were exposed to miR-1227 mimics alone ( $P= 0.0004$ ) (Figure 3-17 B, D). When cells were exposed to the combination treatment of miR-1227 and butyrate NUP62 protein levels were significantly decreased ( $P= 0.0046$ ). Butyrate alone was also able to reduce NUP62 protein levels when comparing NC 0 mM butyrate to NC 2.5 mM butyrate treated cells ( $P=0.0018$ ). Protein loading across all lanes was consistent; however, lane 1 appeared to be slightly underloaded when compared to the other lanes (Figure 3-17 F) (Appendix 3).

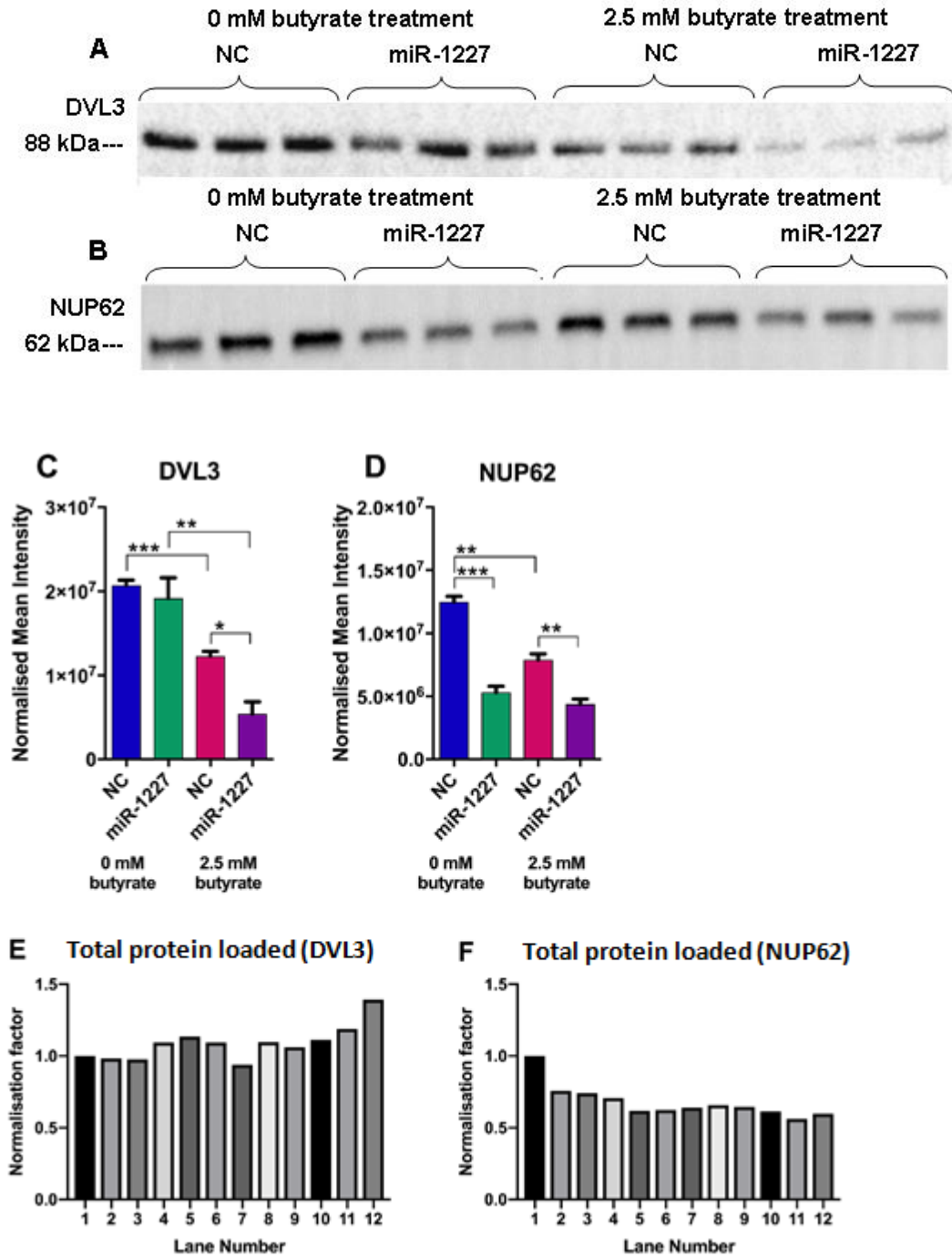


**Figure 3-17 Protein expression of miR-1227 predicted targets**

Western blots of (A) DVL3 and (B) NUP62 in HCT116 cells transfected with miR-1227 or NC mimics for 48 h, followed by 24 h of treatment with 0 mM or 2.5 mM butyrate, over a 72 h post-transfection period. The mean normalised intensity of bands  $\pm$  SEM of the triplicates is represented for the protein analysis of (C) DVL3 and (D) NUP62 and their expression is normalised to (E) total protein loaded (DVL3) and (F) total protein loaded (NUP62) respectively. All significant results are indicated by \* $P < 0.05$ , \*\* $P < 0.01$ , \*\*\* $P < 0.001$ , \*\*\*\* $P < 0.0001$ . NC= Negative Control mimic.

### 3.2.8.3 Effect of miR-125b on predicted target gene protein expression

Protein analysis demonstrated that TRIM29 protein expression levels were unaffected by miR-125b alone or by butyrate alone (Figure 3-18 A, B). When HCT116 cells were exposed to the combination treatment of miRNA and butyrate, the protein expression levels of TRIM29 significantly reduced. Protein loading across all lanes was consistent when compared to reference lane 1 (Figure 3-18 C) (Appendix 3).

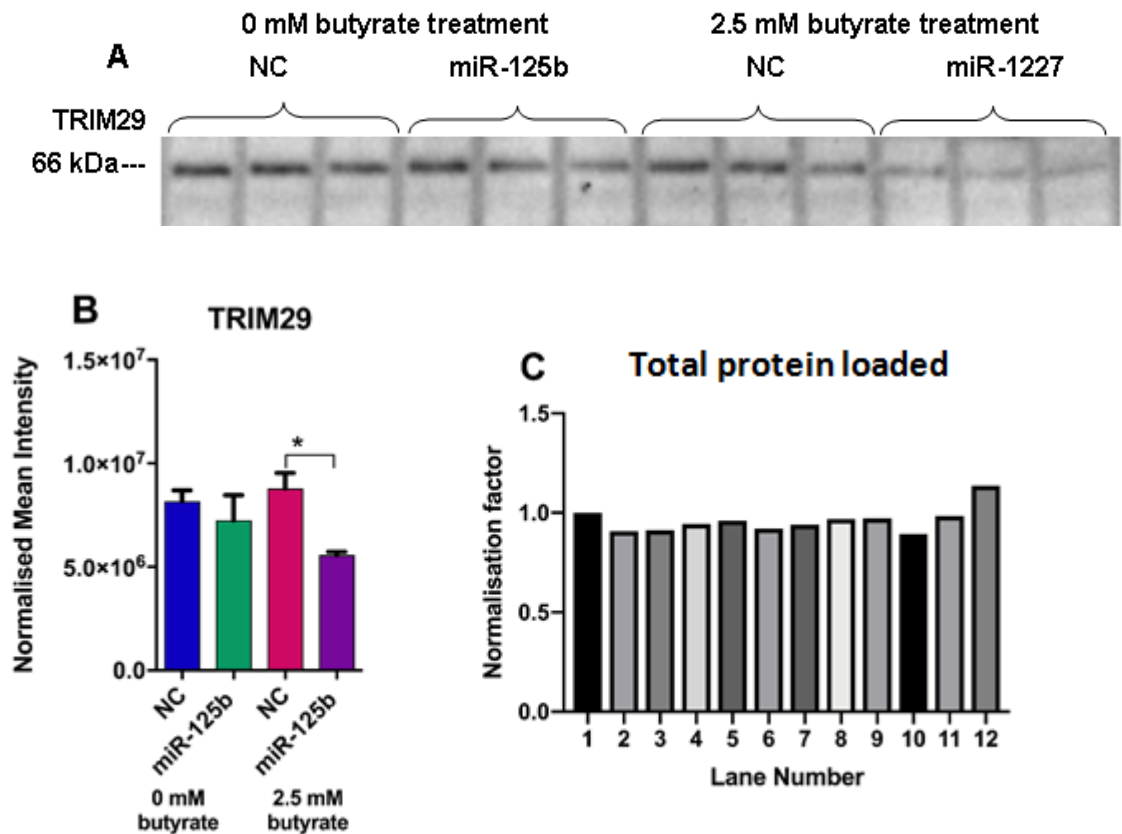


**Figure 3-18 Protein expression of miR-125b predicted targets**

Western blots of (A) TRIM29 in HCT116 cells transfected with miR-125b or NC mimics for 48 h, followed by 24 h of treatment with 0 mM or 2.5 mM butyrate, over a 72 h post-transfection period. The mean normalised intensity of bands  $\pm$  SEM of the triplicates is represented for the protein analysis of (B) TRIM29 and their expression is normalised to (C) total protein loaded. All significant results are indicated by \* $P < 0.05$ , \*\* $P < 0.01$ , \*\*\* $P < 0.001$ , \*\*\*\* $P < 0.0001$ . NC = Negative Control mimic.

**3.2.8.4 Effect of miR-181a on predicted target gene protein expression**

COX2 showed relatively low protein levels in HCT116 cells. miR-181a did not have a significant effect on COX2 protein expression (Figure 3-19 A, C). However, COX2 expression was decreased in the presence of butyrate when comparing NC 0 mM butyrate to NC 2.5 mM butyrate treated cells ( $P=0.0450$ ) and miRNA 0 mM butyrate to miRNA 2.5 mM butyrate treated cells ( $P= 0.0011$ ). When butyrate was combined with miR-181a mimics there was no significant effect on COX2 protein expression; however, a decreasing trend was observed. Protein loading across all lanes was consistent when compared to reference lane 1 (Figure 3-19 E) (Appendix 3).

The protein expression levels of PIK3R3 were significantly reduced when cells were exposed to miR-181a alone ( $P= 0.0033$ ) and in combination with butyrate ( $P=0.0008$ ) (Figure 3-19 B, D). PIK3R3 protein expression did not respond to butyrate alone. Protein loading across all lanes was consistent when compared to reference lane 1; however, lane 12 was slightly underloaded (Figure 3-19 F) (Appendix 3).

Unfortunately, a suitable antibody could not be identified to detect FZD4 or MAP3K8 protein expression levels; therefore, these targets were not further assessed.

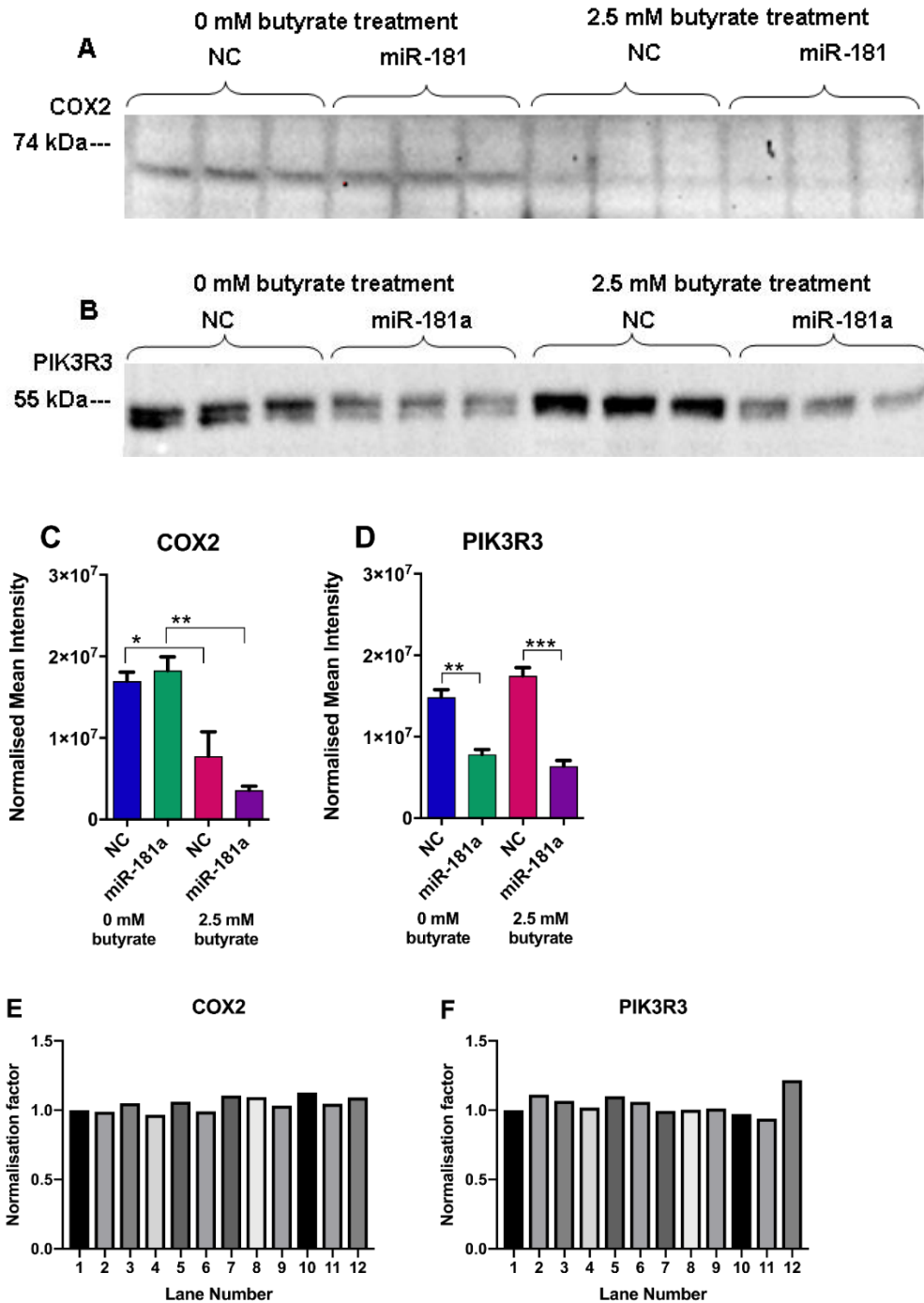


**Figure 3-19 Protein expression of miR-181a predicted targets**

Western blots of (A) COX2 and (B) PIK3R3 in HCT116 cells transfected with miR-181a or NC mimics for 48 h, followed by 24 h of treatment with 0 mM or 2.5 mM butyrate, over a 72 h post-transfection period. The mean normalised intensity of bands  $\pm$  SEM of the triplicates is represented for the protein analysis of (C) COX2 and (D) PIK3R3 and their expression is normalised to total protein (E) COX2 and (F) PIK3R3. All significant results are indicated by \*P<0.05, \*\*P<0.01, \*\*\*P<0.001, \*\*\*\*P<0.0001. NC= Negative Control mimic.

### 3.2.9 miRNA target gene suppression in the butyrate response and effect on proliferation

Predicted miRNA target genes *DVL3* and *PIK3R3* were further investigated due to their significant responses at the mRNA and protein levels when HCT116 cells were exposed to miR-1227 or miR-181a respectively, and when combined with butyrate (Figure 3-12 B, Figure 3-15 E, Figure 3-17 A, C, E, Figure 3-19 B, D, F). These genes were also of interest because they are involved in critical oncogenic pathways: WNT signalling (*DVL3*) and PI3K-AKT signalling (*PIK3R3*). RNA interference (siRNAs) was used to knockdown these target genes in order to determine if siRNAs had a similar effect on cell proliferation as the corresponding miRNA. Knockdown efficiency was determined by exposing HCT116 cells to *DVL3* or *PIK3R3* siRNAs for 72 h without butyrate treatment. *DVL3* mRNA levels were reduced by ~80% ( $P < 0.0001$ ) in HCT116 cells (Figure 3-20 A). *PIK3R3* mRNA levels were reduced by ~73% ( $P = 0.0007$ ) in HCT116 cells (Figure 3-20 B).

HCT116 cells were transfected with *DVL3* or *PIK3R3* siRNAs for 72 h followed by 24 h of 2.5 mM butyrate treatment and cell proliferation was measured using the xCELLigence real-time cell analyser. *DVL3* siRNA did not have a significant effect on cell proliferation alone; however, when combined with butyrate there was a slight but significant reduction in proliferation ( $P = 0.0398$ ) (Figure 3-21 A). Butyrate alone was able to reduce proliferation as expected when comparing NC 0 mM butyrate to 2.5 mM butyrate treated cells ( $P = 0.0003$ ) as well as siRNA 0 mM butyrate to 2.5 mM butyrate treated cells ( $P < 0.0001$ ). *PIK3R3* siRNA significantly reduced cell proliferation alone ( $P < 0.0001$ ) and this was further enhanced in the presence of butyrate ( $P < 0.0001$ ) (Figure 3-21 B). Butyrate alone was able to reduce proliferation as expected when comparing NC 0 mM butyrate to 2.5 mM butyrate treated cells ( $P < 0.0001$ ) as well as siRNA 0 mM butyrate to 2.5 mM butyrate treated cells ( $P < 0.0001$ ). The CDI calculation indicates a synergistic effect when *DVL3* siRNA is combined with butyrate at 0.91, while the *PIK3R3* siRNA effect with butyrate is significantly synergistic at 0.44.

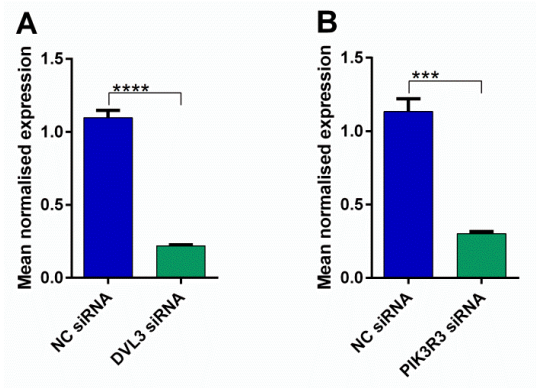


**Figure 3-20 DVL3 and PIK3R3 siRNA knockdown efficiency in HCT116**

mRNA levels of (A) *DVL3* and (B) *PIK3R3* in HCT116 cells transfected with NC, *DVL3* or *PIK3R3* siRNA over a 72 h post-transfection period. The mean mRNA levels  $\pm$  SEM of the triplicates is represented, and their expression is normalised to the geometric mean of three reference genes, *ACTB*, *B2M* and *GAPDH*. Significant values are indicated by \* $P < 0.05$ , \*\* $P < 0.01$ , \*\*\* $P < 0.001$ , \*\*\*\* $P < 0.0001$ . NC= Negative Control mimic.

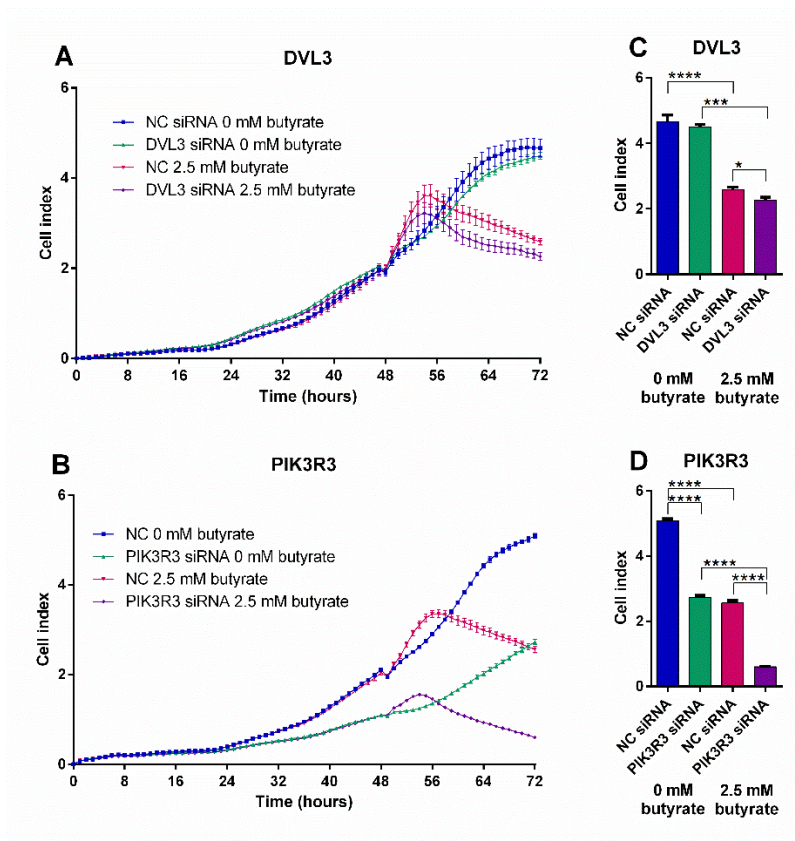


**Figure 3-21 Cell proliferation in DVL3 and PIK3R3 siRNA transfected HCT116 cells after 24 h of butyrate treatment**

Real-time cell index measurements using the xCELLigence RTCA platform, in HCT116 cells transfected with (A) *DVL3* siRNA or (B) *PIK3R3* siRNA for 48 h, followed by 24 h of treatment with 0 mM or 2.5 mM butyrate, over a 72 h post-transfection period. The mean  $\pm$  SEM of 4 replicates is shown at 72 h post-transfection (C) *DVL3* siRNA, (D) *PIK3R3* siRNA. Significant results are indicated by \*  $P < 0.05$ , \*\*  $P < 0.01$ , \*\*\*  $P < 0.001$ , \*\*\*\* $P < 0.0001$ . NC= Negative Control mimic.

### 3.2.10 WNT signalling activity

Following the investigation of predicted miRNA target genes, the WNT signalling pathway was further investigated due to its importance in the development of CRC (Polakis 2000). Many predicted miRNA target genes and butyrate responsive genes identified during the validation process were implicated in this pathway. HCT116 cells have high WNT activity as they have a mutated  $\beta$ -catenin allele leading to constitutive activation of WNT signalling; however, they have a wild type allele for *APC*. RKO cells are classified as low WNT activity cells, as they have wild type alleles for  $\beta$ -catenin and *APC*; however, they have mutant *CDX2* (dominant negative mutation), which is normally involved in APC and AXIN2 activation (Dang et al. 2001). Luciferase reporter plasmids carrying wild type and mutant TCF binding sites (TOPflash and FOPflash respectively) were used to monitor WNT signalling activity in these cells. Treatment of the cells with WNT3A ligand activates the reporter gene by increasing binding of  $\beta$ -catenin to the TCF sites. In this context, the effect of miRNA overexpression and butyrate treatment on WNT pathway activation could be assessed.

When HCT116 cells were not treated with WNT3A, miR-125b, miR-593 and miR-1227 alone did not alter TOPflash reporter activity, indicating that they did not affect the WNT signalling pathway (Figure 3-22). In contrast, miR-181a alone did significantly increase WNT activity ( $P < 0.0001$ ). When the miRNAs were combined with butyrate, only miR-593 showed any effect, producing a significant reduction in WNT activity ( $P < 0.0001$ ). In all cases, butyrate alone significantly induced WNT activity ( $P < 0.0001$ ). HCT116 cells treated with WNT3A alone showed a large induction of the WNT signalling pathway as expected. In the presence of WNT3A, both miR-125b ( $P = 0.0030$ ) and miR-181a ( $P = 0.0003$ ) significantly increased WNT activity, miR-1227 significantly reduced activity ( $P = 0.0438$ ), while miR-593 had no effect. In combination with butyrate, only miR-181a ( $P < 0.0001$ ) was able to significantly induce WNT activity, while miR-593 significantly reduced activity ( $P < 0.0001$ ) and miR-125b and miR-1227 had no effect.

Further analysis was performed using the low WNT activity CRC cell line, RKO. Most interestingly, when RKO cells were not treated with WNT3A, butyrate was unable to induce the TOPflash reporter suggesting that it did not activate the WNT pathway (Figure 3-23). In the absence of WNT3A, miR-1227 ( $P < 0.0001$ ) and miR-181a ( $P = 0.0019$ ) significantly induced the WNT pathway, while miR-125b and miR-593 showed non-significant increasing trends. When combined with butyrate there was a highly significant but subtle reduction in WNT activity for all miRNAs ( $P \leq 0.0005$ ).

When RKO cells were treated with WNT3A, RKO cells did not respond to any of the miRNAs alone. When miR-125b ( $P=0.0167$ ) or miR-1227 ( $P=0.0117$ ) were combined with butyrate there was a significant reduction in WNT activity in the CRC cells; however, no change was seen with miR-181a or miR-593. Butyrate alone significantly induced WNT activity in the presence of WNT3A ( $P<0.0001$ ).

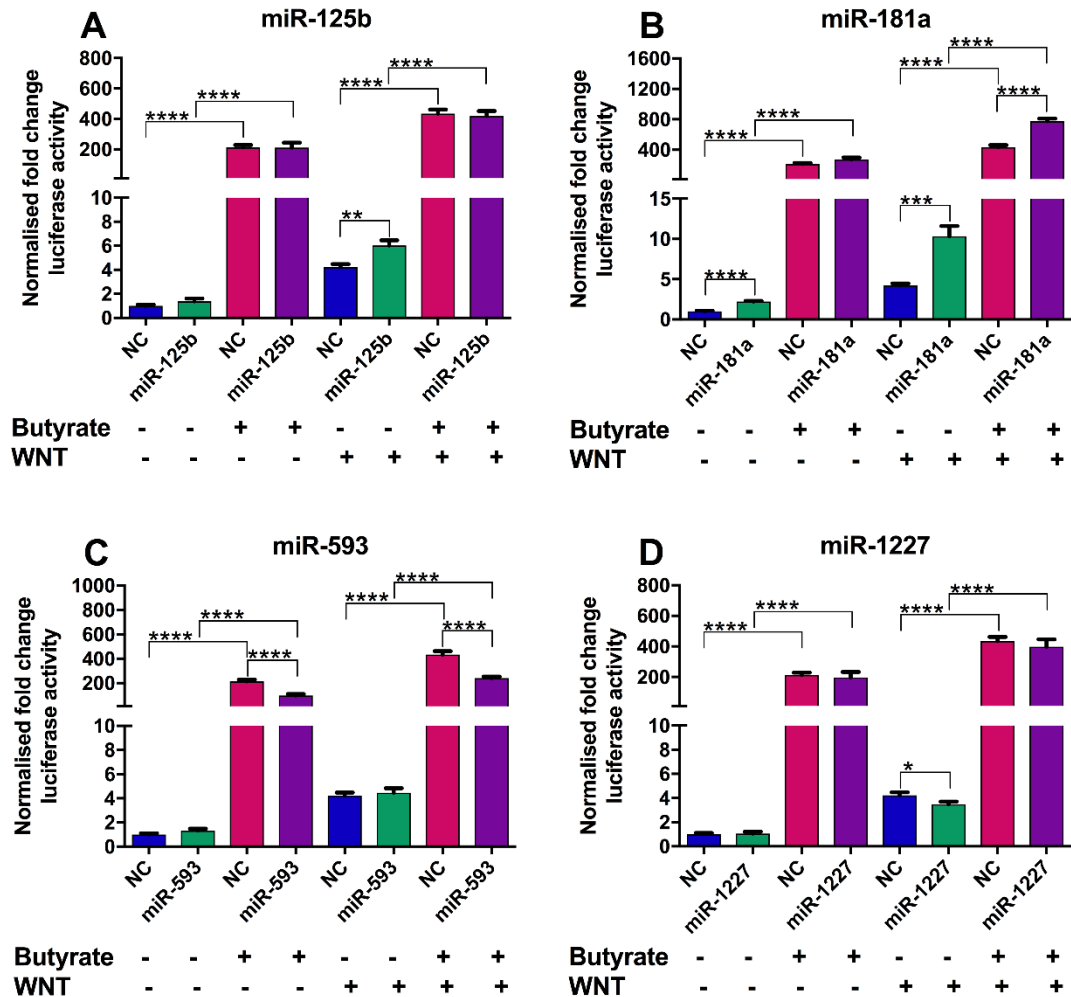


**Figure 3-22 Butyrate responsive miRNAs and butyrate alter WNT reporter activity in HCT116 cells**

WNT reporter activity in HCT116 cells reverse transfected with TOPflash vectors and butyrate-sensitising miRNAs (A) miR-125b, (B) miR-181a, (C) miR-593, (D) miR-1227, for 48 h, followed by 24 h of treatment with 0 mM or 2.5 mM butyrate, over a 72 h post-transfection period. The mean  $\pm$  SEM of 4 replicates is shown. Significant results are indicated by \*  $P<0.05$ , \*\*  $P<0.01$ , \*\*\*  $P<0.001$ , \*\*\*\* $P<0.0001$ . NC= Negative Control mimic.

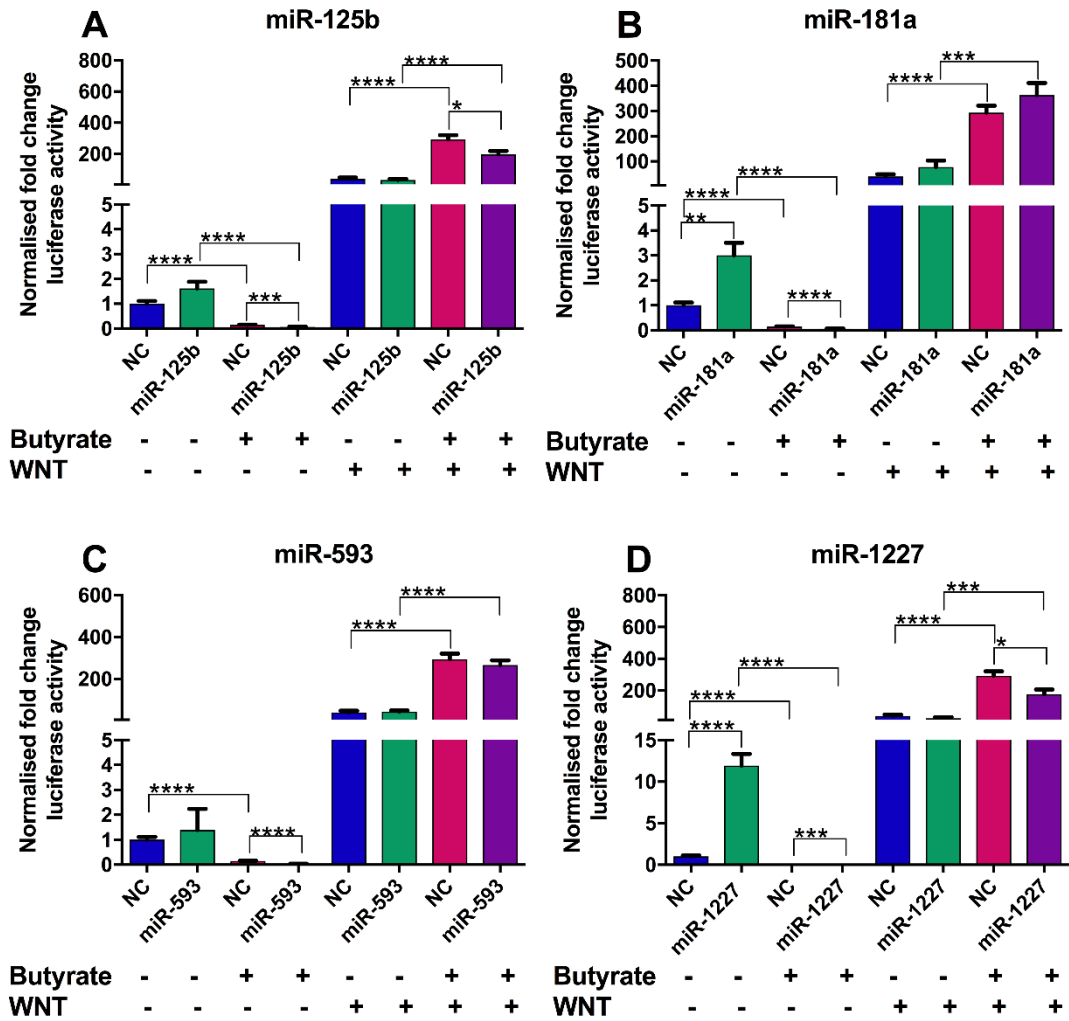


**Figure 3-23 Butyrate responsive miRNAs and butyrate alter WNT reporter activity in RKO cells**

WNT reporter activity in RKO cells reverse transfected with TOPflash vectors and butyrate-sensitising miRNAs (A) miR-125b, (B) miR-181a, (C) miR-593, (D) miR-1227, for 48 h, followed by 24 h of treatment with 0 mM or 2.5 mM butyrate, over a 72 h post-transfection period. The mean  $\pm$  SEM of 4 replicates is shown. Significant results are indicated by \*  $P < 0.05$ , \*\*  $P < 0.01$ , \*\*\*  $P < 0.001$ , \*\*\*\*  $P < 0.0001$ . NC= Negative Control mimic.

### 3.3 Discussion

#### 3.3.1 Summary

Butyrate is a naturally occurring HDACi with the ability to decrease proliferation and increase apoptosis in CRC cells by altering global histone acetylation and consequently global gene expression (Daly & Shirazi-Beechey 2006; Mariadason 2008). Butyrate has been shown to alter non-coding RNA expression, including miRNAs, in order to mediate its anticancer effects in CRC cells through various cellular growth and death pathways (Wu et al. 2018c). It was previously demonstrated that the overexpression of tumour suppressor miRNAs, such as miR-18a, in a combination treatment with butyrate can enhance the anticancer properties of butyrate in CRC cells (Humphreys et al. 2014b). To the best of our knowledge this interesting observation has not been further investigated. A high-throughput functional screen was previously performed and 13 butyrate-sensitising miRNAs were identified (refer to section 1.9) (Ali 2014). The aim of these experiments was to further validate these butyrate-sensitising miRNAs and their target genes in order to reveal their roles in the butyrate response. Several predicted miRNA-mRNA interactions were identified to be involved in key cell growth and death pathways including WNT and PI3K-AKT signalling. The knockdown of some predicted miRNA target genes using siRNAs also revealed potential therapeutic targets.

#### 3.3.2 Butyrate-sensitising miRNAs regulate CRC cell proliferation, apoptosis and the cell cycle

Of the 13 miRNA hits identified from unbiased high-throughput screening, miR-125b, miR-181a, miR-593 and miR-1227 were further investigated based on their strong synergistic effects with butyrate. These miRNAs previously demonstrated the ability to significantly enhance the butyrate response by increasing apoptosis and decreasing proliferation (Ali 2014), indicative of tumour suppressor properties. Apoptotic and viability parameters were further examined using flow cytometry as the previously observed effects of these miRNAs on viability and apoptosis (Ali 2014) were not fully validated.

##### **miR-125b cellular effects**

miR-125b has diverse roles in cancers including oncogenic behaviour in blood cancers such as B-cell leukaemia (Willimott & Wagner 2012) and myeloid leukaemia (Lin et al. 2011) by promoting growth, or tumour suppressor behaviour in breast cancer (Ferracin et al. 2013) and endometrial cancer (Shang et al. 2012) by inhibiting growth and

invasion. Previous studies have suggested that miR-125b may have oncogenic potential in CRC as high expression has been associated with poor prognosis in patients, and also with inhibition of the tumour suppressor p53 (Nishida et al. 2011). However, in contrast to this finding, a tumour suppressor function was demonstrated in HCT116 cells whereby miR-125b mimics induced apoptosis by silencing anti-apoptotic genes *MCL1* and *BCLW* (Gong et al. 2013). This is consistent with the results observed in my previous studies showing apoptosis induction (Ali 2014), but not the current flow cytometry study whereby miR-125b alone did not increase the number of apoptotic cells, nor affect viability. Other reported studies in HCT116 cells did not report changes in cell growth after exposure to miR-125b (Fujino et al. 2017), which do not support previous results (Ali 2014) and requires further investigation. Interestingly, the combination of miR-125b and miR-125a was found to sensitise paclitaxel chemoresistant HT29 CRC cells by inducing apoptosis and reducing growth and survival (Chen et al. 2013b), indicating that miR-125b has the ability to contribute to the anticancer effects of chemotherapeutics. In terms of the cell cycle, miR-125b has been previously shown to induce G2/M phase arrest to inhibit growth in HCT-8 and LOVO cells (Zhang et al. 2017c), although this was not seen in the current study and may be attributed to cell line differences.

#### **miR-181a cellular effects**

miR-181a has been shown to have oncogenic potential in CRC cells and high expression is associated with poor prognosis (Gu et al. 2018). Wei et al. (2014) demonstrated that the overexpression of miR-181a resulted in increased cell proliferation in HCT116 cells. A decrease in proliferation was observed in the previous study (Ali 2014) even though the percentage of viable cells did not change in the current study. It was previously reported that apoptosis was unaffected in HCT116 cells exposed to miR-181a alone (Galluzzi et al. 2010), which was consistent with the current study and my previous study (Ali 2014). miR-181a has also been shown to have diverse functions across cancer cell types. In gastric cancer miR-181a has oncogenic properties as it promotes proliferation (Zhang et al. 2014b). Similarly, another study in gastric cancer cells demonstrated that miR-181 reduced the percentage of cells in the G0/G1 phase and increased those in the S phase, while the G2/M phase cell percentage did not change (Yu et al. 2018b), which is similar to findings in the current study. In contrast to these oncogenic effects, in glioma and lung cancer miR-181a suppresses growth and promotes apoptosis (Shi et al. 2008; Shi et al. 2017) again showing that effects are context specific.

Interestingly, pre-miR-181a was shown to enhance the anticancer properties of cisplatin in lung cancer (Galluzzi et al. 2010), indicating potential benefit for cancer treatment.

#### **miR-593 and miR-1227 cellular effects**

miR-593 and miR-1227 are relatively poorly characterised miRNAs in CRC and other cancers. miR-593 has been shown to inhibit CRC and oesophageal cancer cell proliferation and induce G2/M arrest by silencing a critical cell cycle regulator, PLK1 (Ito et al. 2011; Ma et al. 2019), which coincidentally was used as a control in this high-throughput screen (Ali 2014). Results of the previous study did show that miR-593 had anti-proliferative effects in CRC cells (Ali 2014). However, in the current study miR-593 alone did not affect the percentage of viable cells detected by flow cytometry. The percentage of cells in the G2/M phase only significantly increased when the miRNA was combined with butyrate. Interestingly, CCND1 protein, which is involved in cell cycle regulation, was reduced by miR-593 and butyrate alone. When CRC cells were exposed to miR-593 and butyrate in combination, CCND1 protein increased in expression but it did not reach that of the untreated control group. This may indicate that reduction of CCND1 protein contributes to the accumulation of cells in the G2/M phase. As previously mentioned, miRNAs and butyrate are known to regulate several hundred genes; therefore, other targets may also be involved in this response. Further investigation of other cell cycle-related targets is required to understand this response.

More recently, several studies have implicated miR-593 in circular RNA (circRNA) and lncRNA regulatory axes (Dong et al. 2018b; Han et al. 2019; Song & Xiao 2018). For example, (Song & Xiao 2018) demonstrated that miR-593 was bound (sponged) and inhibited by hsa\_circ\_0007534 circRNA in order to promote the expression of its target MUC19, resulting in cell proliferation and invasion of breast cancer cells; this was reversed upon knockdown of the circRNA.

miR-1227 was demonstrated to be downregulated in HCT116 CRC cells relative to the embryonic kidney cell line HEK293A (Butkytė et al. 2016). Interestingly, in the current study miR-1227 had a strong synergistic effect with butyrate in greatly increasing the cell percentage in the S phase, which was not observed with other miRNAs. Previous studies in HCT116 cells have demonstrated that several drugs can induce S phase arrest such as Daurinol which inhibits topoisomerase 2 $\alpha$  and has a potent anti-proliferative effect (Kang et al. 2011). Chlorophyllin was also shown to increase S phase arrest in HCT116 cells; however, this is a result of decreased DNA damage and induction of checkpoint related proteins including RR, p53, p21, CCDN1, Rb and MDM2 (Chimploy

et al. 2009). S phase accumulation was also found to precede apoptosis which was discovered when CRC cells were treated with 5-fluorouracil (Yamane et al. 1999). This may explain why the combination of miR-1227 transfection and butyrate treatment promotes a large percentage of cells to accumulate in the S phase and strongly induce apoptosis. The phenomenon was also found in human oral cancer cells and lung cancer cells after treatment with celecoxib derivative OSU03012 and pemetrexed respectively which was shown to upregulate and activate ERK1/2 and CDK2/Cyclin A (Ding et al. 2008; Yang et al. 2011b). The findings in this study are novel for miR-1227 and warrants further investigation in the context of cell cycle regulation.

### **Limitations of cell-based studies**

There are several reasons as to why the literature is not fully consistent with the findings of the current study. These reasons include cell line heterogeneity, experimental conditions and assay differences. As mentioned above, variation was seen between previous studies even using the same HCT116 cell line. Recently, Ben-David et al. (2018) identified genetic and transcriptional heterogeneity across 27 MCF7 breast cancer cell lines collected from several laboratories. Most concerning, when the drug response of these cell lines was tested against 321 anticancer compounds, it was revealed that approximately 75% of the compounds which inhibited some MCF7 cell lines had no effect in others (Ben-David et al. 2018). Several approaches can be used to avoid these issues, such as recording passage numbers, examining the diversification of cell lines by genome-wide analyses and maintaining consistent culture conditions in order to maintain the quality and consistency of research (Ben-David et al. 2018). The experimental conditions can also be a source of variation in results. In the current study, a 20 nM concentration of miRNA mimics was used to induce responses in CRC cells; however, concentrations used in other studies vary greatly and were up to 50 nM (Fujino et al. 2017; Gong et al. 2013; Wei et al. 2014). The endogenous concentrations of miRNAs are normally much lower. A cell may have less than 10 copies of a low abundance miRNA and sometimes >10,000 copies per cell for highly abundant cell-type restricted miRNAs (Liang et al. 2007). Generally, miRNA species largely vary within cells. The use of a 20 nM concentration was to maintain consistency with previous studies (Humphreys et al. 2013) and high-throughput screening protocols. The effects of miRNAs are subtle; therefore, the cellular response may be minimal and difficult for real-time platforms such as the xCELLigence or Incucyte FLR to detect. It must be noted that if miRNAs are used therapeutically, cells are likely to be exposed to high

concentrations of miRNAs. miR-16 was delivered to mesothelioma patients in Phase 1 clinical trials at doses of 1.5 µg RNA in  $5 \times 10^9$  minicells across several weeks (van Zandwijk et al. 2017). However, if functional studies are being performed to identify gene targets, results must be carefully considered as highly supraphysiological concentrations of miRNAs can induce non-specific gene expression changes in cells (Jin et al. 2015). Another key point is that different types of assays were used across studies. For example, the Incucyte FLR real-time cell imaging system and CellPlayer™ 96-well Caspase 3/7 reagent were used to detect overall apoptotic events in my previous study (Ali 2014). This system is advantageous because of the real-time monitoring of cells; however, the clumping of cells can make it difficult for the Incucyte software to detect individual cells which fluoresce during apoptosis. Conversely, PI and annexin V stains, which were used for flow cytometry, are specific markers of apoptotic state and can differentiate between early and late apoptosis. Issues can include lack of dye binding to cells resulting in high background signals (Demchenko 2013), which may reduce the sensitivity of the assay. It must be noted that many published studies that have measured miRNA levels in cells do not provide details of the quantitative PCR protocol (for example Taqman assay number) or mention which arm of the mature miRNA was being quantified. As a general issue, many studies do not distinguish between the mature miRNA arms (5p or 3p) generated from the same hairpin precursor. Asymmetrical miRNA arm switching, whereby one strand is dominant, is common but it does not follow that the other arm is not functional (Chen et al. 2018a). Co-accumulation of miR-30e-3p and miR-30e-5p has been shown, though they do target different genes (Ro et al. 2007).

### 3.3.3 Butyrate-sensitising miRNAs regulate cell viability and apoptosis in LIM1215 CRC cells

The cellular effects of the miRNAs studied here were further tested in another CRC cell line, LIM1215, to determine if their effects were consistent in different CRC models. The endpoint ApoLive Multiplex assay was used to determine proliferative and apoptotic changes. In terms of viability and apoptosis, the response of LIM1215 cells to miR-181a, miR-593 and miR-1227 was largely consistent with the response of HCT116 cells (Ali 2014). The key difference observed was when cells were exposed to miR-125b, which resulted in an unexpected increase in cell viability, that was not seen in HCT116 cells (Ali 2014). As previously mentioned, the mutational status of LIM1215 and HCT116 cells are different as LIM1215 cells have wild type *KRAS* and *PIK3CA*, while HCT116 cells have mutant *KRAS* and *PIK3CA* and both have wild type

phenotypes for *BRAF* and *TP53*. The Hke3 cell line is derived from HCT116 cells. The *KRAS* mutant allele has been knocked out by homologous recombination (Shirasawa et al. 1993), while the wild type allele remains active; therefore, this was a suitable model to identify the involvement of *KRAS* in this response. Interestingly, viability was unchanged in this cell line when exposed to miR-125b alone, whereas in HCT116 cells it reduced growth, which indicates that *KRAS* might be implicated in this response. *KRAS* is a key gene involved in RAS signalling, which is mutated in ~40% of CRC cases (Fearon 2011). *KRAS* status in CRC has been shown to be important in the response of cells to several miRNAs. An investigation in HCT116 *KRAS*<sup>WT/-</sup> and HCT116 *KRAS*<sup>WT/G13D</sup> mutant cell lines revealed that the mutant cell line was particularly sensitive to miR-512, miR-618 and miR-1298 mimics, which significantly reduced cell viability compared to the WT cell line (Zhou et al. 2016d). Further examination revealed that lung cancer cell lines with mutant *KRAS* were also highly sensitive to miR-1298 (Zhou et al. 2016d), which highlights the importance of this mutation in specific miRNA responses. Further investigation is required as this emphasises the importance of identifying key mutations that may drive differential miRNA responses in cancers.

### 3.3.4 Butyrate-sensitising miRNAs regulate cell viability and death in 'normal' cell line models

To ensure that the effects of miRNA and butyrate treatments were cancer specific a noncancerous cell line was selected for investigation. Interestingly, HaCaT, MCF10A and HEK293 cells all responded to butyrate and had reduced growth, while HFF cells only slightly increased growth at 5 mM butyrate. Although butyrate has previously been shown to reduce viability and induce apoptosis in HaCaT cells (Daehn et al. 2006), these results were confirmed using a range of more relevant butyrate concentrations before being discounted as a potential cell line for further investigation. Interestingly, previous studies demonstrated that MCF10A cells only responded to butyrate at 2.5, 5, 7.5, 10 and 20 mM when exposed for 72 h, but no effects were seen at 24 h (Salimi et al. 2017), whereas in this study they responded to the same concentrations at 24 h and as low as 0.5 mM butyrate. This may be due to cell line heterogeneity as previously mentioned (Ben-David et al. 2018). HEK293 cells were also shown to previously respond to butyrate with decreasing viability; however, the butyrate concentrations tested were different (0.1, 0.5, 2, 8 mM) as well as the exposure time (96 h) (Li et al. 2015a); therefore, the cells were tested under the new conditions, but they still responded. HFF cells were the only cells that did not respond to butyrate. It is unclear from the literature as to whether butyrate decreases HFF growth alone as several studies have investigated

HFF cells and butyrate; however, in the context of induced pluripotency and viral infection (Radsak et al. 1985; Zhang et al. 2011b; Zhang & Wu 2013). The difference in responses may be due to the expression of butyrate receptors for example GPR41 (FFAR3), GPR43 (FFAR2) and GPR109A, which are not only present in colonic cells but also several other cell types such as macrophages, adipose, pancreatic and spleen cells among others (Koh et al. 2016; Nohr et al. 2013; Thangaraju et al. 2009). These receptors are responsible for activating a wide range of intracellular signalling pathways related to cellular metabolism and immune responses; unsurprisingly they are often silenced in CRC cells to restrict butyrate's activity (Tang et al. 2011; Thangaraju et al. 2009). Based on data available in GEO Profiles (Edgar et al. 2002), these receptors are all expressed in MCF10A (Stinson et al. 2011; Wali et al. 2014), HEK293 (Liu et al. 2008) and HaCat cells (Semini et al. 2011); however, HFF cells appear to express some GPR43 (Behnke et al. 2012), but not GPR41 or GPR109A. This might explain why HFF cells do not significantly respond to butyrate.

Alternatively, butyrate transporters monocarboxylate transporter 1 (MCT1) and sodium monocarboxylate transporter 1 (SMCT1), are important in the absorption of butyrate from the gut into colonocytes (Gopal et al. 2007; Gupta et al. 2006; Ritzhaupt et al. 1998). For butyrate to exert its HDACi effects, to regulate cell growth and death related genes, it must accumulate inside the cell. Not surprisingly, these receptors are silenced in colon cancer to prevent this (Lambert et al. 2002; Li et al. 2003). It must also be noted that colonocytes are efficient at utilising butyrate as it constitutes approximately 60% of their energy requirements (Cummings 1984) whereas other normal cells are less capable of metabolising it. HEK293, MCF10A and HaCaT cells have all been shown to express both MCT1 (Ahlin et al. 2009; Hussien & Brooks 2011; Semini et al. 2011) and SMCT1 (Babu et al. 2011; Liu et al. 2008; Semini et al. 2011) so, butyrate is capable of entering the cells. HFF cells appear to express MCT1 (Behnke et al. 2012), but not SMCT1, which may also explain their lack of response to butyrate in combination with lack of receptor expression mentioned above. Most body cells are not exposed to significant levels of butyrate because it is primarily metabolised by the colonic epithelium and very small amounts are transported into the portal and peripheral blood system (Cummings et al. 1987). Butyrate also has a short-half life (Miller et al. 2005). It must be noted that HFF cells are fibroblasts, not epithelial cells like HEK293 and MCF10A, or epidermal cells like HaCaTs. In future work, it would be useful to compare the response of CRC lines to those of a normal epithelial colon cell line, resected normal colon epithelium or 3D cell models such as organoids (discussed in section 6.5). However, such lines are

difficult to maintain and cells such as FHC cells are also susceptible to tumorigenicity and may have *TP53* mutations (Soucek et al. 2010).

A key issue faced with current cancer therapeutics are the toxic side effects experienced by normal cell types as signalling pathways required by normal cells are often disrupted (Cleeland et al. 2012); therefore, this needs to be considered. HFF cells were selected for further validation with the identified butyrate-sensitising miRNAs. It was demonstrated that no viability changes were observed with any of the miRNAs except a slight increase in growth with miR-1227 and butyrate. All miRNAs were able to induce increases in apoptosis in HFF cells either alone or in combination with butyrate. One way to offset the potential toxicity of the miRNAs to normal cells is by using targeted delivery vectors to reduce non-target cell exposure (Hosseinhali et al. 2018). Several delivery systems have been designed to encapsulate or bind miRNAs including non-viral vectors such as lipid-based carriers, charged polymeric vectors with varying chemical coatings and inorganic materials and viral vectors (adenovirus and lentivirus) (Hosseinhali et al. 2018). In some cases, these vehicles may be modified to selectively target cancer cells (Hosseinhali et al. 2018). Results from a phase 1 clinical trial have supported the potential of targeted miRNA replacement therapy using EGFR-targeted minicells to deliver miR-16 mimics to mesothelioma sufferers, with outcomes including 1 objective response, 1 partial response and 15 stable disease out of 22 patients (van Zandwijk et al. 2017). Further development of these vectors will hopefully help avoid issues with miRNA toxicities and unwanted immune responses.

### 3.3.5 Validation of predicted miRNA target genes

The ability of specific miRNAs to modulate cell proliferation or apoptosis in combination with butyrate is presumably due to modulation of specific downstream target mRNAs. Hence, predicted targets of these miRNAs were investigated. Many target genes were involved in key CRC and butyrate related pathways such as WNT signalling, PI3K-AKT signalling, MAPK signalling, RAS signalling and apoptosis. As described in detail in sections 1.1.3 and 1.3.3.1, several mutations associated with CRC are found within these pathways as well as genes regulated by butyrate to exert its anticancer properties.

#### **miR-593 predicted target genes**

miR-593 was shown to regulate the mRNA level of the target genes *CCND1* and *EEF2K*. A significant reduction in *CCND1* protein expression was also observed while

EEF2K protein was unaffected by miR-593. *CCND1* is a well-known cell cycle regulator which interacts with CDK4 and CDK6 in order to regulate G1 to S phase transition (VanArsdale et al. 2015). *CCND1* gene expression has been associated with metastasis in CRC (Balcerczak et al. 2005), while it has been shown to be downregulated by butyrate (Daly & Shirazi-Beechey 2006). *CCND1* was found to be associated with several pathways including WNT signalling as a target of the  $\beta$ -catenin/TCF/LEF transcriptional complex (Tetsu & McCormick 1999), PI3K-AKT signalling which regulates its degradation by GSK3- $\beta$  (Diehl et al. 1998) and MAPK signalling which promotes *CCND1* expression via the AP-1 transcription factors (Shaulian & Karin 2001). It has been demonstrated that the silencing of *CCND1* via other miRNAs, like miR-374a, in CRC has been able to inhibit proliferation, migration and invasion (Chen et al. 2016c), which is similar in terms of the growth effects induced by miR-593 in the current study.

EEF2K is an elongation factor which is involved in inhibiting protein synthesis and is regulated via mTORC signalling and mTOR phosphorylation, PI3K signalling through GSK3 phosphorylation and MAPK signalling pathways via ERK phosphorylation to inhibit its activity (Wang et al. 2014c). EEF2K expression is upregulated in CRC (Rhodes et al. 2004). EEF2K has been identified as a potential therapeutic target because its inhibition is related to apoptosis induction and reduced growth in cancer (Fu et al. 2014). Although few studies have been performed in CRC cells, other studies have shown that *EEF2K* silencing by tumour suppressor miRNAs in renal cell carcinoma and breast cancer reduces cell growth, migration and invasion (Bayraktar et al. 2017; Shi et al. 2016), which is promising. Previous studies have also shown that silencing *EEF2K* in HCT116 cells induces autophagy (Xie et al. 2014).

### **miR-1227 predicted target genes**

miR-1227 was shown to reduce the transcript levels of predicted target genes *DVL3* and *NUP62*. *NUP62* protein also declined after miRNA exposure; however, *DVL3* protein levels did not change significantly. It is possible that *DVL3* protein has a long half-life or that it is subject to additional levels of regulation. *DVL3* is a phosphoprotein involved in WNT signalling, which negatively regulates the destruction complex in order to release  $\beta$ -catenin to promote gene expression (Gao & Chen 2010). *DVL3* is overexpressed in several cancers including CRC (Hong et al. 2007), lung cancer (Uematsu et al. 2003a) and mesothelioma (Uematsu et al. 2003b). *DVL3* knockdown in several other cancers has revealed promising results, as inhibition resulted in reduced

proliferation in lung cancer (Uematsu et al. 2003a) and breast cancer cells (Castro-Piedras et al. 2018) through regulation of the WNT pathway. Interestingly, DVL1-3 have been shown to contribute to multi-drug resistance (vincristine, 5-fluorouracil and oxaliplatin) in CRC cells; silencing of these genes resensitised the cells to these drugs (Zhang et al. 2017b), indicating DVL proteins are potential therapeutic targets.

NUP62 is a nuclear pore protein which localises to the central channel and assists in nucleocytoplasmic transport as well as pore permeability (Schwarz-Herion et al. 2007). There is some evidence to support the association of NUP62 with  $\beta$ -catenin nuclear import in WNT signalling; however, further investigation is required (Yang et al. 2015d). NUP62 has been detected in CRC cells and patient tissues, although its expression is inconsistent when compared to normal mucosa (Chang et al. 2007; Tsukamoto et al. 2011); however, it is over expressed in squamous cell carcinoma (Hazawa et al. 2018). Recently, NUP62 was shown to promote the nuclear transport of the oncogenic transcription factor P63 and hence its knockdown reduced proliferation and increased differentiation of squamous cell carcinoma (Hazawa et al. 2018). Other nucleoporins have been associated with CRC development, including NUP358 which is involved in mitotic cell death; however, further investigation of NUP62 is required (Wong & D'Angelo 2016) as it may be a potential therapeutic target.

Interestingly, miR-1227 was shown to significantly increase transcript levels of *STAT3*. There are several mechanisms by which miRNAs may induce post-transcriptional up-regulation of their target genes (Vasudevan 2012). For example, miR-369 has been shown to bind the 3'UTR of TNF $\alpha$  and recruit AGO2 and FXR1 in order to activate translation (Vasudevan et al. 2007). Alternatively, miR-125b has been shown to bind to the 3'UTR of  $\kappa$ B-Ras2 to block binding of degradation proteins to the AU-rich element (ARE) thereby enhancing mRNA stability (Murphy et al. 2010). miR-328 can act as a miRNA mediated-decoy by binding hnRNP-E2 to prevent it from silencing c/EBP $\alpha$  (Eiring et al. 2010). Interestingly, *STAT3* is commonly upregulated and associated with poor prognosis in several cancer states including CRC (Corvinus et al. 2005; Wu et al. 2016b). However, particular isoforms (*STAT3 $\beta$* ) can have tumour suppressor properties and are associated with better prognosis in oesophageal cancer and AML (Aigner et al. 2019; Zhang et al. 2016a). Although specific isoforms were not investigated in this study, the tumour suppressor properties of *STAT3 $\beta$*  may provide an explanation as to why miR-1227 and butyrate promote its expression to partly exert their anticancer properties. This requires further investigation.

**miR-125b predicted target genes**

miR-125b was shown to regulate the expression of *TRIM29* (also known as ATDC) at the transcript level but it had no effect at the protein level unless combined with butyrate. *TRIM29* is involved in promoting WNT signalling through the regulation of  $\beta$ -catenin stabilisation, localisation and expression as well as promoting PI3K/AKT signalling through AKT phosphorylation in order to promote cell growth (Sun et al. 2019a; Zhou et al. 2016c). *TRIM29* is overexpressed in CRC (Sun et al. 2019a) and several other cancers such as pancreatic cancer (Wang et al. 2009), lung cancer (Tang et al. 2013) and gastric cancer (Kosaka et al. 2007). Knockdown of *TRIM29* in CRC resulted in decreased cell proliferation, migration, invasion and metastasis as well as inducing cell cycle arrest and apoptosis by reduction of  $\beta$ -catenin expression and nuclear accumulation (Sun et al. 2019a; Xu et al. 2016). As the protein levels did not change with miRNA exposure, it is unclear whether this protein is responsible for the cellular responses observed with the miRNA, although it might be implicated in the butyrate response.

**miR-181a predicted target genes**

miR-181a was shown to regulate the expression of *COX2*, *FZD4*, *MAP3K8* and *PIK3R3* by decreasing transcript levels although interestingly, in the presence of butyrate all genes were significantly induced. *COX2* protein levels did not change with miR-181a exposure although it was reduced in the presence of butyrate, while *PIK3R3* protein levels were reduced by the miRNA and in the combination treatment. *COX2* is a well-studied pro-inflammatory protein; however, it has been implicated in WNT signalling as its promoter region contains a TCF/LEF responsive element which promotes its expression during WNT signalling activation (Nunez et al. 2011). It was also shown that when rat intestinal epithelial cells were created to overexpress *COX2*, this resulted in increased anti-apoptotic protein *BCL2* as well as resistance to butyrate induced apoptosis (Tsujii & DuBois 1995). *COX2* is normally upregulated in CRC and other cancers (Dannenberget al. 2001; Ferrandez et al. 2003; Wang & Dubois 2010), while its expression is reduced by butyrate (Daly & Shirazi-Beechey 2006). Interestingly, knockdown of *COX2* can resensitise CRC cells to cetuximab and induce apoptosis (Lu et al. 2016b), which is supportive of its potential as a therapeutic target. miRNA studies in cancer have also revealed that knockdown of *COX2* inhibits cell proliferation and promotes cell apoptosis (Agra Andrieu et al. 2012).

PIK3R3 is a regulatory subunit of PI3K which is involved in the negative regulation of the tumour suppressor PTEN in PI3K/AKT signalling (Martini et al. 2014). PIK3R3 is upregulated in CRC (Wang et al. 2014b; Zhang et al. 2017a) and other cancers like pancreatic cancer (Peng et al. 2018). miR-212 has been shown to silence *PIK3R3* in order to inhibit viability and invasion of CRC cells (Zhang et al. 2017a), which indicates it may be a good therapeutic target. Conversely, *PIK3R3* overexpression has been shown to promote cell survival but also increase chemotherapeutic sensitivity in HT29 and SW480 CRC cells (Ibrahim et al. 2018); further testing is required understand these dichotomous functions, including in other cell lines.

In the current study, MAP3K8 and FZD4 protein levels were not determined although they appeared to be regulated by miR-181a and butyrate at the mRNA level. Frizzled (FZD) proteins are well known WNT receptors which bind WNT ligands in order to activate the WNT pathway and cell growth (Zeng et al. 2018). However, FZD4 is not a well-studied family member. FZD4 is upregulated in CRC (Hong et al. 2007) and other cancers like glioma (Riva et al. 2018). A previous study demonstrated that miR-493-mediated silencing of FZD4 in bladder cancer inhibited growth and migration (Ueno et al. 2012), which suggests that it may play an oncogenic role. MAP3K8 (also known as COI) is a kinase protein involved in activating MEK kinases in the MAPK signalling pathway which normally promotes growth (Fang & Richardson 2005). MAP3K8 expression is upregulated in CRC and is associated with poor prognosis (Tunca et al. 2013); it is also overexpressed in breast cancer (Sourvinos et al. 1999) and T-cell lymphomas (Patriotis et al. 1993). A previous study revealed that miRNA-mediated silencing of *MAP3K8* in renal cancer inhibited proliferation and migration (Su et al. 2015), although further investigation of this gene is required in CRC cells, it may also be a useful therapeutic target.

### **Limitations of gene expression studies**

As noted previously, in this study miRNA-mediated changes in mRNA and protein expression levels did not always correlate. The lack of correlation is not uncommon and has been discussed in several studies (Liu et al. 2016c; Payne 2015; Vogel & Marcotte 2012). This could be due to the multiple modes of regulation involved including transcriptional, translational and protein degradation. For example, on average less mRNA transcripts are produced compared to their corresponding proteins over one hour in mammalian cells and mRNAs are usually less stable than proteins (Schwanhausser et al. 2011; Sharova et al. 2009). Stability also varies based on function

as many metabolic proteins are more stable than those involved in dynamic processes like transcriptional regulation (Schwanhausser et al. 2011; Vogel et al. 2010). In cancer states, some highly expressed oncogenes experience 3'UTR shortening in order to avoid miRNA mediated translation repression (Mayr & Bartel 2009). miRNAs can regulate protein synthesis by destabilising their target mRNAs in order to decrease mRNA abundance or by inducing translational inhibition that does not affect mRNA levels (Baek et al. 2008). Although, it is important to note that the protein is the effector of the cellular response and so changes in steady-state protein levels are more informative at least in understanding the cellular changes. A limitation of this study was that only the protein level was investigated and not activity or changes such as protein phosphorylation, which may control the cellular response.

### 3.3.6 *PIK3R3* knockdown mimics miR-181a cellular response

The next investigation involved determining if the knockdown of target genes could mimic the effects of the miRNAs, potentially illustrating the importance of these genes in the cellular responses observed. *DVL3* and *PIK3R3* were knocked down using siRNAs and it was revealed that *PIK3R3* knockdown had the most lethal effects on HCT116 cell growth alone and in combination with butyrate, whereas the effects of *DVL3* knockdown were very subtle. A previous study demonstrated that the use of PI3K catalytic subunit inhibitors (Wortmannin or LY294002) and 5 mM butyrate in combination significantly induced a pro-apoptotic and anti-proliferative effect in KM20 (Wang et al. 2002). This highlights the importance of the PI3K signalling pathway in complementing the butyrate response as a strong anticancer effect is induced by targeting both the catalytic subunit (Wang et al. 2002) and regulatory subunit, *PIK3R3*, as identified in the current study. Hence *PIK3R3* could be a good therapeutic target.

### 3.3.7 miR-181a regulates WNT signalling

The final set of studies examined whether the butyrate-sensitising miRNAs modulated key pathways revealed through pathway analysis. All miRNAs had at least one target gene involved in the WNT signalling pathway, which is a critical dysregulated pathway in CRC (Fodde 2002). miR-181a was the only miRNA that appeared to regulate the WNT pathway in both the presence and absence of WNT ligand in high WNT activity HCT116 cells. In contrast, all miRNAs had some effect on WNT signalling in the absence of WNT ligand in low WNT activity RKO cells. These results are difficult to interpret because the mechanisms involved are unclear. Previous studies have implicated miR-181a in WNT signalling as it targets  $\beta$ -catenin and TCF4 in CRC (Lv et al. 2018);

however, this may be expected to decrease WNT activity rather than increase in WNT activity as seen in the current study. However, the earlier study only showed changes in expression of WNT pathway proteins but did not investigate activity changes, and different CRC cell lines were used (Lv et al. 2018). Conversely, another study in CRC cells demonstrated that miR-181a inhibits WIF1 which is a WNT signalling inhibitor, WNT activity was also not determined in this study; however, this may imply miR-181a can increase WNT activity (Ji et al. 2014a). miR-125b has been previously shown to silence WNT inhibitors (APC2 DKK1, DKK3, RNF43, ZNRF3) in CRC in order to promote WNT signalling which induces cetuximab resistance (Lu et al. 2017b). miR-593 and miR-1227 have not been well studied in the context of WNT signalling.

Another interesting observation was that RKO cells did not respond to butyrate without WNT ligands; however, they did show hyperactivation of the WNT pathway when exposed to WNT ligands. Previous studies have demonstrated that when RKO cells were exposed to 5 mM butyrate for 48 h this weakly induced WNT activity (Lazarova et al. 2004), which supports the aforementioned results. It is likely that the differences in responses to WNT between the cell lines are due to  $\beta$ -catenin levels. It was demonstrated that exposure to a dose range of 0-50 ng/ml of WNT3A, induced a dose dependent increase in  $\beta$ -catenin levels in RKO cells, with negligible amounts in the absence of WNT3A; in contrast,  $\beta$ -catenin levels in HCT116 cells were not affected by WNT3A (Song et al. 2014a). HCT116 cells have stabilising mutations in  $\beta$ -catenin, while RKO cells have wild type  $\beta$ -catenin, which contributes to their baseline WNT activity and differential response to WNT3A. Another study demonstrated that P300 interactions with  $\beta$ -catenin are important in butyrate-mediated WNT hyperactivation as the knockdown of P300 repressed the effect of butyrate on WNT activity in HCT116 cells (Lazarova et al. 2013). Interestingly, P300 levels are low in RKO cells (Zhang et al. 2017e). This requires further investigation.

### **Limitations of WNT activity assays**

A key limitation of the WNT activity assay used was that butyrate was hyperactivating WNT activity in the cells providing little capacity for the miRNA to induce further effects on WNT activity (i.e. ceiling effect). Reducing butyrate concentration might have reduced the hyperactivation response; however, this condition would have been inconsistent with the other studies performed. Moreover, previous published studies have shown that the effect of butyrate on HATs and HDAC inhibition is concentration dependent (Donohoe et al. 2012). Although CRC cells primarily rely on aerobic

glycolysis (Warburg effect), they still have the ability to perform oxidative metabolism (Donohoe et al. 2012). CRC cells have the capacity to metabolise butyrate up to approximately 1-2 mM, before it begins to accumulate and act as a HDACi (Andriamihaja et al. 2009). Below this threshold, butyrate can be metabolised into acetyl CoA, where it enters the citric acid cycle to produce citrate, which is shuttled out of the mitochondria and converted to acetyl CoA by ATP citrate lyase (ACL) in the nucleus (Donohoe et al. 2012; Wellen et al. 2009). This free acetyl CoA can be utilised as a co-factor by HATs to transfer acetyl groups to histones and non-histone proteins (Donohoe et al. 2012; Wellen et al. 2009). This results in different cellular effects compared to butyrate when it acts as a HDACi because it was demonstrated that low doses (0.5 mM) of butyrate increased cell growth in CRC cells (Donohoe et al. 2012).

### 3.3.8 Conclusion

In conclusion, this study identified several miRNAs and potential target genes that could enhance the ability of butyrate to reduce CRC cell proliferation and induce apoptosis. These included miR-125b and its target *TRIM29*, miR-181 and targets *COX2*, *FZD4*, *MAP3K8* and *PIK3R3*, miR-593 and targets *CCND1* and *EEF2K* and miR-1227 and targets *NUP62* and *DVL3*. The future directions will involve further validation of the key miRNA targets, including determining if they are directly bound by the miRNAs. In order to define the involvement of key miRNA target genes in WNT signalling, siRNAs could be used to knockdown the targets and determine WNT activity changes. The key outcomes of this study are that several butyrate-sensitising miRNAs have been identified and the PI3K regulatory subunit, *PIK3R3*, has been revealed as a critical target gene that may control proliferation and apoptosis in HCT116 cells. Although further investigation is required, this study may provide the basis to develop these miRNAs and this gene as potential therapeutic targets.

# Chapter 4. Integrative transcriptome network analysis in butyrate treated CRC cells

---

## 4.1 Introduction

CRC development and progression involves the dysregulation of thousands of genes in the transcriptome (Huo et al. 2017; Xu et al. 2017). Butyrate, which is an HDACi that alters global acetylation and consequently global gene expression in CRC cells, can counteract CRC development (Wu et al. 2018c). Through microarray and small-scale profiling studies, it has been shown to regulate thousands of genes involved in apoptosis, proliferation, the cell cycle and differentiation in order to exert its anticancer properties (Daly & Shirazi-Beechey 2006; Iacomino et al. 2001). Of the altered genes, many include non-coding RNAs such as miRNAs which are known to regulate cell proliferation, apoptosis and differentiation. To the best of our knowledge, a systems biology approach has not yet been employed to gain a comprehensive understanding of the complex RNA interactions occurring and contributing to the butyrate response in CRC cells. Next generation sequencing and network analysis has yet to be utilised to reveal the extent of butyrate mediated gene regulation in cancer. Such analyses could identify the key RNA contributors and the networks in which they function to promote the anti-proliferative and pro-apoptotic effects of butyrate. The investigation of these functional networks and RNA molecules may also further reveal the mechanism by which butyrate influences key cell growth and death pathways in CRC and assist in identification of potential therapeutic targets.

To investigate the diverse effects of butyrate and identify key miRNA hubs involved in the butyrate response of CRC cells, Illumina total and small RNA-seq was performed on HCT116 cells which were treated with 2.5 mM butyrate. Differentially expressed (DE) genes were selected and key miRNA-gene hubs were identified in cell death and growth-related pathways including apoptosis and the cell cycle. The expression changes of the selected miRNAs and their predicted target genes were validated using real-time RT-PCR analysis.

## 4.2 Results

### 4.2.1 Identification of butyrate regulated mRNAs

To identify protein-coding genes that were differentially expressed after treatment with butyrate, Illumina total RNA-seq was performed on the RNA of 2.5 mM butyrate treated or untreated HCT116 CRC cells. The total RNA-seq revealed that out of 15,000 protein-coding genes detected, 2447 mRNAs showed altered expression (1110 downregulated and 1337 upregulated) by butyrate when the criteria  $\log_2FC < -1.5$  or  $\log_2FC > 1.5$  and  $p_{adj} < 0.01$  was applied (Figure 4-1). The differentially expressed genes were further investigated for their potential roles in the butyrate response of CRC cells through network and pathway analyses.

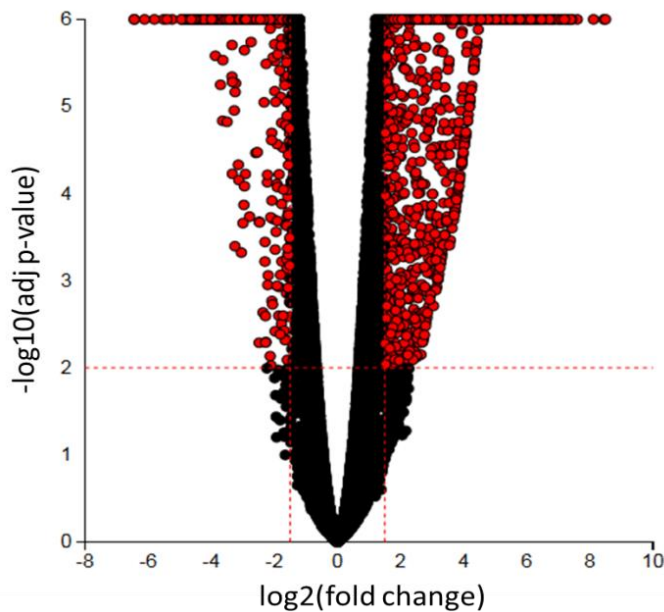


**Figure 4-1 Volcano plot representing the differential expression of butyrate responsive mRNAs**

HCT116 cells (n=2) were treated with 2.5 mM butyrate for 48 h and total RNA sequencing was performed to determine differential mRNA expression. The x-axis represents the differential expression ( $\log_2$  fold change (FC)) and the y-axis represents the significance ( $-\log_{10}$  (p-value)). Highly differentially expressed microRNAs, which have  $\log_2FC \leq -1.5$  or  $\log_2FC \geq 1.5$  and  $adj\ p\text{-value} < 0.01$ , are coloured in red and black dots show miRNAs with no significant change. The plot was generated using Advaita iPathway Guide tool (Ahsan & Draghici 2017).

### 4.2.2 Identification of butyrate regulated miRNAs

To identify miRNAs that were differentially expressed after treatment with butyrate, Illumina small RNA-seq was performed on the RNA of 2.5 mM butyrate treated or untreated HCT116 CRC cells. The small RNA-seq data revealed that out of 845 miRNAs detected, 113 miRNAs were dysregulated (50 downregulated and 63

upregulated) by butyrate when  $\log_2FC < -1$  or  $\log_2FC > 1$  and  $p_{adj} < 0.05$  was applied (Figure 4-2). Criteria were less stringent for miRNA selection due to limited dysregulation of miRNA genes. Previous studies have demonstrated that endogenous concentrations of miRNAs vary greatly within cells. A cell may have less than 10 copies of a low abundance miRNA and sometimes  $>10,000$  copies per cell for highly abundant cell-type restricted miRNAs (Liang et al. 2007). Marginal changes in miRNA expression can lead to repression of hundreds of targets (Selbach et al. 2008); therefore, this subtle variation is considered in the above criteria. The differentially expressed miRNAs were further investigated for their functional role in the butyrate response of CRC cells through network and pathway analyses.

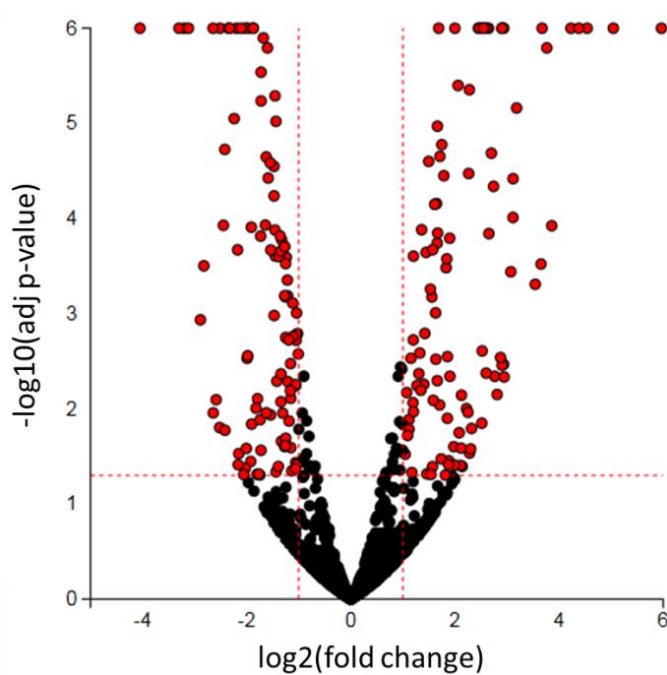


**Figure 4-2** Volcano plot representing the differential expression of butyrate responsive miRNAs

HCT116 cells ( $n=3$ ) were treated with 2.5 mM butyrate for 48 h and small RNA sequencing was performed to determine differential miRNA expression. The x-axis represents the differential expression ( $\log_2$  fold change (FC)) and the y-axis represents the significance ( $-\log_{10}$  (p-value)). Highly differentially expressed miRNAs, which have  $\log_2FC \leq -1$  or  $\log_2FC \geq 1$  and  $adj\ p\text{-value} < 0.05$ , are coloured in red and black dots show miRNAs with no significant change. The plot was generated using Advaita iPathway Guide tool (Ahsan & Draghici 2017).

### 4.2.3 Butyrate regulated protein-protein interaction (PPI) network analysis

The differentially expressed mRNA gene list was further filtered by the criteria mean raw counts  $\geq 25$  in both untreated and butyrate treated samples in order to remove very low expressed genes which may be difficult to validate by real-time RT-PCR. This resulted in a final list of 1623 mRNAs regulated by butyrate (1026 downregulated and 597 upregulated) (refer to Appendix 4).

Network Analyst (<http://www.networkanalyst.ca>) (Xia et al. 2015), an online PPI network analysis tool, was used to further define and construct networks for DE mRNAs to assist in identification of key biological interactions involved in the butyrate response. The PPI database, IMEx Interactome which is a comprehensive literature-curated database from InnateDB, was used to define the network. Only zero-order networks were investigated as these show direct interactions with the input list (seed proteins).

The protein-protein interaction network was visualized using the open source network construction software, Cytoscape (Version 3.4.0) (Shannon et al. 2003) and then analysed (undirected network) using the in-built NetworkAnalyser tool to determine the network properties. A total of 507 DE genes with degree  $\geq 1$  were selected for network visualisation and further investigation (Figure 4-3). Refer to Appendix 5 (Table 7-1) for a list of protein-coding gene nodes within the PPI network with degree  $\geq 1$ . The PPI network identified several hub proteins (greatest degree value) regulated by butyrate including p53 with degree 80 and KIAA0101 and FN1 with degree 75. Proteins with the greatest degree value are the most central to the network i.e. they have the greatest number of protein connections.

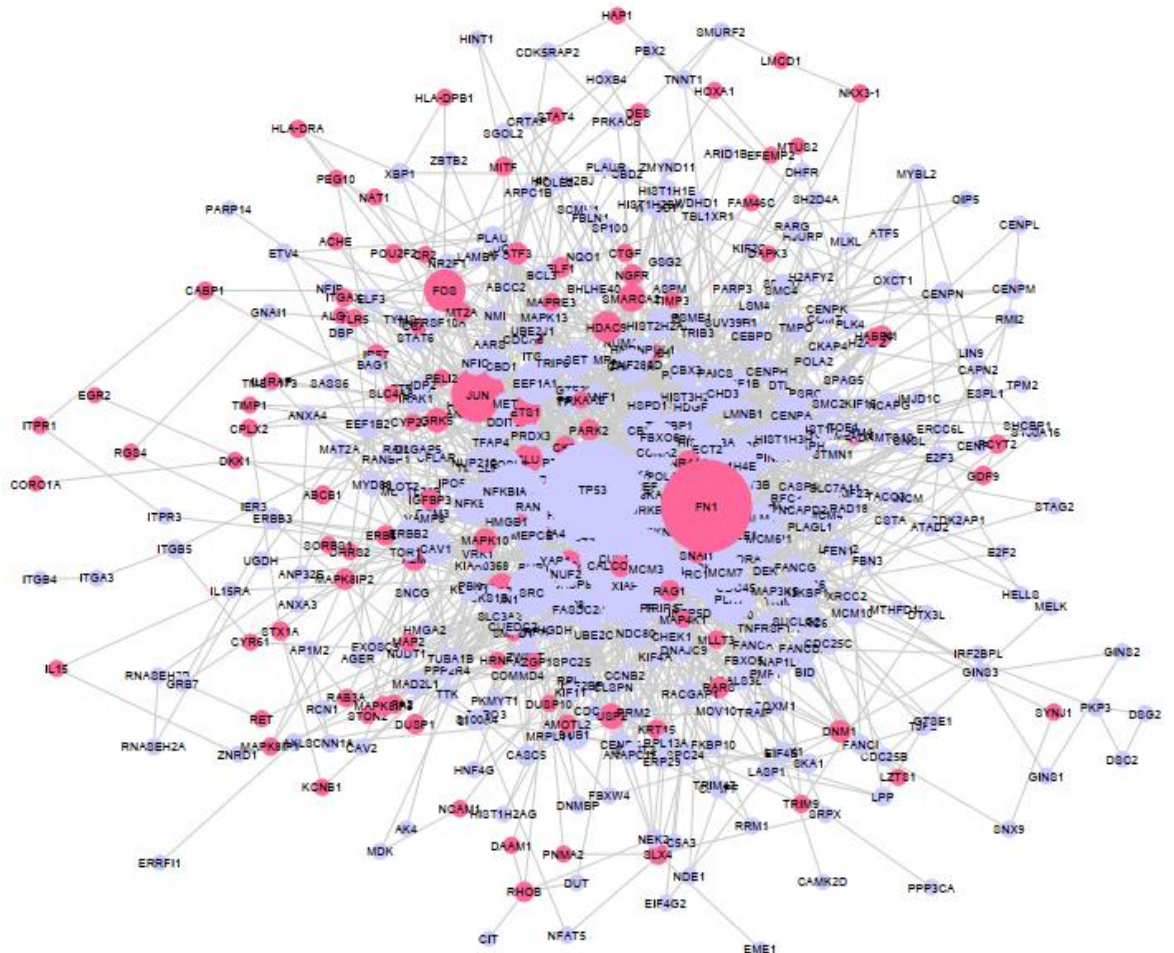


**Figure 4-3 Butyrate regulated PPI network for DE protein-coding genes**

PPI network analysed using NetworkAnalyst and constructed using Cytoscape software. Pink nodes represent the upregulated protein-coding genes and purple nodes represent the downregulated protein-coding genes. Solid grey lines are edges and represent direct protein-protein interactions between two nodes. The size of the nodes is proportional to the number of interactions with other nodes i.e. degree value.

#### 4.2.4 Functional gene ontology (GO) analysis of butyrate regulated genes

Gene ontology (GO) enrichment analysis allows the classification and interpretation of gene lists based on their functional characteristics including molecular function, biological processes and cellular components. GO enrichment analysis was used to further examine the butyrate response in CRC cells at the transcriptomic level based on protein-coding genes identified in the PPI network with degree  $\geq 1$  (Figure 4-3). ClueGO (Bindea et al. 2009) is a Cytoscape plug-in which can be used for GO enrichment analysis of gene lists. ClueGO was used to identify the enriched GO terms for the butyrate response for each of the following classifications: Biological Processes, Molecular Functions, and Cellular Compartments. The functional characteristics for Biological Processes identified 68 significantly enriched terms per group, Molecular Functions identified 26 significantly enriched terms per group, and Cellular Compartments identified 31 significantly enriched terms per group (Figure 4-4). The two most highly represented terms in Biological Processes were ‘cell cycle process’ and ‘positive regulation of macromolecule metabolic processes.’ The ‘cell cycle’ had the lowest term p-value at 6.89E-72 (Table 4-1). Interestingly, ‘DNA binding’ and ‘ATP binding’ were the top two Molecular Functions; however, ‘enzyme binding’ had the lowest term p-value at 1.82E-21 (Appendix 6). The top Cellular Components identified were ‘chromosomal part’ and intracellular ‘non-membrane-bounded organelle’, while the term with the lowest p-value was ‘chromosome’ at 2.79E-61 (Appendix 6).

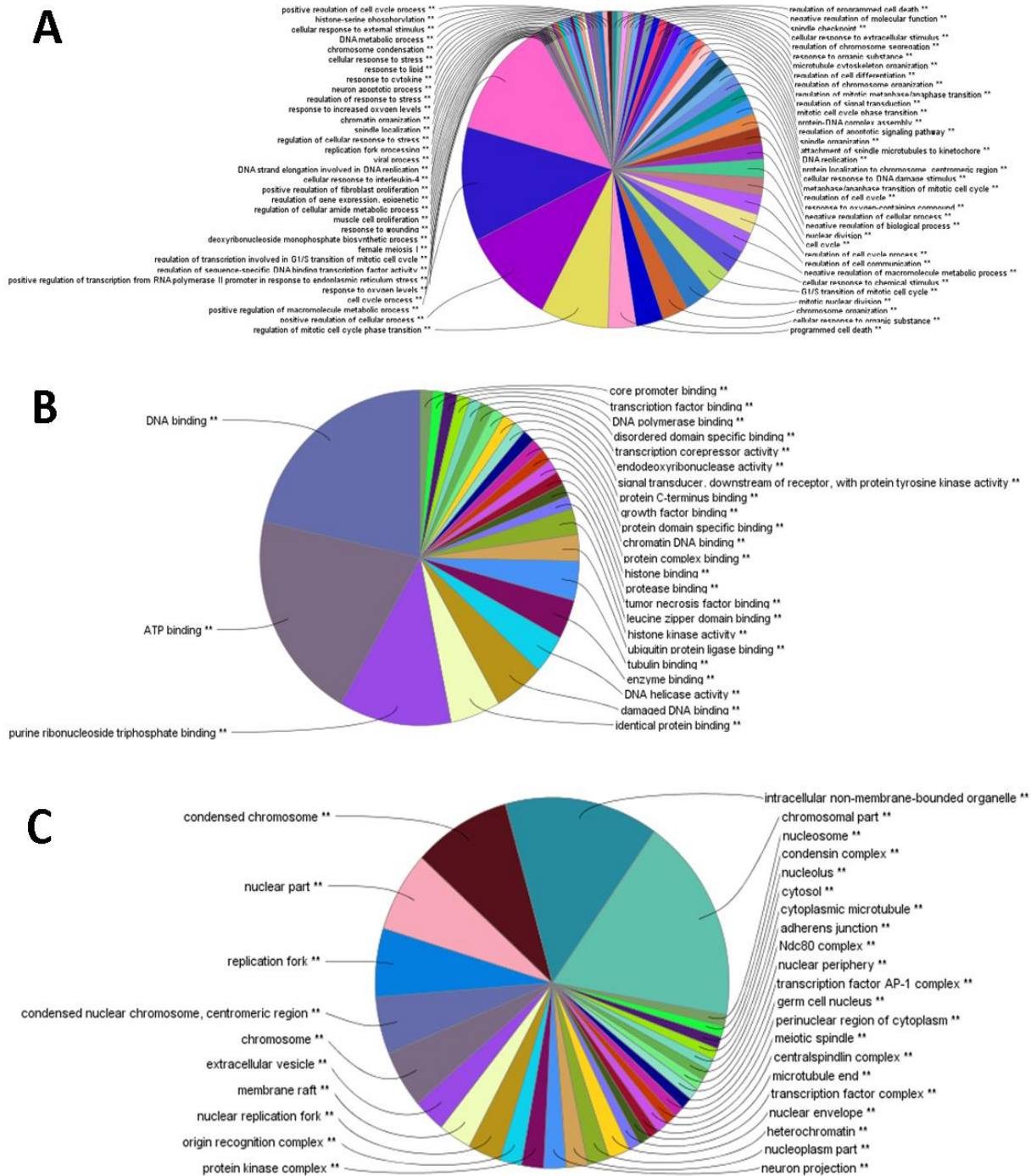


**Figure 4-4 Gene Ontology Enrichment analysis for butyrate DE genes**

Pie charts representing ClueGO enrichment analysis for butyrate regulated genes including the functional characteristics (A) biological processes, (B) molecular functions and (C) cellular compartments illustrating enriched GO terms ( $p$  value  $\leq 0.05$  corrected using Bonferroni step down method and kappa score threshold  $\geq 0.4$ ). The most significant terms in each group are labelled on the graph and the proportion of each pathway indicates the percent terms per group.

CHAPTER 4

**Table 4-1 Top three ‘Biological processes’ identified in GO enrichment analysis**

GO ID	GO Term	Number of Genes	% Associated Genes	Term PValue Corrected with Bonferroni step down	Associated Genes Found
<b>GO:0007049</b>	cell cycle	206	11.41	6.89E-72	<p>                     ABCB1, ANAPC16, APEX1, ASNS, ASPM, ATF5, AURKA, AURKB, BANF1, BID, BIRC5, BLM, BORA, BRCA1, BRCA2, BRIP1, BUB1, BUB1B, CAMK2D, CAV2, CCNA2, CCNB1, CCNB2, CDC20, CDC25A, CDC25B, CDC25C, CDC45, CDC6, CDCA3, CDCA8, CDK1, CDK2AP1, CDK4, CDK5RAP2, CDKN2A, CDT1, CENPA, CENPE, CENPF, CENPH, CENPK, CENPL, CENPM, CENPN, CENPQ, CHAF1A, CHD3, CHEK1, CIT, CKS1B, CLSPN, CTGF, CUL1, DAPK3, DBF4, DDIT3, DHFR, DLGAP5, DSN1, DTL, DUSP1, E2F1, E2F2, E2F3, ECT2, EIF4G2, EME1, ERCC6L, ESPL1, ETS1, FANCA, FANCD2, FANCG, FANCI, FANCM, FBXO5, FBXO6, FEN1, FOSL1, FOXM1, GINS1, GINS2, GNAH1, GRK5, GSG2, GTSE1, H2AFX, HELLS, HJURP, HMGA2, HMMR, HSPA2, ITGB3BP, JUN, KIF11, KIF15, KIF23, KIF2C, KIF4A, KNL1, LIN9, LZTS1, MAD2L1, MAPK13, MAPRE3, MCM10, MCM2, MCM3, MCM4, MCM5, MCM6, MCM7, MELK, MEPCE, MKI67, MYBL2, NCAPD2, NCAPG, NCAPH, NDC80, NDE1, NEK2, NKX3-1, NR2F1, NR4A1, NUF2, NUMA1, NUP210, OIP5, ORC1, ORC6, PARP3, PBK, PCLAF, PHGDH, PKMYT1, PLAGL1, PLK1, PLK4, PMF1, POLA1, POLA2, POLE2, PPP3CA, PRC1, PRKAA2, PRKACB, PSME1, PSRC1, PTPA, PTTG1, RACGAP1, RAD21, RAD51, RAN, RANBP1, RBBP4, RBBP8, RCC1, RCC2, RHOB, RMI2, RNASEH2A, RNASEH2B, RPA1, RRM1, RRM2, SASS6, SGO1, SGO2, SKA1, SKA3, SLX4, SMC2, SMC4, SNX9, SPAG5, SPC24, SPC25, SRC, STAG2, STMN1, SUV39H1, TACC3, TFAP4, THBS1, TIMELESS, TOP2A, TOPBP1, TP53, TP73, TPX2, TRIP13, TTK, TUBA1A, TUBB, TYMS, UBE2C, UBE2E1, USP2, VRK1, WEE1, XRCC2, ZMYND11, ZWINT                 </p>
<b>GO:0022402</b>	cell cycle process	178	12.81	4.97E-68	<p>                     ABCB1, ANAPC16, APEX1, ASPM, ATF5, AURKA, AURKB, BANF1, BID, BIRC5, BLM, BORA, BRCA1, BRCA2, BRIP1, BUB1, BUB1B, CAMK2D, CAV2, CCNA2, CCNB1, CCNB2, CDC20, CDC25A, CDC25B, CDC25C, CDC45, CDC6, CDCA3, CDCA8, CDK1, CDK4, CDK5RAP2, CDKN2A, CDT1, CENPA, CENPE, CENPF, CENPH, CENPK, CENPL, CENPM, CENPN, CENPQ, CHD3, CHEK1, CIT, CKS1B, CLSPN, CTGF, CUL1, DAPK3, DBF4, DDIT3, DHFR, DLGAP5, DSN1, DUSP1, E2F1, ECT2, EIF4G2, EME1, ERCC6L, ESPL1, FANCA, FANCD2, FANCI, FANCM, FBXO5, FEN1, FOXM1, GINS1, GINS2, GSG2, GTSE1, HELLS, HMGA2, HMMR, HSPA2, ITGB3BP, KIF11, KIF15, KIF23, KIF2C, KIF4A, KNL1, LZTS1, MAD2L1, MAPRE3, MCM10, MCM2, MCM3, MCM4, MCM5, MCM6, MCM7, MELK, MEPCE, MKI67, MYBL2, NCAPD2, NCAPG, NCAPH, NDC80, NDE1, NEK2, NKX3-1, NUF2, NUMA1, NUP210, OIP5, ORC1, ORC6, PARP3, PBK, PHGDH, PKMYT1, PLAGL1, PLK1, PLK4, PMF1, POLA1, POLA2, POLE2, PPP3CA, PRC1, PRKAA2, PSME1, PSRC1, PTPA, PTTG1, RACGAP1, RAD21, RAD51, RAN, RANBP1, RBBP8, RCC1, RCC2, RHOB, RMI2, RNASEH2B, RPA1, RRM2, SASS6, SGO1, SGO2, SKA1, SKA3, SLX4, SMC2, SMC4, SNX9, SPAG5, SPC24, SPC25, STAG2, STMN1, TACC3, TFAP4, THBS1, TIMELESS, TOP2A, TOPBP1, TP53, TP73, TPX2, TRIP13, TTK, TUBA1A, TUBB, TYMS, UBE2C, UBE2E1, VRK1, WEE1, XRCC2, ZWINT                 </p>
<b>GO:0000278</b>	mitotic cell cycle	154	14.82	2.90E-66	<p>                     ABCB1, ANAPC16, APEX1, ASNS, ASPM, AURKA, AURKB, BANF1, BID, BIRC5, BLM, BORA, BRCA1, BRCA2, BRIP1, BUB1, BUB1B, CAMK2D, CAV2, CCNA2, CCNB1, CCNB2, CDC20, CDC25A, CDC25B, CDC25C, CDC45, CDC6, CDCA3, CDCA8, CDK1, CDK4, CDK5RAP2, CDKN2A, CDT1, CENPA, CENPE, CENPF, CENPH, CHEK1, CIT, CKS1B, CLSPN, CUL1, DAPK3, DBF4, DHFR, DLGAP5, DSN1, DUSP1, E2F1, EME1, ERCC6L, ESPL1, FANCI, FBXO5, FOXM1, GINS1, GINS2, GSG2, GTSE1, HELLS, HMGA2, HMMR, ITGB3BP, KIF11, KIF15, KIF23, KIF2C, KIF4A, KNL1, LZTS1, MAD2L1, MAPRE3, MCM10, MCM2, MCM3, MCM4, MCM5, MCM6, MCM7, MELK, MEPCE, MKI67, MYBL2, NCAPD2, NCAPG, NCAPH, NDC80, NDE1, NEK2, NKX3-1, NUF2, NUMA1, NUP210, OIP5, ORC1, ORC6, PARP3, PBK, PKMYT1, PLAGL1, PLK1, PLK4, PMF1, POLA1, POLA2, POLE2, PPP3CA, PRC1, PSME1, PSRC1, PTPA, PTTG1, RACGAP1, RAD21, RAN, RANBP1, RBBP8, RCC1, RCC2, RNASEH2B, RPA1, RRM1, RRM2, SGO1, SKA1, SKA3, SMC2, SMC4, SNX9, SPAG5, SPC24, SPC25, STAG2, STMN1, TACC3, TFAP4, TIMELESS, TOP2A, TOPBP1, TP53, TP73, TPX2, TTK, TUBA1A, TUBB, TYMS, UBE2C, UBE2E1, USP2, VRK1, WEE1, XRCC2, ZWINT                 </p>

#### 4.2.5 Pathway enrichment analysis of butyrate regulated genes

ClueGO pathway enrichment analysis was used to further investigate the role of the DE protein-coding genes in the butyrate response of CRC cells. Butyrate is known to have anti-proliferative and pro-apoptotic properties; therefore, genes involved in these processes were of interest. KEGG and WikiPathways pathway analysis programs revealed that DE genes were enriched in key pathways such as the cell cycle and apoptosis as expected (Figure 4-5). KEGG pathway analysis identified 11 significantly enriched pathway groups in which ‘Apoptosis’ had the most percent terms per group allocated. The ‘Cell cycle’ pathway had the lowest term p-value at  $2.53E-21$  followed by ‘DNA replication’ ( $P=8.21E-09$ ) (Table 4-2). WikiPathways pathway analysis identified 9 significantly enriched pathway groups in which ‘ATM signalling pathway’ and ‘Apoptosis modulation and signalling’ had the most percent terms per group allocated (Figure 4-5 B). The ‘Retinoblastoma in Cancer’ pathway had the lowest term p-value at  $1.10E-29$  followed by the ‘Cell cycle’ ( $P=3.62E-17$ ) (Appendix 7). Reactome pathway analysis identified 18 significantly enriched pathway groups in which ‘IRS-mediated signalling’ and ‘oxidative stress induced senescence’ had the most percent terms per group allocated (Figure 4-5 C). Interestingly, the ‘Cell cycle’, ‘Meiosis’ and ‘Meiotic synapsis’ shared the same and lowest term p-values ( $P=6.62E-67$ ) (Appendix 7).

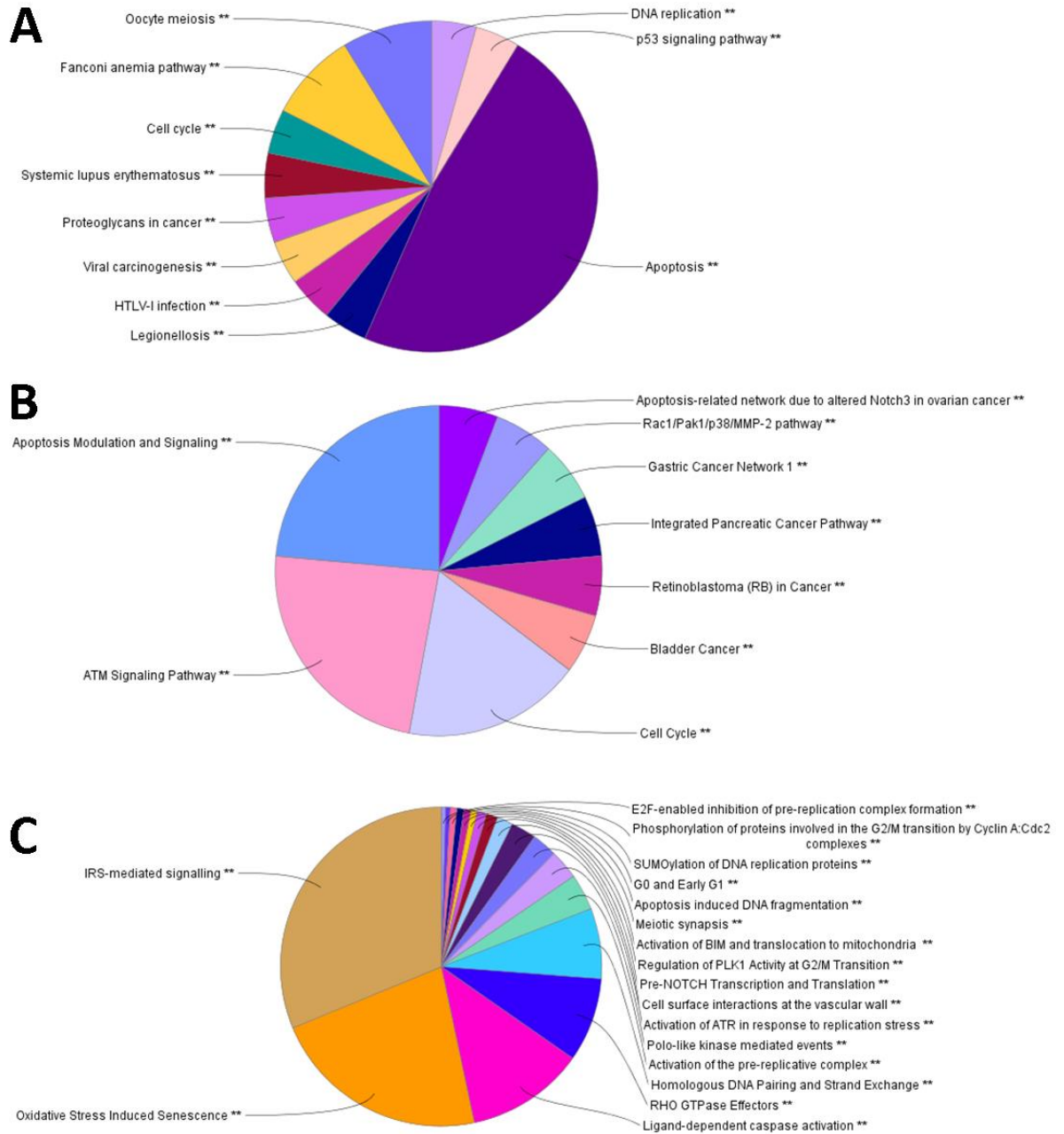


**Figure 4-5 KEGG, WikiPathways and Reactome pathway analysis of differentially expressed butyrate responsive mRNAs**

Pie graph depicting the enriched pathway terms identified after performing ClueGO pathway enrichment analysis in Cytoscape with butyrate responsive genes (A) KEGG, (B) WikiPathways, (C) Reactome. The most significant terms in each group are labelled on the graph and the proportion of each pathway indicates the percent terms per group ( $p$  value  $\leq 0.05$  corrected using Bonferroni step down method and kappa score threshold  $\geq 0.4$ ).

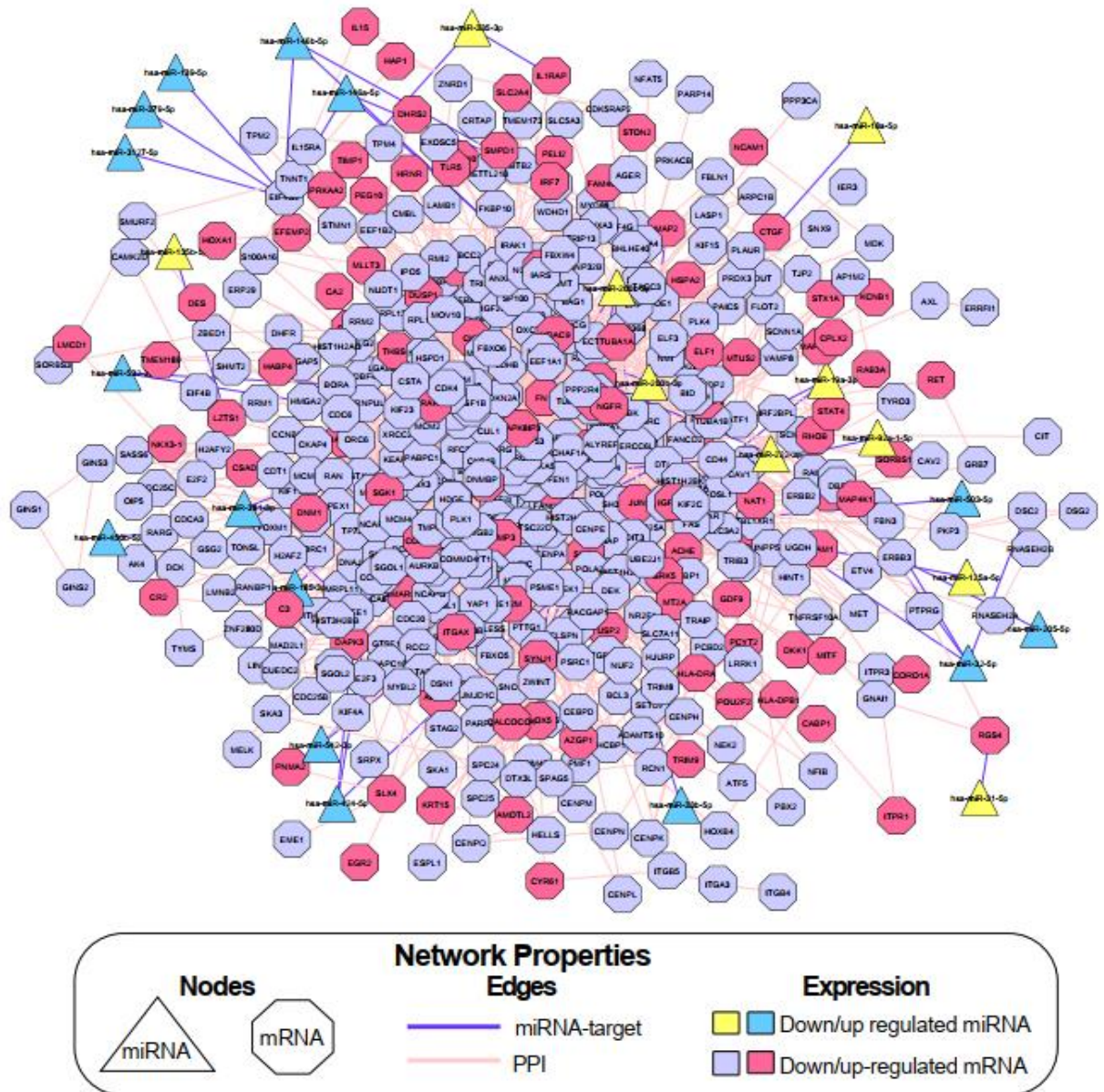
CHAPTER 4

Table 4-2 Enriched pathway terms identified using KEGG in ClueGO

GO ID	GO Term	No. of Genes	% Associated Genes	Term Corrected with Bonferroni down	PValue with step	Associated Genes Found
GO:0004110	Cell cycle	38.00	30.65	2.53E-21		BUB1, BUB1B, CCNA2, CCNB1, CCNB2, CDC20, CDC25A, CDC25B, CDC25C, CDC45, CDC6, CDK1, CDK4, CDKN2A, CHEK1, CUL1, DBF4, E2F1, E2F2, E2F3, ESPL1, MAD2L1, MCM2, MCM3, MCM4, MCM5, MCM6, MCM7, ORC1, ORC6, PKMYT1, PLK1, PTTG1, RAD21, STAG2, TP53, TTK, WEE1
GO:0003030	DNA replication	14.00	38.89	8.21E-09		FEN1, MCM2, MCM3, MCM4, MCM5, MCM6, MCM7, POLA1, POLA2, POLE2, RFC3, RNASEH2A, RNASEH2B, RPA1
GO:0005166	HTLV-I infection	35.00	13.67	4.39E-08		ATF1, ATF3, ATF4, BUB1B, CCNB2, CDC20, CDK4, CDKN2A, CHEK1, E2F1, E2F2, E2F3, EGR2, ETS1, FOS, FOSL1, HLA-DPB1, HLA-DRA, IL15, IL15RA, JUN, MAD2L1, MYBL2, NFKB1, NFKBIA, POLE2, PPP3CA, PRKACB, PTTG1, RAN, RANBP1, TNFRSF1A, TP53, XBP1, XIAP
GO:0004210	Apoptosis	25.00	18.12	4.58E-08		ATF4, BID, BIRC5, CAPN2, CASP8, CFLAR, DDIT3, FAS, FOS, ITPR1, ITPR3, JUN, LMNB1, LMNB2, MAP3K5, MAPK10, NFKB1, NFKBIA, PARP3, TNFRSF10A, TNFRSF1A, TP53, TUBA1A, TUBA1B, XIAP
GO:0003460	Fanconi anaemia pathway	14.00	25.45	4.49E-06		BLM, BRCA1, BRCA2, BRIP1, EME1, FANCA, FANCD2, FANCG, FANCI, FANCM, RAD51, RMI2, RPA1, SLX4
GO:0004115	p53 signalling pathway	15.00	21.74	1.41E-05		BID, CASP8, CCNB1, CCNB2, CDK1, CDK4, CDKN2A, CHEK1, FAS, GTSE1, IGFBP3, RRM2, THBS1, TP53, TP73
GO:0004114	Oocyte meiosis	20.00	16.13	2.12E-05		AURKA, BUB1, CAMK2D, CCNB1, CCNB2, CDC20, CDC25C, CDK1, CUL1, ESPL1, FBXO5, ITPR1, ITPR3, MAD2L1, PKMYT1, PLK1, PPP3CA, PRKACB, PTTG1, SGO1
GO:0005161	Hepatitis B	21.00	14.58	5.94E-05		ATF4, BIRC5, CASP8, CCNA2, CDK4, E2F1, E2F2, E2F3, EGR2, FAS, FOS, IRF7, JUN, MAPK10, MYD88, NFKB1, NFKBIA, SRC, STAT4, STAT6, TP53
GO:0005219	Bladder cancer	11.00	26.83	7.52E-05		CDK4, CDKN2A, DAPK3, E2F1, E2F2, E2F3, ERBB2, RPS6KA5, SRC, THBS1, TP53
GO:0005203	Viral carcinogenesis	25.00	12.44	1.04E-04		ATF4, C3, CASP8, CCNA2, CDC20, CDK1, CDK4, CDKN2A, CHEK1, EGR2, HDAC9, HIST1H2BJ, HIST1H2BK, HIST1H4E, HIST2H2BE, HIST3H2BB, IRF7, JUN, NFKB1, NFKBIA, PRKACB, RANBP1, SP100, SRC, TP53
GO:0003440	Homologous recombination	10.00	24.39	6.31E-04		BLM, BRCA1, BRCA2, BRIP1, EME1, RAD51, RBBP8, RPA1, TOPBP1, XRCC2
GO:0004914	Progesterone-mediated oocyte maturation	15.00	15.63	1.12E-03		BUB1, CCNA2, CCNB1, CCNB2, CDC25A, CDC25B, CDC25C, CDK1, GNAI1, MAD2L1, MAPK10, MAPK13, PKMYT1, PLK1, PRKACB
GO:0004668	TNF signalling pathway	16.00	14.81	1.13E-03		ATF4, BCL3, CASP8, CFLAR, FAS, FOS, IL15, JUN, MAP3K5, MAPK10, MAPK13, MLKL, NFKB1, NFKBIA, RPS6KA5, TNFRSF1A
GO:0005205	Proteoglycans in cancer	23.00	11.33	1.39E-03		CAMK2D, CAV1, CAV2, CD44, EIF4B, ERBB2, ERBB3, ERBB4, FAS, FN1, ITGB5, ITPR1, ITPR3, MAPK13, MET, PLAUR, PLAUR, PRKACB, SRC, TFAP4, THBS1, TIMP3, TP53
GO:0005212	Pancreatic cancer	11.00	17.19	7.16E-03		BRCA2, CDK4, CDKN2A, E2F1, E2F2, E2F3, ERBB2, MAPK10, NFKB1, RAD51, TP53
GO:0005145	Toxoplasmosis	15.00	13.27	7.91E-03		ALOX5, CASP8, GNAI1, HLA-DPB1, HLA-DRA, HSPA2, IRAK1, LAMB1, MAPK10, MAPK13, MYD88, NFKB1, NFKBIA, TNFRSF1A, XIAP
GO:0005142	Chagas disease (American trypanosomiasis)	14.00	13.73	9.51E-03		C3, CASP8, CFLAR, FAS, FOS, GNAI1, IRAK1, JUN, MAPK10, MAPK13, MYD88, NFKB1, NFKBIA, TNFRSF1A
GO:0005168	Herpes simplex infection	20.00	10.81	9.96E-03		ALYREF, C3, CASP8, CDK1, CUL1, FAS, FOS, GTF2I, HLA-DPB1, HLA-DRA, IL15, IRF7, JUN, MAPK10, MYD88, NFKB1, NFKBIA, SP100, TNFRSF1A, TP53
GO:0004010	MAPK signalling pathway	24.00	9.41	1.99E-02		ATF4, CDC25B, DDIT3, DUSP1, DUSP10, FAS, FOS, HSPA2, JUN, MAP3K5, MAP4K1, MAPK10, MAPK13, MAPK8IP1, MAPK8IP2, MAPK8IP3, NFKB1, NR4A1, PPP3CA, PRKACB, RPS6KA5, STMN1, TNFRSF1A, TP53
GO:0005222	Small cell lung cancer	12.00	14.29	2.05E-02		CDK4, CKS1B, E2F1, E2F2, E2F3, FN1, ITGA3, LAMB1, NFKB1, NFKBIA, TP53, XIAP
GO:0005200	Pathways in cancer	32.00	8.10	2.93E-02		BID, BIRC5, BRCA2, CASP8, CDK4, CDKN2A, CKS1B, DAPK3, E2F1, E2F2, E2F3, ERBB2, ETS1, FAS, FN1, FOS, GNAI1, ITGA3, JUN, LAMB1, MAPK10, MET, MIF, NFKB1, NFKBIA, NKX3-1, PPARG, PRKACB, RAD51, RET, TP53, XIAP
GO:0004215	Apoptosis	7.00	21.21	4.08E-02		BID, BIRC5, CASP8, MAPK10, NGFR, TNFRSF1A, XIAP
GO:0005134	Legionellosis	9.00	16.36	4.67E-02		C3, CASP8, EEF1A1, HSPA2, HSPD1, MYD88, NFKB1, NFKBIA, TLR5
GO:0005322	Systemic lupus erythematosus	15.00	11.28	4.68E-02		C3, H2AFX, H2AFY2, H2AFZ, HIST1H2AG, HIST1H2BJ, HIST1H2BK, HIST1H3H, HIST1H4E, HIST2H2AC, HIST2H2BE, HIST2H3A, HIST3H2BB, HLA-DPB1, HLA-DRA

### 4.2.6 Integrative network construction using miRNA target prediction

Butyrate is known to regulate miRNA expression in order to exert its anticancer properties on cell growth and death. For example, butyrate regulates the expression of key members of the miR-17-92 cluster in order to regulate their tumour suppressor targets such as *PTEN* and *CDKN1A* (Humphreys et al. 2013) and this contributes to decreased cell growth and increased apoptosis (Hu et al. 2011). In order to identify key miRNA and mRNA gene interactions regulated by butyrate, a miRNA-mRNA network analysis incorporating PPI was performed using Cytoscape. The differentially expressed miRNA gene lists collected (section 4.2.2) were further filtered by the criteria mean raw counts  $\geq 25$ , in both untreated and butyrate treated samples, to remove low expressed genes that may be difficult to validate using real-time RT-PCR. This resulted in a final list of 77 miRNAs regulated by butyrate (38 downregulated and 39 upregulated) (Appendix 8). The predicted and validated mRNA targets of these selected miRNAs were identified using online target prediction programs or validated target databases. miRTarBase (Chou et al. 2018a) and miRecords (Xiao et al. 2009a) databases identified validated targets based on strong experimental evidence i.e. luciferase reporter assays. TargetScan, miRDB and DIANA microT-CDS were used in combination to identify predicted miRNA target genes based on the thresholds mentioned in the methods section. The miRNA-mRNA interactions were presented in the network if they were predicted or validated by two or more programs or databases respectively and if their expression was negatively correlated. The rationale behind this is that if a miRNA targets an mRNA, its levels are very likely to be reduced due to target degradation. If the miRNA expression is reduced, then the mRNA target expression is expected to increase and vice versa. Based on the above criteria, a total of 52 miRNA-mRNA target pairs were revealed in the miRNA- mRNA integrative network incorporating PPI and of these interactions 16 were both predicted and validated, while 36 were only predicted targets (Figure 4-6). The network had a total of 566 nodes including miRNAs, miRNA targets and non-target proteins.



**Figure 4-6 Integrative miRNA-mRNA interaction network of butyrate regulated genes in CRC**

Butyrate-regulated integrative miRNA-mRNA network constructed using Cytoscape based on interactions between miRNA and target protein-coding genes and PPI. Refer to key for node information and expression profiles. The colour of the node represents the expression changes due to 2.5 mM butyrate treatment and the shape represents the type of molecule for each node. Solid lines are edges and represent direct interactions between two nodes.

### 4.2.7 Investigation of key miRNA-mRNA interactions involved in cell growth and death pathways in the butyrate response

Network interactions were further defined based on pathway enrichment analysis results (Section 4.2.5). As previously mentioned, butyrate is known to regulate cell growth and death pathways including the cell cycle and apoptosis. The 'Cell cycle' pathway was reported as highly enriched by each of the pathway analysis programs and is highly relevant in the butyrate response (Figure 4-5). The protein-coding genes from each of the pathway analysis programs, which mapped to the 'Cell cycle', were collated into lists for further investigation in network analysis. GO functional analysis for 'Biological Processes' was also included in the list to strengthen the cell cycle association and included genes which appeared in the 'Cell cycle' process, which was the top enriched process (Table 4-1). Apoptosis is also another key pathway regulated and induced by butyrate. This pathway was not as prominent in the pathway analysis; however, it appeared as a key group term in both the KEGG and WikiPathways analysis programs (Figure 4-5) and was therefore further investigated. In total 215 cell cycle-related and 143 apoptosis-related protein-coding genes were retrieved. To further elucidate the role of miRNA-mRNA interactions in the butyrate response, these genes were used to select predicted and validated miRNA-mRNA pairs for further investigation (Table 4-3, 4-4). This list was further refined by identifying miRNA-mRNA interactions that were known to have key roles in CRC based on the literature. This resulted in a small list of three anti-correlating miRNA-mRNA pairs including miR-139 and EIF4G2, miR-381 and WEE1 which were cell cycle-related interactions plus miR-542 and BIRC5 which was cell cycle and apoptosis related.

**Table 4-3 Cell cycle related miRNA-mRNA interactions identified by interactive network analysis**

miRNA-mRNA predicted, and validated interactions collated from cell cycle network analysis which were identified in two or more programs or databases. V = validated targets from miRTarBase or miRecords, V (literature) = validated targets that did not appear in miRTarBase or miRecords but were found to be validated in the literature or (-) representing unvalidated targets.

miRNAs	Expression	Genes	Expression	Program/Database	Validated
hsa-miR-542-3p	Up	BIRC5	Down	TargetScan, miRTarBase	V
hsa-miR-532-3p	Up	BORA	Down	microT-CDS, TargetScan	-
hsa-miR-503-5p	Up	CDC25A	Down	miRTarBase, miRecords	V
hsa-miR-424-5p	Up	CHEK1	Down	miRDB, miRTarBase	V
hsa-miR-18a-5p	Down	CTGF	Up	miRDB, miRTarBase	V
hsa-miR-200b-3p	Down	DUSP1	Up	microT-CDS, miRDB	-
hsa-miR-200c-3p	Down	DUSP1	Up	microT-CDS, miRDB	V (literature)
hsa-miR-139-5p	Up	EIF4G2	Down	microT-CDS, miRDB	V (literature)
hsa-miR-146a-5p	Up	EIF4G2	Down	microT-CDS, miRDB	-
hsa-miR-146b-5p	Up	EIF4G2	Down	microT-CDS, miRDB	-
hsa-miR-3127-5p	Up	EIF4G2	Down	microT-CDS, miRDB	-
hsa-miR-379-5p	Up	EIF4G2	Down	microT-CDS, miRDB	V (literature)
hsa-miR-222-3p	Down	ETS1	Up	microT-CDS, miRTarBase	V
hsa-miR-532-3p	Up	HMG2A	Down	miRDB, TargetScan	-
hsa-miR-200b-3p	Down	JUN	Up	microT-CDS, miRDB	V (literature)
hsa-miR-200c-3p	Down	JUN	Up	microT-CDS, miRDB	V (literature)
hsa-miR-381-3p	Up	KIF11	Down	microT-CDS, miRDB	-
hsa-miR-424-5p	Up	KIF23	Down	miRDB, TargetScan, miRTarBase	V
hsa-miR-135b-5p	Down	LZTS1	Up	microT-CDS, miRDB, miRTarBase	V (literature)
hsa-miR-335-3p	Down	PRKAA2	Up	microT-CDS, miRDB	-
hsa-miR-19a-3p	Down	RHOB	Up	microT-CDS, miRDB, TargetScan	V (literature)
hsa-miR-542-3p	Up	UBE2E1	Down	microT-CDS, miRDB	-
hsa-miR-381-3p	Up	WEE1	Down	microT-CDS, miRTarBase	V
hsa-miR-424-5p	Up	WEE1	Down	microT-CDS, miRDB, TargetScan, miRTarBase	V

**Table 4-4 Apoptosis related miRNA-mRNA interactions identified by interactive network analysis**

miRNA-mRNA predicted, and validated interactions collated from apoptosis network analysis which were identified in two or more programs or databases. V = validated targets from miRTarBase or miRecords, V (literature) = validated targets that did not appear in miRTarBase or miRecords but were found to be validated in the literature.

miRNAs	Expression	Genes	Expression	Program/Database	Validated
miR-542-3p	Up	BIRC5	Down	TargetScan, miRTarBase	V
hsa-miR-424-5p	Up	CHEK1	Down	miRDB, miRTarBase	V (literature)
hsa-miR-92a-1-5p	Down	COL1A1	Up	miRDB, TargetScan	-
hsa-miR-125a-5p	Down	DAAM1	Up	microT-CDS, miRDB	-
hsa-miR-200b-3p	Down	DUSP1	Up	microT-CDS, miRDB	V (literature)
hsa-miR-200c-3p	Down	DUSP1	Up	microT-CDS, miRDB	V (literature)
hsa-miR-222-3p	Down	ETS1	Up	microT-CDS, miRTarBase	V (literature)
hsa-miR-200b-3p	Down	FN1	Up	miRDB, miRTarBase	V (literature)
hsa-miR-200c-3p	Down	FN1	Up	miRDB, miRTarBase	V (literature)
hsa-miR-222-3p	Down	FOS	Up	miRTarBase, miRecords	V
hsa-miR-146a-5p	Up	IRAK1	Down	microT-CDS, miRDB, miRTarBase	V
hsa-miR-146b-5p	Up	IRAK1	Down	microT-CDS, miRDB, miRTarBase	V
hsa-miR-200b-3p	Down	JUN	Up	microT-CDS, miRDB	V (literature)
hsa-miR-200c-3p	Down	JUN	Up	microT-CDS, miRDB	V (literature)
hsa-miR-335-3p	Down	PRKAA2	Up	microT-CDS, miRDB	-
hsa-miR-450b-5p	Up	RARG	Down	microT-CDS, miRDB	-
hsa-miR-31-5p	Down	RGS4	Up	miRDB, TargetScan	-
hsa-miR-19a-3p	Down	RHOB	Up	microT-CDS, miRDB, TargetScan	V (literature)
hsa-miR-32-5p	Up	TBL1XR1	Down	microT-CDS, miRDB	-

### 4.2.8 Validation of the butyrate effect on miRNA and mRNA target gene expression

Regulation of selected miRNA and target genes by butyrate was confirmed using real-time RT-PCR. HCT116 cells were treated with 2.5 mM butyrate and RNA was extracted, quantified and the quality confirmed using the Bioanalyzer. Taqman miRNA real time RT-PCRs confirmed that miR-139 ( $P=0.0053$ ) and miR-542 ( $P=0.0065$ ) had significantly increased expression when CRC cells were exposed to butyrate (Figure 4-7). The validated targets for miR-139 and miR-542 including EIF4G2 ( $P=0.0022$ ) and BIRC5 ( $P<0.0001$ ) respectively had significantly decreased expression when CRC cells were treated with butyrate. Unfortunately, miR-381 was not detected using real-time RT-PCR, although expression was significant in the RNA-seq data. The validated target gene of miR-381, WEE1 ( $P<0.0001$ ), was significantly decreased with butyrate treatment which correlates with RNA-seq data. Only miR-139, miR-542 and their target genes were pursued for further analysis.

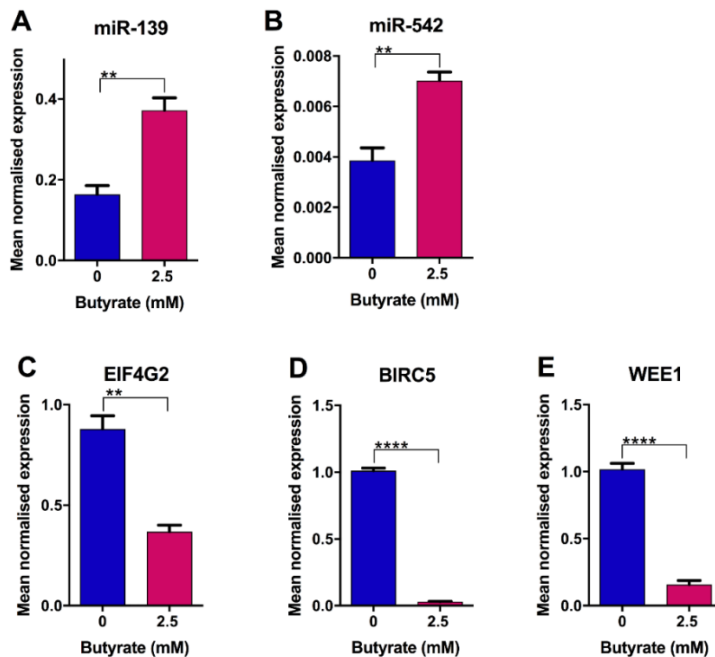


**Figure 4-7 Real-time RT-PCR analysis of networking miRNAs and predicted target gene expression validation in HCT116 cells treated with 2.5 mM butyrate for 24 h**

Expression levels of miRNAs and predicted target genes identified by network analysis (A) miR-139, (B) miR-542, (C) EIF4G2, (D) BIRC5, (E) WEE1 in HCT116 cells treated with 0 mM or 2.5 mM butyrate for 24 h. The mean miRNA or mRNA levels  $\pm$  SEM of the technical triplicates is represented, and their expression is normalised to RNU6B endogenous control (miRNAs only) or the geometric mean of three reference genes, ACTB, B2M and GAPDH (mRNAs only). Significant values are indicated by \* $P<0.05$ , \*\* $P<0.01$ , \*\*\* $P<0.001$ , \*\*\*\* $P<0.0001$ . NC= Negative Control mimic.

### 4.2.9 Effect of miRNA nodes on both cell cycle and cell growth in CRC in the presence of butyrate

miRNA genes were further investigated for their role in the butyrate response in CRC cells by determining their effects on the cell cycle, cell growth and death. HCT116 cells were reverse transfected with miRNA mimics or negative control for 48 h, followed by 24 h with or without 2.5 mM butyrate treatment as described in Chapter 2. Both miR-139 and *EIF4G2* and miR-542 and *BIRC5* miRNA-mRNA pairs were found to be involved in the cell cycle through pathway analysis, therefore, cell cycle analysis using flow cytometry was performed. Cell proliferation changes, which may be a result of direct effects on the cell cycle among other cellular effects, were detected using the real-time cell imaging system, xCELLigence.

#### 4.2.9.1 Effects of miRNAs on the cell cycle in CRC cells after butyrate treatment

The cell cycle was investigated due to the identification of key butyrate regulated genes involved in this pathway that were targeted by DE miRNAs. The Cytotflex Flow Cytometer and propidium iodide staining were used to measure cell cycle phases in HCT116 cells reverse transfected with miRNA mimics for 48 h followed by 24 h butyrate treatment (2.5 mM). The results demonstrated that miR-139 (NC 0 mM butyrate vs miRNA 0 mM butyrate treated) did not appear to have an effect on the G0/G1 phase; however, the miRNA alone significantly induced an increase in the percentage of cells in the S phase ( $P=0.0152$ ) while causing a significant decrease in cell percentage in the G2/M phase ( $P=0.0041$ ) (Figure 4-9). Butyrate alone (NC 0 mM butyrate vs. 2.5 mM butyrate treated) significantly reduced the percentage of cells in the S phase ( $P=0.0361$ ) and increased the percentage in the G2/M phase ( $P=0.0045$ ); however, when combined with miR-139 (NC 2.5 mM butyrate treated vs. miRNA 2.5 mM butyrate treated) a decreasing but non-significant trend was seen in the S phase and increasing trend in the G2/M phase. miR-542 alone (NC 0 mM butyrate vs miRNA 0 mM butyrate) was able to significantly increase the percentage of cells in the G0/G1 phase ( $P=0.0327$ ), while causing a significant decrease in the G2/M phase ( $P=0.0397$ ) (Figure 4-8, 4-9). When miR-542 was combined with butyrate (NC 2.5 mM butyrate treated vs. miRNA 2.5 mM butyrate treated), there was a significant increase in the percentage of cells in the G0/G1 phase ( $P=0.0098$ ), and a significant reduction in the S phase ( $P=0.0152$ ). Only a non-significant increasing trend was observed in the G2/M phase when cells were treated with a combination of miR-542 and butyrate.

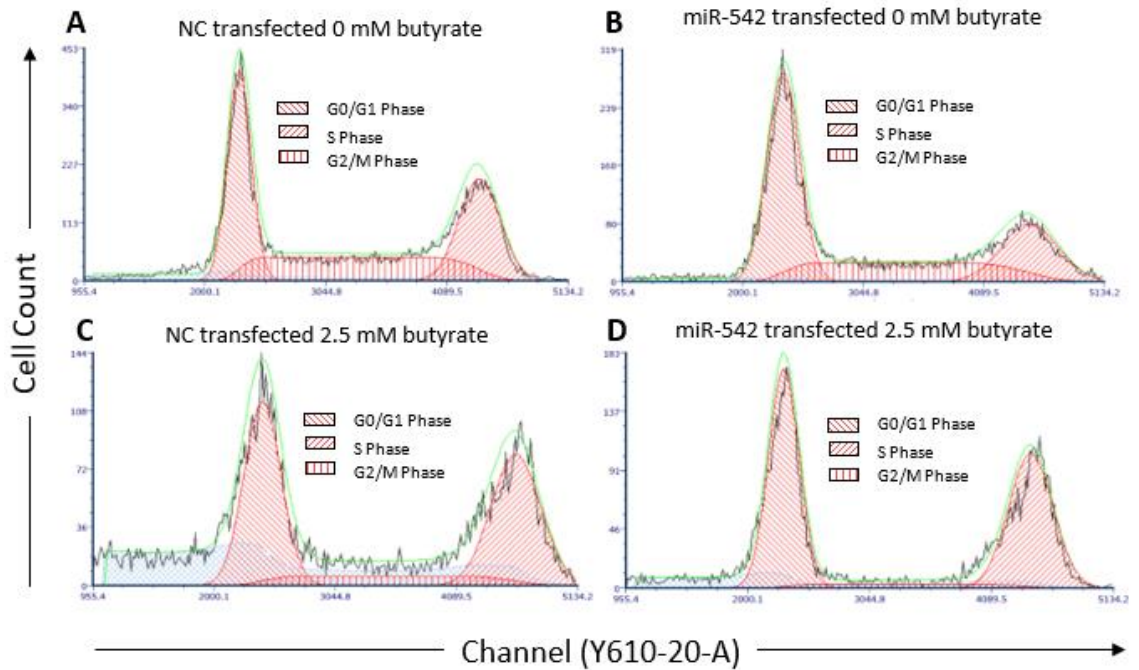


**Figure 4-8** Flow cytometry analysis of the cell cycle in miRNA transfected HCT116 cells after 24 h of butyrate treatment

Examples of flow charts depicting cell cycle analyses of HCT116 cells reverse transfected with NC or miR-542 mimics for 48 h, followed by 24 h of treatment with 0 mM or 2.5 mM butyrate, over a 72 h post-transfection period (A) NC transfected 0 mM butyrate, (B) miR-542 transfected 0 mM butyrate, (C) NC transfected 2.5 mM butyrate, (D) miR-542 transfected 2.5 mM butyrate. Cells were stained with propidium iodide and measured using the Cytotflex Flow Cytometer. NC= Negative Control mimic.

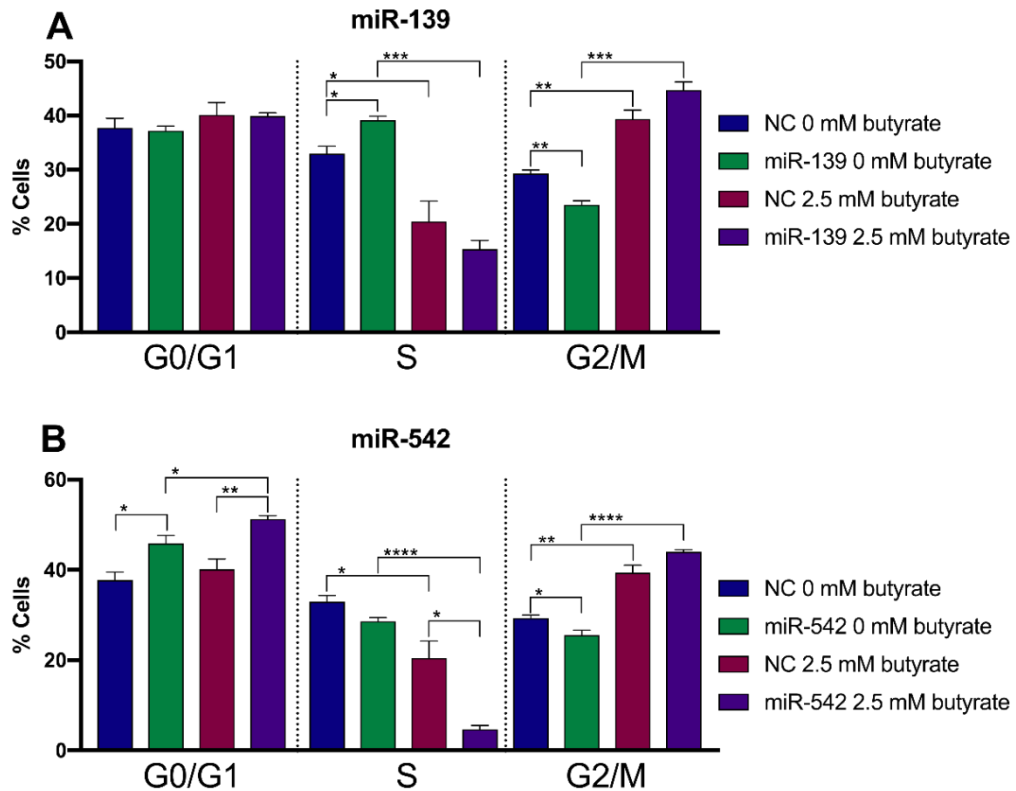


**Figure 4-9 Cell cycle analysis using flow cytometry in miRNA transfected HCT116 cells after 24 h of butyrate treatment**

Bar charts for cell cycle analysis of HCT116 cells reverse transfected with miRNA mimics (A) miR-139, (B) miR-542 for 48 h, followed by 24 h of treatment with 0 mM or 2.5 mM butyrate, over a 72 h post-transfection period. Cells were stained with propidium iodide and cell percentage measured using the Cytoflex Flow Cytometer. The mean  $\pm$  SEM of 3 replicate wells is shown. Significant results are indicated by \*  $P < 0.05$ , \*\*  $P < 0.01$ , \*\*\*  $P < 0.001$ , \*\*\*\*  $P < 0.0001$ . NC = Negative Control mimic.

#### 4.2.9.2 Proliferation of HCT116 CRC cells after miRNA mimic transfection and butyrate treatment

miRNA-mRNA pairs were further investigated for their roles in cell growth by investigating their effects on proliferation in the presence of butyrate using a real-time cell analysis system (xCELLigence instrument). Reverse transfection of HCT116 CRC cells with miRNA mimics (48 h) and treatment with 2.5 mM butyrate (24 h) led to decreased proliferation over a 72 h time period for all miRNAs when compared to 2.5 mM butyrate treated controls. Both miR-139 and miR-542 significantly decreased proliferation of HCT116 cells; both independently of butyrate (NC vs. miRNA transfected 0 mM butyrate treated) but also by enhancing the butyrate effect (NC vs. miRNA transfected 2.5 mM butyrate treated) (Figure 4-10).

miR-139 showed the most significant ability to decrease proliferation of HCT116 cells with  $P$ -values  $< 0.0001$ , for all comparison groups. miR-542 showed the most dramatic

effects on cell proliferation independently of butyrate ( $P = <0.0001$ ). Butyrate alone was able to significantly decrease cell proliferation within all miRNA experiments (NC transfected 0 mM butyrate vs. 2.5 mM butyrate treated and miRNA transfected 0 mM butyrate vs. 2.5 mM butyrate treated) ( $P < 0.05$ ).

CDI calculations illustrated that both miR-139 and miR-542 were acting synergistically with butyrate to enhance its anticancer properties. miR-542 had the lowest CDI indicating synergism with butyrate, followed closely by miR-139 (Table 4-5).

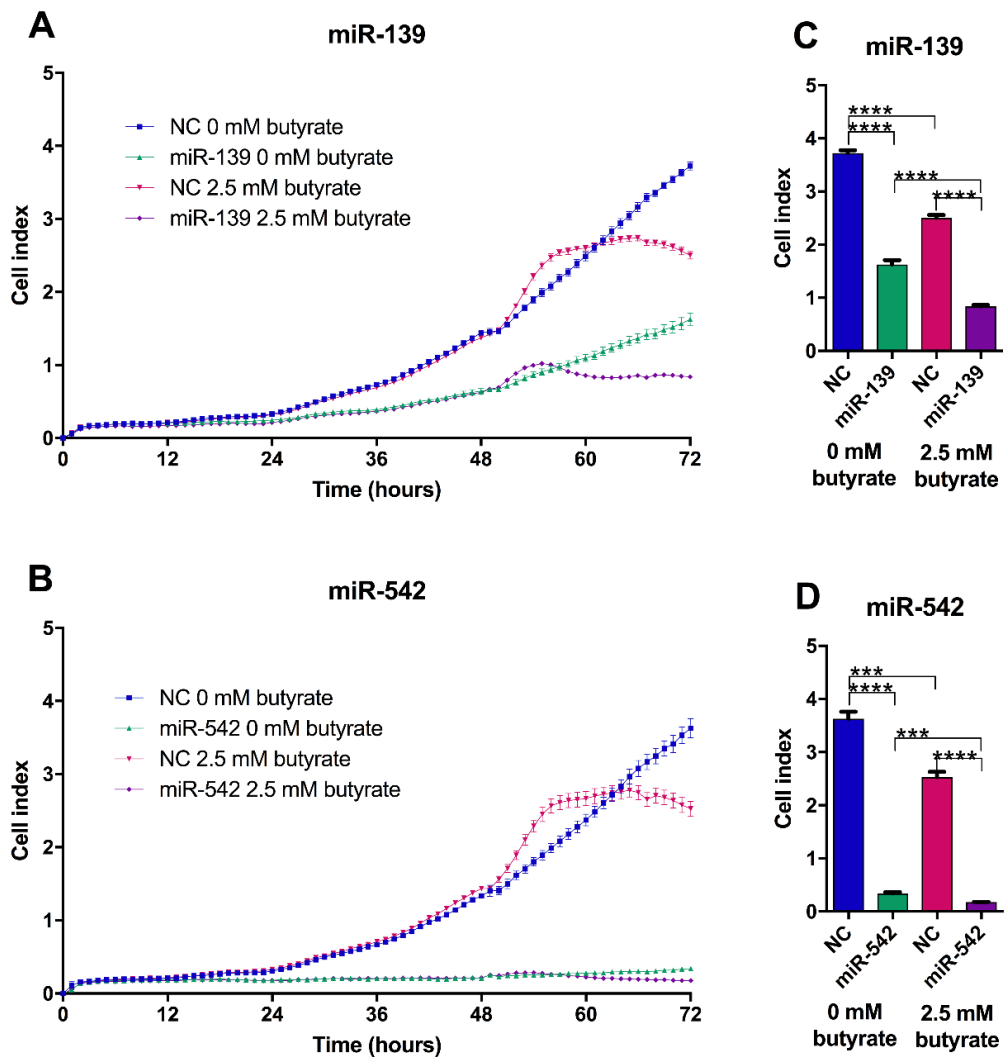


**Figure 4-10 Proliferation of HCT116 cells after transfection with miRNA mimics and butyrate treatment for 24 h**

Real-time cell index measurements using the xCELLigence RTCA platform, in HCT116 cells transfected with miRNAs (A) miR-139, (B) miR-542 for 48 h, followed by 24 h of treatment with 0 mM or 2.5 mM butyrate, over a 72 h post-transfection period. The mean  $\pm$  SEM of 4 replicate wells is shown at 72 h post-transfection (C) miR-139, (D) miR-542. Significant results are indicated by \*  $P < 0.05$ , \*\*  $P < 0.01$ , \*\*\*  $P < 0.001$ , \*\*\*\*  $P < 0.0001$ . NC= Negative Control mimic.

**Table 4-5 Coefficient of drug interaction values for miRNA and butyrate interactions for xCELLigence proliferation data**

Coefficient of drug interaction values were calculated as described in Chapter 2. CDI <1, = 1 or >1 indicates that when the miRNA mimic and butyrate are combined, they behave synergistically, additively or antagonistically together, respectively. CDI <0.7 indicates that the drug is significantly synergistic.

miRNA	CDI value	Classification
<b>miR-139</b>	0.768945052	Synergistic
<b>miR-542</b>	0.742196056	Synergistic

#### 4.2.9.3 Apoptosis of HCT116 CRC cells after miRNA mimic transfection and butyrate treatment

Although miR-542 and *BIRC5* was the only miRNA-mRNA pair identified as being involved in the apoptosis pathway, both miRNAs that synergistically reduced growth of CRC cells with butyrate were examined for their effects on apoptosis using flow cytometry. HCT116 cells were reverse transfected with each miRNA mimic for 48 h followed by 24 h butyrate treatment. Cells were prepared and stained with annexin V and propidium iodide to differentiate between cell death phases: early apoptosis, late apoptosis and necrosis. The Cytoflex Flow Cytometer was used to measure the samples and FSC Express 6 data analysis program was used to analyse the results.

When cells were transfected with the miRNAs alone, only miR-542 induced significant decreases in the percentage of viable cells ( $P=0.0097$ ), while miR-139 had no effect (Figure 4-11, 4-12). Only miR-542 significantly increased early apoptosis ( $P=0.0111$ ) and late apoptosis ( $P=0.0068$ ) alone, while miR-139 significantly reduced late apoptosis ( $P=0.0359$ ), but to a lesser extent. Both miRNAs were able to significantly reduce the percentage of viable cells when combined with butyrate relative to butyrate alone ( $P<0.0001$ ). Early apoptosis was also significantly increased when both miR-139 ( $P=0.0049$ ) and miR-542 ( $P<0.0001$ ) were combined with butyrate. miR-139 ( $P=0.0015$ ) and miR-542 ( $P<0.0001$ ) showed the same trends for late apoptosis when combined with butyrate. miR-139 mimics alone produced a slight but significant increase in necrosis ( $P=0.0047$ ) and in combination with butyrate ( $P=0.0025$ ), while the opposite was seen for miR-542 with the combination treatment ( $P=0.0215$ ).

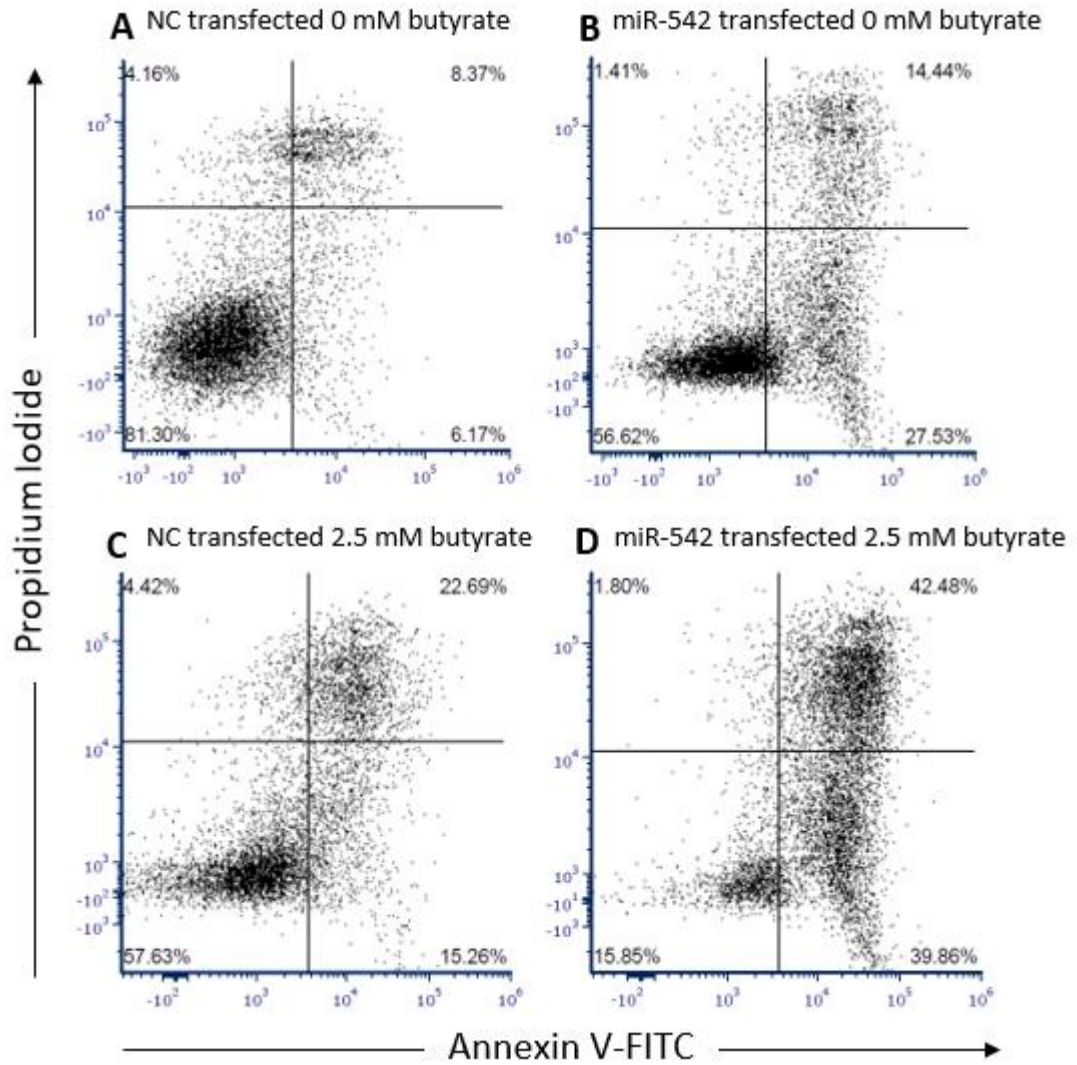


**Figure 4-11** Flow cytometry analysis of apoptosis in miRNA transfected HCT116 cells after 24 h of butyrate treatment

Examples of flow charts depicting the apoptosis analyses of HCT116 cells reverse transfected with NC or miRNA mimics for 48 h, followed by 24 h of treatment with 0 mM or 2.5 mM butyrate, over a 72 h post-transfection period (A) NC transfected 0 mM butyrate, (B) miR-542 transfected 0 mM butyrate, (C) NC transfected 2.5 mM butyrate, (D) miR-542 transfected 2.5 mM butyrate. Cells were stained with propidium iodide and annexin V stain and measured using the Cytoflex Flow Cytometer. NC= Negative Control mimic.

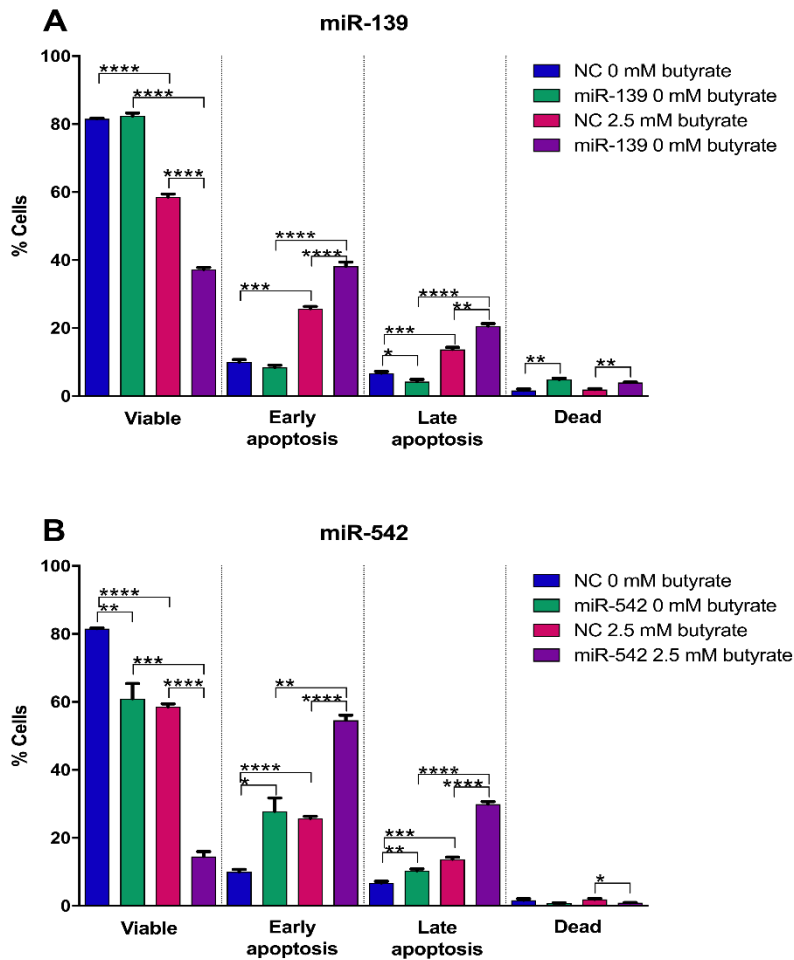


**Figure 4-12 Apoptosis analysis of networking miRNAs using Cytoflex flow cytometry**

Bar charts showing apoptosis analysis of HCT116 cells reverse transfected with miRNA mimics (A) miR-139, (B) miR-542 for 48 h, followed by 24 h of treatment with 0 mM or 2.5 mM butyrate, over a 72 h post-transfection period. Cells were stained with propidium iodide and annexin V stain and measured using the Cytoflex Flow Cytometer. The mean  $\pm$  SEM of 3 replicate wells is shown. Significant results are indicated by \*  $P < 0.05$ , \*\*  $P < 0.01$ , \*\*\*  $P < 0.001$ , \*\*\*\*  $P < 0.0001$ . NC = Negative Control mimic.

#### 4.2.10 Effects of miR-139 and miR-542 on cell growth and death in other cell types

miR-139 and miR-542 were further tested in another CRC cell line model, LIM1215 and a normal but immortalised cell line, HFF, to examine their potential as therapeutic molecules. LIM1215 cells originate from human colorectal carcinoma. This cell line has wild-type *TP53*, *KRAS*, *BRAF* and *PIK3CA* and mutant  $\beta$ -catenin. HFF cells, which are human foreskin fibroblasts, were the only cell line that did not have a significant response to butyrate (except 5 mM butyrate) when examined using crystal violet assays (Section 3.2.5).

In terms of viability, LIM1215 cells did not respond to miR-139 alone (NC 0 mM butyrate vs. miRNA 0 mM butyrate) or their combination with butyrate (NC 2.5 mM butyrate treated vs. miRNA 2.5 mM butyrate treated) (Figure 4-13); however, viability was significantly decreased by miR-542 alone ( $P < 0.0001$ ) and when combined with butyrate treatment ( $P < 0.0001$ ). Butyrate alone was able to reduce cell viability as previously observed with a  $P$ -value  $< 0.001$  or less for all groups (NC 0 mM butyrate vs. NC 2.5 mM butyrate treated and miRNA 0 mM butyrate vs. miRNA 2.5 mM butyrate treated).

Cell apoptosis changes, which were measured following viability measurements in LIM1215 cells, demonstrated that miR-139 significantly increased apoptosis alone ( $P = 0.0107$ ), miR-542 significantly reduced apoptosis alone ( $P = 0.0004$ ) (Figure 4-13). When combined with butyrate miR-139 ( $P = 0.0362$ ) and miR-542 ( $P = 0.0459$ ) significantly increased apoptosis. As expected, butyrate significantly increased apoptosis in all conditions (minimum  $P = 0.0001$ ).

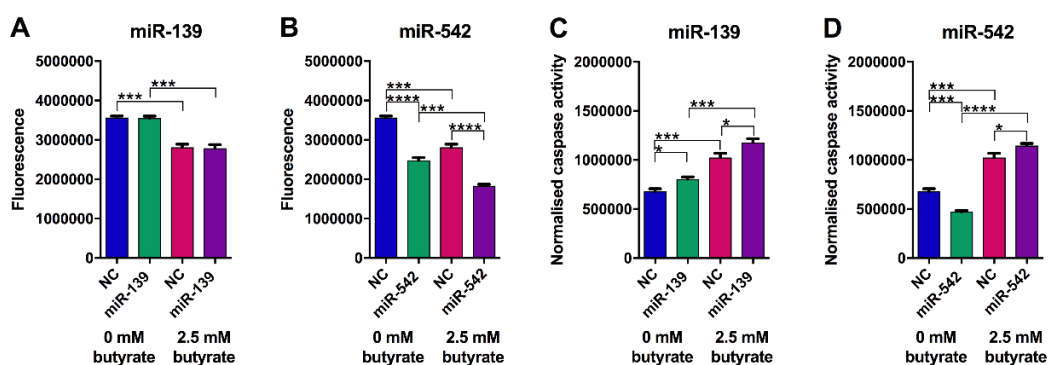


**Figure 4-13 Cell viability and apoptosis in miRNA transfected LIM1215 cells after 24 h of butyrate treatment**

ApoLive-Glo™ Multiplex Assay: fluorescence and luminescent signals for viability changes (A) miR-139, (B) miR-542 and normalised caspase activity for apoptosis changes respectively (C) miR-139, (F) miR-542 in LIM1215 cells transfected with butyrate-sensitising miRNAs for 48 h, followed by 24 h of treatment with 0 mM or 2.5 mM butyrate, over a 72 h post-transfection period. Significant results are indicated by \*  $P < 0.05$ , \*\*  $P < 0.01$ , \*\*\*  $P < 0.001$ , \*\*\*\*  $P < 0.0001$ . NC= Negative Control mimic.

HFF cells did not show any significant viability changes when exposed to miRNA mimics and/or butyrate in any combination (Figure 4-14). miR-139 significantly increased apoptosis alone ( $P = 0.0021$ ); while, miR-542 showed a non-significant increasing trend. Interestingly the comparison of miRNA 0 mM butyrate vs. miRNA 2.5 mM butyrate treated groups for miR-139 ( $P = 0.0028$ ) and miR-542 ( $P = 0.0172$ ) revealed a significant decrease in apoptosis, demonstrating that butyrate antagonized the miRNA effect.

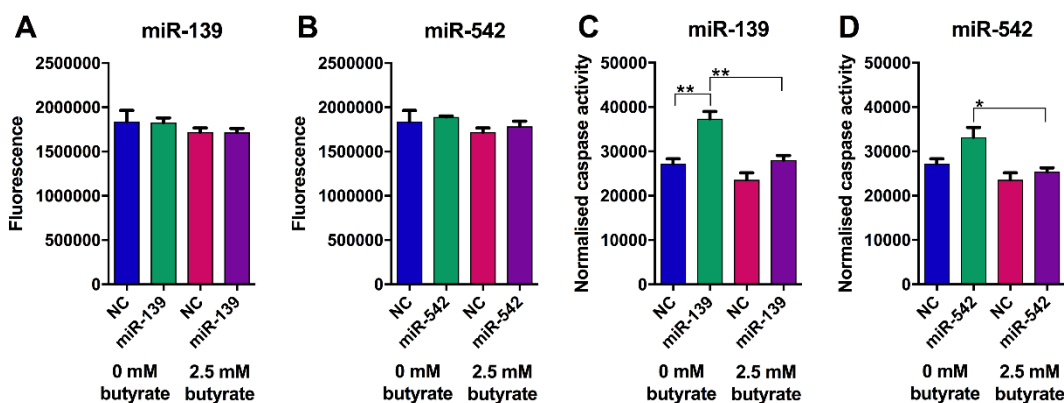


**Figure 4-14 Cell viability and apoptosis in miRNA transfected HFF normal cells after 24 h of butyrate treatment**

ApoLive-Glo™ Multiplex Assay: fluorescence and luminescent signals for viability changes (A) miR-139, (B) miR-542 and normalised caspase activity for apoptosis changes respectively (C) miR-139, (F) miR-542 in HFF cells transfected with butyrate-sensitising miRNAs for 48 h, followed by 24 h of treatment with 0 mM or 2.5 mM butyrate, over a 72 h post-transfection period. The mean  $\pm$  SEM of 4 replicates is shown. Significant results are indicated by \*  $P < 0.05$ , \*\*  $P < 0.01$ , \*\*\*  $P < 0.001$ , \*\*\*\*  $P < 0.0001$ . NC= Negative Control mimic.

#### 4.2.11 miRNA target confirmation using miRNA mimics in HCT116 cells

In order to determine the effect of miRNA mimics on their target genes, each miRNA was individually transfected into HCT116 CRC cells and treated with or without 2.5 mM butyrate. mRNA expression changes of targets were measured using real-time RT-PCR. The miRNAs tested all had previously validated targets that were expected to decrease in expression. miR-139 and miR-542 were confirmed to significantly decrease the expression levels of their targets *EIF4G2* ( $P = 0.0011$ ) and *BIRC5* ( $P < 0.0001$ ) respectively (Figure 4-15). The target gene expression was further reduced in the presence of butyrate for *EIF4G2* and *BIRC5* with  $P < 0.001$  when comparing NC 2.5 mM butyrate treated to miRNA 2.5 mM butyrate treated. Butyrate alone decreased the expression of these genes as previously observed (section 4.2.8).

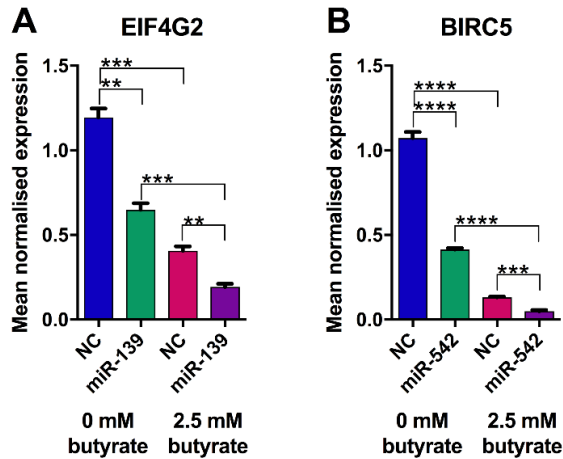


**Figure 4-15 Real-time RT-PCR analysis of miRNA target gene expression in HCT116 cells treated with butyrate for 24 h**

mRNA levels of (A) *EIF4G2* and miR-542 predicted target genes (D) *BIRC5* in HCT116 cells transfected with miRNA or NC mimics for 48 h, followed by 24 h of treatment with 0 mM or 2.5 mM butyrate, over a 72 h post-transfection period. The mean mRNA levels  $\pm$  SEM of the triplicates is represented, and their expression is normalised to the geometric mean of three reference genes, *ACTB*, *B2M* and *GAPDH*. Significant values are indicated by \* $P < 0.05$ , \*\* $P < 0.01$ , \*\*\* $P < 0.001$ , \*\*\*\* $P < 0.0001$ . NC= Negative Control mimic.

#### 4.2.12 Effect of miRNA target gene silencing and butyrate treatment on CRC cell proliferation and the cell cycle

Based on network analysis in section 4.2.7, *EIF4G2* had the greatest number of connections with DE miRNAs including predicted interactions with miR-146a, miR-146b, miR-3127 and validated interactions with miR-139 and miR-379 (Table 4-3). This gene was, therefore, selected for further investigation by RNA interference in CRC cells. Knockdown efficiency was determined by exposing HCT116 cells to *EIF4G2* siRNA for 72 without butyrate treatment. *EIF4G2* mRNA expression was reduced by ~89% ( $P = 0.0001$ ) (Figure 4-16).

HCT116 cells were transfected with *EIF4G2* or NC siRNAs for 72 h and treated with or without 2.5 mM butyrate for 24 h before cell proliferation was measured using the xCELLigence platform. *EIF4G2* siRNA significantly reduced cell proliferation alone ( $P < 0.0001$ ) and when combined with butyrate this effect was further enhanced ( $P < 0.0001$ ) (Figure 4-17). The CDI calculation indicates a significantly synergistic effect when *EIF4G2* siRNA is combined with butyrate at 0.49. Butyrate alone reduced proliferation as expected when comparing NC siRNA 0 mM butyrate vs. 2.5 mM butyrate treated and *EIF4G2* siRNA 0 mM butyrate vs. 2.5 mM butyrate treated ( $P < 0.0001$ ).

Cell cycle analysis was then performed on HCT116 cells that were treated under the same conditions described above. Cells were stained with PI and the Cytoflex Flow Cytometer was used to measure the percentage of cells in each phase. The results demonstrated that when cells were exposed to *EIF4G2* siRNAs alone (NC 0 mM butyrate vs. siRNA 0 mM butyrate) there was a significant increase in cell percentage in the G0/G1 phase ( $P=0.0237$ ) while a significant decrease was observed in the G2/M phase ( $P=0.0251$ ) (Figure 4-18, 4-19). When exposed to butyrate alone (NC 2.5 mM butyrate vs. miRNA 2.5 mM butyrate treated) the same decrease in S phase was observed and there was a significant increase in cells in the G2/M phase ( $P=0.0214$ ) as previously observed (Figure 4-8). The combination of siRNA and butyrate (NC 2.5 mM butyrate treated vs. miRNA 2.5 mM butyrate treated) resulted in a non-significant increase in G0/G1 phase and G2/M phase; however, the cell percentage significantly decreased in S phase ( $P=0.0201$ ).

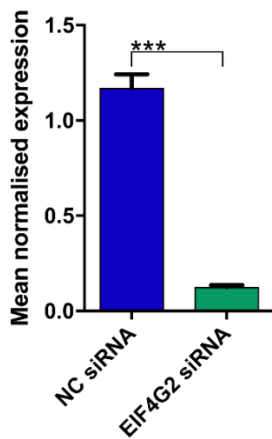


**Figure 4-16 *EIF4G2* siRNA knockdown efficiency in HCT116 cells**

mRNA levels of *EIF4G2* in CRC cells (A) HCT116 cells transfected with NC siRNA or *EIF4G2* siRNA for 72 h. The mean mRNA levels  $\pm$  SEM of the triplicates is represented, and their expression is normalised to the geometric mean of three reference genes, *ACTB*, *B2M* and *GAPDH*. Significant values are indicated by \* $P<0.05$ , \*\* $P<0.01$ , \*\*\* $P<0.001$ , \*\*\*\* $P<0.0001$ . NC= Negative Control mimic.

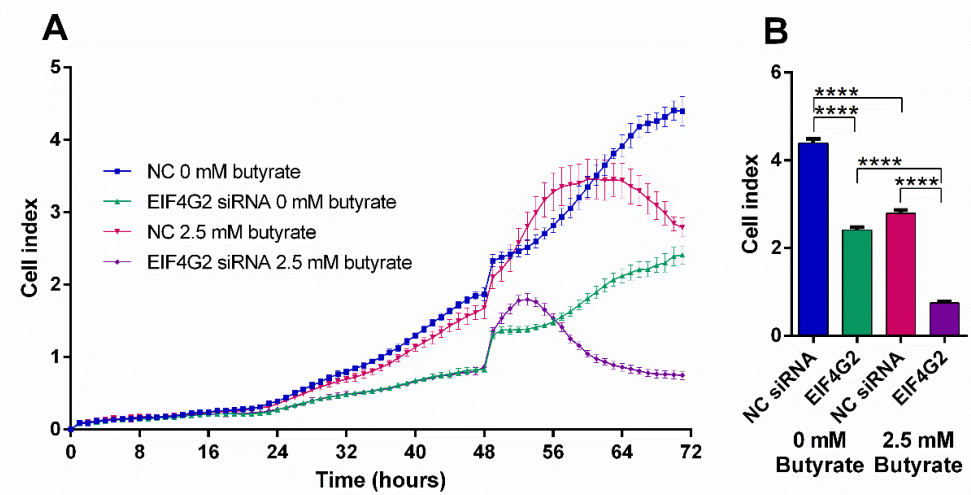


**Figure 4-17** siRNA knockdown of miR-139 target gene *EIF4G2*

Real-time cell index measurements using the xCELLigence RTCA platform, in (A) HCT116 cells transfected with NC or *EIF4G2* siRNA for 48 h, followed by 24 h of treatment with 0 mM or 2.5 mM butyrate, over a 72 h post-transfection period. The mean  $\pm$  SEM of 4 replicates is shown at 72 h post-transfection (B) *EIF4G2* siRNA. Significant results are indicated by \*  $P < 0.05$ , \*\*  $P < 0.01$ , \*\*\*  $P < 0.001$ , \*\*\*\*  $P < 0.0001$ . NC= Negative Control mimic.

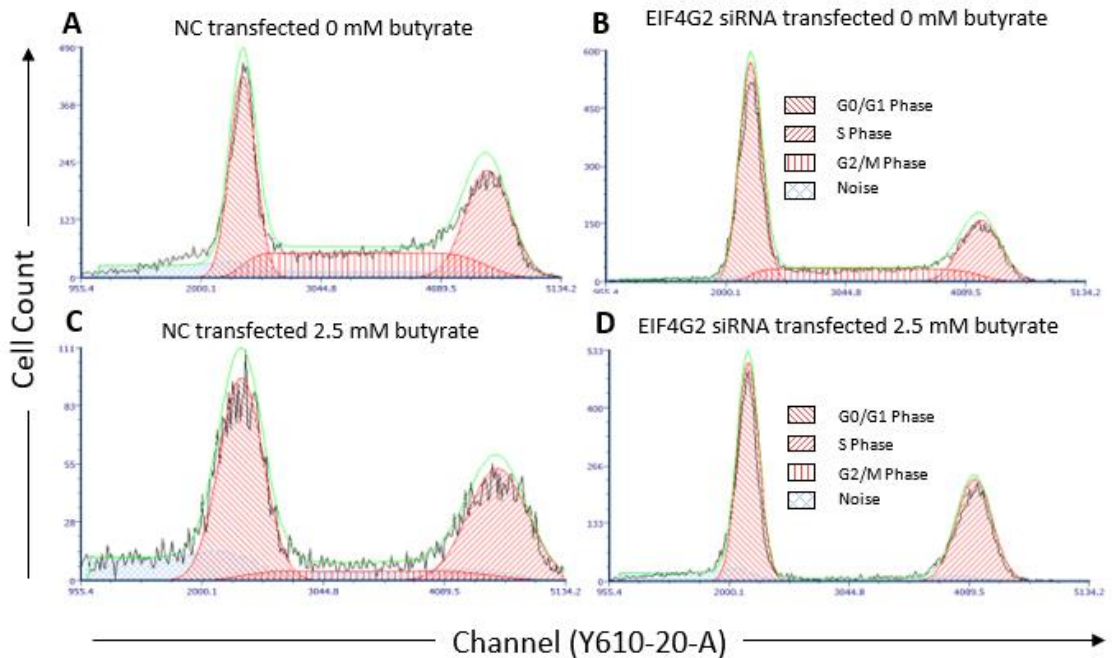


**Figure 4-18** Flow cytometry analysis of the cell cycle in siRNA transfected HCT116 cells after 24 h of butyrate treatment

Examples of flow charts depicting cell cycle analyses of HCT116 cells reverse transfected with NC or *EIF4G2* siRNAs for 48 h, followed by 24 h of treatment with 0 mM or 2.5 mM butyrate, over a 72 h post-transfection period (A) NC transfected 0 mM butyrate, (B) *EIF4G2* siRNA transfected 0 mM butyrate, (C) NC transfected 2.5 mM butyrate, (D) *EIF4G2* siRNA transfected 2.5 mM butyrate. Cells were stained with propidium iodide and measured using the Cytoflex Flow Cytometer. NC= Negative Control siRNA.

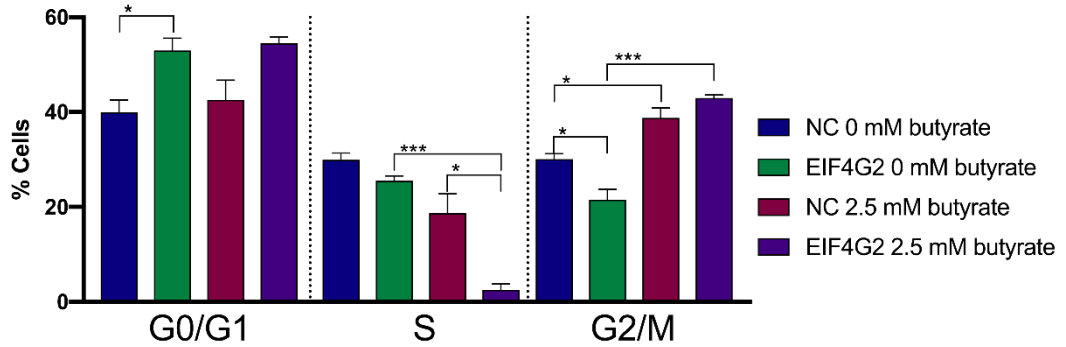


**Figure 4-19 Cell cycle analysis of *EIF4G2* siRNA transfected HCT116 cells using flow cytometry**

Bar charts showing the cell cycle analysis of HCT116 cells reverse transfected with *EIF4G2* siRNAs for 48 h, followed by 24 h of treatment with 0 mM or 2.5 mM butyrate, over a 72 h post-transfection period. Cells were stained with propidium iodide and cell percentage measured using the Cytotex Flow Cytometer. The mean  $\pm$  SEM of 3 replicate wells is shown. Significant results are indicated by \*  $P < 0.05$ , \*\*  $P < 0.01$ , \*\*\*  $P < 0.001$ , \*\*\*\*  $P < 0.0001$ . NC= Negative Control mimic.

## 4.3 Discussion

### 4.3.1 Summary

Butyrate is a well-studied chemo-protective agent, with the ability to induce apoptosis and inhibit cell proliferation in CRC cells through the global regulation of gene expression (Daly & Shirazi-Beechey 2006; Mariadason 2008). miRNAs are commonly dysregulated in CRC and some can enhance the anticancer properties of butyrate (Humphreys et al. 2013); however, the complex interactions and networks that are involved in this response have yet to be elucidated. The aim of these experiments was to investigate the diverse effects of butyrate on the transcriptome profile of CRC cells and to identify key miRNA-target interactions within biological signalling pathways that contribute to the anticancer effects of butyrate. Additionally, butyrate-sensitising miRNAs were also identified (and their target genes) with the ability to enhance the anticancer properties of butyrate in CRC cells. This was done by using a systems biology approach to examine butyrate induced transcriptomic changes through integrative pathway and network analysis. Several miRNA-mRNA interactions were identified to be important in cell cycle regulation and apoptosis in CRC cells.

### 4.3.2 Butyrate regulated gene expression

The global effect of butyrate on the HCT116 cell transcriptome was examined using Illumina total and small RNA-seq analysis. It was revealed that thousands of protein-

coding and non-coding genes are regulated by 2.5 mM butyrate (48 h). From the total RNA-seq, 15,000 protein-coding genes were detected and 1110 were downregulated and 1337 were upregulated when comparing control cells to butyrate treated cells ( $\log_2FC < -1.5$  or  $\log_2FC > 1.5$  and  $p_{adj} < 0.01$ ). From the small RNA-seq, it was revealed that out of 845 miRNAs detected, 50 were downregulated and 63 were upregulated by butyrate ( $\log_2FC < -1$  or  $\log_2FC > 1$  and  $p_{adj} < 0.05$ ). Butyrate is a HDACi known to alter global gene expression through the regulation of global acetylation patterns through H3 and H4 hyperacetylation (Mariadason 2008). This results in a more open chromatin configuration allowing transcription factors to access the DNA more easily, therefore, promoting transcription of cell cycle, apoptosis and differentiation related genes (Gu & Roeder 1997). Interestingly, the total and small RNA-seq data show that the number of genes which are downregulated, although less, are near equal to those upregulated, which was similar to a previous profiling study in CRC (Daly & Shirazi-Beechey 2006). The mechanisms behind this downregulation have been studied in CRC and hepatocellular carcinoma cells, whereby histone acetylation around the promoter regions, and specifically transcription start sites of particular genes can be decreased resulting in decreased gene expression (Rada-Iglesias et al. 2007). Histone deacetylation of selected gene regions was accompanied by reduced RNA polymerase II initiation and elongation and reduced transcription factor binding to regulatory sequences (Duan et al. 2005; Rada-Iglesias et al. 2007). GO analysis revealed that these particular genes were similar in functions and involved in processes promoting cell proliferation (Rada-Iglesias et al. 2007). Of course, butyrate has many other functions including the regulation of non-coding RNAs, transcription factors and heterochromatin factors, which could result in the repression of gene expression (Davie 2003; Taddei et al. 2001).

### 4.3.3 Butyrate regulated PPI networks

Further investigation of the interactions between protein-coding genes using butyrate-regulated PPI networks revealed that the topmost highly connected interactors were p53 with degree 80 and KIAA0101 and FN1 with degree 75. *TP53* is a well-studied tumour suppressor gene which is commonly mutated in ~50% of CRC cases (Liu & Bodmer 2006); however, HCT116 cells have wild type *TP53*. p53 regulates the cell cycle and apoptosis by regulating the expression of p21 cell cycle inhibitor (He et al. 2005) and PUMA pro-apoptotic genes (Nakano & Vousden 2001). *TP53* transcript expression was found to be significantly reduced by butyrate, which is initially counterintuitive. However, several other studies have also found reduced *TP53* transcript expression and p53 protein accumulation after treatment with butyrate and other HDAC inhibitors, for

example Trichostatin A (TSA) (Emenaker et al. 2001; Janson et al. 1997; Taniguchi et al. 2012). Butyrate-regulated p53-independent mechanisms have been identified in CRC cell lines (Hague et al. 1993; Kobayashi et al. 2003; Mahyar-Roemer & Roemer 2001). Kobayashi et al. (2003) demonstrated that butyrate inhibited growth and induced cell cycle arrest in cells such as LS513 (*TP53* wild type), Lovo (*TP53* wild type), HT29 (*TP53* point mutation) and Caco2 (*TP53* truncation), regardless of their *TP53* status. *P21* transcript and protein levels were also increased in all cell lines after butyrate exposure as well as promoter activity in Caco2 and Lovo cells, indicating the mechanism is independent of p53 (Kobayashi et al. 2003). It appears that *TP53* status may not be a limiting variable in the chemo-protective effects of butyrate as it seems not to play a role in the butyrate effect on CRC growth (Kobayashi et al. 2003). Further investigation will need to be done for other genetic aberrations that may influence the butyrate response.

FN1 or fibronectin 1 is a protein involved in cell adhesion, migration, differentiation, and proliferation that has been implicated in CRC development and growth (Saito et al. 2008). Increased expression of *FN1* has been associated with poor prognosis in CRC and several other cancers (Saito et al. 2008; Wang & Hielscher 2017). Interestingly, *FN1* expression was significantly induced in CRC cells by butyrate; however, there is precedent for induction of *FN1* in cancer cells by butyrate. Specifically Halgunset et al. (1988) revealed that exposing prostatic carcinoma cells to butyrate induced up to a 100-fold increase in *FN1* expression and cells produced stress fibres and had decreased proliferation.

KIAA0101 (PCLAF), which is a proliferating cell nuclear antigen (PCNA) clamp associated factor involved in DNA replication, is known to be upregulated in several cancers and have oncogenic functions (Cheng et al. 2013; Su et al. 2014; Zhu et al. 2013). *KIAA0101* was significantly increased in CRC cells by butyrate, which might suggest that it plays no role in the protective effect of butyrate, or that it has a non-oncogenic function in this cell type. As noted previously, it is commonly observed that many genes have oncogenic functions in one cancer type and tumour suppressor functions in another.

#### 4.3.4 GO and pathway enrichment analysis

Further investigation of target genes was performed using gene ontology enrichment analysis to examine the functional roles of genes including biological processes, molecular functions and cellular components. This analysis revealed that butyrate regulated genes that are involved in a wide range of processes including the cell cycle as

well as DNA related functions and components such as DNA binding and chromosomal parts. Previous studies investigating the functional enrichment of butyrate regulated genes also demonstrated that DE genes were significantly enriched in the same or similar pathways including regulation of mismatch repair, cell cycle, DNA replication, and the replication fork (Zhou et al. 2019). Further examination of this gene set was performed to define the biological importance of butyrate DE genes.

Pathway enrichment analysis was achieved using KEGG, WikiPathways and Reactome pathway analysis programs. The analysis revealed that DE genes were enriched in several key pathways including the cell cycle, DNA replication and apoptosis, which correlates with the GO analysis. All of these pathways have previously been shown to have biological relevance in the butyrate response in microarray and small-scale profiling studies (Daly & Shirazi-Beechey 2006; Iacomino et al. 2001), which supports the analysis. As mentioned in section 1.3.3, butyrate is a very well-known regulator of the cell cycle and has been shown to regulate numerous cell cycle related genes and induce G1 phase and G2/M phase arrest in several CRC cell lines (Daly et al. 2005; Daly & Shirazi-Beechey 2006; Mariadason et al. 2000; Saldanha et al. 2014; Siavoshian et al. 2000; Taylor et al. 2014). Butyrate is also a well-known apoptotic inducer of CRC cells (section 1.3.3) which upregulates pro-apoptotic gene *BAK1* and caspase 3, and downregulates anti-apoptotic genes *BIRC5*, *CFLAR* and *BCLXL* (Daly et al. 2005; Daly & Shirazi-Beechey 2006; Taylor et al. 2014). As for the direct effects of butyrate on DNA, animal studies demonstrated that a butyrylated-RS diet protects rat colonocytes from DNA damage (Bajka et al. 2008). Butyrylated-RS diets were shown to be twice as effective as high protein diets in protecting rats against genetic damage (Bajka et al. 2008). Le Leu et al. (2015a) also demonstrated that alkylating agent-induced DNA adducts were reduced by a high butyrylated starch dietary intervention, indicating a key role of butyrate in DNA damage repair.

### **Limitations of GO and pathway enrichment analysis**

GO and pathway enrichment analyses are clearly useful tools, but they have limitations. Well studied genes and pathways are most well represented in functional annotations and, therefore, there is a bias which may result in important information being lost during the analysis process (i.e. poorly characterized genes may be overlooked due to lack of useful annotation). Annotations can be incomplete, and some databases include pseudogenes, predicted and hypothetical genes (Khatri et al. 2012). The most analogous results were observed between KEGG and WikiPathways and these differed from the

Reactome output. Differences may be due to the curation process. Reactome is the most comprehensive database; it is curated by experts using experimental data and the literature and is peer-reviewed to avoid errors (Bauer-Mehren et al. 2009; Croft et al. 2011). KEGG is curated by experts in the field using the literature (Kanehisa et al. 2017). WikiPathways is an open source database which is curated based on public contributions and other databases like KEGG, which would explain some of the overlap in KEGG and WikiPathways output (Pico et al. 2008). The curation process itself is compromised as the literature is used to guide the formation of these pathways; however, they may lack key information about the conditions in which the data was acquired such as cell type and time points (Khatri et al. 2012).

#### 4.3.5 Integrative network analysis

Integrative network construction was then performed in order to identify key miRNA-mRNA interactions in the butyrate response. DE miRNAs were selected, and miRNA target prediction was used to identify mRNA interactors. Only interactors whose response to butyrate (expression change) anti-correlated with that of the miRNA and were present in the PPI network were presented in the final network analysis. This led to the identification of 52 miRNA-mRNA interactions; GO and pathway analysis results were used to refine the list of interactions to those identified in cell cycle and apoptosis pathways. The literature was used to further refine the list to three interactions: miR-139 with *EIF4G2*, miR-381 with *WEE1* and miR-542 with *BIRC5*.

##### **miR-139 interactions**

miR-139 is a known tumour suppressor that is commonly downregulated in CRC and several other cancers, and decreased expression is associated with poor prognosis (Huang et al. 2017; Liu et al. 2013b; Miyoshi et al. 2017; Song et al. 2014b). miR-139 inhibits migration, invasion, growth and induces apoptosis and cell cycle arrest by targeting several genes including *AMFR*, *NOTCH1* and *BCL2* in CRC (Li et al. 2016c; Song et al. 2014b), *EIF4G2* in acute myeloid leukaemia (AML) (Emmrich et al. 2016) and *IGF1R* in lung cancer (Huang et al. 2017). *EIF4G2*, which is a translation initiation complex component has not been well-studied in general. Knockdown studies of *EIF4G2* demonstrated that the cell cycle inhibitor P27 increased in expression to promote cell cycle arrest and inhibit proliferation in glioblastoma, human embryonic kidney and AML cells (Emmrich et al. 2016; Lee & McCormick 2006), which is promising.

**miR-381 interactions**

miR-381 is also a known tumour suppressor that is normally downregulated in CRC and numerous other cancers (Cao et al. 2017; Chen et al. 2013a; He et al. 2016; Liang et al. 2015b). miR-381 inhibits migration, invasion, growth and induces apoptosis and cell cycle arrest through targeting several genes including *TWIST1* in CRC (He et al. 2016), *WEE1* in renal cancer (Chen et al. 2013a), *SETDB1* in breast cancer (Wu et al. 2018b). *WEE1*, which is a cell cycle checkpoint kinase that inhibits G2/M transition, is well-studied (Fasulo et al. 2012). In fact, *WEE1* is already a drug (AZD1775) target due to its importance in cancer development (Fu et al. 2018). Cancer cells bypass the G1 checkpoint in order to accumulate mutations to promote their survival; therefore, cells rely on the G2/M phase checkpoint to repair DNA damage to avoid apoptosis (Matheson et al. 2016). As *WEE1* regulates this checkpoint, *WEE1* inhibition by AZD1775 results in apoptosis (Fu et al. 2018; Matheson et al. 2016).

**miR-542 interactions**

miR-542 is also a known tumour suppressor miRNA that is normally downregulated in CRC and other cancers (Long et al. 2016; Ye et al. 2016a; Yuan et al. 2017; Zhang et al. 2018d). It functions by inhibiting proliferation, migration, invasion and inducing cell cycle arrest by targeting several genes such as *BIRC5*, *OTUB1* and cortactin in CRC (Long et al. 2016; Yang et al. 2017a; Ye et al. 2016a; Yuan et al. 2017) *TGFβ1* in hepatocellular carcinoma (Zhang et al. 2018d), *BIRC5* in breast cancer (Lyu et al. 2018) among others. *BIRC5* (Survivin) is a well-studied member of the Inhibitor of Apoptosis (IAP) family, that is highly expressed in several cancer and is involved in the regulation of several important pathways such as apoptosis, cell cycle, proliferation, metastasis and invasion (Garg et al. 2016; Li et al. 2018a). *BIRC5* has a key role in inhibition of apoptosis by inhibiting caspase 3 and 7 (Altieri 2003) and regulation of cell division by centrosome and mitotic spindle structure (Li et al. 1998). YM155, which is a small molecule inhibitor of *BIRC5* mRNA has also been tested in clinical trials for several cancers including breast cancer (Clemens et al. 2015; Kelly et al. 2013; Kudchadkar et al. 2015). Overall, integrative networking in conjunction with literature-based information was able to provide meaningful miRNA-mRNA interactions that were appropriate for further study.

### **Limitations of gene expression studies**

The expression of the miRNA-mRNA interactors and their response to butyrate was assessed in the HCT116 cell line. Real-time RT-PCR revealed that miR-139 and miR-542 were significantly increased in expression while their target genes EIF4G2 and BIRC5 were significantly decreased by butyrate, consistent with the total and small RNA-seq results. WEE1 transcript levels were significantly decreased with butyrate treatment; however, miR-381 was not detected by real-time RT-PCR. This is not consistent with the literature as miR-381 has been previously detected in HCT116 cells and several other CRC cell lines (He et al. 2016; Liang et al. 2015b). Notably, these articles do not mention whether they measured the 5p or 3p arm of the miRNA although as only the miR-381-3p Taqman assay is available commercially, this is likely the most studied form. It is also possible that different miRNA variants with different 3' end structures (isomiRs) are expressed and as others have reported Taqman assays may not detect all isomiRs (Androvic et al. 2017; Schamberger & Orban 2014; Soundara Pandi et al. 2013). Thus, our inability to detect miR-381-3p may be a technical artefact; other techniques could be explored to resolve this issue in the future. One method is amplification of the primary miRNA; however, this will not identify which mature form (3p and 5p) is produced. Another technique involves the amplification of the mature miRNA by using poly(A) polymerase to add a poly(A) tail to the mature miRNA followed by reverse transcription with a tagged poly(I) primer and finally amplification with two primers using SYBR green master mix (Balcells et al. 2011). The 3' primer can be designed to detect individual isomiRs or they can be designed to sit outside of the regions of variation to detect all variants together (Balcells et al. 2011). Although we have assumed here that the inability to confirm the RNA-seq data using the RT-PCR data is due to technical issues with the latter, it is worth mentioning that small RNA-seq can also produce artefacts. Ultimately, only miR-139 and miR-542 and their target genes were pursued for further analysis as the inability to amplify miR-381 was not resolved due to time constraints.

#### **4.3.6 Butyrate-sensitising miRNAs regulate CRC cell proliferation, apoptosis and cell cycle**

Butyrate is a regulator of the cell cycle as mentioned in section 1.3.3 and it affects the expression of many related genes to induce cell cycle arrest. As the key interactions that were selected were involved in the cell cycle, flow cytometry analysis was used to assess the changes in the cell cycle at 72 h post transfection with miRNA mimics. Further

investigation of the cellular effects of miR-139 and miR-542 in HCT116 cells was determined by using the xCELLigence real-time cell system to determine changes in proliferation. The effects of these miRNAs on apoptosis were also examined.

### **miR-139 cellular effects**

miR-139 is a known tumour suppressor in several cancers that inhibits migration, invasion, growth and induces apoptosis and cell cycle arrest by targeting key growth and death related genes such as *NOTCH1*, *BCL2*, *EIF4G2*, *IGFR1* (Emmrich et al. 2016; Huang et al. 2017; Li et al. 2016c; Song et al. 2014b). Results supported the tumour suppressor function of miR-139 which significantly reduced HCT116 cell growth both alone and in combination with butyrate through a synergistic mechanism. miR-139 was previously shown to decrease growth to a similar extent in HCT116 cells (Zhang et al. 2014a); however, there are some contradictory data in other studies indicating it has no effect on growth in HCT116 cells (Li et al. 2016c; Song et al. 2014b). Interestingly, the contradictory studies both used the same type of endpoint assay (Cell Counting Kit-8 assay) (Li et al. 2016c; Song et al. 2014b), while Zhang et al. (2014a) used a metabolic 3-(4,5-Dimethylthiazol-2-yl)-5-(3-carboxymethoxyphenyl)-2-(4-sulfophenyl)-2H-tetrazolium (MTS) assay which may account for the differences observed.

Examination of the cell cycle revealed that miR-139 did not affect G0/G1 phase alone or in combination with butyrate. However, previous studies revealed that overexpression of miR-139 suppressed proliferation in HCT116 cells and prostate cancer cells by promoting G0/G1 phase arrest (Sun et al. 2018b; Zhang et al. 2014a), which is contradictory to the current study. Furthermore, the current study showed miR-139 alone increased the percentage of cells in S phase, while butyrate reduced this effect; however, the opposite effect was induced in the G2/M phase. miR-139 was found to decrease the percentage of cells in the S and G2 phases in prostate cancer cells (Sun et al. 2018b), while miR-139 decreased the percentage of cells in S phase and induced G2/M phase arrest in AML to inhibit growth (Zhang et al. 2019c). It is unclear why the G0/G1 phase is unaffected by miR-139 in the current study as the knockdown of the miR-139 target, *EIF4G2*, was shown to increase protein levels of the G0/G1 phase inhibitor cyclin-dependent kinase inhibitor CDKN1B (p27Kip1) (Lee & McCormick 2006). The cell cycle responses to miR-139 are varied across cancer cell types; however, changes in this process may still contribute to proliferative effects observed in the current study. Thus, this requires further investigation.

Further examination of miR-139-mediated cellular responses revealed that miR-139 had no effect on the percentage of viable HCT116 cells, which is supported by previous evidence that miR-139 does not affect viability (Li et al. 2016c; Song et al. 2014b). miR-139 alone did not affect apoptosis in the current study. miR-139 has been previously shown to induce cell cycle arrest and inhibit of migration and invasion (Li et al. 2016c; Song et al. 2014b; Zhang et al. 2014a), which could explain cell index changes seen using the xCELLigence platform and lack of change in apoptotic analysis. Interestingly, miR-139 significantly enhanced the anti-apoptotic effects of butyrate, even though it had no effect on apoptosis alone. The mechanism behind this response was not further investigated; however, this combinatorial effect with butyrate has been observed previously with other molecules. For example, the epigenetic regulatory molecule epigallocatechin gallate (EGCG) was unable to reduce HCT116 cell proliferation alone at concentrations of 10  $\mu$ M, but when combined with various concentrations of butyrate it was able to enhance butyrate's anti-proliferative effects (Saldanha et al. 2014). Several experiments revealed that this enhancement effect is due to numerous changes induced by the combination treatment including reduced BIRC5, increased p53 and p21 protein expression as well as epigenetic changes that were not strongly induced by the drugs alone (Saldanha et al. 2014). This highlights the importance of investigating combination treatments as some agents may be useful therapeutically only in conjunction with another drug.

#### **miR-542 cellular effects**

miR-542 is a known tumour suppressor in several cancers that functions by inhibiting proliferation, migration, invasion and inducing cell cycle arrest by silencing several growth related genes such as *BIRC5*, *OTUB1*, *TGF $\beta$ 1* and cortactin (Long et al. 2016; Lyu et al. 2018; Yang et al. 2017a; Ye et al. 2016a; Yuan et al. 2017; Zhang et al. 2018d). Results revealed the tumour suppressor capabilities of miR-542 which was able to significantly reduce CRC cell growth both alone and in combination with butyrate through a synergistic mechanism. Interestingly, miR-542 had very dramatic effects even in the absence of butyrate. Previous studies have shown that miR-542 significantly reduced proliferation in several CRC cells lines including HCT116 cells (Long et al. 2016; Yuan et al. 2017); however, not to the same extent seen in this study. This may be attributed to the differences in the assays used to assess cell proliferation as Yuan et al. (2017) used a colorimetric based Cell Counting Kit-8 assay for proliferation while Long et al. (2016) used a BrdU colorimetric based assay which is based on changes in DNA synthesis. These are both endpoint assays. The advantage of the xCELLigence platform

is that it is a real-time cell analysis system which monitors growth over a period. It does, however, have its limitations as the cell index values are an indication of several cellular changes, not just proliferation, including adherence, morphology, cell cycle arrest, apoptosis, necrosis or a combination of these events.

Cell cycle analysis revealed that miR-542 alone and in combination with butyrate significantly increased the percentage of cells in the G<sub>0</sub>/G<sub>1</sub> phase. A previous study demonstrated that miR-542 inhibits lung cancer cell growth by inducing G<sub>1</sub> phase arrest (Yoon et al. 2010). Similarly, miR-542 inhibited hepatocellular carcinoma cell growth by increasing cells in G<sub>1</sub> phase (Chen et al. 2018d). This indicates G<sub>1</sub> phase regulation is a likely contributing factor to reduced HCT116 cell growth induced by miR-542. The current study revealed that miR-542 enhanced the reduction in the percentage of cells in the S-phase in combination with butyrate and similarly miR-542 was shown to decrease cells in S phase in hepatocellular carcinoma cells to reduce growth (Chen et al. 2018d). miR-542 also induced G<sub>2</sub>/M cell cycle arrest in lung cancer cells (Yoon et al. 2010); however, in contrast miR-542 without butyrate reduced percentage of HCT116 cells in the G<sub>2</sub>/M phase. This effect was counteracted by butyrate which increased the percentage of cells in the G<sub>2</sub>/M phase. As miR-542 has strong anti-proliferative effects independently of butyrate, effects on the G<sub>2</sub>/M phase are likely not as critical in the cell response. This is further supported by the fact that a target of miR-542, *BIRC5*, is a critical regulator of the cell cycle and its inhibition in several cancer types was demonstrated to induce G<sub>1</sub> phase arrest (Ai et al. 2006; Bian et al. 2012). In liver cancer cells *BIRC5* has been shown to promote resistance to G<sub>1</sub> phase arrest (Suzuki et al. 2000).

Further investigations revealed that miR-542 without butyrate induced significant decreases in percentage of viable cells, which may partly explain the reduction seen in cell index using the xCELLigence platform. Previous studies also demonstrated a reduction in HCT116 cell viability after miR-542 mimic transfection (Yuan et al. 2017). miR-542 significantly increased early and late apoptosis and this was further enhanced in the presence of butyrate. This effect is not unexpected as both miR-542 and butyrate are known to downregulate genes such as *BIRC5* which is implicated in the reduction of apoptosis via caspase inhibition (Altieri 2003). Further repression of this gene when both molecules are combined might explain the enhanced reduction in apoptosis.

#### **Limitations of cell studies**

It is difficult to determine exactly what is happening to the cell cycle due to the limitations of using a single dye. The protocol used during this study was only able to determine the percentage of cells within a phase as PI only stains the DNA. To observe if cell cycle arrest was occurring would have required further optimisation of the protocol with another dye. One approach of determining resting or proliferating cells is to use proliferation associated proteins like Ki-67 or nuclear proliferation antigens like proliferating cell nuclear antigen (PCNA) (Kim & Sederstrom 2015). Ki-67 is present in proliferating cells specifically those in G2 and early M phase, but is not normally detected in the G0 phase and decreases in anaphase and telophase (mitosis) (Gerdes et al. 1984). Alternatively, PCNA indicates cells are proliferating and can be found in the S-phase (Kurki et al. 1986). Cell cycle status can also be studied by examining RNA levels within cells, which are normally higher in proliferating cells (G1 to M phase) compared to resting cells (G0 phase) (Kim & Sederstrom 2015). This involves the use of Hoechst 33342 and Pyronin Y to double stain the cells (Kim & Sederstrom 2015).

#### 4.3.7 Butyrate-sensitising miRNAs regulate cell viability and apoptosis in LIM1215 cells

The cellular effects of these miRNAs were further examined in another CRC cell line, LIM1215. The endpoint ApoLive Multiplex assay was used to determine viability and apoptotic changes. In terms of viability, LIM1215 cells did not respond to miR-139 alone which was also seen in HCT116 cells during flow cytometry apoptotic analysis; however, the cells did not respond to the combination with butyrate unlike the HCT116 response. Interestingly, miR-139 significantly increased apoptosis alone (not seen in HCT116) and when combined with butyrate (also seen in HCT116). LIM1215 cell viability was significantly decreased by miR-542 alone and this was enhanced when combined with butyrate treatment. Interestingly, in the absence of butyrate, miR-542 significantly reduced apoptosis in LIM1215 cells, which was not seen in HCT116 cells; however, it significantly enhanced the pro-apoptotic effects of butyrate. LIM1215 cells may be more sensitive to miRNA-induced apoptosis than HCT116 cells due to differences in mutational status. LIM1215 cells have wild-type *TP53*, *KRAS*, *BRAF* and *PIK3CA*, while HCT116 cells have mutant *KRAS* and *PIK3CA* and wild-type phenotypes for *BRAF* and *TP53*. KRAS and PI3K are critical regulators of the PI3K signalling pathway (section 1.4.3.1) which regulates cell growth and death. PI3K is especially critical in this pathway as it is one of the main effectors of the RAS signalling component; however, it is involved in several other signalling pathways which makes it an ideal drug target (Castellano & Downward 2011). For example, previous studies have

shown that CRC cell lines with *PI3KCA* mutations are resistant to growth factor deprivation induced apoptosis; however, they are particularly sensitive to apoptosis induced by PI3K inhibitors (Wang et al. 2007). Interestingly, *KRAS* mutations in CRC have been associated with increased spontaneous apoptosis (Liu et al. 2011c). This highlights the importance of identifying key mutations involved in the response to combination treatments as not all CRCs may respond in the same way.

#### 4.3.8 Butyrate-sensitising miRNAs regulate cell viability and apoptosis in 'normal' cell line models

A key issue faced with current cancer therapeutics are the toxic side effects experienced by normal cell types as signalling pathways required by normal cells are often disrupted (Cleeland et al. 2012). Hence, miRNAs were further investigated in a normal but immortalised cell line, HFF, to test their potential as therapeutic molecules. miR-139 significantly increased apoptosis alone, but this was reduced by butyrate, hence the combined effect was non-significant, while miR-542 had no significant effect alone or in combination with butyrate. As mentioned in chapter 3 (section 3.2.5), butyrate-sensitising miRNAs identified through the screen were also able to induce similar effects in HFF cells. Toxicity related effects of chemotherapies are a well-studied issue; therefore, it is important to address this problem in the development of miRNA therapies. As previously mentioned, the systemic effects of miRNA therapy may be avoided by using targeted delivery systems and has previously been shown to be used in the treatment of mesothelioma patients (van Zandwijk et al. 2017); however, more research is required.

#### 4.3.9 Butyrate regulates target gene expression

Real-time RT-PCR was used to confirm the effect of the miRNA on the target mRNA, alone and in combination with butyrate. As previously demonstrated in section 4.2.8, butyrate significantly reduced the expression of *BIRC5* and *EIF4G2*. miR-139 and miR-542 significantly reduced *EIF4G2* and *BIRC5* transcript levels respectively, as expected (section 4.2.11). When combined with butyrate, both transcript levels were further reduced. This may explain some of the combinatorial effects that were mentioned previously including enhancement of reduced proliferation, increased apoptosis and reduced percentage of cells in the S-phase, which were achieved by both miRNAs in combination with butyrate. The mechanisms responsible for the reduction in gene expression may be due to several factors including indirect regulation of transcription factors and co-regulators or repressors induced by butyrate or other miRNA targets.

#### 4.3.10 Effect of target gene knockdown and butyrate treatment on cell proliferation and the cell cycle

To further investigate the roles of specific target mRNAs in the observed cellular responses, RNA interference was used to mimic the effects of the miRNAs. Specifically, *EIF4G2* was further examined based on network analysis in section 4.2.7. *EIF4G2* had the greatest number of connections with DE miRNAs (miR-146a, miR-146b, miR-3127, miR-139 and miR-379). *EIF4G2* is not a well-studied gene, but it appeared to be a key target in the butyrate regulated network, and it has been shown to regulate key proteins in the cell cycle (Lee & McCormick 2006). Interestingly, *EIF4G2* inhibition significantly reduced cell proliferation in the absence of butyrate. When combined with butyrate this effect was further enhanced. This result is very similar to that observed following transfection of miR-139 mimics in HCT116 cells (section 4.2.9.2). The CDI calculation indicated a significantly synergistic effect when *EIF4G2* siRNA was combined with butyrate.

Cell cycle analysis was performed to determine if *EIF4G2* regulates the cell cycle as previously described in other cancers including AML and glioblastoma cells (Emmrich et al. 2016; Lee & McCormick 2006). The cell cycle effects of *EIF4G2* knockdown were similar to those produced by miR-139 mimics; however, there were some differences. *EIF4G2* siRNAs alone and in combination with butyrate increased the percentage of cells in the G<sub>0</sub>/G<sub>1</sub> phase, but miR-139 had no effect. *EIF4G2* has previously been shown to regulate G<sub>1</sub> cell cycle progression by inhibiting the activation of cyclin E-CDK2 or cyclin D-CDK4 complexes (Lee & McCormick 2006), which is consistent with the observed results. The siRNA alone had no effect on S phase, while miR-139 increased the percentage of cells in this phase in the absence of butyrate. Butyrate alone reduced the percentage of cells in S phase, while the combination with *EIF4G2* siRNA or miR-139 mimic further reduced the percentage of cells in S phase. *EIF4G2* siRNA then reduced cells in G<sub>2</sub>/M phase but enhanced the cell percentage when in combination with butyrate, in a similar pattern to miR-139. The differences that were observed between the siRNA and miRNA response may be due to the fact that the miRNA only induced a 50% knockdown of *EIF4G2* compared to the ~89% induced by the siRNA. miRNAs have also been shown to regulate hundreds of target genes (Muljo et al. 2010), hence other target genes in similar pathways may also contribute to the response of the cells to the miRNA.

### 4.3.11 Conclusion

In conclusion, this study identified several miRNAs and predicted target genes that could enhance the ability of butyrate to reduce CRC cell proliferation and induce apoptosis. These included miR-139 and its target *EIF4G2* and miR-542 and its target *BIRC5*. There are several future directions for this work, including further investigating other key interactions that were identified during integrative network analysis such as members of the oncogenic miR-17-92 cluster, miR-18a and miR-19a, which are known to have key roles in CRC development and progression (Ng et al. 2009a; Tsuchida et al. 2011; Yu et al. 2012). Target confirmation in this cell line should also be performed to ensure *EIF4G2* is a true target of miR-139 which can be done using target protectors or luciferase reporter gene studies. While *EIF4G2* seems promising as a future therapeutic target, its effects on CRC cell growth and survival will need to be further elucidated in cell studies and more physiologically relevant 3D models such as organoids before proceeding to animal studies (Duval et al. 2017). While further investigation is necessary, this study may provide the basis to develop these miRNAs and this gene as potential therapeutic targets.

# Chapter 5. High-throughput functional lncRNA screen and validation

---

## 5.1 Introduction

As previously discussed, butyrate has anticancer properties in CRC cells by altering global acetylation and consequently global gene expression. The previous chapters focused on miRNAs that can be regulated by butyrate, and may enhance its anticancer properties in CRC. Other non-coding RNAs, such as lncRNAs, have not been investigated in the context of butyrate; however, they may regulate miRNAs, in particular by acting as miRNA sponges to regulate miRNA target genes (Li et al. 2016e; Liang et al. 2017; Pa et al. 2017). The RNA-seq data, described in Chapter 4, were also analysed for lncRNA expression and revealed that lncRNAs are regulated by butyrate treatment of CRC cells, which has not been previously reported. lncRNAs are also known to directly regulate key genes in cell death and growth pathways such as apoptosis and the cell cycle and they may act as tumour suppressors or oncogenes. Given their known involvement in key cancer related pathways, lncRNAs are potential novel therapeutic targets. Here the study sought to identify lncRNAs that influenced the response of CRC cells to butyrate to gain further insight into how butyrate influences key cell growth and death pathways in CRC and assist in identification of potential therapeutic target genes.

In order to investigate lncRNAs with the ability to sensitise CRC cells to butyrate, a high-throughput functional screen was utilised, employing lncRNA-targeting RNA interference. The effect of suppressed lncRNA function was validated using real-time cell analysis assays. The response of the lncRNAs to butyrate was assessed by real-time RT-PCR. In addition, predicted miRNA targets of these lncRNAs (interactors) were also investigated using real-time RT-PCR.

## 5.2 Results

### 5.2.1 Primary high-throughput screen

An unbiased high-throughput functional screen was performed in 2016, involving the analysis of 2231 siRNAs that target lncRNAs in HCT116 colorectal carcinoma cells

(Figure 5-1) (Methods section 2.2.1). Cells were reverse transfected with the Human Lincode siRNA SMARTpool Library V54 (GE Healthcare Dharmacon, Colorado, USA) for 48 h and treated with 0 mM or 2.5 mM butyrate for 24 h (48 h post-transfection) using the SciClone ALH3000 Lab Automation Liquid handler (Caliper Life Sciences) and BioTek liquid dispenser (BioTek). At 72 h post-transfection, the fluorescent and luminescent endpoint assay ApoLive-Glo Multiplex assay (Promega) was used to determine cellular changes in cell viability (CellTiter-Fluor reagent) and apoptosis (Caspase-Glo reagent) as described in Chapter 2. Controls included a positive death control siRNA (siPLK1) and miRNA mimic control (miR-18a), negative scrambled sequence siRNA control (OPT-NT) and mock transfection control. All experiments were performed in duplicate plates. Screen quality control was performed to determine the performance and reliability of the screen as described in Chapter 2 and values were within the acceptable ranges (Appendix 9).

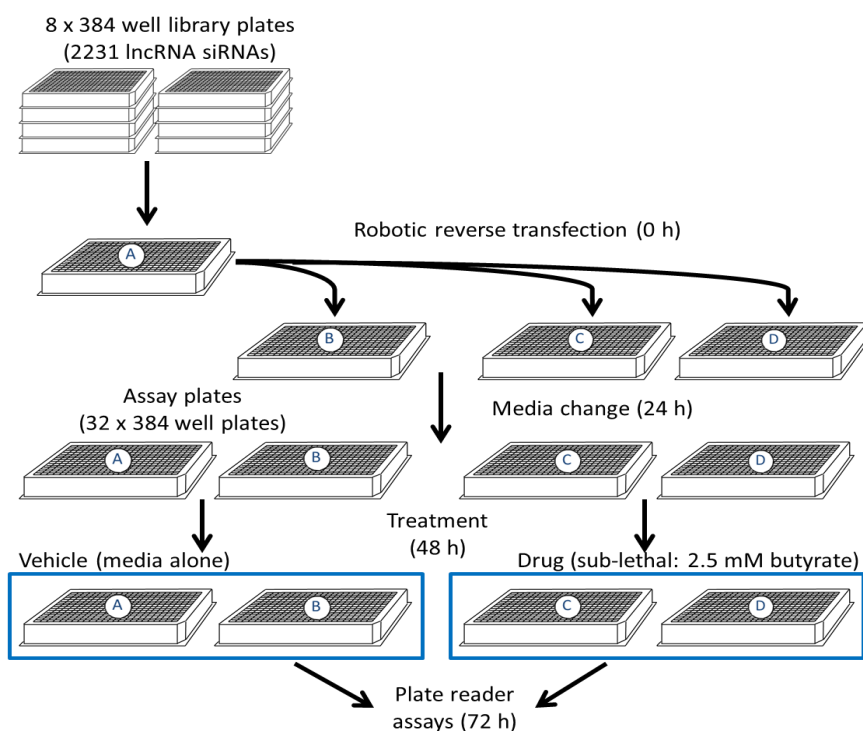


**Figure 5-1 High-throughput screen workflow summary**

HCT116 cells were reverse transfected with lncRNA-targeting siRNAs at 0 h; followed by a media change at 24 h. Cells were treated with 0 mM or 2.5 mM butyrate at 48 h. Plate reader assays were performed at 72 h for cell viability and apoptosis changes.

### 5.2.1.1 Hit selection

lncRNA hits were selected for validation based on their ability to induce changes in cell viability and apoptosis, ideally with the ability to enhance the anticancer properties of butyrate (Figure 5-2). Hits were allocated to 5 groups including changes to viability and

apoptosis together or alone. Significant decreases in viability were labelled as synthetic lethal (SL) hits if they were  $\geq 20\%$  difference between siRNA 0 mM butyrate vs siRNA 2.5 mM butyrate treated fold change, while significant changes in normalised caspase activity were classified as robust Z-score above 1.5 representing significantly increased apoptosis and below 1.5 representing significantly decreased apoptosis. A Z-score represents the comparison of two different standard distributions of data sets.

**List 1:**

- Synthetic lethal hit at least  $\geq 20\%$  difference between siRNA 0 mM butyrate vs siRNA 2.5 mM butyrate treated fold change (decreased viability)
- Z-score  $> 1.5$  (siRNA 0 mM butyrate vs siRNA 2.5 mM butyrate treated) ranked as Hi (increased apoptosis)
- Assumption: Cause for decline in viability is likely due to death by apoptosis

**List 2:**

- Synthetic lethal hit at least  $\geq 20\%$  difference between siRNA 0 mM butyrate vs drug fold change (decreased viability)
- No change in apoptosis
- Assumption: Cause for decline in viability, but no change in apoptosis, is likely due to an alternative form of cell death i.e. necrosis, senescence/cell cycle arrest

**List 3:**

- No change in viability
- Z-score  $> 1.5$  Z-score (siRNA 0 mM butyrate vs siRNA 2.5 mM butyrate treated) was ranked as Hi (increased apoptosis)
- Assumption: Cells may be in early apoptosis (viability signal is still detected within cells up until the proteases are released whereupon they become inactivated; therefore, during early apoptosis cells are still alive and can still be detected)

**List 4:**

- Synthetic lethal hit at least  $\geq 20\%$  difference between siRNA 0 mM butyrate vs siRNA 2.5 mM butyrate treated fold change (decreased viability)
- Z-score  $< -1.5$  (siRNA 0 mM butyrate vs siRNA 2.5 mM butyrate treated) for apoptosis (decreased apoptosis)

- Assumption: Cells may be undergoing a form of cell death other than apoptosis (apoptosis may decrease as caspase activity is affected by the siRNAs/drug, but other forms of cell death or senescence/cell cycle arrest are occurring)

**List 5:**

- No change in viability
- Z-score  $< -1.5$  (siRNA 0 mM butyrate vs siRNA 2.5 mM butyrate treated) for apoptosis (decreased apoptosis)
- Assumption: Caspases may be affected by siRNAs/drug and they are less active; however, this does not translate to any change in viability.

lncRNAs were selected for further investigation if they fit the criteria for any of the five groups listed. Due to the low hit percentage, various scenarios were considered in hit selection criteria. In order to refine the final hit list, total RNA-seq data were used to identify lncRNAs present in the HCT116 cell line to maintain biological relevance. If lncRNAs were expressed with a  $p\text{-adj} < 0.05$ , then they were considered for the secondary screen. This identified 3 hits in List 1, 15 hits in List 2, 22 hits in List 3, 2 hits in List 4, plus 7 cherry picked hits based on literature review from List 5 (least relevant list). The top 49 hits were selected for a secondary screen (Table 5-1).

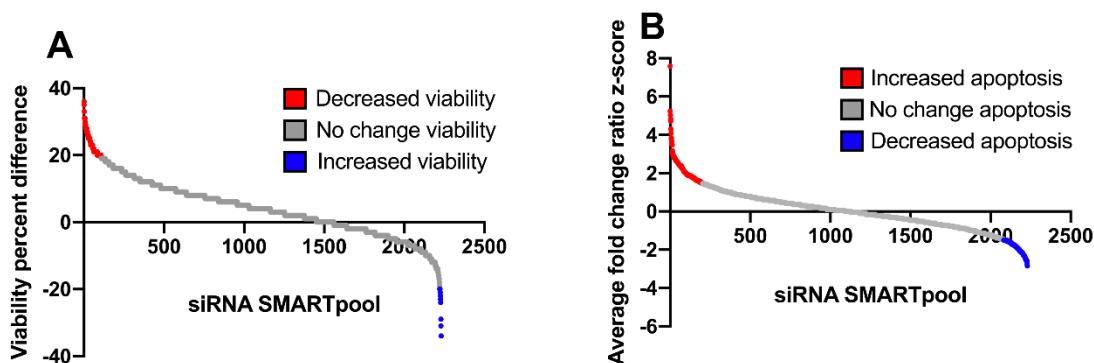


**Figure 5-2 Summary of primary screen data**

Graphical summaries of (A) viability and (B) apoptosis data depicting viability percent difference and average fold change ratio z-score (y-axis) for each siRNA SMARTpool (x-axis). Decreased viability (red)  $\geq 20\%$  difference and increased viability (blue)  $\leq -20\%$  difference. Increased apoptosis (red) z-score  $> 1.5$  and decreased apoptosis (blue) z-score  $< -1.5$ .

**Table 5-1 Selected lncRNA hits from the primary high-throughput functional siRNA screen**

List Number	lncRNA	Normalised viability (siRNA vs NC) 0 mM butyrate	Normalised viability (siRNA vs NC) 2.5 mM butyrate	Viability percent difference	Normalised caspase activity (siRNA vs NC) 0 mM butyrate	Normalised caspase activity (siRNA vs NC) 2.5 mM butyrate	Average fold change ratio z-score (caspase activity)	Padj Value
1	LINC00487	1	0.8	20	0.8	1.06	2.54	2.84E-02
1	LINC00971	1	0.72	28	0.94	1.23	2.49	4.61E-02
1	LINC-PINT	1.09	0.89	20	0.8	1.04	2.44	7.65E-25
2	AQP4-AS1	0.86	0.66	20	1.19	1.28	1.3	4.05E-10
2	LINC00944	0.94	0.72	22	0.82	0.84	0.99	3.65E-02
2	LINC01123	0.91	0.68	23	1.09	1.09	0.88	9.56E-06
2	LINC00898	1.11	0.9	21	0.92	0.84	0.42	6.53E-04
2	ST3GAL4-AS1	1	0.78	22	0.97	0.84	0.21	1.85E-02
2	PRR7-AS1	1.08	0.84	24	0.8	0.68	0.1	8.11E-03
2	PAXIP1-AS2	1.04	0.83	21	1.37	1.16	0.1	2.89E-08
2	LINC00936	1.02	0.81	21	1.54	1.24	-0.1	1.31E-02
2	LINC01098	1.01	0.76	25	1.47	1.15	-0.26	5.79E-03
2	ATP6V0E2-AS1	1.06	0.83	23	1.33	1.04	-0.26	3.58E-09
2	KIAA0125	1.02	0.82	20	1.43	1.04	-0.52	1.38E-08
2	DNAJC9-AS1	1.01	0.72	29	1.06	0.76	-0.57	3.42E-02
2	SPANXA2-OT1	0.9	0.62	28	1.27	0.88	-0.73	2.53E-02
2	MIR22HG	0.71	0.5	21	0.98	0.64	-0.93	1.38E-03
2	FGD5-AS1	0.9	0.66	24	1.21	0.77	-0.99	1.01E-02
3	MIR503HG	0.74	0.58	16	0.94	1.25	2.59	2.47E-05
3	LINC00608	0.86	0.74	12	1.27	1.62	2.33	1.88E-04
3	BHLHE40-AS1	1.06	0.94	12	0.98	1.24	2.28	5.95E-04
3	GAS5	0.96	0.84	12	1.29	1.5	1.71	3.04E-04
3	CECR7	0.76	0.65	11	0.72	0.98	2.75	8.19E-11
3	FAM83H-AS1	0.78	0.71	7	0.88	1.23	2.96	1.03E-03
3	PAXBP1-AS1	1.02	0.95	7	0.95	1.12	1.82	1.03E-05
3	PDCD4-AS1	0.9	0.87	3	1.01	1.54	3.58	1.12E-04
3	CHKB-AS1	0.88	0.85	3	0.76	1.02	2.65	8.20E-03
3	LINC00271	0.99	0.96	3	1.08	1.3	1.92	1.34E-09
3	WWTR1-AS1	0.76	0.76	0	1.08	1.52	3.01	5.52E-05
3	PRC1-AS1	0.89	0.89	0	0.76	0.92	1.97	1.15E-03
3	LINC00482	0.84	0.84	0	1	1.19	1.87	1.75E-10
3	DIAPH3-AS2	0.8	0.82	-2	1.14	1.52	2.59	3.56E-09
3	DKFZP434K028	0.76	0.78	-2	0.9	1.04	1.71	3.46E-05
3	LINC00941	0.75	0.78	-3	0.94	1.64	4.72	2.95E-02
3	CCDC148-AS1	0.85	0.88	-3	0.94	1.52	4.1	1.71E-03
3	KMT2E-AS1	0.76	0.79	-3	0.98	1.17	1.87	1.21E-23
3	RNASEH2B-AS1	0.98	1.04	-6	0.97	1.16	1.92	3.01E-07
3	SLC8A1-AS1	0.96	1.04	-8	0.88	1.04	1.82	4.77E-02
3	SH3PXD2A-AS1	0.32	0.41	-9	0.31	0.38	2.08	8.16E-16
3	LOXL1-AS1	0.86	1	-14	0.97	1.16	1.92	4.67E-03
4	SNHG5	0.64	0.35	29	1.99	0.83	-2.13	3.53E-05
4	LINC01012	0.94	0.69	25	1.66	0.75	-1.97	3.17E-02
5	MALAT1	0.78	0.83	-5	1.21	0.61	-1.71	6.70E-03
5	MKNK1-AS1	0.98	1	-2	1.52	0.74	-1.76	2.58E-06
5	MIR17HG	0.71	0.72	-1	2.45	0.98	-2.23	7.97E-17
5	MIRLET7BHG	1.02	0.96	6	1.21	0.62	-1.66	3.00E-07
5	HOXA-AS3	0.73	0.64	9	1.84	0.86	-1.87	5.36E-04
5	ZFAS1	0.84	0.71	13	1.18	0.59	-1.71	9.92E-07
5	ST7-AS2	0.59	0.53	6	2.41	1.29	-1.5	1.83E-07

### 5.2.2 Secondary lncRNA-targeting siRNA screen

To confirm the cellular responses induced by lncRNA-targeting siRNAs in HCT116 CRC cells and identify siRNAs for further testing, cells were individually transfected with duplexes from each lncRNA siRNA SMARTpool (a mixture of 4 individual siRNAs designed against a single lncRNA) and their effect on cell viability and apoptosis determined. Cells were also transfected with the SMARTpool and with

negative control siRNA as reference standards. Hits (individual siRNAs) were selected based on their concordance to SMARTpool data which were used to confirm positive results. If the siRNA 0 mM butyrate siRNA 2.5 mM butyrate treated fold change ratios of individual duplexes were <25% discordant when compared to the SMARTpool 0 mM butyrate SMARTpool 2.5 mM butyrate treated fold change ratios, then the individual siRNA was selected for further investigation. Validation outcomes were based on the confidence that the phenotypes produced by individual siRNAs were on-target and reflected those phenotypes observed in the primary screen (Simpson et al. 2008). These included high confidence hits for which 3/4 or 4/4 siRNAs validated, moderate confidence hits for which 2/4 siRNAs validated and low confidence hits or off-target effects for which only 1/4 siRNAs validated (Simpson et al. 2008). Low confidence hits were initially kept in the analysis to assess their relevance in pathway analysis as a phenotype was observed for 1 out of 4 siRNAs tested (Thomas et al. 2014). As lncRNA-targeted siRNA efficacy varies, a single siRNA out of 4 could still be a valid hit, and not assessing low confidence hits may omit critical data (Lennox & Behlke 2016). This resulted in the identification of 17 hits with 1 or more duplexes that validated (1 with 3 validated siRNAs, 7 with 2 validated siRNAs and 9 with 1 validated siRNA) (Table 5-2, Figure 5-3). HOXA-AS3 had the greatest number of individual siRNAs validate when compared to the SMARTpool results, with a total of 3 validated siRNAs. Other well-studied lncRNAs, including GAS5 tumour suppressor lncRNA and MALAT1 oncogene lncRNA, had 2 validated siRNAs.

**Table 5-2 Secondary screen hits**

Summary of secondary screen data presenting average drug/control normalised caspase ratios for lncRNA-targeting siRNA SMARTpools (SP) and individual siRNAs (Du).

Entrez gene symbol	Primary hit list	screen	Validation apoptosis (No. siRNAs)	outcome	Average drug/control normalised caspase ratio SP	Average drug/control normalised caspase ratio Du (+/-25% of SP)
HOXA-AS3	5		3		0.99	<b>0.93</b> , 0.68, <b>0.77</b> , <b>1.01</b>
DKFZP434K028	3		2		0.82	<b>0.69</b> , 0.47, <b>0.87</b> , 1.26
GAS5	3		2		1.39	<b>1.47</b> , 1.68, 1.05, <b>1.41</b>
PAXBP1-AS1	3		2		1.39	<b>1.56</b> , <b>1.24</b> , 0.75, 1.03
SLC8A1-AS1	3		2		1.07	0.77, <b>1.21</b> , <b>1.13</b> , 0.76
PRC1-AS1	3		2		0.74	<b>0.9</b> , 0.28, 1.11, <b>0.52</b>
MALAT1	5		2		0.72	0.42, <b>0.67</b> , 1.19, <b>0.86</b>
ZFAS1	5		2		0.92	<b>0.97</b> , <b>1.05</b> , 1.25, 0.64
DIAPH3-AS2	3		1		1.73	<b>1.67</b> , 1.02, 0.87, 0.58
BHLHE40-AS1	3		1		1.64	<b>1.59</b> , 1.05, 0.63, 0.73
MIR503HG	3		1		1.47	<b>1.28</b> , 0.43, 0.95, 0.59
CECR7	3		1		1.27	0.98, 0.72, <b>1.5</b> , 0.88
KMT2E-AS1	3		1		1.12	<b>0.88</b> , 0.27, 0.78, 0.47
CHKB-AS1	3		1		0.95	1.5, 0.49, <b>0.81</b> , 0.62
FAM83H-AS1	3		1		0.63	0.93, 2.08, 1.04, <b>0.47</b>
ST7-AS2	5		1		1.97	1.05, 1.41, 1.4, <b>2.19</b>
MIRLET7BHG	5		1		0.96	0.4, 0.44, 1.56, <b>1.02</b>

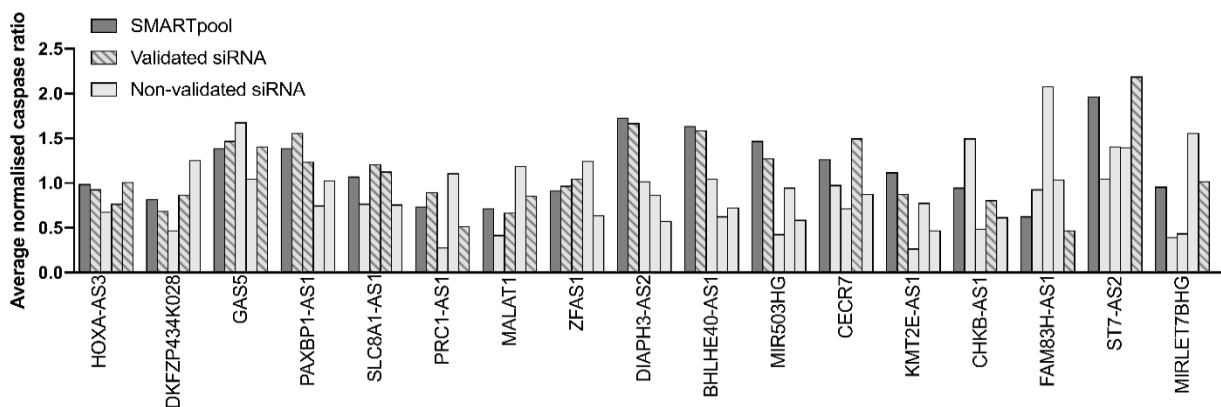


**Figure 5-3 lncRNA siRNA secondary screen SMARTpool validation of apoptosis data**

The average normalised caspase ratio representing apoptosis changes for lncRNA siRNAs which validated  $\geq 1$  siRNA compared to the Dharmacon lncRNA siRNA SMARTpools (4 siRNAs per pool) BHLHE40-AS1, CECR7, CHKB-AS1, DIAPH3-AS2, DKFZP434K028, FAM83H-AS1, GAS5, HOXA-AS3, KMT2E-AS1, MALAT1, MIR503HG, MIRLET7BHG, PAXBP1-AS1, PRC1-AS1, SLC8A1-AS1, ST7-AS2, ZFAS1 representing apoptotic change after 2.5 mM butyrate treatment of HCT116 cells. Validated siRNAs with  $\pm 25\%$  discrepancy threshold for hit selection.

### 5.2.3 lncRNA-miRNA-mRNA interaction networking using Cytoscape

In order to elucidate the role of the lncRNA-targeting siRNA hits in the butyrate response, lncRNA-miRNA-mRNA interactions were further investigated due to the known role of lncRNAs as miRNA sponges and the ability of miRNAs to regulate lncRNAs (Li et al. 2016e; Liang et al. 2017; Pa et al. 2017). Identified hits were only shown to alter apoptosis; therefore, miRNA-mRNA interactions involved in apoptosis were collated from the Chapter 4 analysis to assist in the construction of a lncRNA-miRNA-mRNA apoptotic network with differentially expressed (DE) lncRNAs. This resulted in a list of 19 miRNA-mRNA interactions that were potential interactors with the secondary screen lncRNAs.

lncRNA-miRNA interactions were predicted using a sequence based algorithm called DIANA-LncBase V2 (Paraskevopoulou et al. 2016). Some lncRNAs were excluded as they were not listed within the prediction program or their targets were not within the list of butyrate dysregulated miRNAs. The network was constructed using 8 lncRNAs: CECR7, GAS5, HOXA-AS3, KMT2E-AS1, MALAT1, PAXBP1-AS1, PRC1-AS1 and ZFAS1. MALAT1 was identified as a key hub with 15 miRNA interactions, of which three had down-stream mRNA targets that were associated with apoptosis (Figure 5-4, Table 5-3 and Appendix 10). Interestingly 5/15 MALAT1-miRNA interactions which appeared in the networking analysis were already validated in the literature, which is very supportive of this analysis that incorporates prediction data.

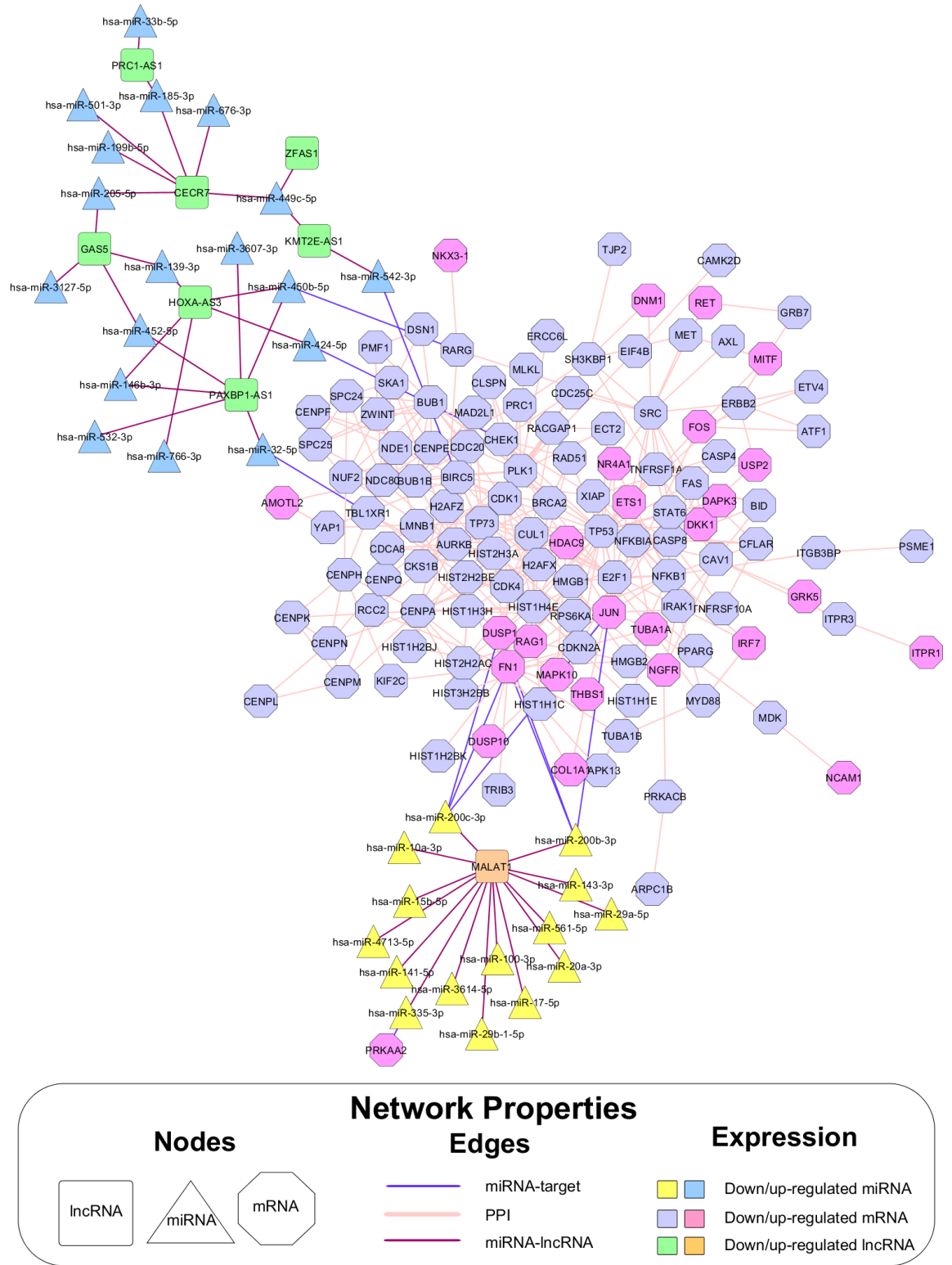


**Figure 5-4 Integrative apoptotic lncRNA-miRNA-mRNA interaction network of butyrate regulated genes in CRC**

Butyrate-regulated integrative lncRNA-miRNA-mRNA network constructed using Cytoscape based on interactions between lncRNAs-miRNA- target protein-coding genes and Protein-protein interactions (PPI). Refer to key for node information and expression profiles. The colour of the node represents the expression changes due to 2.5 mM butyrate treatment and the shape represents the type of molecule for each node. Solid lines are edges and represent direct interactions between two nodes.

**Table 5-3 Interaction table representing anti-correlating lncRNA-miRNA-mRNA interactors only**

lncRNAs	Expression	miRNAs	Expression	Validated lncRNA-miRNA interaction	miRNA targets	Expression
<b>HOXA-AS3</b>	Down	hsa-miR-424-5p	Up	-	CHEK1	Down
<b>HOXA-AS3</b>	Down	hsa-miR-450b-5p	Up	-	RARG	Down
<b>KMT2E-AS1</b>	Down	hsa-miR-542-3p	Up	-	BIRC5	Down
<b>MALAT1</b>	Up	hsa-miR-200b-3p	Down	V	DUSP1, FN1, JUN	Up
<b>MALAT1</b>	Up	hsa-miR-200c-3p	Down	V	DUSP1, FN1, JUN	Up
<b>MALAT1</b>	Up	hsa-miR-335-3p	Down	-	PRKAA2	Up
<b>PAXBPI-AS1</b>	Down	hsa-miR-32-5p	Up	-	TBL1XR1	Down
<b>PAXBPI-AS1</b>	Down	hsa-miR-450b-5p	Up	-	RARG	Down

## 5.2.4 MALAT1 functional investigation

### 5.2.4.1 Butyrate regulation of MALAT1 expression

MALAT1 was selected for further investigation due to its high relevance in CRC and known involvement in cell growth and death. MALAT1 also has known sponge interactions (described in section 1.6.2.2) with key miRNAs including the miR-200 family miRNAs including miR-200b and miR-200c (Li et al. 2016e; Liang et al. 2017; Pa et al. 2017) but it has not been studied in the context of butyrate, nor have they been studied with respect to the three predicted target genes *DUSP1*, *FN1* and *JUN*. Another well-known tumour suppressor miRNA in CRC, miR-335, was also identified as a potential interactor, along with its predicted target gene *PRKAA2*. The expression of MALAT1, as determined by RNA-seq, was confirmed using real-time RT-PCR before any further functional validation was performed to ensure biological relevance and to determine a suitable primer set to measure MALAT1 expression changes. Real-time RT-PCR results revealed that the transcript levels of MALAT1 significantly increased (P=0.0017) (Figure 5-5) in the presence of 2.5 mM of butyrate as observed in the RNA-seq results (Appendix 11).

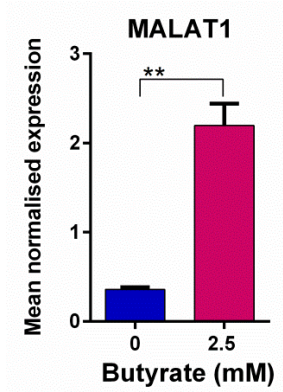


**Figure 5-5 Real-time RT-PCR analysis of MALAT1 expression in HCT116 CRC cells**

MALAT1 lncRNA levels in HCT116 cells treated with 0 mM or 2.5 mM butyrate for 24 h. The mean lncRNA expression  $\pm$  SEM of 4 technical replicates is represented and expression is normalised to the geometric mean of three reference genes, *ACTB*, *B2M* and *GAPDH*. Significant values are indicated by \* $P < 0.05$ , \*\* $P < 0.01$ , \*\*\* $P < 0.001$ , \*\*\*\* $P < 0.0001$ .

#### 5.2.4.2 MALAT1 siRNA knockdown efficiency

Based on the secondary screen data the MALAT1 siRNA with the most similar effect to the MALAT1 SMARTpool was used in subsequent experimentation to reproduce the phenotype (Figure 5-3, Table 5-2). Knockdown efficiency was determined prior to further investigation to ensure MALAT1 was being adequately targeted. HCT116 cells were reverse transfected with 20 nM of MALAT1 siRNA or NC siRNA for 72 h resulting in 65% knockdown of MALAT1 ( $P < 0.0001$ ) (Figure 5-6).

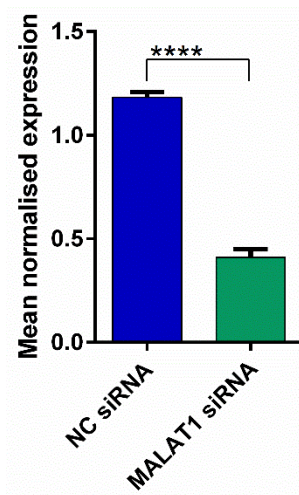


**Figure 5-6 MALAT1 siRNA knockdown efficiency in HCT116 CRC cells**

MALAT1 expression levels in CRC cells (A) HCT116 cells transfected with NC siRNA or MALAT1 siRNA for 72 h. The mean relative RNA levels  $\pm$  SEM of the triplicates is represented, and their expression is normalised to the geometric mean of three reference genes, *ACTB*, *B2M* and *GAPDH*. Significant values are indicated by \* $P < 0.05$ , \*\* $P < 0.01$ , \*\*\* $P < 0.001$ , \*\*\*\* $P < 0.0001$ . NC = Negative Control siRNA.

### 5.2.4.3 Effect of MALAT1 RNAi and butyrate on apoptosis, proliferation and viability in CRC cells

MALAT1 knockdown has previously been shown to increase CRC apoptosis and reduce proliferation in the absence of butyrate (Xu et al. 2018). However, the screen demonstrated that when combined with butyrate treatment the ability of MALAT1 to induce apoptosis was significantly decreased, but viability did not change. The screen results were validated using the same endpoint ApoLive-Glo™ Multiplex Assay and flow cytometry. HCT116 cells were reverse transfected with lncRNA or NC siRNAs for 48 h and treated with 0 mM or 2.5 mM butyrate for 24 h, as per previous experiments. After transfection with MALAT1 siRNAs alone, there were no significant effects on apoptosis (Figure 5-7 B). As expected, butyrate significantly induced apoptosis of HCT116 cells ( $P < 0.0001$ ). When MALAT1 siRNA was combined with butyrate treatment, apoptosis levels were significantly increased ( $P < 0.0001$ ). These results do not correlate with the screen data, which showed the opposing effects. The viability measurements in the ApoLive-Glo™ Multiplex Assay demonstrated that MALAT1 siRNA alone did not induce a decrease in viability (Figure 5-7 A). When MALAT1 siRNA was combined with butyrate treatment there was a slight but significant increase in cell viability ( $P = 0.0045$ ).

Flow cytometry was used to further validate apoptotic changes in HCT116 cells. These results demonstrated that MALAT1 siRNA alone caused a significant increase in viability ( $P = 0.0144$ ), while the combination of MALAT1 siRNA and butyrate cause a significant decrease in viability ( $P = 0.0245$ ) (Figure 5-8, 5-9). When MALAT1 siRNA was combined with butyrate, early apoptosis significantly increased ( $P = 0.0011$ ) which correlates with the ApoLive-Glo™ Multiplex Assay results; however, alone the MALAT1 siRNA caused a slight but significant decrease in early apoptosis ( $P = 0.0021$ ). In terms of late apoptosis, the siRNA caused no significant effects in the absence of butyrate, although a slight but non-significant decrease is observed, while the combination with butyrate had no significant effects. MALAT1 siRNA alone caused a slight but significant decrease in necrosis ( $P = 0.0145$ ). Butyrate alone was able to significantly reduce viability and increase apoptosis as expected ( $P \leq 0.0024$ ).

Further investigation was undertaken to confirm the growth effects observed in the initial screen. HCT116 cells were reverse transfected with NC or MALAT1 siRNAs and treated with 0 mM or 2.5 mM butyrate as previously mentioned and real-time cell growth was measured using the xCELLigence. It was observed that MALAT1 siRNA

alone had no significant effect on the growth of HCT116 cells and butyrate alone significantly decreased growth as expected ( $P < 0.0001$ ) (Figure 5-10). When MALAT1 siRNAs were combined with butyrate treatment a significant enhancement effect ( $P = 0.0003$ ) was observed and cell growth was further decreased. This was not observed in the primary or secondary screen. The viability effects were investigated by performing crystal violet assays. This assay showed that the MALAT1 siRNA alone did not influence cell viability at 72 h (Figure 5-11), which correlates with the xCELLigence results (Figure 5-10). When MALAT1 siRNAs were combined with butyrate a significant effect was not observed, which does not correlate with xCELLigence results or ApoLive-Glo™ assay results. Butyrate induced a significant decrease in viability as previously observed ( $P = 0.0006$ ).

To further characterise the changes observed, flow cytometry was used to identify changes in the cell cycle, which might contribute to changes observed in proliferation using the xCELLigence. It was demonstrated that alone MALAT1 siRNAs had no significant effect on accumulation of cells in the G0/G1 phase; however, percentage of cells significantly increased in the S phase ( $P = 0.0174$ ), while it significantly decreased in the G2/M phase ( $P = 0.0002$ ) (Figure 5-11, 5-12). When the siRNA was combined with butyrate, again no significant effects were seen in G0/G1 phase, while cells significantly accumulated in the G2/M phase ( $P = 0.0489$ ) but decreased in the S phase ( $P = 0.0007$ ). Butyrate alone was able to reduce the percentage of cells in the S phase and increase the percentage of cells in the G2/M phase as shown in previous experiments ( $P \leq 0.0361$ ).

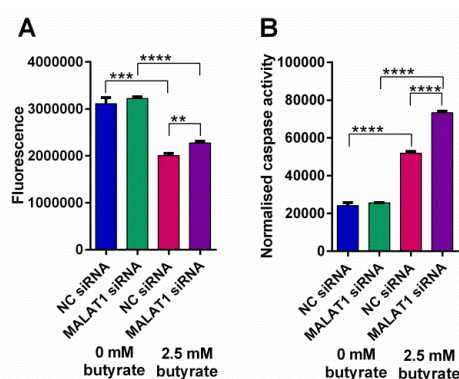


**Figure 5-7 Cell viability and apoptosis in MALAT1 siRNA transfected HCT116 cells after 24 h of butyrate treatment**

ApoLive-Glo™ Multiplex Assay: fluorescence and luminescent signals for (A) viability changes and (B) normalised caspase activity for apoptosis changes respectively, for HCT116 cells reverse transfected with MALAT1 siRNAs for 48 h, followed by 24 h of treatment with 0 mM or 2.5 mM butyrate, over a 72 h post-transfection period. The mean  $\pm$  SEM of 4 technical replicates is shown. Significant results are indicated by \*  $P < 0.05$ , \*\*  $P < 0.01$ , \*\*\*  $P < 0.001$ , \*\*\*\*  $P < 0.0001$ . NC = Negative Control siRNA.

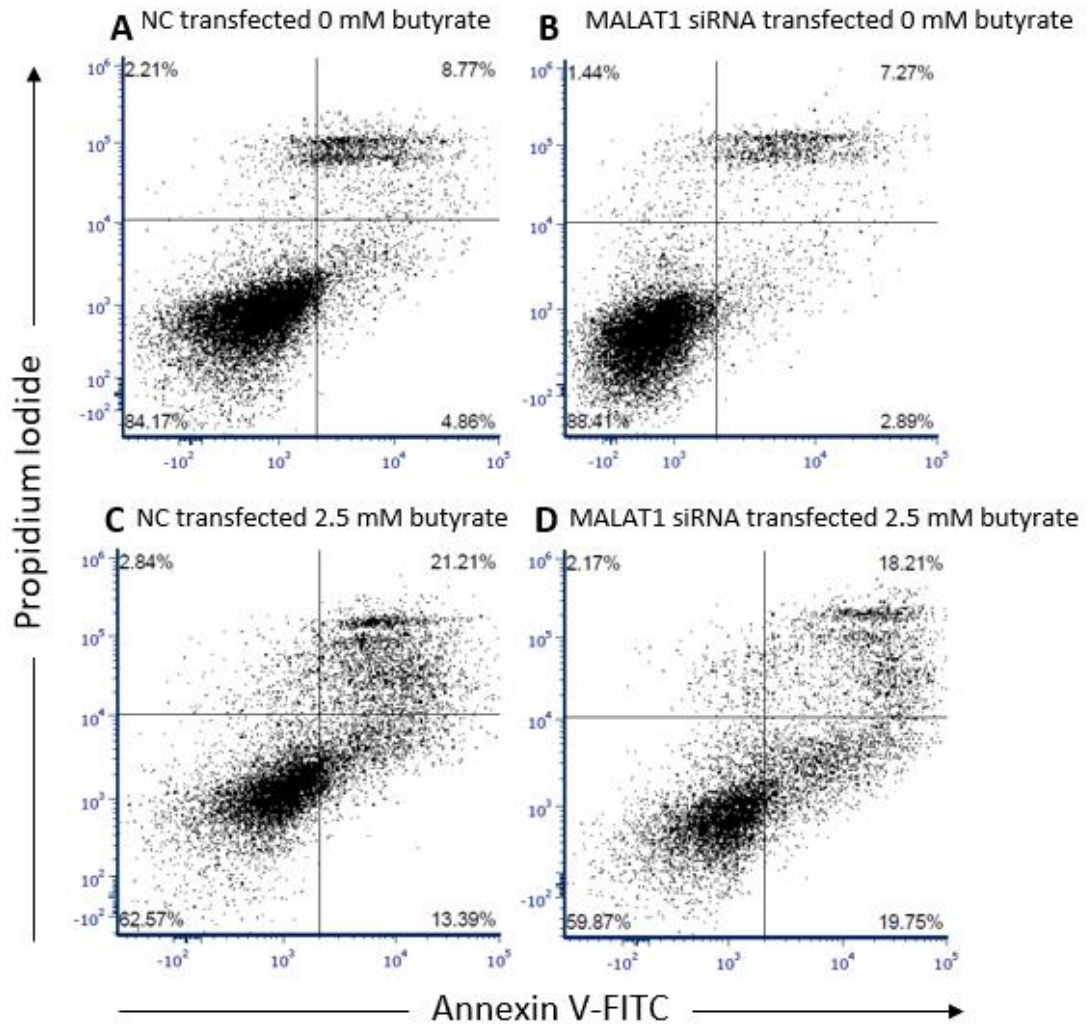


**Figure 5-8** Flow cytometry analysis of apoptosis in siRNA transfected HCT116 cells after 24 h of butyrate treatment

Examples of flow charts depicting the apoptosis analyses of HCT116 cells reverse transfected with NC or MALAT1 siRNAs for 48 h, followed by 24 h of treatment with 0 mM or 2.5 mM butyrate, over a 72 h post-transfection period (A) NC transfected 0 mM butyrate, (B) MALAT1 siRNA transfected 0 mM butyrate, (C) NC transfected 2.5 mM butyrate, (D) MALAT1 siRNA transfected 2.5 mM butyrate. Cells were stained with propidium iodide and annexin V stain and measured using the Cytoflex Flow Cytometer. NC= Negative Control siRNA.

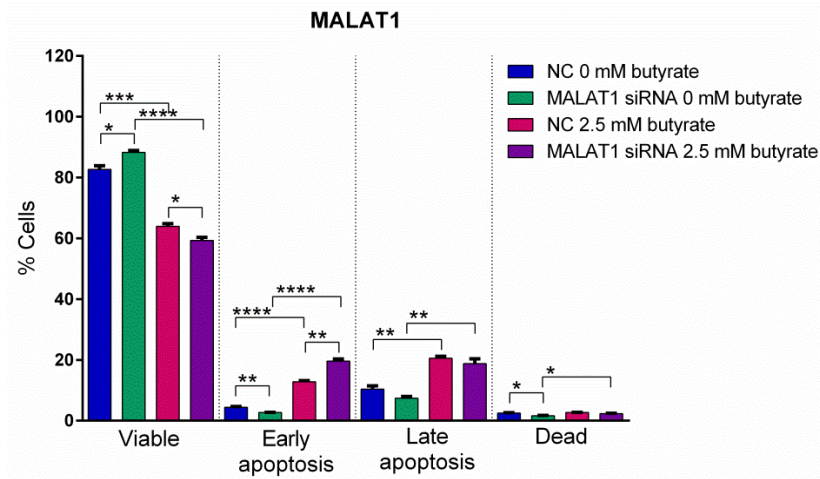


**Figure 5-9 Apoptosis analysis of MALAT1 siRNA using Cytoflex flow cytometry**

Bar chart depicting apoptosis analysis of HCT116 cells reverse transfected with MALAT1 siRNAs for 48 h, followed by 24 h of treatment with 0 mM or 2.5 mM butyrate, over a 72 h post-transfection period. Cells were stained with propidium iodide and annexin V stain and measured using the Cytoflex Flow Cytometer. The mean  $\pm$  SEM of 3 replicate wells is shown. Significant results are indicated by \*  $P < 0.05$ , \*\*  $P < 0.01$ , \*\*\*  $P < 0.001$ , \*\*\*\*  $P < 0.0001$ . NC= Negative Control siRNA.

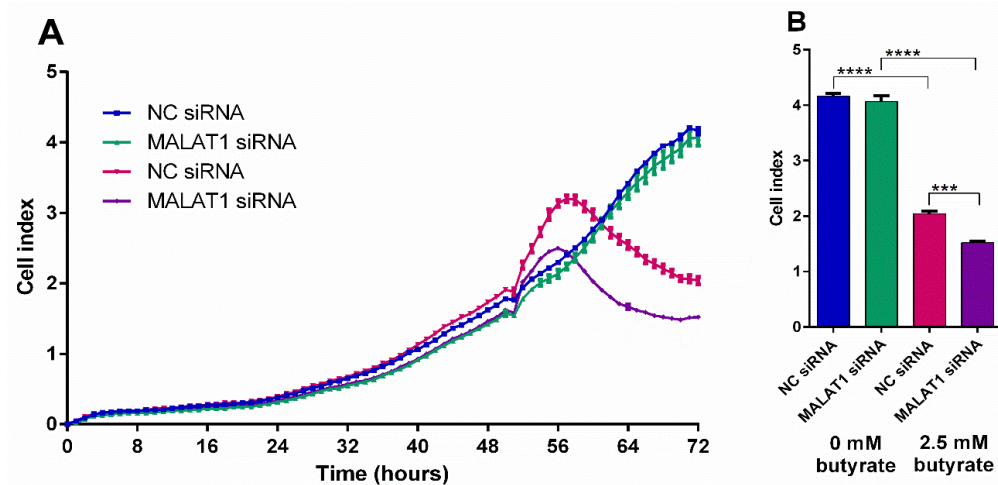


**Figure 5-10 Proliferation of HCT116 cells after transfection with MALAT1 siRNAs and 24 h butyrate treatment**

Real-time cell index measurements using the xCELLigence RTCA platform, in HCT116 cells transfected with (A) MALAT1 siRNAs for 48 h, followed by 24 h of treatment with 0 mM or 2.5 mM butyrate, over a 72 h post-transfection period. The mean  $\pm$  SEM of 4 replicates is shown at 72 h post-transfection (B) MALAT1 siRNAs. Significant results are indicated by \*  $P < 0.05$ , \*\*  $P < 0.01$ , \*\*\*  $P < 0.001$ , \*\*\*\*  $P < 0.0001$ . NC= Negative Control siRNA.

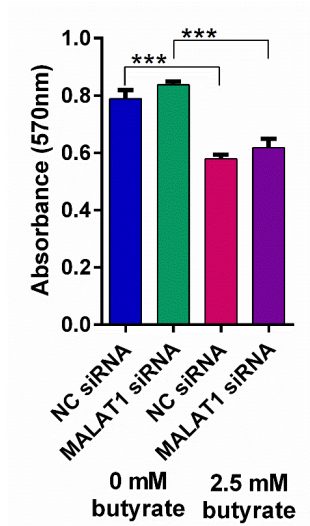


**Figure 5-11 Viability of HCT116 cells after transfection with MALAT1 siRNAs and 24 h butyrate treatment**

Crystal violet assay: Absorbance signal at 570 nm indicates viability changes in HCT116 cells reverse transfected with NC or MALAT1 siRNAs for 48 h, followed by 24 h of treatment with 0 mM or 2.5 mM butyrate, over a 72 h post-transfection period. The mean  $\pm$  SEM of 4 replicate wells is shown. Significant results are indicated by \*  $P < 0.05$ , \*\*  $P < 0.01$ , \*\*\*  $P < 0.001$ , \*\*\*\*  $P < 0.0001$ . NC= Negative Control siRNA.

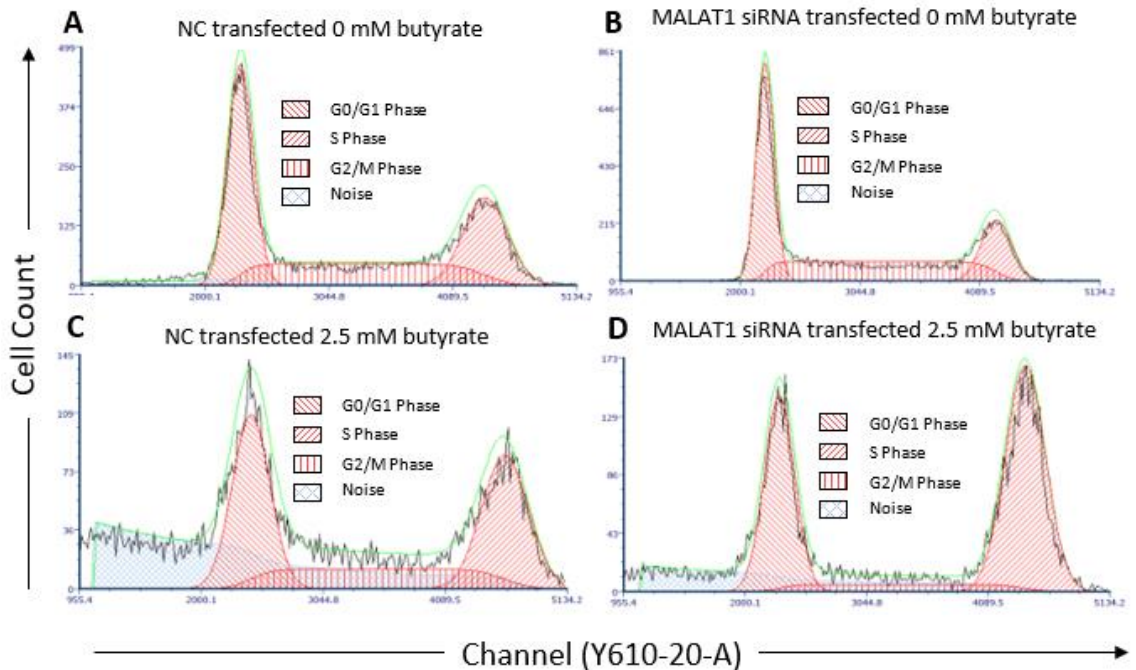


**Figure 5-12 Flow cytometry analysis of the cell cycle in siRNA transfected and butyrate treated HCT116 cells**

Examples of flow charts depicting cell cycle analyses of HCT116 cells reverse transfected with NC or MALAT1 siRNAs for 48 h, followed by 24 h of treatment with 0 mM or 2.5 mM butyrate, over a 72 h post-transfection period (A) NC transfected 0 mM butyrate, (B) MALAT1 siRNA transfected 0 mM butyrate, (C) NC transfected 2.5 mM butyrate, (D) MALAT1 siRNA transfected 2.5 mM butyrate. Cells were stained with propidium iodide and measured using the Cytoflex Flow Cytometer. NC= Negative Control siRNA.

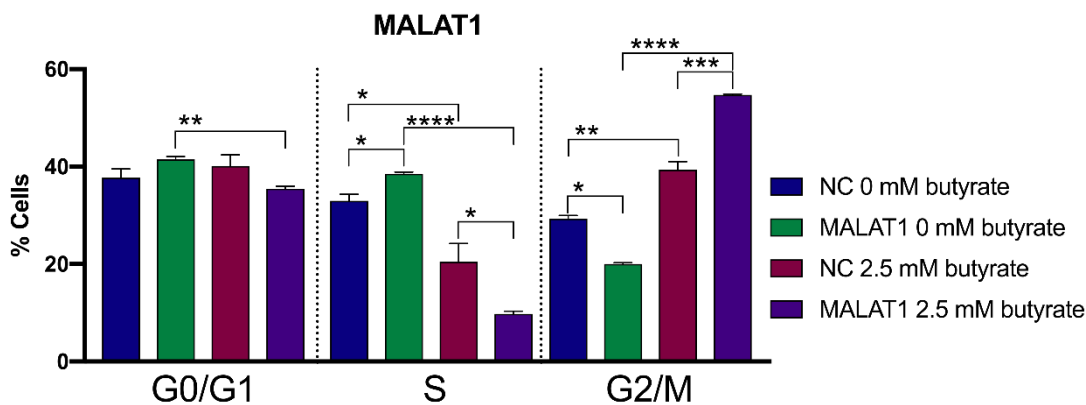


**Figure 5-13 Cell cycle analysis using flow cytometry in butyrate treated HCT116 cells**

Bar chart depicting cell cycle analysis of HCT116 cells reverse transfected with MALAT1 siRNAs for 48 h, followed by 24 h of treatment with 0 mM or 2.5 mM butyrate, over a 72 h post-transfection period. Cells were stained with propidium iodide and cell percentage measured using the Cytoflex Flow Cytometer. The mean  $\pm$  SEM of 3 replicate wells is shown. Significant results are indicated by \*  $P < 0.05$ , \*\*  $P < 0.01$ , \*\*\*  $P < 0.001$ , \*\*\*\*  $P < 0.0001$ . NC= Negative Control siRNA.

#### 5.2.4.4 Effect of MALAT1 siRNA on miRNA and mRNA expression

To further elucidate the role of MALAT1 in the butyrate response of HCT116 cells the lncRNA-miRNA-mRNA axis was investigated. MALAT1 interactions with miR-200b, miR-200c and miR-335 were investigated by examining whether the expression of these miRNAs is altered by MALAT1 knockdown. Using LncBase version 2, MALAT1 was identified to have 10 binding sites each for miR-200b (Table 5-4) and miR-200c (Table 5-5), while miR-335 was identified to have 11 sites (Table 5-6). HCT116 cells were transfected with MALAT1 siRNAs and treated with 2.5 mM butyrate as previously mentioned and RNA collected for real-time RT-PCR. Knockdown of MALAT1 alone resulted in a significant increase in miR-200b ( $P = 0.0018$ ), miR-200c ( $P = 0.0283$ ) and miR-335 ( $P = 0.0006$ ) (Figure 5-14). When the siRNA was combined with butyrate the expression levels for miR-200b ( $P = 0.0078$ ) and miR-335 ( $P < 0.0001$ ) were significantly increased, but not miR-200c. Knockdown of MALAT1 alone only caused a significant reduction in *JUN* ( $P = 0.0348$ ) expression, but not *DUSP1*, *FN1* or *PRKAA2*. When the siRNA was combined with butyrate, there was a significant reduction in *JUN* ( $P = 0.0029$ ) expression and a non-significant increase in *PRKAA2* expression, but no change in *DUSP1* and *FN1*. MALAT1 knockdown was confirmed ( $P = 0.0004$ ).

CHAPTER 5

Table 5-4 Binding sites for miR-200b in MALAT1

miRNA binding category	Transcript position	Binding area with target lncRNA transcript (top) and miRNA (bottom)	Binding score
<b>8mer</b>	5445-5457	5'GAUAAGUUUAACUUG U CAUC GCAGUAUUG        GUAG CGUCAUAAU 3' A UAAUGGUC	0.008
<b>7mer</b>	3443-3464	ACUGA G GGGGAGUUUU U G CGGG CAGUAUU .  .      U GUCC GUCAUAA A G U	0.003
<b>6mer</b>	7969-7988	GCCUGCAA A AAG AUUGUUA CAG GGUAUUA   . .         .       UAGUAAU GUC UCAUAAU G G CG	0.003
<b>6mer</b>	1079-1095	CUUUCCACAC UAAUUUA U GCUAG AGUAUU .  .      UGGUC UCAUAA A CG U	0.002
<b>6mer</b>	3920-3937	GAGCUGCUU C GA C UUAUC UUG AG AGUAUU  .       .          AGUAG AAU UC UCAUAA U GG CG U	0.002
<b>6mer</b>	7296-7318	GUCAG A G ACAA AUC GUUAU GG UAGUAUUG     .    . .   .       UAG UAAUG UC GUCAUAAU G G C	0.002
<b>6mer</b>	4604-4627	GAUU U UGA G CUUUU UC UC UG UAG GUAUUA        . .      AG AG AU GUC CAUAAU U UA G CGU	0.002
<b>6mer</b>	4409-4419	UAUAGAGCUUUUGGGGA AA AGG AGUAUUG           UCC UCAUAAU G G	0.002
<b>6mer</b>	3334-3359	G GU GU G AAUGA U UAU UUA U GGGU AGUAUU .        . .   .   GUA AAU G UCCG UCAUAA A GU G U	0.002
<b>8mer+mismatch</b>	4901-4921	UCUGA A GCCU GA GUCAU ACCA GGCAGUAU .             UAGUA UGGU CCGUCAUA G A A	0.002

CHAPTER 5

Table 5-5 Binding sites for miR-200c in MALAT1

miRNA binding category	Transcript position	Binding area with target lncRNA transcript (top) and miRNA (bottom)	Binding score
8mer	5436-5457	GAUAAG      A      A      U UUA C UUGC UC GCAGUAUUG  . .       .   .         AGGU G AAUG GG CGUCAUAAU A U                      C	0.008
7mer	3445-3464	ACUGAGG      GGGGGAGUUU      U CGG                      CAGUAUU                                GCC                      GUCAUAA G                                      U	0.003
6mer	7962-7988	G    UGCAA      AACAGAA CC      AUUGUU      GG    GUAUUA            . . .                  GG      UAAUGG      CC    CAUAAU A    UAG                      G                      GU	0.003
6mer	1072-1095	CUU      CA    C    G    AAUUUA      U UCCA    CG    UA    U                      AGUAUU          .          .                            AGGU    GU    AU    G                      UCAUAA A      A    G    GCCG                      U	0.002
6mer	3919-3937	GAGCUGCU                                      AAG      C UUUUUC      CUUGG      AGUAUU  . .           . .               AGGUAG      GGGCC      UCAUAA UAAU                      G                      U	0.002
6mer	7296-7318	G    GA      GUUA      GACAA UCA    UCA                      UGG      UAGUAUUG .                                .         .       GGU    AGU                      GCC      GUCAUAAU A                      AAUGG	0.002
6mer	4603-4627	GAU    U    UGA                      GCUUUU UUC    UC                      UGGUA      GUAUUA  .                           .   .              AGG    AG                      GCCGU      CAUAAU U    UAAUGG	0.002
6mer	4392-4419	AGAGCU      GGAAGGAA UAU                      UUUGG                      AGUAUUG .                         . . .                               GUA                      GGGCC                      UCAUAAU G    GUAAU                      G	0.002
6mer	3334-3359	G    GU    G      GGUAAUGA      U UAU    UUA    UUGG                      AGUAUU .              . .                               GUA    AAU    GGCC                      UCAUAA G    GU    G      G                      U	0.001
8mer+mismatch	4902-4921	UCUGAG      AACCA                      GA UCAU                      GCCUGGCAGUAU .                          .   .       GGUA                      UGGGCCGUCAU A      GUAA                      A	0.001

CHAPTER 5

**Table 5-6 Binding sites for miR-335 in MALAT1**

miRNA binding category	Transcript position	Binding area with target lncRNA transcript (top) and miRNA (bottom)	Binding score
<b>8mer</b>	5218-5243	G AAUAAA AAAGA U CAG AGCGA AAUGAAAA        .         GUC UCGUU UUACUUUU A C A U	0.008
<b>6mer</b>	8650-8668	GUGUUUUG A CC CUGC C AG AGC UA UGAAAA                UC UCG AU ACUUUU G C UU U U	0.007
<b>8mer</b>	2099-2115	AAGAUAGAAA A UA A U CA GA GA AAUGAAAA        .         GU CU UU UUACUUUU A C CG A U	0.006
<b>7mer</b>	521-544	ACUU AGCC AAGC UCAGGAG UGG UGAAAAA        .         AGUCCUC AUU ACUUUUU C GUU	0.006
<b>7mer</b>	2487-2505	CCUAAAUA U UUAGUU UAG AGC UGAAAAA .              GUC UCG ACUUUUU A C UUAUU	0.005
<b>9mer</b>	2121-2148	A UUCA AGAA GUCA GAGU GAU AAUGAAAAA          .            CAGU CUCG UUA UUACUUUUU C C	0.005
<b>7mer</b>	2208-2227	CAAAAUU UAA CAC GGA AAUAG UGAAAAA         .         CCU UUAUU ACUUUUU U CG	0.003
<b>6mer</b>	529-555	A C U A UGAAAAAC A G C GGA GC GGU GAAAAA             .         C G CCU CG UUA CUUUUU C A U UUA	0.002
<b>6mer</b>	3941-3956	GAAGAGUAUCC UUGA CAG AGC UGAAAAG               .   GUC UCG ACUUUUU A C UUAUU	0.002
<b>6mer</b>	1992-2011	AGAAAAAA UA UUAACC GA AAU UGAAAAG             .   CU UUA ACUUUUU C CG UU	0.002
<b>6mer</b>	2832-2850	UAACGAUUU G U A UAG GGU G GA GC GAAAAA      .              CCA U CU CG CUUUUU G C UUAUUA	0.002

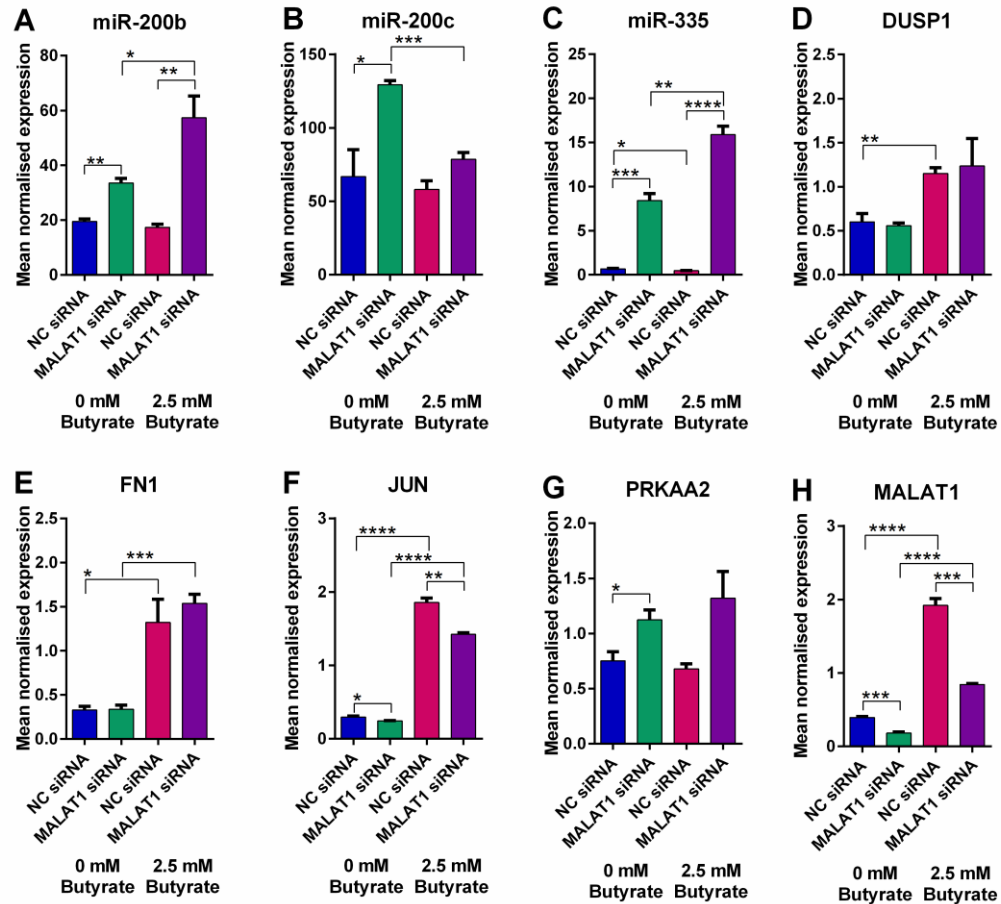


**Figure 5-14** mRNA and miRNA expression changes in HCT116 cells exposed to MALAT1 siRNAs and butyrate

miRNA and mRNA levels of (A) miR-200b, (B) miR-200c, (C) miR-335, (D) *DUSP1*, (E) *FN1*, (F) *JUN* and (G) *PRKAA2*, (H) MALAT1 in HCT116 cells transfected with NC or MALAT1 siRNAs for 48 h, followed by 24 h of treatment with 0 mM or 2.5 mM butyrate, over a 72 h post-transfection period. The mean mRNA and miRNA levels  $\pm$  SEM of the triplicates is represented. mRNA expression is normalised to the geometric mean of three reference genes, *ACTB*, *B2M* and *GAPDH*. miRNA expression is normalised to *RNU6B* reference gene. Significant values are indicated by \*P<0.05, \*\*P<0.01, \*\*\*P<0.001, \*\*\*\*P<0.0001. NC= Negative Control siRNA.

## 5.3 Discussion

### 5.3.1 Summary

This work focused on another subset of non-coding RNAs, lncRNAs, which have not previously been implicated in the butyrate response in CRC cells. The aim of these experiments was to systematically identify lncRNAs that enhance the anti-cancer effects of butyrate and reveal critical lncRNA-miRNA-mRNA interactions involved in the butyrate response of CRC cells. This study was done using unbiased high-throughput functional screening and integrative pathway and network analyses. RNA interference of

several different lncRNAs was shown to increase the pro-apoptotic potential of butyrate. Further investigation of MALAT1 knockdown suggested that this lncRNA has anti-proliferative and pro-apoptotic effects. MALAT1 was confirmed to act as a sponge for tumour suppressor miRNAs, miR-200b and miR-200c and potentially miR-335, and have critical potential downstream targets including *FN1*, *DUSP1*, *JUN* and *PRKAA2* involved in apoptosis.

### 5.3.2 Primary high-throughput screen

The primary high-throughput screen revealed 49 hits (siRNA SMARTpools) which were selected for further investigation in the secondary screen. Of the hits identified, only 3 were found to reduce viability and induce apoptosis together (list 1), while 15 reduced viability without changing apoptosis (list 2), 22 increased apoptosis but did not change viability (list 3), 2 reduced viability and apoptosis (list 4) and 7 cherry picked hits decreased apoptosis without changing viability (list 5). The hit lists were carefully created to consider several cellular responses which may have been detected via the use of the ApoLive Multiplex assay. It was important to note that even with no changes in viability or increases in apoptosis as measured by caspase activity, the data were still valuable and could have indicated that cells were undergoing early apoptosis. The assay utilises a live cell protease marker for viability. This marker remains active in the cell until the cell membrane becomes compromised and proteases are exposed to the extracellular environment. The proteases are still active during early apoptosis when cells are shrinking and organelles are being tightly packed as cell membrane integrity is maintained until later stages (Elmore 2007). Alternatively, no changes in apoptosis, but decreases in viability were important to consider as other cellular changes such as necrosis, senescence or cell cycle arrest could have occurred. In order to avoid the presumption of these effects, additional cellular parameters might have been useful to detect during the screen such as dead-cell protease markers (Riss et al. 2011), which would indicate if cells had passed early apoptosis in combination with caspase data.

### 5.3.3 Secondary screen investigating RNA interference of lncRNAs

Of the 49 lncRNAs that showed a phenotype when silenced by SMARTpools in the primary screen, 17 of these validated in the secondary screen. This included a range of well-studied oncogenic and tumour suppressor lncRNAs such as MALAT1 (Sun & Ma 2019), GAS5 (Gao et al. 2017) and ZFAS1 (Dong et al. 2018a) as well as uncharacterised lncRNA species including DKFZP434K028. Interestingly, HOXA-AS3 had the greatest number of siRNAs validate at 3/4. The lncRNA HOXA-AS3 regulates

key cell cycle related proteins including cyclin A, D and E and CDK1, CDK2 and CDK3 in order to promote cell proliferation (Zhang et al. 2018a). Previous studies have demonstrated that HOXA-AS3 is upregulated in cancer states including lung cancer (Zhang et al. 2018a) and glioma (Wu et al. 2017a) and interestingly it is upregulated by HDAC inhibitors such as Trichostatin A (TSA) in lung cancer (Zhang et al. 2018a), although reduced in expression by butyrate in CRC. Knockdown of this lncRNA has been shown to inhibit proliferation, migration and invasion and induce cell cycle arrest and apoptosis in lung cancer and glioma cells (Wu et al. 2017a; Zhang et al. 2018a).

### 5.3.4 Integrative network and pathway analyses

Further investigation of these hits was performed using integrative network and pathway analysis in order to examine lncRNA function and involvement in the butyrate response. A lncRNA-miRNA-mRNA network was constructed to identify lncRNAs which might be acting as sponges (decoy archetype) (section 1.5.2.2). As all lncRNA-targeting siRNAs were shown to affect apoptosis in the primary screen, only apoptotic interactions from chapter 4 were identified for further examination and combined with DE lncRNAs. MALAT1 was the most highly connected lncRNA with the greatest number of miRNA interactions (15 interactions) in the apoptotic network, of which 5 were already validated in several cancers and disease types, which was very supportive of this network, although the interactions still need to be validated in CRC. These included miR-143-3p in liver cancer (Chen et al. 2017), miR-15b-5p in heart disease (Zhu et al. 2019), miR-20a-3p in breast cancer (Zhao et al. 2018a), miR-200b-3p in kidney cancer (Xiao et al. 2015) and miR-200c-3p in endometrial and ovarian cancer (Li et al. 2016e; Liang et al. 2017; Pa et al. 2017). miR-29b has also been shown to interact with MALAT1 in a non-sponge interaction whereby the promoter region of the miRNA gene is silenced by the addition of H3K27me3 marks via MALAT1 and EZH2 interactions (Stamato et al. 2017). Further examination revealed that of these miRNAs, only 3 had interactions with apoptosis related genes including miR-200b and miR-200c with *FN1*, *DUSP1* and *JUN* and miR-335 with *PRKAA2*.

#### miR-200b and miR-200c interactions

miR-200b and miR-200c are well known inhibitors of EMT in several cancer types (Korpala & Kang 2008). miR-200b has been shown to be decreased in CRC tissues and cell lines when compared to normal tissues and cell lines (Chen et al. 2018b), although other studies have shown it is upregulated in CRC tissues when compared to normal tissues (Pan et al. 2015). Discrepancies might be due to CRC stage which was not

mentioned in most studies. miR-200c expression varies in CRC based on tumour stage as it is often upregulated in later stages (III-IV) and associated with poor prognosis, and downregulated in earlier stages (I-II) (Chen et al. 2014; Toiyama et al. 2014). The overexpression of miR-200b was demonstrated to inhibit proliferation and induce apoptosis in HCT116 CRC cells (Chen et al. 2018b). miR-200c downregulation was revealed to decrease apoptosis and increase invasion (Karimi Mazraehshah et al. 2018), whereas overexpression of miR-200b and miR-200c has also been shown to promote proliferation in other CRC cell lines, SW420, Caco2 and HT29 (Pan et al. 2015), which may be due to mutational differences in cell lines. miR-200b and miR-200c have already been shown to target *FN1* in breast and endometrial cancer resulting in inhibition of migration and invasion via EMT (Howe et al. 2011; Yang et al. 2017c). As mentioned in section 4.2.3, *FN1* was one of the most highly connected interactors in the butyrate regulated PPI network. *FN1* is involved in several processes including migration, differentiation, and proliferation that have been implicated in CRC development and growth (Saito et al. 2008). It has been shown that knockdown of this gene in CRC inhibits proliferation, migration and invasion (Cai et al. 2018b), which is promising. *DUSP1* is another target that is known to dephosphorylate MAPK proteins including p38, JNK, and ERK (Wu et al. 2006). *DUSP1* is a confirmed target of miR-200b in HEK293T cells and miR-200c in rats with diabetic cardiomyopathy (Singh et al. 2017); however, this interaction and function has yet to be investigated in CRC. *JUN* is a protein that forms the AP-1 transcription factor with *FOS*, which has a key role in differentiation, proliferation and migration (Dunn et al. 2002). *JUN* has already been identified as a target of miR-200b and miR-200c in mouse hepatocytes (Guo et al. 2016) and HEK293T cells (Del Vecchio et al. 2016), although this has not been confirmed in CRC. These are all promising interactions which may have key roles in the butyrate response.

### **miR-335 interactions**

The other miRNA investigated was miR-335. miR-335 is a well-known tumour suppressor miRNA which has reduced expression in several cancer types such as CRC, lung cancer and breast cancer (Gao et al. 2015; Liu et al. 2018a; Wang et al. 2017). miR-335 has been shown to inhibit CRC cell growth, migration and invasion by targeting genes in EMT such as *ZEB1* (Sun et al. 2014; Wang et al. 2017) as well as reduce proliferation and migration in lung and breast cancer (Gao et al. 2015; Liu et al. 2018a). *PRKAA2* was predicted to be a novel interactor with miR-335 that has not previously

been reported. Other lncRNAs had limited interactions or their target miRNAs were not associated with apoptosis genes.

### 5.3.5 MALAT1 butyrate regulation and knockdown

MALAT1 was selected for further investigation based on its extensive connections in the apoptosis network. Moreover, MALAT1 is typically overexpressed in cancers (Xu et al. 2018; Yang et al. 2015c) and is a known oncogene in CRC and other cancers such as lung, gastric, and pancreatic, where it has been shown to promote proliferation, migration and invasion (Miao et al. 2016; Xu et al. 2018; Yang et al. 2015c; Zhao et al. 2018b). MALAT1 overexpression has also been associated with poor prognosis in patients and resistance to oxaliplatin in CRC (Li et al. 2017a; Li et al. 2016b; Zheng et al. 2014). In the present study, butyrate significantly increased MALAT1 expression, which was unexpected as butyrate has anti-proliferative and anti-survival effects in CRC. However, it is not without precedent as TSA and vorinostat, other HDAC inhibitors, have also been shown to upregulate MALAT1 in gastric cancer cells and aortic endothelial cells (Rafehi & El-Osta 2016; YiRen et al. 2017).

MALAT1 knockdown was confirmed using the siRNA from the secondary screen which had the most similar cellular response to the initial SMARTpool phenotype, in order to mimic the initial effects detected in the primary screen. The screen siRNA reduced MALAT1 levels by 65%. Given that MALAT1 is a nuclear localised lncRNA that aggregates into nuclear speckles that are involved in splicing regulation (Hutchinson et al. 2007; Tripathi et al. 2010); it was unclear whether a siRNA would be effective in mediating MALAT1 knockdown. The silencing of a nuclear lncRNA requires the presence of nuclear RNAi machinery such as AGO2 which normally facilitates miRNA-mediated silencing in the RISC complex (Gagnon et al. 2014). It has been demonstrated that AGO2, DICER and TRBP RNAi machinery are present in the nuclei of some cancer cells (HeLa and A549) in multiprotein complexes (Gagnon et al. 2014). However, the localisation of AGO2 greatly depends on the cell type and tissues (Sharma et al. 2016) and this should be examined in the model of interest to confirm the siRNA effects are not off-target effects. It was previously demonstrated that MALAT1 siRNAs significantly reduce the amount of MALAT1 localised in nuclear speckles in HeLa cells using fluorescence in situ hybridization (FISH) (Gagnon et al. 2014). Hence these data provide further support that siRNAs mediate efficient RNAi of MALAT1 in the nucleus.

### 5.3.6 Effects of MALAT1 knockdown on proliferation, apoptosis and the cell cycle

After the confirmation of siRNA knockdown, the growth and apoptotic effects of MALAT1 siRNA were validated using a range of assays and real-time cell systems. MALAT1 siRNAs in combination with butyrate significantly induced apoptosis in several assays including the same Apo-Live Multiplex assay used in the screen. However, the latter conflicted with the screen results which showed that early apoptosis was reduced during the combination treatment. The primary screen showed that viability was unaffected by MALAT1 RNAi and butyrate. However, the validation results were varied with both marginal significant increases and decreases in viability seen in different assays. The conflicts are likely related to the different parameters measured in the different assays. In particular, the xCELLigence measures cell impedance which can be affected by morphological changes as well as changes in cell number. Such morphological changes may not be unexpected given the effects MALAT1 has on EMT (Yang et al. 2015c). Although previous studies demonstrated that MALAT1 knockdown inhibits proliferation of CRC cells (Yang et al. 2015c), the effect is clearly marginal even in the presence of butyrate. Interestingly, cell cycle studies were supportive of growth changes as MALAT1 knockdown resulted in accumulation of cells in the S phase and decreases in the G2/M phase although this effect was reversed when combined with butyrate. MALAT1 siRNA had no effect on the G0/G1 phase. A previous study demonstrated similar results in SW620 and SW480 CRC cells, whereby MALAT1 knockdown increased cells in the S phase but also the G0/G1 phase resulting in inhibition of proliferation (Yang et al. 2015c). Although the same changes in the G0/G1 phase did not occur in this study. Further investigation is required to elucidate the different responses.

#### Screen limitations

The observation that MALAT1 screen results were contradictory to the validation results may have several technical and biological explanations. Further investigation will need to be performed to determine if this contradictory pattern is consistent for other hits. An interesting phenomenon identified in the screen was the low apoptotic signal in the *PLK1* siRNA group. *PLK1* was used as a positive control as it is a potent repressor of growth and inducer of death in CRC (Driscoll et al. 2014). *PLK1* siRNA potently induced cell death in HCT116 cells; the effectiveness of the caspase assay was believed to be compromised by the large amount of cell debris. This same effect may have led to

underestimation of the pro-apoptotic effects of other siRNAs, although this could have been overcome by using a dead-cell protease marker in the screen (Riss et al. 2011). Lesser effects on cell death were detectable and comparable to the other positive control, miR-18a (Humphreys et al. 2014b). Another observation was an unexpected decline in viability and increase in apoptosis in control wells on butyrate treated plates. Although samples are normalised to their own plate controls to account for interplate variation, it was concerning to observe such variation across plates. The screen sought to identify differences between the lncRNA-targeting siRNA alone and the siRNA plus butyrate combination. As a butyrate only control was not included, there was no comparison to butyrate only treated cells to determine the drug effect alone. This also may have omitted valuable data about the combinatorial effects of these molecules, in whether they were acting synergistically or antagonistically to butyrate.

Previous studies have demonstrated that the method of screening and normalisation can affect RNAi and drug screen hit rates and reproducibility (Barrows et al. 2010; Mpindi et al. 2015). Several normalisation techniques are used to analyse HTS data, but there is no standard normalisation method (Birmingham et al. 2009). Interestingly, three independent RNAi screening studies investigating human host factors in the HIV lifecycle revealed dissimilar lists of key factors involved in this process (Brass et al. 2008; Konig et al. 2008; Zhou et al. 2008) and although differences in the methodologies may account for some variation, it is questionable whether there should have been greater cross-over in hit outcomes. Another study investigated factors affecting RNAi screen reproducibility and hit list outcomes for host factors promoting yellow fever virus infection by repeating the same methods of the screen 5 months apart (Barrows et al. 2010). This study revealed that the analysis method significantly affected the hit list outcome, which astoundingly ranged from 82 to 1,140 hits depending on the method as well as intra- and inter-screen reproducibility which varied from 32% to 99% (Barrows et al. 2010). Another study also revealed that the placement of controls on the screen plates can affect the normalisation as those controls in the end columns (column 1 and 24) may experience evaporation compared to those on the interior the plate (Mpindi et al. 2015). Scattering controls throughout the plate is a useful approach but may add technical difficulty. Earlier investigations revealed that there are clear systematic row, column and border effects on well signals (Brideau et al. 2003), again highlighting the importance of control and sample placement, but also that normalisation methods need to take this into account to prevent false positives. Murie et al. (2014) developed a control-plate regression (CPR) method which involves normalising the treatment plate

data to a control plate which contains the same feature across all wells to estimate systematic error for each individual well, which bypasses this issue.

Several other systematic errors may have contributed to data differences including butyrate evaporation, robotic liquid handling and pipetting issues, incubation and signal measurement time variations and the use of different plate readers (Makarenkov et al. 2007), which often happens due to the large number of plates to be processed. Other considerations must also be noted when selecting plates for high-throughput screening as there is the possibility of optical crosstalk between wells, whereby small amounts of light can travel between wells, even if the wells have black sides (Jones et al. 2004). White coloured plates are optimal for luminescent assays as they absorb less light and black plates can quench the signal (Jones et al. 2004). In this study, black clear-bottom plates were used which may have reduced caspase luminescent signals, but were the optimal colour for the fluorescent viability signals.

Overall, our validation data for MALAT1 (showing that RNAi increases apoptosis in combination with butyrate) was broadly consistent with literature. In particular, a previous study has shown that knockdown of MALAT1 in CRC induces apoptosis (Xu et al. 2018), which is consistent with its proposed oncogenic role. While the cellular effects of MALAT1 in combination with butyrate have not been characterised, a previous study treated MALAT1-knockout gastric cells with TSA, and this resulted in increased sensitivity to TSA and autophagy, although the effects on apoptosis are unknown (YiRen et al. 2017). It was previously shown that knockdown of MALAT1 reversed the chemoresistance of glioblastoma cells to temozolomide (TMZ) and promoted apoptosis (Cai et al. 2018a), so its knockdown may have potential in future treatments.

### 5.3.7 Effect of MALAT1 RNAi on miRNA and mRNA interactors

MALAT1 interactions were examined by using real-time RT-PCR to determine if MALAT1 RNAi affects expression of key mRNA interactors. MALAT1 RNAi significantly increased miR-200b, miR-200c and miR-335 expression levels alone and this was further enhanced in the presence of butyrate. This result was consistent with previous evidence that MALAT1 can sponge miR-200b (Xiao et al. 2015) and miR-200c (Li et al. 2016e; Pa et al. 2017); however, miR-200b and miR-200c predicted targets, *FN1* and *DUSP1* did not respond to MALAT1 knockdown alone. This was unexpected as MALAT1 is known to sponge these miRNAs but also *DUSP1* and *FN1* are confirmed targets of miR-200b and miR-200c (Howe et al. 2011; Singh et al. 2017),

although these interactions have yet to be investigated in CRC. Lack of response may have indicated an issue with the MALAT1 siRNA; however, MALAT1 knockdown was confirmed indicating MALAT1 RNAi was not an issue. Interestingly, *JUN* expression was significantly reduced after MALAT1 knockdown in the absence of butyrate, providing evidence for the MALAT1-miR-200b/c-*JUN* axis. JUN is a confirmed target of miR-200b and miR-200c (Del Vecchio et al. 2016; Guo et al. 2016), although this has not been confirmed in CRC.

The effect on miR-335 expression was a novel finding in CRC. However, the interaction has been proposed to have a role in acute lymphoblastic leukaemia in a lncRNA-miRNA-mRNA axis, whereby MALAT1 and *ABCA3* were upregulated and miR-335 downregulated (Pouyanrad et al. 2019). *PRK4A2* was found to be significantly upregulated after MALAT1 knockdown, which does not support the existence of the MALAT1-miR-335-*PRK4A2* axis and may indicate it is not a direct target of miR-335. *PRK4A2* was predicted to be a novel interactor with miR-335 which has not previously been reported; therefore, target confirmation is required to confirm the interaction. MALAT1 has been previously implicated in the regulation of mRNA stability and expression (Tripathi et al. 2013; Xiao et al. 2019), which may provide an alternative mechanism by which *PRK4A2* is upregulated.

The effect of overexpressing or inhibiting the target miRNAs on MALAT1 levels and target gene expression has yet to be investigated. miRNAs have been shown to induce silencing of lncRNAs, and for example, miR-9 was shown to silence MALAT1 in the nucleus by binding to two miRNA-binding sites within MALAT1 (Leucci et al. 2013). Furthermore, the reciprocal repression of MALAT1 and miR-200c has been identified in endometrial carcinoma (Li et al. 2016e). Further investigation is warranted to provide insight into whether miR-200b, miR-200c and miR-335 are regulating MALAT1 expression in CRC.

### 5.3.8 Conclusion

This study identified several butyrate-sensitising, lncRNA-targeting siRNAs. MALAT1 knockdown was revealed to enhance the pro-apoptotic effects of butyrate. MALAT1 was identified to be potentially involved in three lncRNA-miRNA-mRNA axes including miR-200b, miR-200c and miR-335, as well as targets *FN1*, *DUSP1*, *JUN* and *PRK4A2*. The future directions of this work will involve elucidating whether miR-200b, miR-200c and miR-335 regulate the expression of MALAT1, validation of the MALAT1 and miR-335 interaction as well as miR-335 regulation of *PRK4A2*. In the

## CHAPTER 5

long term, other screen hits including HOXA-AS3 and PAXBP1-AS1 should also be further investigated to validate their cellular responses and apoptosis-related target interactors. Those lncRNAs which did not have apoptotic downstream miRNA interactors may also be studied in the future to reveal other mechanisms by which they may influence cancer cell growth or apoptosis. lncRNAs functioning as miRNA sponges were the primary focus of this study; however, future investigations should also include elucidating other functions including guide, scaffolding, signalling and enhancer mechanisms (described section 1.6.2.2) involved in the butyrate response. Although further investigation is required, this study provides the basis to study the utility of lncRNA inhibition as future potential therapeutic targets.

# Chapter 6. Summary and conclusions

---

## 6.1 Thesis summary

Epigenetic dysregulation, including alterations to histone modification patterns, DNA methylation and non-coding RNA gene expression, is important in the development and progression of CRC. CRC has been commonly associated with aberrant changes in global histone acetylation and methylation, DNA hypomethylation of repeat sequences and increased promoter DNA methylation as well as reduction of tumour suppressor functioning miRNAs and upregulation of miRNAs with oncogenic potential (Cummins et al. 2006; Qin et al. 2019; Tse et al. 2017). Diet-related molecules, such as butyrate, have been shown to have chemo-protective effects against CRC through the alteration of global histone acetylation and consequently global gene expression through HDAC inhibition (Daly & Shirazi-Beechey 2006; Davie 2003). Although it is known that butyrate can alter non-coding RNA expression in order to exert its anticancer properties in CRC (Cummins et al. 2006), the effects of manipulating these molecules on the butyrate response requires further investigation. On the basis that miR-18a overexpression was found to enhance the anti-proliferative and pro-apoptotic effects of butyrate in CRC (Humphreys et al. 2014b), it was hypothesised that manipulation of non-coding RNA expression would have the ability to sensitise CRC cells to butyrate.

The purpose of the work in this thesis was to perform cell-based studies to determine the ability of specific non-coding RNAs, including miRNAs and lncRNAs that had been identified in a functional screen, to enhance the anticancer properties of the HDACi, butyrate. This study also aimed to further elucidate the role of non-coding RNAs, their targets and critical cell growth and death pathways in the butyrate response of CRC cells. This could support the potential therapeutic value and feasibility of RNAi and HDACi combinatorial therapies in CRC cells. The key results of this study are summarised below.

## 6.2 Functional high-throughput screen identifies miRNAs sensitise CRC cells to butyrate

In Chapter 3, several miRNAs were shown to enhance the anti-proliferative and pro-apoptotic effects of butyrate. This is supportive of previous data, whereby the tumour

suppressor miR-18a was able to promote the anticancer properties of butyrate (Humphreys et al. 2014b). Of the miRNAs identified, miR-1227 which is not a well characterised miRNA was found to have the most potent effects on cell growth and death in combination with butyrate. Three other miRNAs were also found to modulate the butyrate response to varying degrees: miR-593, miR-125b and miR-181a. miR-593 is not well studied; however, miR-125b and miR-181a, are both well studied dual-acting miRNAs (oncogenic and tumour suppressor roles in different contexts) in several cancers including CRC (Gong et al. 2013; Gu et al. 2018; Nishida et al. 2011). Interestingly, the potential of the miRNAs to act as an oncogene or tumour suppressor in CRC did not determine their effects when combined with butyrate. In contrast, the miRNA previously shown by our laboratory to enhance the anticancer effects of butyrate, miR-18a, was a likely tumour suppressor (Humphreys et al. 2014b). Further examination revealed that all four studied miRNAs were involved in critical cell growth and death pathways including WNT signalling, PI3K-AKT signalling and MAPK signalling indicating overlap with the pathways regulated by butyrate (Daly & Shirazi-Beechey 2006). It was revealed that targeting of the regulatory subunit of PI3K, *PIK3R3* (an identified miR-181a target gene), could reduce CRC proliferation and should be further investigated for therapeutic potential. The catalytic subunit of PI3K has previously been confirmed as a potent target for drug treatment (Wortmannin or LY294002) in CRC cells (Wang et al. 2002), which highlights the importance of PI3K signalling in CRC. Other miRNA targets of interest included *TRIM29* (miR-125b), *CCND1* and *EEF2K* (miR-593), *DVL3* and *NUP62* (miR-1227) which were all related to WNT signalling. WNT signalling, which is a key dysregulated pathway in CRC (Fodde 2002), was also demonstrated to be regulated by the butyrate-sensitising miRNAs, specifically miR-181a, in a context-specific manner; however, this requires further investigation.

### **6.3 Systems biology approach reveals butyrate-sensitising miRNAs and their involvement in the cell cycle**

In Chapter 4, integrative network and pathway analyses revealed that butyrate regulates the expression of numerous protein-coding and non-coding genes. These butyrate-regulated genes were all significantly involved in the cell cycle pathway as highlighted in past profiling studies in CRC (Daly & Shirazi-Beechey 2006), which reiterates the key role of butyrate in the promotion of cell cycle arrest and inhibition of cell growth in CRC (Wu et al. 2018c). Further examination revealed key butyrate-regulated miRNA-

mRNA interactions involved in the cell cycle, including known tumour suppressors miR-139 and miR-542 and their target genes *EIF4G2* and *BIRC5* respectively. In particular, mimics corresponding to miR-542 were highly lethal in HCT116 cells. Its target BIRC5 (Survivin) is likely a key contributor to this cellular response due to its critical role in the inhibition of caspase proteins in apoptosis (Altieri 2003) and regulation of cell division (Li et al. 1998). *BIRC5* has already been identified as a potential therapeutic target (Garg et al. 2016), hence its role in the butyrate effect warrants further investigation. HCT116 cells were much more sensitive to miR-542 than LIM1215 cells suggesting that the function of this miRNA may depend on mutational status in CRC and this is worthy of further study. miR-139 and miR-542 were confirmed to regulate the cell cycle, which is likely a key contributor to their anti-proliferative and pro-apoptotic effects in combination with butyrate in CRC as seen in previous studies (Li et al. 2016d; Long et al. 2016). miR-139 and miR-542 were identified as new butyrate-sensitising miRNAs in this study, which act synergistically with butyrate to enhance its anticancer properties. Networking analysis revealed that *EIF4G2* was the most highly connected gene in the butyrate-regulated cell cycle network. Further investigation revealed that *EIF4G2* knockdown was highly effective in reducing proliferation both alone and in combination with butyrate. These effects likely relate to the role of *EIF4G2* in regulating synthesis of cell cycle proteins (Lee & McCormick 2006). The novel findings in the present study, together with previous reports that *EIF4G2* knockdown significantly reduces cell growth and survival of other cancers (Emmrich et al. 2016), suggests that *EIF4G2* could be a future therapeutic target.

#### **6.4 Functional RNAi screen identifies butyrate-sensitising lncRNAs in CRC cells**

In Chapter 5, functional RNAi screening revealed that several combinations of lncRNA-targeting siRNAs can regulate proliferation and apoptosis of CRC in combination with butyrate. This chapter presents the first evidence for the feasibility of a combined lncRNA-targeting and HDACi cell treatment. Bioinformatic analysis of selected targets revealed that MALAT1 was a critical hub in the integrative apoptotic network. MALAT1 is a well-studied oncogenic lncRNA in CRC and several other cancers (Miao et al. 2016; Xu et al. 2018; Yang et al. 2015c; Zhao et al. 2018b); however, its role in the butyrate response in CRC had not been previously elucidated. This study demonstrated that MALAT1 knockdown in combination with butyrate significantly increased apoptosis of CRC cells. MALAT1 knockdown was previously shown to increase the

expression of miR-200b and miR-200c, which are known MALAT1 interactors in kidney cancer (Xiao et al. 2015) and endometrial and ovarian cancer (Li et al. 2016e; Liang et al. 2017; Pa et al. 2017) respectively, although interactions will need to be confirmed in CRC. The same effect was observed for miR-335 which is a novel target identified in the present study. Interestingly, miR-335 is also an EMT regulator and has been shown to inhibit CRC cell growth, migration and invasion by targeting genes such as *ZEB1* (Sun et al. 2014; Wang et al. 2017), as do the EMT regulators miR-200b and miR-200c (Mongroo & Rustgi 2010). Of the downstream targets investigated, only the miR-200b and miR-200c predicted target *JUN* responded with reduced expression upon MALAT1 knockdown. *JUN* is a confirmed target of miR-200b and miR-200c (Del Vecchio et al. 2016; Guo et al. 2016), although this has not been established in CRC. *FN1* and *DUSP1* did not respond to MALAT1 knockdown. However, although it does not support the MALAT1-miR-200b/c-*FN1*/*DUSP1* axis, *FN1* and *DUSP1* responses to miR-200b and miR-200c mimics should be investigated in the future. The expression of miR-335 predicted target, *PRKAA2*, increased after MALAT1 knockdown. This indicates that an alternative mechanism may be responsible for its regulation, rather than miR-335, such as direct regulation of mRNA stability via MALAT1 (Tripathi et al. 2013; Xiao et al. 2019). Targeting lncRNAs with siRNAs may be a viable therapeutic approach in cancer as it has previously been validated in other contexts (Modarresi et al. 2012), as discussed further below.

## 6.5 Future directions and applications

These studies have provided insight into the role of non-coding RNAs in the butyrate response and their ability to enhance the anticancer properties of this HDACi. This study has also revealed some limitations that could be addressed in future work, as well as opening up new avenues for further investigation.

Further work should investigate the functional RNA interactions using 3D cell culture methods such as organoids to confirm cellular responses, before potentially moving on to *in vivo* studies. The use of 2D cell monolayers limits the extrapolation of data as they lack the physiological features of tumours such as vasculature, tissue-specific structures, interactions with the extracellular matrix, mechanical and biochemical signals, and cell-cell and cell-matrix interactions (Fang & Eglen 2017). This can lead to poor predictions of drug responses in some cancer cell types.

In terms of the physiological relevance of the miRNA screens, future screens should identify combinations of miRNAs to treat cells at lower concentrations rather than single miRNAs at supraphysiological levels. It is not reflective of the natural cellular system as miRNAs usually work in combination and this may be reflected in their pattern of co-regulation. A previous study demonstrated that exposing breast cancer cells to a set of co-regulated pro-epithelial miRNAs could promote mesenchymal to epithelial (MET) transition at much lower concentrations than a single overexpressed miRNA, with fewer off-target effects (Cursons et al. 2018). Therapeutic advantages of lower-dose miRNA combinations may include the reduction of toxic side effects on surrounding healthy tissues, increased treatment efficiency, and reduced acquired resistance as multiple miRNAs can target several pathways and targets. The same might be considered for siRNA therapies.

Future work should also investigate metabolic regulation of the butyrate response in combination with miRNA/lncRNA treatments. Glucose concentration has been shown to affect the fate of butyrate in CRC cell lines and, therefore their cellular response (Donohoe et al. 2012). At high concentrations of glucose (25 mM), low concentrations of butyrate (0.5 mM) modestly increased HCT116 cell proliferation or had negligible effects (1 mM), while 2 and 5 mM butyrate reduced proliferation (Donohoe et al. 2012). Conversely, at low concentrations of glucose (0.5 mM), low concentrations of butyrate (0.5 and 1 mM) greatly stimulated HCT116 cell proliferation, while 2 and 5 mM butyrate reduce proliferation (Donohoe et al. 2012). In this study, the recommended media for HCT116 cells, McCoy's media, was used which has high glucose levels (16.7 mM); however, more physiologically relevant levels (~5 mM) should also be investigated. Further investigation of key interactions will need to be performed in order to elucidate the exact mechanisms of butyrate-sensitisation by non-coding RNAs (Figure 6-1). WNT hyperactivation is a key mechanism by which butyrate reduces growth and induces apoptosis in CRC cells; however, the mechanism by which this happens is poorly understood (Bordonaro et al. 2002; Bordonaro et al. 2008; Lazarova et al. 2014). Interestingly, across all xCELLigence experiments in this study, an initial rise in cell index was observed in the first few hours after butyrate was added to the wells; however, not with the addition of unsupplemented media. Previous studies demonstrated that the rapid increase and then decrease in cell index is cell type and treatment dependent (Kho et al. 2015). NT2 astrocytes were exposed to a range of concentrations of pro-inflammatory cytokines which resulted in a rapid increase and then decrease in cell index for treatment only wells which indicated transient loss of

adhesion (Kho et al. 2015). This phenomenon should be further investigated as it may indicate a link between butyrate-induced WNT hyperactivation and apoptosis (Bordonaro et al. 2002; Bordonaro et al. 2008; Lazarova et al. 2014), which is not well studied. The initial activation of growth could be due to WNT hyperactivation, whereby cells rapidly respond to WNT signalling and proliferate before reaching a threshold and undergo cell death as pro-apoptotic genes are activated. Previous studies have shown that the balance of WNT activity is critical in the cell fate, whereby high WNT activity can induce apoptosis, moderate WNT activity maintains a proliferative cell state and low WNT activity promotes differentiation followed by apoptosis (Albuquerque et al. 2002; Lazarova et al. 2004; Wong et al. 2002). Several critical signalling molecules can also regulate the sensitivity of cells to WNT hyperactivation.  $\beta$ -catenin mutations are important in the constitutive activation of WNT signalling; however, this leaves cells vulnerable to butyrate making them more sensitive to WNT hyperactivation and apoptosis induction (Lazarova et al. 2004). Interestingly, loss of *TP53* and miR-34 in CRC cell lines was shown to hyperactivate WNT signalling and promote CRC progression, while overexpression of miR-34a reduced  $\beta$ -catenin abundance by targeting its UTR (Kim et al. 2011). Another study also identified miR-552 as a hyper-activator of WNT signalling via the targeting of *TP53* in CRC (Kwak et al. 2018). Clearly there is a balance between WNT activity,  $\beta$ -catenin and p53 levels and activity and the promotion of growth or death (Kim et al. 2011; Lazarova et al. 2004). Based on results collected in this study, it is possible that butyrate-sensitising miRNAs miR-125b, miR-1227, miR-593 and miR-181a are fine tuning WNT signalling activity via their targets *TRIM29*, *DVL3* and *NUP62*, *CCND1* and *COX2* and *FZD4* respectively; however, the key regulator is butyrate. In future studies, it would be interesting to investigate  $\beta$ -catenin and p53 protein levels and activity after miRNA and butyrate combination treatments, which may give insight into the mechanisms by which the treatments modulate WNT related pathways. It must also be acknowledged that miRNAs can target up to several hundred genes within a cell across numerous pathways (Bartel 2009; Friedman et al. 2009); therefore, these miRNAs are likely targeting other CRC related pathways that can also contribute to their anticancer effects.

PI3K and MAPK signalling pathways were also key pathways found to be regulated by butyrate-sensitizing miRNAs in this study (Figure 6-1). Previous studies have demonstrated that butyrate and PI3K inhibitors (Wortmannin or LY294002) induced significant pro-apoptotic and anti-proliferative effects in CRC (Wang et al. 2002). As butyrate downregulates the expression of several components of this pathway (*PIK3CG*,

*IRS1*, *MATK*) (Daly & Shirazi-Beechey 2006; Zhang et al. 2010), it is not unexpected that targeting of the regulatory subunit, *PIK3R3*, by miR-181a also caused enhancement of the butyrate response synergistically. Butyrate has also been shown to enhance the anticancer effects of SIRT1 inhibition through reducing activity of mTOR/S6K1 signalling and cell proliferation (Cao et al. 2019). Targeting EIF4G2, a critical effector of this pathway and butyrate-inhibited gene (Daly & Shirazi-Beechey 2006; Zhang et al. 2010), using miR-139 further reduced its expression and enhanced the butyrate response synergistically. EEF2K is also part of the mTOR signalling pathway; however, is it normally inhibited by mTORC1 indirectly. In this study, *EEF2K* RNAi was not investigated; however, previous studies have identified it as a potential therapeutic target as its inhibition led to apoptosis and reduced growth in cancer (Fu et al. 2014). EEF2K inhibits protein synthesis by preventing elongation and similarly butyrate normally inhibits protein synthesis by mTOR signalling in CRC to impede cell growth (Cao et al. 2019). As miR-593 is predicted to silence *EEF2K*, alternative mechanisms may be responsible for the anticancer effects of miR-593 observed in combination with butyrate, rather than its effects on *EEF2K*. Interestingly, *PRKAA2* which is an upstream inhibitor of mTORC1 was shown to be upregulated through MALAT1 knockdown; therefore, this further highlights the importance of protein synthesis in CRC cells (Francipane & Lagasse 2014). Butyrate was also shown to regulate MAPK signalling by decreasing ERK3 expression, ERK1/2 phosphorylation and upregulating MAPK12 expression (Daly & Shirazi-Beechey 2006; Zhang et al. 2010). Silencing of another MAPK signalling member, MAP3K8, with miR-181a may also have contributed to the butyrate response from this miRNA. A previous miRNA study revealed that silencing of MAP3K8 in renal cancer inhibited proliferation and migration (Su et al. 2015), although further investigation is required in CRC. Other investigations revealed that butyrate activated JNK protein through increased phosphorylation and inhibition of JNK reversed the anti-apoptotic effects of butyrate (Zhang et al. 2010). ERK1/2 phosphorylation was also reduced by butyrate, indicating that ERK signalling is likely inhibited to allow JNK signalling pathways to promote cell death (Zhang et al. 2010). Interestingly, *JUN*, which is downstream of JNK, was identified as a predicted target in the MALAT1-miR-200b/*JUN* axis. *JUN* has been identified as an immediate-early gene induced by HDAC inhibitors including butyrate, vorinostat and valproic acid (VPA) to promote cell death (Wilson et al. 2010). Therefore, enhanced pro-apoptotic effects observed with MALAT1 RNAi, combined with butyrate, may not be attributed to this interaction.

Other butyrate-sensitising non-coding RNAs and their targets should also be evaluated in future studies to reveal other potential therapeutic targets. Those miRNAs and lncRNAs, which desensitised cells to butyrate (not reported in this study), may also provide further insight into the butyrate response. As discussed further below, future studies should also investigate the effects of other HDAC inhibitors such as vorinostat and panobinostat which are already used to treat Cutaneous T cell lymphoma (CTCL) (Mann et al. 2007) and Multiple Myeloma (MM) (Richardson et al. 2015) respectively.

There are various potential therapeutic applications based on data collected during this study. Several HDAC inhibitors have already been approved to treat blood cancers as previously mentioned. Butyrate alone was shown to reduce growth and induce apoptosis in CRC cells throughout this study and as shown in previous studies (Daly & Shirazi-Beechey 2006; Hague et al. 1997; Mariadason 2008). Butyrate, although a cheap and reliable model for HDAC inhibition in CRC cells *in vitro*, is not stable and has a short half-life which is not suitable for a systemic cancer therapeutic (Miller et al. 1987). Other HDAC inhibitors which are FDA approved, such as vorinostat, panobinostat and romidepsin, are stable synthetic HDAC inhibitors that have already proven to be efficacious in the treatment of Cutaneous T cell lymphoma (CTCL) (Mann et al. 2007), Multiple Myeloma (MM) (Richardson et al. 2015) and Peripheral T cell lymphoma (PTCL) (Piekarz et al. 2011), respectively. HDAC inhibitors are being further investigated for use in solid cancers, although they have been shown to have poor efficacy alone (Qiu et al. 2013), they have shown greater efficacy in combination therapies. For example with topoisomerase inhibitors, platinum-based chemotherapeutics and proteasome inhibitors (Suraweera et al. 2018). However, cell-based studies on HDAC inhibition help broaden our understanding of the mechanism of action behind these molecules and potentially assist in improving current treatment approaches.

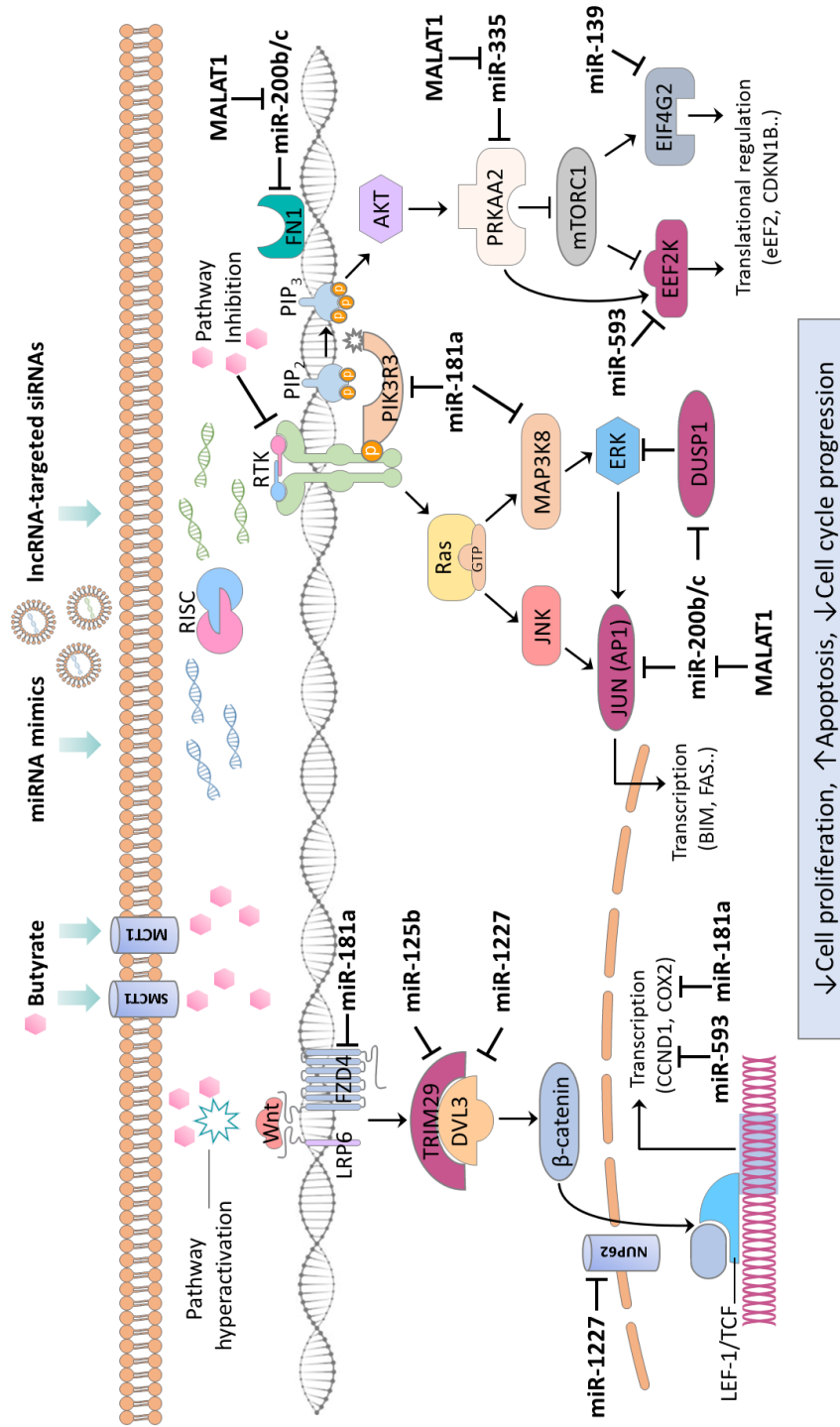


**Figure 6-1 Summary of non-coding RNA interactions contributing to butyrate sensitisation of CRC cells**

Butyrate-sensitising non-coding RNAs were identified to target several genes across WNT, MAPK and PI3K signalling pathways. The relationship between miRNA-mediated gene regulation and butyrate regulation is complex. Butyrate hyperactivates the WNT pathway, by unclear mechanisms, to induce apoptosis while key miRNAs silence the expression of WNT and cell cycle promoters. PI3K and MAPK signalling pathways are inhibited by the HDACi mechanisms of butyrate and they are further exacerbated by the silencing of key proteins in these pathways using miRNAs. Overall these interactions promote cell proliferation, induce apoptosis and decrease cell cycle progression.

miRNA replacement therapies and anti-miR therapy have been shown to have therapeutic potential due to well-studied dysregulation and causative roles of miRNAs in various cancer states (Peng & Croce 2016; Tan et al. 2018). As highlighted in section 1.4.4, re-introducing downregulated tumour suppressor miRNAs or reducing the expression of upregulated oncogenic miRNAs may inhibit disease progression when healthy concentrations are reached. miRNA replacement therapies have already been tested in clinical trials. As previously mentioned, miR-34a (MRX34) replacement therapy demonstrated efficacy in some hepatocellular carcinoma patients including 1 partial response and 6 stable disease states (Beg et al. 2017); however, further investigation is required in CRC. Anti-miR therapies have also been tested in phase 2 clinical trials in hepatitis C virus (HCV) sufferers using anti-miR-122 (Miravirsen) to block the pro-viral miRNA miR-122 (Janssen et al. 2013). It was demonstrated that anti-miR-122 induced dose-dependent reductions in HCV RNA levels in patients and there has been no viral resistance (Janssen et al. 2013).

Several types of lncRNA-targeting therapies have also shown therapeutic potential as summarised in section 1.5.4. Silencing oncogenic lncRNAs and overexpressing tumour suppressor lncRNAs has been shown to prevent disease progression. For example, antisense oligonucleotides (ASOs), AntagoNATs, siRNAs, and lncRNA replacement therapy using gene therapy vectors are currently being investigated in pre-clinical stages. ASOs targeting MALAT1 in mouse models demonstrated reduced metastasis (Gutschner et al. 2013), while ASOs targeting TUG1 in mouse models with glioma demonstrated reduced tumour growth (Katsushima et al. 2016). As previously mentioned in this section, Modarresi et al. (2012) revealed that siRNA and AntagoNAT targeting of the lncRNA, *BDNF-AS*, resulted in the restoration of *BDNF* expression in mouse models and promoted neuronal outgrowth and differentiation. The introduction of lncRNA-422 lentiviral vectors in CRC cells and *in vivo* models induced apoptosis, suppressed migration and invasion and reduced tumour growth (Shao et al. 2018). With the ability to reduce oncogenic lncRNA expression, re-activate gene expression by targeted inhibition of lncRNAs and increase tumour suppressor lncRNA expression, these molecules certainly show therapeutic potential.

Delivery systems to improve the efficacy and specificity of these potential RNAi therapeutics are continuously being developed and improved. Numerous delivery particles have been designed to encapsulate or bind RNAi molecules, including non-viral vectors such as lipid-based carriers, charged polymeric vectors with varying chemical coatings and inorganic materials and viral vectors (adenovirus and lentivirus)

(Hosseinahli et al. 2018). A recent phase 1 clinical trial testing miR-16 loaded minicells revealed some success whereby 1 patient had an objective response, 1 had partial response and 15 had stable disease out of 22 patients (van Zandwijk et al. 2017). However, it must be noted that dose-limiting toxicities were experienced by patients ranging from grade 1-4, including infusion-related inflammation and coronary ischaemia, anaphylaxis and cardiomyopathy and non-cardiac pain (van Zandwijk et al. 2017). In the context of this study, the protective miRNAs identified could be delivered to CRC patients in the future; however, miR-16 is a very well-studied tumour suppressor miRNA across many cancers (Cui 2015); therefore, thorough examination of other potential miRNAs should be performed across many pre-clinical models before considering clinical trials. Tissue specificity issues would also have to be addressed as miRNAs such as miR-125b and miR-181a are known to act as tumour suppressors and oncogenes in different cell types (Ferracin et al. 2013; Gu et al. 2018; Nishida et al. 2011; Shi et al. 2017). For example, a tissue specific miRNA-targeted therapy was developed whereby a cardio-specific  $\alpha$ -MHC promoter was cloned into a vector to create a miR-181-sponge construct; this revealed loss of miR-181 in the heart but no other organs using *in vivo* models (Kent et al. 2018). Issues with tumour penetration of RNA therapeutics also need to be addressed. Currently, several strategies to enhance tumour penetration efficacy are being investigated including reducing particle size, functionalising particles and regulating the tumour microenvironment (Su & Hu 2018).

## 6.6 Conclusion

This project examined the role of non-coding RNAs, including miRNAs and lncRNAs, in the butyrate sensitisation of CRC cells. The combination of miRNA mimics or lncRNA-targeting siRNAs and butyrate could reduce CRC cell proliferation and increase apoptosis through changes in target gene expression. High-throughput screening revealed that miR-125b, miR-181a, miR-593 and miR-1227 work synergistically with butyrate to enhance its anticancer properties. Butyrate sensitisation by these miRNAs seems to function through a range of oncogenes involved in cell growth and death pathways; however, PIK3R3 was a key target and may be a valuable therapeutic target. Integrative network and pathway analyses revealed the involvement of thousands of butyrate regulated genes in CRC cell cycle regulation and identified butyrate-sensitising miRNAs, miR-139 and miR-542. The miR-139 target, *EIF4G2* seems to be an ideal target for potential therapeutics due to its potent anti-proliferative effects in combination with butyrate. Furthermore, this study is the first to show that

## CHAPTER 6

lncRNA-targeting siRNAs can enhance the anticancer effects of butyrate in CRC cells. MALAT1 RNA interference resulted in apoptosis of CRC cells, which may be due to its predicted interactions with miR-200b, miR-200c and miR-335 and downstream effectors *FN1*, *DUSP1*, *JUN* and *PRKAA2*. In conclusion, this study has provided a basis for the future investigation of RNA-based and HDACi combinatorial treatments as potential therapeutics as well as the identification of PI3K signalling molecules as potential therapeutic targets.



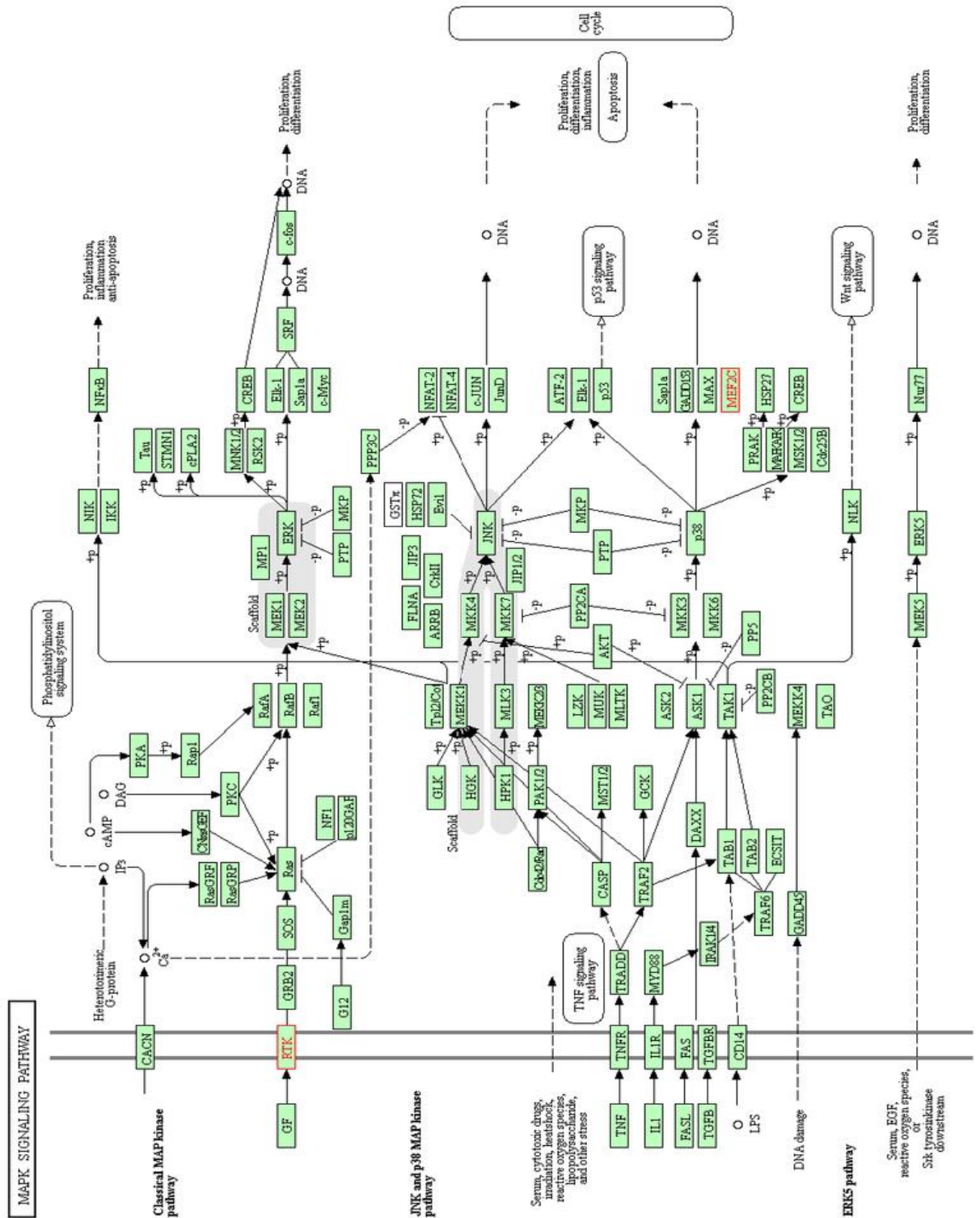


Figure A1-2 KEGG mapper canonical pathway analysis miR-125b: MAPK Signalling Pathway

MAPK Signalling Pathway was present in the top canonical pathways related to CRC for miR-125b predicted target genes. Predicted target genes are highlighted in red. Example target genes in MAPK Signalling Pathway include *IGF1R*, *MEF2C* and *PRKCA*.

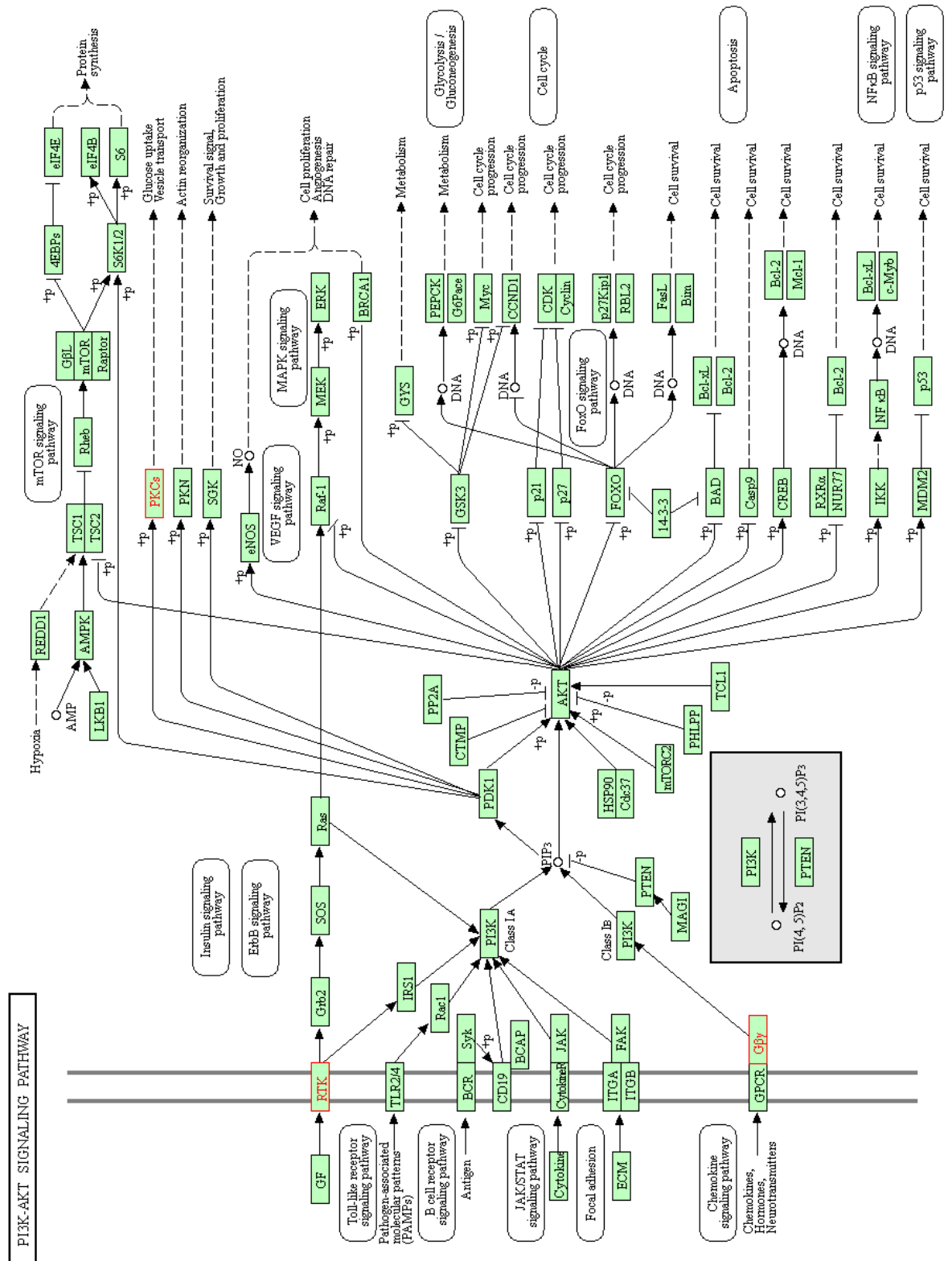


Figure A1-3 KEGG mapper canonical pathway analysis miR-125b: PI3K-AKT Signalling pathway

PI3K-AKT Signalling Pathway was present in the top canonical pathways related to CRC for miR-125b predicted target genes. Predicted target genes are highlighted in red. Example target genes in PI3K-AKT Signalling Pathway include *IGF1R*, *MEF2C* and *PRKCA*.

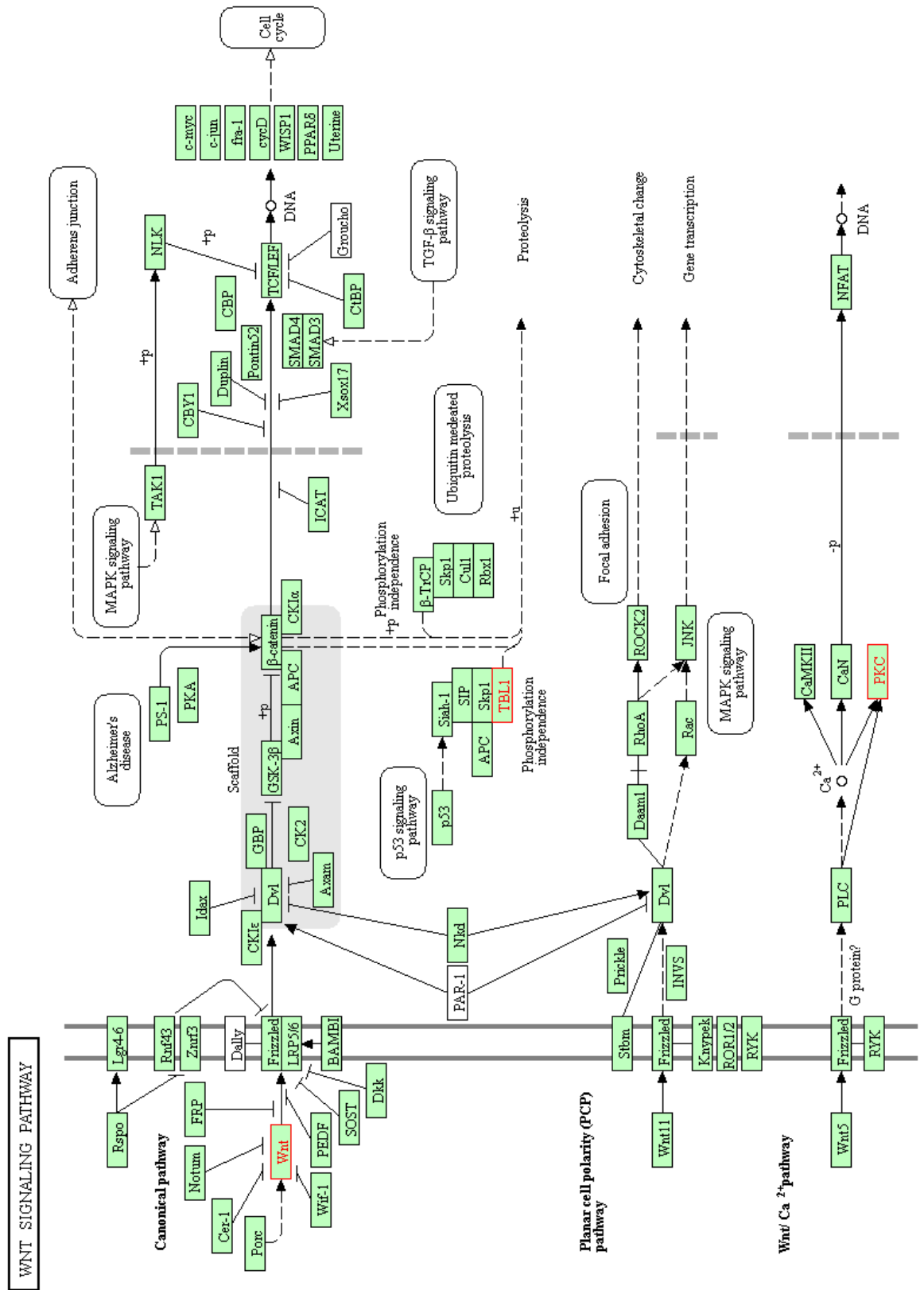
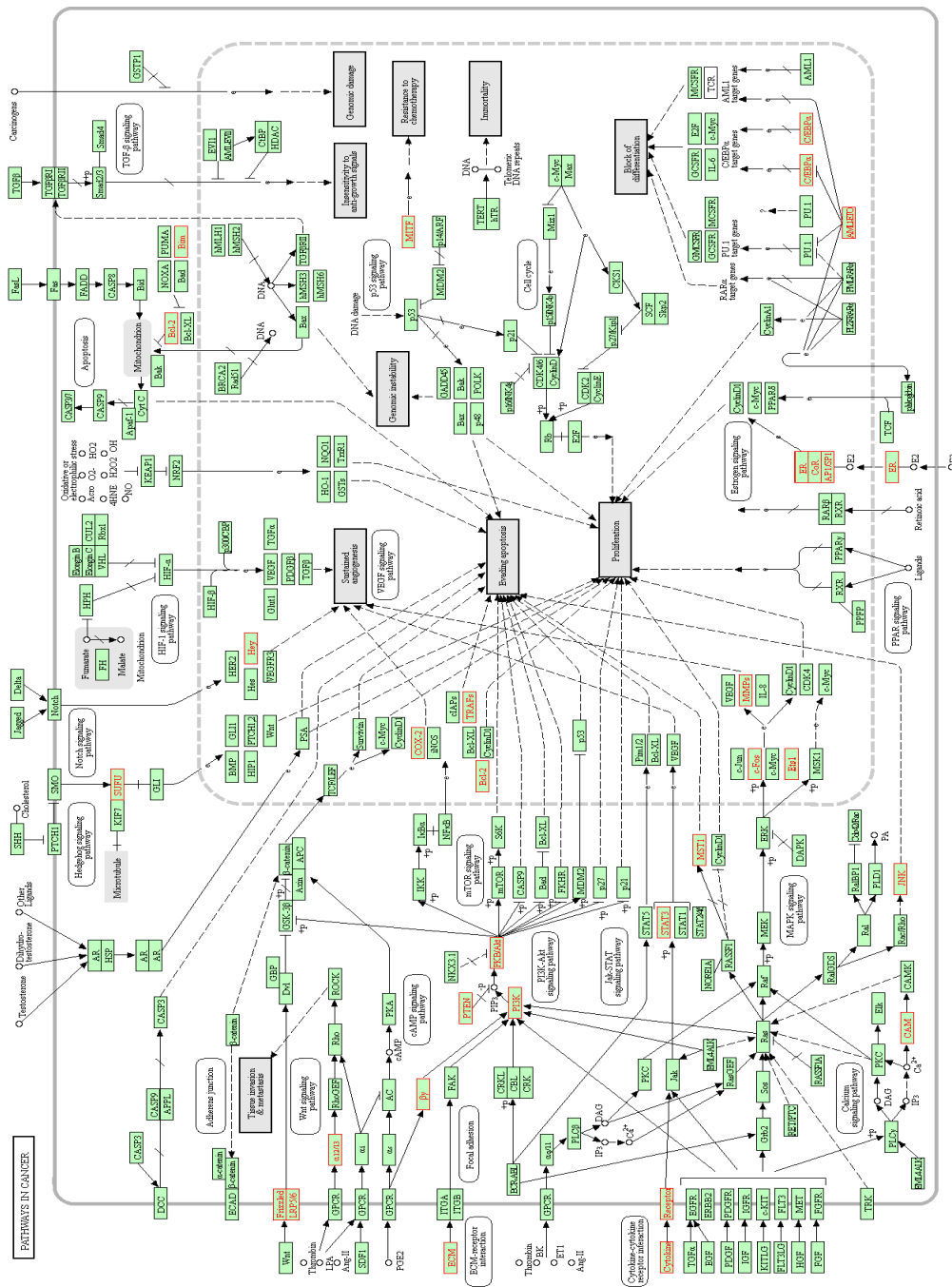


Figure A1-4 KEGG mapper canonical pathway analysis miR-125b: WNT Signalling pathway

WNT Signalling Pathway was present in the top canonical pathways related to CRC for miR-125b predicted target genes. Predicted target genes are highlighted in red. Example target genes in WNT Signalling Pathway include *PRKCA*, *TBL1X* and *WNT8B*.

# Appendix 2: Canonical pathway analysis for miR-181a predicted target gene



**Figure A2-1 KEGG mapper canonical pathway analysis miR-181a: Pathways in Cancer**

Pathways in Cancer was present in the top canonical pathways related to CRC for miR-181a predicted target genes. Predicted target genes are highlighted in red. Example target genes in Pathways in Cancer include *FZD4*, *COX2*, *PIK3R3* and *PTEN*.

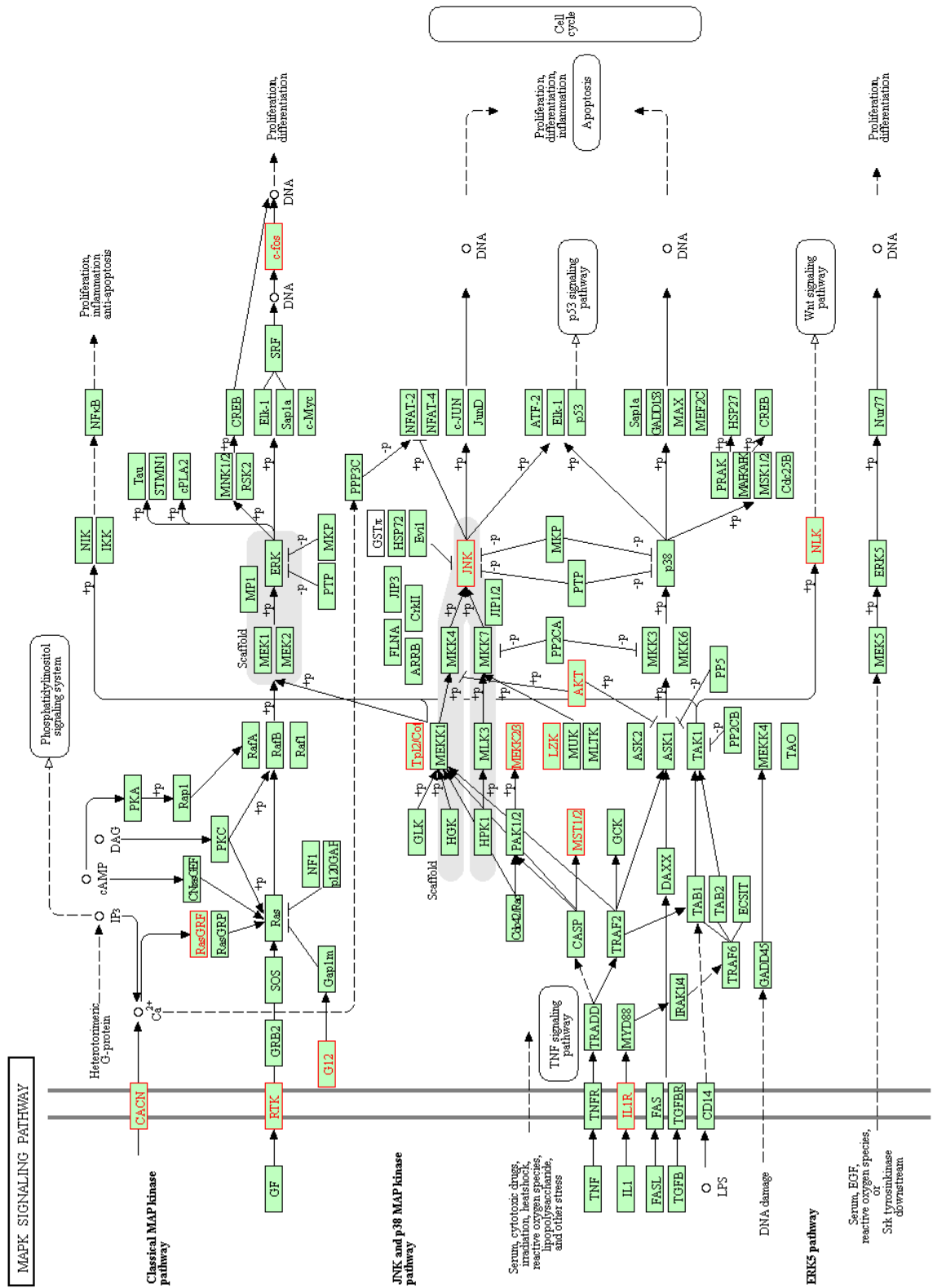


Figure A2-2 KEGG mapper canonical pathway analysis miR-181a: MAPK Signalling Pathway

MAPK Signalling Pathway was present in the top canonical pathways related to CRC for miR-181a predicted target genes. Predicted target genes are highlighted in red. Example target genes in the MAPK Signalling Pathway include *MAP3K8*, *AKT3* and *FOS*.

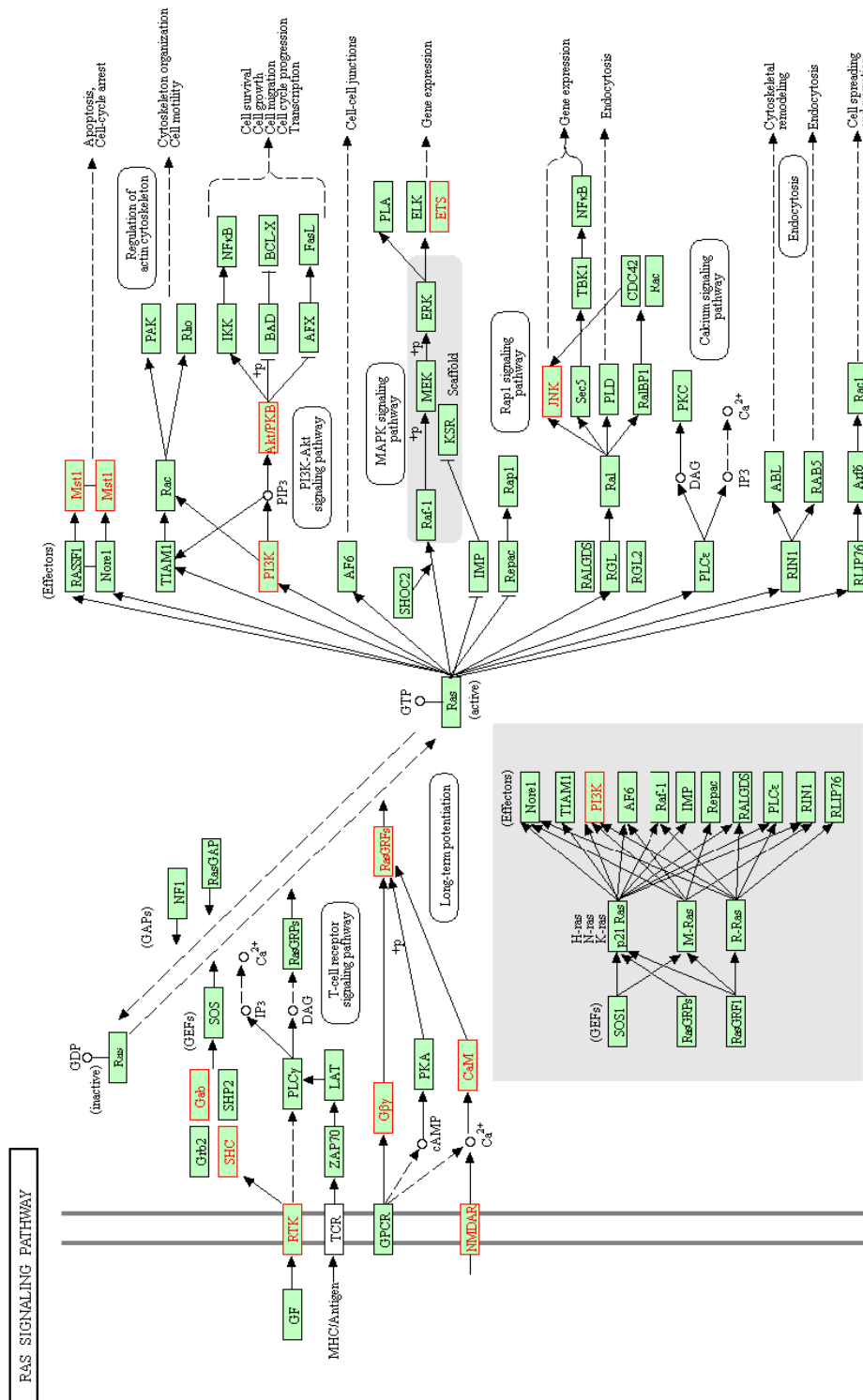


Figure A2-3 KEGG mapper canonical pathway analysis miR-181a: RAS Signalling Pathway

RAS Signalling Pathway was present in the top canonical pathways related to CRC for miR-181a predicted target genes. Predicted target genes are highlighted in red. Example target genes in the RAS Signalling Pathway include *ETS1* and *GNB4*.

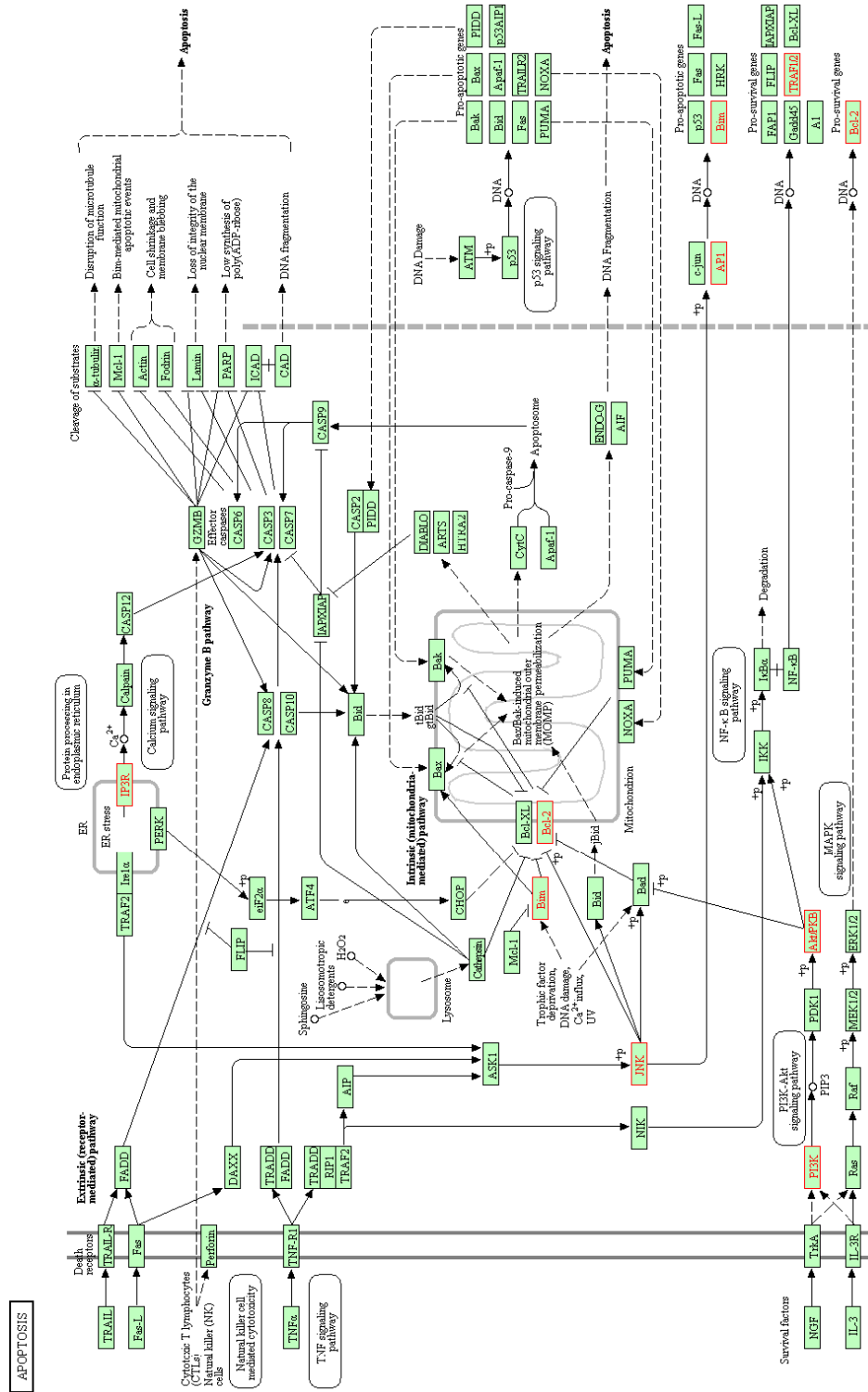
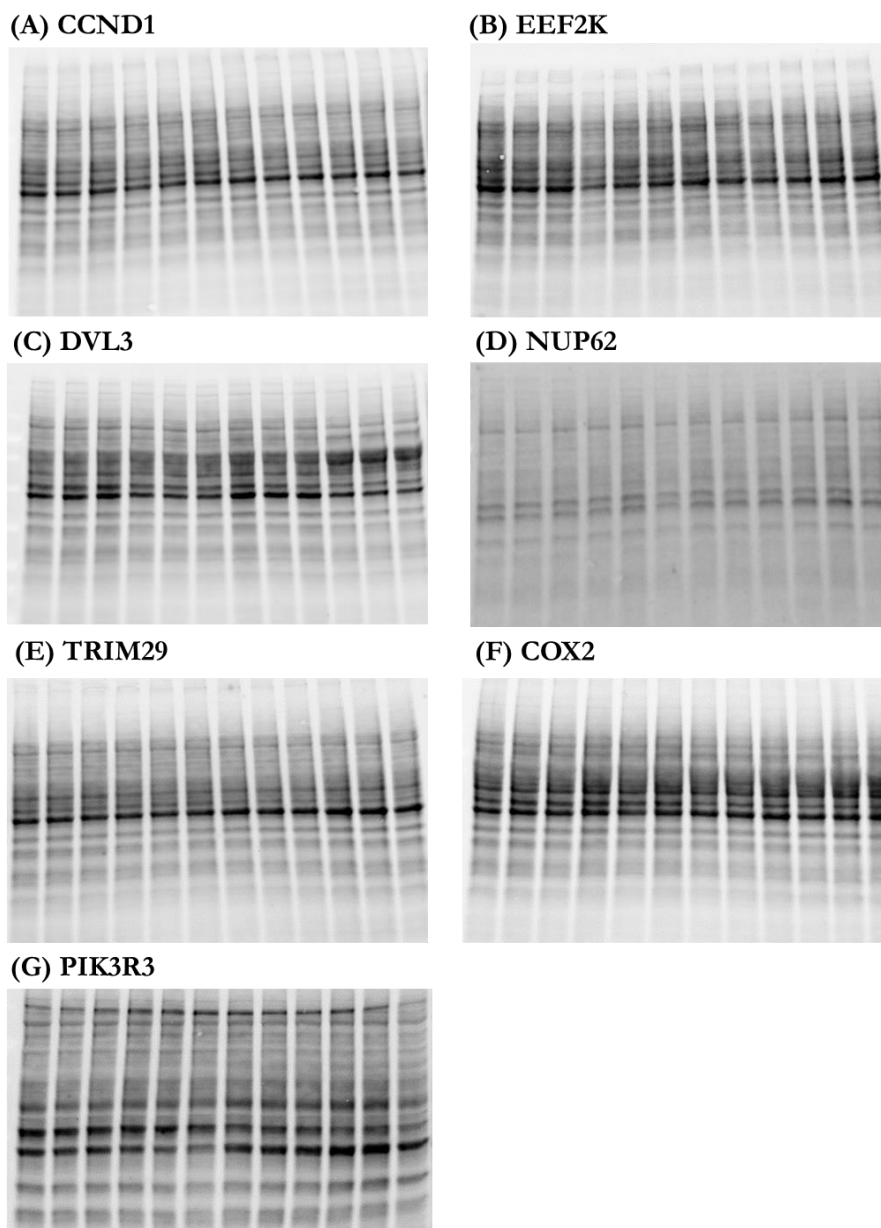


Figure A2-4 KEGG mapper canonical pathway analysis miR-181a: Apoptosis

Apoptosis was present in the top canonical pathways related to CRC for miR-181a predicted target genes. Predicted target genes are highlighted in red. Example target genes in the Apoptosis include *BCL2* and *BCL2L1*.

## Appendix 3: Protein loading images

---



**Figure A3-1 Protein loading for total protein normalisation**

Blots used to determine total protein loading for total protein normalisation for each protein investigated (A) CCND1, (B) EEF2K, (C) DVL3, (D) NUP62, (E) TRIM29, (F) COX2 and (G) PIK3R3.

# Appendix 4: Differentially expressed mRNA genes

Table A4-1 Top 100 mRNA differentially expressed genes

Gene name	Mean Counts 0 mM Butyrate	Mean Counts 2.5 mM Butyrate	log2FoldChange	Padj value
CPA4	554.5	35813	5.617672797	1.0216E-105
ADGRF1	3035	37	-6.436710729	2.2463E-104
SYT11	25	3291.5	6.54027685	1.13019E-93
CTGF	59.5	5560	6.119683629	1.05603E-89
ABCC2	9702	364	-4.891076297	3.54632E-89
TFPI	2358.5	45	-5.802296923	3.73129E-88
ARRDC4	1380	48423	4.753020888	3.73129E-88
NCAM1	51.5	5363	6.227681746	2.57255E-85
MTIX	520.5	18015	4.752337804	3.57543E-84
LIF	4910	218	-4.657957726	2.18761E-79
CEND1	30	1986	5.657539023	4.33143E-70
CRISPLD2	190.5	5871	4.57335066	5.00409E-69
HMGA2	7984	417.5	-4.420692144	1.41121E-68
EFR3B	107.5	2964.5	4.422460682	8.6293E-67
PCDH7	6865.5	405.5	-4.287535774	3.32814E-66
PDE4B	7133.5	159	-5.513649851	4.43014E-66
NR2F1	2325	117	-4.483986375	1.02667E-63
EHF	3068.5	150	-4.496823012	5.66495E-63
KCNN4	2484	144.5	-4.26745763	1.86644E-61
EMP1	1317	47	-4.929032823	2.64717E-60
ABCC3	2964.5	84	-5.236720896	1.25196E-57
TEX19	117	2856	4.289392456	5.16309E-57
PEG10	868	20750	4.212344851	7.40453E-57
AKAP12	197463.5	18117	-3.649999527	1.73086E-56
SLC4A8	144	3181	4.102200091	1.08324E-55
MKX	1675	97	-4.290069997	8.58356E-55
PAG1	124.5	2464	3.96083646	2.0377E-54
SCNN1A	1548.5	54.5	-4.893347132	2.38096E-54
EREG	25721.5	945.5	-4.865577676	6.47595E-54
LARGE	41.5	1292.5	4.56387544	8.95143E-54
THBS1	399	6635	3.738343883	7.74318E-53
CNTNAP2	34.5	1170	4.695076453	2.85806E-52
JADE2	1963	149	-3.896354936	2.23166E-51
NQO1	20038.5	1289.5	-4.076541821	2.99527E-51
ACSBG1	30	1186	4.850836886	5.73175E-51
NRXN2	26.5	984.5	4.805327688	7.86118E-51
CLU	3403.5	62477	3.855832132	9.21792E-51
S100A14	3114.5	179	-4.231238629	7.79744E-49
IQGAP3	2582.5	109.5	-4.629986779	2.21362E-48
PLAU	3053	209	-4.000141244	2.32332E-48
FMN1	51.5	1713	4.597344124	2.86049E-48
CYBRD1	1649.5	79	-4.468218136	4.41789E-48
SMIM3	2352	156	-4.034563052	2.46227E-46
ANXA3	7658	541	-3.989297837	3.81622E-46
UBE2C	2679.5	115	-4.589501993	5.40493E-46
PHOSPHO1	52	1285	4.288845329	1.07786E-45
FAM49A	48	1335	4.363915795	9.65925E-45
TENM3	108.5	1946	3.808856781	1.99602E-44
AXL	3098	264	-3.70392256	2.022E-44
ARMC4	1716.5	166.5	-3.558616827	2.68577E-44
KCNK9	46	1069.5	4.162580041	3.17355E-44
MALL	2125.5	125	-4.188017942	3.76728E-44
TRIP6	2740	203.5	-3.894704697	4.37845E-44
IFITM2	1309	60.5	-4.53611605	3.25632E-43
CCNB2	2626.5	122	-4.513376212	4.12453E-43
SLC7A11	10497.5	367	-4.948495903	7.01482E-43
HOXB6	821	52	-4.116692063	1.50518E-42
PMEPA1	38	1055.5	4.383977185	1.5587E-42
SLC38A5	1095	48.5	-4.54272487	2.41103E-42
RGMA	133.5	2226.5	3.679301385	4.45563E-42
PRKACB	10875.5	1001.5	-3.633709312	5.44901E-42
SLC38A1	18562	1665.5	-3.64348726	1.06475E-41
CYSRT1	77.5	1300.5	3.709171986	2.22987E-41

APPENDIX 4

CENPF	19208	1167.5	-4.13469453	2.94013E-41
NLRP4	47	1203.5	4.292692681	3.80785E-41
BIRC5	4966	221.5	-4.495623831	4.49138E-41
CASP4	986	78	-3.812199279	8.43082E-41
C6orf141	1497.5	99	-4.075981464	1.17594E-40
KIF20A	3871	163	-4.602084659	2.18518E-40
CKS1B	1890	179.5	-3.565666488	6.85285E-40
RGL1	178	2305	3.346524789	1.59663E-39
RNF152	57.5	1017.5	3.799858606	4.77294E-39
TNFRSF19	45.5	893.5	3.944052682	1.148E-38
HMMR	3118.5	137.5	-4.542115399	2.98608E-38
CD44	29460	3180.5	-3.36474144	1.19205E-37
BUB1B	3577	200	-4.201757755	2.12333E-37
DEPDC1	5148	326.5	-4.060882394	4.41624E-37
EMP3	1514	138	-3.602945288	6.95864E-37
PARP14	2165	289.5	-3.114562244	1.61468E-36
HMGB2	11997.5	794	-4.061388677	1.61611E-36
NUF2	1506	78	-4.345986541	2.2441E-36
AURKB	1838	81.5	-4.494201186	3.07934E-36
CNTN1	288.5	3074	3.099705683	3.21545E-36
SPAG5	3060	342.5	-3.343472393	8.43651E-36
DHRS3	1882.5	175.5	-3.590217881	1.1141E-35
RCAN2	57	920	3.648917117	2.21877E-35
MLLT3	343.5	3438	2.999397322	2.26031E-35
ARHGAP11A	3879	353	-3.606758536	2.74076E-35
HS3ST1	3723	391	-3.403404762	5.12769E-35
VGF	980	24900.5	4.354513085	9.13712E-35
ASPM	5915.5	401	-3.948423467	1.36396E-34
ATP8A1	284.5	3328.5	3.183813504	1.44035E-34
S100A4	8659	911.5	-3.37795435	1.95701E-34
KIF23	4217.5	407.5	-3.527466203	2.12986E-34
KIF18B	1264.5	72.5	-4.173873686	2.41923E-34
KIF15	1751	138.5	-3.780059806	2.58741E-34
H2AFY2	1441.5	152.5	-3.393020859	4.98672E-34
MKI67	15644	1151.5	-3.825565112	6.67691E-34
SEMA3A	1328.5	136.5	-3.439035625	8.6E-34
BHLHE40	1514	191	-3.169073906	9.58347E-34

# Appendix 5: Protein-protein interaction network interactors

**Table A5-1 Protein-protein interaction network interactions**

Ensembl ID	Gene Name	Mean Counts 0 mM butyrate	Mean Counts 2.5 mM butyrate	log2FC	Padj Value	Degree
ENSG00000141510.16	TP53	2604	642	-2.14	9.80E-11	80
ENSG00000166803.10	KIAA0101	659	56	-3.59	4.55E-17	75
ENSG00000115414.18	FN1	1016	3620.5	1.54	1.91E-10	75
ENSG00000055130.15	CUL1	3376	1204	-1.70	2.36E-11	53
ENSG0000012048.20	BRCA1	3044.5	392	-3.04	4.01E-21	49
ENSG00000276966.2	HIST1H4E	8883	1824.5	-2.44	7.73E-15	44
ENSG00000170312.15	CDK1	5356	272.5	-4.27	2.86E-31	42
ENSG00000177606.6	JUN	734	5158	2.53	3.61E-21	38
ENSG00000188486.3	H2AFX	3024.5	1032	-1.66	5.03E-06	38
ENSG00000132383.11	RPA1	6478	2502	-1.53	1.52E-06	34
ENSG00000197122.11	SRC	905.5	326	-1.72	5.54E-11	34
ENSG00000166851.14	PLK1	1844.5	163	-3.61	1.81E-24	33
ENSG00000278828.1	HIST1H3H	11465.5	1073	-2.97	1.35E-04	30
ENSG00000109320.11	NFKB1	1682	344	-2.47	1.15E-17	27
ENSG00000156508.17	EEF1A1	221514.5	68818.5	-1.89	2.37E-14	27
ENSG00000170345.9	FOS	561.5	3884.5	2.44	9.52E-17	26
ENSG00000094916.13	CBX5	7973.5	2079	-2.19	1.72E-19	26
ENSG00000164754.12	RAD21	13039.5	4663.5	-1.70	3.72E-10	25
ENSG00000178999.12	AURKB	1838	81.5	-4.49	3.08E-36	25
ENSG00000101412.12	E2F1	962.5	196	-2.34	1.03E-09	25
ENSG00000143321.18	HDGF	7630	930	-3.19	2.29E-30	25
ENSG00000162521.18	RBBP4	7359.5	2914	-1.55	5.05E-10	24
ENSG00000134057.14	CCNB1	6582.5	567	-3.58	4.76E-23	23
ENSG00000112118.17	MCM3	10569.5	2390	-2.32	2.98E-18	23
ENSG00000145386.9	CCNA2	3469	283.5	-3.73	6.32E-32	22
ENSG00000115163.14	CENPA	721	48	-3.94	3.60E-25	22
ENSG00000073111.13	MCM2	7809.5	1458	-2.54	3.16E-16	22
ENSG00000076003.4	MCM6	5302	1894.5	-1.63	1.48E-07	22
ENSG00000166508.17	MCM7	14614	1857	-3.13	6.20E-29	21
ENSG00000117399.13	CDC20	3763	502.5	-3.00	1.12E-19	21
ENSG00000087586.17	AURKA	2229	263	-3.17	3.24E-20	20
ENSG00000196230.12	TUBB	20689	7402	-1.69	7.98E-12	20
ENSG00000170004.16	CHD3	3779.5	971.5	-2.20	9.37E-20	19
ENSG00000122565.18	CBX3	10151.5	3893.5	-1.59	1.28E-08	19
ENSG00000147889.16	CDKN2A	721.5	177	-2.21	3.37E-14	19
ENSG00000147010.17	SH3KBP1	3200	879	-2.07	1.08E-15	19
ENSG00000167670.15	CHAF1A	2203	499.5	-2.22	1.55E-10	19
ENSG00000203852.3	HIST2H3A	20916.5	887	-3.64	1.46E-05	19
ENSG00000156970.12	BUB1B	3577	200	-4.20	2.12E-37	19
ENSG00000119335.16	SET	18529.5	6910.5	-1.64	1.55E-10	18
ENSG00000146834.13	MEPCE	1890.5	662.5	-1.72	2.64E-10	18
ENSG00000078900.14	TP73	398	99.5	-2.08	9.73E-08	17
ENSG00000167900.11	TK1	8249.5	1538	-2.11	0.0093779	17
ENSG00000197299.10	BLM	1799	336	-2.54	5.94E-16	17
ENSG00000114346.13	ECT2	6163	1456	-2.27	1.27E-14	17
ENSG00000116663.10	FBXO6	537.5	222	-1.51	1.37E-07	17
ENSG00000105974.11	CAV1	8805.5	1414	-2.81	4.30E-24	16
ENSG00000149554.12	CHEK1	2055.5	284.5	-2.97	7.06E-23	16
ENSG00000134954.14	ETS1	271.5	1660	2.28	6.01E-16	16
ENSG00000094804.9	CDC6	3744.5	991.5	-2.03	4.33E-10	16
ENSG00000080986.12	NDC80	2019	112.5	-4.17	7.05E-29	16
ENSG00000184678.9	HIST2H2BE	11594	1557	-3.03	1.56E-19	16
ENSG00000100906.10	NFKBIA	1484	346.5	-2.31	5.37E-17	15
ENSG00000144381.16	HSPD1	33356	11661.5	-1.72	1.20E-10	15
ENSG00000139618.14	BRCA2	1987.5	392.5	-2.50	4.49E-19	15
ENSG00000048052.21	HDAC9	152	683	1.84	3.47E-10	15
ENSG00000067182.7	TNFRSF1A	2189	434	-2.47	1.29E-15	15
ENSG00000104738.16	MCM4	10827	2150.5	-2.47	3.57E-18	15
ENSG00000180198.15	RCC1	4708	1457.5	-1.89	1.72E-12	14
ENSG00000169679.14	BUB1	4162.5	456.5	-3.26	2.21E-21	14

## APPENDIX 5

ENSG0000088305.18	DNMT3B	1219.5	390	-1.82	7.24E-09	14
ENSG0000100297.15	MCM5	6441.5	799.5	-3.10	1.61E-21	14
ENSG0000167552.13	TUBA1A	3211	12072	1.63	2.29E-10	14
ENSG0000120885.19	CLU	3403.5	62477	3.86	9.22E-51	14
ENSG0000070756.13	PABPC1	28057.5	9188.5	-1.78	1.75E-10	14
ENSG0000135446.16	CDK4	3574	991.5	-2.04	7.90E-14	14
ENSG0000167513.8	CDT1	2180	398	-2.52	5.60E-12	14
ENSG0000141736.13	ERBB2	3137.5	938	-1.95	2.07E-14	14
ENSG0000122952.16	ZWINT	2350	455	-2.49	4.29E-16	14
ENSG0000221869.4	CEBPD	141	39	-1.98	3.01E-06	14
ENSG0000102804.14	TSC22D1	17526.5	4994.5	-2.03	5.97E-18	13
ENSG0000090447.11	TFAP4	822.5	221.5	-2.08	3.44E-13	13
ENSG0000136824.18	SMC2	2212.5	534	-2.25	2.83E-16	13
ENSG0000093009.9	CDC45	1086.5	150	-2.98	3.73E-22	13
ENSG0000145335.15	SNCA	58.5	260.5	1.79	1.25E-06	13
ENSG0000156711.16	MAPK13	1660.5	247.5	-2.93	4.17E-26	13
ENSG0000087077.11	TRIP6	2740	203.5	-3.89	4.38E-44	13
ENSG0000051180.16	RAD51	561	82	-2.88	3.57E-18	12
ENSG0000080503.20	SMARCA2	600.5	2592.5	1.81	2.96E-13	12
ENSG0000064012.21	CASP8	1561.5	532	-1.78	2.16E-12	12
ENSG0000026508.16	CD44	29460	3180.5	-3.36	1.19E-37	12
ENSG0000085840.12	ORC1	1273.5	236.5	-2.55	3.25E-16	12
ENSG0000128272.14	ATF4	21724	7571	-1.74	3.05E-09	12
ENSG0000175197.10	DDIT3	2255	675	-1.95	7.41E-09	12
ENSG0000132341.11	RAN	18086	7321	-1.51	3.86E-08	12
ENSG0000184260.5	HIST2H2AC	2236.5	372	-2.27	0.0050666	12
ENSG0000189403.14	HMGB1	12347	2708.5	-2.38	1.90E-15	11
ENSG0000144554.10	FANCD2	3204.5	212.5	-3.96	2.85E-33	11
ENSG0000113368.11	LMNB1	4716	865.5	-2.59	9.35E-18	11
ENSG0000166228.8	PCBD1	2118.5	322.5	-2.89	3.45E-28	11
ENSG0000184216.11	IRAK1	2605	553	-2.42	2.48E-19	11
ENSG0000114942.13	EEF1B2	10471.5	2539.5	-2.23	1.99E-18	11
ENSG0000164104.11	HMGB2	11997.5	794	-4.06	1.62E-36	11
ENSG0000143228.12	NUF2	1506	78	-4.35	2.24E-36	11
ENSG0000123358.19	NR4A1	255.5	2000	2.62	1.82E-22	10
ENSG0000105323.16	HNRNPUL1	3794.5	1454.5	-1.59	5.15E-10	10
ENSG0000149257.13	SERPINH1	3617.5	673	-2.61	1.66E-22	10
ENSG0000026103.19	FAS	572.5	201.5	-1.70	6.34E-09	10
ENSG0000187109.13	NAP1L1	15190.5	3629	-2.26	1.67E-19	10
ENSG0000121152.9	NCAPH	2020	163.5	-3.68	3.22E-27	10
ENSG0000131747.14	TOP2A	11712	829.5	-3.86	2.86E-30	10
ENSG0000036672.15	USP2	106	538	2.07	9.87E-10	10
ENSG0000196305.17	IARS	28607	11377	-1.55	2.26E-08	10
ENSG0000089685.14	BIRC5	4966	221.5	-4.50	4.49E-41	10
ENSG0000091651.8	ORC6	883.5	147.5	-2.66	1.07E-14	10
ENSG000006634.7	DBF4	1557.5	483.5	-1.88	3.00E-10	10
ENSG0000168496.3	FEN1	4351	854	-2.46	3.17E-15	10
ENSG0000175592.8	FOSL1	458	140.5	-1.91	2.95E-10	10
ENSG0000101966.12	XIAP	2717	979.5	-1.72	7.24E-12	10
ENSG0000138778.11	CENPE	3734	484.5	-3.09	3.08E-22	10
ENSG0000111716.12	LDHB	38024	14041	-1.64	5.89E-09	10
ENSG0000109339.18	MAPK10	30	145.5	1.90	1.33E-05	9
ENSG0000100823.11	APEX1	5388	1769	-1.76	9.34E-09	9
ENSG0000141905.17	NFIC	742	156.5	-2.37	7.89E-12	9
ENSG0000166888.10	STAT6	2149.5	543.5	-2.22	6.78E-20	9
ENSG0000101868.10	POLA1	2881	1201	-1.51	1.92E-09	9
ENSG0000175334.7	BANF1	2289.5	732	-1.82	7.81E-09	9
ENSG0000148773.12	MKI67	15644	1151.5	-3.83	6.68E-34	9
ENSG0000065328.16	MCM10	2266	351.5	-2.72	3.05E-13	9
ENSG0000198873.11	GRK5	205.5	885.5	1.72	1.15E-05	9
ENSG0000175899.14	A2M	52.5	265.5	1.95	2.11E-07	9
ENSG0000187741.14	FANCA	2452	774.5	-1.91	2.84E-15	9
ENSG0000221829.9	FANCG	1664	364.5	-2.36	1.07E-16	9
ENSG0000161800.12	RACGAP1	4877	700	-2.94	4.23E-22	9
ENSG0000105011.8	ASF1B	2063	297	-2.86	3.89E-17	9
ENSG0000132170.19	PPARG	1039.5	229.5	-2.38	8.17E-19	9
ENSG0000117592.8	PRDX6	8707.5	3294.5	-1.61	2.55E-10	9
ENSG0000183684.7	ALYREF	4556.5	1385.5	-1.90	6.17E-11	9
ENSG0000172936.12	MYD88	538.5	204.5	-1.53	2.55E-05	9
ENSG0000173207.12	CKS1B	1890	179.5	-3.57	6.85E-40	9
ENSG0000120802.13	TMPO	11616.5	2998.5	-2.18	6.26E-15	9
ENSG0000100749.7	VRK1	2080	807.5	-1.55	2.02E-08	8

APPENDIX 5

ENSG00000134690.10	CDCA8	1543.5	178	-3.15	1.26E-16	8
ENSG00000164045.11	CDC25A	966	202	-2.32	4.77E-10	8
ENSG00000100784.9	RPS6KA5	2391	606	-2.23	2.17E-19	8
ENSG00000198901.13	PRC1	6690.5	729.5	-3.32	4.68E-28	8
ENSG00000160949.16	TONSL	2197	618	-1.98	2.50E-11	8
ENSG00000109805.9	NCAPG	5777.5	372	-3.99	1.27E-30	8
ENSG00000197442.9	MAP3K5	2264.5	924.5	-1.51	1.63E-08	8
ENSG00000164109.13	MAD2L1	3592	259	-3.83	5.60E-28	8
ENSG00000079999.13	KEAP1	3149.5	944.5	-1.94	8.00E-14	8
ENSG00000128050.8	PAICS	11704.5	3534.5	-1.93	1.86E-13	7
ENSG00000162772.16	ATF3	902.5	3912	1.76	2.90E-06	7
ENSG00000164611.12	PTTG1	2046.5	507	-2.18	5.19E-12	7
ENSG00000015475.18	BID	1400.5	278.5	-2.47	1.09E-16	7
ENSG00000165672.6	PRDX3	10724	4337.5	-1.53	2.77E-08	7
ENSG00000263001.5	GTF2I	3048.5	1058.5	-1.74	1.74E-12	7
ENSG00000077312.8	SNRPA	2687.5	703	-2.12	7.17E-13	7
ENSG00000101773.16	RBBP8	4427	1565	-1.72	1.55E-11	7
ENSG00000163781.12	TOPBP1	4081	1325.5	-1.83	4.53E-13	7
ENSG00000088325.15	TPX2	6846.5	832.5	-3.13	1.07E-21	7
ENSG00000089157.15	RPLP0	45039.5	13826.5	-1.89	2.05E-12	7
ENSG00000070950.9	RAD18	1274	297	-2.26	9.74E-15	7
ENSG00000106976.19	DNM1	269	1199	1.81	5.75E-09	7
ENSG00000153044.9	CENPH	577	109.5	-2.57	1.02E-15	7
ENSG00000161888.11	SPC24	1202	110	-3.49	3.82E-23	7
ENSG00000122861.15	PLAU	3053	209	-4.00	2.32E-48	7
ENSG00000071539.13	TRIP13	1348	320	-2.26	6.82E-17	7
ENSG00000123416.15	TUBA1B	9699.5	2675.5	-2.06	3.21E-16	7
ENSG00000113810.15	SMC4	5895	883	-2.85	4.05E-18	7
ENSG00000175063.16	UBE2C	2679.5	115	-4.59	5.40E-46	7
ENSG00000010292.12	NCAPD2	10913	3115.5	-2.00	1.07E-11	7
ENSG00000166451.13	CENPN	1654	328	-2.48	3.21E-16	7
ENSG00000092010.14	PSME1	5221.5	1848	-1.71	6.81E-12	6
ENSG00000101255.10	TRIB3	6886.5	772	-3.28	9.95E-19	6
ENSG00000171206.13	TRIM8	1367	324	-2.19	4.35E-11	6
ENSG00000113643.8	RARS	5386	18818.5	1.52	1.07E-10	6
ENSG00000168918.13	INPP5D	105.5	26	-2.08	2.01E-05	6
ENSG00000083720.12	OXCT1	2213.5	845	-1.61	7.95E-09	6
ENSG00000149636.15	DSN1	1241.5	398	-1.82	2.00E-10	6
ENSG00000129810.14	SGOL1	452.5	45	-3.42	1.89E-21	6
ENSG00000092621.11	PHGDH	7014.5	1480	-2.38	2.16E-11	6
ENSG00000064300.8	NGFR	479	4356	2.89	2.31E-19	6
ENSG00000187790.10	FANCM	1004.5	376.5	-1.58	1.50E-07	6
ENSG00000136938.8	ANP32B	1692.5	285	-2.62	2.48E-11	6
ENSG00000158402.18	CDC25C	753.5	49	-3.97	5.20E-25	6
ENSG00000188827.10	SLX4	447	1656	1.58	7.22E-09	6
ENSG00000118515.11	SGK1	198.5	1417	2.56	5.45E-19	6
ENSG00000166349.9	RAG1	49.5	182	1.54	8.24E-05	6
ENSG00000147403.16	RPL10	19054.5	5819	-1.88	5.52E-12	6
ENSG00000008735.13	MAPK8IP2	178	718	1.74	4.01E-09	6
ENSG00000070669.16	ASNS	14650.5	4983.5	-1.77	1.68E-06	6
ENSG00000090861.15	AARS	17377	5953.5	-1.75	1.85E-09	6
ENSG00000012822.15	CALCOCO1	1436	8447	2.16	3.17E-13	6
ENSG00000185345.18	PARK2	41.5	159.5	1.60	1.29E-04	6
ENSG00000065361.14	ERBB3	2065.5	503.5	-2.27	1.19E-20	6
ENSG00000105976.14	MET	28482	5280.5	-2.63	8.42E-29	6
ENSG00000119383.19	PPP2R4	6285.5	1637.5	-2.13	1.05E-16	6
ENSG00000108821.13	COL1A1	398.5	1625	1.67	4.33E-09	6
ENSG00000002834.17	LASP1	5825	2095.5	-1.66	4.92E-09	6
ENSG00000137812.19	CASC5	4755	472	-3.45	1.05E-28	6
ENSG00000137807.13	KIF23	4217.5	407.5	-3.53	2.13E-34	6
ENSG00000112242.14	E2F3	1508	570.5	-1.60	2.80E-09	6
ENSG00000123609.10	NMI	176.5	35.5	-2.44	4.34E-10	6
ENSG00000166165.12	CKB	8372.5	29490.5	1.57	1.19E-06	6
ENSG00000187837.3	HIST1H1C	33326.5	6637.5	-2.50	4.82E-15	6
ENSG00000123219.12	CENPK	561.5	112.5	-2.52	4.02E-18	6
ENSG00000109685.17	WHSC1	8465.5	2165.5	-2.15	4.70E-15	6
ENSG00000124795.14	DEK	6983.5	1972	-2.05	2.44E-15	6
ENSG00000136813.14	KIAA0368	6199	1884	-1.94	8.85E-16	6
ENSG00000136231.13	IGF2BP3	5423.5	1044.5	-2.52	1.12E-16	6
ENSG00000164032.11	H2AFZ	14618.5	3855.5	-2.12	8.67E-13	6
ENSG00000100162.14	CENPM	623	83.5	-3.04	1.27E-22	6
ENSG00000142731.10	PLK4	1839	247.5	-3.04	2.18E-24	5

## APPENDIX 5

ENSG00000146674.14	IGFBP3	116.5	1022	2.84	1.89E-23	5
ENSG00000003402.19	CFLAR	1474.5	243.5	-2.81	7.53E-29	5
ENSG00000196154.11	S100A4	8659	911.5	-3.38	1.96E-34	5
ENSG00000120129.5	DUSP1	333	1476.5	1.85	1.63E-11	5
ENSG00000178568.13	ERBB4	28	407.5	3.44	3.38E-22	5
ENSG00000107262.17	BAG1	1509	518	-1.75	4.08E-11	5
ENSG00000140525.17	FANCI	4706.5	475	-3.42	5.42E-32	5
ENSG00000168298.6	HIST1H1E	31041	5722	-2.59	4.18E-16	5
ENSG00000101945.16	SUV39H1	381	59.5	-2.78	3.47E-14	5
ENSG00000102317.17	RBM3	9044.5	2969.5	-1.81	6.47E-10	5
ENSG00000136492.8	BRIP1	2177.5	338	-2.84	1.77E-24	5
ENSG00000142856.16	ITGB3BP	1171	332	-2.03	7.00E-13	5
ENSG00000112029.9	FBXO5	1704.5	324	-2.54	7.15E-18	5
ENSG00000092853.13	CLSPN	1553	496	-1.76	2.54E-07	5
ENSG00000138834.12	MAPK8IP3	2143	7704	1.51	3.95E-08	5
ENSG00000170142.11	UBE2E1	2253	570	-2.19	3.85E-16	5
ENSG00000152253.8	SPC25	523	43.5	-2.99	2.18E-04	5
ENSG00000179051.13	RCC2	4911.5	1783.5	-1.67	3.37E-08	5
ENSG00000123268.8	ATF1	1201	444.5	-1.67	5.04E-10	5
ENSG00000136026.13	CKAP4	2886	877.5	-1.91	2.90E-13	5
ENSG00000196954.12	CASP4	986	78	-3.81	8.43E-41	5
ENSG00000132182.11	NUP210	5949	1110	-2.64	4.47E-29	5
ENSG00000166295.8	ANAPC16	2876	953	-1.81	7.79E-13	5
ENSG00000108679.12	LGALS3BP	11473	3543	-1.87	4.07E-12	5
ENSG00000143878.9	RHOB	2922.5	21041.5	2.55	2.66E-23	5
ENSG00000137497.17	NUMA1	6060.5	2065	-1.76	4.02E-11	5
ENSG00000100219.16	XBP1	3603.5	1291.5	-1.69	1.95E-09	5
ENSG00000120690.14	ELF1	807	3396	1.78	1.12E-12	5
ENSG00000137693.13	YAP1	4761	1290.5	-2.09	4.50E-17	5
ENSG00000164404.8	GDF9	33	163	1.93	2.60E-05	4
ENSG00000185813.10	PCYT2	1602	6482	1.73	3.14E-13	4
ENSG00000160783.19	PMF1	520.5	82.5	-2.79	6.09E-18	4
ENSG00000143476.17	DTL	2243	357	-2.71	6.35E-15	4
ENSG00000145391.13	SETD7	6989	2130	-1.89	4.13E-12	4
ENSG00000112742.9	TTK	3149.5	320.5	-3.38	1.34E-23	4
ENSG00000067066.16	SP100	1625	629	-1.60	7.27E-10	4
ENSG00000175745.11	NR2F1	2325	117	-4.48	1.03E-63	4
ENSG00000196890.4	HIST3H2BB	3325.5	1261	-1.55	4.70E-05	4
ENSG00000162909.17	CAPN2	12712	4183	-1.84	5.10E-15	4
ENSG00000171346.13	KRT15	539	3542	2.38	4.64E-21	4
ENSG00000011422.11	PLAUR	1826	371	-2.53	1.07E-24	4
ENSG00000126803.9	HSPA2	76.5	1110	3.42	3.32E-19	4
ENSG00000168003.16	SLC3A2	14858.5	4977	-1.77	1.89E-07	4
ENSG00000117724.12	CENPF	19208	1167.5	-4.13	2.94E-41	4
ENSG00000111206.12	FOXO1	1117.5	98.5	-3.63	2.69E-33	4
ENSG00000166483.10	WEE1	2019.5	383	-2.54	3.59E-18	4
ENSG00000127564.16	PKMYT1	730.5	161.5	-2.30	8.95E-12	4
ENSG00000063046.17	EIF4B	34596.5	12715	-1.66	5.50E-11	4
ENSG00000031691.6	CENPQ	569.5	140	-2.16	2.26E-10	4
ENSG00000181938.13	GINS3	616	249	-1.51	1.96E-07	4
ENSG00000099901.16	RANBP1	3680	1043	-1.99	7.05E-12	4
ENSG00000142541.16	RPL13A	32443	11439.5	-1.69	1.75E-10	4
ENSG00000145012.12	LPP	5484	2059.5	-1.65	3.51E-09	4
ENSG00000014138.8	POLA2	864	334	-1.58	1.23E-08	4
ENSG00000106089.11	STX1A	621	2362	1.57	4.41E-08	4
ENSG00000168906.12	MAT2A	14875.5	5879.5	-1.58	2.63E-11	4
ENSG00000172819.16	RARG	1521.5	353	-2.27	1.73E-15	4
ENSG00000198554.11	WDHD1	2867	1054	-1.68	5.64E-12	4
ENSG00000196975.15	ANXA4	2398.5	714	-1.94	3.82E-13	4
ENSG00000154839.9	SKA1	1229.5	122.5	-3.37	9.28E-19	4
ENSG00000082781.11	ITGB5	3960.5	887	-2.34	1.79E-19	4
ENSG00000141756.18	FKBP10	3012.5	581	-2.61	2.25E-26	4
ENSG00000117650.12	NEK2	1853	113.5	-4.05	1.84E-26	4
ENSG00000117632.20	STMN1	13673.5	2821	-2.46	1.07E-17	4
ENSG00000163435.15	ELF3	2017	728.5	-1.68	5.35E-10	4
ENSG00000085563.14	ABCB1	178.5	2226	3.28	3.19E-24	4
ENSG00000132589.15	FLOT2	2306	777	-1.76	1.21E-10	4
ENSG00000130520.10	LSM4	6377.5	2314.5	-1.65	2.00E-09	4
ENSG00000133119.12	RFC3	1612	292.5	-2.58	4.47E-16	4
ENSG00000213551.4	DNAJC9	1332.5	399	-1.96	4.13E-14	4
ENSG00000132570.14	PCBD2	542	120	-2.41	3.68E-16	4
ENSG00000111602.11	TIMELESS	3963	845	-2.39	6.60E-17	4

APPENDIX 5

ENSG00000187098.14	MITF	60	517	2.74	2.66E-16	4
ENSG00000125730.16	C3	86.5	340	1.66	2.88E-07	4
ENSG00000142945.12	KIF2C	4551	223.5	-4.34	9.87E-33	4
ENSG00000104689.9	TNFRSF10A	1668	575	-1.76	5.70E-12	4
ENSG00000101057.15	MYBL2	1558	195.5	-3.05	5.29E-18	4
ENSG00000130429.12	ARPC1B	5217.5	1839.5	-1.68	5.19E-09	4
ENSG00000077348.8	EXOSC5	1102	359	-1.79	1.82E-09	4
ENSG00000185507.19	IRF7	404.5	2237.5	2.13	1.63E-16	4
ENSG00000172340.14	SUCLG2	1945.5	575	-1.95	2.78E-11	4
ENSG00000069399.12	BCL3	194.5	49.5	-2.11	5.09E-08	4
ENSG00000156802.12	ATAD2	11098.5	2100.5	-2.54	2.57E-18	4
ENSG00000137801.10	THBS1	399	6635	3.74	7.74E-53	4
ENSG00000125148.6	MT2A	4874.5	44753	2.91	9.45E-30	4
ENSG00000175832.12	ETV4	1339.5	475	-1.72	4.53E-11	4
ENSG00000028277.20	POU2F2	25.5	171.5	2.35	1.38E-08	4
ENSG00000134107.4	BHLHE40	1514	191	-3.17	9.58E-34	3
ENSG00000105048.16	TNNT1	4469	1355	-1.92	3.08E-13	3
ENSG00000168078.9	PBK	2813	114.5	-4.57	5.79E-33	3
ENSG00000066279.16	ASPM	5915.5	401	-3.95	1.36E-34	3
ENSG00000187554.11	TLR5	60	405.5	2.38	8.87E-13	3
ENSG00000181019.12	NQO1	20038.5	1289.5	-4.08	3.00E-51	3
ENSG00000171848.13	RRM2	8602.5	876.5	-2.92	5.96E-05	3
ENSG00000198833.6	UBE2J1	1926	666	-1.75	1.34E-11	3
ENSG00000228716.6	DHFR	2609	430.5	-2.74	3.59E-21	3
ENSG00000156136.9	DCK	1030.5	416.5	-1.50	1.16E-07	3
ENSG00000137871.19	ZNF280D	2239	859.5	-1.62	3.95E-11	3
ENSG00000142449.12	FBN3	334	57	-2.72	1.17E-16	3
ENSG00000171843.15	MLLT3	343.5	3438	3.00	2.26E-35	3
ENSG00000140044.12	JDP2	574	205.5	-1.69	4.41E-09	3
ENSG00000136861.17	CDK5RAP2	3287.5	1313.5	-1.57	6.14E-10	3
ENSG00000142303.13	ADAMTS10	318	95.5	-1.92	1.49E-07	3
ENSG00000077942.18	FBLN1	425	129	-1.87	1.11E-06	3
ENSG00000134222.16	PSRC1	1111.5	397.5	-1.69	2.92E-07	3
ENSG00000136122.15	BORA	960	258	-2.11	1.73E-11	3
ENSG00000157456.7	CCNB2	2626.5	122	-4.51	4.12E-43	3
ENSG00000204305.13	AGER	184.5	70.5	-1.61	1.69E-05	3
ENSG00000175084.11	DES	152	1079	2.54	1.90E-17	3
ENSG00000167460.14	TPM4	7587	1515.5	-2.52	3.21E-25	3
ENSG00000121653.11	MAPK8IP1	256.5	1915	2.62	3.38E-22	3
ENSG00000108557.17	RAI1	1154	384	-1.77	1.61E-09	3
ENSG00000111319.12	SCNN1A	1548.5	54.5	-4.89	2.38E-54	3
ENSG00000118640.10	VAMP8	923.5	210.5	-2.25	3.28E-11	3
ENSG00000145920.14	CPLX2	26	115.5	1.69	0.0012155	3
ENSG00000163840.9	DTX3L	1255	206	-2.81	2.87E-26	3
ENSG00000109814.11	UGDH	3094	1123	-1.67	7.42E-10	3
ENSG00000167601.11	AXL	3098	264	-3.70	2.02E-44	3
ENSG00000078018.19	MAP2	414	3312.5	2.67	2.69E-23	3
ENSG00000104267.9	CA2	556.5	2959.5	2.12	3.26E-18	3
ENSG00000084764.10	MAPRE3	359	1654	1.85	5.72E-11	3
ENSG00000093010.11	COMT	2000	632.5	-1.84	3.13E-10	3
ENSG00000118523.5	CTGF	59.5	5560	6.12	1.06E-89	3
ENSG00000119139.16	TJP2	1437.5	319	-2.38	3.33E-19	3
ENSG00000105649.9	RAB3A	74.5	344.5	1.90	1.90E-06	3
ENSG00000129354.11	AP1M2	2436.5	448.5	-2.61	1.84E-22	3
ENSG00000141738.13	GRB7	1137.5	253.5	-2.36	4.76E-18	3
ENSG00000100505.13	TRIM9	177.5	1839.5	3.04	2.33E-29	3
ENSG00000065150.18	IPO5	15115.5	5120.5	-1.77	4.24E-12	3
ENSG00000142875.19	PRKACB	10875.5	1001.5	-3.63	5.45E-42	3
ENSG00000114019.14	AMOTL2	1484	5255.5	1.54	2.09E-06	3
ENSG00000188643.10	S100A16	3668.5	511.5	-3.01	1.37E-29	3
ENSG00000164237.8	CMBL	1451.5	322.5	-2.30	2.16E-13	3
ENSG00000173267.13	SNCG	1228	154.5	-3.13	1.41E-27	3
ENSG00000175643.8	RMI2	391	109	-2.01	3.69E-10	3
ENSG00000101224.17	CDC25B	4491	1079	-2.28	5.78E-20	3
ENSG00000154237.12	LRRK1	888	269	-1.92	1.47E-11	3
ENSG00000136827.11	TOR1A	1163.5	367.5	-1.87	1.22E-12	3
ENSG00000176619.10	LMNB2	12697	4806	-1.59	1.64E-08	3
ENSG00000163535.17	SGOL2	1904	375	-2.46	1.22E-12	3
ENSG00000123485.11	HJURP	2346	135.5	-4.11	4.28E-29	3
ENSG00000090889.11	KIF4A	2241	129.5	-4.14	8.42E-31	3
ENSG00000140678.16	ITGAX	76	420	2.08	2.41E-09	3
ENSG00000151012.13	SLC7A11	10497.5	367	-4.95	7.01E-43	3

APPENDIX 5

ENSG00000108854.15	SMURF2	14195.5	4419.5	-1.89	7.13E-14	3
ENSG00000123427.15	MEITL21B	208	34.5	-2.67	2.78E-11	3
ENSG00000157782.9	CABP1	27	143.5	2.04	2.12E-06	3
ENSG00000107554.15	DNMBP	5732	2297.5	-1.56	3.87E-11	3
ENSG00000091136.13	LAMB1	5432.5	1576.5	-1.99	1.28E-14	3
ENSG00000072571.19	HMMR	3118.5	137.5	-4.54	2.99E-38	3
ENSG00000167034.9	NKX3-1	194.5	827	1.83	1.50E-09	3
ENSG00000168404.12	MLKL	379.5	84.5	-2.35	5.71E-14	3
ENSG00000184584.12	TMEM173	735.5	67.5	-3.59	1.03E-33	3
ENSG00000184363.9	PKP3	3419.5	987.5	-1.95	6.57E-11	3
ENSG00000177565.15	TBL1XR1	8894.5	3159.5	-1.73	1.70E-11	3
ENSG00000124635.8	HIST1H2BJ	8923.5	464.5	-3.63	2.94E-06	3
ENSG00000171960.10	PPIH	1377.5	347.5	-2.18	1.28E-14	3
ENSG00000204287.13	HLA-DRA	119	445	1.62	5.63E-06	3
ENSG00000143401.14	ANP32E	4142	1719.5	-1.50	1.54E-08	3
ENSG00000120334.15	CENPL	760	199.5	-2.10	1.20E-11	3
ENSG00000163808.16	KIF15	1751	138.5	-3.78	2.59E-34	2
ENSG00000130956.13	HABP4	710.5	2567	1.55	1.13E-06	2
ENSG00000138772.12	ANXA3	7658	541	-3.99	3.82E-46	2
ENSG00000172638.12	EFEMP2	135	508.5	1.52	2.01E-05	2
ENSG00000107984.9	DKK1	9262.5	78737	2.75	6.99E-25	2
ENSG00000167657.11	DAPK3	682.5	4621.5	2.41	7.61E-13	2
ENSG00000124216.3	SNAI1	163	722	1.89	6.32E-09	2
ENSG00000015171.18	ZMYND11	2069.5	583	-2.05	1.40E-14	2
ENSG00000117322.16	CR2	228.5	860.5	1.63	4.94E-09	2
ENSG00000132773.11	TOE1	728	221.5	-1.90	1.01E-10	2
ENSG00000118495.18	PLAGL1	958.5	290.5	-1.92	1.45E-12	2
ENSG00000181472.4	ZBTB2	637.5	188	-1.96	5.03E-12	2
ENSG00000100592.15	DAAM1	555	2765	1.99	2.17E-15	2
ENSG00000099284.13	H2AFY2	1441.5	152.5	-3.39	4.99E-34	2
ENSG00000100479.12	POLE2	776.5	170	-2.37	5.47E-16	2
ENSG00000023839.10	ABCC2	9702	364	-4.89	3.55E-89	2
ENSG00000173805.15	HAP1	299.5	1496	1.99	6.88E-14	2
ENSG00000171988.17	JMJD1C	6745	2458	-1.71	2.95E-12	2
ENSG00000139631.18	CSAD	391	1565.5	1.65	6.23E-09	2
ENSG00000120254.15	MTHFD1L	4099.5	704.5	-2.72	1.80E-24	2
ENSG00000169136.8	ATF5	370.5	63	-2.68	1.36E-12	2
ENSG00000134470.19	IL15RA	203	62	-1.91	1.00E-07	2
ENSG00000101972.18	STAG2	8278	2287.5	-2.06	1.73E-12	2
ENSG00000075218.18	GTSE1	1089.5	70.5	-3.98	5.58E-27	2
ENSG00000186871.6	ERCC6L	972.5	157.5	-2.77	5.24E-20	2
ENSG00000101955.14	SRPX	496.5	186.5	-1.58	1.89E-06	2
ENSG00000176890.15	TYMS	1811	136.5	-3.80	2.00E-28	2
ENSG00000242265.5	PEG10	868	20750	4.21	7.40E-57	2
ENSG00000155363.18	MOV10	3349.5	1253.5	-1.64	5.64E-11	2
ENSG00000181856.14	SLC2A4	71	357	2.02	1.38E-09	2
ENSG00000104611.11	SH2D4A	1456	483	-1.80	7.71E-12	2
ENSG00000158445.8	KCNB1	96.5	377.5	1.67	5.07E-07	2
ENSG00000143507.17	DUSP10	107	824	2.62	6.29E-21	2
ENSG00000013810.18	TACC3	2321.5	420.5	-2.56	1.85E-14	2
ENSG00000104889.4	RNASEH2A	1814	433	-2.22	1.21E-13	2
ENSG00000196584.2	XRCC2	1192	295	-2.16	1.11E-12	2
ENSG00000105971.14	CAV2	4515.5	1224	-2.11	4.56E-16	2
ENSG00000095637.21	SORBS1	271	2710.5	2.98	2.61E-32	2
ENSG00000165731.17	RET	358.5	1245	1.54	3.41E-08	2
ENSG00000104814.12	MAP4K1	95	330.5	1.50	5.49E-06	2
ENSG00000092445.11	TYRO3	1505	535	-1.69	2.55E-10	2
ENSG00000164749.11	HNF4G	210	30.5	-2.89	1.32E-12	2
ENSG00000050438.16	SLC4A8	144	3181	4.10	1.08E-55	2
ENSG00000160862.12	AZGP1	25	264.5	3.04	5.63E-15	2
ENSG00000102265.11	TIMP1	3298	11558	1.50	4.60E-10	2
ENSG00000177602.5	GSG2	492	89.5	-2.55	3.54E-12	2
ENSG00000165480.15	SKA3	1117.5	150.5	-2.98	1.76E-19	2
ENSG00000107829.13	FBXW4	642	157	-2.24	5.80E-15	2
ENSG00000076382.16	SPAG5	3060	342.5	-3.34	8.44E-36	2
ENSG00000117152.13	RGS4	34.5	127	1.57	3.89E-04	2
ENSG00000167325.14	RRM1	6682	1542	-2.29	1.37E-16	2
ENSG00000100867.14	DHRS2	485	30698.5	4.82	1.25E-11	2
ENSG00000198467.13	TPM2	8213.5	1191	-2.89	5.92E-21	2
ENSG00000182199.10	SHMT2	9240	3349	-1.67	5.50E-08	2
ENSG00000012779.10	ALOX5	60	419.5	2.46	1.07E-14	2
ENSG00000096433.10	ITPR3	8886	3054.5	-1.73	2.86E-10	2

## APPENDIX 5

ENSG00000107874.10	CUEDC2	2330.5	688	-1.95	9.42E-13	2
ENSG0000049618.21	ARID1B	1197.5	299	-2.22	6.19E-13	2
ENSG00000197915.5	HRNR	33.5	449	3.31	2.90E-20	2
ENSG0000041880.14	PARP3	772	295	-1.63	1.21E-09	2
ENSG00000165304.7	MELK	2462.5	389.5	-2.81	5.45E-23	2
ENSG00000105991.7	HOXA1	74.5	468.5	2.33	4.23E-12	2
ENSG00000162409.10	PRKAA2	410	1650.5	1.66	3.69E-08	2
ENSG00000183508.4	FAM46C	172.5	1307	2.61	9.60E-21	2
ENSG00000110321.15	EIF4G2	23709.5	8172.5	-1.76	3.06E-13	2
ENSG00000119969.14	HELLS	4711	1800	-1.62	2.12E-11	2
ENSG00000111665.11	CDCA3	835	119	-3.02	1.15E-23	2
ENSG00000106268.15	NUDT1	571	161.5	-1.95	7.94E-08	2
ENSG00000132481.6	TRIM47	1345.5	256.5	-2.52	1.11E-15	2
ENSG00000174547.13	MRPL11	2153	551.5	-2.13	1.09E-12	2
ENSG00000196787.3	HIST1H2AG	13820	1454	-3.33	1.25E-19	2
ENSG00000128951.13	DUT	1640	594	-1.71	1.32E-10	2
ENSG00000140022.9	STON2	145.5	1449	2.99	8.75E-30	2
ENSG00000010803.16	SCMH1	743.5	237.5	-1.88	4.24E-12	2
ENSG00000169567.11	HINT1	6624	2503.5	-1.62	6.52E-10	2
ENSG00000111328.6	CDK2AP1	1888.5	295	-2.82	1.95E-20	2
ENSG00000183814.15	LIN9	526.5	147.5	-2.01	2.91E-10	2
ENSG00000089248.6	ERP29	4855.5	1880.5	-1.57	3.34E-08	2
ENSG00000147862.14	NFIB	795.5	264	-1.79	4.78E-08	2
ENSG00000132938.18	MTUS2	35.5	598	3.66	1.65E-26	2
ENSG00000126787.12	DLGAP5	3454.5	233.5	-3.89	1.81E-25	2
ENSG00000183763.8	TRAIP	648	137.5	-2.37	6.35E-13	2
ENSGR0000214717.10	ZBED1	681.5	188.5	-1.81	8.11E-11	2
ENSG00000105516.10	DBP	1283	455	-1.64	5.12E-07	2
ENSG00000171241.8	SHCBP1	1554.5	121.5	-3.14	4.67E-05	2
ENSG00000066379.14	ZNRD1	575	185	-1.88	1.64E-10	2
ENSG00000164136.16	IL15	129.5	543	1.76	7.20E-09	2
ENSG00000138378.17	STAT4	138.5	755	2.12	1.95E-10	2
ENSG00000196083.9	IL1RAP	158	1257.5	2.64	4.53E-21	2
ENSG00000102908.20	NFAT5	7653	2375.5	-1.95	4.02E-12	2
ENSG00000156876.9	SASS6	1009	214.5	-2.45	2.15E-18	2
ENSG00000071282.11	LMCD1	156.5	918	2.26	4.13E-16	2
ENSG00000150995.18	ITPR1	892	5649.5	2.33	9.01E-22	2
ENSG00000127955.15	GNAI1	5229.5	2128	-1.51	1.24E-08	2
ENSG00000100234.11	TIMP3	69.5	873.5	3.33	2.59E-29	2
ENSG00000104147.8	OIP5	332.5	44	-3.04	1.46E-17	2
ENSG00000119669.4	IRF2BPL	3122.5	699.5	-2.25	1.46E-09	2
ENSG00000110492.15	MDK	3418	1174.5	-1.69	1.17E-07	2
ENSG00000149294.16	NCAM1	51.5	5363	6.23	2.57E-85	2
ENSG00000149948.13	HMGA2	7984	417.5	-4.42	1.41E-68	2
ENSG00000140365.15	COMMD4	1765	676	-1.62	2.63E-10	2
ENSG00000138160.5	KIF11	3185.5	346.5	-3.33	2.92E-28	2
ENSG00000072864.12	NDE1	1813.5	527	-1.99	6.20E-13	2
ENSG00000139946.9	PEL12	115	453	1.65	2.94E-07	2
ENSG00000135476.11	ESPL1	2081	197.5	-3.50	3.74E-26	2
ENSG00000121552.3	CSTA	456.5	50.5	-3.28	2.05E-20	2
ENSG00000240694.8	PNMA2	87	362	1.77	1.14E-07	2
ENSG00000061337.15	LZTS1	172	1057.5	2.33	7.73E-15	2
ENSG00000204304.11	PBX2	1539.5	502	-1.82	8.21E-12	2
ENSG00000130340.14	SNX9	3321.5	1249	-1.63	7.43E-10	2
ENSG00000159082.17	SYNJ1	319	1332.5	1.73	1.96E-10	2
ENSG00000049449.8	RCN1	4945	911.5	-2.63	1.84E-22	2
ENSG00000142871.15	CYR61	252.5	1975.5	2.65	1.47E-13	2
ENSG00000144724.18	PTPRG	4281	1546	-1.63	3.23E-08	2
ENSG00000170275.14	CRTAP	3240	906	-2.00	1.05E-11	2
ENSG00000005884.17	ITGA3	18414.5	6634.5	-1.67	6.79E-10	2
ENSG00000197903.7	HIST1H2BK	12974.5	1024.5	-3.73	4.27E-27	2
ENSG00000198743.5	SLC5A3	4212.5	1516	-1.70	2.69E-12	2
ENSG00000171428.13	NAT1	113.5	1014	2.84	7.31E-23	2
ENSG00000134716.9	CYP2J2	39	170.5	1.80	6.23E-06	2
ENSG00000223865.10	HLA-DPB1	46	215.5	1.92	5.84E-07	2
ENSG00000046604.12	DSG2	6265.5	2521	-1.55	4.54E-09	2
ENSG00000134755.14	DSC2	2236.5	501.5	-2.36	1.91E-19	2
ENSG00000087085.13	ACHE	57.5	292	2.04	2.56E-08	2
ENSG00000182742.5	HOXB4	530	110.5	-2.43	1.49E-15	2
ENSG00000007968.6	E2F2	813.5	128.5	-2.79	6.09E-19	2
ENSG00000136104.18	RNASEH2B	1102.5	421	-1.59	3.96E-08	2
ENSG00000240849.10	TMEM189	995	3752.5	1.61	3.30E-11	2

## APPENDIX 5

ENSG00000166311.9	SMPD1	108.5	768.5	2.48	2.01E-15	2
ENSG00000131153.8	GINS2	1666	540	-1.77	1.29E-08	2
ENSG00000101003.9	GINS1	1506	388.5	-2.09	7.38E-12	2
ENSG00000145349.16	CAMK2D	4976	993.5	-2.51	1.55E-22	1
ENSG00000122877.13	EGR2	44	348.5	2.61	1.69E-13	1
ENSG00000102879.15	CORO1A	136	1072.5	2.66	5.84E-20	1
ENSG00000120896.13	SORBS3	487.5	144	-1.93	6.38E-10	1
ENSG00000138814.16	PPP3CA	7365.5	3057	-1.53	4.41E-08	1
ENSG00000162433.14	AK4	1983.5	733.5	-1.64	2.18E-08	1
ENSG00000173193.13	PARP14	2165	289.5	-3.11	1.61E-36	1
ENSG00000116285.12	ERRFI1	36563.5	6143.5	-2.78	9.44E-29	1
ENSG00000132470.13	ITGB4	12348	1846	-2.88	6.66E-23	1
ENSG00000137331.11	IER3	12072.5	4768.5	-1.55	2.19E-07	1
ENSG00000122966.13	CIT	2114.5	368	-2.68	5.73E-21	1
ENSG00000154920.14	EME1	845	197	-2.25	1.14E-13	1

# Appendix 6: GO analysis Molecular Functions and Cellular Components

**Table A6-1 Top three enriched Molecular Functions identified in ClueGO**

GO ID	GO Term	Number of Genes	% Associated Genes	Term PValue Corrected with Bonferroni step down	Associated Genes Found
<b>GO:0019899</b>	enzyme binding	136	6.98	1.82E-21	A2M, ANP32B, ATF5, AURKA, BANF1, BID, BIRC5, BORA, BRCA1, BRCA2, CAMK2D, CASP8, CAV1, CAV2, CBX3, CBX5, CCNA2, CCNB1, CDC20, CDC25A, CDC25B, CDC25C, CDC6, CDK2AP1, CDK5RAP2, CDKN2A, CFLAR, CIT, CKB, CKS1B, CLU, COL1A1, CSTA, CUL1, DAAM1, DAPK3, DNMI, DNMT3B, E2F1, ECT2, EEF1A1, EGR2, ERBB2, ERBB3, ERFF1, ETS1, FANCD2, FANCI, FAS, FBXO5, FLOT2, FN1, FOXM1, GRB7, GRK5, GTF2I, H2AFX, HDAC9, HINT1, HIST1H2AG, HMGA2, HMGB1, HNRNPUL1, HSPA2, HSPD1, IARS, IL1RAP, IPO5, ITGA3, JUN, KIF11, LDHB, LMNB1, LZTS1, MAP3K5, MAPK8IP1, MAPK8IP2, MAPK8IP3, MCM10, MCM2, MCM7, MET, MLKL, NCAPH, NEK2, NFKBIA, NGFR, NKX3-1, PKP3, PLAUR, PLK1, POLA1, PPARG, PPP3CA, PRC1, PRDX3, PRDX6, PRKACB, PRKN, PTPA, RAB3A, RACGAP1, RAD18, RAD51, RANBP1, RBBP4, RCC1, RCC2, SGO1, SH2D4A, SNAI1, SNCA, SNX9, SP100, SRC, STAT6, STX1A, TFAP4, TIMP1, TIMP3, TMEM173, TMEM189, TNFRSF10A, TOP2A, TP53, TP73, TPX2, TRIB3, TRIP6, TUBA1B, TUBB, UBE2C, UBE2J1, USP2, VRK1, XBP1
<b>GO:0042802</b>	identical protein binding	106	6.99	6.56E-16	ACHE, AGER, AMOTL2, ANXA4, ASNS, ATF3, BANF1, BHLHE40, BIRC5, CAMK2D, CASP8, CAV1, CAV2, CBX3, CBX5, CEBPD, CENPF, CHAF1A, COL1A1, CORO1A, CR2, DAAM1, DAPK3, DCK, DDI3, DES, DNMI, ECT2, ERBB2, ERBB3, ERBB4, ERP29, ETS1, FAS, FBLN1, FN1, GRB7, HJURP, HOXA1, HRNR, IRAK1, JUN, KEAP1, LDHB, LRRK1, MAD2L1, MAP3K5, MAPRE3, MAT2A, MCM10, MCM6, MTHFD1L, MTUS2, MYD88, NCAM1, NDC80, NDE1, NFKB1, NFKBIA, NMI, NQO1, NR2F1, NR4A1, OIP5, OXCT1, PAICS, PCBD1, PLK4, PPARG, PRC1, PRDX3, PRDX6, PRKN, PTPA, PTPRG, RAD18, RAD51, RAG1, RRM2, S100A16, S100A4, SHMT2, SMURF2, SNCA, SNRPA, SNX9, SP100, STAT6, TFAP4, THBS1, TIMELESS, TK1, TMEM173, TOP2A, TOPBP1, TP53, TP73, TRIM8, TRIM9, TRIP13, TTK, TYMS, USP2, XBP1, XIAP, ZBED1
<b>GO:0046983</b>	protein dimerization activity	93	7.35	4.20E-15	ACHE, ASNS, ATF1, ATF3, ATF4, AURKA, AXIL, BANF1, BHLHE40, BID, BIRC5, CAMK2D, CAPN2, CAV1, CAV2, CBX5, CEBPD, CENPA, CENPF, CORO1A, CR2, DAPK3, DCK, DDI3, DNMI, E2F1, E2F2, E2F3, ECT2, ERBB2, ERBB3, ERBB4, ERP29, FLOT2, FOS, H2AFX, H2AFY2, H2AFZ, HIST1H2AG, HIST1H2BJ, HIST1H2BK, HIST2H2AC, HIST2H2BE, HIST2H3A, HIST3H2BB, HRNR, HSPD1, IRAK1, ITGA3, JDP2, JUN, KCNB1, KEAP1, MAD2L1, MAP3K5, MITF, MTHFD1L, MTUS2, NFKB1, NR2F1, NR4A1, NUP210, OXCT1, POLA1, POLA2, PPARG, PPP3CA, PRDX6, PTPA, RAG1, RAN, RCC1, RRM2, S100A16, SMC2, SMC4, SNX9, SP100, STX1A, SUCLG2, TFAP4, TIMELESS, TMEM173, TOP2A, TP53, TRIM8, TRIM9, TTK, TYMS, TYRO3, XBP1, YAP1, ZBED1

APPENDIX 6

Table A6-2 Top three enriched Cellular Components identified in ClueGO

GO ID	GO Term	Number of Genes	% Associated Genes	Term PValue Corrected with Bonferroni step down	Associated Genes Found
<b>GO:0005694</b>	chromosome	140	14.31	2.79E-61	ALYREF, ANAPC16, ANP32E, APEX1, ASF1B, AURKA, AURKB, BANF1, BIRC5, BLM, BRCA1, BRCA2, BUB1, BUB1B, CALCOCO1, CAPN2, CBX3, CBX5, CCNB1, CDC45, CDCA8, CDK1, CDK4, CDKN2A, CDT1, CENPA, CENPE, CENPF, CENPH, CENPK, CENPL, CENPM, CENPN, CENPQ, CHAF1A, CHEK1, DSN1, DTL, E2F1, EME1, ERCC6L, EXOSC5, FANCD2, FEN1, GINS1, GINS2, GSG2, H2AFX, H2AFY2, H2AFZ, HELLS, HIST1H1C, HIST1H1E, HIST1H2AG, HIST1H2BJ, HIST1H2BK, HIST2H2AC, HIST2H2BE, HIST2H3A, HIST3H2BB, HJURP, HMGA2, HMGB1, HMGB2, ITGB3BP, JMJD1C, JUN, KIF2C, KIF4A, KNL1, MAD2L1, MCM10, MCM2, MCM3, MCM4, MCM5, MCM6, MCM7, MKI67, MYBL2, NCAPD2, NCAPG, NCAPH, NDC80, NDE1, NEK2, NSD2, NUF2, NUMA1, OIP5, ORC1, ORC6, PARP3, PLK1, PLK4, PMF1, POLA1, POLA2, POLE2, RAD18, RAD21, RAD51, RAN, RARG, RBBP4, RBBP8, RCC1, RCC2, RFC3, RNASEH2A, RPA1, SCMH1, SETD7, SGO1, SGO2, SKA1, SKA3, SLX4, SMARCA2, SMC2, SMC4, SP100, SPAG5, SPC24, SPC25, STAG2, STAT6, SUV39H1, TIMELESS, TMPO, TONSL, TOP2A, TOPBP1, TP53, TP73, TTK, XRCC2, ZBED1, ZMYND11, ZWINT
<b>GO:0044428</b>	nuclear part	290	6.57	5.45E-59	AGER, ALOX5, ALYREF, ANAPC16, ANP32B, ANP32E, ANXA4, APEX1, ARID1B, ASF1B, ATAD2, ATF1, ATF3, ATF4, ATF5, AURKA, AURKB, BANF1, BCL3, BHLHE40, BIRC5, BLM, BRCA1, BRCA2, BRIP1, BUB1, BUB1B, CALCOCO1, CAMK2D, CASP8, CBX3, CBX5, CCNA2, CCNB1, CCNB2, CDC20, CDC25A, CDC25B, CDC25C, CDC45, CDC6, CDCA8, CDK1, CDK2AP1, CDK4, CDKN2A, CDT1, CEBPD, CENPA, CENPF, CENPH, CENPK, CENPL, CENPM, CENPN, CENPQ, CHAF1A, CHD3, CHEK1, CKAP4, CKS1B, CLSPN, CUEDC2, CUL1, DAPK3, DBF4, DDI3, DEK, DHFR, DHRS2, DNJC9, DNMT3B, DTL, DTX3L, DUSP10, DUT, E2F1, E2F2, E2F3, EEF1A1, EGR2, ELF3, EME1, ERBB4, ETS1, ETV4, EXOSC5, FANCA, FANCD2, FANCG, FANCI, FANCM, FAS, FBXO5, FEN1, FOS, FOSL1, FOXM1, GINS1, GINS2, GINS3, GNAI1, GRK5, GTF2I, GTSE1, H2AFX, H2AFY2, H2AFZ, HABP4, HAP1, HDAC9, HDGF, HINT1, HIST1H1C, HIST1H1E, HIST1H2AG, HIST1H2BJ, HIST1H2BK, HIST2H2AC, HIST2H2BE, HIST2H3A, HIST3H2BB, HJURP, HMGA2, HMGB1, HMGB2, HNF4G, HNRNPUL1, HRNR, HSPD1, IGF2BP3, IL15, IL15RA, IPO5, IRF2BPL, IRF7, ITGB3BP, ITPR1, ITPR3, JMJD1C, JUN, KEAP1, KIF23, KIF2C, KIF4A, KNL1, LIN9, LMCD1, LMNB1, LMNB2, LSM4, MAD2L1, MAP2, MAPK10, MCM10, MCM2, MCM3, MCM4, MCM5, MCM6, MCM7, MITF, MKI67, MLLT3, MYBL2, NCAPD2, NCAPG, NCAPH, NDC80, NEK2, NFAT5, NFIB, NFIC, NFKB1, NGFR, NMI, NR2F1, NR4A1, NSD2, NUDT1, NUMA1, NUP210, OIP5, ORC1, ORC6, OXCT1, PABPC1, PARP3, PCBD1, PCLAF, PKMYT1, PKP3, PLAGL1, PLK1, PLK4, PMF1, PNMA2, POLA1, POLA2, POLE2, POU2F2, PPARG, PPIH, PPP3CA, PRC1, PRKAA2, PRKACB, PSME1, PSRC1, PTPA, RACGAP1, RAD18, RAD21, RAD51, RAG1, RAI1, RAN, RANBP1, RARG, RARS, RBBP4, RBBP8, RBM3, RCC1, RCC2, RFC3, RMI2, RNASEH2A, RPA1, RPL13A, RPS6KA5, RRM1, RRM2, S100A16, SCMH1, SET, SETD7, SGK1, SGO1, SGO2, SHMT2, SLX4, SMARCA2, SMC2, SMC4, SMURF2, SNCA, SNRPA, SORBS1, SP100, SPC24, STAG2, STAT6, STON2, STX1A, SUV39H1, TBL1XR1, TIMELESS, TJP2, TMEM173, TMPO, TOE1, TONSL, TOP2A, TOPBP1, TOR1A, TP53, TP73, TPX2, TRAP, TRIB3, TRIM8, TUBB, TYMS, TYRO3, UBE2C, UBE2E1, UGDH, USP2, VRK1, WDHD1, WEE1, XBP1, XIAP, XRCC2, YAP1, ZBED1, ZMYND11, ZNRD1, ZWINT
<b>GO:0031981</b>	nuclear lumen	274	6.77	6.15E-57	AGER, ALOX5, ALYREF, ANAPC16, ANP32B, ANP32E, APEX1, ARID1B, ASF1B, ATAD2, ATF1, ATF3, ATF4, ATF5, AURKA, AURKB, BANF1, BCL3, BHLHE40, BIRC5, BLM, BRCA1, BRCA2, BRIP1, BUB1, BUB1B, CALCOCO1, CAMK2D, CASP8, CBX3, CBX5, CCNA2, CCNB1, CCNB2, CDC20, CDC25A, CDC25B, CDC25C,

## APPENDIX 6

CDC45, CDC6, CDCA8, CDK1, CDK2AP1, CDK4, CDKN2A, CDT1, CEBPD, CENPA, CENPF, CENPH, CENPK, CENPL, CENPM, CENPN, CENPQ, CHAF1A, CHD3, CHEK1, CKAP4, CKS1B, CLSPN, CUEDC2, CUL1, DAPK3, DBF4, DDIT3, DEK, DHFR, DNAJC9, DNMT3B, DTL, DTX3L, DUSP10, DUT, E2F1, E2F2, E2F3, EEF1A1, EGR2, ELF3, EME1, ERBB4, ETS1, ETV4, EXOSC5, FANCA, FANCD2, FANCG, FANCI, FANCM, FAS, FBXO5, FEN1, FOS, FOSL1, FOXM1, GINS1, GINS2, GINS3, GNAI1, GRK5, GTF2I, GTSE1, H2AFX, H2AFY2, H2AFZ, HABP4, HAP1, HDAC9, HDGF, HINT1, HIST1H1C, HIST1H1E, HIST1H2AG, HIST1H2BJ, HIST1H2BK, HIST2H2AC, HIST2H2BE, HIST2H3A, HIST3H2BB, HJURP, HMGA2, HMGB1, HMGB2, HNF4G, HNRNPUL1, HRNR, IGF2BP3, IL15, IPO5, IRF2BP1, IRF7, ITGB3BP, ITPR1, ITPR3, JMJD1C, JUN, KEAP1, KIF23, KIF2C, KIF4A, KNL1, LIN9, LMCD1, LMNB1, LMNB2, LSM4, MAD2L1, MAP2, MAPK10, MCM10, MCM2, MCM3, MCM4, MCM5, MCM6, MCM7, MTF, MKI67, MLLT3, MYBL2, NCAPD2, NCAPG, NCAPH, NDC80, NEK2, NFAT5, NFIB, NFIC, NFKB1, NGFR, NMI, NR2F1, NR4A1, NSD2, NUMA1, OIP5, ORC1, ORC6, OXCT1, PARP3, PCBD1, PCLAF, PKMYT1, PKP3, PLAGL1, PLK1, PLK4, PMF1, PNMA2, POLA1, POLA2, POLE2, POU2F2, PPARG, PPIH, PPP3CA, PRC1, PRKAA2, PRKACB, PSME1, PSRC1, PTPA, RACGAP1, RAD18, RAD21, RAD51, RAG1, RAI1, RAN, RARG, RARS, RBBP4, RBBP8, RBM3, RCC1, RCC2, RFC3, RMI2, RNASEH2A, RPA1, RPL13A, RPS6KA5, RRM2, S100A16, SCMH1, SET, SETD7, SGK1, SGO1, SGO2, SLX4, SMARCA2, SMC2, SMC4, SMURF2, SNRPA, SORBS1, SP100, SPC24, STAG2, STAT6, STON2, SUV39H1, TBL1XR1, TIMELESS, TJP2, TMEM173, TOE1, TONSL, TOP2A, TOPBP1, TP53, TP73, TPX2, TRAP, TRIB3, TRIM8, TYMS, UBE2C, UBE2E1, UGDH, USP2, VRK1, WDHD1, WEE1, XBP1, XIAP, XRCC2, YAP1, ZBED1, ZMYND11, ZNRD1, ZWINT

# Appendix 7: WikiPathways and Reactome GO pathway analysis

**Table A7-1 Enriched pathway terms identified using WikiPathways in ClueGO**

All enriched pathways from WikiPathways are presented.

GO ID	GO Term	Number of Genes	% Associated Genes	Term PValue Corrected with Bonferroni step down	Associated Genes Found
GO:0002446	Retinoblastoma (RB) in Cancer	43	48.86	1.1E-29	CCNA2, CCNB1, CCNB2, CDC25A, CDC25B, CDC45, CDK1, CDK4, CDT1, CHEK1, DCK, DHFR, E2F1, E2F2, E2F3, FANCG, H2AFZ, HMGB1, HMGB2, KIF4A, MAPK13, MCM3, MCM4, MCM6, MCM7, ORC1, PLK4, POLA1, POLE2, RBBP4, RFC3, RPA1, RRM1, RRM2, SMARCA2, SMC2, STMN1, SUV39H1, TOP2A, TP53, TTK, TYMS, WEE1
GO:0000179	Cell Cycle	35	33.33	3.62E-17	BUB1, BUB1B, CCNA2, CCNB1, CCNB2, CDC20, CDC25A, CDC25B, CDC25C, CDC45, CDC6, CDK1, CDK4, CDKN2A, CHEK1, DBF4, E2F1, E2F2, E2F3, ESPL1, MAD2L1, MCM10, MCM2, MCM3, MCM4, MCM5, MCM6, MCM7, ORC1, ORC6, PKMYT1, PLK1, PTTG1, TP53, WEE1
GO:0000466	DNA Replication	18	42.86	1.59E-10	CDC45, CDC6, CDT1, DBF4, MCM10, MCM2, MCM3, MCM4, MCM5, MCM6, MCM7, ORC1, ORC6, POLA1, POLA2, POLE2, RFC3, RPA1
GO:0000045	G1 to S cell cycle control	22	32.35	4.16E-10	CCNB1, CDC25A, CDC45, CDK1, CDK4, CDKN2A, E2F1, E2F2, E2F3, MCM2, MCM3, MCM4, MCM5, MCM6, MCM7, ORC1, ORC6, POLA2, POLE2, RPA1, TP53, WEE1
GO:0002377	Integrated Pancreatic Cancer Pathway	33	16.75	5.54E-07	ABCB1, ACHE, BID, BLM, BRCA1, BRCA2, BUB1B, CASP8, CCNA2, CDC25C, CDK4, CHEK1, E2F1, ERBB2, FAS, IGFBP3, JUN, MAP3K5, NFKB1, NFKBIA, PLK1, POLA1, PRKAA2, PTTG1, RAD51, RRM1, SRC, STMN1, THBS1, TNFRSF1A, TOP2A, TP53, TYMS
GO:0002516	ATM Signalling Pathway	14	35.00	1.26E-06	BID, BRCA1, CCNB1, CDC25A, CDC25C, CDK1, CHEK1, FANCD2, H2AFX, JUN, NFKBIA, RAD51, TP53, TP73
GO:0000707	DNA Damage Response	16	23.19	7.22E-05	BID, BRCA1, CASP8, CCNB1, CCNB2, CDC25A, CDC25C, CDK1, CDK4, CHEK1, E2F1, FANCD2, FAS, H2AFX, RAD51, TP53
GO:0001971	Integrated Cancer Pathway	13	28.26	7.3E-05	ATF1, BLM, BRCA1, CASP8, CDC25A, CDC25B, CDK1, CDK4, CHEK1, E2F1, MAP3K5, PLK1, TP53
GO:0002361	Gastric Cancer Network 1	10	34.48	0.000196	AURKA, CENPF, ECT2, KIF15, LIN9, MCM4, MYBL2, TOP2A, TPX2, UBE2C
GO:0001772	Apoptosis Modulation and Signalling	18	19.15	0.000281	BID, BIRC5, CASP4, CASP8, CDKN2A, CFLAR, FAS, FOS, IRAK1, JUN, MAP3K5, MYD88, NFKB1, NFKBIA, TNFRSF10A, TNFRSF1A, TP53, XIAP
GO:0000254	Apoptosis	17	19.77	0.000338	BID, BIRC5, CASP4, CASP8, CDKN2A, CFLAR, FAS, HELLS, IRF7, JUN, MAPK10, NFKB1, NFKBIA, TNFRSF1A, TP53, TP73, XIAP
GO:0001530	miRNA Regulation of DNA Damage Response	17	18.28	0.001023	BID, BRCA1, CASP8, CCNB1, CCNB2, CDC25A, CDC25C, CDK1, CDK4, CHEK1, E2F1, FANCD2, FAS, H2AFX, MCM7, RAD51, TP53
GO:0003611	Photodynamic therapy-induced AP-1 survival signaling.	12	23.53	0.001548	BCL3, BID, CCNA2, CDKN2A, CFLAR, FAS, FOS, JUN, MAP3K5, MAPK13, TNFRSF1A, TP53
GO:0002864	Apoptosis-related network due to altered Notch3 in ovarian cancer	11	20.37	0.014514	BCL3, BIRC5, CUL1, ERBB3, ETS1, HELLS, HSPD1, IER3, NFKB1, NQO1, THBS1
GO:0002828	Bladder Cancer	8	25.00	0.027564	CDK4, CDKN2A, DAPK3, E2F1, ERBB2, RPS6KA5, THBS1, TP53
GO:0003303	Rac1/Pak1/p38/MMP-2 pathway	12	17.65	0.029857	BIRC5, ERBB2, FN1, GRB7, MAPK13, NFKB1, NFKBIA, RAD51, SRC, STMN1, TP53, YAP1
GO:0000384	Apoptosis Modulation by HSP70	6	31.58	0.042086	BID, CASP8, FAS, MAPK10, NFKB1, TNFRSF1A

APPENDIX 7

**Table A7-2 Enriched pathway terms identified using Reactome in ClueGO**

The top three enriched pathways from Reactome are presented, from a total of 435 pathways.

GO ID	GO Term	Number of Genes	% Associated Genes	Term PValue Corrected with Bonferroni step down	Associated Genes Found
<b>GO:0000080</b>	Meiotic synapsis	136	22.11	6.62E-67	ANAPC16, AURKA, AURKB, BANF1, BIRC5, BLM, BORA, BRCA1, BRCA2, BRIP1, BUB1, BUB1B, CCNA2, CCNB1, CCNB2, CDC20, CDC25A, CDC25B, CDC25C, CDC45, CDC6, CDCA8, CDK1, CDK4, CDK5RAP2, CDKN2A, CDT1, CENPA, CENPE, CENPF, CENPH, CENPK, CENPL, CENPM, CENPN, CENPQ, CHEK1, CKS1B, CLSPN, CUL1, DBF4, DHFR, DSN1, E2F1, E2F2, E2F3, ERCC6L, ESPL1, FBXO5, FEN1, FOXM1, GINS1, GINS2, GINS3, GTSE1, H2AFX, H2AFZ, HIST1H2BJ, HIST1H2BK, HIST1H3H, HIST1H4E, HIST2H2AC, HIST2H2BE, HIST2H3A, HIST3H2BB, HJURP, HMMR, HSPA2, ITGB3BP, KIF23, KIF2C, KNL1, LIN9, LMNB1, MAD2L1, MCM10, MCM2, MCM3, MCM4, MCM5, MCM6, MCM7, MYBL2, NCAPD2, NCAPG, NCAPH, NDC80, NDE1, NEK2, NSD2, NUF2, NUMA1, NUP210, OIP5, ORC1, ORC6, PKMYT1, PLK1, PLK4, PMF1, POLA1, POLA2, POLE2, PSME1, PTTG1, RAD21, RAD51, RBBP4, RBBP8, RCC2, RFC3, RMI2, RPA1, RRM2, SET, SGO1, SGO2, SKA1, SMC2, SMC4, SPC24, SPC25, STAG2, TOP2A, TOPBP1, TP53, TPX2, TUBA1A, TUBA1B, TUBB, TYMS, UBE2C, UBE2E1, VRK1, WEE1, ZWINT
<b>GO:0000201</b>	Meiosis	136	22.11	6.62E-67	ANAPC16, AURKA, AURKB, BANF1, BIRC5, BLM, BORA, BRCA1, BRCA2, BRIP1, BUB1, BUB1B, CCNA2, CCNB1, CCNB2, CDC20, CDC25A, CDC25B, CDC25C, CDC45, CDC6, CDCA8, CDK1, CDK4, CDK5RAP2, CDKN2A, CDT1, CENPA, CENPE, CENPF, CENPH, CENPK, CENPL, CENPM, CENPN, CENPQ, CHEK1, CKS1B, CLSPN, CUL1, DBF4, DHFR, DSN1, E2F1, E2F2, E2F3, ERCC6L, ESPL1, FBXO5, FEN1, FOXM1, GINS1, GINS2, GINS3, GTSE1, H2AFX, H2AFZ, HIST1H2BJ, HIST1H2BK, HIST1H3H, HIST1H4E, HIST2H2AC, HIST2H2BE, HIST2H3A, HIST3H2BB, HJURP, HMMR, HSPA2, ITGB3BP, KIF23, KIF2C, KNL1, LIN9, LMNB1, MAD2L1, MCM10, MCM2, MCM3, MCM4, MCM5, MCM6, MCM7, MYBL2, NCAPD2, NCAPG, NCAPH, NDC80, NDE1, NEK2, NSD2, NUF2, NUMA1, NUP210, OIP5, ORC1, ORC6, PKMYT1, PLK1, PLK4, PMF1, POLA1, POLA2, POLE2, PSME1, PTTG1, RAD21, RAD51, RBBP4, RBBP8, RCC2, RFC3, RMI2, RPA1, RRM2, SET, SGO1, SGO2, SKA1, SMC2, SMC4, SPC24, SPC25, STAG2, TOP2A, TOPBP1, TP53, TPX2, TUBA1A, TUBA1B, TUBB, TYMS, UBE2C, UBE2E1, VRK1, WEE1, ZWINT
<b>GO:0000275</b>	Cell Cycle	136	22.11	6.62E-67	ANAPC16, AURKA, AURKB, BANF1, BIRC5, BLM, BORA, BRCA1, BRCA2, BRIP1, BUB1, BUB1B, CCNA2, CCNB1, CCNB2, CDC20, CDC25A, CDC25B, CDC25C, CDC45, CDC6, CDCA8, CDK1, CDK4, CDK5RAP2, CDKN2A, CDT1, CENPA, CENPE, CENPF, CENPH, CENPK, CENPL, CENPM, CENPN, CENPQ, CHEK1, CKS1B, CLSPN, CUL1, DBF4, DHFR, DSN1, E2F1, E2F2, E2F3, ERCC6L, ESPL1, FBXO5, FEN1, FOXM1, GINS1, GINS2, GINS3, GTSE1, H2AFX, H2AFZ, HIST1H2BJ, HIST1H2BK, HIST1H3H, HIST1H4E, HIST2H2AC, HIST2H2BE, HIST2H3A, HIST3H2BB, HJURP, HMMR, HSPA2, ITGB3BP, KIF23, KIF2C, KNL1, LIN9, LMNB1, MAD2L1, MCM10, MCM2, MCM3, MCM4, MCM5, MCM6, MCM7, MYBL2, NCAPD2, NCAPG, NCAPH, NDC80, NDE1, NEK2, NSD2, NUF2, NUMA1, NUP210, OIP5, ORC1, ORC6, PKMYT1, PLK1, PLK4, PMF1, POLA1, POLA2, POLE2, PSME1, PTTG1, RAD21, RAD51, RBBP4, RBBP8, RCC2, RFC3, RMI2, RPA1, RRM2, SET, SGO1, SGO2, SKA1, SMC2, SMC4, SPC24, SPC25, STAG2, TOP2A, TOPBP1, TP53, TPX2, TUBA1A, TUBA1B, TUBB, TYMS, UBE2C, UBE2E1, VRK1, WEE1, ZWINT

# Appendix 8: Differentially expressed miRNA list

Table A8-1 Differentially expressed miRNA genes selected for network analysis

miRNA ID	Mean Counts 0 mM Butyrate	Mean Counts 2.5 mM Butyrate	log2FC	Padj value
hsa-let-7a-2-3p	91	31	-1.91	3.38E-07
hsa-let-7a-5p	2433	1361	-1.16	2.48E-04
hsa-let-7b-5p	30518	18729	-1.06	6.17E-05
hsa-let-7e-3p	127	61	-1.39	1.55E-04
hsa-let-7e-5p	23395	12355	-1.24	8.84E-04
hsa-miR-100-3p	3340	377	-3.46	3.09E-28
hsa-miR-10a-3p	493	278	-1.15	3.29E-04
hsa-miR-1247-5p	523	1438	1.06	3.53E-03
hsa-miR-125a-3p	220	110	-1.32	3.11E-03
hsa-miR-125a-5p	34770	18250	-1.27	2.10E-05
hsa-miR-125b-1-3p	3780	1150	-2.05	1.48E-10
hsa-miR-132-5p	129	359	1.07	4.58E-03
hsa-miR-135b-3p	178	113	-1.02	7.21E-04
hsa-miR-135b-5p	390	230	-1.11	8.25E-05
hsa-miR-139-3p	146	529	1.41	2.80E-03
hsa-miR-139-5p	322	1174	1.46	2.80E-03
hsa-miR-141-5p	2503	793	-1.98	4.74E-10
hsa-miR-143-3p	1766	903	-1.30	2.10E-05
hsa-miR-146a-5p	98	304	1.21	2.16E-02
hsa-miR-146b-3p	35	120	1.39	1.71E-02
hsa-miR-146b-5p	20070	53615	1.03	1.10E-02
hsa-miR-147b	37	114	1.24	2.97E-03
hsa-miR-15b-5p	1647	1013	-1.05	1.14E-04
hsa-miR-17-5p	12386	7724	-1.01	1.04E-03
hsa-miR-181c-3p	626	305	-1.37	1.65E-05
hsa-miR-185-3p	213	650	1.21	6.22E-03
hsa-miR-187-3p	25	72	1.21	1.49E-02
hsa-miR-18a-5p	1249	695	-1.17	1.31E-04
hsa-miR-190a-5p	2366	7391	1.25	1.80E-02
hsa-miR-191-5p	466575	1314675	1.11	3.62E-03
hsa-miR-192-5p	8038	29002	1.44	2.60E-03
hsa-miR-199b-5p	164	479	1.17	3.09E-04
hsa-miR-19a-3p	1711	932	-1.21	2.10E-05
hsa-miR-200b-3p	34285	18628	-1.22	5.60E-04
hsa-miR-200c-3p	39700	22093	-1.18	4.75E-05
hsa-miR-200c-5p	80	37	-1.47	6.06E-03
hsa-miR-205-5p	32	83	1.01	1.84E-02
hsa-miR-20a-3p	90	37	-1.61	2.10E-05
hsa-miR-215-5p	30	111	1.48	3.16E-03
hsa-miR-222-3p	237187	127676	-1.23	1.81E-04
hsa-miR-222-5p	649	316	-1.37	6.06E-05
hsa-miR-25-5p	700	412	-1.11	2.95E-04
hsa-miR-296-3p	64	198	1.22	6.86E-03
hsa-miR-29a-5p	793	229	-2.14	1.56E-12
hsa-miR-29b-1-5p	1124	196	-2.85	3.50E-10
hsa-miR-3127-5p	81	244	1.23	5.69E-03
hsa-miR-31-3p	3045	1316	-1.55	8.42E-08
hsa-miR-31-5p	195963	118387	-1.06	4.56E-04
hsa-miR-32-5p	286	765	1.03	5.94E-03
hsa-miR-335-3p	2943	1695	-1.14	1.55E-04
hsa-miR-33b-5p	647	1782	1.08	3.61E-03
hsa-miR-3607-3p	65	190	1.24	1.33E-02
hsa-miR-3613-5p	129	71	-1.17	7.67E-03
hsa-miR-3614-5p	151	59	-1.65	1.09E-03
hsa-miR-362-5p	158	414	1.01	2.25E-03
hsa-miR-374a-3p	1055	639	-1.06	4.55E-05
hsa-miR-379-5p	45	120	1.02	1.88E-02
hsa-miR-381-3p	292	789	1.04	1.01E-02
hsa-miR-382-5p	110	295	1.06	2.80E-03
hsa-miR-409-3p	263	823	1.27	3.83E-03
hsa-miR-411-5p	226	685	1.20	4.97E-03
hsa-miR-424-5p	90	366	1.61	8.47E-03
hsa-miR-425-3p	4218	11449	1.04	5.57E-03
hsa-miR-449c-5p	739	2030	1.08	3.16E-03

## APPENDIX 8

hsa-miR-450b-5p	79	216	1.08	5.27E-04
hsa-miR-452-5p	129	390	1.22	2.56E-03
hsa-miR-4707-5p	166	63	-1.73	2.06E-04
hsa-miR-4713-5p	92	58	-1.03	8.95E-03
hsa-miR-500a-3p	2020	5356	1.03	8.84E-04
hsa-miR-501-3p	1085	3877	1.47	1.03E-02
hsa-miR-503-5p	384	1571	1.60	3.13E-03
hsa-miR-532-3p	336	920	1.04	1.18E-02
hsa-miR-542-3p	128	352	1.07	5.69E-03
hsa-miR-561-5p	3257	1874	-1.13	2.65E-05
hsa-miR-676-3p	89	310	1.39	2.80E-03
hsa-miR-766-3p	178	489	1.07	6.87E-03
hsa-miR-92a-1-5p	357	81	-2.46	2.54E-07

# Appendix 9: lncRNA screen quality control

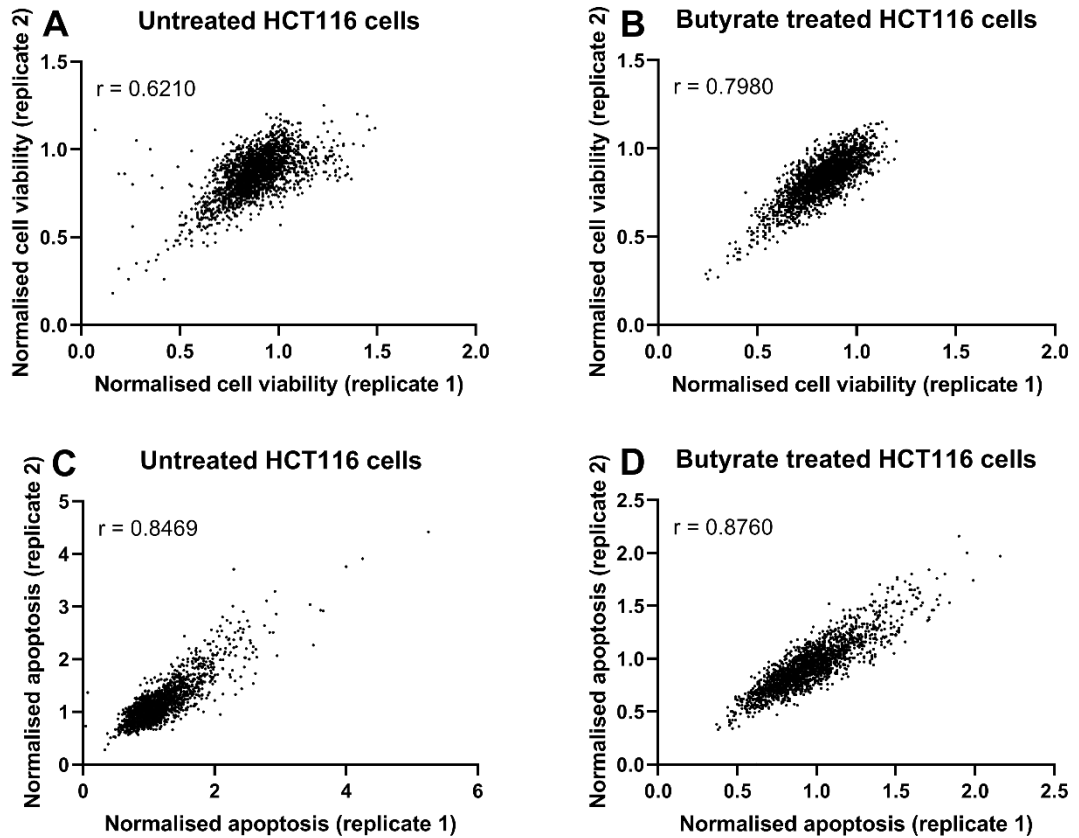


**Figure A9-1** Correlation analysis of lncRNA-targeting siRNA primary high-throughput screen

Quality control analysis of primary lncRNA high-throughput screen. The graphs plot normalized viability and apoptosis replicate 1 and 2 values for each lncRNA siRNA SMARTpool investigated in the primary screen. Correlation analysis was performed, and the Pearson correlation coefficient is displayed.

# Appendix 10: lncRNA-miRNA interactions

**Table A10-1 lncRNA-miRNA interactions**

lncRNA-miRNA interactions which did not have apoptotic gene targets.

miRNAs	Expression	Genes	Expression	Validated
CECR7	Down	hsa-miR-185-3p	Up	-
CECR7	Down	hsa-miR-199b-5p	Up	-
CECR7	Down	hsa-miR-205-5p	Up	-
CECR7	Down	hsa-miR-449c-5p	Up	-
CECR7	Down	hsa-miR-501-3p	Up	-
CECR7	Down	hsa-miR-676-3p	Up	-
GAS5	Down	hsa-miR-139-3p	Up	-
GAS5	Down	hsa-miR-205-5p	Up	V
GAS5	Down	hsa-miR-3127-5p	Up	-
GAS5	Down	hsa-miR-452-5p	Up	-
HOXA-AS3	Down	hsa-miR-139-3p	Up	-
HOXA-AS3	Down	hsa-miR-146b-3p	Up	-
HOXA-AS3	Down	hsa-miR-766-3p	Up	-
KMT2E-AS1	Down	hsa-miR-449c-5p	Up	-
MALAT1	Up	hsa-miR-100-3p	Down	-
MALAT1	Up	hsa-miR-10a-3p	Down	-
MALAT1	Up	hsa-miR-141-5p	Down	-
MALAT1	Up	hsa-miR-143-3p	Down	V
MALAT1	Up	hsa-miR-15b-5p	Down	V
MALAT1	Up	hsa-miR-17-5p	Down	-
MALAT1	Up	hsa-miR-20a-3p	Down	V
MALAT1	Up	hsa-miR-29a-5p	Down	-
MALAT1	Up	hsa-miR-29b-1-5p	Down	-
MALAT1	Up	hsa-miR-3614-5p	Down	-
MALAT1	Up	hsa-miR-4713-5p	Down	-
MALAT1	Up	hsa-miR-561-5p	Down	-
PAXBP1-AS1	Down	hsa-miR-146b-3p	Up	-
PAXBP1-AS1	Down	hsa-miR-3607-3p	Up	-
PAXBP1-AS1	Down	hsa-miR-452-5p	Up	-
PAXBP1-AS1	Down	hsa-miR-532-3p	Up	-
PRC1-AS1	Down	hsa-miR-185-3p	Up	-
PRC1-AS1	Down	hsa-miR-33b-5p	Up	-
ZFAS1	Down	hsa-miR-449c-5p	Up	-

# Appendix 11: MALAT1 RNA-seq data

---

## Figure A11-1 MALAT1 RNA-seq data

MALAT1 expression in HCT116 cells treated with 0 mM or 2.5 mM butyrate for 48 h.

Gene name	Mean Counts 0 mM Butyrate	Mean Counts 2.5 mM Butyrate	log2FoldChange	Padj value
<b>MALAT1</b>	200528	985600	1.63	2.58E-06

# References

---

- Aartsma-Rus, A, Janson, AA, Kaman, WE, Bremmer-Bout, M, den Dunnen, JT, Baas, F, van Ommen, GJ & van Deutekom, JC 2003, 'Therapeutic antisense-induced exon skipping in cultured muscle cells from six different DMD patients', *Hum Mol Genet*, vol. 12, no. 8, pp. 907-14.
- Agarwal, V, Bell, GW, Nam, JW & Bartel, DP 2015, 'Predicting effective microRNA target sites in mammalian mRNAs', *eLife*, vol. 4.
- Agra Andrieu, N, Motino, O, Mayoral, R, Llorente Izquierdo, C, Fernandez-Alvarez, A, Bosca, L, Casado, M & Martin-Sanz, P 2012, 'Cyclooxygenase-2 is a target of microRNA-16 in human hepatoma cells', *PLoS One*, vol. 7, no. 11, p. e50935.
- Aguilo, F, Zhou, M-M & Walsh, MJ 2011, 'Long noncoding RNA, polycomb, and the ghosts haunting INK4b-ARF-INK4a expression', *Cancer Research*, vol. 71, no. 16, pp. 5365-9.
- Ahlin, G, Hilgendorf, C, Karlsson, J, Szigartyo, CA, Uhlen, M & Artursson, P 2009, 'Endogenous gene and protein expression of drug-transporting proteins in cell lines routinely used in drug discovery programs', *Drug Metab Dispos*, vol. 37, no. 12, pp. 2275-83.
- Ahmed, D, Eide, PW, Eilertsen, IA, Danielsen, SA, Eknaes, M, Hektoen, M, Lind, GE & Lothe, RA 2013, 'Epigenetic and genetic features of 24 colon cancer cell lines', *Oncogenesis*, vol. 2, p. e71.
- Ahmed, SBM & Prigent, SA 2017, 'Insights into the Shc Family of Adaptor Proteins', *Journal of molecular signaling*, vol. 12, pp. 2-.
- Ahsan, S & Draghici, S 2017, 'Identifying Significantly Impacted Pathways and Putative Mechanisms with iPathwayGuide', *Curr Protoc Bioinformatics*, vol. 57, pp. 7.15.1-7..30.
- Ai, Z, Yin, L, Zhou, X, Zhu, Y, Zhu, D, Yu, Y & Feng, Y 2006, 'Inhibition of survivin reduces cell proliferation and induces apoptosis in human endometrial cancer', *Cancer*, vol. 107, no. 4, pp. 746-56.
- Aigner, P, Mizutani, T, Horvath, J, Eder, T, Heber, S, Lind, K, Just, V, Moll, HP, Yeroslaviz, A, Fischer, MJM, Kenner, L, Gyorffy, B, Sill, H, Grebien, F, Moriggl, R, Casanova, E & Stoiber, D 2019, 'STAT3beta is a tumor suppressor in acute myeloid leukemia', *Blood Adv*, vol. 3, no. 13, pp. 1989-2002.
- AIHW 2018, *Colorectal and other digestive-tract cancers*, Australian Institute of Health and Welfare, Canberra.
- AIHW 2019, *Cancer in Australia 2019*, Australian Institute of Health and Welfare, Canberra.
- Akao, Y, Nakagawa, Y, Hirata, I, Iio, A, Itoh, T, Kojima, K, Nakashima, R, Kitade, Y & Naoe, T 2010, 'Role of anti-oncomirs miR-143 and -145 in human colorectal tumors', *Cancer Gene Ther*, vol. 17, no. 6, pp. 398-408.

## REFERENCES

- Akao, Y, Nakagawa, Y & Naoe, T 2006, 'let-7 microRNA functions as a potential growth suppressor in human colon cancer cells', *Biol Pharm Bull*, vol. 29, no. 5, pp. 903-6.
- Alaiyan, B, Ilyayev, N, Stojadinovic, A, Izadjoo, M, Roistacher, M, Pavlov, V, Tzivin, V, Halle, D, Pan, H, Trink, B, Gure, AO & Nissan, A 2013, 'Differential expression of colon cancer associated transcript1 (CCAT1) along the colonic adenoma-carcinoma sequence', *BMC Cancer*, vol. 13, pp. 196-.
- Albuquerque, C, Breukel, C, van der Luijt, R, Fidalgo, P, Lage, P, Slors, FJ, Leitao, CN, Fodde, R & Smits, R 2002, 'The 'just-right' signaling model: APC somatic mutations are selected based on a specific level of activation of the beta-catenin signaling cascade', *Hum Mol Genet*, vol. 11, no. 13, pp. 1549-60.
- Aldridge, GM, Podrebarac, DM, Greenough, WT & Weiler, IJ 2008, 'The use of total protein stains as loading controls: an alternative to high-abundance single-protein controls in semi-quantitative immunoblotting', *Journal of neuroscience methods*, vol. 172, no. 2, pp. 250-4.
- Alessi, DR, James, SR, Downes, CP, Holmes, AB, Gaffney, PR, Reese, CB & Cohen, P 1997, 'Characterization of a 3-phosphoinositide-dependent protein kinase which phosphorylates and activates protein kinase Balpha', *Curr Biol*, vol. 7, no. 4, pp. 261-9.
- Ali, SR 2014, 'Butyrate sensitising microRNAs in colorectal cancer cells', (Unpublished Honours Thesis) thesis.
- Alter, J, Lou, F, Rabinowitz, A, Yin, H, Rosenfeld, J, Wilton, SD, Partridge, TA & Lu, QL 2006, 'Systemic delivery of morpholino oligonucleotide restores dystrophin expression bodywide and improves dystrophic pathology', *Nat Med*, vol. 12, no. 2, pp. 175-7.
- Altieri, DC 2003, 'Survivin, versatile modulation of cell division and apoptosis in cancer', *Oncogene*, vol. 22, no. 53, pp. 8581-9.
- Amin, MB, Greene, FL, Edge, SB, Compton, CC, Gershenwald, JE, Brookland, RK, Meyer, L, Gress, DM, Byrd, DR & Winchester, DP 2017, 'The Eighth Edition AJCC Cancer Staging Manual: Continuing to build a bridge from a population-based to a more "personalized" approach to cancer staging', *CA Cancer J Clin*, vol. 67, no. 2, pp. 93-9.
- Anders, S, Pyl, PT & Huber, W 2015, 'HTSeq—a Python framework to work with high-throughput sequencing data', *Bioinformatics*, vol. 31, no. 2, pp. 166-9.
- Andriamihaja, M, Chaumontet, C, Tome, D & Blachier, F 2009, 'Butyrate metabolism in human colon carcinoma cells: implications concerning its growth-inhibitory effect', *J Cell Physiol*, vol. 218, no. 1, pp. 58-65.
- Androvic, P, Valihrach, L, Elling, J, Sjoback, R & Kubista, M 2017, 'Two-tailed RT-qPCR: a novel method for highly accurate miRNA quantification', *Nucleic Acids Res*, vol. 45, no. 15, p. e144.
- Armaghany, T, Wilson, JD, Chu, Q & Mills, G 2012, 'Genetic Alterations in Colorectal Cancer', *Gastrointestinal Cancer Research : GCR*, vol. 5, no. 1, pp. 19-27.

## REFERENCES

- Arun, G, Diermeier, SD & Spector, DL 2018, 'Therapeutic Targeting of Long Non-Coding RNAs in Cancer', *Trends Mol Med*, vol. 24, no. 3, pp. 257-77.
- Babu, E, Ramachandran, S, CoothanKandaswamy, V, Elangovan, S, Prasad, PD, Ganapathy, V & Thangaraju, M 2011, 'Role of SLC5A8, a plasma membrane transporter and a tumor suppressor, in the antitumor activity of dichloroacetate', *Oncogene*, vol. 30, no. 38, pp. 4026-37.
- Back, D, Villen, J, Shin, C, Camargo, FD, Gygi, SP & Bartel, DP 2008, 'The impact of microRNAs on protein output', *Nature*, vol. 455, no. 7209, pp. 64-71.
- Bakirtzi, K, Hatziapostolou, M, Karagiannides, I, Polytarchou, C, Jaeger, S, Iliopoulos, D & Pothoulakis, C 2011, 'Neurotensin signaling activates microRNAs-21 and -155 and Akt, promotes tumor growth in mice, and is increased in human colon tumors', *Gastroenterology*, vol. 141, no. 5, pp. 1749-61.e1.
- Balcells, I, Cirera, S & Busk, PK 2011, 'Specific and sensitive quantitative RT-PCR of miRNAs with DNA primers', *BMC biotechnology*, vol. 11, pp. 70-.
- Balcerczak, E, Pasz-Walczak, G, Kumor, P, Panczyk, M, Kordek, R, Wierzbicki, R & Mirowski, M 2005, 'Cyclin D1 protein and CCND1 gene expression in colorectal cancer', *Eur J Surg Oncol*, vol. 31, no. 7, pp. 721-6.
- Bandrés, E, Cubedo, E, Agirre, X, Malumbres, R, Zárata, R, Ramirez, N, Abajo, A, Navarro, A, Moreno, I, Monzó, M & García-Foncillas, J 2006, 'Identification by Real-time PCR of 13 mature microRNAs differentially expressed in colorectal cancer and non-tumoral tissues', *Molecular Cancer*, vol. 5, pp. 29-.
- Barrows, NJ, Le Sommer, C, Garcia-Blanco, MA & Pearson, JL 2010, 'Factors affecting reproducibility between genome-scale siRNA-based screens', *Journal of biomolecular screening*, vol. 15, no. 7, pp. 735-47.
- Bartel, DP 2004, 'MicroRNAs: genomics, biogenesis, mechanism, and function', *Cell*, vol. 116, no. 2, pp. 281-97.
- Bartel, DP 2009, 'MicroRNAs: target recognition and regulatory functions', *Cell*, vol. 136, no. 2, pp. 215-33.
- Bartolomei, MS, Webber, AL, Brunkow, ME & Tilghman, SM 1993, 'Epigenetic mechanisms underlying the imprinting of the mouse H19 gene', *Genes Dev*, vol. 7, no. 9, pp. 1663-73.
- Bartolomei, MS, Zemel, S & Tilghman, SM 1991, 'Parental imprinting of the mouse H19 gene', *Nature*, vol. 351, no. 6322, pp. 153-5.
- Bartova, E, Pachernik, J, Harnicarova, A, Kovarik, A, Kovarikova, M, Hofmanova, J, Skalnikova, M, Kozubek, M & Kozubek, S 2005, 'Nuclear levels and patterns of histone H3 modification and HP1 proteins after inhibition of histone deacetylases', *J Cell Sci*, vol. 118, no. Pt 21, pp. 5035-46.
- Battle, E, Henderson, JT, Beghtel, H, van den Born, MM, Sancho, E, Huls, G, Meeldijk, J, Robertson, J, van de Wetering, M, Pawson, T & Clevers, H 2002, 'Beta-catenin and

## REFERENCES

- TCF mediate cell positioning in the intestinal epithelium by controlling the expression of EphB/ephrinB', *Cell*, vol. 111, no. 2, pp. 251-63.
- Bauer-Mehren, A, Furlong, LI & Sanz, F 2009, 'Pathway databases and tools for their exploitation: benefits, current limitations and challenges', *Molecular systems biology*, vol. 5, pp. 290-.
- Bayraktar, R, Pichler, M, Kanlikilicer, P, Ivan, C, Bayraktar, E, Kahraman, N, Aslan, B, Oguztuzun, S, Ulasli, M, Arslan, A, Calin, G, Lopez-Berestein, G & Ozpolat, B 2017, 'MicroRNA 603 acts as a tumor suppressor and inhibits triple-negative breast cancer tumorigenesis by targeting elongation factor 2 kinase', *Oncotarget*, vol. 8, no. 7, pp. 11641-58.
- Beg, MS, Brenner, AJ, Sachdev, J, Borad, M, Kang, YK, Stoudemire, J, Smith, S, Bader, AG, Kim, S & Hong, DS 2017, 'Phase I study of MRX34, a liposomal miR-34a mimic, administered twice weekly in patients with advanced solid tumors', *Invest New Drugs*, vol. 35, no. 2, pp. 180-8.
- Behm-Ansmant, I, Rehwinkel, J, Doerks, T, Stark, A, Bork, P & Izaurralde, E 2006, 'mRNA degradation by miRNAs and GW182 requires both CCR4:NOT deadenylase and DCP1:DCP2 decapping complexes', *Genes Dev*, vol. 20, no. 14, pp. 1885-98.
- Behnke, MS, Fentress, SJ, Mashayekhi, M, Li, LX, Taylor, GA & Sibley, LD 2012, 'The polymorphic pseudokinase ROP5 controls virulence in *Toxoplasma gondii* by regulating the active kinase ROP18', *PLoS Pathog*, vol. 8, no. 11, p. e1002992.
- Ben-David, U, Siranosian, B, Ha, G, Tang, H, Oren, Y, Hinohara, K, Strathdee, CA, Dempster, J, Lyons, NJ, Burns, R, Nag, A, Kugener, G, Cimini, B, Tsvetkov, P, Maruvka, YE, O'Rourke, R, Garrity, A, Tubelli, AA, Bandopadhyay, P, Tsherniak, A, Vazquez, F, Wong, B, Birger, C, Ghandi, M, Thorner, AR, Bittker, JA, Meyerson, M, Getz, G, Beroukhi, R & Golub, TR 2018, 'Genetic and transcriptional evolution alters cancer cell line drug response', *Nature*, vol. 560, no. 7718, pp. 325-30.
- Bendardaf, R, El-Serafi, A, Syrjänen, K, Collan, Y & Pyrhönen, S 2017, 'The effect of vascular endothelial growth factor-1 expression on survival of advanced colorectal cancer patients', *The Libyan journal of medicine*, vol. 12, no. 1, pp. 1290741-.
- Bian, K, Fan, J, Zhang, X, Yang, XW, Zhu, HY, Wang, L, Sun, JY, Meng, YL, Cui, PC, Cheng, SY, Zhang, J, Zhao, J, Yang, AG & Zhang, R 2012, 'MicroRNA-203 leads to G1 phase cell cycle arrest in laryngeal carcinoma cells by directly targeting survivin', *FEBS Lett*, vol. 586, no. 6, pp. 804-9.
- Bian, Z, Jin, L, Zhang, J, Yin, Y, Quan, C, Hu, Y, Feng, Y, Liu, H, Fei, B, Mao, Y, Zhou, L, Qi, X, Huang, S, Hua, D, Xing, C & Huang, Z 2016, 'LncRNA-UCA1 enhances cell proliferation and 5-fluorouracil resistance in colorectal cancer by inhibiting miR-204-5p', *Sci Rep*, vol. 6, p. 23892.
- Bian, Z, Zhang, J, Li, M, Feng, Y, Wang, X, Zhang, J, Yao, S, Jin, G, Du, J, Han, W, Yin, Y, Huang, S, Fei, B, Zou, J & Huang, Z 2018, 'LncRNA-FEZF1-AS1 Promotes Tumor Proliferation and Metastasis in Colorectal Cancer by Regulating PKM2 Signaling', *Clin Cancer Res*, vol. 24, no. 19, pp. 4808-19.

## REFERENCES

- Bindea, G, Galon, J & Mlecnik, B 2013, 'CluePedia Cytoscape plugin: pathway insights using integrated experimental and in silico data', *Bioinformatics*, vol. 29, no. 5, pp. 661-3.
- Bindea, G, Mlecnik, B, Hackl, H, Charoentong, P, Tosolini, M, Kirilovsky, A, Fridman, W-H, Pagès, F, Trajanoski, Z & Galon, J 2009, 'ClueGO: a Cytoscape plug-in to decipher functionally grouped gene ontology and pathway annotation networks', *Bioinformatics*, vol. 25, no. 8, pp. 1091-3.
- Birmingham, A, Selfors, LM, Forster, T, Wrobel, D, Kennedy, CJ, Shanks, E, Santoyo-Lopez, J, Dunican, DJ, Long, A, Kelleher, D, Smith, Q, Beijersbergen, RL, Ghazal, P & Shamu, CE 2009, 'Statistical methods for analysis of high-throughput RNA interference screens', *Nat Methods*, vol. 6, no. 8, pp. 569-75.
- Biswas, SC & Greene, LA 2002, 'Nerve growth factor (NGF) down-regulates the Bcl-2 homology 3 (BH3) domain-only protein Bim and suppresses its proapoptotic activity by phosphorylation', *J Biol Chem*, vol. 277, no. 51, pp. 49511-6.
- Bleeker, FE, Felicioni, L, Buttitta, F, Lamba, S, Cardone, L, Rodolfo, M, Scarpa, A, Leenstra, S, Frattini, M, Barbareschi, M, Grammastro, MD, Sciarrotta, MG, Zanon, C, Marchetti, A & Bardelli, A 2008, 'AKT1(E17K) in human solid tumours', *Oncogene*, vol. 27, no. 42, pp. 5648-50.
- Bodmer, WF 2006, 'Cancer genetics: colorectal cancer as a model', *J Hum Genet*, vol. 51, no. 5, pp. 391-6.
- Boffa, LC, Gruss, RJ & Allfrey, VG 1981, 'Manifold effects of sodium butyrate on nuclear function. Selective and reversible inhibition of phosphorylation of histones H1 and H2A and impaired methylation of lysine and arginine residues in nuclear protein fractions', *J Biol Chem*, vol. 256, no. 18, pp. 9612-21.
- Boland, CR & Goel, A 2010, 'Microsatellite Instability in Colorectal Cancer', *Gastroenterology*, vol. 138, no. 6, pp. 2073-87.e3.
- Bolger, AM, Lohse, M & Usadel, B 2014, 'Trimmomatic: a flexible trimmer for Illumina sequence data', *Bioinformatics*, vol. 30, no. 15, pp. 2114-20.
- Bommi, PV, Dimri, M, Sahasrabudde, AA, Khandekar, J & Dimri, GP 2010, 'The polycomb group protein BMI1 is a transcriptional target of HDAC inhibitors', *Cell Cycle*, vol. 9, no. 13, pp. 2663-73.
- Bordonaro, M, Lazarova, DL, Augenlicht, LH & Sartorelli, AC 2002, 'Cell type- and promoter-dependent modulation of the Wnt signaling pathway by sodium butyrate', *Int J Cancer*, vol. 97, no. 1, pp. 42-51.
- Bordonaro, M, Lazarova, DL & Sartorelli, AC 2008, 'Butyrate and Wnt signaling: a possible solution to the puzzle of dietary fiber and colon cancer risk?', *Cell Cycle*, vol. 7, no. 9, pp. 1178-83.
- Bordonaro, M, Mariadason, JM, Aslam, F, Heerdt, BG & Augenlicht, LH 1999, 'Butyrate-induced apoptotic cascade in colonic carcinoma cells: modulation of the beta-catenin-Tcf pathway and concordance with effects of sulindac and trichostatin A but not curcumin', *Cell Growth Differ*, vol. 10, no. 10, pp. 713-20.

## REFERENCES

- Boukamp, P, Petrussevska, RT, Breitkreutz, D, Hornung, J, Markham, A & Fusenig, NE 1988, 'Normal keratinization in a spontaneously immortalized aneuploid human keratinocyte cell line', *J Cell Biol*, vol. 106, no. 3, pp. 761-71.
- Brannan, CI, Dees, EC, Ingram, RS & Tilghman, SM 1990, 'The product of the H19 gene may function as an RNA', *Mol Cell Biol*, vol. 10, no. 1, pp. 28-36.
- Brass, AL, Dykxhoorn, DM, Benita, Y, Yan, N, Engelman, A, Xavier, RJ, Lieberman, J & Elledge, SJ 2008, 'Identification of host proteins required for HIV infection through a functional genomic screen', *Science*, vol. 319, no. 5865, pp. 921-6.
- Brattain, MG, Fine, WD, Khaled, FM, Thompson, J & Brattain, DE 1981, 'Heterogeneity of malignant cells from a human colonic carcinoma', *Cancer Res*, vol. 41, no. 5, pp. 1751-6.
- Brattain, MG, Levine, AE, Chakrabarty, S, Yeoman, LC, Willson, JK & Long, B 1984, 'Heterogeneity of human colon carcinoma', *Cancer Metastasis Rev*, vol. 3, no. 3, pp. 177-91.
- Bray, F, Ferlay, J, Soerjomataram, I, Siegel, RL, Torre, LA & Jemal, A 2018, 'Global cancer statistics 2018: GLOBOCAN estimates of incidence and mortality worldwide for 36 cancers in 185 countries', *CA Cancer J Clin*, vol. 68, no. 6, pp. 394-424.
- Brenner, C, Deplus, R, Didelot, C, Lorient, A, Vire, E, De Smet, C, Gutierrez, A, Danovi, D, Bernard, D, Boon, T, Pelicci, PG, Amati, B, Kouzarides, T, de Launoit, Y, Di Croce, L & Fuks, F 2005, 'Myc represses transcription through recruitment of DNA methyltransferase corepressor', *Embo j*, vol. 24, no. 2, pp. 336-46.
- Breuer, RI, Soergel, KH, Lashner, BA, Christ, ML, Hanauer, SB, Vanaganas, A, Harig, JM, Keshavarzian, A, Robinson, M, Sellin, JH, Weinberg, D, Vidican, DE, Flemal, KL & Rademaker, AW 1997, 'Short chain fatty acid rectal irrigation for left-sided ulcerative colitis: a randomised, placebo controlled trial', *Gut*, vol. 40, no. 4, pp. 485-91.
- Brideau, C, Gunter, B, Pikounis, B & Liaw, A 2003, 'Improved statistical methods for hit selection in high-throughput screening', *Journal of biomolecular screening*, vol. 8, no. 6, pp. 634-47.
- Brink, M, de Goeij, AFPM, Weijenberg, MP, Roemen, GMJM, Lentjes, MHFM, Pachen, MMM, Smits, KM, de Bruïne, AP, Goldbohm, RA & van den Brandt, PA 2003, 'K-ras oncogene mutations in sporadic colorectal cancer in The Netherlands Cohort Study', *Carcinogenesis*, vol. 24, no. 4, pp. 703-10.
- Brockdorff, N, Ashworth, A, Kay, GF, McCabe, VM, Norris, DP, Cooper, PJ, Swift, S & Rastan, S 1992, 'The product of the mouse Xist gene is a 15 kb inactive X-specific transcript containing no conserved ORF and located in the nucleus', *Cell*, vol. 71, no. 3, pp. 515-26.
- Brown, CJ, Hendrich, BD, Rupert, JL, Lafreniere, RG, Xing, Y, Lawrence, J & Willard, HF 1992, 'The human XIST gene: analysis of a 17 kb inactive X-specific RNA that contains conserved repeats and is highly localized within the nucleus', *Cell*, vol. 71, no. 3, pp. 527-42.

## REFERENCES

- Brown, JA, Valenstein, ML, Yario, TA, Tycowski, KT & Steitz, JA 2012, 'Formation of triple-helical structures by the 3'-end sequences of MALAT1 and MENbeta noncoding RNAs', *Proc Natl Acad Sci U S A*, vol. 109, no. 47, pp. 19202-7.
- Brunet, A, Bonni, A, Zigmond, MJ, Lin, MZ, Juo, P, Hu, LS, Anderson, MJ, Arden, KC, Blenis, J & Greenberg, ME 1999, 'Akt promotes cell survival by phosphorylating and inhibiting a Forkhead transcription factor', *Cell*, vol. 96, no. 6, pp. 857-68.
- Buller, NV, Rosekrans, SL, Westerlund, J & van den Brink, GR 2012, 'Hedgehog signaling and maintenance of homeostasis in the intestinal epithelium', *Physiology (Bethesda)*, vol. 27, no. 3, pp. 148-55.
- Burn, J, Bishop, DT, Chapman, PD, Elliott, F, Bertario, L, Dunlop, MG, Eccles, D, Ellis, A, Evans, DG, Fodde, R, Maher, ER, Möslein, G, Vasen, HFA, Coaker, J, Phillips, RKS, Bülow, S & Mathers, JC 2011, 'A Randomized Placebo-Controlled Prevention Trial of Aspirin and/or Resistant Starch in Young People with Familial Adenomatous Polyposis', *Cancer Prevention Research*, vol. 4, no. 5, pp. 655-65.
- Bussemakers, MJ, van Bokhoven, A, Verhaegh, GW, Smit, FP, Karthaus, HF, Schalken, JA, Debruyne, FM, Ru, N & Isaacs, WB 1999, 'DD3: a new prostate-specific gene, highly overexpressed in prostate cancer', *Cancer Res*, vol. 59, no. 23, pp. 5975-9.
- Butkytė, S, Čiupas, L, Jakubauskienė, E, Vilys, L, Mocevicius, P, Kanopka, A & Vilkaitis, G 2016, 'Splicing-dependent expression of microRNAs of mirtron origin in human digestive and excretory system cancer cells', *Clinical Epigenetics*, vol. 8, pp. 33-.
- Cai, T, Liu, Y & Xiao, J 2018a, 'Long noncoding RNA MALAT1 knockdown reverses chemoresistance to temozolomide via promoting microRNA-101 in glioblastoma', *Cancer Med*, vol. 7, no. 4, pp. 1404-15.
- Cai, X, Liu, C, Zhang, TN, Zhu, YW, Dong, X & Xue, P 2018b, 'Down-regulation of FN1 inhibits colorectal carcinogenesis by suppressing proliferation, migration, and invasion', *J Cell Biochem*, vol. 119, no. 6, pp. 4717-28.
- Calin, GA, Dumitru, CD, Shimizu, M, Bichi, R, Zupo, S, Noch, E, Aldler, H, Rattan, S, Keating, M, Rai, K, Rassenti, L, Kipps, T, Negrini, M, Bullrich, F & Croce, CM 2002, 'Frequent deletions and down-regulation of micro- RNA genes miR15 and miR16 at 13q14 in chronic lymphocytic leukemia', *Proc Natl Acad Sci U S A*, vol. 99, no. 24, pp. 15524-9.
- Calin, GA, Liu, CG, Ferracin, M, Hyslop, T, Spizzo, R, Sevignani, C, Fabbri, M, Cimmino, A, Lee, EJ, Wojcik, SE, Shimizu, M, Tili, E, Rossi, S, Taccioli, C, Pichiorri, F, Liu, X, Zupo, S, Herlea, V, Gramantieri, L, Lanza, G, Alder, H, Rassenti, L, Volinia, S, Schmittgen, TD, Kipps, TJ, Negrini, M & Croce, CM 2007, 'Ultraconserved regions encoding ncRNAs are altered in human leukemias and carcinomas', *Cancer Cell*, vol. 12, no. 3, pp. 215-29.
- Calin, GA, Sevignani, C, Dumitru, CD, Hyslop, T, Noch, E, Yendamuri, S, Shimizu, M, Rattan, S, Bullrich, F, Negrini, M & Croce, CM 2004, 'Human microRNA genes are frequently located at fragile sites and genomic regions involved in cancers', *Proc Natl Acad Sci U S A*, vol. 101, no. 9, pp. 2999-3004.

## REFERENCES

- Cao, D, Ding, Q, Yu, W, Gao, M & Wang, Y 2016, 'Long noncoding RNA SPRY4-IT1 promotes malignant development of colorectal cancer by targeting epithelial–mesenchymal transition', *Oncotargets and therapy*, vol. 9, pp. 5417-25.
- Cao, M, Zhang, Z, Han, S & Lu, X 2019, 'Butyrate inhibits the proliferation and induces the apoptosis of colorectal cancer HCT116 cells via the deactivation of mTOR/S6K1 signaling mediated partly by SIRT1 downregulation', *Mol Med Rep*.
- Cao, Q, Liu, F, Ji, K, Liu, N, He, Y, Zhang, W & Wang, L 2017, 'MicroRNA-381 inhibits the metastasis of gastric cancer by targeting TMEM16A expression', *Journal of Experimental & Clinical Cancer Research : CR*, vol. 36, no. 1, pp. 29-.
- Cao, SS & Zhen, YS 1989, 'Potentiation of antimetabolite antitumor activity in vivo by dipyrindamole and amphotericin B', *Cancer Chemother Pharmacol*, vol. 24, no. 3, pp. 181-6.
- Cao, Y 2009, 'Positive and negative modulation of angiogenesis by VEGFR1 ligands', *Sci Signal*, vol. 2, no. 59, p. re1.
- Cappell, MS 2005, 'The pathophysiology, clinical presentation, and diagnosis of colon cancer and adenomatous polyps', *Med Clin North Am*, vol. 89, no. 1, pp. 1-42, vii.
- Cappuzzo, F, Sacconi, A, Landi, L, Ludovini, V, Biagioni, F, D'Incecco, A, Capodanno, A, Salvini, J, Corgna, E, Cupini, S, Barbara, C, Fontanini, G, Crino, L & Blandino, G 2014, 'MicroRNA signature in metastatic colorectal cancer patients treated with anti-EGFR monoclonal antibodies', *Clin Colorectal Cancer*, vol. 13, no. 1, pp. 37-45.e4.
- Carrier, F, Smith, ML, Bae, I, Kilpatrick, KE, Lansing, TJ, Chen, CY, Engelstein, M, Friend, SH, Henner, WD, Gilmer, TM & et al. 1994, 'Characterization of human Gadd45, a p53-regulated protein', *J Biol Chem*, vol. 269, no. 51, pp. 32672-7.
- Castellano, E & Downward, J 2011, 'RAS Interaction with PI3K: More Than Just Another Effector Pathway', *Genes Cancer*, vol. 2, no. 3, pp. 261-74.
- Castro-Piedras, I, Sharma, M, den Bakker, M, Molehin, D, Martinez, EG, Vartak, D, Pruitt, WM, Deitrick, J, Almodovar, S & Pruitt, K 2018, 'DVL1 and DVL3 differentially localize to CYP19A1 promoters and regulate aromatase mRNA in breast cancer cells', *Oncotarget*, vol. 9, no. 86, pp. 35639-54.
- Catela Ivkovic, T, Aralica, G, Cacev, T, Loncar, B & Kapitanovic, S 2013, 'miR-106a overexpression and pRB downregulation in sporadic colorectal cancer', *Exp Mol Pathol*, vol. 94, no. 1, pp. 148-54.
- Center, MM, Jemal, A, Smith, RA & Ward, E 2009a, 'Worldwide variations in colorectal cancer', *CA Cancer J Clin*, vol. 59, no. 6, pp. 366-78.
- Center, MM, Jemal, A & Ward, E 2009b, 'International trends in colorectal cancer incidence rates', *Cancer Epidemiol Biomarkers Prev*, vol. 18, no. 6, pp. 1688-94.
- Chai, Y, Liu, J, Zhang, Z & Liu, L 2016, 'HuR-regulated lncRNA NEAT1 stability in tumorigenesis and progression of ovarian cancer', *Cancer Med*, vol. 5, no. 7, pp. 1588-98.

## REFERENCES

- Chandrasekaran, KS, Sathyanarayanan, A & Karunakaran, D 2016, 'Downregulation of HMGB1 by miR-34a is sufficient to suppress proliferation, migration and invasion of human cervical and colorectal cancer cells', *Tumour Biol*, vol. 37, no. 10, pp. 13155-66.
- Chang, H, Wang, GN & Tao, YL 2019, 'The expression of long noncoding RNA CRCAL-3 in colorectal cancer and its impacts on cell proliferation and migration', *J Cell Biochem*.
- Chang, KH, Miller, N, Kheirelseid, EA, Ingoldsby, H, Hennessy, E, Curran, CE, Curran, S, Smith, MJ, Regan, M, McAnena, OJ & Kerin, MJ 2011, 'MicroRNA-21 and PDCD4 expression in colorectal cancer', *Eur J Surg Oncol*, vol. 37, no. 7, pp. 597-603.
- Chang, TC, Wentzel, EA, Kent, OA, Ramachandran, K, Mullendore, M, Lee, KH, Feldmann, G, Yamakuchi, M, Ferlito, M, Lowenstein, CJ, Arking, DE, Beer, MA, Maitra, A & Mendell, JT 2007, 'Transactivation of miR-34a by p53 broadly influences gene expression and promotes apoptosis', *Mol Cell*, vol. 26, no. 5, pp. 745-52.
- Chen, B, Duan, L, Yin, G, Tan, J & Jiang, X 2013a, 'Simultaneously expressed miR-424 and miR-381 synergistically suppress the proliferation and survival of renal cancer cells--Cdc2 activity is up-regulated by targeting WEE1', *Clinics (Sao Paulo, Brazil)*, vol. 68, no. 6, pp. 825-33.
- Chen, C, Li, Z, Yang, Y, Xiang, T, Song, W & Liu, S 2015, 'Microarray expression profiling of dysregulated long non-coding RNAs in triple-negative breast cancer', *Cancer Biol Ther*, vol. 16, no. 6, pp. 856-65.
- Chen, J, Chen, Y & Chen, Z 2013b, 'MiR-125a/b regulates the activation of cancer stem cells in paclitaxel-resistant colon cancer', *Cancer Invest*, vol. 31, no. 1, pp. 17-23.
- Chen, J, Wang, W, Zhang, Y, Hu, T & Chen, Y 2014, 'The roles of miR-200c in colon cancer and associated molecular mechanisms', *Tumour Biol*, vol. 35, no. 7, pp. 6475-83.
- Chen, L, Sun, H, Wang, C, Yang, Y, Zhang, M & Wong, G 2018a, 'miRNA arm switching identifies novel tumour biomarkers', *EBioMedicine*, vol. 38, pp. 37-46.
- Chen, L, Wang, X, Zhu, Y, Zhu, J & Lai, Q 2018b, 'miR-200b-3p inhibits proliferation and induces apoptosis in colorectal cancer by targeting Wnt1', *Mol Med Rep*, vol. 18, no. 3, pp. 2571-80.
- Chen, L, Yao, H, Wang, K & Liu, X 2017, 'Long Non-Coding RNA MALAT1 Regulates ZEB1 Expression by Sponging miR-143-3p and Promotes Hepatocellular Carcinoma Progression', *J Cell Biochem*, vol. 118, no. 12, pp. 4836-43.
- Chen, L, Zhang, W, Li, DY, Wang, X, Tao, Y, Zhang, Y, Dong, C, Zhao, J, Zhang, L, Zhang, X, Guo, J, Zhang, X & Liao, Q 2018c, 'Regulatory network analysis of LINC00472, a long noncoding RNA downregulated by DNA hypermethylation in colorectal cancer', *Clin Genet*, vol. 93, no. 6, pp. 1189-98.
- Chen, N, Guo, D, Xu, Q, Yang, M, Wang, D, Peng, M, Ding, Y, Wang, S & Zhou, J 2016a, 'Long non-coding RNA FEZF1-AS1 facilitates cell proliferation and migration in colorectal carcinoma', *Oncotarget*, vol. 7, no. 10, pp. 11271-83.

## REFERENCES

- Chen, X, Guo, X, Zhang, H, Xiang, Y, Chen, J, Yin, Y, Cai, X, Wang, K, Wang, G, Ba, Y, Zhu, L, Wang, J, Yang, R, Zhang, Y, Ren, Z, Zen, K, Zhang, J & Zhang, CY 2009, 'Role of miR-143 targeting KRAS in colorectal tumorigenesis', *Oncogene*, vol. 28, no. 10, pp. 1385-92.
- Chen, X, Zhang, Q, Ma, W, Lan, T, Hong, Z & Yuan, Y 2018d, 'The Abnormal Expression of MicroRNA-542-3p in Hepatocellular Carcinoma and Its Clinical Significance', *Disease markers*, vol. 2018, pp. 3973250-.
- Chen, X, Zhu, H, Wu, X, Xie, X, Huang, G, Xu, X, Li, S & Xing, C 2016b, 'Downregulated pseudogene CTNNAP1 promote tumor growth in human cancer by downregulating its cognate gene CTNNA1 expression', *Oncotarget*.
- Chen, Y, Jiang, J, Zhao, M, Luo, X, Liang, Z, Zhen, Y, Fu, Q, Deng, X, Lin, X, Li, L, Luo, R, Liu, Z & Fang, W 2016c, 'microRNA-374a suppresses colon cancer progression by directly reducing CCND1 to inactivate the PI3K/AKT pathway', *Oncotarget*, vol. 7, no. 27, pp. 41306-19.
- Cheng, Y, Li, K, Diao, D, Zhu, K, Shi, L, Zhang, H, Yuan, D, Guo, Q, Wu, X, Liu, D & Dang, C 2013, 'Expression of KIAA0101 protein is associated with poor survival of esophageal cancer patients and resistance to cisplatin treatment in vitro', *Lab Invest*, vol. 93, no. 12, pp. 1276-87.
- Chimploy, K, Díaz, GD, Li, Q, Carter, O, Dashwood, W-M, Mathews, CK, Williams, DE, Bailey, GS & Dashwood, RH 2009, 'E2F4 and ribonucleotide reductase mediate S-phase arrest in colon cancer cells treated with chlorophyllin', *International Journal of Cancer*, vol. 125, no. 9, pp. 2086-94.
- Choi, SW, Kim, HW & Nam, JW 2018, 'The small peptide world in long noncoding RNAs', *Brief Bioinform.*
- Chou, C-H, Shrestha, S, Yang, C-D, Chang, N-W, Lin, Y-L, Liao, K-W, Huang, W-C, Sun, T-H, Tu, S-J, Lee, W-H, Chiew, M-Y, Tai, C-S, Wei, T-Y, Tsai, T-R, Huang, H-T, Wang, C-Y, Wu, H-Y, Ho, S-Y, Chen, P-R, Chuang, C-H, Hsieh, P-J, Wu, Y-S, Chen, W-L, Li, M-J, Wu, Y-C, Huang, X-Y, Ng, FL, Buddhakosai, W, Huang, P-C, Lan, K-C, Huang, C-Y, Weng, S-L, Cheng, Y-N, Liang, C, Hsu, W-L & Huang, H-D 2018a, 'miRTarBase update 2018: a resource for experimentally validated microRNA-target interactions', *Nucleic Acids Research*, vol. 46, no. D1, pp. D296-D302.
- Chou, CH, Shrestha, S, Yang, CD, Chang, NW, Lin, YL, Liao, KW, Huang, WC, Sun, TH, Tu, SJ, Lee, WH, Chiew, MY, Tai, CS, Wei, TY, Tsai, TR, Huang, HT, Wang, CY, Wu, HY, Ho, SY, Chen, PR, Chuang, CH, Hsieh, PJ, Wu, YS, Chen, WL, Li, MJ, Wu, YC, Huang, XY, Ng, FL, Buddhakosai, W, Huang, PC, Lan, KC, Huang, CY, Weng, SL, Cheng, YN, Liang, C, Hsu, WL & Huang, HD 2018b, 'miRTarBase update 2018: a resource for experimentally validated microRNA-target interactions', *Nucleic Acids Res*, vol. 46, no. D1, pp. D296-d302.
- Cimmino, A, Calin, GA, Fabbri, M, Iorio, MV, Ferracin, M, Shimizu, M, Wojcik, SE, Aqeilan, RI, Zupo, S, Dono, M, Rassenti, L, Alder, H, Volinia, S, Liu, CG, Kipps, TJ, Negrini, M & Croce, CM 2005, 'miR-15 and miR-16 induce apoptosis by targeting BCL2', *Proc Natl Acad Sci U S A*, vol. 102, no. 39, pp. 13944-9.

## REFERENCES

- Clapé, C, Fritz, V, Henriquet, C, Apparailly, F, Fernandez, PL, Iborra, F, Avancès, C, Villalba, M, Culine, S & Fajas, L 2009, 'miR-143 Interferes with ERK5 Signaling, and Abrogates Prostate Cancer Progression in Mice', *PLoS One*, vol. 4, no. 10, p. e7542.
- Clark, MB, Johnston, RL, Inostroza-Ponta, M, Fox, AH, Fortini, E, Moscato, P, Dinger, ME & Mattick, JS 2012, 'Genome-wide analysis of long noncoding RNA stability', *Genome Res*, vol. 22, no. 5, pp. 885-98.
- Clarke, JM, Bird, AR, Topping, DL & Cobiac, L 2007, 'Excretion of starch and esterified short-chain fatty acids by ileostomy subjects after the ingestion of acylated starches', *Am J Clin Nutr*, vol. 86, no. 4, pp. 1146-51.
- Cleeland, CS, Allen, JD, Roberts, SA, Brell, JM, Giralt, SA, Khakoo, AY, Kirch, RA, Kwitkowski, VE, Liao, Z & Skillings, J 2012, 'Reducing the toxicity of cancer therapy: recognizing needs, taking action', *Nat Rev Clin Oncol*, vol. 9, no. 8, pp. 471-8.
- Clemens, MR, Gladkov, OA, Gartner, E, Vladimirov, V, Crown, J, Steinberg, J, Jie, F & Keating, A 2015, 'Phase II, multicenter, open-label, randomized study of YM155 plus docetaxel as first-line treatment in patients with HER2-negative metastatic breast cancer', *Breast Cancer Res Treat*, vol. 149, no. 1, pp. 171-9.
- Clemson, CM, McNeil, JA, Willard, HF & Lawrence, JB 1996, 'XIST RNA paints the inactive X chromosome at interphase: evidence for a novel RNA involved in nuclear/chromosome structure', *J Cell Biol*, vol. 132, no. 3, pp. 259-75.
- Compton, T 1993, 'An immortalized human fibroblast cell line is permissive for human cytomegalovirus infection', *J Virol*, vol. 67, no. 6, pp. 3644-8.
- Corvinus, FM, Orth, C, Moriggl, R, Tsareva, SA, Wagner, S, Pfitzner, EB, Baus, D, Kaufmann, R, Huber, LA, Zatloukal, K, Beug, H, Ohlschläger, P, Schütz, A, Halbhuber, K-J & Friedrich, K 2005, 'Persistent STAT3 activation in colon cancer is associated with enhanced cell proliferation and tumor growth', *Neoplasia*, vol. 7, no. 6, pp. 545-55.
- Croft, D, O'Kelly, G, Wu, G, Haw, R, Gillespie, M, Matthews, L, Caudy, M, Garapati, P, Gopinath, G, Jassal, B, Jupe, S, Kalatskaya, I, Mahajan, S, May, B, Ndegwa, N, Schmidt, E, Shamovsky, V, Yung, C, Birney, E, Hermjakob, H, D'Eustachio, P & Stein, L 2011, 'Reactome: a database of reactions, pathways and biological processes', *Nucleic Acids Research*, vol. 39, no. Database issue, pp. D691-D7.
- Cui, J 2015, 'MiR-16 family as potential diagnostic biomarkers for cancer: a systematic review and meta-analysis', *International Journal of Clinical and Experimental Medicine*, vol. 8, no. 2, pp. 1703-14.
- Cui, M, Chen, M, Shen, Z, Wang, R, Fang, X & Song, B 2019, 'LncRNA-UCA1 modulates progression of colon cancer through regulating the miR-28-5p/HOXB3 axis', *J Cell Biochem*.
- Cui, S, Yang, X, Zhang, L, Zhao, Y & Yan, W 2018, 'LncRNA MAFG-AS1 promotes the progression of colorectal cancer by sponging miR-147b and activation of NDUFA4', *Biochem Biophys Res Commun*, vol. 506, no. 1, pp. 251-8.
- Cummings, JH 1981, 'Short chain fatty acids in the human colon', *Gut*, vol. 22, no. 9, pp. 763-79.

## REFERENCES

- Cummings, JH 1984, 'Colonic absorption: the importance of short chain fatty acids in man', *Scandinavian journal of gastroenterology. Supplement*, vol. 93, pp. 89-99.
- Cummings, JH, Pomare, EW, Branch, WJ, Naylor, CP & Macfarlane, GT 1987, 'Short chain fatty acids in human large intestine, portal, hepatic and venous blood', *Gut*, vol. 28, no. 10, pp. 1221-7.
- Cummins, JM, He, Y, Leary, RJ, Pagliarini, R, Diaz, LA, Jr., Sjoblom, T, Barad, O, Bentwich, Z, Szafranska, AE, Labourier, E, Raymond, CK, Roberts, BS, Juhl, H, Kinzler, KW, Vogelstein, B & Velculescu, VE 2006, 'The colorectal microRNAome', *Proc Natl Acad Sci U S A*, vol. 103, no. 10, pp. 3687-92.
- Cursons, J, Pillman, KA, Scheer, KG, Gregory, PA, Foroutan, M, Hadiyah-Zadeh, S, Toubia, J, Crampin, EJ, Goodall, GJ, Bracken, CP & Davis, MJ 2018, 'Combinatorial Targeting by MicroRNAs Co-ordinates Post-transcriptional Control of EMT', *Cell Syst*, vol. 7, no. 1, pp. 77-91.e7.
- Daehn, IS, Varelias, A & Rayner, TE 2006, 'Sodium butyrate induced keratinocyte apoptosis', *Apoptosis*, vol. 11, no. 8, pp. 1379-90.
- Dai, M, Chen, X, Mo, S, Li, J, Huang, Z, Huang, S, Xu, J, He, B, Zou, Y, Chen, J & Dai, S 2017, 'Meta-signature LncRNAs serve as novel biomarkers for colorectal cancer: integrated bioinformatics analysis, experimental validation and diagnostic evaluation', *Sci Rep*, vol. 7, p. 46572.
- Daly, K, Cuff, MA, Fung, F & Shirazi-Beechey, SP 2005, 'The importance of colonic butyrate transport to the regulation of genes associated with colonic tissue homeostasis', *Biochem Soc Trans*, vol. 33, no. Pt 4, pp. 733-5.
- Daly, K & Shirazi-Beechey, SP 2006, 'Microarray analysis of butyrate regulated genes in colonic epithelial cells', *DNA Cell Biol*, vol. 25, no. 1, pp. 49-62.
- Danese, E & Montagnana, M 2017, 'Epigenetics of colorectal cancer: emerging circulating diagnostic and prognostic biomarkers', *Annals of translational medicine*, vol. 5, no. 13, pp. 279-.
- Dang, DT, Mahatan, CS, Dang, LH, Agboola, IA & Yang, VW 2001, 'Expression of the gut-enriched Kruppel-like factor (Kruppel-like factor 4) gene in the human colon cancer cell line RKO is dependent on CDX2', *Oncogene*, vol. 20, no. 35, pp. 4884-90.
- Daniel, NN & Korsmeyer, SJ 2004, 'Cell death: critical control points', *Cell*, vol. 116, no. 2, pp. 205-19.
- Danielsen, SA, Lind, GE, Bjornstlett, M, Meling, GI, Rognum, TO, Heim, S & Lothe, RA 2008, 'Novel mutations of the suppressor gene PTEN in colorectal carcinomas stratified by microsatellite instability- and TP53 mutation- status', *Hum Mutat*, vol. 29, no. 11, pp. E252-62.
- Dannenber, AJ, Altorki, NK, Boyle, JO, Dang, C, Howe, LR, Weksler, BB & Subbaramaiah, K 2001, 'Cyclo-oxygenase 2: a pharmacological target for the prevention of cancer', *Lancet Oncol*, vol. 2, no. 9, pp. 544-51.

## REFERENCES

- Datta, SR, Dudek, H, Tao, X, Masters, S, Fu, H, Gotoh, Y & Greenberg, ME 1997, 'Akt phosphorylation of BAD couples survival signals to the cell-intrinsic death machinery', *Cell*, vol. 91, no. 2, pp. 231-41.
- Davido, DJ, Richter, F, Boxberger, F, Stahl, A, Menzel, T, Luhrs, H, Loffler, S, Dusel, G, Rapp, UR & Scheppach, W 2001, 'Butyrate and propionate downregulate ERK phosphorylation in HT-29 colon carcinoma cells prior to differentiation', *Eur J Cancer Prev*, vol. 10, no. 4, pp. 313-21.
- Davie, JR 2003, 'Inhibition of Histone Deacetylase Activity by Butyrate', *The Journal of Nutrition*, vol. 133, no. 7, pp. 2485S-93S.
- Davies, H, Bignell, GR, Cox, C, Stephens, P, Edkins, S, Clegg, S, Teague, J, Woffendin, H, Garnett, MJ, Bottomley, W, Davis, N, Dicks, E, Ewing, R, Floyd, Y, Gray, K, Hall, S, Hawes, R, Hughes, J, Kosmidou, V, Menzies, A, Mould, C, Parker, A, Stevens, C, Watt, S, Hooper, S, Wilson, R, Jayatilake, H, Gusterson, BA, Cooper, C, Shipley, J, Hargrave, D, Pritchard-Jones, K, Maitland, N, Chenevix-Trench, G, Riggins, GJ, Bigner, DD, Palmieri, G, Cossu, A, Flanagan, A, Nicholson, A, Ho, JW, Leung, SY, Yuen, ST, Weber, BL, Seigler, HF, Darrow, TL, Paterson, H, Marais, R, Marshall, CJ, Wooster, R, Stratton, MR & Futreal, PA 2002, 'Mutations of the BRAF gene in human cancer', *Nature*, vol. 417, no. 6892, pp. 949-54.
- Davies, RJ, Miller, R & Coleman, N 2005, 'Colorectal cancer screening: prospects for molecular stool analysis', *Nature Reviews Cancer*, vol. 5, no. 3, pp. 199-209.
- Davis, PK, Ho, A & Dowdy, SF 2001, 'Biological methods for cell-cycle synchronization of mammalian cells', *Biotechniques*, vol. 30, no. 6, pp. 1322-6, 8, 30-1.
- Day, FL, Jorissen, RN, Lipton, L, Mouradov, D, Sakthianandeswaren, A, Christie, M, Li, S, Tsui, C, Tie, J, Desai, J, Xu, ZZ, Molloy, P, Whitehall, V, Leggett, BA, Jones, IT, McLaughlin, S, Ward, RL, Hawkins, NJ, Ruzskiewicz, AR, Moore, J, Busam, D, Zhao, Q, Strausberg, RL, Gibbs, P & Sieber, OM 2013, 'PIK3CA and PTEN gene and exon mutation-specific clinicopathologic and molecular associations in colorectal cancer', *Clin Cancer Res*, vol. 19, no. 12, pp. 3285-96.
- de Voer, RM, Hahn, MM, Weren, RD, Mensenkamp, AR, Gilissen, C, van Zelst-Stams, WA, Spruijt, L, Kets, CM, Zhang, J, Venselaar, H, Vreede, L, Schubert, N, Tychon, M, Derks, R, Schackert, HK, Geurts van Kessel, A, Hoogerbrugge, N, Ligtenberg, MJ & Kuiper, RP 2016, 'Identification of Novel Candidate Genes for Early-Onset Colorectal Cancer Susceptibility', *PLoS Genet*, vol. 12, no. 2, p. e1005880.
- Del Vecchio, G, De Vito, F, Saunders, SJ, Risi, A, Mannironi, C, Bozzoni, I & Presutti, C 2016, 'RNA-binding protein HuR and the members of the miR-200 family play an unconventional role in the regulation of c-Jun mRNA', *Rna*, vol. 22, no. 10, pp. 1510-21.
- Demchenko, AP 2013, 'Beyond annexin V: fluorescence response of cellular membranes to apoptosis', *Cytotechnology*, vol. 65, no. 2, pp. 157-72.
- Deng, B, Wang, B, Fang, J, Zhu, X, Cao, Z, Lin, Q, Zhou, L & Sun, X 2016, 'MiRNA-203 suppresses cell proliferation, migration and invasion in colorectal cancer via targeting of EIF5A2', *Sci Rep*, vol. 6, p. 28301.

## REFERENCES

- Deng, Q, He, B, Gao, T, Pan, Y, Sun, H, Xu, Y, Li, R, Ying, H, Wang, F, Liu, X, Chen, J & Wang, S 2014, 'Up-regulation of 91H promotes tumor metastasis and predicts poor prognosis for patients with colorectal cancer', *PLoS One*, vol. 9, no. 7, p. e103022.
- Denli, AM, Tops, BB, Plasterk, RH, Ketting, RF & Hannon, GJ 2004, 'Processing of primary microRNAs by the Microprocessor complex', *Nature*, vol. 432, no. 7014, pp. 231-5.
- Derrien, T, Johnson, R, Bussotti, G, Tanzer, A, Djebali, S, Tilgner, H, Guernec, G, Martin, D, Merkel, A, Knowles, DG, Lagarde, J, Veeravalli, L, Ruan, X, Ruan, Y, Lassmann, T, Carninci, P, Brown, JB, Lipovich, L, Gonzalez, JM, Thomas, M, Davis, CA, Shiekhattar, R, Gingeras, TR, Hubbard, TJ, Notredame, C, Harrow, J & Guigo, R 2012, 'The GENCODE v7 catalog of human long noncoding RNAs: analysis of their gene structure, evolution, and expression', *Genome Res*, vol. 22, no. 9, pp. 1775-89.
- Dhir, A, Dhir, S, Proudfoot, NJ & Jopling, CL 2015, 'Microprocessor mediates transcriptional termination of long noncoding RNA transcripts hosting microRNAs', *Nat Struct Mol Biol*, vol. 22, no. 4, pp. 319-27.
- Di Fiore, F, Blanchard, F, Charbonnier, F, Le Pessot, F, Lamy, A, Galais, MP, Bastit, L, Killian, A, Sesboue, R, Tuech, JJ, Queuniet, AM, Paillot, B, Sabourin, JC, Michot, F, Michel, P & Frebourg, T 2007, 'Clinical relevance of KRAS mutation detection in metastatic colorectal cancer treated by Cetuximab plus chemotherapy', *Br J Cancer*, vol. 96, no. 8, pp. 1166-9.
- Diehl, JA, Cheng, M, Roussel, MF & Sherr, CJ 1998, 'Glycogen synthase kinase-3beta regulates cyclin D1 proteolysis and subcellular localization', *Genes Dev*, vol. 12, no. 22, pp. 3499-511.
- Dijkers, PF, Medema, RH, Pals, C, Banerji, L, Thomas, NS, Lam, EW, Burgering, BM, Raaijmakers, JA, Lammers, JW, Koenderman, L & Coffey, PJ 2000, 'Forkhead transcription factor FKHR-L1 modulates cytokine-dependent transcriptional regulation of p27(KIP1)', *Mol Cell Biol*, vol. 20, no. 24, pp. 9138-48.
- Ding, H, Han, C, Guo, D, Wang, D, Chen, CS & D'Ambrosio, SM 2008, 'OSU03012 activates Erk1/2 and Cdks leading to the accumulation of cells in the S-phase and apoptosis', *Int J Cancer*, vol. 123, no. 12, pp. 2923-30.
- Ding, J, Li, J, Wang, H, Tian, Y, Xie, M, He, X, Ji, H, Ma, Z, Hui, B, Wang, K & Ji, G 2017, 'Long noncoding RNA CRNDE promotes colorectal cancer cell proliferation via epigenetically silencing DUSP5/CDKN1A expression', *Cell Death Dis*, vol. 8, no. 8, pp. e2997-e.
- Ding, J, Lu, B, Wang, J, Wang, J, Shi, Y, Lian, Y, Zhu, Y, Wang, J, Fan, Y, Wang, Z, De, W & Wang, K 2015, 'Long non-coding RNA Loc554202 induces apoptosis in colorectal cancer cells via the caspase cleavage cascades', *J Exp Clin Cancer Res*, vol. 34, p. 100.
- Dinger, ME, Pang, KC, Mercer, TR & Mattick, JS 2008, 'Differentiating Protein-Coding and Noncoding RNA: Challenges and Ambiguities', *PLoS Computational Biology*, vol. 4, no. 11, p. e1000176.
- Diosdado, B, van de Wiel, MA, Terhaar Sive Droste, JS, Mongera, S, Postma, C, Meijerink, WJ, Carvalho, B & Meijer, GA 2009, 'MiR-17-92 cluster is associated with

## REFERENCES

- 13q gain and c-myc expression during colorectal adenoma to adenocarcinoma progression', *Br J Cancer*, vol. 101, no. 4, pp. 707-14.
- Dobin, A, Davis, CA, Schlesinger, F, Drenkow, J, Zaleski, C, Jha, S, Batut, P, Chaisson, M & Gingeras, TR 2013, 'STAR: ultrafast universal RNA-seq aligner', *Bioinformatics*, vol. 29, no. 1, pp. 15-21.
- Domina, AM, Vrana, JA, Gregory, MA, Hann, SR & Craig, RW 2004, 'MCL1 is phosphorylated in the PEST region and stabilized upon ERK activation in viable cells, and at additional sites with cytotoxic okadaic acid or taxol', *Oncogene*, vol. 23, no. 31, pp. 5301-15.
- Dong, D, Mu, Z, Zhao, C & Sun, M 2018a, 'ZFAS1: a novel tumor-related long non-coding RNA', *Cancer Cell International*, vol. 18, p. 125.
- Dong, H, Hu, J, Zou, K, Ye, M, Chen, Y, Wu, C, Chen, X & Han, M 2019, 'Activation of LncRNA TINCR by H3K27 acetylation promotes Trastuzumab resistance and epithelial-mesenchymal transition by targeting MicroRNA-125b in breast Cancer', *Mol Cancer*, vol. 18, no. 1, p. 3.
- Dong, L, Hong, H, Chen, X, Huang, Z, Wu, W & Wu, F 2018b, 'LINC02163 regulates growth and epithelial-to-mesenchymal transition phenotype via miR-593-3p/FOXK1 axis in gastric cancer cells', *Artif Cells Nanomed Biotechnol*, vol. 46, no. sup2, pp. 607-15.
- Dong, L, Lin, W, Qi, P, Xu, MD, Wu, X, Ni, S, Huang, D, Weng, WW, Tan, C, Sheng, W, Zhou, X & Du, X 2016, 'Circulating Long RNAs in Serum Extracellular Vesicles: Their Characterization and Potential Application as Biomarkers for Diagnosis of Colorectal Cancer', *Cancer Epidemiol Biomarkers Prev*, vol. 25, no. 7, pp. 1158-66.
- Donohoe, DR, Collins, LB, Wali, A, Bigler, R, Sun, W & Bultman, SJ 2012, 'The Warburg Effect Dictates the Mechanism of Butyrate Mediated Histone Acetylation and Cell Proliferation', *Molecular Cell*, vol. 48, no. 4, pp. 612-26.
- Donohoe, DR, Holley, D, Collins, LB, Montgomery, SA, Whitmore, AC, Hillhouse, A, Curry, KP, Renner, SW, Greenwalt, A, Ryan, EP, Godfrey, V, Heise, MT, Threadgill, DS, Han, A, Swenberg, JA, Threadgill, DW & Bultman, SJ 2014, 'A Gnotobiotic Mouse Model Demonstrates that Dietary Fiber Protects Against Colorectal Tumorigenesis in a Microbiota- and Butyrate-Dependent Manner', *Cancer discovery*, vol. 4, no. 12, pp. 1387-97.
- Driscoll, DL, Chakravarty, A, Bowman, D, Shinde, V, Lasky, K, Shi, J, Vos, T, Stringer, B, Amidon, B, D'Amore, N & Hyer, ML 2014, 'Plk1 inhibition causes post-mitotic DNA damage and senescence in a range of human tumor cell lines', *PLoS One*, vol. 9, no. 11, pp. e111060-e.
- Dronamraju, SS, Coxhead, JM, Kelly, SB, Burn, J & Mathers, JC 2009, 'Cell kinetics and gene expression changes in colorectal cancer patients given resistant starch: a randomised controlled trial', *Gut*, vol. 58, no. 3, pp. 413-20.
- Duan, H, Heckman, CA & Boxer, LM 2005, 'Histone deacetylase inhibitors down-regulate bcl-2 expression and induce apoptosis in t(14;18) lymphomas', *Mol Cell Biol*, vol. 25, no. 5, pp. 1608-19.

## REFERENCES

- Duan, W, Du, L, Jiang, X, Wang, R, Yan, S, Xie, Y, Yan, K, Wang, Q, Wang, L, Zhang, X, Pan, H, Yang, Y & Wang, C 2016, 'Identification of a serum circulating lncRNA panel for the diagnosis and recurrence prediction of bladder cancer', *Oncotarget*, vol. 7, no. 48, pp. 78850-8.
- Dunn, C, Wiltshire, C, MacLaren, A & Gillespie, DA 2002, 'Molecular mechanism and biological functions of c-Jun N-terminal kinase signalling via the c-Jun transcription factor', *Cell Signal*, vol. 14, no. 7, pp. 585-93.
- Duval, K, Grover, H, Han, L-H, Mou, Y, Pegoraro, AF, Fredberg, J & Chen, Z 2017, 'Modeling Physiological Events in 2D vs. 3D Cell Culture', *Physiology (Bethesda)*, vol. 32, no. 4, pp. 266-77.
- Dweep, H, Sticht, C, Pandey, P & Gretz, N 2011, 'miRWalk--database: prediction of possible miRNA binding sites by "walking" the genes of three genomes', *J Biomed Inform*, vol. 44, no. 5, pp. 839-47.
- Edgar, R, Domrachev, M & Lash, AE 2002, 'Gene Expression Omnibus: NCBI gene expression and hybridization array data repository', *Nucleic Acids Res*, vol. 30, no. 1, pp. 207-10.
- Eiring, AM, Harb, JG, Neviani, P, Garton, C, Oaks, JJ, Spizzo, R, Liu, S, Schwind, S, Santhanam, R, Hickey, CJ, Becker, H, Chandler, JC, Andino, R, Cortes, J, Hokland, P, Huettner, CS, Bhatia, R, Roy, DC, Liebhaber, SA, Caligiuri, MA, Marcucci, G, Garzon, R, Croce, CM, Calin, GA & Perrotti, D 2010, 'miR-328 functions as an RNA decoy to modulate hnRNP E2 regulation of mRNA translation in leukemic blasts', *Cell*, vol. 140, no. 5, pp. 652-65.
- Ellis, BC, Molloy, PL & Graham, LD 2012, 'CRNDE: A Long Non-Coding RNA Involved in Cancer, Neurobiology, and DEvelopment', *Front Genet*, vol. 3, p. 270.
- Elmore, S 2007, 'Apoptosis: a review of programmed cell death', *Toxicologic pathology*, vol. 35, no. 4, pp. 495-516.
- Emenaker, NJ, Calaf, GM, Cox, D, Basson, MD & Qureshi, N 2001, 'Short-chain fatty acids inhibit invasive human colon cancer by modulating uPA, TIMP-1, TIMP-2, mutant p53, Bcl-2, Bax, p21 and PCNA protein expression in an in vitro cell culture model', *J Nutr*, vol. 131, no. 11 Suppl, pp. 3041s-6s.
- Emmrich, S, Engeland, F, El-Khatib, M, Henke, K, Obulkasim, A, Schoning, J, Katsman-Kuipers, JE, Michel Zwaan, C, Pich, A, Stary, J, Baruchel, A, de Haas, V, Reinhardt, D, Fornerod, M, van den Heuvel-Eibrink, MM & Klusmann, JH 2016, 'miR-139-5p controls translation in myeloid leukemia through EIF4G2', *Oncogene*, vol. 35, no. 14, pp. 1822-31.
- Enright, A, John, B, Gaul, U, Tuschl, T, Sander, C & Marks, D 2003, 'MicroRNA targets in Drosophila', *Genome Biology*, vol. 5, no. 1, p. R1.
- Fabian, MR, Sonenberg, N & Filipowicz, W 2010, 'Regulation of mRNA translation and stability by microRNAs', *Annu Rev Biochem*, vol. 79, pp. 351-79.

## REFERENCES

- Fan, H, Zhu, JH & Yao, XQ 2018, 'Knockdown of long noncoding RNA PVT1 reverses multidrug resistance in colorectal cancer cells', *Mol Med Rep*, vol. 17, no. 6, pp. 8309-15.
- Fang, JY & Richardson, BC 2005, 'The MAPK signalling pathways and colorectal cancer', *Lancet Oncol*, vol. 6, no. 5, pp. 322-7.
- Fang, Y & Eglen, RM 2017, 'Three-Dimensional Cell Cultures in Drug Discovery and Development', *SLAS discovery : advancing life sciences R & D*, vol. 22, no. 5, pp. 456-72.
- Farin, HF, Jordens, I, Mosa, MH, Basak, O, Korving, J, Tauriello, DV, de Punder, K, Angers, S, Peters, PJ, Maurice, MM & Clevers, H 2016, 'Visualization of a short-range Wnt gradient in the intestinal stem-cell niche', *Nature*, vol. 530, no. 7590, pp. 340-3.
- Fasulo, B, Koyama, C, Yu, KR, Homola, EM, Hsieh, TS, Campbell, SD & Sullivan, W 2012, 'Chk1 and Wee1 kinases coordinate DNA replication, chromosome condensation, and anaphase entry', *Mol Biol Cell*, vol. 23, no. 6, pp. 1047-57.
- Fearnhead, NS, Britton, MP & Bodmer, WF 2001, 'The ABC of APC', *Hum Mol Genet*, vol. 10, no. 7, pp. 721-33.
- Fearon & Vogelstein, B 1990, 'A genetic model for colorectal tumorigenesis', *Cell*, vol. 61, no. 5, pp. 759-67.
- Fearon, ER 2011, 'Molecular Genetics of Colorectal Cancer', *Annual Review of Pathology: Mechanisms of Disease*, vol. 6, no. 1, pp. 479-507.
- Ferracin, M, Bassi, C, Pedriali, M, Pagotto, S, D'Abundo, L, Zagatti, B, Corra, F, Musa, G, Callegari, E, Lupini, L, Volpato, S, Querzoli, P & Negrini, M 2013, 'miR-125b targets erythropoietin and its receptor and their expression correlates with metastatic potential and ERBB2/HER2 expression', *Mol Cancer*, vol. 12, no. 1, p. 130.
- Ferrandez, A, Prescott, S & Burt, RW 2003, 'COX-2 and colorectal cancer', *Curr Pharm Des*, vol. 9, no. 27, pp. 2229-51.
- Fesler, A, Liu, H & Ju, J 2017, 'Modified miR-15a has therapeutic potential for improving treatment of advanced stage colorectal cancer through inhibition of BCL2, BMI1, YAP1 and DCLK1', *Oncotarget*, vol. 9, no. 2, pp. 2367-83.
- Filipowicz, W, Bhattacharyya, SN & Sonenberg, N 2008, 'Mechanisms of post-transcriptional regulation by microRNAs: are the answers in sight?', *Nat Rev Genet*, vol. 9, no. 2, pp. 102-14.
- Fodde, R 2002, 'The APC gene in colorectal cancer', *European Journal of Cancer*, vol. 38, no. 7, pp. 867-71.
- Forbes, SA, Bindal, N, Bamford, S, Cole, C, Kok, CY, Beare, D, Jia, M, Shepherd, R, Leung, K, Menzies, A, Teague, JW, Campbell, PJ, Stratton, MR & Futreal, PA 2011, 'COSMIC: mining complete cancer genomes in the Catalogue of Somatic Mutations in Cancer', *Nucleic Acids Research*, vol. 39, no. Database issue, pp. D945-D50.
- Francipane, MG & Lagasse, E 2014, 'mTOR pathway in colorectal cancer: an update', *Oncotarget*, vol. 5, no. 1, pp. 49-66.

## REFERENCES

- Fre, S, Huyghe, M, Mourikis, P, Robine, S, Louvard, D & Artavanis-Tsakonas, S 2005, 'Notch signals control the fate of immature progenitor cells in the intestine', *Nature*, vol. 435, no. 7044, pp. 964-8.
- Fretheim, K 1983, 'Polycyclic aromatic hydrocarbons in grilled meat products—A review', *Food Chemistry*, vol. 10, no. 2, pp. 129-39.
- Friedman, RC, Farh, KK, Burge, CB & Bartel, DP 2009, 'Most mammalian mRNAs are conserved targets of microRNAs', *Genome Res*, vol. 19, no. 1, pp. 92-105.
- Fu, LL, Xie, T, Zhang, SY & Liu, B 2014, 'Eukaryotic elongation factor-2 kinase (eEF2K): a potential therapeutic target in cancer', *Apoptosis*, vol. 19, no. 10, pp. 1527-31.
- Fu, Q, Zhang, J, Xu, X, Qian, F, Feng, K & Ma, J 2016, 'miR-203 is a predictive biomarker for colorectal cancer and its expression is associated with BIRC5', *Tumour Biol*.
- Fu, S, Wang, Y, Keyomarsi, K, Meric-Bernstam, F & Meric-Bernstein, F 2018, 'Strategic development of AZD1775, a Wee1 kinase inhibitor, for cancer therapy', *Expert Opin Investig Drugs*, vol. 27, no. 9, pp. 741-51.
- Fuchs, P, Strehl, S, Dworzak, M, Himmler, A & Ambros, PF 1992, 'Structure of the human TNF receptor 1 (p60) gene (TNFR1) and localization to chromosome 12p13 [corrected]', *Genomics*, vol. 13, no. 1, pp. 219-24.
- Fujino, Y, Takeishi, S, Nishida, K, Okamoto, K, Mugeruma, N, Kimura, T, Kitamura, S, Miyamoto, H, Fujimoto, A, Higashijima, J, Shimada, M, Rokutan, K & Takayama, T 2017, 'Downregulation of microRNA-100/microRNA-125b is associated with lymph node metastasis in early colorectal cancer with submucosal invasion', *Cancer Sci*, vol. 108, no. 3, pp. 390-7.
- Fung, KY, Cosgrove, L, Lockett, T, Head, R & Topping, DL 2012, 'A review of the potential mechanisms for the lowering of colorectal oncogenesis by butyrate', *Br J Nutr*, vol. 108, no. 5, pp. 820-31.
- Furi, I, Kalmar, A, Wichmann, B, Spisak, S, Scholler, A, Bartak, B, Tulassay, Z & Molnar, B 2015, 'Cell Free DNA of Tumor Origin Induces a 'Metastatic' Expression Profile in HT-29 Cancer Cell Line', *PLoS One*, vol. 10, no. 7, p. e0131699.
- Fuziwara, CS & Kimura, ET 2015, 'Insights into Regulation of the miR-17-92 Cluster of miRNAs in Cancer', *Frontiers in medicine*, vol. 2, pp. 64-.
- Gagnon, KT, Li, L, Chu, Y, Janowski, BA & Corey, DR 2014, 'RNAi factors are present and active in human cell nuclei', *Cell Rep*, vol. 6, no. 1, pp. 211-21.
- Galluzzi, L, Morselli, E, Vitale, I, Kepp, O, Senovilla, L, Criollo, A, Servant, N, Paccard, C, Hupe, P, Robert, T, Ripoche, H, Lazar, V, Harel-Bellan, A, Dessen, P, Barillot, E & Kroemer, G 2010, 'miR-181a and miR-630 regulate cisplatin-induced cancer cell death', *Cancer Res*, vol. 70, no. 5, pp. 1793-803.
- Gao, C & Chen, YG 2010, 'Dishevelled: The hub of Wnt signaling', *Cell Signal*, vol. 22, no. 5, pp. 717-27.

## REFERENCES

- Gao, F & Wang, W 2015, 'MicroRNA-96 promotes the proliferation of colorectal cancer cells and targets tumor protein p53 inducible nuclear protein 1, forkhead box protein O1 (FOXO1) and FOXO3a', *Mol Med Rep*, vol. 11, no. 2, pp. 1200-6.
- Gao, Q, Xie, H, Zhan, H, Li, J, Liu, Y & Huang, W 2017, 'Prognostic Values of Long Noncoding RNA GAS5 in Various Carcinomas: An Updated Systematic Review and Meta-Analysis', *Frontiers in physiology*, vol. 8, pp. 814-.
- Gao, Y, Zeng, F, Wu, JY, Li, HY, Fan, JJ, Mai, L, Zhang, J, Ma, DM, Li, Y & Song, FZ 2015, 'MiR-335 inhibits migration of breast cancer cells through targeting oncoprotein c-Met', *Tumour Biol*, vol. 36, no. 4, pp. 2875-83.
- Garg, H, Suri, P, Gupta, JC, Talwar, GP & Dubey, S 2016, 'Survivin: a unique target for tumor therapy', *Cancer Cell International*, vol. 16, p. 49.
- Garzon, R, Fabbri, M, Cimmino, A, Calin, GA & Croce, CM 2006, 'MicroRNA expression and function in cancer', *Trends Mol Med*, vol. 12, no. 12, pp. 580-7.
- Ge, X, Chen, Y, Liao, X, Liu, D, Li, F, Ruan, H & Jia, W 2013, 'Overexpression of long noncoding RNA PCAT-1 is a novel biomarker of poor prognosis in patients with colorectal cancer', *Med Oncol*, vol. 30, no. 2, p. 588.
- George, ML, Tutton, MG, Janssen, F, Arnaout, A, Abulafi, AM, Eccles, SA & Swift, RI 2001, 'VEGF-A, VEGF-C, and VEGF-D in colorectal cancer progression', *Neoplasia (New York, N.Y.)*, vol. 3, no. 5, pp. 420-7.
- Gerdes, J, Lemke, H, Baisch, H, Wacker, HH, Schwab, U & Stein, H 1984, 'Cell cycle analysis of a cell proliferation-associated human nuclear antigen defined by the monoclonal antibody Ki-67', *J Immunol*, vol. 133, no. 4, pp. 1710-5.
- Gibson, PR, Rosella, O, Wilson, AJ, Mariadason, JM, Rickard, K, Byron, K & Barkla, DH 1999, 'Colonic epithelial cell activation and the paradoxical effects of butyrate', *Carcinogenesis*, vol. 20, no. 4, pp. 539-44.
- Goel, HL & Mercurio, AM 2013, 'VEGF targets the tumour cell', *Nat Rev Cancer*, vol. 13, no. 12, pp. 871-82.
- Gong, J, Zhang, JP, Li, B, Zeng, C, You, K, Chen, MX, Yuan, Y & Zhuang, SM 2013, 'MicroRNA-125b promotes apoptosis by regulating the expression of Mcl-1, Bcl-w and IL-6R', *Oncogene*, vol. 32, no. 25, pp. 3071-9.
- Gopal, E, Miyauchi, S, Martin, PM, Ananth, S, Roon, P, Smith, SB & Ganapathy, V 2007, 'Transport of nicotinate and structurally related compounds by human SMCT1 (SLC5A8) and its relevance to drug transport in the mammalian intestinal tract', *Pharm Res*, vol. 24, no. 3, pp. 575-84.
- Gopalan, V, Ebrahimi, F, Islam, F, Vider, J, Qallandar, OB, Pillai, S, Lu, CT & Lam, AK 2018, 'Tumour suppressor properties of miR-15a and its regulatory effects on BCL2 and SOX2 proteins in colorectal carcinomas', *Exp Cell Res*, vol. 370, no. 2, pp. 245-53.
- Goss, KH & Groden, J 2000, 'Biology of the adenomatous polyposis coli tumor suppressor', *J Clin Oncol*, vol. 18, no. 9, pp. 1967-79.

## REFERENCES

- Graham, FL, Smiley, J, Russell, WC & Nairn, R 1977, 'Characteristics of a human cell line transformed by DNA from human adenovirus type 5', *J Gen Virol*, vol. 36, no. 1, pp. 59-74.
- Graham, LD, Pedersen, SK, Brown, GS, Ho, T, Kassir, Z, Moynihan, AT, Vizgofit, EK, Dunne, R, Pimlott, L, Young, GP, Lapointe, LC & Molloy, PL 2011, 'Colorectal Neoplasia Differentially Expressed (CRNDE), a Novel Gene with Elevated Expression in Colorectal Adenomas and Adenocarcinomas', *Genes Cancer*, vol. 2, no. 8, pp. 829-40.
- Grant, P 2001, 'A tale of histone modifications', *Genome Biology*, vol. 2, no. 4, pp. reviews0003.1 - reviews.6.
- Gregorieff, A & Clevers, H 2005, 'Wnt signaling in the intestinal epithelium: from endoderm to cancer', *Genes Dev*, vol. 19, no. 8, pp. 877-90.
- Grimson, A, Farh, KK-H, Johnston, WK, Garrett-Engele, P, Lim, LP & Bartel, DP 2007, 'MicroRNA Targeting Specificity in Mammals: Determinants beyond Seed Pairing', *Molecular Cell*, vol. 27, no. 1, pp. 91-105.
- Gu, W & Roeder, RG 1997, 'Activation of p53 Sequence-Specific DNA Binding by Acetylation of the p53 C-Terminal Domain', *Cell*, vol. 90, no. 4, pp. 595-606.
- Gu, X, Jin, R, Mao, X, Wang, J, Yuan, J & Zhao, G 2018, 'Prognostic value of miRNA-181a/b in colorectal cancer: a meta-analysis', *Biomark Med*, vol. 12, no. 3, pp. 299-308.
- Guil, S & Esteller, M 2012, 'Cis-acting noncoding RNAs: friends and foes', *Nat Struct Mol Biol*, vol. 19, no. 11, pp. 1068-75.
- Guo, H, Ingolia, NT, Weissman, JS & Bartel, DP 2010a, 'Mammalian microRNAs predominantly act to decrease target mRNA levels', *Nature*, vol. 466, no. 7308, pp. 835-40.
- Guo, J, Fang, W, Sun, L, Lu, Y, Dou, L, Huang, X, Sun, M, Pang, C, Qu, J, Liu, G & Li, J 2016, 'Reduced miR-200b and miR-200c expression contributes to abnormal hepatic lipid accumulation by stimulating JUN expression and activating the transcription of srebpl1', *Oncotarget*, vol. 7, no. 24, pp. 36207-19.
- Guo, J, Miao, Y, Xiao, B, Huan, R, Jiang, Z, Meng, D & Wang, Y 2009, 'Differential expression of microRNA species in human gastric cancer versus non-tumorous tissues', *Journal of Gastroenterology and Hepatology*, vol. 24, no. 4, pp. 652-7.
- Guo, K, Yao, J, Yu, Q, Li, Z, Huang, H, Cheng, J, Wang, Z & Zhu, Y 2017, 'The expression pattern of long non-coding RNA PVT1 in tumor tissues and in extracellular vesicles of colorectal cancer correlates with cancer progression', *Tumour Biol*, vol. 39, no. 4, p. 1010428317699122.
- Guo, Q, Zhao, Y, Chen, J, Hu, J, Wang, S, Zhang, D & Sun, Y 2014, 'BRAF-activated long non-coding RNA contributes to colorectal cancer migration by inducing epithelial-mesenchymal transition', *Oncol Lett*, vol. 8, no. 2, pp. 869-75.
- Guo, RJ, Funakoshi, S, Lee, HH, Kong, J & Lynch, JP 2010b, 'The intestine-specific transcription factor Cdx2 inhibits beta-catenin/TCF transcriptional activity by

## REFERENCES

- disrupting the beta-catenin-TCF protein complex', *Carcinogenesis*, vol. 31, no. 2, pp. 159-66.
- Guo, XB, Hua, Z, Li, C, Peng, LP, Wang, JS, Wang, B & Zhi, QM 2015, 'Biological significance of long non-coding RNA FTX expression in human colorectal cancer', *Int J Clin Exp Med*, vol. 8, no. 9, pp. 15591-600.
- Gupta, N, Martin, PM, Prasad, PD & Ganapathy, V 2006, 'SLC5A8 (SMCT1)-mediated transport of butyrate forms the basis for the tumor suppressive function of the transporter', *Life Sci*, vol. 78, no. 21, pp. 2419-25.
- Gupta, RA, Shah, N, Wang, KC, Kim, J, Horlings, HM, Wong, DJ, Tsai, MC, Hung, T, Argani, P, Rinn, JL, Wang, Y, Brzoska, P, Kong, B, Li, R, West, RB, van de Vijver, MJ, Sukumar, S & Chang, HY 2010, 'Long non-coding RNA HOTAIR reprograms chromatin state to promote cancer metastasis', *Nature*, vol. 464, no. 7291, pp. 1071-6.
- Gutschner, T, Hämmerle, M, Eißmann, M, Hsu, J, Kim, Y, Hung, G, Revenko, A, Arun, G, Stenrup, M, Groß, M, Zörnig, M, MacLeod, AR, Spector, DL & Diederichs, S 2013, 'The non-coding RNA MALAT1 is a critical regulator of the metastasis phenotype of lung cancer cells', *Cancer Research*, vol. 73, no. 3, pp. 1180-9.
- Guttman, M, Amit, I, Garber, M, French, C, Lin, MF, Feldser, D, Huarte, M, Zuk, O, Carey, BW, Cassady, JP, Cabili, MN, Jaenisch, R, Mikkelsen, TS, Jacks, T, Hacohen, N, Bernstein, BE, Kellis, M, Regev, A, Rinn, JL & Lander, ES 2009, 'Chromatin signature reveals over a thousand highly conserved large non-coding RNAs in mammals', *Nature*, vol. 458, no. 7235, pp. 223-7.
- Hagggar, FA & Boushey, RP 2009, 'Colorectal cancer epidemiology: incidence, mortality, survival, and risk factors', *Clin Colon Rectal Surg*, vol. 22, no. 4, pp. 191-7.
- Hague, A, Diaz, GD, Hicks, DJ, Krajewski, S, Reed, JC & Paraskeva, C 1997, 'bcl-2 and bak may play a pivotal role in sodium butyrate-induced apoptosis in colonic epithelial cells; however overexpression of bcl-2 does not protect against bak-mediated apoptosis', *Int J Cancer*, vol. 72, no. 5, pp. 898-905.
- Hague, A, Manning, AM, Hanlon, KA, Hart, D, Paraskeva, C & Huschtscha, LI 1993, 'Sodium butyrate induces apoptosis in human colonic tumour cell lines in a p53-independent pathway: Implications for the possible role of dietary fibre in the prevention of large-bowel cancer', *International Journal of Cancer*, vol. 55, no. 3, pp. 498-505.
- Hajjari, M & Salavaty, A 2015, 'HOTAIR: an oncogenic long non-coding RNA in different cancers', *Cancer Biology & Medicine*, vol. 12, no. 1, pp. 1-9.
- Halgunset, J, Lamvik, T & Espevik, T 1988, 'Butyrate effects on growth, morphology, and fibronectin production in PC-3 prostatic carcinoma cells', *Prostate*, vol. 12, no. 1, pp. 65-77.
- Hamer, HM, Jonkers, D, Venema, K, Vanhoutvin, S, Troost, FJ & Brummer, RJ 2008, 'Review article: the role of butyrate on colonic function', *Aliment Pharmacol Ther*, vol. 27, no. 2, pp. 104-19.

## REFERENCES

- Hamford, J, Stangeland, AM, Hughes, T, Skrede, ML, Tveit, KM, Ikdahl, T & Kure, EH 2012, 'Differential Expression of miRNAs in Colorectal Cancer: Comparison of Paired Tumor Tissue and Adjacent Normal Mucosa Using High-Throughput Sequencing', *PLoS One*, vol. 7, no. 4, p. e34150.
- Han, D, Gao, X, Wang, M, Qiao, Y, Xu, Y, Yang, J, Dong, N, He, J, Sun, Q, Lv, G, Xu, C, Tao, J & Ma, N 2016a, 'Long noncoding RNA H19 indicates a poor prognosis of colorectal cancer and promotes tumor growth by recruiting and binding to eIF4A3', *Oncotarget*, vol. 7, no. 16, pp. 22159-73.
- Han, R, Sun, Q, Wu, J, Zheng, P & Zhao, G 2016b, 'Sodium Butyrate Upregulates miR-203 Expression to Exert Anti-Proliferation Effect on Colorectal Cancer Cells', *Cell Physiol Biochem*, vol. 39, no. 5, pp. 1919-29.
- Han, W, Wang, L, Zhang, L, Wang, Y & Li, Y 2019, 'Circular RNA circ-RAD23B promotes cell growth and invasion by miR-593-3p/CCND2 and miR-653-5p/TIAM1 pathways in non-small cell lung cancer', *Biochem Biophys Res Commun*, vol. 510, no. 3, pp. 462-6.
- Han, X, Wang, L, Ning, Y, Li, S & Wang, Z 2016c, 'Long non-coding RNA AFAP1-AS1 facilitates tumor growth and promotes metastasis in colorectal cancer', *Biol Res*, vol. 49, no. 1, p. 36.
- Han, Y, Yang, YN, Yuan, HH, Zhang, TT, Sui, H, Wei, XL, Liu, L, Huang, P, Zhang, WJ & Bai, YX 2014, 'UCA1, a long non-coding RNA up-regulated in colorectal cancer influences cell proliferation, apoptosis and cell cycle distribution', *Pathology*, vol. 46, no. 5, pp. 396-401.
- Handra-Luca, A, Olschwang, S & Flejou, JF 2011, 'SMAD4 protein expression and cell proliferation in colorectal adenocarcinomas', *Virchows Arch*, vol. 459, no. 5, pp. 511-9.
- Hanna, N, Ohana, P, Konikoff, FM, Leichtmann, G, Hubert, A, Appelbaum, L, Kopelman, Y, Czerniak, A & Hochberg, A 2012, 'Phase 1/2a, dose-escalation, safety, pharmacokinetic and preliminary efficacy study of intratumoral administration of BC-819 in patients with unresectable pancreatic cancer', *Cancer Gene Ther*, vol. 19, no. 6, pp. 374-81.
- Hao, H, Xia, G, Wang, C, Zhong, F, Liu, L & Zhang, D 2017, 'miR-106a suppresses tumor cells death in colorectal cancer through targeting ATG7', *Med Mol Morphol*, vol. 50, no. 2, pp. 76-85.
- Hasenpusch, G, Pfeifer, C, Aneja, MK, Wagner, K, Reinhardt, D, Gilon, M, Ohana, P, Hochberg, A & Rudolph, C 2011, 'Aerosolized BC-819 Inhibits Primary but Not Secondary Lung Cancer Growth', *PLoS One*, vol. 6, no. 6, p. e20760.
- Hazawa, M, Lin, DC, Kobayashi, A, Jiang, YY, Xu, L, Dewi, FRP, Mohamed, MS, Hartono, Nakada, M, Meguro-Horike, M, Horike, SI, Koeffler, HP & Wong, RW 2018, 'ROCK-dependent phosphorylation of NUP62 regulates p63 nuclear transport and squamous cell carcinoma proliferation', *EMBO Rep*, vol. 19, no. 1, pp. 73-88.
- He, G, Siddik, ZH, Huang, Z, Wang, R, Koomen, J, Kobayashi, R, Khokhar, AR & Kuang, J 2005, 'Induction of p21 by p53 following DNA damage inhibits both Cdk4 and Cdk2 activities', *Oncogene*, vol. 24, no. 18, pp. 2929-43.

## REFERENCES

- He, TC, Sparks, AB, Rago, C, Hermeking, H, Zawel, L, da Costa, LT, Morin, PJ, Vogelstein, B & Kinzler, KW 1998, 'Identification of c-MYC as a target of the APC pathway', *Science*, vol. 281, no. 5382, pp. 1509-12.
- He, X, Tan, X, Wang, X, Jin, H, Liu, L, Ma, L, Yu, H & Fan, Z 2014, 'C-Myc-activated long noncoding RNA CCAT1 promotes colon cancer cell proliferation and invasion', *Tumour Biol*, vol. 35, no. 12, pp. 12181-8.
- He, X, Wei, Y, Wang, Y, Liu, L, Wang, W & Li, N 2016, 'MiR-381 functions as a tumor suppressor in colorectal cancer by targeting Twist1', *Oncotargets and therapy*, vol. 9, pp. 1231-9.
- He, XC, Zhang, J, Tong, WG, Tawfik, O, Ross, J, Scoville, DH, Tian, Q, Zeng, X, He, X, Wiedemann, LM, Mishina, Y & Li, L 2004, 'BMP signaling inhibits intestinal stem cell self-renewal through suppression of Wnt-beta-catenin signaling', *Nat Genet*, vol. 36, no. 10, pp. 1117-21.
- Hecht, A, Vlemminckx, K, Stemmler, MP, van Roy, F & Kemler, R 2000, 'The p300/CBP acetyltransferases function as transcriptional coactivators of beta-catenin in vertebrates', *Embo j*, vol. 19, no. 8, pp. 1839-50.
- Hibi, K, Nakamura, H, Hirai, A, Fujikake, Y, Kasai, Y, Akiyama, S, Ito, K & Takagi, H 1996, 'Loss of H19 imprinting in esophageal cancer', *Cancer Res*, vol. 56, no. 3, pp. 480-2.
- Hinnebusch, BF, Meng, S, Wu, JT, Archer, SY & Hodin, RA 2002, 'The effects of short-chain fatty acids on human colon cancer cell phenotype are associated with histone hyperacetylation', *J Nutr*, vol. 132, no. 5, pp. 1012-7.
- Hoeben, A, Landuyt, B, Highley, MS, Wildiers, H, Van Oosterom, AT & De Bruijn, EA 2004, 'Vascular endothelial growth factor and angiogenesis', *Pharmacol Rev*, vol. 56, no. 4, pp. 549-80.
- Hong, S, Zhao, B, Lombard, DB, Fingar, DC & Inoki, K 2014, 'Cross-talk between sirtuin and mammalian target of rapamycin complex 1 (mTORC1) signaling in the regulation of S6 kinase 1 (S6K1) phosphorylation', *J Biol Chem*, vol. 289, no. 19, pp. 13132-41.
- Hong, Y, Ho, KS, Eu, KW & Cheah, PY 2007, 'A susceptibility gene set for early onset colorectal cancer that integrates diverse signaling pathways: implication for tumorigenesis', *Clin Cancer Res*, vol. 13, no. 4, pp. 1107-14.
- Hong, YK, Ontiveros, SD & Strauss, WM 2000, 'A revision of the human XIST gene organization and structural comparison with mouse Xist', *Mamm Genome*, vol. 11, no. 3, pp. 220-4.
- Hosseinahli, N, Aghapour, M, Duijf, PHG & Baradaran, B 2018, 'Treating cancer with microRNA replacement therapy: A literature review', *J Cell Physiol*, vol. 233, no. 8, pp. 5574-88.
- Howe, EN, Cochrane, DR & Richer, JK 2011, 'Targets of miR-200c mediate suppression of cell motility and anoikis resistance', *Breast Cancer Res*, vol. 13, no. 2, p. R45.

## REFERENCES

- Hu, L, Ye, H, Huang, G, Luo, F, Liu, Y, Liu, Y, Yang, X, Shen, J, Liu, Q & Zhang, J 2016a, 'Long noncoding RNA GAS5 suppresses the migration and invasion of hepatocellular carcinoma cells via miR-21', *Tumour Biol*, vol. 37, no. 2, pp. 2691-702.
- Hu, S, Dong, TS, Dalal, SR, Wu, F, Bissonnette, M, Kwon, JH & Chang, EB 2011, 'The microbe-derived short chain fatty acid butyrate targets miRNA-dependent p21 gene expression in human colon cancer', *PLoS One*, vol. 6, no. 1, p. e16221.
- Hu, S, Liu, L, Chang, EB, Wang, J-Y & Raufman, J-P 2015, 'Butyrate inhibits pro-proliferative miR-92a by diminishing c-Myc-induced miR-17-92a cluster transcription in human colon cancer cells', *Molecular Cancer*, vol. 14, p. 180.
- Hu, X, Du, S, Yu, J, Yang, X, Yang, C, Zhou, D, Wang, Q, Qin, S, Yan, X, He, L, Han, D & Wan, C 2016b, 'Common housekeeping proteins are upregulated in colorectal adenocarcinoma and hepatocellular carcinoma, making the total protein a better "housekeeper"', *Oncotarget*, vol. 7, no. 41, pp. 66679-88.
- Huang, CH, Mandelker, D, Schmidt-Kittler, O, Samuels, Y, Velculescu, VE, Kinzler, KW, Vogelstein, B, Gabelli, SB & Amzel, LM 2007, 'The structure of a human p110alpha/p85alpha complex elucidates the effects of oncogenic PI3Kalpha mutations', *Science*, vol. 318, no. 5857, pp. 1744-8.
- Huang, G, Wu, X, Li, S, Xu, X, Zhu, H & Chen, X 2016, 'The long noncoding RNA CASC2 functions as a competing endogenous RNA by sponging miR-18a in colorectal cancer', *Sci Rep*, vol. 6, p. 26524.
- Huang, L-L, Huang, L-W, Wang, L, Tong, B-D, Wei, Q & Ding, X-S 2017, 'Potential role of miR-139-5p in cancer diagnosis, prognosis and therapy', *Oncol Lett*, vol. 14, no. 2, pp. 1215-22.
- Huang, Z, Huang, D, Ni, S, Peng, Z, Sheng, W & Du, X 2010, 'Plasma microRNAs are promising novel biomarkers for early detection of colorectal cancer', *Int J Cancer*, vol. 127, no. 1, pp. 118-26.
- Huarte, M 2015, 'The emerging role of lncRNAs in cancer', *Nat Med*, vol. 21, no. 11, pp. 1253-61.
- Huarte, M, Guttman, M, Feldser, D, Garber, M, Koziol, MJ, Kenzelmann-Broz, D, Khalil, AM, Zuk, O, Amit, I, Rabani, M, Attardi, LD, Regev, A, Lander, ES, Jacks, T & Rinn, JL 2010, 'A large intergenic noncoding RNA induced by p53 mediates global gene repression in the p53 response', *Cell*, vol. 142, no. 3, pp. 409-19.
- Huels, DJ & Sansom, OJ 2015, 'Stem vs non-stem cell origin of colorectal cancer', *Br J Cancer*, vol. 113, no. 1, pp. 1-5.
- Humphreys, KJ, Cobiac, L, Le Leu, RK, Van der Hoek, MB & Michael, MZ 2013, 'Histone deacetylase inhibition in colorectal cancer cells reveals competing roles for members of the oncogenic miR-17-92 cluster', *Mol Carcinog*, vol. 52, no. 6, pp. 459-74.
- Humphreys, KJ, Conlon, MA, Young, GP, Topping, DL, Hu, Y, Winter, JM, Bird, AR, Cobiac, L, Kennedy, NA, Michael, MZ & Le Leu, RK 2014a, 'Dietary manipulation of

## REFERENCES

- oncogenic microRNA expression in human rectal mucosa: a randomized trial', *Cancer Prev Res (Phila)*, vol. 7, no. 8, pp. 786-95.
- Humphreys, KJ, McKinnon, RA & Michael, MZ 2014b, 'miR-18a inhibits CDC42 and plays a tumour suppressor role in colorectal cancer cells', *PLoS One*, vol. 9, no. 11, pp. e112288-e.
- Hung, T, Wang, Y, Lin, MF, Koegel, AK, Kotake, Y, Grant, GD, Horlings, HM, Shah, N, Umbricht, C, Wang, P, Wang, Y, Kong, B, Langerod, A, Borresen-Dale, AL, Kim, SK, van de Vijver, M, Sukumar, S, Whitfield, ML, Kellis, M, Xiong, Y, Wong, DJ & Chang, HY 2011, 'Extensive and coordinated transcription of noncoding RNAs within cell-cycle promoters', *Nat Genet*, vol. 43, no. 7, pp. 621-9.
- Huo, T, Canepa, R, Sura, A, Modave, F & Gong, Y 2017, 'Colorectal cancer stages transcriptome analysis', *PLoS One*, vol. 12, no. 11, pp. e0188697-e.
- Hussien, R & Brooks, GA 2011, 'Mitochondrial and plasma membrane lactate transporter and lactate dehydrogenase isoform expression in breast cancer cell lines', *Physiological genomics*, vol. 43, no. 5, pp. 255-64.
- Hutchinson, JN, Ensminger, AW, Clemson, CM, Lynch, CR, Lawrence, JB & Chess, A 2007, 'A screen for nuclear transcripts identifies two linked noncoding RNAs associated with SC35 splicing domains', *BMC Genomics*, vol. 8, p. 39.
- Hwang, HW & Mendell, JT 2006, 'MicroRNAs in cell proliferation, cell death, and tumorigenesis', *Br J Cancer*, vol. 94, no. 6, pp. 776-80.
- Iacomino, G, Tecce, MF, Grimaldi, C, Tosto, M & Russo, GL 2001, 'Transcriptional response of a human colon adenocarcinoma cell line to sodium butyrate', *Biochem Biophys Res Commun*, vol. 285, no. 5, pp. 1280-9.
- Ibrahim, AF, Weirauch, U, Thomas, M, Grünweller, A, Hartmann, RK & Aigner, A 2011, 'MicroRNA Replacement Therapy for miR-145 and miR-33a Is Efficacious in a Model of Colon Carcinoma', *Cancer Research*, vol. 71, no. 15, pp. 5214-24.
- Ibrahim, S, Li, G, Hu, F, Hou, Z, Chen, Q, Li, G, Luo, X, Hu, J & Feng, Y 2018, 'PIK3R3 promotes chemotherapeutic sensitivity of colorectal cancer through PIK3R3/NF-kB/IP pathway', *Cancer Biol Ther*, vol. 19, no. 3, pp. 222-9.
- Igene, JO, King, JA, Pearson, AM & Gray, JI 1979, 'Influence of heme pigments, nitrite, and non-heme iron on development of warmed-over flavor (WOF) in cooked meat', *Journal of Agricultural and Food Chemistry*, vol. 27, no. 4, pp. 838-42.
- Imajo, M, Tsuchiya, Y & Nishida, E 2006, 'Regulatory mechanisms and functions of MAP kinase signaling pathways', *IUBMB Life*, vol. 58, no. 5-6, pp. 312-7.
- Ip, YT & Davis, RJ 1998, 'Signal transduction by the c-Jun N-terminal kinase (JNK)--from inflammation to development', *Curr Opin Cell Biol*, vol. 10, no. 2, pp. 205-19.
- Ishikawa, S, Tamaki, S, Ohata, M, Arihara, K & Itoh, M 2010, 'Heme induces DNA damage and hyperproliferation of colonic epithelial cells via hydrogen peroxide produced by heme oxygenase: a possible mechanism of heme-induced colon cancer', *Mol Nutr Food Res*, vol. 54, no. 8, pp. 1182-91.

## REFERENCES

- Ito, T, Sato, F, Kan, T, Cheng, Y, David, S, Agarwal, R, Paun, BC, Jin, Z, Oлару, AV, Hamilton, JP, Selaru, FM, Yang, J, Matsumura, N, Shimizu, K, Abraham, JM, Shimada, Y, Mori, Y & Meltzer, SJ 2011, 'Polo-like kinase 1 regulates cell proliferation and is targeted by miR-593\* in esophageal cancer', *Int J Cancer*, vol. 129, no. 9, pp. 2134-46.
- Itoh, N, Yonehara, S, Ishii, A, Yonehara, M, Mizushima, S, Sameshima, M, Hase, A, Seto, Y & Nagata, S 1991, 'The polypeptide encoded by the cDNA for human cell surface antigen Fas can mediate apoptosis', *Cell*, vol. 66, no. 2, pp. 233-43.
- Jaenisch, R & Bird, A 2003, 'Epigenetic regulation of gene expression: how the genome integrates intrinsic and environmental signals', *Nat Genet*, vol. 33 Suppl, pp. 245-54.
- James de Bony, E, Bizet, M, Van Grembergen, O, Hassabi, B, Calonne, E, Putmans, P, Bontempi, G & Fuks, F 2018, 'Comprehensive identification of long noncoding RNAs in colorectal cancer', *Oncotarget*, vol. 9, no. 45, pp. 27605-29.
- Janout, V & Kollarova, H 2001, 'Epidemiology of colorectal cancer', *Biomed Pap Med Fac Univ Palacky Olomouc Czech Repub*, vol. 145, no. 1, pp. 5-10.
- Janson, W, Brandner, G & Siegel, J 1997, 'Butyrate modulates DNA-damage-induced p53 response by induction of p53-independent differentiation and apoptosis', *Oncogene*, vol. 15, no. 12, pp. 1395-406.
- Janssen, HL, Reesink, HW, Lawitz, EJ, Zeuzem, S, Rodriguez-Torres, M, Patel, K, van der Meer, AJ, Patick, AK, Chen, A, Zhou, Y, Persson, R, King, BD, Kauppinen, S, Levin, AA & Hodges, MR 2013, 'Treatment of HCV infection by targeting microRNA', *N Engl J Med*, vol. 368, no. 18, pp. 1685-94.
- Ji, D, Chen, Z, Li, M, Zhan, T, Yao, Y, Zhang, Z, Xi, J, Yan, L & Gu, J 2014a, 'MicroRNA-181a promotes tumor growth and liver metastasis in colorectal cancer by targeting the tumor suppressor WIF-1', *Molecular Cancer*, vol. 13, pp. 86-.
- Ji, P, Diederichs, S, Wang, W, Boing, S, Metzger, R, Schneider, PM, Tidow, N, Brandt, B, Buerger, H, Bulk, E, Thomas, M, Berdel, WE, Serve, H & Muller-Tidow, C 2003, 'MALAT-1, a novel noncoding RNA, and thymosin beta4 predict metastasis and survival in early-stage non-small cell lung cancer', *Oncogene*, vol. 22, no. 39, pp. 8031-41.
- Ji, Q, Liu, X, Fu, X, Zhang, L, Sui, H, Zhou, L, Sun, J, Cai, J, Qin, J, Ren, J & Li, Q 2013, 'Resveratrol inhibits invasion and metastasis of colorectal cancer cells via MALAT1 mediated Wnt/beta-catenin signal pathway', *PLoS One*, vol. 8, no. 11, p. e78700.
- Ji, Q, Zhang, L, Liu, X, Zhou, L, Wang, W, Han, Z, Sui, H, Tang, Y, Wang, Y, Liu, N, Ren, J, Hou, F & Li, Q 2014b, 'Long non-coding RNA MALAT1 promotes tumour growth and metastasis in colorectal cancer through binding to SFPQ and releasing oncogene PTBP2 from SFPQ/PTBP2 complex', *Br J Cancer*, vol. 111, no. 4, pp. 736-48.
- Ji, Z, Song, R, Regev, A & Struhl, K 2015, 'Many lncRNAs, 5'UTRs, and pseudogenes are translated and some are likely to express functional proteins', *eLife*, vol. 4, p. e08890.
- Jin, C, Shi, W, Wang, F, Shen, X, Qi, J, Cong, H, Yuan, J, Shi, L, Zhu, B, Luo, X, Zhang, Y & Ju, S 2016, 'Long non-coding RNA HULC as a novel serum biomarker for

## REFERENCES

- diagnosis and prognosis prediction of gastric cancer', *Oncotarget*, vol. 7, no. 32, pp. 51763-72.
- Jin, H, Shi, X, Zhao, Y, Peng, M, Kong, Y, Qin, D & Lv, X 2018, 'MicroRNA-30a Mediates Cell Migration and Invasion by Targeting Metadherin in Colorectal Cancer', *Technology in cancer research & treatment*, vol. 17, pp. 1533033818758108-.
- Jin, HY, Gonzalez-Martin, A, Miletic, AV, Lai, M, Knight, S, Sabouri-Ghomi, M, Head, SR, Macauley, MS, Rickert, RC & Xiao, C 2015, 'Transfection of microRNA Mimics Should Be Used with Caution', *Front Genet*, vol. 6, pp. 340-.
- John, B, Enright, AJ, Aravin, A, Tuschl, T, Sander, C & Marks, DS 2004, 'Human MicroRNA targets', *PLoS Biol*, vol. 2, no. 11, p. e363.
- Jones, E, Michael, S & Sittampalam, GS 2004, 'Basics of Assay Equipment and Instrumentation for High Throughput Screening', in GS Sittampalam, NP Coussens, K Brimacombe, A Grossman, M Arkin, D Auld, C Austin, J Baell, B Bejcek, JMM Caaveiro, TDY Chung, JL Dahlin, V Devanaryan, TL Foley, M Glicksman, MD Hall, JV Haas, J Inglese, PW Iversen, SD Kahl, SC Kales, M Lal-Nag, Z Li, J McGee, O McManus, T Riss, OJ Trask, Jr., JR Weidner, MJ Wildey, M Xia & X Xu (eds), *Assay Guidance Manual*, Eli Lilly & Company and the National Center for Advancing Translational Sciences, Bethesda (MD).
- Jorissen, RN, Walker, F, Pouliot, N, Garrett, TP, Ward, CW & Burgess, AW 2003, 'Epidermal growth factor receptor: mechanisms of activation and signalling', *Exp Cell Res*, vol. 284, no. 1, pp. 31-53.
- Kaiko, GE, Ryu, SH, Koues, OI, Collins, PL, Solnica-Krezel, L, Pearce, EJ, Pearce, EL, Oltz, EM & Stappenbeck, TS 2016, 'The Colonic Crypt Protects Stem Cells from Microbiota-Derived Metabolites', *Cell*, vol. 165, no. 7, pp. 1708-20.
- Kali, A & Shetty, KSR 2014, 'Endocan: a novel circulating proteoglycan', *Indian journal of pharmacology*, vol. 46, no. 6, pp. 579-83.
- Kam, Y, Rubinstein, A, Naik, S, Djavsarov, I, Halle, D, Ariel, I, Gure, AO, Stojadinovic, A, Pan, H, Tsivin, V, Nissan, A & Yavin, E 2014, 'Detection of a long non-coding RNA (CCAT1) in living cells and human adenocarcinoma of colon tissues using FIT-PNA molecular beacons', *Cancer Lett*, vol. 352, no. 1, pp. 90-6.
- Kanaan, Z, Rai, SN, Eichenberger, MR, Barnes, C, Dworkin, AM, Weller, C, Cohen, E, Roberts, H, Keskey, B, Petras, RE, Crawford, NP & Galandiuk, S 2012, 'Differential microRNA expression tracks neoplastic progression in inflammatory bowel disease-associated colorectal cancer', *Hum Mutat*, vol. 33, no. 3, pp. 551-60.
- Kanehisa, M, Furumichi, M, Tanabe, M, Sato, Y & Morishima, K 2017, 'KEGG: new perspectives on genomes, pathways, diseases and drugs', *Nucleic Acids Res*, vol. 45, no. D1, pp. D353-d61.
- Kanehisa, M & Goto, S 2000, 'KEGG: kyoto encyclopedia of genes and genomes', *Nucleic Acids Res*, vol. 28, no. 1, pp. 27-30.

## REFERENCES

- Kanehisa, M, Sato, Y, Kawashima, M, Furumichi, M & Tanabe, M 2016, 'KEGG as a reference resource for gene and protein annotation', *Nucleic Acids Res*, vol. 44, no. D1, pp. D457-62.
- Kang, K, Oh, SH, Yun, JH, Jho, EH, Kang, JH, Batsuren, D, Tunsag, J, Park, KH, Kim, M & Nho, CW 2011, 'A novel topoisomerase inhibitor, daurinol, suppresses growth of HCT116 cells with low hematological toxicity compared to etoposide', *Neoplasia*, vol. 13, no. 11, pp. 1043-57.
- Kapinas, K & Delany, AM 2011, 'MicroRNA biogenesis and regulation of bone remodeling', *Arthritis Res Ther*, vol. 13, no. 3, p. 220.
- Kapranov, P, Cheng, J, Dike, S, Nix, DA, Dutttagupta, R, Willingham, AT, Stadler, PF, Hertel, J, Hackermuller, J, Hofacker, IL, Bell, I, Cheung, E, Drenkow, J, Dumais, E, Patel, S, Helt, G, Ganesh, M, Ghosh, S, Piccolboni, A, Sementchenko, V, Tammana, H & Gingeras, TR 2007, 'RNA maps reveal new RNA classes and a possible function for pervasive transcription', *Science*, vol. 316, no. 5830, pp. 1484-8.
- Karapetis, CS, Khambata-Ford, S, Jonker, DJ, O'Callaghan, CJ, Tu, D, Tebbutt, NC, Simes, RJ, Chalchal, H, Shapiro, JD, Robitaille, S, Price, TJ, Shepherd, L, Au, HJ, Langer, C, Moore, MJ & Zalberg, JR 2008, 'K-ras mutations and benefit from cetuximab in advanced colorectal cancer', *N Engl J Med*, vol. 359, no. 17, pp. 1757-65.
- Karimi Mazraehshah, M, Tavangar, SM, Saidijam, M, Amini, R, Bahreini, F, Karimi Dermani, F & Najafi, R 2018, 'Anticancer effects of miR-200c in colorectal cancer through BMI1', *J Cell Biochem*, vol. 119, no. 12, pp. 10005-12.
- Kasinski, AL, Kelnar, K, Stahlhut, C, Orellana, E, Zhao, J, Shimer, E, Dysart, S, Chen, X, Bader, AG & Slack, FJ 2015, 'A combinatorial microRNA therapeutics approach to suppressing non-small cell lung cancer', *Oncogene*, vol. 34, no. 27, pp. 3547-55.
- Katsushima, K, Natsume, A, Ohka, F, Shinjo, K, Hatanaka, A, Ichimura, N, Sato, S, Takahashi, S, Kimura, H, Totoki, Y, Shibata, T, Naito, M, Kim, HJ, Miyata, K, Kataoka, K & Kondo, Y 2016, 'Targeting the Notch-regulated non-coding RNA TUG1 for glioma treatment', *Nat Commun*, vol. 7, p. 13616.
- Kawahara, K, Morishita, T, Nakamura, T, Hamada, F, Toyoshima, K & Akiyama, T 2000, 'Down-regulation of beta-catenin by the colorectal tumor suppressor APC requires association with Axin and beta-catenin', *J Biol Chem*, vol. 275, no. 12, pp. 8369-74.
- Kelly, RJ, Thomas, A, Rajan, A, Chun, G, Lopez-Chavez, A, Szabo, E, Spencer, S, Carter, CA, Guha, U, Khozin, S, Poondru, S, Van Sant, C, Keating, A, Steinberg, SM, Figg, W & Giaccone, G 2013, 'A phase I/II study of sepantronium bromide (YM155, survivin suppressor) with paclitaxel and carboplatin in patients with advanced non-small-cell lung cancer', *Ann Oncol*, vol. 24, no. 10, pp. 2601-6.
- Keniry, A, Oxley, D, Monnier, P, Kyba, M, Dandolo, L, Smits, G & Reik, W 2012, 'The H19 lincRNA is a developmental reservoir of miR-675 which suppresses growth and Igf1r', *Nat Cell Biol*, vol. 14, no. 7, pp. 659-65.
- Kent, OA & Mendell, JT 2006, 'A small piece in the cancer puzzle: microRNAs as tumor suppressors and oncogenes', *Oncogene*, vol. 25, no. 46, pp. 6188-96.

## REFERENCES

- Kent, OA, Steenbergen, C & Das, S 2018, 'In Vivo Nanovector Delivery of a Heart-specific MicroRNA-sponge', *Journal of visualized experiments : JoVE*, no. 136, p. 57845.
- Keppler, BR & Archer, TK 2008, 'Chromatin-modifying enzymes as therapeutic targets-Part 1', *Expert opinion on therapeutic targets*, vol. 12, no. 10, pp. 1301-12.
- Kertesz, M, Iovino, N, Unnerstall, U, Gaul, U & Segal, E 2007, 'The role of site accessibility in microRNA target recognition', *Nat Genet*, vol. 39, no. 10, pp. 1278-84.
- Khalek, FJA, Gallicano, GI & Mishra, L 2010, 'Colon Cancer Stem Cells', *Gastrointestinal Cancer Research : GCR*, no. Suppl 1, pp. S16-S23.
- Khalil, AM, Guttman, M, Huarte, M, Garber, M, Raj, A, Rivea Morales, D, Thomas, K, Presser, A, Bernstein, BE, van Oudenaarden, A, Regev, A, Lander, ES & Rinn, JL 2009, 'Many human large intergenic noncoding RNAs associate with chromatin-modifying complexes and affect gene expression', *Proc Natl Acad Sci U S A*, vol. 106, no. 28, pp. 11667-72.
- Khatri, P, Sirota, M & Butte, AJ 2012, 'Ten years of pathway analysis: current approaches and outstanding challenges', *PLoS Comput Biol*, vol. 8, no. 2, p. e1002375.
- Kho, D, MacDonald, C, Johnson, R, Unsworth, CP, O'Carroll, SJ, du Mez, E, Angel, CE & Graham, ES 2015, 'Application of xCELLigence RTCA Biosensor Technology for Revealing the Profile and Window of Drug Responsiveness in Real Time', *Biosensors*, vol. 5, no. 2, pp. 199-222.
- Kim, KH & Sederstrom, JM 2015, 'Assaying Cell Cycle Status Using Flow Cytometry', *Curr Protoc Mol Biol*, vol. 111, pp. 28.6.1-11.
- Kim, NH, Kim, HS, Kim, N-G, Lee, I, Choi, H-S, Li, X-Y, Kang, SE, Cha, SY, Ryu, JK, Na, JM, Park, C, Kim, K, Lee, S, Gumbiner, BM, Yook, JI & Weiss, SJ 2011, 'p53 and microRNA-34 are suppressors of canonical Wnt signaling', *Sci Signal*, vol. 4, no. 197, pp. ra71-ra.
- Kim, PJ, Plescia, J, Clevers, H, Fearon, ER & Altieri, DC 2003, 'Survivin and molecular pathogenesis of colorectal cancer', *Lancet*, vol. 362, no. 9379, pp. 205-9.
- Kim, VN, Han, J & Siomi, MC 2009, 'Biogenesis of small RNAs in animals', *Nat Rev Mol Cell Biol*, vol. 10, no. 2, pp. 126-39.
- Kingston, RE & Tamkun, JW 2014, 'Transcriptional Regulation by Trithorax-Group Proteins', *Cold Spring Harb Perspect Biol*, vol. 6, no. 10.
- Kino, T, Hurt, DE, Ichijo, T, Nader, N & Chrousos, GP 2010, 'Noncoding RNA gas5 is a growth arrest- and starvation-associated repressor of the glucocorticoid receptor', *Sci Signal*, vol. 3, no. 107, p. ra8.
- Kobayashi, H, Tan, EM & Fleming, SE 2003, 'Sodium butyrate inhibits cell growth and stimulates p21WAF1/CIP1 protein in human colonic adenocarcinoma cells independently of p53 status', *Nutr Cancer*, vol. 46, no. 2, pp. 202-11.

## REFERENCES

- Koduru, SV, Tiwari, AK, Hazard, SW, Mahajan, M & Ravnic, DJ 2017, 'Exploration of small RNA-seq data for small non-coding RNAs in Human Colorectal Cancer', *J Genomics*, vol. 5, pp. 16-31.
- Kogo, R, Shimamura, T, Mimori, K, Kawahara, K, Imoto, S, Sudo, T, Tanaka, F, Shibata, K, Suzuki, A, Komune, S, Miyano, S & Mori, M 2011, 'Long noncoding RNA HOTAIR regulates polycomb-dependent chromatin modification and is associated with poor prognosis in colorectal cancers', *Cancer Res*, vol. 71, no. 20, pp. 6320-6.
- Koh, A, De Vadder, F, Kovatcheva-Datchary, P & Backhed, F 2016, 'From Dietary Fiber to Host Physiology: Short-Chain Fatty Acids as Key Bacterial Metabolites', *Cell*, vol. 165, no. 6, pp. 1332-45.
- Konig, R, Zhou, Y, Elleder, D, Diamond, TL, Bonamy, GM, Irelan, JT, Chiang, CY, Tu, BP, De Jesus, PD, Lilley, CE, Seidel, S, Opaluch, AM, Caldwell, JS, Weitzman, MD, Kuhen, KL, Bandyopadhyay, S, Ideker, T, Orth, AP, Miraglia, LJ, Bushman, FD, Young, JA & Chanda, SK 2008, 'Global analysis of host-pathogen interactions that regulate early-stage HIV-1 replication', *Cell*, vol. 135, no. 1, pp. 49-60.
- Koo, BK, Lim, HS, Chang, HJ, Yoon, MJ, Choi, Y, Kong, MP, Kim, CH, Kim, JM, Park, JG & Kong, YY 2009, 'Notch signaling promotes the generation of EphrinB1-positive intestinal epithelial cells', *Gastroenterology*, vol. 137, no. 1, pp. 145-55, 55.e1-3.
- Korpala, M & Kang, Y 2008, 'The emerging role of miR-200 family of microRNAs in epithelial-mesenchymal transition and cancer metastasis', *RNA Biology*, vol. 5, no. 3, pp. 115-9.
- Kosaka, Y, Inoue, H, Ohmachi, T, Yokoe, T, Matsumoto, T, Mimori, K, Tanaka, F, Watanabe, M & Mori, M 2007, 'Tripartite motif-containing 29 (TRIM29) is a novel marker for lymph node metastasis in gastric cancer', *Ann Surg Oncol*, vol. 14, no. 9, pp. 2543-9.
- Kozomara, A & Griffiths-Jones, S 2014, 'miRBase: annotating high confidence microRNAs using deep sequencing data', *Nucleic Acids Research*, vol. 42, no. Database issue, pp. D68-D73.
- Kramps, T, Peter, O, Brunner, E, Nellen, D, Froesch, B, Chatterjee, S, Murone, M, Zullig, S & Basler, K 2002, 'Wnt/wingless signaling requires BCL9/legless-mediated recruitment of pygopus to the nuclear beta-catenin-TCF complex', *Cell*, vol. 109, no. 1, pp. 47-60.
- Krek, A, Grun, D, Poy, MN, Wolf, R, Rosenberg, L, Epstein, EJ, MacMenamin, P, da Piedade, I, Gunsalus, KC, Stoffel, M & Rajewsky, N 2005, 'Combinatorial microRNA target predictions', *Nat Genet*, vol. 37, no. 5, pp. 495-500.
- Kruidering, M & Evan, GI 2000, 'Caspase-8 in apoptosis: the beginning of "the end"?', *IUBMB Life*, vol. 50, no. 2, pp. 85-90.
- Kudchadkar, R, Ernst, S, Chmielowski, B, Redman, BG, Steinberg, J, Keating, A, Jie, F, Chen, C, Gonzalez, R & Weber, J 2015, 'A phase 2, multicenter, open-label study of sepantronium bromide (YM155) plus docetaxel in patients with stage III (unresectable) or stage IV melanoma', *Cancer Med*, vol. 4, no. 5, pp. 643-50.

## REFERENCES

- Kurki, P, Vanderlaan, M, Dolbeare, F, Gray, J & Tan, EM 1986, 'Expression of proliferating cell nuclear antigen (PCNA)/cyclin during the cell cycle', *Exp Cell Res*, vol. 166, no. 1, pp. 209-19.
- Kwak, B, Kim, DU, Kim, TO, Kim, HS & Kim, SW 2018, 'MicroRNA-552 links Wnt signaling to p53 tumor suppressor in colorectal cancer', *Int J Oncol*, vol. 53, no. 4, pp. 1800-8.
- Kyriakis, JM & Avruch, J 2012, 'Mammalian MAPK signal transduction pathways activated by stress and inflammation: a 10-year update', *Physiol Rev*, vol. 92, no. 2, pp. 689-737.
- Lambert, DW, Wood, IS, Ellis, A & Shirazi-Beechey, SP 2002, 'Molecular changes in the expression of human colonic nutrient transporters during the transition from normality to malignancy', *Br J Cancer*, vol. 86, no. 8, pp. 1262-9.
- Lan, Y, Xiao, X, He, Z, Luo, Y, Wu, C, Li, L & Song, X 2018, 'Long noncoding RNA OCC-1 suppresses cell growth through destabilizing HuR protein in colorectal cancer', *Nucleic Acids Research*, vol. 46, no. 11, pp. 5809-21.
- Landthaler, M, Yalcin, A & Tuschl, T 2004, 'The human DiGeorge syndrome critical region gene 8 and Its D. melanogaster homolog are required for miRNA biogenesis', *Curr Biol*, vol. 14, no. 23, pp. 2162-7.
- Lao, VV & Grady, WM 2011, 'Epigenetics and colorectal cancer', *Nature reviews. Gastroenterology & hepatology*, vol. 8, no. 12, pp. 686-700.
- Latres, E, Chiaur, DS & Pagano, M 1999, 'The human F box protein beta-Trecp associates with the Cul1/Skp1 complex and regulates the stability of beta-catenin', *Oncogene*, vol. 18, no. 4, pp. 849-54.
- Lavie, O, Edelman, D, Levy, T, Fishman, A, Hubert, A, Segev, Y, Raveh, E, Gilon, M & Hochberg, A 2017, 'A phase 1/2a, dose-escalation, safety, pharmacokinetic, and preliminary efficacy study of intraperitoneal administration of BC-819 (H19-DTA) in subjects with recurrent ovarian/peritoneal cancer', *Archives of Gynecology and Obstetrics*, vol. 295, no. 3, pp. 751-61.
- Lavoie, H & Therrien, M 2015, 'Regulation of RAF protein kinases in ERK signalling', *Nat Rev Mol Cell Biol*, vol. 16, no. 5, pp. 281-98.
- Lavoie, JN, L'Allemain, G, Brunet, A, Muller, R & Pouyssegur, J 1996, 'Cyclin D1 expression is regulated positively by the p42/p44MAPK and negatively by the p38/HOGMAPK pathway', *J Biol Chem*, vol. 271, no. 34, pp. 20608-16.
- Lazarova, DL, Bordonaro, M, Carbone, R & Sartorelli, AC 2004, 'Linear relationship between Wnt activity levels and apoptosis in colorectal carcinoma cells exposed to butyrate', *Int J Cancer*, vol. 110, no. 4, pp. 523-31.
- Lazarova, DL, Chiaro, C & Bordonaro, M 2014, 'Butyrate induced changes in Wnt-signaling specific gene expression in colorectal cancer cells', *BMC Res Notes*, vol. 7, p. 226.

## REFERENCES

- Lazarova, DL, Wong, T, Chiaro, C, Drago, E & Bordonaro, M 2013, 'p300 Influences Butyrate-Mediated WNT Hyperactivation In Colorectal Cancer Cells', *Journal of Cancer*, vol. 4, no. 6, pp. 491-501.
- Le Leu, RK, Winter, JM, Christophersen, CT, Young, GP, Humphreys, KJ, Hu, Y, Gratz, SW, Miller, RB, Topping, DL, Bird, AR & Conlon, MA 2015a, 'Butyrylated starch intake can prevent red meat-induced O6-methyl-2-deoxyguanosine adducts in human rectal tissue: a randomised clinical trial', *Br J Nutr*, vol. 114, no. 2, pp. 220-30.
- Le Leu, RK, Winter, JM, Christophersen, CT, Young, GP, Humphreys, KJ, Hu, Y, Gratz, SW, Miller, RB, Topping, DL, Bird, AR & Conlon, MA 2015b, 'Butyrylated starch intake can prevent red meat-induced O(6)-methyl-2-deoxyguanosine adducts in human rectal tissue: a randomised clinical trial', *Br J Nutr*, vol. 114, no. 2, pp. 220-30.
- Lee, HY, Zhou, K, Smith, AM, Noland, CL & Doudna, JA 2013, 'Differential roles of human Dicer-binding proteins TRBP and PACT in small RNA processing', *Nucleic Acids Research*, vol. 41, no. 13, pp. 6568-76.
- Lee, RC, Feinbaum, RL & Ambros, V 1993, 'The *C. elegans* heterochronic gene *lin-4* encodes small RNAs with antisense complementarity to *lin-14*', *Cell*, vol. 75, no. 5, pp. 843-54.
- Lee, SH & McCormick, F 2006, 'p97/DAP5 is a ribosome-associated factor that facilitates protein synthesis and cell proliferation by modulating the synthesis of cell cycle proteins', *Embo j*, vol. 25, no. 17, pp. 4008-19.
- Lee, Y, Kim, M, Han, J, Yeom, KH, Lee, S, Baek, SH & Kim, VN 2004, 'MicroRNA genes are transcribed by RNA polymerase II', *Embo j*, vol. 23, no. 20, pp. 4051-60.
- Lee, YS & Dutta, A 2009, 'MicroRNAs in cancer', *Annual review of pathology*, vol. 4, pp. 199-227.
- Lennox, KA & Behlke, MA 2016, 'Cellular localization of long non-coding RNAs affects silencing by RNAi more than by antisense oligonucleotides', *Nucleic Acids Res*, vol. 44, no. 2, pp. 863-77.
- Leslie, NR & Downes, CP 2004, 'PTEN function: how normal cells control it and tumour cells lose it', *Biochem J*, vol. 382, no. Pt 1, pp. 1-11.
- Leucci, E, Patella, F, Waage, J, Holmstrom, K, Lindow, M, Porse, B, Kauppinen, S & Lund, AH 2013, 'microRNA-9 targets the long non-coding RNA MALAT1 for degradation in the nucleus', *Sci Rep*, vol. 3, p. 2535.
- Levin, B, Lieberman, DA, McFarland, B, Smith, RA, Brooks, D, Andrews, KS, Dash, C, Giardiello, FM, Glick, S, Levin, TR, Pickhardt, P, Rex, DK, Thorson, A & Winawer, SJ 2008, 'Screening and surveillance for the early detection of colorectal cancer and adenomatous polyps, 2008: a joint guideline from the American Cancer Society, the US Multi-Society Task Force on Colorectal Cancer, and the American College of Radiology', *CA Cancer J Clin*, vol. 58, no. 3, pp. 130-60.
- Levine, B, Sinha, S & Kroemer, G 2008, 'Bcl-2 family members: dual regulators of apoptosis and autophagy', *Autophagy*, vol. 4, no. 5, pp. 600-6.

## REFERENCES

- Lewin, MH, Bailey, N, Bandaletova, T, Bowman, R, Cross, AJ, Pollock, J, Shuker, DEG & Bingham, SA 2006, 'Red Meat Enhances the Colonic Formation of the DNA Adduct O6-Carboxymethyl Guanine: Implications for Colorectal Cancer Risk', *Cancer Research*, vol. 66, no. 3, pp. 1859-65.
- Lewis, BP, Burge, CB & Bartel, DP 2005, 'Conserved seed pairing, often flanked by adenosines, indicates that thousands of human genes are microRNA targets', *Cell*, vol. 120, no. 1, pp. 15-20.
- Li, C, Liu, T, Zhang, Y, Li, Q & Jin, LK 2019a, 'LncRNA-ZDHHC8P1 promotes the progression and metastasis of colorectal cancer by targeting miR-34a', *Eur Rev Med Pharmacol Sci*, vol. 23, no. 4, pp. 1476-86.
- Li, C, Zhou, L, He, J, Fang, XQ, Zhu, SW & Xiong, MM 2016a, 'Increased long noncoding RNA SNHG20 predicts poor prognosis in colorectal cancer', *BMC Cancer*, vol. 16, p. 655.
- Li, D, Hu, C & Li, H 2018a, 'Survivin as a novel target protein for reducing the proliferation of cancer cells', *Biomed Rep*, vol. 8, no. 5, pp. 399-406.
- Li, F, Ambrosini, G, Chu, EY, Plescia, J, Tognin, S, Marchisio, PC & Altieri, DC 1998, 'Control of apoptosis and mitotic spindle checkpoint by survivin', *Nature*, vol. 396, no. 6711, pp. 580-4.
- Li, H, Myeroff, L, Smiraglia, D, Romero, MF, Pretlow, TP, Kasturi, L, Lutterbaugh, J, Rerko, RM, Casey, G, Issa, JP, Willis, J, Willson, JK, Plass, C & Markowitz, SD 2003, 'SLC5A8, a sodium transporter, is a tumor suppressor gene silenced by methylation in human colon aberrant crypt foci and cancers', *Proc Natl Acad Sci U S A*, vol. 100, no. 14, pp. 8412-7.
- Li, J, Wang, Y, Zhang, C-G, Xiao, H-J, Hou, J-M & He, J-D 2018b, 'Effect of long non-coding RNA Gas5 on proliferation, migration, invasion and apoptosis of colorectal cancer HT-29 cell line', *Cancer Cell International*, vol. 18, pp. 4-.
- Li, L, Sun, R, Liang, Y, Pan, X, Li, Z, Bai, P, Zeng, X, Zhang, D, Zhang, L & Gao, L 2013a, 'Association between polymorphisms in long non-coding RNA PRNCR1 in 8q24 and risk of colorectal cancer', *J Exp Clin Cancer Res*, vol. 32, p. 104.
- Li, L, Sun, Y, Liu, J, Wu, X, Chen, L, Ma, L & Wu, P 2015a, 'Histone deacetylase inhibitor sodium butyrate suppresses DNA double strand break repair induced by etoposide more effectively in MCF-7 cells than in HEK293 cells', *BMC biochemistry*, vol. 16, pp. 2-.
- Li, P, Zhang, X, Wang, H, Wang, L, Liu, T, Du, L, Yang, Y & Wang, C 2017a, 'MALAT1 Is Associated with Poor Response to Oxaliplatin-Based Chemotherapy in Colorectal Cancer Patients and Promotes Chemoresistance through EZH2', *Mol Cancer Ther*, vol. 16, no. 4, pp. 739-51.
- Li, Q, Dai, Y, Wang, F & Hou, S 2016b, 'Differentially expressed long non-coding RNAs and the prognostic potential in colorectal cancer', *Neoplasma*, vol. 63, no. 6, pp. 977-83.

## REFERENCES

- Li, Q, Ding, C, Meng, T, Lu, W, Liu, W, Hao, H & Cao, L 2017b, 'Butyrate suppresses motility of colorectal cancer cells via deactivating Akt/ERK signaling in histone deacetylase dependent manner', *J Pharmacol Sci*, vol. 135, no. 4, pp. 148-55.
- Li, Q, Liang, X, Wang, Y, Meng, X, Xu, Y, Cai, S, Wang, Z, Liu, J & Cai, G 2016c, 'miR-139-5p Inhibits the Epithelial-Mesenchymal Transition and Enhances the Chemotherapeutic Sensitivity of Colorectal Cancer Cells by Downregulating BCL2', *Sci Rep*, vol. 6, p. 27157.
- Li, Q, Liang, X, Wang, Y, Meng, X, Xu, Y, Cai, S, Wang, Z, Liu, J & Cai, G 2016d, 'miR-139-5p Inhibits the Epithelial-Mesenchymal Transition and Enhances the Chemotherapeutic Sensitivity of Colorectal Cancer Cells by Downregulating BCL2', *Sci Rep*, vol. 6, p. 27157.
- Li, Q, Zhang, C, Chen, R, Xiong, H, Qiu, F, Liu, S, Zhang, M, Wang, F, Wang, Y, Zhou, X, Xiao, G, Wang, X & Jiang, Q 2016e, 'Disrupting MALAT1/miR-200c sponge decreases invasion and migration in endometrioid endometrial carcinoma', *Cancer Lett*, vol. 383, no. 1, pp. 28-40.
- Li, Q, Zou, C, Zou, C, Han, Z, Xiao, H, Wei, H, Wang, W, Zhang, L, Zhang, X, Tang, Q, Zhang, C, Tao, J, Wang, X & Gao, X 2013b, 'MicroRNA-25 functions as a potential tumor suppressor in colon cancer by targeting Smad7', *Cancer Lett*, vol. 335, no. 1, pp. 168-74.
- Li, T, Yang, J, Lv, X, Liu, K, Gao, C, Xing, Y & Xi, T 2014a, 'miR-155 regulates the proliferation and cell cycle of colorectal carcinoma cells by targeting E2F2', *Biotechnol Lett*, vol. 36, no. 9, pp. 1743-52.
- Li, T, Zhu, J, Wang, X, Chen, G, Sun, L, Zuo, S, Zhang, J, Chen, S, Ma, J, Yao, Z, Zheng, Y, Chen, Z, Liu, Y & Wang, P 2017c, 'Long non-coding RNA lncTCF7 activates the Wnt/beta-catenin pathway to promote metastasis and invasion in colorectal cancer', *Oncol Lett*, vol. 14, no. 6, pp. 7384-90.
- Li, Y, Huang, S, Li, Y, Zhang, W, He, K, Zhao, M, Lin, H, Li, D, Zhang, H, Zheng, Z & Huang, C 2016f, 'Decreased expression of LncRNA SLC25A25-AS1 promotes proliferation, chemoresistance, and EMT in colorectal cancer cells', *Tumour Biol*.
- Li, Y, Li, C, Li, D, Yang, L, Jin, J & Zhang, B 2019b, 'lncRNA KCNQ1OT1 enhances the chemoresistance of oxaliplatin in colon cancer by targeting the miR-34a/ATG4B pathway', *Onco Targets Ther*, vol. 12, pp. 2649-60.
- Li, Y, Li, Y, Chen, W, He, F, Tan, Z, Zheng, J, Wang, W, Zhao, Q & Li, J 2015b, 'NEAT expression is associated with tumor recurrence and unfavorable prognosis in colorectal cancer', *Oncotarget*, vol. 6, no. 29, pp. 27641-50.
- Li, Z, Wang, Y, Yuan, C, Zhu, Y, Qiu, J, Zhang, W, Qi, B, Wu, H, Ye, J, Jiang, H, Yang, J & Cheng, J 2014b, 'Oncogenic roles of Bmi1 and its therapeutic inhibition by histone deacetylase inhibitor in tongue cancer', *Lab Invest*.
- Liang, WC, Fu, WM, Wong, CW, Wang, Y, Wang, WM, Hu, GX, Zhang, L, Xiao, LJ, Wan, DC, Zhang, JF & Waye, MM 2015a, 'The lncRNA H19 promotes epithelial to mesenchymal transition by functioning as miRNA sponges in colorectal cancer', *Oncotarget*, vol. 6, no. 26, pp. 22513-25.

## REFERENCES

- Liang, Y, Ridzon, D, Wong, L & Chen, C 2007, 'Characterization of microRNA expression profiles in normal human tissues', *BMC Genomics*, vol. 8, p. 166.
- Liang, Y, Zhao, Q, Fan, L, Zhang, Z, Tan, B, Liu, Y & Li, Y 2015b, 'Down-regulation of MicroRNA-381 promotes cell proliferation and invasion in colon cancer through up-regulation of LRH-1', *Biomed Pharmacother*, vol. 75, pp. 137-41.
- Liang, Z, Chen, Y, Zhao, Y, Xu, C, Zhang, A, Zhang, Q, Wang, D, He, J, Hua, W & Duan, P 2017, 'miR-200c suppresses endometriosis by targeting MALAT1 in vitro and in vivo', *Stem Cell Res Ther*, vol. 8, no. 1, p. 251.
- Lievre, A, Bachet, JB, Le Corre, D, Boige, V, Landi, B, Emile, JF, Cote, JF, Tomasic, G, Penna, C, Ducreux, M, Rougier, P, Penault-Llorca, F & Laurent-Puig, P 2006, 'KRAS mutation status is predictive of response to cetuximab therapy in colorectal cancer', *Cancer Res*, vol. 66, no. 8, pp. 3992-5.
- Lijinsky, W 1999, 'N-Nitroso compounds in the diet', *Mutation Research/Genetic Toxicology and Environmental Mutagenesis*, vol. 443, no. 1-2, pp. 129-38.
- Lim, DHK & Maher, ER 2011, 'DNA methylation: A form of epigenetic control of gene expression', vol. 12, pp. 37-42.
- Lim, S & Kaldis, P 2013, 'Cdks, cyclins and CKIs: roles beyond cell cycle regulation', *Development*, vol. 140, no. 15, pp. 3079-93.
- Lin, K-Y, Zhang, X-J, Feng, D-D, Zhang, H, Zeng, C-W, Han, B-W, Zhou, A-D, Qu, L-H, Xu, L & Chen, Y-Q 2011, 'miR-125b, a target of CDX2, regulates cell differentiation through repression of the core binding factor in hematopoietic malignancies', *J Biol Chem*, vol. 286, no. 44, pp. 38253-63.
- Ling, H, Spizzo, R, Atlasi, Y, Nicoloso, M, Shimizu, M, Redis, RS, Nishida, N, Gafà, R, Song, J, Guo, Z, Ivan, C, Barbarotto, E, De Vries, I, Zhang, X, Ferracin, M, Churchman, M, van Galen, JF, Beverloo, BH, Shariati, M, Haderk, F, Estecio, MR, Garcia-Manero, G, Patijn, GA, Gotley, DC, Bhardwaj, V, Shureiqi, I, Sen, S, Multani, AS, Welsh, J, Yamamoto, K, Taniguchi, I, Song, M-A, Gallinger, S, Casey, G, Thibodeau, SN, Le Marchand, L, Tiirikainen, M, Mani, SA, Zhang, W, Davuluri, RV, Mimori, K, Mori, M, Sieuwerts, AM, Martens, JWM, Tomlinson, I, Negrini, M, Berindan-Neagoe, I, Foekens, JA, Hamilton, SR, Lanza, G, Kopetz, S, Fodde, R & Calin, GA 2013, 'CCAT2, a novel noncoding RNA mapping to 8q24, underlies metastatic progression and chromosomal instability in colon cancer', *Genome Res*, vol. 23, no. 9, pp. 1446-61.
- Link, A, Balaguer, F, Shen, Y, Nagasaka, T, Lozano, JJ, Boland, CR & Goel, A 2010, 'Fecal MicroRNAs as novel biomarkers for colon cancer screening', *Cancer Epidemiol Biomarkers Prev*, vol. 19, no. 7, pp. 1766-74.
- Liu, C, Kelnar, K, Liu, B, Chen, X, Calhoun-Davis, T, Li, H, Patrawala, L, Yan, H, Jeter, C, Honorio, S, Wiggins, JF, Bader, AG, Fagin, R, Brown, D & Tang, DG 2011a, 'The microRNA miR-34a inhibits prostate cancer stem cells and metastasis by directly repressing CD44', *Nat Med*, vol. 17, no. 2, pp. 211-5.

## REFERENCES

- Liu, C, Li, Y, Semenov, M, Han, C, Baeg, GH, Tan, Y, Zhang, Z, Lin, X & He, X 2002, 'Control of beta-catenin phosphorylation/degradation by a dual-kinase mechanism', *Cell*, vol. 108, no. 6, pp. 837-47.
- Liu, J, Bian, T, Feng, J, Qian, L, Zhang, J, Jiang, D, Zhang, Q, Li, X, Liu, Y & Shi, J 2018a, 'miR-335 inhibited cell proliferation of lung cancer cells by target Tra2beta', *Cancer Sci*, vol. 109, no. 2, pp. 289-96.
- Liu, L, Ji, C, Chen, J, Li, Y, Fu, X, Xie, Y, Gu, S & Mao, Y 2008, 'A global genomic view of MIF knockdown-mediated cell cycle arrest', *Cell Cycle*, vol. 7, no. 11, pp. 1678-92.
- Liu, M, Lang, N, Qiu, M, Xu, F, Li, Q, Tang, Q, Chen, J, Chen, X, Zhang, S, Liu, Z, Zhou, J, Zhu, Y, Deng, Y, Zheng, Y & Bi, F 2011b, 'miR-137 targets Cdc42 expression, induces cell cycle G1 arrest and inhibits invasion in colorectal cancer cells', *Int J Cancer*, vol. 128, no. 6, pp. 1269-79.
- Liu, Q, Huang, J, Zhou, N, Zhang, Z, Zhang, A, Lu, Z, Wu, F & Mo, YY 2013a, 'LncRNA loc285194 is a p53-regulated tumor suppressor', *Nucleic Acids Res*, vol. 41, no. 9, pp. 4976-87.
- Liu, R, Yang, M, Meng, Y, Liao, J, Sheng, J, Pu, Y, Yin, L & Kim, SJ 2013b, 'Tumor-suppressive function of miR-139-5p in esophageal squamous cell carcinoma', *PLoS One*, vol. 8, no. 10, p. e77068.
- Liu, S, Xu, B & Yan, D 2016a, 'Enhanced expression of long non-coding RNA Sox2ot promoted cell proliferation and motility in colorectal cancer', *Minerva Med*, vol. 107, no. 5, pp. 279-86.
- Liu, T, Yu, T, Hu, H & He, K 2018b, 'Knockdown of the long non-coding RNA HOTTIP inhibits colorectal cancer cell proliferation and migration and induces apoptosis by targeting SGK1', *Biomed Pharmacother*, vol. 98, pp. 286-96.
- Liu, T, Zhang, X, Yang, Y-m, Du, L-t & Wang, C-x 2016b, 'Increased expression of the long noncoding RNA CRNDE-h indicates a poor prognosis in colorectal cancer, and is positively correlated with IRX5 mRNA expression', *OncoTargets and therapy*, vol. 9, pp. 1437-48.
- Liu, X, Jakubowski, M & Hunt, JL 2011c, 'KRAS gene mutation in colorectal cancer is correlated with increased proliferation and spontaneous apoptosis', *Am J Clin Pathol*, vol. 135, no. 2, pp. 245-52.
- Liu, Y, Beyer, A & Aebersold, R 2016c, 'On the Dependency of Cellular Protein Levels on mRNA Abundance', *Cell*, vol. 165, no. 3, pp. 535-50.
- Liu, Y & Bodmer, WF 2006, 'Analysis of P53 mutations and their expression in 56 colorectal cancer cell lines', *Proc Natl Acad Sci U S A*, vol. 103, no. 4, pp. 976-81.
- Long, HC, Gao, X, Lei, CJ, Zhu, B, Li, L, Zeng, C, Huang, JB & Feng, JR 2016, 'miR-542-3p inhibits the growth and invasion of colorectal cancer cells through targeted regulation of cortactin', *Int J Mol Med*, vol. 37, no. 4, pp. 1112-8.
- Louis, P, Hold, GL & Flint, HJ 2014, 'The gut microbiota, bacterial metabolites and colorectal cancer', *Nat Rev Microbiol*, vol. 12, no. 10, pp. 661-72.

## REFERENCES

- Love, MI, Huber, W & Anders, S 2014, 'Moderated estimation of fold change and dispersion for RNA-seq data with DESeq2', *Genome Biol*, vol. 15, no. 12, p. 550.
- Lu, J, Getz, G, Miska, EA, Alvarez-Saavedra, E, Lamb, J, Peck, D, Sweet-Cordero, A, Ebert, BL, Mak, RH, Ferrando, AA, Downing, JR, Jacks, T, Horvitz, HR & Golub, TR 2005, 'MicroRNA expression profiles classify human cancers', *Nature*, vol. 435, no. 7043, pp. 834-8.
- Lu, M, Liu, Z, Li, B, Wang, G, Li, D & Zhu, Y 2016a, 'The high expression of long non-coding RNA PANDAR indicates a poor prognosis for colorectal cancer and promotes metastasis by EMT pathway', *J Cancer Res Clin Oncol*.
- Lu, M, Liu, Z, Li, B, Wang, G, Li, D & Zhu, Y 2017a, 'The high expression of long non-coding RNA PANDAR indicates a poor prognosis for colorectal cancer and promotes metastasis by EMT pathway', *J Cancer Res Clin Oncol*, vol. 143, no. 1, pp. 71-81.
- Lu, X, Liu, Z, Ning, X, Huang, L & Jiang, B 2018, 'The Long Noncoding RNA HOTAIR Promotes Colorectal Cancer Progression by Sponging miR-197', *Oncol Res*, vol. 26, no. 3, pp. 473-81.
- Lu, X, Yu, Y & Tan, S 2019, 'Long non-coding XIAP-AS1 regulates cell proliferation, invasion and cell cycle in colon cancer', *Artif Cells Nanomed Biotechnol*, vol. 47, no. 1, pp. 767-75.
- Lu, Y, Shi, C, Qiu, S & Fan, Z 2016b, 'Identification and validation of COX-2 as a co-target for overcoming cetuximab resistance in colorectal cancer cells', *Oncotarget*, vol. 7, no. 40, pp. 64766-77.
- Lu, Y, Zhao, X, Liu, Q, Li, C, Graves-Deal, R, Cao, Z, Singh, B, Franklin, JL, Wang, J, Hu, H, Wei, T, Yang, M, Yeatman, TJ, Lee, E, Saito-Diaz, K, Hinger, S, Patton, JG, Chung, CH, Emrich, S, Klusmann, J-H, Fan, D & Coffey, RJ 2017b, 'lncRNA MIR100HG-derived miR-100 and miR-125b mediate cetuximab resistance via Wnt/ $\beta$ -catenin signaling', *Nat Med*, vol. 23, no. 11, pp. 1331-41.
- Luo, J, Qu, J, Wu, D-K, Lu, Z-L, Sun, Y-S & Qu, Q 2017, 'Long non-coding RNAs: a rising biotarget in colorectal cancer', *Oncotarget*, vol. 8, no. 13, pp. 22187-202.
- Lv, SY, Shan, TD, Pan, XT, Tian, ZB, Liu, XS, Liu, FG, Sun, XG, Xue, HG, Li, XH, Han, Y, Sun, LJ, Chen, L & Zhang, LY 2018, 'The lncRNA ZEB1-AS1 sponges miR-181a-5p to promote colorectal cancer cell proliferation by regulating Wnt/beta-catenin signaling', *Cell Cycle*, vol. 17, no. 10, pp. 1245-54.
- Lyu, H, Wang, S, Huang, J, Wang, B, He, Z & Liu, B 2018, 'Survivin-targeting miR-542-3p overcomes HER3 signaling-induced chemoresistance and enhances the antitumor activity of paclitaxel against HER2-overexpressing breast cancer', *Cancer Lett*, vol. 420, pp. 97-108.
- Ma, J, Zhu, Y, Wang, Z, Zan, J, Cao, L, Feng, Z, Wang, S, Fan, Q & Yan, L 2019, '[miR-593 inhibits proliferation of colon cancer cells in vitro by down-regulating PLK1]', *Nan Fang Yi Ke Da Xue Xue Bao*, vol. 39, no. 2, pp. 144-9.

## REFERENCES

- Ma, S, Yang, D, Liu, Y, Wang, Y, Lin, T, Li, Y, Yang, S, Zhang, W & Zhang, R 2018, 'LncRNA BANC1 promotes tumorigenesis and enhances adriamycin resistance in colorectal cancer', *Aging*, vol. 10, no. 8, pp. 2062-78.
- Ma, Y, Yang, Y, Wang, F, Moyer, MP, Wei, Q, Zhang, P, Yang, Z, Liu, W, Zhang, H, Chen, N, Wang, H, Wang, H & Qin, H 2015, 'Long non-coding RNA CCAL regulates colorectal cancer progression by activating Wnt/beta-catenin signalling pathway via suppression of activator protein 2alpha', *Gut*.
- MacFarlane, L-A & Murphy, PR 2010, 'MicroRNA: Biogenesis, Function and Role in Cancer', *Current Genomics*, vol. 11, no. 7, pp. 537-61.
- Mahyar-Roemer, M & Roemer, K 2001, 'p21 Waf1/Cip1 can protect human colon carcinoma cells against p53-dependent and p53-independent apoptosis induced by natural chemopreventive and therapeutic agents', *Oncogene*, vol. 20, no. 26, pp. 3387-98.
- Major, ML, Lepe, R & Costa, RH 2004, 'Forkhead box M1B transcriptional activity requires binding of Cdk-cyclin complexes for phosphorylation-dependent recruitment of p300/CBP coactivators', *Mol Cell Biol*, vol. 24, no. 7, pp. 2649-61.
- Makarenkov, V, Zentilli, P, Kevorkov, D, Gagarin, A, Malo, N & Nadon, R 2007, 'An efficient method for the detection and elimination of systematic error in high-throughput screening', *Bioinformatics*, vol. 23, no. 13, pp. 1648-57.
- Mandal, M, Adam, L, Mendelsohn, J & Kumar, R 1998, 'Nuclear targeting of Bax during apoptosis in human colorectal cancer cells', *Oncogene*, vol. 17, no. 8, pp. 999-1007.
- Mann, BS, Johnson, JR, Cohen, MH, Justice, R & Pazdur, R 2007, 'FDA approval summary: vorinostat for treatment of advanced primary cutaneous T-cell lymphoma', *Oncologist*, vol. 12, no. 10, pp. 1247-52.
- Maragkakis, M, Reczko, M, Simossis, VA, Alexiou, P, Papadopoulos, GL, Dalamagas, T, Giannopoulos, G, Goumas, G, Koukis, E, Kourtis, K, Vergoulis, T, Koziris, N, Sellis, T, Tsanakas, P & Hatzigeorgiou, AG 2009, 'DIANA-microT web server: elucidating microRNA functions through target prediction', *Nucleic Acids Research*, vol. 37, no. suppl 2, pp. W273-W6.
- Mariadason, JM 2008, 'HDACs and HDAC inhibitors in colon cancer', *Epigenetics*, vol. 3, no. 1, pp. 28-37.
- Mariadason, JM, Corner, GA & Augenlicht, LH 2000, 'Genetic reprogramming in pathways of colonic cell maturation induced by short chain fatty acids: comparison with trichostatin A, sulindac, and curcumin and implications for chemoprevention of colon cancer', *Cancer Res*, vol. 60, no. 16, pp. 4561-72.
- Marin-Bejar, O, Marchese, FP, Athie, A, Sanchez, Y, Gonzalez, J, Segura, V, Huang, L, Moreno, I, Navarro, A, Monzo, M, Garcia-Foncillas, J, Rinn, JL, Guo, S & Huarte, M 2013, 'Pint lincRNA connects the p53 pathway with epigenetic silencing by the Polycomb repressive complex 2', *Genome Biol*, vol. 14, no. 9, p. R104.
- Martini, M, De Santis, MC, Braccini, L, Gulluni, F & Hirsch, E 2014, 'PI3K/AKT signaling pathway and cancer: an updated review', *Ann Med*, vol. 46, no. 6, pp. 372-83.

## REFERENCES

- Matheson, CJ, Backos, DS & Reigan, P 2016, 'Targeting WEE1 Kinase in Cancer', *Trends Pharmacol Sci*, vol. 37, no. 10, pp. 872-81.
- Matsumura, T, Sugimachi, K, Inuma, H, Takahashi, Y, Kurashige, J, Sawada, G, Ueda, M, Uchi, R, Ueo, H, Takano, Y, Shinden, Y, Eguchi, H, Yamamoto, H, Doki, Y, Mori, M, Ochiya, T & Mimori, K 2015, 'Exosomal microRNA in serum is a novel biomarker of recurrence in human colorectal cancer', *Br J Cancer*, vol. 113, no. 2, pp. 275-81.
- Mayo, LD & Donner, DB 2001, 'A phosphatidylinositol 3-kinase/Akt pathway promotes translocation of Mdm2 from the cytoplasm to the nucleus', *Proc Natl Acad Sci U S A*, vol. 98, no. 20, pp. 11598-603.
- Mayr, C & Bartel, DP 2009, 'Widespread shortening of 3'UTRs by alternative cleavage and polyadenylation activates oncogenes in cancer cells', *Cell*, vol. 138, no. 4, pp. 673-84.
- Mazzoni, SM & Fearon, ER 2014, 'AXIN1 and AXIN2 variants in gastrointestinal cancers', *Cancer Lett*, vol. 355, no. 1, pp. 1-8.
- McIntyre, A, Gibson, PR & Young, GP 1993, 'Butyrate production from dietary fibre and protection against large bowel cancer in a rat model', *Gut*, vol. 34, no. 3, pp. 386-91.
- Medema, RH, Kops, GJ, Bos, JL & Burgering, BM 2000, 'AFX-like Forkhead transcription factors mediate cell-cycle regulation by Ras and PKB through p27kip1', *Nature*, vol. 404, no. 6779, pp. 782-7.
- Metz, HE & Houghton, AM 2011, 'Insulin receptor substrate regulation of phosphoinositide 3-kinase', *Clin Cancer Res*, vol. 17, no. 2, pp. 206-11.
- Miao, Y, Fan, R, Chen, L & Qian, H 2016, 'Clinical Significance of Long Non-coding RNA MALAT1 Expression in Tissue and Serum of Breast Cancer', *Ann Clin Lab Sci*, vol. 46, no. 4, pp. 418-24.
- Michael, MZ, SM, OC, van Holst Pellekaan, NG, Young, GP & James, RJ 2003, 'Reduced accumulation of specific microRNAs in colorectal neoplasia', *Mol Cancer Res*, vol. 1, no. 12, pp. 882-91.
- Milla, PJ 2009, 'Advances in understanding colonic function', *J Pediatr Gastroenterol Nutr*, vol. 48 Suppl 2, pp. S43-5.
- Miller, AA, Kurschel, E, Osieka, R & Schmidt, CG 1987, 'Clinical pharmacology of sodium butyrate in patients with acute leukemia', *Eur J Cancer Clin Oncol*, vol. 23, no. 9, pp. 1283-7.
- Miller, CJ, Li, Q, Abel, K, Kim, EY, Ma, ZM, Wietgreffe, S, La Franco-Scheuch, L, Compton, L, Duan, L, Shore, MD, Zupancic, M, Busch, M, Carlis, J, Wolinsky, S & Haase, AT 2005, 'Propagation and dissemination of infection after vaginal transmission of simian immunodeficiency virus', *J Virol*, vol. 79, no. 14, pp. 9217-27.
- Mima, K, Nishihara, R, Yang, J, Dou, R, Masugi, Y, Shi, Y, da Silva, A, Cao, Y, Song, M, Nowak, J, Gu, M, Li, W, Morikawa, T, Zhang, X, Wu, K, Baba, H, Giovannucci, EL, Meyerhardt, JA, Chan, AT, Fuchs, CS, Qian, ZR & Ogino, S 2016, 'MicroRNA MIR21 (miR-21) and PTGS2 Expression in Colorectal Cancer and Patient Survival', *Clin Cancer Res*, vol. 22, no. 15, pp. 3841-8.

## REFERENCES

- Miranda, KC, Huynh, T, Tay, Y, Ang, YS, Tam, WL, Thomson, AM, Lim, B & Rigoutsos, I 2006, 'A pattern-based method for the identification of MicroRNA binding sites and their corresponding heteroduplexes', *Cell*, vol. 126, no. 6, pp. 1203-17.
- Miyoshi, J, Toden, S, Yoshida, K, Toiyama, Y, Alberts, SR, Kusunoki, M, Sinicrope, FA & Goel, A 2017, 'MiR-139-5p as a novel serum biomarker for recurrence and metastasis in colorectal cancer', *Sci Rep*, vol. 7, p. 43393.
- Modarresi, F, Faghihi, MA, Lopez-Toledano, MA, Fatemi, RP, Magistri, M, Brothers, SP, van der Brug, MP & Wahlestedt, C 2012, 'Natural Antisense Inhibition Results in Transcriptional De-Repression and Gene Upregulation', *Nature biotechnology*, vol. 30, no. 5, pp. 453-9.
- Mojarad, EN, Kuppen, PJK, Aghdaei, HA & Zali, MR 2013, 'The CpG island methylator phenotype (CIMP) in colorectal cancer', *Gastroenterology and Hepatology From Bed to Bench*, vol. 6, no. 3, pp. 120-8.
- Molinari, M 2000, 'Cell cycle checkpoints and their inactivation in human cancer', *Cell Prolif*, vol. 33, no. 5, pp. 261-74.
- Mongroo, PS & Rustgi, AK 2010, 'The role of the miR-200 family in epithelial-mesenchymal transition', *Cancer Biology & Therapy*, vol. 10, no. 3, pp. 219-22.
- Morin, PJ, Sparks, AB, Korinek, V, Barker, N, Clevers, H, Vogelstein, B & Kinzler, KW 1997, 'Activation of beta-catenin-Tcf signaling in colon cancer by mutations in beta-catenin or APC', *Science*, vol. 275, no. 5307, pp. 1787-90.
- Morlando, M, Ballarino, M & Fatica, A 2015, 'Long Non-Coding RNAs: New Players in Hematopoiesis and Leukemia', *Frontiers in medicine*, vol. 2, pp. 23-.
- Moss, EG, Lee, RC & Ambros, V 1997, 'The cold shock domain protein LIN-28 controls developmental timing in *C. elegans* and is regulated by the lin-4 RNA', *Cell*, vol. 88, no. 5, pp. 637-46.
- Mpindi, JP, Swapnil, P, Dmitrii, B, Jani, S, Saeed, K, Wennerberg, K, Aittokallio, T, Ostling, P & Kallioniemi, O 2015, 'Impact of normalization methods on high-throughput screening data with high hit rates and drug testing with dose-response data', *Bioinformatics*, vol. 31, no. 23, pp. 3815-21.
- Muljo, SA, Kanellopoulou, C & Aravind, L 2010, 'MicroRNA targeting in mammalian genomes: genes and mechanisms', *Wiley interdisciplinary reviews. Systems biology and medicine*, vol. 2, no. 2, pp. 148-61.
- Muller, PY, Janovjak, H, Miserez, AR & Dobbie, Z 2002, 'Processing of gene expression data generated by quantitative real-time RT-PCR', *Biotechniques*, vol. 32, no. 6, pp. 1372-4, 6, 8-9.
- Murie, C, Barette, C, Lafanechere, L & Nadon, R 2014, 'Control-Plate Regression (CPR) Normalization for High-Throughput Screens with Many Active Features', *Journal of biomolecular screening*, vol. 19, no. 5, pp. 661-71.

## REFERENCES

- Murphy, AJ, Guyre, PM & Pioli, PA 2010, 'Estradiol suppresses NF-kappa B activation through coordinated regulation of let-7a and miR-125b in primary human macrophages', *J Immunol*, vol. 184, no. 9, pp. 5029-37.
- Naemura, M, Tsunoda, T, Inoue, Y, Okamoto, H, Shirasawa, S & Kotake, Y 2016, 'ANRIL regulates the proliferation of human colorectal cancer cells in both two- and three-dimensional culture', *Mol Cell Biochem*, vol. 412, no. 1-2, pp. 141-6.
- Nagano, T, Mitchell, JA, Sanz, LA, Pauler, FM, Ferguson-Smith, AC, Feil, R & Fraser, P 2008, 'The Air noncoding RNA epigenetically silences transcription by targeting G9a to chromatin', *Science*, vol. 322, no. 5908, pp. 1717-20.
- Nagao, M, Honda, M, Seino, Y, Yahagi, T & Sugimura, T 1977, 'Mutagenicities of smoke condensates and the charred surface of fish and meat', *Cancer Lett*, vol. 2, no. 4-5, pp. 221-6.
- Nagel, R, le Sage, C, Diosdado, B, van der Waal, M, Oude Vrielink, JA, Bolijn, A, Meijer, GA & Agami, R 2008, 'Regulation of the adenomatous polyposis coli gene by the miR-135 family in colorectal cancer', *Cancer Res*, vol. 68, no. 14, pp. 5795-802.
- Nakano, K & Vousden, KH 2001, 'PUMA, a novel proapoptotic gene, is induced by p53', *Mol Cell*, vol. 7, no. 3, pp. 683-94.
- Nasevicius, A & Ekker, SC 2000, 'Effective targeted gene 'knockdown' in zebrafish', *Nat Genet*, vol. 26, no. 2, pp. 216-20.
- Nave, BT, Ouwens, M, Withers, DJ, Alessi, DR & Shepherd, PR 1999, 'Mammalian target of rapamycin is a direct target for protein kinase B: identification of a convergence point for opposing effects of insulin and amino-acid deficiency on protein translation', *Biochem J*, vol. 344 Pt 2, pp. 427-31.
- Neerincx, M, Sie, DLS, van de Wiel, MA, van Grieken, NCT, Burggraaf, JD, Dekker, H, Eijk, PP, Ylstra, B, Verhoef, C, Meijer, GA, Buffart, TE & Verheul, HMW 2015, 'MiR expression profiles of paired primary colorectal cancer and metastases by next-generation sequencing', *Oncogenesis*, vol. 4, no. 10, pp. e170-e.
- Ng, EK, Chong, WW, Jin, H, Lam, EK, Shin, VY, Yu, J, Poon, TC, Ng, SS & Sung, JJ 2009a, 'Differential expression of microRNAs in plasma of patients with colorectal cancer: a potential marker for colorectal cancer screening', *Gut*, vol. 58, no. 10, pp. 1375-81.
- Ng, EK, Chong, WW, jin, h, Lam, EK, Shin, VY, Yu, J, Poon, TCW, Ng, SS & Sung, JJY 2009b, 'Differential expression of microRNAs in plasma of colorectal cancer patients: A potential marker for colorectal cancer screening', *Gut*.
- Ni, B, Yu, X, Guo, X, Fan, X, Yang, Z, Wu, P, Yuan, Z, Deng, Y, Wang, J, Chen, D & Wang, L 2015, 'Increased urothelial cancer associated 1 is associated with tumor proliferation and metastasis and predicts poor prognosis in colorectal cancer', *Int J Oncol*, vol. 47, no. 4, pp. 1329-38.
- Nie, J, Liu, L, Zheng, W, Chen, L, Wu, X, Xu, Y, Du, X & Han, W 2012a, 'microRNA-365, down-regulated in colon cancer, inhibits cell cycle progression and promotes

## REFERENCES

- apoptosis of colon cancer cells by probably targeting Cyclin D1 and Bcl-2', *Carcinogenesis*, vol. 33, no. 1, pp. 220-5.
- Nie, L, Wu, HJ, Hsu, JM, Chang, SS, Labaff, AM, Li, CW, Wang, Y, Hsu, JL & Hung, MC 2012b, 'Long non-coding RNAs: versatile master regulators of gene expression and crucial players in cancer', *Am J Transl Res*, vol. 4, no. 2, pp. 127-50.
- Nishida, N, Yano, H, Nishida, T, Kamura, T & Kojiro, M 2006, 'Angiogenesis in cancer', *Vascular health and risk management*, vol. 2, no. 3, pp. 213-9.
- Nishida, N, Yokobori, T, Mimori, K, Sudo, T, Tanaka, F, Shibata, K, Ishii, H, Doki, Y, Kuwano, H & Mori, M 2011, 'MicroRNA miR-125b is a prognostic marker in human colorectal cancer', *Int J Oncol*, vol. 38, no. 5, pp. 1437-43.
- Nissan, A, Stojadinovic, A, Mitrani-Rosenbaum, S, Halle, D, Grinbaum, R, Roistacher, M, Bochem, A, Dayanc, BE, Ritter, G, Gomceli, I, Bostanci, EB, Akoglu, M, Chen, YT, Old, LJ & Gure, AO 2012, 'Colon cancer associated transcript-1: a novel RNA expressed in malignant and pre-malignant human tissues', *Int J Cancer*, vol. 130, no. 7, pp. 1598-606.
- Nohr, MK, Pedersen, MH, Gille, A, Egerod, KL, Engelstoft, MS, Husted, AS, Sichlau, RM, Grunddal, KV, Poulsen, SS, Han, S, Jones, RM, Offermanns, S & Schwartz, TW 2013, 'GPR41/FFAR3 and GPR43/FFAR2 as cosensors for short-chain fatty acids in enteroendocrine cells vs FFAR3 in enteric neurons and FFAR2 in enteric leukocytes', *Endocrinology*, vol. 154, no. 10, pp. 3552-64.
- Nunez, F, Bravo, S, Cruzat, F, Montecino, M & De Ferrari, GV 2011, 'Wnt/beta-catenin signaling enhances cyclooxygenase-2 (COX2) transcriptional activity in gastric cancer cells', *PLoS One*, vol. 6, no. 4, p. e18562.
- Ochiumi, T, Kitadai, Y, Tanaka, S, Akagi, M, Yoshihara, M & Chayama, K 2006, 'Neuropilin-1 is involved in regulation of apoptosis and migration of human colon cancer', *Int J Oncol*, vol. 29, no. 1, pp. 105-16.
- Ogawa, H, Rafiee, P, Fisher, PJ, Johnson, NA, Otterson, MF & Binion, DG 2003, 'Sodium butyrate inhibits angiogenesis of human intestinal microvascular endothelial cells through COX-2 inhibition', *FEBS Lett*, vol. 554, no. 1-2, pp. 88-94.
- Olive, V, Jiang, I & He, L 2010, 'mir-17-92, a cluster of miRNAs in the midst of the cancer network', *Int J Biochem Cell Biol*, vol. 42, no. 8, pp. 1348-54.
- Olschwang, S, Laurent-Puig, P, Groden, J, White, R & Thomas, G 1993, 'Germ-line mutations in the first 14 exons of the adenomatous polyposis coli (APC) gene', *Am J Hum Genet*, vol. 52, no. 2, pp. 273-9.
- Orang, AV & Barzegari, A 2014, 'MicroRNAs in colorectal cancer: from diagnosis to targeted therapy', *Asian Pac J Cancer Prev*, vol. 15, no. 17, pp. 6989-99.
- Pa, M, Naizaer, G, Seyiti, A & Kuerbang, G 2017, 'Long Noncoding RNA MALAT1 Functions as a Sponge of MiR-200c in Ovarian Cancer', *Oncol Res*.

## REFERENCES

- Pachnis, V, Belayew, A & Tilghman, SM 1984, 'Locus unlinked to alpha-fetoprotein under the control of the murine raf and Rif genes', *Proc Natl Acad Sci U S A*, vol. 81, no. 17, pp. 5523-7.
- Padua Alves, C, Fonseca, AS, Muys, BR, de Barros, ELBR, Burger, MC, de Souza, JE, Valente, V, Zago, MA & Silva, WA, Jr. 2013, 'Brief report: The lincRNA Hotair is required for epithelial-to-mesenchymal transition and stemness maintenance of cancer cell lines', *Stem Cells*, vol. 31, no. 12, pp. 2827-32.
- Paine, PL, Moore, LC & Horowitz, SB 1975, 'Nuclear envelope permeability', *Nature*, vol. 254, no. 5496, pp. 109-14.
- Pan, Y, Liang, H, Chen, W, Zhang, H, Wang, N, Wang, F, Zhang, S, Liu, Y, Zhao, C, Yan, X, Zhang, J, Zhang, C-Y, Gu, H, Zen, K & Chen, X 2015, 'microRNA-200b and microRNA-200c promote colorectal cancer cell proliferation via targeting the reversion-inducing cysteine-rich protein with Kazal motifs', *RNA Biology*, vol. 12, no. 3, pp. 276-89.
- Papadopoulos, N & Lindblom, A 1997, 'Molecular basis of HNPCC: Mutations of MMR genes', *Human Mutation*, vol. 10, no. 2, pp. 89-99.
- Paraskevopoulou, MD, Georgakilas, G, Kostoulas, N, Vlachos, IS, Vergoulis, T, Reczko, M, Filippidis, C, Dalamagas, T & Hatzigeorgiou, AG 2013, 'DIANA-microT web server v5.0: service integration into miRNA functional analysis workflows', *Nucleic Acids Research*, vol. 41, no. Web Server issue, pp. W169-W73.
- Paraskevopoulou, MD, Vlachos, IS, Karagkouni, D, Georgakilas, G, Kanellos, I, Vergoulis, T, Zagganas, K, Tsanakas, P, Floros, E, Dalamagas, T & Hatzigeorgiou, AG 2016, 'DIANA-LncBase v2: indexing microRNA targets on non-coding transcripts', *Nucleic Acids Research*, vol. 44, no. D1, pp. D231-D8.
- Parikh, AA, Fan, F, Liu, WB, Ahmad, SA, Stoeltzing, O, Reinmuth, N, Bielenberg, D, Bucana, CD, Klagsbrun, M & Ellis, LM 2004, 'Neuropilin-1 in human colon cancer: expression, regulation, and role in induction of angiogenesis', *Am J Pathol*, vol. 164, no. 6, pp. 2139-51.
- Parker, R & Sheth, U 2007, 'P Bodies and the Control of mRNA Translation and Degradation', *Molecular Cell*, vol. 25, no. 5, pp. 635-46.
- Pasquale, EB 2010, 'Eph receptors and ephrins in cancer: bidirectional signalling and beyond', *Nat Rev Cancer*, vol. 10, no. 3, pp. 165-80.
- Pasquinelli, AE, Reinhart, BJ, Slack, F, Martindale, MQ, Kuroda, MI, Maller, B, Hayward, DC, Ball, EE, Degnan, B, Muller, P, Spring, J, Srinivasan, A, Fishman, M, Finnerty, J, Corbo, J, Levine, M, Leahy, P, Davidson, E & Ruvkun, G 2000, 'Conservation of the sequence and temporal expression of let-7 heterochronic regulatory RNA', *Nature*, vol. 408, no. 6808, pp. 86-9.
- Patel, PH, Barbee, SA & Blankenship, JT 2016, 'GW-Bodies and P-Bodies Constitute Two Separate Pools of Sequestered Non-Translating RNAs', *PLoS One*, vol. 11, no. 3, p. e0150291.

## REFERENCES

- Patriotis, C, Makris, A, Bear, SE & Tschlis, PN 1993, 'Tumor progression locus 2 (Tpl-2) encodes a protein kinase involved in the progression of rodent T-cell lymphomas and in T-cell activation', *Proc Natl Acad Sci U S A*, vol. 90, no. 6, pp. 2251-5.
- Payne, SH 2015, 'The utility of protein and mRNA correlation', *Trends Biochem Sci*, vol. 40, no. 1, pp. 1-3.
- Pellizzaro, C, Coradini, D & Daidone, MG 2002, 'Modulation of angiogenesis-related proteins synthesis by sodium butyrate in colon cancer cell line HT29', *Carcinogenesis*, vol. 23, no. 5, pp. 735-40.
- Peng, L, Bian, XW, Li, DK, Xu, C, Wang, GM, Xia, QY & Xiong, Q 2015, 'Large-scale RNA-Seq Transcriptome Analysis of 4043 Cancers and 548 Normal Tissue Controls across 12 TCGA Cancer Types', *Sci Rep*, vol. 5, p. 13413.
- Peng, Y & Croce, CM 2016, 'The role of MicroRNAs in human cancer', *Signal Transduct Target Ther*, vol. 1, p. 15004.
- Peng, YP, Zhu, Y, Yin, LD, Wei, JS, Liu, XC, Zhu, XL & Miao, Y 2018, 'PIK3R3 Promotes Metastasis of Pancreatic Cancer via ZEB1 Induced Epithelial-Mesenchymal Transition', *Cell Physiol Biochem*, vol. 46, no. 5, pp. 1930-8.
- Philp, AJ, Campbell, IG, Leet, C, Vincan, E, Rockman, SP, Whitehead, RH, Thomas, RJ & Phillips, WA 2001, 'The phosphatidylinositol 3'-kinase p85alpha gene is an oncogene in human ovarian and colon tumors', *Cancer Res*, vol. 61, no. 20, pp. 7426-9.
- Pibouin, L, Villaudy, J, Ferbus, D, Muleris, M, Prosperi, MT, Remvikos, Y & Goubin, G 2002, 'Cloning of the mRNA of overexpression in colon carcinoma-1: a sequence overexpressed in a subset of colon carcinomas', *Cancer Genet Cytogenet*, vol. 133, no. 1, pp. 55-60.
- Pico, AR, Kelder, T, van Iersel, MP, Hanspers, K, Conklin, BR & Evelo, C 2008, 'WikiPathways: pathway editing for the people', *PLoS Biol*, vol. 6, no. 7, p. e184.
- Piekarz, RL, Frye, R, Prince, HM, Kirschbaum, MH, Zain, J, Allen, SL, Jaffe, ES, Ling, A, Turner, M, Peer, CJ, Figg, WD, Steinberg, SM, Smith, S, Joske, D, Lewis, I, Hutchins, L, Craig, M, Fojo, AT, Wright, JJ & Bates, SE 2011, 'Phase 2 trial of romidepsin in patients with peripheral T-cell lymphoma', *Blood*, vol. 117, no. 22, pp. 5827-34.
- Ping, G, Xiong, W, Zhang, L, Li, Y, Zhang, Y & Zhao, Y 2018, 'Silencing long noncoding RNA PVT1 inhibits tumorigenesis and cisplatin resistance of colorectal cancer', *Am J Transl Res*, vol. 10, no. 1, pp. 138-49.
- Pino, MS & Chung, DC 2010, 'The chromosomal instability pathway in colon cancer', *Gastroenterology*, vol. 138, no. 6, pp. 2059-72.
- Polakis, P 2000, 'Wnt signaling and cancer', *Genes & Development*, vol. 14, no. 15, pp. 1837-51.
- Pouyanrad, S, Rahgozar, S & Ghodousi, ES 2019, 'Dysregulation of miR-335-3p, targeted by NEAT1 and MALAT1 long non-coding RNAs, is associated with poor prognosis in childhood acute lymphoblastic leukemia', *Gene*, vol. 692, pp. 35-43.

## REFERENCES

- Pramanik, D, Campbell, NR, Karikari, C, Chivukula, R, Kent, OA, Mendell, JT & Maitra, A 2011, 'Restitution of tumor suppressor microRNAs using a systemic nanovector inhibits pancreatic cancer growth in mice', *Mol Cancer Ther*, vol. 10, no. 8, pp. 1470-80.
- Prasanth, KV & Spector, DL 2007, 'Eukaryotic regulatory RNAs: an answer to the 'genome complexity' conundrum', *Genes Dev*, vol. 21, no. 1, pp. 11-42.
- Pratt, MM, John, K, MacLean, AB, Afework, S, Phillips, DH & Poirier, MC 2011, 'Polycyclic Aromatic Hydrocarbon (PAH) Exposure and DNA Adduct Semi-Quantitation in Archived Human Tissues', *International Journal of Environmental Research and Public Health*, vol. 8, no. 7, pp. 2675-91.
- Prensner, JR & Chinnaiyan, AM 2011, 'The emergence of lncRNAs in cancer biology', *Cancer discovery*, vol. 1, no. 5, pp. 391-407.
- Pritchard, CC, Cheng, HH & Tewari, M 2012, 'MicroRNA profiling: approaches and considerations', *Nat Rev Genet*, vol. 13, no. 5, pp. 358-69.
- Qi, P, Xu, MD, Ni, SJ, Huang, D, Wei, P, Tan, C, Zhou, XY & Du, X 2013, 'Low expression of LOC285194 is associated with poor prognosis in colorectal cancer', *J Transl Med*, vol. 11, p. 122.
- Qi, P, Xu, MD, Ni, SJ, Shen, XH, Wei, P, Huang, D, Tan, C, Sheng, WQ, Zhou, XY & Du, X 2015, 'Down-regulation of ncRAN, a long non-coding RNA, contributes to colorectal cancer cell migration and invasion and predicts poor overall survival for colorectal cancer patients', *Mol Carcinog*, vol. 54, no. 9, pp. 742-50.
- Qiao, L, Liu, X, Tang, Y, Zhao, Z, Zhang, J & Feng, Y 2017, 'Down regulation of the long non-coding RNA PCAT-1 induced growth arrest and apoptosis of colorectal cancer cells', *Life Sci*, vol. 188, pp. 37-44.
- Qin, J, Wen, B, Liang, Y, Yu, W & Li, H 2019, 'Histone Modifications and their Role in Colorectal Cancer (Review)', *Pathol Oncol Res*.
- Qiu, T, Zhou, L, Zhu, W, Wang, T, Wang, J, Shu, Y & Liu, P 2013, 'Effects of treatment with histone deacetylase inhibitors in solid tumors: a review based on 30 clinical trials', *Future Oncol*, vol. 9, no. 2, pp. 255-69.
- Rada-Iglesias, A, Enroth, S, Ameer, A, Koch, CM, Clelland, GK, Respuela-Alonso, P, Wilcox, S, Dovey, OM, Ellis, PD, Langford, CF, Dunham, I, Komorowski, J & Wadelius, C 2007, 'Butyrate mediates decrease of histone acetylation centered on transcription start sites and down-regulation of associated genes', *Genome Res*, vol. 17, no. 6, pp. 708-19.
- Radsak, K, Wiegandt, H, Unterdorfer, G, Wagner, C & Kaiser, CJ 1985, 'Sodium butyrate selectively inhibits host cell glycoprotein synthesis in human fibroblasts infected with cytomegalovirus', *Biosci Rep*, vol. 5, no. 7, pp. 589-99.
- Rafehi, H & El-Osta, A 2016, 'HDAC Inhibition in Vascular Endothelial Cells Regulates the Expression of ncRNAs', *Non-coding RNA*, vol. 2, no. 2, p. 4.

## REFERENCES

- Rajagopalan, H, Bardelli, A, Lengauer, C, Kinzler, KW, Vogelstein, B & Velculescu, VE 2002, 'Tumorigenesis: RAF/RAS oncogenes and mismatch-repair status', *Nature*, vol. 418, no. 6901, p. 934.
- Reid, JF, Sokolova, V, Zoni, E, Lampis, A, Pizzamiglio, S, Bertan, C, Zanutto, S, Perrone, F, Camerini, T, Gallino, G, Verderio, P, Leo, E, Pilotti, S, Gariboldi, M & Pierotti, MA 2012, 'miRNA profiling in colorectal cancer highlights miR-1 involvement in MET-dependent proliferation', *Mol Cancer Res*, vol. 10, no. 4, pp. 504-15.
- Reinhart, BJ, Slack, FJ, Basson, M, Pasquinelli, AE, Bettinger, JC, Rougvie, AE, Horvitz, HR & Ruvkun, G 2000, 'The 21-nucleotide let-7 RNA regulates developmental timing in *Caenorhabditis elegans*', *Nature*, vol. 403, no. 6772, pp. 901-6.
- Ren, YK, Xiao, Y, Wan, XB, Zhao, YZ, Li, J, Li, Y, Han, GS, Chen, XB, Zou, QY, Wang, GC, Lu, CM, Xu, YC & Wang, YC 2015, 'Association of long non-coding RNA HOTTIP with progression and prognosis in colorectal cancer', *Int J Clin Exp Pathol*, vol. 8, no. 9, pp. 11458-63.
- Rhodes, DR, Yu, J, Shanker, K, Deshpande, N, Varambally, R, Ghosh, D, Barrette, T, Pandey, A & Chinnaiyan, AM 2004, 'ONCOMINE: a cancer microarray database and integrated data-mining platform', *Neoplasia*, vol. 6, no. 1, pp. 1-6.
- Rice, JC & Allis, CD 2001, 'Histone methylation versus histone acetylation: new insights into epigenetic regulation', *Curr Opin Cell Biol*, vol. 13, no. 3, pp. 263-73.
- Richardson, PG, Laubach, JP, Lonial, S, Moreau, P, Yoon, SS, Hungria, VT, Dimopoulos, MA, Beksac, M, Alsina, M & San-Miguel, JF 2015, 'Panobinostat: a novel pan-deacetylase inhibitor for the treatment of relapsed or relapsed and refractory multiple myeloma', *Expert Rev Anticancer Ther*, vol. 15, no. 7, pp. 737-48.
- Rinn, JL, Kertesz, M, Wang, JK, Squazzo, SL, Xu, X, Bruggmann, SA, Goodnough, LH, Helms, JA, Farnham, PJ, Segal, E & Chang, HY 2007, 'Functional demarcation of active and silent chromatin domains in human HOX loci by noncoding RNAs', *Cell*, vol. 129, no. 7, pp. 1311-23.
- Riss, TL, Moravec, RA & Niles, AL 2011, 'Cytotoxicity testing: measuring viable cells, dead cells, and detecting mechanism of cell death', *Methods Mol Biol*, vol. 740, pp. 103-14.
- Ritzhaupt, A, Wood, IS, Ellis, A, Hosie, KB & Shirazi-Beechey, SP 1998, 'Identification and characterization of a monocarboxylate transporter (MCT1) in pig and human colon: its potential to transport L-lactate as well as butyrate', *J Physiol*, vol. 513 ( Pt 3), pp. 719-32.
- Riva, G, Cilibrasi, C, Bazzoni, R, Cadamuro, M, Negroni, C, Butta, V, Strazzabosco, M, Dalpra, L, Lavitrano, M & Bentivegna, A 2018, 'Valproic Acid Inhibits Proliferation and Reduces Invasiveness in Glioma Stem Cells Through Wnt/beta Catenin Signalling Activation', *Genes (Basel)*, vol. 9, no. 11.
- Ro, S, Park, C, Young, D, Sanders, KM & Yan, W 2007, 'Tissue-dependent paired expression of miRNAs', *Nucleic Acids Research*, vol. 35, no. 17, pp. 5944-53.

## REFERENCES

- Rodd, AL, Ververis, K & Karagiannis, TC 2012, 'Current and Emerging Therapeutics for Cutaneous T-Cell Lymphoma: Histone Deacetylase Inhibitors %J Lymphoma', vol. 2012, p. 10.
- Rodrigues, NR, Rowan, A, Smith, ME, Kerr, IB, Bodmer, WF, Gannon, JV & Lane, DP 1990, 'p53 mutations in colorectal cancer', *Proceedings of the National Academy of Sciences*, vol. 87, no. 19, pp. 7555-9.
- Roediger, WE 1982, 'Utilization of nutrients by isolated epithelial cells of the rat colon', *Gastroenterology*, vol. 83, no. 2, pp. 424-9.
- Rohr, C, Kerick, M, Fischer, A, Kuhn, A, Kashofer, K, Timmermann, B, Daskalaki, A, Meinel, T, Drichel, D, Borno, ST, Nowka, A, Krobitch, S, McHardy, AC, Kratsch, C, Becker, T, Wunderlich, A, Barmeyer, C, Viertler, C, Zatloukal, K, Wierling, C, Lehrach, H & Schweiger, MR 2013, 'High-throughput miRNA and mRNA sequencing of paired colorectal normal, tumor and metastasis tissues and bioinformatic modeling of miRNA-1 therapeutic applications', *PLoS One*, vol. 8, no. 7, p. e67461.
- Romashkova, JA & Makarov, SS 1999, 'NF-kappaB is a target of AKT in anti-apoptotic PDGF signalling', *Nature*, vol. 401, no. 6748, pp. 86-90.
- Ronchetti, D, Manzoni, M, Agnelli, L & Vinci, C 2016, 'lncRNA profiling in early-stage chronic lymphocytic leukemia identifies transcriptional fingerprints with relevance in clinical outcome', vol. 6, no. 9, p. e468.
- Rossetto, D, Avvakumov, N & Côté, J 2012, 'Histone phosphorylation: a chromatin modification involved in diverse nuclear events', *Epigenetics*, vol. 7, no. 10, pp. 1098-108.
- Rudy, DR & Zdon, MJ 2000, 'Update on colorectal cancer', *Am Fam Physician*, vol. 61, no. 6, pp. 1759-70, 73-4.
- Rui, Y, Hu, M, Wang, P, Zhang, C, Xu, H, Li, Y, Zhang, Y, Gu, J & Wang, Q 2018, 'lncRNA HOTTIP mediated DKK1 downregulation confers metastasis and invasion in colorectal cancer cells', *Histol Histopathol*, p. 18043.
- Rusanescu, G, Gotoh, T, Tian, X & Feig, LA 2001, 'Regulation of Ras signaling specificity by protein kinase C', *Mol Cell Biol*, vol. 21, no. 8, pp. 2650-8.
- Sachdeva, M, Zhu, S, Wu, F, Wu, H, Walia, V, Kumar, S, Elble, R, Watabe, K & Mo, YY 2009, 'p53 represses c-Myc through induction of the tumor suppressor miR-145', *Proc Natl Acad Sci U S A*, vol. 106, no. 9, pp. 3207-12.
- Saeinasab, M, Bahrami, AR, Gonzalez, J, Marchese, FP, Martinez, D, Mowla, SJ, Matin, MM & Huarte, M 2019, 'SNHG15 is a bifunctional MYC-regulated noncoding locus encoding a lncRNA that promotes cell proliferation, invasion and drug resistance in colorectal cancer by interacting with AIF', *J Exp Clin Cancer Res*, vol. 38, no. 1, p. 172.
- Saito, N, Nishimura, H & Kameoka, S 2008, 'Clinical significance of fibronectin expression in colorectal cancer', *Mol Med Rep*, vol. 1, no. 1, pp. 77-81.
- Saito, Y, Suzuki, H & Hibi, T 2009, 'The role of microRNAs in gastrointestinal cancers', *J Gastroenterol*, vol. 44 Suppl 19, pp. 18-22.

## REFERENCES

- Saldanha, SN, Kala, R & Tollefsbol, TO 2014, 'Molecular mechanisms for inhibition of colon cancer cells by combined epigenetic-modulating epigallocatechin gallate and sodium butyrate', *Exp Cell Res*, vol. 324, no. 1, pp. 40-53.
- Salimi, V, Shahsavari, Z, Safizadeh, B, Hosseini, A, Khademian, N & Tavakoli-Yaraki, M 2017, 'Sodium butyrate promotes apoptosis in breast cancer cells through reactive oxygen species (ROS) formation and mitochondrial impairment', *Lipids in health and disease*, vol. 16, no. 1, pp. 208-.
- Salvador, MA, Wicinski, J, Cabaud, O, Toiron, Y, Finetti, P, Josselin, E, Lelievre, H, Kraus-Berthier, L, Depil, S, Bertucci, F, Collette, Y, Birnbaum, D, Charafe-Jauffret, E & Ginestier, C 2013, 'The histone deacetylase inhibitor abexinostat induces cancer stem cells differentiation in breast cancer with low Xist expression', *Clin Cancer Res*, vol. 19, no. 23, pp. 6520-31.
- Samuels, Y, Diaz, LA, Jr., Schmidt-Kittler, O, Cummins, JM, DeLong, L, Cheong, I, Rago, C, Huso, DL, Lengauer, C, Kinzler, KW, Vogelstein, B & Velculescu, VE 2005, 'Mutant PIK3CA promotes cell growth and invasion of human cancer cells', *Cancer Cell*, vol. 7, no. 6, pp. 561-73.
- Samuels, Y, Wang, Z, Bardelli, A, Silliman, N, Ptak, J, Szabo, S, Yan, H, Gazdar, A, Powell, SM, Riggins, GJ, Willson, JK, Markowitz, S, Kinzler, KW, Vogelstein, B & Velculescu, VE 2004, 'High frequency of mutations of the PIK3CA gene in human cancers', *Science*, vol. 304, no. 5670, p. 554.
- Saridaki, Z, Weidhaas, JB, Lenz, HJ, Laurent-Puig, P, Jacobs, B, De Schutter, J, De Roock, W, Salzman, DW, Zhang, W, Yang, D, Pilati, C, Bouche, O, Piessevaux, H & Tejpar, S 2014, 'A let-7 microRNA-binding site polymorphism in KRAS predicts improved outcome in patients with metastatic colorectal cancer treated with salvage cetuximab/panitumumab monotherapy', *Clin Cancer Res*, vol. 20, no. 17, pp. 4499-510.
- Sati, S, Ghosh, S, Jain, V, Scaria, V & Sengupta, S 2012, 'Genome-wide analysis reveals distinct patterns of epigenetic features in long non-coding RNA loci', *Nucleic Acids Res*, vol. 40, no. 20, pp. 10018-31.
- Schamberger, A & Orban, TI 2014, '3' IsomiR species and DNA contamination influence reliable quantification of microRNAs by stem-loop quantitative PCR', *PLoS One*, vol. 9, no. 8, p. e106315.
- Schee, K, Lorenz, S, Worren, MM, Gunther, CC, Holden, M, Hovig, E, Fodstad, O, Meza-Zepeda, LA & Flatmark, K 2013, 'Deep Sequencing the MicroRNA Transcriptome in Colorectal Cancer', *PLoS One*, vol. 8, no. 6, p. e66165.
- Scheffzek, K, Ahmadian, MR, Kabsch, W, Wiesmuller, L, Lautwein, A, Schmitz, F & Wittinghofer, A 1997, 'The Ras-RasGAP complex: structural basis for GTPase activation and its loss in oncogenic Ras mutants', *Science*, vol. 277, no. 5324, pp. 333-8.
- Schlormann, W, Naumann, S, Renner, C & Gleib, M 2015, 'Influence of miRNA-106b and miRNA-135a on butyrate-regulated expression of p21 and Cyclin D2 in human colon adenoma cells', *Genes Nutr*, vol. 10, no. 6, p. 50.
- Schmitt, AM & Chang, HY 2016, 'Long Noncoding RNAs in Cancer Pathways', *Cancer Cell*, vol. 29, no. 4, pp. 452-63.

## REFERENCES

- Schneider, P & Tschopp, J 2000, 'Apoptosis induced by death receptors', *Pharm Acta Heb*, vol. 74, no. 2-3, pp. 281-6.
- Schroeder, A, Mueller, O, Stocker, S, Salowsky, R, Leiber, M, Gassmann, M, Lightfoot, S, Menzel, W, Granzow, M & Ragg, T 2006, 'The RIN: an RNA integrity number for assigning integrity values to RNA measurements', *BMC Mol Biol*, vol. 7, p. 3.
- Schwanhausser, B, Busse, D, Li, N, Dittmar, G, Schuchhardt, J, Wolf, J, Chen, W & Selbach, M 2011, 'Global quantification of mammalian gene expression control', *Nature*, vol. 473, no. 7347, pp. 337-42.
- Schwarz-Herion, K, Maco, B, Sauder, U & Fahrenkrog, B 2007, 'Domain topology of the p62 complex within the 3-D architecture of the nuclear pore complex', *J Mol Biol*, vol. 370, no. 4, pp. 796-806.
- Sealy, L & Chalkley, R 1978, 'The effect of sodium butyrate on histone modification', *Cell*, vol. 14, no. 1, pp. 115-21.
- Selbach, M, Schwanhausser, B, Thierfelder, N, Fang, Z, Khanin, R & Rajewsky, N 2008, 'Widespread changes in protein synthesis induced by microRNAs', *Nature*, vol. 455, no. 7209, pp. 58-63.
- Semini, G, Klein, A & Danker, K 2011, 'Impact of alkylphospholipids on the gene expression profile of HaCaT cells', *Pharmacogenet Genomics*, vol. 21, no. 7, pp. 375-87.
- Shakoori, A, Ougolkov, A, Yu, ZW, Zhang, B, Modarressi, MH, Billadeau, DD, Mai, M, Takahashi, Y & Minamoto, T 2005, 'Deregulated GSK3beta activity in colorectal cancer: its association with tumor cell survival and proliferation', *Biochem Biophys Res Commun*, vol. 334, no. 4, pp. 1365-73.
- Shan, Y, Ma, J, Pan, Y, Hu, J, Liu, B & Jia, L 2018, 'LncRNA SNHG7 sponges miR-216b to promote proliferation and liver metastasis of colorectal cancer through upregulating GALNT1', *Cell Death Dis*, vol. 9, no. 7, p. 722.
- Shang, C, Lu, YM & Meng, LR 2012, 'MicroRNA-125b down-regulation mediates endometrial cancer invasion by targeting ERBB2', *Med Sci Monit*, vol. 18, no. 4, pp. Br149-55.
- Shannon, P, Markiel, A, Ozier, O, Baliga, NS, Wang, JT, Ramage, D, Amin, N, Schwikowski, B & Ideker, T 2003, 'Cytoscape: a software environment for integrated models of biomolecular interaction networks', *Genome Res*, vol. 13, no. 11, pp. 2498-504.
- Shao, Q, Xu, J, Deng, R, Wei, W, Zhou, B, Yue, C, Zhu, M, Huang, X & Zhu, H 2018, 'Long non-coding RNA-422 acts as a tumor suppressor in colorectal cancer', *Biochem Biophys Res Commun*, vol. 495, no. 1, pp. 539-45.
- Sharma, NR, Wang, X, Majerciak, V, Ajiro, M, Kruhlak, M, Meyers, C & Zheng, ZM 2016, 'Cell Type- and Tissue Context-dependent Nuclear Distribution of Human Ago2', *J Biol Chem*, vol. 291, no. 5, pp. 2302-9.
- Sharova, LV, Sharov, AA, Nedorezov, T, Piao, Y, Shaik, N & Ko, MS 2009, 'Database for mRNA half-life of 19 977 genes obtained by DNA microarray analysis of

## REFERENCES

- pluripotent and differentiating mouse embryonic stem cells', *DNA Res*, vol. 16, no. 1, pp. 45-58.
- Shaulian, E & Karin, M 2001, 'AP-1 in cell proliferation and survival', *Oncogene*, vol. 20, no. 19, pp. 2390-400.
- Shen, F, Cai, WS, Feng, Z, Chen, JW, Feng, JH, Liu, QC, Fang, YP, Li, KP, Xiao, HQ, Cao, J & Xu, B 2017, 'Long non-coding RNA SPRY4-IT1 promotes colorectal cancer metastasis by regulate epithelial-mesenchymal transition', *Oncotarget*, vol. 8, no. 9, pp. 14479-86.
- Shi, L, Cheng, Z, Zhang, J, Li, R, Zhao, P, Fu, Z & You, Y 2008, 'hsa-mir-181a and hsa-mir-181b function as tumor suppressors in human glioma cells', *Brain Res*, vol. 1236, pp. 185-93.
- Shi, Q, Xu, X, Liu, Q, Luo, F, Shi, J & He, X 2016, 'MicroRNA-877 acts as a tumor suppressor by directly targeting eEF2K in renal cell carcinoma', *Oncol Lett*, vol. 11, no. 2, pp. 1474-80.
- Shi, Q, Zhou, Z, Ye, N, Chen, Q, Zheng, X & Fang, M 2017, 'MiR-181a inhibits non-small cell lung cancer cell proliferation by targeting CDK1', *Cancer Biomark*, vol. 20, no. 4, pp. 539-46.
- Shi, X, Sun, M, Liu, H, Yao, Y, Kong, R, Chen, F & Song, Y 2015a, 'A critical role for the long non-coding RNA GAS5 in proliferation and apoptosis in non-small-cell lung cancer', *Mol Carcinog*, vol. 54 Suppl 1, pp. E1-e12.
- Shi, Y, Liu, Y, Wang, J, Jie, D, Yun, T, Li, W, Yan, L, Wang, K & Feng, J 2015b, 'Downregulated Long Noncoding RNA BANCR Promotes the Proliferation of Colorectal Cancer Cells via Downregulation of p21 Expression', *PLoS One*, vol. 10, no. 4, p. e0122679.
- Shirasawa, S, Furuse, M, Yokoyama, N & Sasazuki, T 1993, 'Altered growth of human colon cancer cell lines disrupted at activated Ki-ras', *Science*, vol. 260, no. 5104, pp. 85-8.
- Siavoshian, S, Segain, JP, Kornprobst, M, Bonnet, C, Cherbut, C, Galmiche, JP & Blottiere, HM 2000, 'Butyrate and trichostatin A effects on the proliferation/differentiation of human intestinal epithelial cells: induction of cyclin D3 and p21 expression', *Gut*, vol. 46, no. 4, pp. 507-14.
- Sicard, F, Gayral, M, Lulka, H, Buscail, L & Cordelier, P 2013, 'Targeting miR-21 for the therapy of pancreatic cancer', *Mol Ther*, vol. 21, no. 5, pp. 986-94.
- Sidi, AA, Shalva, B, Leibovitch, I, Shalev, M, Hochberg, A & Ohana, P 2008, 'Phase 1/2a, dose-escalation, safety and efficacy of intravesical plasmid (BC-819) in patients with superficial transitional cell cancer of the bladder (STCCB)', *The Journal of Urology*, vol. 179, no. 4, Supplement, p. 613.
- Simpson, KJ, Selfors, LM, Bui, J, Reynolds, A, Leake, D, Khvorova, A & Brugge, JS 2008, 'Identification of genes that regulate epithelial cell migration using an siRNA screening approach', *Nat Cell Biol*, vol. 10, no. 9, pp. 1027-38.

## REFERENCES

- Singh, B, Halestrap, AP & Paraskeva, C 1997, 'Butyrate can act as a stimulator of growth or inducer of apoptosis in human colonic epithelial cell lines depending on the presence of alternative energy sources', *Carcinogenesis*, vol. 18, no. 6, pp. 1265-70.
- Singh, GB, Raut, SK, Khanna, S, Kumar, A, Sharma, S, Prasad, R & Khullar, M 2017, 'MicroRNA-200c modulates DUSP-1 expression in diabetes-induced cardiac hypertrophy', *Mol Cell Biochem*, vol. 424, no. 1-2, pp. 1-11.
- Singh, R, Zorrón Cheng Tao Pu, L, Koay, D & Burt, A 2016, 'Sessile serrated adenoma/polyps: Where are we at in 2016?', *World Journal of Gastroenterology*, vol. 22, no. 34, pp. 7754-9.
- Sivaprakasam, S, Bhutia, YD, Yang, S & Ganapathy, V 2017, 'Short-Chain Fatty Acid Transporters: Role in Colonic Homeostasis', *Compr Physiol*, vol. 8, no. 1, pp. 299-314.
- Skalsky, RL & Cullen, BR 2010, 'Viruses, microRNAs, and host interactions', *Annu Rev Microbiol*, vol. 64, pp. 123-41.
- Smaldone, MC & Davies, BJ 2010, 'BC-819, a plasmid comprising the H19 gene regulatory sequences and diphtheria toxin A, for the potential targeted therapy of cancers', *Curr Opin Mol Ther*, vol. 12, no. 5, pp. 607-16.
- Soh, JW, Mao, Y, Liu, L, Thompson, WJ, Pamukcu, R & Weinstein, IB 2001, 'Protein kinase G activates the JNK1 pathway via phosphorylation of MEKK1', *J Biol Chem*, vol. 276, no. 19, pp. 16406-10.
- Song, J, Wang, Z & Ewing, RM 2014a, 'Integrated analysis of the Wnt responsive proteome in human cells reveals diverse and cell-type specific networks', *Molecular bioSystems*, vol. 10, no. 1, pp. 45-53.
- Song, L & Xiao, Y 2018, 'Downregulation of hsa\_circ\_0007534 suppresses breast cancer cell proliferation and invasion by targeting miR-593/MUC19 signal pathway', *Biochem Biophys Res Commun*, vol. 503, no. 4, pp. 2603-10.
- Song, M, Yin, Y, Zhang, J, Zhang, B, Bian, Z, Quan, C, Zhou, L, Hu, Y, Wang, Q, Ni, S, Fei, B, Wang, W, Du, X, Hua, D & Huang, Z 2014b, 'MiR-139-5p inhibits migration and invasion of colorectal cancer by downregulating AMFR and NOTCH1', *Protein Cell*, vol. 5, no. 11, pp. 851-61.
- Soucek, K, Gajduskova, P, Brazdova, M, Hyzd'alova, M, Koci, L, Vydra, D, Trojanec, R, Pernicova, Z, Lentvorska, L, Hajduch, M, Hofmanova, J & Kozubik, A 2010, 'Fetal colon cell line FHC exhibits tumorigenic phenotype, complex karyotype, and TP53 gene mutation', *Cancer Genet Cytogenet*, vol. 197, no. 2, pp. 107-16.
- Soule, HD, Maloney, TM, Wolman, SR, Peterson, WD, Jr., Brenz, R, McGrath, CM, Russo, J, Pauley, RJ, Jones, RF & Brooks, SC 1990, 'Isolation and characterization of a spontaneously immortalized human breast epithelial cell line, MCF-10', *Cancer Res*, vol. 50, no. 18, pp. 6075-86.
- Soundara Pandi, SP, Chen, M, Guduric-Fuchs, J, Xu, H & Simpson, DA 2013, 'Extremely complex populations of small RNAs in the mouse retina and RPE/choroid', *Invest Ophthalmol Vis Sci*, vol. 54, no. 13, pp. 8140-51.

## REFERENCES

- Sourvinos, G, Tsatsanis, C & Spandidos, DA 1999, 'Overexpression of the Tpl-2/Cot oncogene in human breast cancer', *Oncogene*, vol. 18, no. 35, pp. 4968-73.
- Spit, M, Koo, BK & Maurice, MM 2018, 'Tales from the crypt: intestinal niche signals in tissue renewal, plasticity and cancer', *Open Biol*, vol. 8, no. 9.
- Srikantan, V, Zou, Z, Petrovics, G, Xu, L, Augustus, M, Davis, L, Livezey, JR, Connell, T, Sesterhenn, IA, Yoshino, K, Buzard, GS, Mostofi, FK, McLeod, DG, Moul, JW & Srivastava, S 2000, 'PCGEM1, a prostate-specific gene, is overexpressed in prostate cancer', *Proc Natl Acad Sci U S A*, vol. 97, no. 22, pp. 12216-21.
- Stamato, MA, Juli, G, Romeo, E, Ronchetti, D, Arbitrio, M, Caracciolo, D, Neri, A, Tagliaferri, P, Tassone, P & Amodio, N 2017, 'Inhibition of EZH2 triggers the tumor suppressive miR-29b network in multiple myeloma', *Oncotarget*, vol. 8, no. 63, pp. 106527-37.
- Staton, CA, Koay, I, Wu, JM, Hoh, L, Reed, MW & Brown, NJ 2013, 'Neuropilin-1 and neuropilin-2 expression in the adenoma-carcinoma sequence of colorectal cancer', *Histopathology*, vol. 62, no. 6, pp. 908-15.
- Stinson, S, Lackner, MR, Adai, AT, Yu, N, Kim, HJ, O'Brien, C, Spoerke, J, Jhunjhunwala, S, Boyd, Z, Januario, T, Newman, RJ, Yue, P, Bourgon, R, Modrusan, Z, Stern, HM, Warming, S, de Sauvage, FJ, Amler, L, Yeh, RF & Dornan, D 2011, 'TRPS1 targeting by miR-221/222 promotes the epithelial-to-mesenchymal transition in breast cancer', *Sci Signal*, vol. 4, no. 177, p. ra41.
- Stoffel, EM & Kastrinos, F 2014, 'Familial colorectal cancer, beyond Lynch syndrome', *Clin Gastroenterol Hepatol*, vol. 12, no. 7, pp. 1059-68.
- Stoian, M, Stoica, V & Radulian, G 2016, 'Stem cells and colorectal carcinogenesis', *Journal of Medicine and Life*, vol. 9, no. 1, pp. 6-11.
- Strillacci, A, Griffoni, C, Sansone, P, Paterini, P, Piazzzi, G, Lazzarini, G, Spisni, E, Pantaleo, MA, Biasco, G & Tomasi, V 2009, 'MiR-101 downregulation is involved in cyclooxygenase-2 overexpression in human colon cancer cells', *Exp Cell Res*, vol. 315, no. 8, pp. 1439-47.
- Su, J, Zhang, E, Han, L, Yin, D, Liu, Z, He, X, Zhang, Y, Lin, F, Lin, Q, Mao, P, Mao, W & Shen, D 2017, 'Long noncoding RNA BLACAT1 indicates a poor prognosis of colorectal cancer and affects cell proliferation by epigenetically silencing of p15', *Cell Death Dis*, vol. 8, no. 3, p. e2665.
- Su, X, Zhang, T, Cheng, P, Zhu, Y, Li, H, Li, D, Liu, Z, Gao, H, Zhao, Z, Zhao, Y & Liu, H 2014, 'KIAA0101 mRNA overexpression in peripheral blood mononuclear cells acts as predictive marker for hepatic cancer', *Tumour Biol*, vol. 35, no. 3, pp. 2681-6.
- Su, YL & Hu, SH 2018, 'Functional Nanoparticles for Tumor Penetration of Therapeutics', *Pharmaceutics*, vol. 10, no. 4.
- Su, Z, Chen, D, Zhang, E, Li, Y, Yu, Z, Shi, M, Jiang, Z, Ni, L, Yang, S, Gui, Y, Ye, J & Lai, Y 2015, 'MicroRNA-509-3p inhibits cancer cell proliferation and migration by targeting the mitogen-activated protein kinase kinase kinase 8 oncogene in renal cell carcinoma', *Mol Med Rep*, vol. 12, no. 1, pp. 1535-43.

## REFERENCES

- Subramanian, M, Rao, SR, Thacker, P, Chatterjee, S & Karunagaran, D 2014, 'MiR-29b downregulates canonical Wnt signaling by suppressing coactivators of beta-catenin in human colorectal cancer cells', *J Cell Biochem*, vol. 115, no. 11, pp. 1974-84.
- Sun, D, Yu, F, Ma, Y, Zhao, R, Chen, X, Zhu, J, Zhang, CY, Chen, J & Zhang, J 2013, 'MicroRNA-31 activates the RAS pathway and functions as an oncogenic MicroRNA in human colorectal cancer by repressing RAS p21 GTPase activating protein 1 (RASA1)', *J Biol Chem*, vol. 288, no. 13, pp. 9508-18.
- Sun, J, Ding, C, Yang, Z, Liu, T, Zhang, X, Zhao, C & Wang, J 2016a, 'The long non-coding RNA TUG1 indicates a poor prognosis for colorectal cancer and promotes metastasis by affecting epithelial-mesenchymal transition', *J Transl Med*, vol. 14, p. 42.
- Sun, J, Zhang, T, Cheng, M, Hong, L, Zhang, C, Xie, M, Sun, P, Fan, R, Wang, Z, Wang, L & Zhong, J 2019a, 'TRIM29 facilitates the epithelial-to-mesenchymal transition and the progression of colorectal cancer via the activation of the Wnt/beta-catenin signaling pathway', *J Exp Clin Cancer Res*, vol. 38, no. 1, p. 104.
- Sun, L, Xue, H, Jiang, C, Zhou, H, Gu, L, Liu, Y, Xu, C & Xu, Q 2016b, 'LncRNA DQ786243 contributes to proliferation and metastasis of colorectal cancer both in vitro and in vivo', *Biosci Rep*, vol. 36, no. 3.
- Sun, N, Zhang, G & Liu, Y 2018a, 'Long non-coding RNA XIST sponges miR-34a to promotes colon cancer progression via Wnt/beta-catenin signaling pathway', *Gene*, vol. 665, pp. 141-8.
- Sun, Q, Weng, D, Li, K, Li, S, Bai, X, Fang, C, Luo, D, Wu, P, Chen, G & Wei, J 2018b, 'MicroRNA-139-5P inhibits human prostate cancer cell proliferation by targeting Notch1', *Oncol Lett*, vol. 16, no. 1, pp. 793-800.
- Sun, Y & Ma, L 2019, 'New Insights into Long Non-Coding RNA MALAT1 in Cancer and Metastasis', *Cancers*, vol. 11, no. 2, p. 216.
- Sun, Y, Zheng, ZP, Li, H, Zhang, HQ & Ma, FQ 2016c, 'ANRIL is associated with the survival rate of patients with colorectal cancer, and affects cell migration and invasion in vitro', *Mol Med Rep*, vol. 14, no. 2, pp. 1714-20.
- Sun, Z, Ou, C, Liu, J, Chen, C, Zhou, Q, Yang, S, Li, G, Wang, G, Song, J, Li, Z, Zhang, Z, Yuan, W & Li, X 2019b, 'YAP1-induced MALAT1 promotes epithelial-mesenchymal transition and angiogenesis by sponging miR-126-5p in colorectal cancer', *Oncogene*, vol. 38, no. 14, pp. 2627-44.
- Sun, Z, Zhang, Z, Liu, Z, Qiu, B, Liu, K & Dong, G 2014, 'MicroRNA-335 inhibits invasion and metastasis of colorectal cancer by targeting ZEB2', *Med Oncol*, vol. 31, no. 6, p. 982.
- Sun, ZQ, Chen, C, Zhou, QB, Liu, JB, Yang, SX, Li, Z, Ou, CL, Sun, XT, Wang, GX, Song, JM, Zhang, ZY & Yuan, WT 2017, 'Long non-coding RNA LINC00959 predicts colorectal cancer patient prognosis and inhibits tumor progression', *Oncotarget*, vol. 8, no. 57, pp. 97052-60.

## REFERENCES

- Suraweera, A, O'Byrne, KJ & Richard, DJ 2018, 'Combination Therapy With Histone Deacetylase Inhibitors (HDACi) for the Treatment of Cancer: Achieving the Full Therapeutic Potential of HDACi', *Frontiers in oncology*, vol. 8, pp. 92-.
- Suzuki, A, Hayashida, M, Ito, T, Kawano, H, Nakano, T, Miura, M, Akahane, K & Shiraki, K 2000, 'Survivin initiates cell cycle entry by the competitive interaction with Cdk4/p16(INK4a) and Cdk2/cyclin E complex activation', *Oncogene*, vol. 19, no. 29, pp. 3225-34.
- Svoboda, M, Slyskova, J, Schneiderova, M, Makovicky, P, Bielik, L, Levy, M, Lipska, L, Hemmelova, B, Kala, Z, Protivankova, M, Vycital, O, Liska, V, Schwarzova, L, Vodickova, L & Vodicka, P 2014, 'HOTAIR long non-coding RNA is a negative prognostic factor not only in primary tumors, but also in the blood of colorectal cancer patients', *Carcinogenesis*, vol. 35, no. 7, pp. 1510-5.
- Taddei, A, Maison, C, Roche, D & Almouzni, G 2001, 'Reversible disruption of pericentric heterochromatin and centromere function by inhibiting deacetylases', *Nat Cell Biol*, vol. 3, no. 2, pp. 114-20.
- Taylor, D, Hahm, E-R, Kale, RK, Singh, SV & Singh, RP 2014, 'Sodium butyrate induces DRP1-mediated mitochondrial fusion and apoptosis in human colorectal cancer cells', *Mitochondrion*, vol. 16, pp. 55-64.
- Takahashi, Y, Sawada, G, Kurashige, J, Uchi, R, Matsumura, T, Ueo, H, Takano, Y, Eguchi, H, Sudo, T, Sugimachi, K, Yamamoto, H, Doki, Y, Mori, M & Mimori, K 2014, 'Amplification of PVT-1 is involved in poor prognosis via apoptosis inhibition in colorectal cancers', *Br J Cancer*, vol. 110, no. 1, pp. 164-71.
- Tam, S, de Borja, R, Tsao, MS & McPherson, JD 2014, 'Robust global microRNA expression profiling using next-generation sequencing technologies', *Lab Invest*, vol. 94, no. 3, pp. 350-8.
- Tamagawa, H, Oshima, T, Shiozawa, M, Morinaga, S, Nakamura, Y, Yoshihara, M, Sakuma, Y, Kameda, Y, Akaike, M, Masuda, M, Imada, T & Miyagi, Y 2012, 'The global histone modification pattern correlates with overall survival in metachronous liver metastasis of colorectal cancer', *Oncol Rep*, vol. 27, no. 3, pp. 637-42.
- Tamborero, D, Gonzalez-Perez, A, Perez-Llamas, C, Deu-Pons, J, Kandoth, C, Reimand, J, Lawrence, MS, Getz, G, Bader, GD, Ding, L & Lopez-Bigas, N 2013, 'Comprehensive identification of mutational cancer driver genes across 12 tumor types', *Sci Rep*, vol. 3, p. 2650.
- Tan, W, Liu, B, Qu, S, Liang, G, Luo, W & Gong, C 2018, 'MicroRNAs and cancer: Key paradigms in molecular therapy', *Oncol Lett*, vol. 15, no. 3, pp. 2735-42.
- Tang, Q, Zou, Z, Zou, C, Zhang, Q, Huang, R, Guan, X, Li, Q, Han, Z, Wang, D, Wei, H, Gao, X & Wang, X 2015, 'MicroRNA-93 suppress colorectal cancer development via Wnt/beta-catenin pathway downregulating', *Tumour Biol*, vol. 36, no. 3, pp. 1701-10.
- Tang, Y, Chen, Y, Jiang, H, Robbins, GT & Nie, D 2011, 'G-protein-coupled receptor for short-chain fatty acids suppresses colon cancer', *Int J Cancer*, vol. 128, no. 4, pp. 847-56.

## REFERENCES

- Tang, ZP, Dong, QZ, Cui, QZ, Papavassiliou, P, Wang, ED & Wang, EH 2013, 'Ataxia-telangiectasia group D complementing gene (ATDC) promotes lung cancer cell proliferation by activating NF-kappaB pathway', *PLoS One*, vol. 8, no. 6, p. e63676.
- Taniguchi, T, Iwashita, J, Murata, J, Ueda, K & Abe, T 2012, 'The histone deacetylase inhibitor trichostatin A induces cell cycle arrest and rapid upregulation of gadd45 $\beta$  in LS174T human colon cancer cells', *Advances in Biological Chemistry*, vol. 2, pp. 43-50.
- Tazawa, H, Tsuchiya, N, Izumiya, M & Nakagama, H 2007, 'Tumor-suppressive miR-34a induces senescence-like growth arrest through modulation of the E2F pathway in human colon cancer cells', *Proc Natl Acad Sci U S A*, vol. 104, no. 39, pp. 15472-7.
- Tetsu, O & McCormick, F 1999, 'Beta-catenin regulates expression of cyclin D1 in colon carcinoma cells', *Nature*, vol. 398, no. 6726, pp. 422-6.
- Thangaraju, M, Cresci, GA, Liu, K, Ananth, S, Gnanaprakasam, JP, Browning, DD, Mellinger, JD, Smith, SB, Digby, GJ, Lambert, NA, Prasad, PD & Ganapathy, V 2009, 'GPR109A is a G-protein-coupled receptor for the bacterial fermentation product butyrate and functions as a tumor suppressor in colon', *Cancer Res*, vol. 69, no. 7, pp. 2826-32.
- Thomas, DW, Gould, CM, Handoko, Y & Simpson, KJ 2014, 'Functional genomics down under: RNAi screening in the Victorian Centre for Functional Genomics', *Comb Chem High Throughput Screen*, vol. 17, no. 4, pp. 343-55.
- Thorenoor, N, Faltejskova-Vychytilova, P, Hombach, S, Mlcochova, J, Kretz, M, Svoboda, M & Slaby, O 2015, 'Long non-coding RNA ZFAS1 interacts with CDK1 and is involved in p53-dependent cell cycle control and apoptosis in colorectal cancer', *Oncotarget*.
- Tian, W, Du, Y, Ma, Y, Gu, L, Zhou, J & Deng, D 2018, 'MALAT1-miR663a negative feedback loop in colon cancer cell functions through direct miRNA-lncRNA binding', *Cell Death Dis*, vol. 9, no. 9, p. 857.
- Toiyama, Y, Hur, K, Tanaka, K, Inoue, Y, Kusunoki, M, Boland, CR & Goel, A 2014, 'Serum miR-200c is a novel prognostic and metastasis-predictive biomarker in patients with colorectal cancer', *Ann Surg*, vol. 259, no. 4, pp. 735-43.
- Tomari, Y & Zamore, PD 2005, 'MicroRNA Biogenesis: Drosha Can't Cut It without a Partner', *Current Biology*, vol. 15, no. 2, pp. R61-R4.
- Trang, P, Wiggins, JF, Daige, CL, Cho, C, Omotola, M, Brown, D, Weidhaas, JB, Bader, AG & Slack, FJ 2011, 'Systemic delivery of tumor suppressor microRNA mimics using a neutral lipid emulsion inhibits lung tumors in mice', *Mol Ther*, vol. 19, no. 6, pp. 1116-22.
- Treisman, R 1994, 'Ternary complex factors: growth factor regulated transcriptional activators', *Curr Opin Genet Dev*, vol. 4, no. 1, pp. 96-101.
- Tripathi, V, Ellis, JD, Shen, Z, Song, DY, Pan, Q, Watt, AT, Freier, SM, Bennett, CF, Sharma, A, Bubulya, PA, Blencowe, BJ, Prasanth, SG & Prasanth, KV 2010, 'The nuclear-retained noncoding RNA MALAT1 regulates alternative splicing by modulating SR splicing factor phosphorylation', *Mol Cell*, vol. 39, no. 6, pp. 925-38.

## REFERENCES

- Tripathi, V, Shen, Z, Chakraborty, A, Giri, S, Freier, SM, Wu, X, Zhang, Y, Gorospe, M, Prasanth, SG, Lal, A & Prasanth, KV 2013, 'Long noncoding RNA MALAT1 controls cell cycle progression by regulating the expression of oncogenic transcription factor B-MYB', *PLoS Genet*, vol. 9, no. 3, p. e1003368.
- Tsai, KW, Lo, YH, Liu, H, Yeh, CY, Chen, YZ, Hsu, CW, Chen, WS & Wang, JH 2018, 'Linc00659, a long noncoding RNA, acts as novel oncogene in regulating cancer cell growth in colorectal cancer', *Mol Cancer*, vol. 17, no. 1, p. 72.
- Tsai, MC, Manor, O, Wan, Y, Mosammamarast, N, Wang, JK, Lan, F, Shi, Y, Segal, E & Chang, HY 2010, 'Long noncoding RNA as modular scaffold of histone modification complexes', *Science*, vol. 329, no. 5992, pp. 689-93.
- Tsang, WP, Ng, EK, Ng, SS, Jin, H, Yu, J, Sung, JJ & Kwok, TT 2010a, 'Oncofetal H19-derived miR-675 regulates tumor suppressor RB in human colorectal cancer', *Carcinogenesis*, vol. 31, no. 3, pp. 350-8.
- Tsang, WP, Ng, EKO, Ng, SSM, Jin, H, Yu, J, Sung, JJY & Kwok, TT 2010b, 'Oncofetal H19-derived miR-675 regulates tumor suppressor RB in human colorectal cancer', *Carcinogenesis*, vol. 31, no. 3, pp. 350-8.
- Tse, JWT, Jenkins, LJ, Chionh, F & Mariadason, JM 2017, 'Aberrant DNA Methylation in Colorectal Cancer: What Should We Target?', *Trends Cancer*, vol. 3, no. 10, pp. 698-712.
- Tseng, YY, Moriarity, BS, Gong, W, Akiyama, R, Tiwari, A, Kawakami, H, Ronning, P, Reuland, B, Guenther, K, Beadnell, TC, Essig, J, Otto, GM, O'Sullivan, MG, Largaespada, DA, Schwertfeger, KL, Marahrens, Y, Kawakami, Y & Bagchi, A 2014, 'PVT1 dependence in cancer with MYC copy-number increase', *Nature*, vol. 512, no. 7512, pp. 82-6.
- Tsuchida, A, Ohno, S, Wu, W, Borjigin, N, Fujita, K, Aoki, T, Ueda, S, Takanashi, M & Kuroda, M 2011, 'miR-92 is a key oncogenic component of the miR-17-92 cluster in colon cancer', *Cancer Sci*, vol. 102, no. 12, pp. 2264-71.
- Tsujii, M & DuBois, RN 1995, 'Alterations in cellular adhesion and apoptosis in epithelial cells overexpressing prostaglandin endoperoxide synthase 2', *Cell*, vol. 83, no. 3, pp. 493-501.
- Tsukamoto, S, Ishikawa, T, Iida, S, Ishiguro, M, Mogushi, K, Mizushima, H, Uetake, H, Tanaka, H & Sugihara, K 2011, 'Clinical significance of osteoprotegerin expression in human colorectal cancer', *Clin Cancer Res*, vol. 17, no. 8, pp. 2444-50.
- Tunca, B, Tezcan, G, Cecener, G, Egeli, U, Zorluoglu, A, Yilmazlar, T, Ak, S, Yerci, O, Ozturk, E, Umut, G & Evrensel, T 2013, 'Overexpression of CK20, MAP3K8 and EIF5A correlates with poor prognosis in early-onset colorectal cancer patients', *J Cancer Res Clin Oncol*, vol. 139, no. 4, pp. 691-702.
- Uematsu, K, He, B, You, L, Xu, Z, McCormick, F & Jablons, DM 2003a, 'Activation of the Wnt pathway in non small cell lung cancer: evidence of dishevelled overexpression', *Oncogene*, vol. 22, no. 46, pp. 7218-21.

## REFERENCES

- Uematsu, K, Kanazawa, S, You, L, He, B, Xu, Z, Li, K, Peterlin, BM, McCormick, F & Jablons, DM 2003b, 'Wnt pathway activation in mesothelioma: evidence of Dishevelled overexpression and transcriptional activity of beta-catenin', *Cancer Res*, vol. 63, no. 15, pp. 4547-51.
- Ueno, K, Hirata, H, Majid, S, Yamamura, S, Shahryari, V, Tabatabai, ZL, Hinoda, Y & Dahiya, R 2012, 'Tumor suppressor microRNA-493 decreases cell motility and migration ability in human bladder cancer cells by downregulating RhoC and FZD4', *Mol Cancer Ther*, vol. 11, no. 1, pp. 244-53.
- van Loo, G, Saelens, X, van Gorp, M, MacFarlane, M, Martin, SJ & Vandenabeele, P 2002, 'The role of mitochondrial factors in apoptosis: a Russian roulette with more than one bullet', *Cell Death Differ*, vol. 9, no. 10, pp. 1031-42.
- van Zandwijk, N, Pavlakis, N, Kao, SC, Linton, A, Boyer, MJ, Clarke, S, Huynh, Y, Chrzanowska, A, Fulham, MJ, Bailey, DL, Cooper, WA, Kritharides, L, Ridley, L, Pattison, ST, MacDiarmid, J, Brahmbhatt, H & Reid, G 2017, 'Safety and activity of microRNA-loaded minicells in patients with recurrent malignant pleural mesothelioma: a first-in-man, phase 1, open-label, dose-escalation study', *Lancet Oncol*, vol. 18, no. 10, pp. 1386-96.
- VanArsdale, T, Boshoff, C, Arndt, KT & Abraham, RT 2015, 'Molecular Pathways: Targeting the Cyclin D-CDK4/6 Axis for Cancer Treatment', *Clin Cancer Res*, vol. 21, no. 13, pp. 2905-10.
- Vander Heiden, MG, Cantley, LC & Thompson, CB 2009, 'Understanding the Warburg effect: the metabolic requirements of cell proliferation', *Science*, vol. 324, no. 5930, pp. 1029-33.
- Vanhaesebroeck, B & Alessi, DR 2000, 'The PI3K-PDK1 connection: more than just a road to PKB', *Biochem J*, vol. 346 Pt 3, pp. 561-76.
- Vasudevan, S 2012, 'Posttranscriptional upregulation by microRNAs', *Wiley Interdiscip Rev RNA*, vol. 3, no. 3, pp. 311-30.
- Vasudevan, S, Tong, Y & Steitz, JA 2007, 'Switching from repression to activation: microRNAs can up-regulate translation', *Science*, vol. 318, no. 5858, pp. 1931-4.
- Vermeulen, K, Van Bockstaele, DR & Berneman, ZN 2003, 'The cell cycle: a review of regulation, deregulation and therapeutic targets in cancer', *Cell Prolif*, vol. 36, no. 3, pp. 131-49.
- Vivanco, I & Sawyers, CL 2002, 'The phosphatidylinositol 3-Kinase AKT pathway in human cancer', *Nat Rev Cancer*, vol. 2, no. 7, pp. 489-501.
- Vogel, C, Abreu Rde, S, Ko, D, Le, SY, Shapiro, BA, Burns, SC, Sandhu, D, Boutz, DR, Marcotte, EM & Penalva, LO 2010, 'Sequence signatures and mRNA concentration can explain two-thirds of protein abundance variation in a human cell line', *Molecular systems biology*, vol. 6, p. 400.
- Vogel, C & Marcotte, EM 2012, 'Insights into the regulation of protein abundance from proteomic and transcriptomic analyses', *Nat Rev Genet*, vol. 13, no. 4, pp. 227-32.

## REFERENCES

- Volinia, S, Calin, GA, Liu, C-G, Ambros, S, Cimmino, A, Petrocca, F, Visone, R, Iorio, M, Roldo, C, Ferracin, M, Prueitt, RL, Yanaihara, N, Lanza, G, Scarpa, A, Vecchione, A, Negrini, M, Harris, CC & Croce, CM 2006, 'A microRNA expression signature of human solid tumors defines cancer gene targets', *Proc Natl Acad Sci U S A*, vol. 103, no. 7, pp. 2257-61.
- Von Renteln, D, Bouin, M & Barkun, AN 2017, 'Current standards and new developments of colorectal polyp management and resection techniques', *Expert Rev Gastroenterol Hepatol*, pp. 1-8.
- Waby, JS, Chirakkal, H, Yu, C, Griffiths, GJ, Benson, RS, Bingle, CD & Corfe, BM 2010, 'Sp1 acetylation is associated with loss of DNA binding at promoters associated with cell cycle arrest and cell death in a colon cell line', *Mol Cancer*, vol. 9, p. 275.
- Wahlestedt, C 2013, 'Targeting long non-coding RNA to therapeutically upregulate gene expression', *Nat Rev Drug Discov*, vol. 12, no. 6, pp. 433-46.
- Wali, VB, Haskins, JW, Gilmore-Hebert, M, Platt, JT, Liu, Z & Stern, DF 2014, 'Convergent and divergent cellular responses by ErbB4 isoforms in mammary epithelial cells', *Mol Cancer Res*, vol. 12, no. 8, pp. 1140-55.
- Wan, L, Kong, J, Tang, J, Wu, Y, Xu, E, Lai, M & Zhang, H 2016, 'HOTAIRM1 as a potential biomarker for diagnosis of colorectal cancer functions the role in the tumour suppressor', *J Cell Mol Med*.
- Wang, C, Zhu, X, Pu, C & Song, X 2018, 'Upregulated plasmacytoma variant translocation 1 promotes cell proliferation, invasion and metastasis in colorectal cancer', *Mol Med Rep*, vol. 17, no. 5, pp. 6598-604.
- Wang, D & Dubois, RN 2010, 'The role of COX-2 in intestinal inflammation and colorectal cancer', *Oncogene*, vol. 29, no. 6, pp. 781-8.
- Wang, G, Li, Z, Zhao, Q, Zhu, Y, Zhao, C, Li, X, Ma, Z, Li, X & Zhang, Y 2014a, 'LincRNA-p21 enhances the sensitivity of radiotherapy for human colorectal cancer by targeting the Wnt/beta-catenin signaling pathway', *Oncol Rep*, vol. 31, no. 4, pp. 1839-45.
- Wang, G, Yang, X, Li, C, Cao, X, Luo, X & Hu, J 2014b, 'PIK3R3 induces epithelial-to-mesenchymal transition and promotes metastasis in colorectal cancer', *Mol Cancer Ther*, vol. 13, no. 7, pp. 1837-47.
- Wang, H, Wu, J, Meng, X, Ying, X, Zuo, Y, Liu, R, Pan, Z, Kang, T & Huang, W 2011, 'MicroRNA-342 inhibits colorectal cancer cell proliferation and invasion by directly targeting DNA methyltransferase 1', *Carcinogenesis*, vol. 32, no. 7, pp. 1033-42.
- Wang, J, Kuropatwinski, K, Hauser, J, Rossi, MR, Zhou, Y, Conway, A, Kan, JL, Gibson, NW, Willson, JK, Cowell, JK & Brattain, MG 2007, 'Colon carcinoma cells harboring PIK3CA mutations display resistance to growth factor deprivation induced apoptosis', *Mol Cancer Ther*, vol. 6, no. 3, pp. 1143-50.
- Wang, J, Lei, ZJ, Guo, Y, Wang, T, Qin, ZY, Xiao, HL, Fan, LL, Chen, DF, Bian, XW, Liu, J & Wang, B 2015, 'miRNA-regulated delivery of lincRNA-p21 suppresses beta-catenin signaling and tumorigenicity of colorectal cancer stem cells', *Oncotarget*, vol. 6, no. 35, pp. 37852-70.

## REFERENCES

- Wang, J, Wang, X, Liu, F & Fu, Y 2017, 'microRNA-335 inhibits colorectal cancer HCT116 cells growth and epithelial-mesenchymal transition (EMT) process by targeting Twist1', *Pharmazie*, vol. 72, no. 8, pp. 475-81.
- Wang, JP & Hielscher, A 2017, 'Fibronectin: How Its Aberrant Expression in Tumors May Improve Therapeutic Targeting', *Journal of Cancer*, vol. 8, no. 4, pp. 674-82.
- Wang, KC & Chang, HY 2011, 'Molecular mechanisms of long noncoding RNAs', *Molecular Cell*, vol. 43, no. 6, pp. 904-14.
- Wang, L, Duan, W, Yan, S, Xie, Y & Wang, C 2019a, 'Circulating long non-coding RNA colon cancer-associated transcript 2 protected by exosome as a potential biomarker for colorectal cancer', *Biomed Pharmacother*, vol. 113, p. 108758.
- Wang, L, Heidt, DG, Lee, CJ, Yang, H, Logsdon, CD, Zhang, L, Fearon, ER, Ljungman, M & Simeone, DM 2009, 'Oncogenic function of ATDC in pancreatic cancer through Wnt pathway activation and beta-catenin stabilization', *Cancer Cell*, vol. 15, no. 3, pp. 207-19.
- Wang, L, Zhao, Z, Feng, W, Ye, Z, Dai, W, Zhang, C, Peng, J & Wu, K 2016a, 'Long non-coding RNA TUG1 promotes colorectal cancer metastasis via EMT pathway', *Oncotarget*.
- Wang, Q, Li, N, Wang, X, Kim, MM & Evers, BM 2002, 'Augmentation of sodium butyrate-induced apoptosis by phosphatidylinositol 3'-kinase inhibition in the KM20 human colon cancer cell line', *Clin Cancer Res*, vol. 8, no. 6, pp. 1940-7.
- Wang, R, Du, L, Yang, X, Jiang, X, Duan, W, Yan, S, Xie, Y, Zhu, Y, Wang, Q, Wang, L, Yang, Y & Wang, C 2016b, 'Identification of long noncoding RNAs as potential novel diagnosis and prognosis biomarkers in colorectal cancer', *J Cancer Res Clin Oncol*.
- Wang, W & Xing, C 2016, 'Upregulation of long noncoding RNA ZFAS1 predicts poor prognosis and prompts invasion and metastasis in colorectal cancer', *Pathol Res Pract*, vol. 212, no. 8, pp. 690-5.
- Wang, X-D, Lu, J, Lin, Y-S, Gao, C & Qi, F 2019b, 'Functional role of long non-coding RNA CASC19/miR-140-5p/CEMIP axis in colorectal cancer progression in vitro', *World Journal of Gastroenterology*, vol. 25, no. 14, pp. 1697-714.
- Wang, X 2008, 'miRDB: a microRNA target prediction and functional annotation database with a wiki interface', *Rna*, vol. 14, no. 6, pp. 1012-7.
- Wang, X, Liu, Z, Tong, H, Peng, H, Xian, Z, Li, L, Hu, B & Xie, S 2019c, 'Linc01194 acts as an oncogene in colorectal carcinoma and is associated with poor survival outcome', *Cancer Manag Res*, vol. 11, pp. 2349-62.
- Wang, X, Regufe da Mota, S, Liu, R, Moore, CE, Xie, J, Lanucara, F, Agarwala, U, Pyrdit Ruys, S, Vertommen, D, Rider, MH, Evers, CE & Proud, CG 2014c, 'Eukaryotic elongation factor 2 kinase activity is controlled by multiple inputs from oncogenic signaling', *Mol Cell Biol*, vol. 34, no. 22, pp. 4088-103.

## REFERENCES

- Warburg, O 1956, 'On respiratory impairment in cancer cells', *Science*, vol. 124, no. 3215, pp. 269-70.
- Wei, W, Yang, Y, Cai, J, Cui, K, Li, RX, Wang, H, Shang, X & Wei, D 2016, 'MiR-30a-5p Suppresses Tumor Metastasis of Human Colorectal Cancer by Targeting ITGB3', *Cell Physiol Biochem*, vol. 39, no. 3, pp. 1165-76.
- Wei, Z, Cui, L, Mei, Z, Liu, M & Zhang, D 2014, 'miR-181a mediates metabolic shift in colon cancer cells via the PTEN/AKT pathway', *FEBS Lett*, vol. 588, no. 9, pp. 1773-9.
- Wellen, KE, Hatzivassiliou, G, Sachdeva, UM, Bui, TV, Cross, JR & Thompson, CB 2009, 'ATP-citrate lyase links cellular metabolism to histone acetylation', *Science*, vol. 324, no. 5930, pp. 1076-80.
- Whitehead, RH, Macrae, FA, St John, DJ & Ma, J 1985, 'A colon cancer cell line (LIM1215) derived from a patient with inherited nonpolyposis colorectal cancer', *J Natl Cancer Inst*, vol. 74, no. 4, pp. 759-65.
- Wiggins, JF, Ruffino, L, Kelnar, K, Omotola, M, Patrawala, L, Brown, D & Bader, AG 2010, 'Development of a lung cancer therapeutic based on the tumor suppressor microRNA-34', *Cancer Res*, vol. 70, no. 14, pp. 5923-30.
- Wightman, B, Ha, I & Ruvkun, G 1993, 'Posttranscriptional regulation of the heterochronic gene lin-14 by lin-4 mediates temporal pattern formation in *C. elegans*', *Cell*, vol. 75, no. 5, pp. 855-62.
- Willimott, S & Wagner, SD 2012, 'miR-125b and miR-155 contribute to BCL2 repression and proliferation in response to CD40 ligand (CD154) in human leukemic B-cells', *J Biol Chem*, vol. 287, no. 4, pp. 2608-17.
- Wilson, AJ, Chueh, AC, Tögel, L, Corner, GA, Ahmed, N, Goel, S, Byun, D-S, Nasser, S, Houston, MA, Jhaver, M, Smartt, HJM, Murray, LB, Nicholas, C, Heerdt, BG, Arango, D, Augenlicht, LH & Mariadason, JM 2010, 'Apoptotic Sensitivity of Colon Cancer Cells to Histone Deacetylase Inhibitors Is Mediated by an Sp1/Sp3-Activated Transcriptional Program Involving Immediate-Early Gene Induction', *Cancer Research*, vol. 70, no. 2, pp. 609-20.
- Wilusz, JE, Freier, SM & Spector, DL 2008, '3' end processing of a long nuclear-retained noncoding RNA yields a tRNA-like cytoplasmic RNA', *Cell*, vol. 135, no. 5, pp. 919-32.
- Wilusz, JE, JnBaptiste, CK, Lu, LY, Kuhn, CD, Joshua-Tor, L & Sharp, PA 2012, 'A triple helix stabilizes the 3' ends of long noncoding RNAs that lack poly(A) tails', *Genes Dev*, vol. 26, no. 21, pp. 2392-407.
- Winawer, SJ 2007, 'Colorectal cancer screening', *Best Practice & Research Clinical Gastroenterology*, vol. 21, no. 6, pp. 1031-48.
- Winawer, SJ, Zauber, AG, Ho, MN, O'Brien, MJ, Gottlieb, LS, Sternberg, SS, Waye, JD, Schapiro, M, Bond, JH, Panish, JF & et al. 1993, 'Prevention of colorectal cancer by colonoscopic polypectomy. The National Polyp Study Workgroup', *N Engl J Med*, vol. 329, no. 27, pp. 1977-81.

## REFERENCES

- Witkos, TM, Koscianska, E & Krzyzosiak, WJ 2011, 'Practical Aspects of microRNA Target Prediction', *Curr Mol Med*, vol. 11, no. 2, pp. 93-109.
- Wong, MH, Huelsken, J, Birchmeier, W & Gordon, JI 2002, 'Selection of multipotent stem cells during morphogenesis of small intestinal crypts of Lieberkuhn is perturbed by stimulation of Lef-1/beta-catenin signaling', *J Biol Chem*, vol. 277, no. 18, pp. 15843-50.
- Wong, N & Wang, X 2015, 'miRDB: an online resource for microRNA target prediction and functional annotations', *Nucleic Acids Res*, vol. 43, no. Database issue, pp. D146-52.
- Wong, RSY 2011, 'Apoptosis in cancer: from pathogenesis to treatment', *Journal of Experimental & Clinical Cancer Research : CR*, vol. 30, no. 1, pp. 87-.
- Wong, RW & D'Angelo, M 2016, 'Linking Nucleoporins, Mitosis, and Colon Cancer', *Cell Chem Biol*, vol. 23, no. 5, pp. 537-9.
- Wu, C, Zheng, X, Li, X, Fesler, A, Hu, W, Chen, L, Xu, B, Wang, Q, Tong, A, Burke, S, Ju, J & Jiang, J 2016a, 'Reduction of gastric cancer proliferation and invasion by miR-15a mediated suppression of Bmi-1 translation', *Oncotarget*, vol. 7, no. 12, pp. 14522-36.
- Wu, F, Zhang, C, Cai, J, Yang, F, Liang, T, Yan, X, Wang, H, Wang, W, Chen, J & Jiang, T 2017a, 'Upregulation of long noncoding RNA HOXA-AS3 promotes tumor progression and predicts poor prognosis in glioma', *Oncotarget*, vol. 8, no. 32, pp. 53110-23.
- Wu, JJ, Roth, RJ, Anderson, EJ, Hong, EG, Lee, MK, Choi, CS, Neuffer, PD, Shulman, GI, Kim, JK & Bennett, AM 2006, 'Mice lacking MAP kinase phosphatase-1 have enhanced MAP kinase activity and resistance to diet-induced obesity', *Cell Metab*, vol. 4, no. 1, pp. 61-73.
- Wu, K, Xu, K, Liu, K, Huang, J, Chen, J, Zhang, J & Zhang, N 2018a, 'Long noncoding RNA BC200 regulates cell growth and invasion in colon cancer', *Int J Biochem Cell Biol*, vol. 99, pp. 219-25.
- Wu, M, Fan, B, Guo, Q, Li, Y, Chen, R, Lv, N, Diao, Y & Luo, Y 2018b, 'Knockdown of SETDB1 inhibits breast cancer progression by miR-381-3p-related regulation', *Biol Res*, vol. 51, no. 1, p. 39.
- Wu, M, Zhang, S, Chen, X, Xu, H & Li, X 2019, 'Expression and function of lncRNA MALAT-1 in the embryonic development of zebrafish', *Gene*, vol. 680, pp. 65-71.
- Wu, P, Wu, D, Zhao, L, Huang, L, Shen, G, Huang, J & Chai, Y 2016b, 'Prognostic role of STAT3 in solid tumors: a systematic review and meta-analysis', *Oncotarget*, vol. 7, no. 15, pp. 19863-83.
- Wu, X, He, X, Li, S, Xu, X, Chen, X & Zhu, H 2016c, 'Long Non-Coding RNA uc002kmd.1 Regulates CD44-Dependent Cell Growth by Competing for miR-211-3p in Colorectal Cancer', *PLoS One*, vol. 11, no. 3, p. e0151287.
- Wu, X, Wu, Y, He, L, Wu, L, Wang, X & Liu, Z 2018c, 'Effects of the intestinal microbial metabolite butyrate on the development of colorectal cancer', *Journal of Cancer*, vol. 9, no. 14, pp. 2510-7.

## REFERENCES

- Wu, Y, Song, Y, Xiong, Y, Wang, X, Xu, K, Han, B, Bai, Y, Li, L, Zhang, Y & Zhou, L 2017b, 'MicroRNA-21 (Mir-21) Promotes Cell Growth and Invasion by Repressing Tumor Suppressor PTEN in Colorectal Cancer', *Cell Physiol Biochem*, vol. 43, no. 3, pp. 945-58.
- Wu, Y, Yang, L, Zhao, J, Li, C, Nie, J, Liu, F, Zhuo, C, Zheng, Y, Li, B, Wang, Z & Xu, Y 2015, 'Nuclear-enriched abundant transcript 1 as a diagnostic and prognostic biomarker in colorectal cancer', *Mol Cancer*, vol. 14, no. 1, p. 191.
- Wu, ZH, Wang, XL, Tang, HM, Jiang, T, Chen, J, Lu, S, Qiu, GQ, Peng, ZH & Yan, DW 2014, 'Long non-coding RNA HOTAIR is a powerful predictor of metastasis and poor prognosis and is associated with epithelial-mesenchymal transition in colon cancer', *Oncol Rep*, vol. 32, no. 1, pp. 395-402.
- Xia, J, Benner, MJ & Hancock, REW 2014, 'NetworkAnalyst - integrative approaches for protein-protein interaction network analysis and visual exploration', *Nucleic Acids Research*, vol. 42, no. Web Server issue, pp. W167-W74.
- Xia, J, Gill, EE & Hancock, RE 2015, 'NetworkAnalyst for statistical, visual and network-based meta-analysis of gene expression data', *Nat Protoc*, vol. 10, no. 6, pp. 823-44.
- Xiang, J-F, Yin, Q-F, Chen, T, Zhang, Y, Zhang, X-O, Wu, Z, Zhang, S, Wang, H-B, Ge, J, Lu, X, Yang, L & Chen, L-L 2014, 'Human colorectal cancer-specific CCAT1-L lncRNA regulates long-range chromatin interactions at the MYC locus', *Cell Res*, vol. 24, no. 5, pp. 513-31.
- Xiao, F, Zuo, Z, Cai, G, Kang, S, Gao, X & Li, T 2009a, 'miRecords: an integrated resource for microRNA-target interactions', *Nucleic Acids Research*, vol. 37, no. Database issue, pp. D105-D10.
- Xiao, F, Zuo, Z, Cai, G, Kang, S, Gao, X & Li, T 2009b, 'miRecords: an integrated resource for microRNA-target interactions', *Nucleic Acids Research*, vol. 37, no. Database issue, pp. D105-D10.
- Xiao, H, Tang, K, Liu, P, Chen, K, Hu, J, Zeng, J, Xiao, W, Yu, G, Yao, W, Zhou, H, Li, H, Pan, Y, Li, A, Ye, Z, Wang, J, Xu, H & Huang, Q 2015, 'LncRNA MALAT1 functions as a competing endogenous RNA to regulate ZEB2 expression by sponging miR-200s in clear cell kidney carcinoma', *Oncotarget*, vol. 6, no. 35, pp. 38005-15.
- Xiao, M, Liu, YG, Zou, MC & Zou, F 2014, 'Sodium butyrate induces apoptosis of human colon cancer cells by modulating ERK and sphingosine kinase 2', *Biomed Environ Sci*, vol. 27, no. 3, pp. 197-203.
- Xiao, Y, Pan, J, Geng, Q & Wang, G 2019, 'LncRNA MALAT1 increases the stemness of gastric cancer cells via enhancing SOX2 mRNA stability', *FEBS Open Bio*, vol. 9, no. 7, pp. 1212-22.
- Xie, C-M, Liu, X-Y, Sham, KWY, Lai, JMY & Cheng, CHK 2014, 'Silencing of EEF2K (eukaryotic elongation factor-2 kinase) reveals AMPK-ULK1-dependent autophagy in colon cancer cells', *Autophagy*, vol. 10, no. 9, pp. 1495-508.

## REFERENCES

- Xie, M, Qin, H, Luo, Q, Huang, Q, He, X, Yang, Z, Lan, P & Lian, L 2017, 'MicroRNA-30a regulates cell proliferation and tumor growth of colorectal cancer by targeting CD73', *BMC Cancer*, vol. 17, no. 1, pp. 305-.
- Xiong, WC, Han, N, Wu, N, Zhao, KL, Han, C, Wang, HX, Ping, GF, Zheng, PF, Feng, H, Qin, L & He, P 2018, 'Interplay between long noncoding RNA ZEB1-AS1 and miR-101/ZEB1 axis regulates proliferation and migration of colorectal cancer cells', *Am J Transl Res*, vol. 10, no. 2, pp. 605-17.
- Xu, C, Yang, M, Tian, J, Wang, X & Li, Z 2011, 'MALAT-1: a long non-coding RNA and its important 3' end functional motif in colorectal cancer metastasis', *Int J Oncol*, vol. 39, no. 1, pp. 169-75.
- Xu, L, Wang, R, Ziegelbauer, J, Wu, WW, Shen, R-F, Juhl, H, Zhang, Y, Pelosof, L & Rosenberg, AS 2017, 'Transcriptome analysis of human colorectal cancer biopsies reveals extensive expression correlations among genes related to cell proliferation, lipid metabolism, immune response and collagen catabolism', *Oncotarget*, vol. 8, no. 43, pp. 74703-19.
- Xu, MD, Qi, P, Weng, WW, Shen, XH, Ni, SJ, Dong, L, Huang, D, Tan, C, Sheng, WQ, Zhou, XY & Du, X 2014, 'Long non-coding RNA LSINCT5 predicts negative prognosis and exhibits oncogenic activity in gastric cancer', *Medicine (Baltimore)*, vol. 93, no. 28, p. e303.
- Xu, W, Xu, B, Yao, Y, Yu, X, Cao, H, Zhang, J, Liu, J & Sheng, H 2016, 'RNA interference against TRIM29 inhibits migration and invasion of colorectal cancer cells', *Oncol Rep*, vol. 36, no. 3, pp. 1411-8.
- Xu, Y, Zhang, X, Hu, X, Zhou, W, Zhang, P, Zhang, J, Yang, S & Liu, Y 2018, 'The effects of lncRNA MALAT1 on proliferation, invasion and migration in colorectal cancer through regulating SOX9', *Mol Med*, vol. 24, no. 1, p. 52.
- Xue, W, Dahlman, JE, Tammela, T, Khan, OF, Sood, S, Dave, A, Cai, W, Chirino, LM, Yang, GR, Bronson, R, Crowley, DG, Sahay, G, Schroeder, A, Langer, R, Anderson, DG & Jacks, T 2014, 'Small RNA combination therapy for lung cancer', *Proc Natl Acad Sci U S A*, vol. 111, no. 34, pp. E3553-61.
- Xue, Y, Gu, D, Ma, G, Zhu, L, Hua, Q, Chu, H, Tong, N, Chen, J, Zhang, Z & Wang, M 2015a, 'Genetic variants in lncRNA HOTAIR are associated with risk of colorectal cancer', *Mutagenesis*, vol. 30, no. 2, pp. 303-10.
- Xue, Y, Ma, G, Gu, D, Zhu, L, Hua, Q, Du, M, Chu, H, Tong, N, Chen, J, Zhang, Z & Wang, M 2015b, 'Genome-wide analysis of long noncoding RNA signature in human colorectal cancer', *Gene*, vol. 556, no. 2, pp. 227-34.
- Xue, Y, Ma, G, Gu, D, Zhu, L, Hua, Q, Du, M, Chu, H, Tong, N, Chen, J, Zhang, Z & Wang, M 2015c, 'Genome-wide analysis of long noncoding RNA signature in human colorectal cancer', *Gene*, vol. 556, no. 2, pp. 227-34.
- Yamada, A, Yu, P, Lin, W, Okugawa, Y, Boland, CR & Goel, A 2018, 'A RNA-Sequencing approach for the identification of novel long non-coding RNA biomarkers in colorectal cancer', *Sci Rep*, vol. 8, no. 1, pp. 575-.

## REFERENCES

- Yamane, N, Makino, M & Kaibara, N 1999, 'S-phase accumulation precedes apoptosis induced by preoperative treatment with 5-fluorouracil in human colorectal carcinoma cells', *Cancer*, vol. 85, no. 2, pp. 309-17.
- Yan, X, Hu, Z, Feng, Y, Hu, X, Yuan, J, Zhao, SD, Zhang, Y, Yang, L, Shan, W, He, Q, Fan, L, Kandalaft, LE, Tanyi, JL, Li, C, Yuan, CX, Zhang, D, Yuan, H, Hua, K, Lu, Y, Katsaros, D, Huang, Q, Montone, K, Fan, Y, Coukos, G, Boyd, J, Sood, AK, Rebbeck, T, Mills, GB, Dang, CV & Zhang, L 2015, 'Comprehensive Genomic Characterization of Long Non-coding RNAs across Human Cancers', *Cancer Cell*, vol. 28, no. 4, pp. 529-40.
- Yang, C, Wang, MH, Zhou, JD & Chi, Q 2017a, 'Upregulation of miR-542-3p inhibits the growth and invasion of human colon cancer cells through PI3K/AKT/survivin signaling', *Oncol Rep*, vol. 38, no. 6, pp. 3545-53.
- Yang, F, Huo, X-s, Yuan, S-x, Zhang, L, Zhou, W-p, Wang, F & Sun, S-h 2013a, 'Repression of the Long Noncoding RNA-LET by Histone Deacetylase 3 Contributes to Hypoxia-Mediated Metastasis', *Molecular Cell*, vol. 49, no. 6, pp. 1083-96.
- Yang, H, Li, Q, Niu, J, Li, B, Jiang, D, Wan, Z, Yang, Q, Jiang, F, Wei, P & Bai, S 2015a, 'microRNA-342-5p and miR-608 inhibit colon cancer tumorigenesis by targeting NAA10', *Oncotarget*, vol. 7, no. 3, pp. 2709-20.
- Yang, H, Wang, S, Kang, Y-J, Wang, C, Xu, Y, Zhang, Y & Jiang, Z 2018a, 'Long non-coding RNA SNHG1 predicts a poor prognosis and promotes colon cancer tumorigenesis', *Oncol Rep*, vol. 40, no. 1, pp. 261-71.
- Yang, H, Zhong, Y, Xie, H, Lai, X, Xu, M, Nie, Y, Liu, S & Wan, Y-JY 2013b, 'Induction of the liver cancer-down-regulated long noncoding RNA uc002mbe.2 mediates trichostatin-induced apoptosis of liver cancer cells', *Biochemical Pharmacology*, vol. 85, no. 12, pp. 1761-9.
- Yang, J, Zhang, W, Evans, PM, Chen, X, He, X & Liu, C 2006, 'Adenomatous polyposis coli (APC) differentially regulates beta-catenin phosphorylation and ubiquitination in colon cancer cells', *J Biol Chem*, vol. 281, no. 26, pp. 17751-7.
- Yang, L, Lin, C, Liu, W, Zhang, J, Ohgi, KA, Grinstein, JD, Dorrestein, PC & Rosenfeld, MG 2011a, 'ncRNA- and Pc2 methylation-dependent gene relocation between nuclear structures mediates gene activation programs', *Cell*, vol. 147, no. 4, pp. 773-88.
- Yang, L, Qiu, M, Xu, Y, Wang, J, Zheng, Y, Li, M, Xu, L & Yin, R 2015b, 'Upregulation of long non-coding RNA PRNCR1 in colorectal cancer promotes cell proliferation and cell cycle progression', *Oncol Rep*.
- Yang, L, Qiu, M, Xu, Y, Wang, J, Zheng, Y, Li, M, Xu, L & Yin, R 2016a, 'Upregulation of long non-coding RNA PRNCR1 in colorectal cancer promotes cell proliferation and cell cycle progression', *Oncol Rep*, vol. 35, no. 1, pp. 318-24.
- Yang, MH, Hu, ZY, Xu, C, Xie, LY, Wang, XY, Chen, SY & Li, ZG 2015c, 'MALAT1 promotes colorectal cancer cell proliferation/migration/invasion via PRKA kinase anchor protein 9', *Biochim Biophys Acta*, vol. 1852, no. 1, pp. 166-74.

## REFERENCES

- Yang, MH, Yu, J, Chen, N, Wang, XY, Liu, XY, Wang, S & Ding, YQ 2013c, 'Elevated microRNA-31 expression regulates colorectal cancer progression by repressing its target gene SATB2', *PLoS One*, vol. 8, no. 12, p. e85353.
- Yang, P, Xu, Z-P, Chen, T & He, Z-Y 2016b, 'Long noncoding RNA expression profile analysis of colorectal cancer and metastatic lymph node based on microarray data', *Oncotargets and therapy*, vol. 9, pp. 2465-78.
- Yang, TY, Chang, GC, Chen, KC, Hung, HW, Hsu, KH, Sheu, GT & Hsu, SL 2011b, 'Sustained activation of ERK and Cdk2/cyclin-A signaling pathway by pemetrexed leading to S-phase arrest and apoptosis in human non-small cell lung cancer A549 cells', *Eur J Pharmacol*, vol. 663, no. 1-3, pp. 17-26.
- Yang, W, Ning, N & Jin, X 2017b, 'The lncRNA H19 Promotes Cell Proliferation by Competitively Binding to miR-200a and Derepressing beta-Catenin Expression in Colorectal Cancer', *Biomed Res Int*, vol. 2017, p. 2767484.
- Yang, X, Gu, Q, Lin, L, Li, S, Zhong, S, Li, Q & Cui, Z 2015d, 'Nucleoporin 62-like protein activates canonical Wnt signaling through facilitating the nuclear import of  $\beta$ -catenin in zebrafish', *Mol Cell Biol*, vol. 35, no. 7, pp. 1110-24.
- Yang, X, Hu, Q, Hu, LX, Lin, XR, Liu, JQ, Lin, X, Dinglin, XX, Zeng, JY, Hu, H, Luo, ML & Yao, HR 2017c, 'miR-200b regulates epithelial-mesenchymal transition of chemo-resistant breast cancer cells by targeting FN1', *Discov Med*, vol. 24, no. 131, pp. 75-85.
- Yang, X, Liu, W, Xu, X, Zhu, J, Wu, Y, Zhao, K, He, S, Li, M, Wu, Y, Zhang, S, Cao, J, Ye, Z & Xing, C 2018b, 'Downregulation of long noncoding RNA UCA1 enhances the radiosensitivity and inhibits migration via suppression of epithelialmesenchymal transition in colorectal cancer cells', *Oncol Rep*, vol. 40, no. 3, pp. 1554-64.
- Yang, XD, Xu, HT, Xu, XH, Ru, G, Liu, W, Zhu, JJ, Wu, YY, Zhao, K, Wu, Y, Xing, CG, Zhang, SY, Cao, JP & Li, M 2015e, 'Knockdown of long non-coding RNA HOTAIR inhibits proliferation and invasiveness and improves radiosensitivity in colorectal cancer', *Oncol Rep*.
- Yang, Y, Junjie, P, Sanjun, C & Ma, Y 2017d, 'Long non-coding RNAs in Colorectal Cancer: Progression and Future Directions', *Journal of Cancer*, vol. 8, no. 16, pp. 3212-25.
- Yang, Y, Zhang, J, Chen, X, Xu, X, Cao, G, Li, H & Wu, T 2018c, 'LncRNA FTX sponges miR-215 and inhibits phosphorylation of vimentin for promoting colorectal cancer progression', *Gene Ther*, vol. 25, no. 5, pp. 321-30.
- Yao, YX, Xu, BH & Zhang, Y 2018, 'CX-3543 Promotes Cell Apoptosis through Downregulation of CCAT1 in Colon Cancer Cells', *Biomed Res Int*, vol. 2018, p. 9701957.
- Yashiro, M, Carethers, JM, Laghi, L, Saito, K, Slezak, P, Jaramillo, E, Rubio, C, Koizumi, K, Hirakawa, K & Boland, CR 2001, 'Genetic Pathways in the Evolution of Morphologically Distinct Colorectal Neoplasms', *Cancer Research*, vol. 61, no. 6, pp. 2676-83.
- Ye, C, Yue, G, Shen, Z, Wang, B, Yang, Y, Li, T, Mao, S, Jiang, K, Ye, Y & Wang, SJTCR 2016a, 'miR-542-3p suppresses colorectal cancer progression through targeting survivin', *2016*, vol. 5, no. 6, pp. 817-26.

## REFERENCES

- Ye, LC, Chen, T, Zhu, DX, Lv, SX, Qiu, JJ, Xu, J, Yuan, FL & Wei, Y 2016b, 'Downregulated long non-coding RNA CLMAT3 promotes the proliferation of colorectal cancer cells by targeting regulators of the cell cycle pathway', *Oncotarget*.
- Ye, Z, Zhou, M, Tian, B, Wu, B & Li, J 2015, 'Expression of lncRNA-CCAT1, E-cadherin and N-cadherin in colorectal cancer and its clinical significance', *International Journal of Clinical and Experimental Medicine*, vol. 8, no. 3, pp. 3707-15.
- Yeh, JJ, Routh, ED, Rubinas, T, Peacock, J, Martin, TD, Shen, XJ, Sandler, RS, Kim, HJ, Keku, TO & Der, CJ 2009, 'KRAS/BRAF mutation status and ERK1/2 activation as biomarkers for MEK1/2 inhibitor therapy in colorectal cancer', *Molecular Cancer Therapeutics*, vol. 8, no. 4, pp. 834-43.
- Yi, R, Qin, Y, Macara, IG & Cullen, BR 2003, 'Exportin-5 mediates the nuclear export of pre-microRNAs and short hairpin RNAs', *Genes & Development*, vol. 17, no. 24, pp. 3011-6.
- Yin, D, He, X, Zhang, E, Kong, R, De, W & Zhang, Z 2014, 'Long noncoding RNA GAS5 affects cell proliferation and predicts a poor prognosis in patients with colorectal cancer', *Med Oncol*, vol. 31, no. 11, p. 253.
- Yin, DD, Liu, ZJ, Zhang, E, Kong, R, Zhang, ZH & Guo, RH 2015, 'Decreased expression of long noncoding RNA MEG3 affects cell proliferation and predicts a poor prognosis in patients with colorectal cancer', *Tumour Biol*, vol. 36, no. 6, pp. 4851-9.
- Yin, QF, Yang, L, Zhang, Y, Xiang, JF, Wu, YW, Carmichael, GG & Chen, LL 2012, 'Long noncoding RNAs with snoRNA ends', *Mol Cell*, vol. 48, no. 2, pp. 219-30.
- YiRen, H, YingCong, Y, Sunwu, Y, Keqin, L, Xiaochun, T, Senrui, C, Ende, C, XiZhou, L & Yanfan, C 2017, 'Long noncoding RNA MALAT1 regulates autophagy associated chemoresistance via miR-23b-3p sequestration in gastric cancer', *Molecular Cancer*, vol. 16, no. 1, pp. 174-.
- Yoon, JH, Abdelmohsen, K, Srikantan, S, Yang, X, Martindale, JL, De, S, Huarte, M, Zhan, M, Becker, KG & Gorospe, M 2012, 'LincRNA-p21 suppresses target mRNA translation', *Mol Cell*, vol. 47, no. 4, pp. 648-55.
- Yoon, S, Choi, YC, Lee, S, Jeong, Y, Yoon, J & Baek, K 2010, 'Induction of growth arrest by miR-542-3p that targets survivin', *FEBS Lett*, vol. 584, no. 18, pp. 4048-52.
- Young, LE, Moore, AE, Sokol, L, Meisner-Kober, N & Dixon, DA 2012, 'The mRNA stability factor HuR inhibits microRNA-16 targeting of COX-2', *Mol Cancer Res*, vol. 10, no. 1, pp. 167-80.
- Yu, DC, Bury, JP, Tiernan, J, Waby, JS, Staton, CA & Corfe, BM 2011, 'Short-chain fatty acid level and field cancerization show opposing associations with enteroendocrine cell number and neuropilin expression in patients with colorectal adenoma', *Mol Cancer*, vol. 10, p. 27.
- Yu, DC, Waby, JS, Chirakkal, H, Staton, CA & Corfe, BM 2010a, 'Butyrate suppresses expression of neuropilin I in colorectal cell lines through inhibition of Sp1 transactivation', *Mol Cancer*, vol. 9, p. 276.

## REFERENCES

- Yu, DCW, Waby, JS, Chirakkal, H, Staton, CA & Corfe, BM 2010b, 'Butyrate suppresses expression of neuropilin I in colorectal cell lines through inhibition of Sp1 transactivation', *Molecular Cancer*, vol. 9, pp. 276-.
- Yu, G, Liu, G, Yuan, D, Dai, J, Cui, Y & Tang, X 2018a, 'Long non-coding RNA ANRIL is associated with a poor prognosis of osteosarcoma and promotes tumorigenesis via PI3K/Akt pathway', *Journal of bone oncology*, vol. 11, pp. 51-5.
- Yu, G, Tang, JQ, Tian, ML, Li, H, Wang, X, Wu, T, Zhu, J, Huang, SJ & Wan, YL 2012, 'Prognostic values of the miR-17-92 cluster and its paralogs in colon cancer', *J Surg Oncol*, vol. 106, no. 3, pp. 232-7.
- Yu, J, Qi, J, Sun, X, Wang, W, Wei, G, Wu, Y, Gao, Q & Zheng, J 2018b, 'MicroRNA181a promotes cell proliferation and inhibits apoptosis in gastric cancer by targeting RASSF1A', *Oncol Rep*, vol. 40, no. 4, pp. 1959-70.
- Yu, X, Zhao, J & He, Y 2018c, 'Long non-coding RNA PVT1 functions as an oncogene in human colon cancer through miR-30d-5p/RUNX2 axis', *J buon*, vol. 23, no. 1, pp. 48-54.
- Yuan, L, Yuan, P, Yuan, H, Wang, Z, Run, Z, Chen, G, Zhao, P & Xu, B 2017, 'miR-542-3p inhibits colorectal cancer cell proliferation, migration and invasion by targeting OTUB1', *American Journal of Cancer Research*, vol. 7, no. 1, pp. 159-72.
- Yue, B, Qiu, S, Zhao, S, Liu, C, Zhang, D, Yu, F, Peng, Z & Yan, D 2016, 'LncRNA-ATB mediated E-cadherin repression promotes the progression of colon cancer and predicts poor prognosis', *J Gastroenterol Hepatol*, vol. 31, no. 3, pp. 595-603.
- Yue, B, Sun, B, Liu, C, Zhao, S, Zhang, D, Yu, F & Yan, D 2015, 'Long non-coding RNA Fer-1-like protein 4 suppresses oncogenesis and exhibits prognostic value by associating with miR-106a-5p in colon cancer', *Cancer Sci*, vol. 106, no. 10, pp. 1323-32.
- Yuen, ST, Davies, H, Chan, TL, Ho, JW, Bignell, GR, Cox, C, Stephens, P, Edkins, S, Tsui, WW, Chan, AS, Futreal, PA, Stratton, MR, Wooster, R & Leung, SY 2002, 'Similarity of the phenotypic patterns associated with BRAF and KRAS mutations in colorectal neoplasia', *Cancer Res*, vol. 62, no. 22, pp. 6451-5.
- Zeng, C-M, Chen, Z & Fu, L 2018, 'Frizzled Receptors as Potential Therapeutic Targets in Human Cancers', *Int J Mol Sci*, vol. 19, no. 5, p. 1543.
- Zhai, H, Fesler, A, Schee, K, Fodstad, O, Flatmark, K & Ju, J 2013, 'Clinical significance of long intergenic noncoding RNA-p21 in colorectal cancer', *Clin Colorectal Cancer*, vol. 12, no. 4, pp. 261-6.
- Zhai, HY, Sui, MH, Yu, X, Qu, Z, Hu, JC, Sun, HQ, Zheng, HT, Zhou, K & Jiang, LX 2016, 'Overexpression of Long Non-Coding RNA TUG1 Promotes Colon Cancer Progression', *Med Sci Monit*, vol. 22, pp. 3281-7.
- Zhang, B, Pan, X, Cobb, GP & Anderson, TA 2006a, 'Plant microRNA: a small regulatory molecule with big impact', *Dev Biol*, vol. 289, no. 1, pp. 3-16.

## REFERENCES

- Zhang, BH & Guan, KL 2000, 'Activation of B-Raf kinase requires phosphorylation of the conserved residues Thr598 and Ser601', *Embo j*, vol. 19, no. 20, pp. 5429-39.
- Zhang, H, Liu, Y, Yan, L, Zhang, M, Yu, X, Du, W, Wang, S, Li, Q, Chen, H, Zhang, Y, Sun, H, Tang, Z & Zhu, D 2018a, 'Increased levels of the long noncoding RNA, HOXA-AS3, promote proliferation of A549 cells', *Cell Death Dis*, vol. 9, no. 6, p. 707.
- Zhang, H, Song, Y, Yang, C & Wu, X 2019a, 'Overexpression of lncRNA TUSC7 reduces cell migration and invasion in colorectal cancer', *Oncol Rep*, vol. 41, no. 6, pp. 3386-92.
- Zhang, HF, Chen, Y, Wu, C, Wu, ZY, Tweardy, DJ, Alshareef, A, Liao, LD, Xue, YJ, Wu, JY, Chen, B, Xu, XE, Gopal, K, Gupta, N, Li, EM, Xu, LY & Lai, R 2016a, 'The Opposing Function of STAT3 as an Oncoprotein and Tumor Suppressor Is Dictated by the Expression Status of STAT3beta in Esophageal Squamous Cell Carcinoma', *Clin Cancer Res*, vol. 22, no. 3, pp. 691-703.
- Zhang, J, Guo, H, Zhang, H, Wang, H, Qian, G, Fan, X, Hoffman, AR, Hu, JF & Ge, S 2011a, 'Putative tumor suppressor miR-145 inhibits colon cancer cell growth by targeting oncogene Friend leukemia virus integration 1 gene', *Cancer*, vol. 117, no. 1, pp. 86-95.
- Zhang, J, Li, XY, Hu, P & Ding, YS 2018b, 'LncRNA NORAD contributes to colorectal cancer progression by inhibition of miR-202-5p', *Oncol Res*.
- Zhang, J, Sun, Q, Zhang, Z, Ge, S, Han, ZG & Chen, WT 2013, 'Loss of microRNA-143/145 disturbs cellular growth and apoptosis of human epithelial cancers by impairing the MDM2-p53 feedback loop', *Oncogene*, vol. 32, no. 1, pp. 61-9.
- Zhang, J, Zhang, Y, Li, X, Wang, H, Li, Q & Liao, X 2017a, 'MicroRNA212 inhibits colorectal cancer cell viability and invasion by directly targeting PIK3R3', *Mol Med Rep*, vol. 16, no. 5, pp. 7864-72.
- Zhang, K, Li, M, Huang, H, Li, L, Yang, J, Feng, L, Gou, J, Jiang, M, Peng, L, Chen, L, Li, T, Yang, P, Yang, Y, Wang, Y, Peng, Q, Dai, X & Zhang, T 2017b, 'Dishevelled1-3 contribute to multidrug resistance in colorectal cancer via activating Wnt/ $\beta$ -catenin signaling', *Oncotarget*, vol. 8, no. 70, pp. 115803-16.
- Zhang, L, Dong, Y, Zhu, N, Tsoi, H, Zhao, Z, Wu, CW, Wang, K, Zheng, S, Ng, SS, Chan, FK, Sung, JJ & Yu, J 2014a, 'microRNA-139-5p exerts tumor suppressor function by targeting NOTCH1 in colorectal cancer', *Molecular Cancer*, vol. 13, pp. 124-.
- Zhang, L, Huang, J, Yang, N, Greshock, J, Megraw, MS, Giannakakis, A, Liang, S, Naylor, TL, Barchetti, A, Ward, MR, Yao, G, Medina, A, O'Brien-Jenkins, A, Katsaros, D, Hatzigeorgiou, A, Gimotty, PA, Weber, BL & Coukos, G 2006b, 'microRNAs exhibit high frequency genomic alterations in human cancer', *Proc Natl Acad Sci U S A*, vol. 103, no. 24, pp. 9136-41.
- Zhang, L, Zhang, Y, Zhu, H, Sun, X, Wang, X, Wu, P & Xu, X 2019b, 'Overexpression of miR-301a-3p promotes colorectal cancer cell proliferation and metastasis by targeting deleted in liver cancer-1 and runt-related transcription factor 3', *J Cell Biochem*, vol. 120, no. 4, pp. 6078-89.

## REFERENCES

- Zhang, R, Li, J, Yan, X, Jin, K, Li, W, Liu, X, Zhao, J, Shang, W & Liu, Y 2018c, 'Long Noncoding RNA Plasmacytoma Variant Translocation 1 (PVT1) Promotes Colon Cancer Progression via Endogenous Sponging miR-26b', *Med Sci Monit*, vol. 24, pp. 8685-92.
- Zhang, R, Tang, P, Wang, F, Xing, Y, Jiang, Z, Chen, S, Meng, X, Liu, L, Cao, W, Zhao, H, Ma, P, Chen, Y, An, C & Sun, L 2019c, 'Tumor suppressor miR-139-5p targets Tspan3 and regulates the progression of acute myeloid leukemia through the PI3K/Akt pathway', *J Cell Biochem*, vol. 120, no. 3, pp. 4423-32.
- Zhang, T, Liu, W, Meng, W, Zhao, H, Yang, Q, Gu, S-J, Xiao, C-C, Jia, C-C & Fu, B-S 2018d, 'Downregulation of miR-542-3p promotes cancer metastasis through activating TGF- $\beta$ /Smad signaling in hepatocellular carcinoma', *Oncotargets and therapy*, vol. 11, pp. 1929-39.
- Zhang, X, Ma, X, An, H, Xu, C, Cao, W, Yuan, W & Ma, J 2017c, 'Upregulation of microRNA-125b by G-CSF promotes metastasis in colorectal cancer', *Oncotarget*, vol. 8, no. 31, pp. 50642-54.
- Zhang, X, Nie, Y, Li, X, Wu, G, Huang, Q, Cao, J, Du, Y, Li, J, Deng, R, Huang, D, Chen, B, Li, S & Wei, B 2014b, 'MicroRNA-181a functions as an oncomir in gastric cancer by targeting the tumour suppressor gene ATM', *Pathol Oncol Res*, vol. 20, no. 2, pp. 381-9.
- Zhang, Y, Zhou, L, Bao, YL, Wu, Y, Yu, CL, Huang, YX, Sun, Y, Zheng, LH & Li, YX 2010, 'Butyrate induces cell apoptosis through activation of JNK MAP kinase pathway in human colon cancer RKO cells', *Chem Biol Interact*, vol. 185, no. 3, pp. 174-81.
- Zhang, Z, Fu, C, Xu, Q & Wei, X 2017d, 'Long non-coding RNA CASC7 inhibits the proliferation and migration of colon cancer cells via inhibiting microRNA-21', *Biomed Pharmacother*, vol. 95, pp. 1644-53.
- Zhang, Z, Gao, Y, Gordon, A, Wang, ZZ, Qian, Z & Wu, WS 2011b, 'Efficient generation of fully reprogrammed human iPS cells via polycistronic retroviral vector and a new cocktail of chemical compounds', *PLoS One*, vol. 6, no. 10, p. e26592.
- Zhang, Z & Wu, W-S 2013, 'Sodium butyrate promotes generation of human induced pluripotent stem cells through induction of the miR302/367 cluster', *Stem cells and development*, vol. 22, no. 16, pp. 2268-77.
- Zhang, Z, Zheng, F, Yu, Z, Hao, J, Chen, M, Yu, W, Guo, W, Chen, Y, Huang, W, Duan, Z & Deng, W 2017e, 'XRCC5 cooperates with p300 to promote cyclooxygenase-2 expression and tumor growth in colon cancers', *PLoS One*, vol. 12, no. 10, pp. e0186900-e.
- Zhang, Z, Zhou, C, Chang, Y, Zhang, Z, Hu, Y, Zhang, F, Lu, Y, Zheng, L, Zhang, W, Li, X & Li, X 2016b, 'Long non-coding RNA CASC11 interacts with hnRNP-K and activates the WNT/beta-catenin pathway to promote growth and metastasis in colorectal cancer', *Cancer Lett*, vol. 376, no. 1, pp. 62-73.
- Zhang, ZY, Lu, YX, Zhang, ZY, Chang, YY, Zheng, L, Yuan, L, Zhang, F, Hu, YH, Zhang, WJ & Li, XN 2016c, 'Loss of TINCR expression promotes proliferation,

## REFERENCES

- metastasis through activating EpCAM cleavage in colorectal cancer', *Oncotarget*, vol. 7, no. 16, pp. 22639-49.
- Zhao, L, Zhao, Y, He, Y, Li, Q & Mao, Y 2018a, 'The functional pathway analysis and clinical significance of miR-20a and its related lncRNAs in breast cancer', *Cell Signal*, vol. 51, pp. 152-65.
- Zhao, M, Wang, S, Li, Q, Ji, Q, Guo, P & Liu, X 2018b, 'MALAT1: A long non-coding RNA highly associated with human cancers', *Oncol Lett*, vol. 16, no. 1, pp. 19-26.
- Zhao, W, Song, M, Zhang, J, Kuerban, M & Wang, H 2015, 'Combined identification of long non-coding RNA CCAT1 and HOTAIR in serum as an effective screening for colorectal carcinoma', *Int J Clin Exp Pathol*, vol. 8, no. 11, pp. 14131-40.
- Zheng, HT, Shi, DB, Wang, YW, Li, XX, Xu, Y, Tripathi, P, Gu, WL, Cai, GX & Cai, SJ 2014, 'High expression of lncRNA MALAT1 suggests a biomarker of poor prognosis in colorectal cancer', *Int J Clin Exp Pathol*, vol. 7, no. 6, pp. 3174-81.
- Zhong, M, Bian, Z & Wu, Z 2013, 'miR-30a suppresses cell migration and invasion through downregulation of PIK3CD in colorectal carcinoma', *Cell Physiol Biochem*, vol. 31, no. 2-3, pp. 209-18.
- Zhong, X, Lu, M, Wan, J, Zhou, T & Qin, B 2018, 'Long noncoding RNA kcna3 inhibits the progression of colorectal carcinoma through down-regulating YAP1 expression', *Biomed Pharmacother*, vol. 107, pp. 382-9.
- Zhou, BP, Liao, Y, Xia, W, Zou, Y, Spohn, B & Hung, MC 2001, 'HER-2/neu induces p53 ubiquitination via Akt-mediated MDM2 phosphorylation', *Nat Cell Biol*, vol. 3, no. 11, pp. 973-82.
- Zhou, H, Xu, M, Huang, Q, Gates, AT, Zhang, XD, Castle, JC, Stec, E, Ferrer, M, Strulovici, B, Hazuda, DJ & Espeseth, AS 2008, 'Genome-scale RNAi screen for host factors required for HIV replication', *Cell Host Microbe*, vol. 4, no. 5, pp. 495-504.
- Zhou, J, Li, X, Wu, M, Lin, C, Guo, Y & Tian, B 2016a, 'Knockdown of Long Noncoding RNA GHET1 Inhibits Cell Proliferation and Invasion of Colorectal Cancer', *Oncol Res*, vol. 23, no. 6, pp. 303-9.
- Zhou, P, Sun, L, Liu, D, Liu, C & Sun, L 2016b, 'Long Non-Coding RNA lincRNA-ROR Promotes the Progression of Colon Cancer and Holds Prognostic Value by Associating with miR-145', *Pathol Oncol Res*, vol. 22, no. 4, pp. 733-40.
- Zhou, Q, Li, G, Zuo, S, Zhu, W & Yuan, X 2019, 'RNA Sequencing Analysis of Molecular Basis of Sodium Butyrate-Induced Growth Inhibition on Colorectal Cancer Cell Lines', *Biomed Res Int*, vol. 2019, p. 1427871.
- Zhou, W, Li, X, Liu, F, Xiao, Z, He, M, Shen, S & Liu, S 2012a, 'MiR-135a promotes growth and invasion of colorectal cancer via metastasis suppressor 1 in vitro', *Acta Biochim Biophys Sin (Shanghai)*, vol. 44, no. 10, pp. 838-46.
- Zhou, W, Shi, G, Zhang, Q, Wu, Q, Li, B & Zhang, Z 2014, 'MicroRNA-20b promotes cell growth of breast cancer cells partly via targeting phosphatase and tensin homologue (PTEN)', *Cell & Bioscience*, vol. 4, p. 62.

## REFERENCES

- Zhou, X-M, Sun, R, Luo, D-H, Sun, J, Zhang, M-Y, Wang, M-H, Yang, Y, Wang, H-Y & Mai, S-J 2016c, 'Upregulated TRIM29 promotes proliferation and metastasis of nasopharyngeal carcinoma via PTEN/AKT/mTOR signal pathway', *Oncotarget*, vol. 7, no. 12, pp. 13634-50.
- Zhou, Y, Dang, J, Chang, KY, Yau, E, Aza-Blanc, P, Moscat, J & Rana, TM 2016d, 'miR-1298 Inhibits Mutant KRAS-Driven Tumor Growth by Repressing FAK and LAMB3', *Cancer Res*, vol. 76, no. 19, pp. 5777-87.
- Zhou, Y, Zhang, X & Klibanski, A 2012b, 'MEG3 noncoding RNA: a tumor suppressor', *Journal of molecular endocrinology*, vol. 48, no. 3, pp. R45-R53.
- Zhou, Y, Zhong, Y, Wang, Y, Zhang, X, Batista, DL, Gejman, R, Ansell, PJ, Zhao, J, Weng, C & Klibanski, A 2007, 'Activation of p53 by MEG3 non-coding RNA', *J Biol Chem*, vol. 282, no. 34, pp. 24731-42.
- Zhu, K, Diao, D, Dang, C, Shi, L, Wang, J, Yan, R, Yuan, D & Li, K 2013, 'Elevated KIAA0101 expression is a marker of recurrence in human gastric cancer', *Cancer Sci*, vol. 104, no. 3, pp. 353-9.
- Zhu, Y, Wu, G, Yan, W, Zhan, H & Sun, P 2017, 'miR-146b-5p regulates cell growth, invasion, and metabolism by targeting PDHB in colorectal cancer', *American Journal of Cancer Research*, vol. 7, no. 5, pp. 1136-50.
- Zhu, Y, Yang, T, Duan, J, Mu, N & Zhang, T 2019, 'MALAT1/miR-15b-5p/MAPK1 mediates endothelial progenitor cells autophagy and affects coronary atherosclerotic heart disease via mTOR signaling pathway', *Aging*, vol. 11, no. 4, pp. 1089-109.
- Zhuo, M, Yuan, C, Han, T, Cui, J, Jiao, F & Wang, L 2018, 'A novel feedback loop between high MALAT-1 and low miR-200c-3p promotes cell migration and invasion in pancreatic ductal adenocarcinoma and is predictive of poor prognosis', *BMC Cancer*, vol. 18, no. 1, p. 1032.
- Zuo, L, Lu, M, Zhou, Q, Wei, W & Wang, Y 2013, 'Butyrate suppresses proliferation and migration of RKO colon cancer cells through regulating endocan expression by MAPK signaling pathway', *Food Chem Toxicol*, vol. 62, pp. 892-900.
- Zuo, L, Zhang, S-M, Hu, R-L, Zhu, H-Q, Zhou, Q, Gui, S-Y, Wu, Q & Wang, Y 2008, 'Correlation between expression and differentiation of endocan in colorectal cancer', *World Journal of Gastroenterology*, vol. 14, no. 28, pp. 4562-8.